Studies Toward the Synthesis of Salvinorin A

Anthony Lingham

B.App.Sc. (App. Chem.)

B.App.Sc. (App. Chem. Hons.)

A thesis presented in fulfillment for

the Degree of Doctorate of Philosophy in Applied Chemistry.

School of Applied Sciences

Royal Melbourne Institute of Technology

September 2007

Statement of Authenticity

I certify that except where due acknowledgement has been made, the work is that of the author alone; the work has not been submitted previously, in whole or in part, to qualify for any other academic award; the content of the thesis is the result of work which has been carried out since the official commencement date of the approved research program; and, any editorial work, paid or unpaid, carried out by a third party is acknowledged.

Anthony Lingham.

15/9/2007

Acknowledgements

To Helmut Hügel for accepting to supervise a project not of his own creation and having the patients to persist with this extrodinarily difficult project. A very large thank-you to Trevor Rook for brainstorming suggestions, drafting and assistance with environmental and political hurdles. A lasting thank-you to Julie Niere for continuing help with technical trouble-shooting, NMR maintenance, interpretation of NMR spectra and teachings of scientific literacy skills far into my PhD years. Also thank-you for my basic and most essential knowledge of organic chemicals in the undergraduate years, then listening to my seemingly endless PhD chemistry rants, then keeping it real! Throughout my research I have gained a much appreciation for the knowledge passed on by Peter McKay and Gary Amiet in synthetic/retro-synthetic strategies, laboratory skills and pericyclic reactions. I would like to take this opportunity to thank them for making this synthesis project possible. I would also like to thank my colleagues who have contributed towards my experience at RMIT; Nathan Toovey, Robert Shellie, Daniel Beck, Bill Lording, Leigh Ford, Steven Privér, Samantha Gakias, Sylvia Tan, Rachael Clarke, Daniel Dias, Margaret Glewis, and Almar Postma.

I would like to extend a sincere thank you to Paul Morrison for his supreme GC/GC-MS maintenance and also for a shared interest in music and science. Our casual but educational chats have imbedded many practical GC skills that made many make-or-break results possible and pleasurable. Also thanks to Frank Antolasic for GC-MS maintenance and for various scientific and GC-MS related computational programs that made the presentation of GC data in this thesis very easy.

For technical consulting I would also like to thank Sally Duck from Monash University for high resolution mass spectral analysis, Roger Mulder and Jo Cosgriff (CSIRO) for NMR analysis and Jonathon White from the University of Melbourne for crystal structure analysis. Also an extended thanks to Karl Lang, Vioretta Harris, Peter Laming and Zarah Homann for the supply of chemicals and equipment and of course Howard Anderson for store service.

It has taken a mighty effort from my parents to understand what in the world I have been doing these past years but they have always seen me through the rotten moods, inconsistent living schedules and periods of panic and stress. Thank-you for the emotional and financial support for all these years, I really feel lucky not to be out on my rear! My brothers too have stuck this out with me and although they might not understand much from this work I'm positive I have filled them full of enough science lingo to entertain them. I am eternally proud that I have such a loving family. And finally my loving girlfriend and companion Britta, I know I helped you in the lab a bit, but I am still in awe that such a capable and beautiful woman would train herself at home in organic synthesis to be by my side.

Publications.

A. R. Lingham, T. J. Rook, H. M. Hügel. Synthesis of Some 3-Furylamine Derivatives. *Australian Journal of Chemistry*, **2002**, *55*, 795-798.

A. R. Lingham, H. M. Hügel, T. J. Rook. Diels-Alder Reactions of 3-Furylamines in Organic and Aqueous Solvents. *Australian Journal of Chemistry*, **2006**, *59*, 336-339.

A. R. Lingham, H. M. Hügel, T. J. Rook. Studies Towards the Synthesis of Salvinorin A. *Australian Journal of Chemistry*, **2006**, *59*, 340-348.

Abstract

Salvinorin A [(2*S*,4a*R*,6a*R*,7*R*,9*S*,10a*S*,10b*R*)-9-(acetyloxy)-2-(3-furanyl)-dodecahydro-6a,10b-dimethyl-4,10-dioxo-2H-naptho[2,1-*c*]pyran-7-carboxylic acid methyl ester] is a *trans*-neoclerodane diterpene from the leaves of the hallucinogenic Mexican sage *Salvia divinorum* and has been identified as the principal psychoactive component in this plant of traditional spiritual importance. Salvinorin A is the most potent naturally occurring hallucinogen found so far, and is reported to act selectively as a κ-opioid receptor agonist. Synthetic modification of the natural product has contributed to a number of proposed pharmacophores to identify the key structural features necessary for biological activity and a direct strategy for the asymmetric synthesis of the natural product is desirable since it allows access to a more flexible range of analogues. A recent synthesis of salvinorin A and effort towards many other clerodane diterpenoid natural products have followed a linear methodology. A convergent approach for the synthesis of neo-clerodane natural products is not yet reported in literature and would be of value for the facile preparation of salvinorin A.

An ambitious retrosynthetic study of salvinorin A indicated the C(3)-heterosubstituted furan as an appropriate starting material for a Diels-Alder approach towards the ketone ring of the natural product. An expedient and high yielding methodology for the preparation of 3-furylamines is described, allowing the flexible introduction of alkyl substituents in the C(5) position. A variety of non-chiral aza heterosubstituents were incorporated at C(3) of the furan ring including amine and amide functionalities, facilitating the examination of the chemical stability of these previously unreported compounds. Optically pure ephedrine isomers have been explored as chiral amine auxiliaries and have been successfully attached as 3-furylamine substituents using the general methodology described.

The 3-furylamines are electron rich dienes that are highly reactive towards Diels-Alder cycloaddition reactions. By reacting a selection of non-chiral 3-furylamines with methyl acrylate, the Diels-Alder cycloaddition products were prepared in high yield and diastereomeric outcomes were partially controlled using amine substituents of increased size and changes in reaction media polarity. A study involving Diels-Alder reactions in a range of solvents identified water as a general and optimum reaction medium for [4π+2π] electron cycloadditon reactions involving 3-furylamines, due to kinetic enhancement experienced in heterogeneous conditions and the potential for hydrolysis of reactive enamine cycloadduct intermediates. Diastereoisomers of the 7-oxanorbornane species methyl 1-methyl-5-oxo-7-oxa-bicyclo[2.2.1]heptane-2-carboxylate were prepared as new compounds from the hydrolysis of Diels-Alder cycloadducts and are functionalised bicyclic intermediates to access the ketone of the natural product. Diels-Alder reactions between the non-racemic (1*S*,2*S*)-pseudoephedrine-derived furan

and methyl acrylate gave solely the *endo* diatereoisomeric adduct as a spiro-oxazolidine system that underwent hydrolysis at pH = 5.5 to give the desired ketone. Reduction of the Diels-Alder spiro adduct to the bicyclic amine allowed for purification of the major diastereoisomer by crystallization as the perchlorate salt and the single product was identified by X-ray crystallography as the (1*S*,2*S*,4*S*,5*S*)-diastereoisomer. In Diels-Alder reactions involving the (2*S*)-ephedrine derived furans, face selectivity was established to favor the (1*S*,4*S*)-enantiomer as desired for the asymmetric natural product synthesis.

A procedure for the ether cleavage of methyl 1-methyl-5-oxo-7-oxa-bicyclo[2.2.1]heptane-2-carboxylate was required to access the convergent precursor methyl 5-acetoxy-2-methyl-4-oxocyclohex-2-enecarboxylate. Base mediated ether ring opening was discovered to yield C-C cleavage products as a consequence of anionic rearrangement. Successful C-O cleavage was achieved using Lewis-acid catalysis with BBr_3 followed by mixing with the hindered base 2,4,6-collidine to yield methyl 5-hydroxy-2-methyl-4-oxocyclohex-2-enecarboxylate albeit only at high dilution. Acetylation proceeded in excellent yield in the same reaction vessel to give methyl 1-methyl-5-oxo-7-oxa-bicyclo[2.2.1]heptane-2-carboxylate in excellent yield. Both cyclohexenone containing ether cleavage products required isolation by HPLC and found to be facile towards epimerization at C(5) under non-neutral conditions. The devised synthetic pathway is shown to successfully construct the ketone ring of salvinorin A and stereoselectivity for the (1*S*,4*S*)-enantiomer can be achieved using the ephedrine derived furans as desired for the asymmetric natural product synthesis. This molecule can be used directly as a precursor to salvinorin A by enolate trapping of the vinyl Gilman 1,4-addition product followed by reaction with a second molecule with the desired δ-lactone structure.

The δ-lactone ring 6-(furan-3-yl)-5,6-dihydro-4-methyl-3-vinylpyran-2-one was derived from rudimentary precursors as a convergent reagent to introduce the lactone ring of salvinorin A, as hypothesized from retrosynthetic analysis. A short synthesis for the racemic compound is described starting from the aldol reaction between 3-furaldehyde and acetone to give the 3-furfurol, 4-(furan-3-yl)-4-hydroxybutan-2-one in quantitative yield. The 3-furfurol was reacted to form the α-bromovinyl ester, 1-(furan-3-yl)-3-oxobutyl 2-bromobut-3-enoate using a deconjugation/esterification protocol with 2-bromobut-3-enoyl chloride. Intramolecular ring closure to the δ-lactone was achieved using a Reformatsky reaction and dehydration under acidic conditions yielded the racemic convergent precursor 6-(furan-3-yl)-5,6-dihydro-4-methyl-3-vinylpyran-2-one in high yield. A possible strategy for joining the ketone and lactone fragments for the total synthesis of salvinorin A is proposed.

Table of Contents.

List of Abbreviations

Chapter 1.0

DMT	*N*,*N*-dimethyltryptamine
LSD	Lysergic acid diethylamide
CD	Circular dichroism
NMR	Nuclear Magnetic Resonance
D	Dextrorotatory
L	Laevorotatory
R	*rectus*
S	*sinister*
DNA	Deoxyribose nucleic acid
CNS	Central nervous system
GPCRS	G-protein coupled receptors
GABA	γ-aminobutyrate
ACh	Acetylcholine
KOR	κ-opioid receptor
MOR	μ-opioid receptor
DOR	δ-opioid receptor
MEP	Methylerythritol phosphate
DOXP	1-deoxy-d-xylulose-5-phosphate
GPP	Geranyl diphosphate
GGPP	Geranylgeranyl diphosphate
TIPSO	Trisopropylsilyl ether
THF	Tetrahydrofuran
PDC	Pyridinium chloride
NaOMe	Sodium methoxide
NMP	1-methyl-2-pyrrolidinone
NPSP	*N*-phenylselenophthalimide
TPP	5,10,15,20-Tetraphenyl-21*H*,23*H*-porphine
MAC	Methyl acrylate

Chapter 2.0

MO	Molecular orbital
HOMO	Highest occupied molecular orbital
LUMO	Lowest unoccupied molecular orbital
EWG	Electron withdrawing group
EDG	Electron donating group
MeOH	Methanol
CH_3I	Iodomethane
$LiAlH_4$	Lithium aluminium hydride
$AlCl_3$	Aluminium chloride
DCE	1,2-dichloroethane
Et_2O	Diethyl ether
GC-MS	Gas chromatography-mass spectrometry
NH_2NH_2	Hydrazine
KOH	Potassium hydroxide
CCl_4	Carbon tetrachloride
$CHCl_3$	Chloroform
NaOH	Sodium hydroxide
LDA	Lithium diisopropylamine
Pd	Palladium
OAc	Acetate
Dba	Dibenzylidene acetone

$NaO^{+}Bu$	Sodium tertiary-butoxide
BINAP	2,2-bis-diphenylphosphanyl-[1,1']binaphthalenyl
NaH	Sodium hydride
DMAD	Dimethylacetylene dicarboxylate
EtOAc	Ethyl acetate
p-TsOH	*para*-Toluene sulphonic acid
THP	Tetrahydropyran
$POCl_2$	Phosphoryl chloride
TMS	Tetramethylsilyl
TES	Tetraethylsilyl
Ac_2O	Acetic anhydride
n-BuLi	n-butyl lithium
DMF	*N*,*N*-dimethylformamide
KH_2PO_4	Potassium dihydrogen orthophosphate
EIMS	Electron ionization mass spectrometry
HCl	Hydrochloric acid
H_2SO_4	Sulphuric acid
HNO_3	Nitric acid
EtOH	Ethanol
H_2O	Water
$NaHCO_3$	Sodium hydrogen carbonate
TFA	Trifluoroacetic acid
HETCOR	^{1}H-^{13}C Heteronuclear correlared spectroscopy
DEPT	Distortionless enhancement by polarization transfer
ESI-HRMS	Electrospray ionization-high resolution spectrometry
$CDCl_3$	Deutero-chloroform
BnOH	Benzyl alcohol
FTIR	Fourier transform infrared
KHMDS	Potassium bis(trimethylsilyl)amide
TIPSCl	Triisopropyl silylchloride
HMQC	Heteronuclear multiple quantum coherence
COSY	Correlated spectroscopy

Chapter 3.0

FMO	Frontier molecular orbital
SHMO	Simple Hückel molecular orbital theory
D-A	Diels-Alder
LCAO	Linear combination of atomic orbitals
F	Fock
IEA	Independent election assumption
A	Asymmetric
LiCl	Lithium chloride
GnCl	Guanidium chloride
ZnI_2	Zinc iodide
TBDMS	*tert*-Butyldimethylsiloxy
LiHMDS	Lithium bis(trimethylsilyl)amide
PBr_3	Phosphorous tribromide
$^{i}PrOH$	Isopropanol
DMAD	Dimethylacetylenedicarboxylate
$NaBH_4$	Sodium borohydride
DMAP	4-Dimethylaminopyridine
HMBC	Heteronuclear multiple bond correlation
DIMCARB	*N*',*N*'-dimethylamino-*N*,*N*-dimethyl carbamate
GC x GC	Two dimensional gas chromatography
$NaBH(OAc)_3$	Sodium triacetoxyborohydride
MeCN	Acetonitrile
$AgClO_4$	Silver perchlorate

NaOAc	Sodium acetate
TBAI	Tetrabutyl ammonium iodide

Chapter 4.0

TBDMSOTf	*Tert*-butyl-dimethylsilyl triflate
TfOH	Trifluoromethane sulphonic acid
BBr_3	Boron tribromide
FCC	Flash column chromatography
SiO_2	Silica
TLC	Thin layer chromatography
HPLC	High performane liquid chromatography
NOE	Nuclear overhauser effect
AcCl	Acetyl chloride
BCl_3	Boron trichloride
NH_4Cl	Ammonium chloride
TMSCl	Tetramethylsilyl chloride
TBAF	Tetrabutyl ammonium fluoride
$FeCl_3.6H_2O$	Ferric(III) chloride hexahydrate
$ZrCl_4$	Zirconium(IV) chloride
$BF_3.(Et_2O)$	Boron trifluoride etherate
TBAI	Tetrabutylammonium iodide
An	Anisoate
DMAP	4-Dimethylaminopyridine
Piv	Pivaloate
NOESY	NOE correlated spectroscopy
MeMgBr	Methylmagnesiumbromide
MeLi	Methyllithium
MeMgCl	Methylmagnesiumchloride
CuI	Cuprous(I) iodide

Chapter 5.0

HIO_4	Periodic acid
$SOCl_2$	Thionyl chloride
BINOL	1,1'-Bi-2-naphthol
K_2CO_3	Potassium carbonate
NaOH	Sodium hydroxide
DEAD	Diethyl azodicarboxylate
Ph_3P	Triphenyl phosphine
TEA	Triethylamine
(PO(OEt)3)	Triethyl phosphite
1,2-DME	1,2-Dimethoxyethane
HCOOH	Formic acid
RCM	Ring closing metathesis

List of Figures

Chapter 4

List of Schemes

Chapter 3

List of Tables

Chapter 1
Introduction

1.1 Salvia divinorum, a Brief Background of the Unique Mexican Sage

Salvia divinorum is a perennial herb which grows best in humid, shaded areas, and struggles to survive in intense direct sunlight or heavy frost. Although wild and cultivated populations have been found in elevated areas (300 – 1800 m) in the highlands of northern Mexico, it is not known whether the species is native to the area or was introduced. *S. divinorum* thrives in tropical evergreen forests and ravines and reproduces vegetatively, with roots striking from the fresh or dried nodes [1]. Distinct physical features of the plant include a hollow quadrangular stem, with serrated elliptic leaves as long as 30 cm on a mature plant, growing in an opposite arrangement on the stem. A slight 'musty' odour can be noticed from the large green leaves, which vary in shape and shade in different climates. Rarely does the plant set seed or flower, and those grown from seeds are reported to sometimes lack vigour [2]. The mint grows to over 1 m in height and blossoms with white flowers and purple calyces [3]. Reports on cultivated populations of the 'sacred' plant, carefully hidden by the Mazatec Indians of Oaxca, suggest that many populations of the plant are clonal, hence inbreeding depression may account for the low number of successfully developed seedlings in cross-pollination studies [3].

Figure 1.1: *Salvia divinorum* growing in Melbourne (Photo; J. Lingham 2001)

Historically, *S. divinorum* (known as *hojas de la Pastora* – 'Leaves of the Shepherdess' and variations thereof) has been used in traditional societies of the Mazatec Indians for healing and divinatory rituals [4], and as the weakest of three hallucinogens used in shamanic training. The leaves are prepared for ingestion as an infusion or alternately chewed as a 'quid' and held under the tongue, although the fresh leaf material is extremely bitter in taste. Dried leaf material is popular amongst younger indigenous people and in this case is more commonly smoked. Common dosage is in the range of 20 to 100 leaves, sometimes mentioned as 10 to 50 'pairs' of leaves, and is dependant on the method of ingestion [5]. A detailed description of the bioactive effects and botanical history of *S. divinorum* is found in research by Siebert *et al.* [6] and identification of the active components relative to the periodic discovery of other naturally occurring hallucinogens from Mexican plant of traditional and sacramental use is summarised.

The first of the psychoactive Mexican plants to be studied in detail was the *péyotl* cactus *Lophophora williamsii* from which Heffter (1897) isolated the hallucinogenic phenethylamine mescaline (Figure 1.2), a comprehensive list of bioactive cactus alkaloids is found in more recent literature by Shulgin *et al.* [7]. The indole ethylamine, *N*,*N*-dimethyltryptamine (DMT) has been found as an active component in *Psychotria viridis* or '*Chacruna'* used in an admixure of plants to prepare 'ayahuasca', a south American drink used in the Amazon Basin. β-Carboline alkaloids present in *Banisteropsis caapi* act to inhibit DMT metabolism via monoamine oxidase in the gut and liver, allowing the DMT to be orally active [8]. DMT had been synthesised in 1931 by Richard Manske before being uncovered as a bioactive natural product and has since been identified in many plant species including Phalaris grasses such as *Phalaris tuberosa,* and various acacias [9]. *S. divinorum* was first referenced in botanical literature by Jean B. Johnson in 1939 along with other Mexican plants of traditional Aztec use [10] during an expedition to establish the existence of traditional ceremonies involving 'sacred' mushrooms. An ethnobotanist, R. Gordon Wasson obtained samples of mushrooms, referred to as '*Teonanácatl'* in the language native to the Mazatecs (Nahuatl), for identification and analysis [5, 6]. The hallucinogenic mushroom was identified as a new species *Psilocybe mexicana* (Strophariaceae family) by mycologist Roger Heim [11]. The psilocybian mushrooms are the more potent of ceremonial inebriants and investigations into the mushrooms psychoactive components by Albert Hofmann in 1958, revealed the indole ethylamines psilocibin and psilocin (Figure 1.2)[12]. It has since been suggested that psilocibin metabolises in the gut to psilocin, so the latter may actually be the active drug [13]. In 1959 Wasson and Hofmann had collaborative success in the isolation of psychoactive lysergic acid amides from '*Ololiuhqui'*, seeds of the morning glory *Turbina corymbosa*, many of which had already been synthesised by Hofmann from naturally occurring rye ergot alkaloids leading to the discovery of the prototype hallucinogen LSD-25 (Figure 1.2) in 1943 [14]. The samples of *S. divinorum* obtained by

Wasson and Hofmann were later identified by Epling & Játiva (1962) [15] as a new species of salvia from the Labiatae family (now the Lamiaceae family). Leaf extract of *S. divinorum* was retrieved and preserved in alcohol, upon storage the extract decreased in potency and it was concluded that the psychoactive component was unstable. The role of *S. divinorum* in ritualistic use as compared to the other inebriants mentioned is discussed by Valdés *et al.* [16] in an account of the plants effects and significance to indigenous culture.

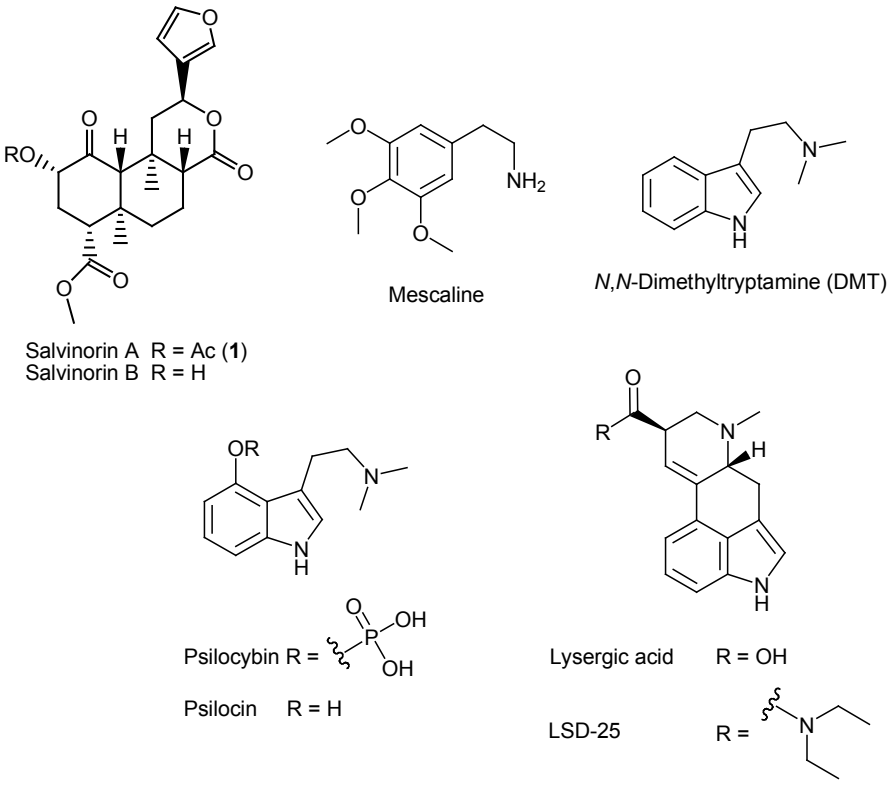

Figure 1.2: Hallucinogenic natural products: Salvinorin A (**1**), Mescaline, *N*,*N*-Dimethyltryptamine (DMT), Psilocybin, Psilocin, Lysergic acid and the semi-synthetic prototypical hallucinogen LSD-25.

It was not until 1982 that a research group led by Alfredo Ortega reported the isolation of a secondary metabolite from *S. divinorum*, present in high concentration in the leaf, and elucidated its structure as (2*S*,4a*R*,6a*R*,7*R*,9*S*,10a*S*,10b*R*)-9-(acetyloxy)-2-(3-furanyl)-dodecahydro-6a,10b-dimethyl-4,10-dioxo-2H-naptho[2,1-*c*]pyran-7-carboxylic acid methyl ester using ^{1}H and ^{13}C nuclear magnetic resonance (NMR) studies as well as single crystal X-ray crystallography [17]. The newly discovered *trans*-neoclerodane diterpene was called salvinorin (Figure 1.2). Valdés *et al.* [18] independently isolated the same compound in 1984 along with its deacetyl derivative and allocated the names divinorin A and divinorin B, respectively. Although both names are used interchangeably in the literature, salvinorin remains the more common name to describe the compound and its analogues. Through *in vivo* studies in

mice, Valdés and co-workers confirmed that salvinorin A (**1**) was indeed a main psychoactive component of the leaves with high potency, and concentrations of **1** have since been reported to range between 0.89-3.70 mg/g (dry weight leaf) [19]. The absolute stereochemistry of **1** was first postulated using circular dichroism (CD) spectroscopy and based on the observed negative n → π* Cotton effect of the ketone around 295 nm by comparison to the effect of isofructtcolone [17], then was later verified by Koreeda *et al.* [20] using the non-empirical exciton chirality CD method. Dedicated study to describe unambiguous NMR spectral assignments of **1** was published by Giner *et al.* [21] at the time of this thesis. Salvinorin A presents itself as an attractive synthetic target for natural product synthesis as it is the first reported non-nitrogenous hallucinogen and is also dissimilar in structure to the psychoactive alkaloids shown in Figure 1.2.

The location of **1** and related diterpenes in *S. divinorum* has been reported by Siebert [22] in resinous secretion accumulating in the subcuticular space of peltate glandular trichomes, which are present in highest levels in the leaves but also present most other parts of the plant in lower concentration. Elucidation of the pathway for the biosynthesis of **1** in *S. divinorum* has been studied by Kutrzeba *et al.* [23] and is discussed in Section 1.4.3. The search for other biologically active compounds from *S. divinorum* has produced improvements in the isolation of secondary metabolites from the leaves, leading Munro *et al.* [24] to report the isolation of commonly encountered plant metabolites such as presqualene alcohol, (E)-phytol and peplusol [24]. The structurally related metabolites salvinorin C [25], D-F [24], G [26] and divinatorins A-C [27], D-E [26] have been isolated in low concentrations (Figure 1.3) along with the tetrahydrofuran analogues salvinicin A and B [28]. Recent studies by Shirota et al. [29] have identified salvinorins H-I, divinorin F as well as a range of metabolites Salvidivin A-D featuring an oxidised furan moiety (Figure 1.3). Known terpenoids hardwickiic acid [27] and loliolide [30] have also been isolated. So far no other isolated metabolites have shown the same potency as **1**.

When thus research was commenced no synthetic studies addressing the stereoselective synthesis of salvinorin A had been reported in the literature. During revisions of this thesis, Scheerer *et al.* [31] published the first asymmetric synthesis of the target compound **1** and their approach is discussed in Section 1.6.4.

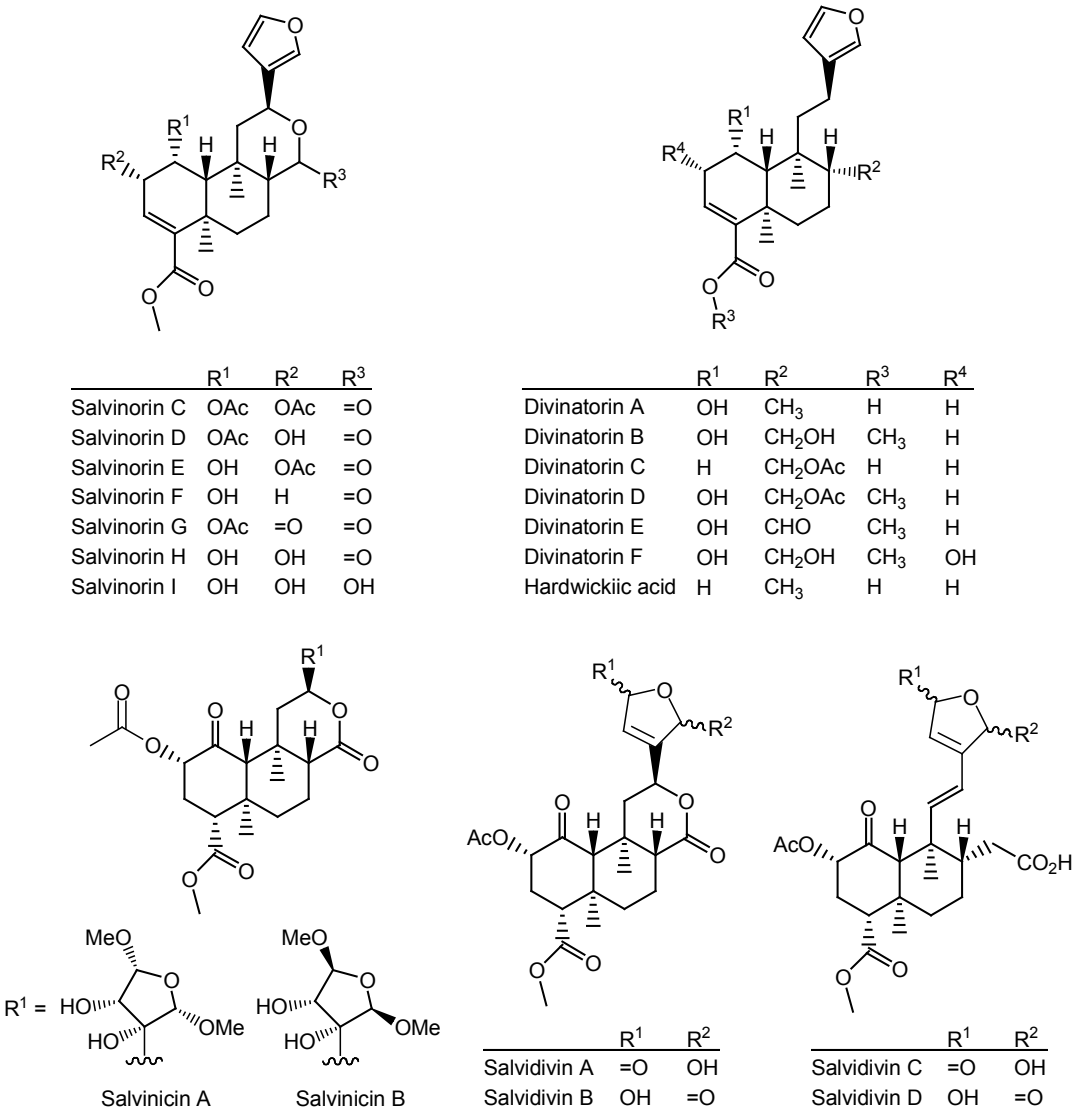

Figure 1.3: Compounds isolated and characterised from *Salvia divinorum* [22-28].

The aim of this thesis is to design a novel stereoselective approach to **1** and its analogues for further research into these newly recognised bioactive diterpenoids. In the remainder of this introduction, the implication of chirality in biological systems and organic synthesis of the *trans*-neoclerodane **1** are discussed. The importance of bioactive natural products to ongoing pharmacological research is mentioned followed by a short review of clerodanes isolated from bioactive plants that feature similar *trans*-neoclerodane connectivity to **1**. Publications related to the mode of action of **1** are reviewed and descriptions of bioactive analogues prepared by synthetic transformation on the natural product **1** are included. Relevant synthetic principals used throughout later chapters are described and previously established chemistry for the asymmetric synthesis of clerodane diterpenes is also outlined.

1.2 Chirality and Neurotransmission

1.2.1 Chirality

In 1874, both Van't Hoff and Le Bel proposed that when four different groups are connected to a non-planar central carbon the molecule can exist in two non-superimposable forms [34]. These two forms are mirror images of each other and are called enantiomers or 'optical isomers' (Figure 1.4) [35]. In likeness to the symmetry of two hands when held side by side, the phenomena as a whole is called chirality, from the greek term 'Cheiros' meaning handedness. In 1913, Bragg demonstrated through the use of X-ray analysis that these four groups are distributed in a tetrahedral arrangement, hence giving chemists a visual model to represent chiral compounds. The central carbon in the tetrahedron is referred to as a *stereogenic* or *chiral* center, from which the four different atoms are arranged at or near the tetrahedral angle of 109^0 28'.

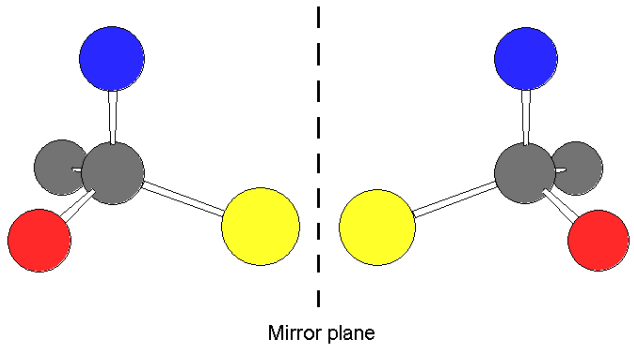

Figure 1.4: Enantiomers

Years before the quadrivalency of carbon had been conceived and the tetrahedral arrangement confirmed, extensive investigation into the properties of chiral compounds had already commenced. In 1848, after slowly crystallizing a racemic mixture of the tartaric acid salts, Louis Pasteur physically separated enantiomers of individual crystals according to their hemihedral shapes [34]. The separated tartrate salts were found to possess identical physical and chemical properties but were metabolised at different rates by the mould *Penicillium glaucum* [35]. For the first time the importance of chirality in biochemical processes was realised. In 1860, Pasteur concluded that the asymmetric arrangement of groups within a molecule is responsible for optical activity, whereby mirror images of the same molecule can rotate the plane of polarised light in opposite directions when viewed through a polarimeter [35] (Figure 1.5).

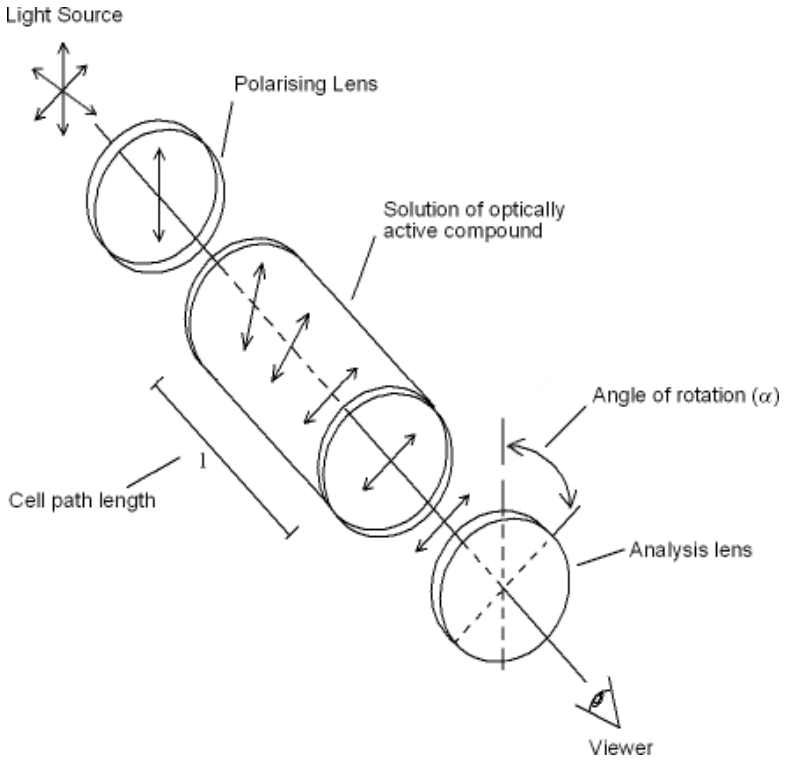

Figure 1.5: Diagram of a polarimeter adapted from McMurry [36]. Incident light is polarised through a slotted lens before being passed through a solution of optically active compound. The analysis lens is also slotted and is rotated to find the maximum intensity of light passing from the light source. The rotation of the analysis lens provides the angle of rotation α.

The optical activity of a pure enantiomer is unique to the compound and the opposite enantiomer will give an equal but opposite angle of rotation. The observed optical rotation is dependent on the cell length (*l* in dm.), sample concentration (c) expressed in g/100 mL and temperature [35]. Results for pure compounds are reported as their specific rotation $[\alpha]_D^T$ calculated as shown in Equation 1.1;

$$[\alpha]_D^T = \frac{100\alpha}{l \times c} \qquad (1.1)$$

To distinguish between enantiomers in chemical nomenclature, those rotating the plane of polarised light to the left are called *laevorotatory* and are given the prefix L or (-), and to the right are called *dextrorotatory* and are given the prefix D or (+). However this convention is not always strictly used; in carbohydrates the D, L prefixes describe the configuration relative to that in (D)-(+)-glyceraldehyde. Alternately the Cahn Ingold Prelog rules [36] determine by substituent ranking whether a compound is right handed or *rectus* thus given the prefix (*R*), or left handed (*sinister*) and given the prefix (*S*). L and D do not indicate absolute stereochemistry of the compound whereas the Cahn-Ingold-Prelog convention does.

The presence of multiple stereocentres introduces the concept of diastereoisomers, or diastereomers, whereby geometric isomers no longer have a mirror image relationship and posses different physical and chemical properties. A good example of this can be seen in saturated ring structures. The *trans*- isomer of 1,2-cyclohexanediol has a non-superimposable mirror image and hence enantiomers exist as the (*R*,*R*) and (*S*,*S*) forms. The *cis*- diastereomer (*R*,*S*) has C-2 plane of symmetry whereby mirror images are identical. This is referred to as the *meso*-form and in the case of 1,2-cyclohexanediol the *meso*-*cis*-isomer has a lower melting point to the *trans*- isomer (Figure 1.6). It is also of interest to note that the racemic *trans*- mixture of 1,2-cyclohexanediol, consisting of an equal ratio of both (*R*,*R*) and (*S*,*S*)-enantiomers, has a lower melting point compared to the enantiomerically pure products.

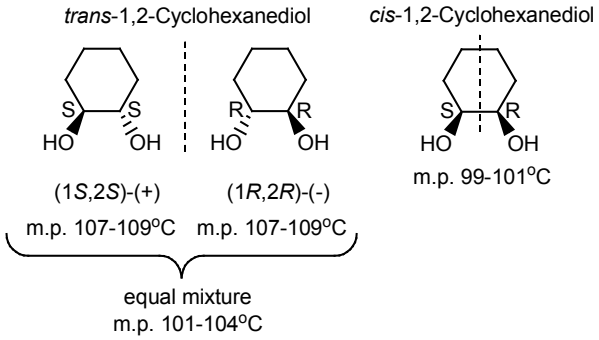

Figure 1.6: Mixtures of *trans*-1,2-cyclohexanol enantiomers possess lower melting points than their optically pure counterparts. The *cis*-diastereomer is in fact a different compound and possesses different chemical and physical properties from the *trans*- isomer.

Attempts to chemically differentiate, separate or form one optical isomer preferentially often involve the interaction with another optically active compound. It is the diastereo-interaction between enantiomers and an optically pure molecule or substrate that allows them to be distinguished (Section 1.5.2). To describe the purity of an enantiomer with respect to the abundance of its antipode the percent enantiomeric excess (% *ee*) is calculated as shown below in Equation 1.2:

$$\%\,ee\ enantiomer\ A = \frac{enantiomer\ A - enantiomer\ B}{enantiomer\ A + enantiomer\ B} \times 100 \qquad (1.2)$$

It follows, a 70:30 mixture of enantiomers A and B, respectively would be expressed as 40% excess of enantiomer A (or 40% *ee*).

1.2.2 Chirality in Biological Systems

As suggested in early experiments conducted by Pasteur, the biology of individual enantiomers are often significantly different. When taken into consideration that natural amino acids exist as the L-enantiomer and carbohydrates are found as D-carbohydrates, it is evident that biological systems provide a chiral environment for chemical processes. Asymmetry in the essential building blocks for life puts into effect the crucial role of chirality in metabolic pathways, enzyme-substrate binding, neural receptor binding and the structure and function of the DNA chiral helix, to name but a few. Olfactory receptors are an everyday example of this, (*R*) and (*S*)-limonene, although differing only at their chiral center, smell like orange and lemon, respectively (Figure 1.7) [37].

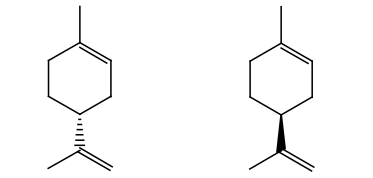

Figure 1.7: (*R*) and (*S*) enantiomers of limonene have orange and lemon fragrances demonstrating the importance of chirality in the olfactory system.

Optical isomers of some medicinal drugs have been shown to have distinctly different physiological effects in the body. Thalidomide (Figure 1.8) was prescribed as a racemic mixture in the 1960s to treat nausea associated with morning sickness. After a high occurrence of birth defects was linked to the use of thalidomide, biological evaluations on individual enantiomers identified (*R*)-(+)-thalidomide as responsible for therapeutic action, however the (*S*)-(-)-enantiomer proved to cause the teratogenic side effects. Incidentally, racemisation between enantiomers has been demonstrated in *in vivo* studies indicating that the drug cannot be reliably administered [38].

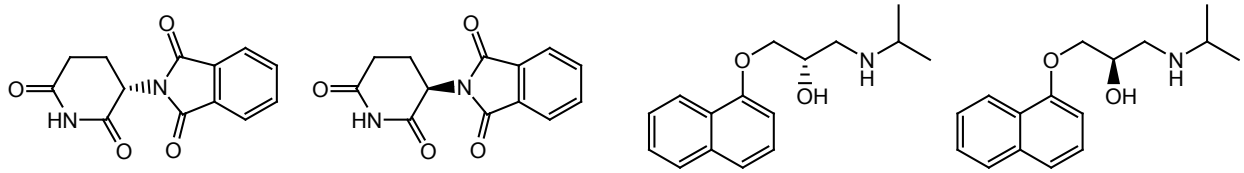

Figure 1.8: Chiral drugs (*S*)/(*R*)-Thalidomide and (*S*)/(*R*)-Propranolol.

Not all racemic drugs have ended with such detrimental effects. Propranolol (Figure 1.8) is a β-adrenergic drug that blocks or 'antagonises' the action of epinephrine and nor-epinephrine, which are neurotransmitters released when the body is under physical or emotional stress [39], to prevent increased heart rate and blood pressure. The β-blocking activity has been found to reside in the (*S*)-enantiomer, however the (*R*)-enantiomer has a reduced capability to produce these effects but exhibits potent antioxidative activity [40]. Activity testing on individual drug enantiomers is now mandatory.

Chirality has a crucial role in biological functions, of which signal transmission and reception are relevant examples, and is regularly discussed throughout the following chapters of this thesis from an organic chemistry perspective.

1.2.3 Neurotransmitters and Psychoactive Ligands

Signal processes of the central nervous system (CNS), which includes the spinal cord and brain, and the peripheral nervous system, rely on nerve cells called neurons. Nerve cells pass an electric signal down the length of the cell and transmission between neurons occurs by the release of neurotransmitters in the junction or 'synapse' between neural cells. Exogenous psychoactive ligands act on the CNS by mimicking the endogenous neurotransmitters responsible for homeostasis, signal transduction and the regulation of emotional and physiological states. Although some ligands directly affect cell wall ion channels, others can bind to G-protein coupled receptors (GPCRs), which consist of seven transmembrane-spanning helices with intra and extra cellular loops of varying lengths. These receptors are coupled to the release of "secondary messengers", which in turn act at ion gates (Appendix 1.1). Endogenous neurotransmitters are synthesised within the body and can be separated into four categories:

Amino acid neurotransmitters.

- Glycine, aspartate, glutamate, γ-aminobutyrate (GABA).

Monoamine neurotransmitters.

- Serotonin (5-HT), dopamine, norepinephrine, epinephrine.

Acetylcholine.

- Acetylcholine (ACh).

Peptides neurotransmitters (neuropeptides).

- Substance P, leu- and met-enkephalin, dynorphin.

The nitrogen containing or 'alkaloid' hallucinogens LSD, DMT, psilocybin and psilocin possess an indole ethylamine backbone and closely resemble the monoamine neurotransmitter serotonin (Figure 1.9). Serotonin (5-HT) governs body temperature, sleep and feeding and acts at an array of receptors that

are found in both the central and peripheral nervous systems [41]. 5-HT imbalances has been implicated in depression, anxiety, social phobia and obsessive-compulsive disorders. The other effects of 5-HT are felt most predominately in the cardiovascular system, with additional activity in the respiratory system and the intestines [42]. Dopamine (Figure 1.9) is involved in mood, motor activity and cognitive functions (learning and memory). It also plays a crucial role in reward-reinforcement, and reward-related incentive learning. Dopamine receptors modulate hippocampal ACh release [43] and receptor signaling pathways in the nucleus accumbens (brain) caused by cumulative drug abuse, are hypothesised to produce tolerance to the rewarding effects of receptor stimulation, leading to increased drug intake to satisfy the reward-reinforcement pathway [43]. Dopamine, norepinephrine and ephinephrine share a phenylethylamine backbone similar to the psychoactive natural product mescaline (Figure 1.2).

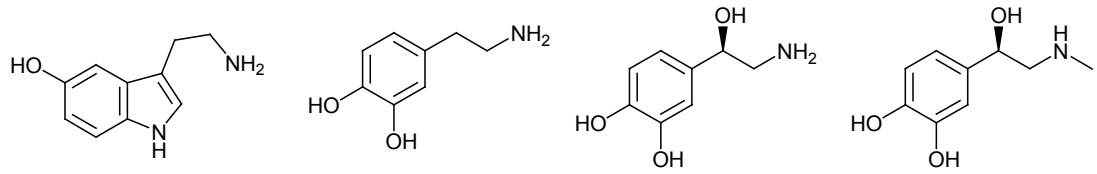

Figure 1.9: The monoamine neurotransmitters serotonin (5-HT), dopamine, norepinephrine and epinephrine.

Extensive research on the preparation of bioactive compounds that mimic the function of neurotransmitters has been achieved through structural modification on the indole ethylamine and phenylethylamine backbones. Hundreds of compounds with unique CNS activity [44, 45] (Figure 1.10) have been prepared, allowing for successful studies of computer generated pharmacophore assessment and receptor mapping through the conformational analysis of a range of structurally related agonists of differing potency [45, 46, 47].

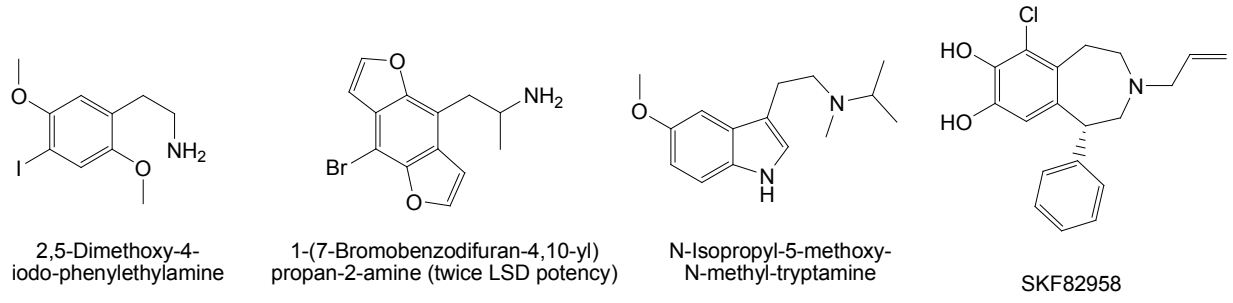

Figure 1.10: Psychotomimetic structures based on endogenous neurotransmitter skeletons. Potent 5-HT agonists 2,5-dimethoxy-4-iodo-phenylethylamine (DOI) [44] and 1-(7-Bromobenzodifuran-4,10-yl) propan-2-amine [45], serotonin type 5-HT agonist N-isopropyl-5-methoxy-N-methyl-tryptamine [7] and the potent dopamine agonist SKF82958 [46].

Neuropeptides consist of amino acids, the majority of which contain stereogenic centers. Almost all of the neuropeptide receptors belong to the rhodopsin or glucagon-vasoactive calcitonin GPCR family. Neuropeptides are far more potent than other neurotransmitters and are responsible for mediating sensory and emotional responses including hunger, thirst, sex drive, pleasure and pain and can be predominately found in the brain and gut. The earliest neuropeptide to be studied was substance P, which is a sensory neurotransmitter in the spinal chord involved in the perception of pain [48]. Opioid neuropeptides include endorphins, enkephalins and dynorphins (Figure 1.11) and are so called since they bind to the same postsynaptic receptors as opium derivatives (Section 1.3.1). The release of substance P is inhibited by opioid peptides, which hyperpolarise the postsynaptic membrane and prevent transmission of pain signals back to the brain, resulting in analgesia [42].

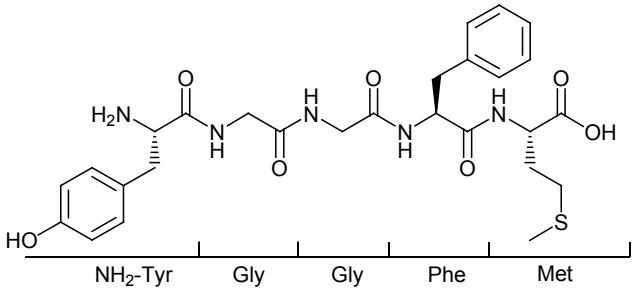

Met-Enkephalin

Leu-Enkephalin NH_2-Tyr-Gly-Gly-Phe-Leu

β-Endorphin NH_2-Tyr-Gly-Gly-Phe-Met-Thr-Ser-Glu-Lys-Ser-Gln-Thr-Pro-Leu-Val-Thr-Leu-Phe-Lys-Asn-Ala-Ile-Ile-Lys-Asn-Ala-Tyr-Lys-Lys-Gly-Glu

Dynorphin NH_2-Tyr-Gly-Gly-Phe-Leu-Arg-Arg-Ile-Arg-Pro-Lys-Leu-Lys-Trp-Asp-Asn-Gln

Substance P NH_2-Met-Leu-Gly-Phe-Phe-Gln-Gln-Pro-Lys-Pro-Arg

Figure 1.11: The peptide neurotransmitters are constructed from amino acids as shown [48, 49].

1.3 Investigation into the Mode of Action of Salvinorin A

In 1994-1995, Siebert and Ott both reported the effects of the *S. divinorum* leaf material to be subjectively identical to those experienced from salvinorin A (**1**) [4, 50]. A sample of the purified diterpene was submitted to a commercial bio-receptor screening service, NovaScreen™ to screen for binding activity at a range of known receptors [51]. Curiously although the drug had no affinity for all screened receptors, including 5-HT_{2A}, the main molecular target for LSD, N,N'-dimethyltryptamine, mescaline, psilocybin, and DOI [52, 53], it was apparent that the documented activity profile reported effects had a distinctive profile compared to the prototypical hallucinogens. An increase in the interest of the pharmacology occurred in the new millennium and in 2002 Roth *et al.* [54] published their findings on the pharmacology of **1**, revealing inactivity at a range of 50 receptors, transporters and ion channels. Functional studies on cloned κ-opioid receptors expressed in human embryonic kidney-293 cells and at

native κ-opioid receptors (KOR) expressed in guinea pig brain indicated that **1** was a KOR agonist with extremely high potency and efficacy. High selectivity for the KOR was demonstrated by *in situ* radioligand binding assays at μ- and δ-opioid receptors that show negligible activity [54], proving **1** to be unique diterpene KOR agonist and a new template for ligand-based drug development. A short review covering the many years of trial and error based receptor assays involved for establishing **1** as a potent KOR agonist can be found in studies by Sheffler *et al.* [55].

1.3.1 The Role and Function of the Opioid Receptors

Opioid receptors belong to the superfamily of GPCRs known to mediate many of the actions of hormones and neurotransmitters responsible for psychological states and an excellent review covering the general biology of opioid receptors is in the literature by Waldhoer *et al.* [56]. The κ- receptor is one of three major subclasses of opioid receptors that have been identified to act on endogenous and synthetic ligands.

The three major subclasses of opioid receptors, types μ-, δ- and κ-, are widely expressed in the central nervous system. The μ-opioid receptors (MOR) are located throughout the central nervous system in areas involved with sensory and motor function, such as the cerebral cortex and amygdala, and are located in high density in the caudate putamen of the basal ganglia also in the brain [49]. MOR agonists derive their name from the prototype morphine for which the affinities for κ- and δ- receptors are substantially lower [57]. μ-Agonists display analgesic effects and are of high importance in clinical medicine for the treatment of severe pain, especially that experienced by terminally ill patients. Morphine and codeine are MOR agonists from the biological extracts of the opium poppy *Papaver somniferum*. Heroin, the 3,6-diacetylmorphine derivative of morphine, has greater potency due to increased lipid solubility, facilitating more rapid penetration through the blood-brain barrier and into the CNS. A number of synthetic MOR agonists have been prepared for clinical use and are structurally dissimilar to the opiate MOR agonists, one example is fentanyl shown in Figure 1.12. MOR agonists often demonstrate physical and psychological dependence and side effects such as respiratory depression, nausea and euphoria [58]. β-Endorphin is the most potent endogenous MOR ligand, although it is not selective and exhibits agonist activity at all μ-, δ- and κ-, opioid receptor sites.

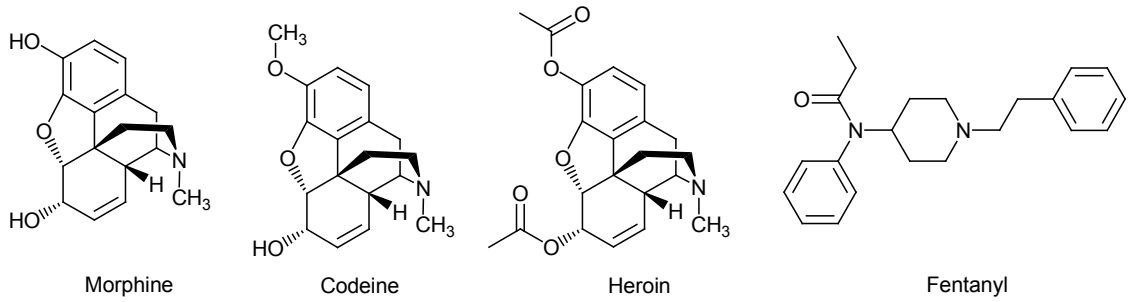

Figure 1.12: MOR agonists morphine, codeine, heroin and fentanyl.

Distribution of the δ-opioid receptor (DOR) is less extensive than the MOR. It is present in high density in the olfactory bulb, cerebral cortex, nucleus accumbens and caudate putamen at the brains cortices. The term δ- is derived from *vas deferens* since the DOR was first identified in the *vas deferens* of mice. DORs play a functional role in the autonomic nervous system, neuroendocrine system as well as mood regulation and olfaction [49]. δ-Receptor agonists mediate analgesia and potentiate the analgesic and euphoric effects produced by MOR ligands [59]. The δ-opioid binding site is also involved in the development of opiate tolerance, dependence and co-administration of morphine and a δ-opioid antagonist has been shown to attenuate the development of tolerances [60]. The endogenous ligands for the DOR are the met-enkephalin and leu-enkephalin peptides, and prototypical agonists include DPDPE and (-)-TAN67 [60] (Figure 1.13).

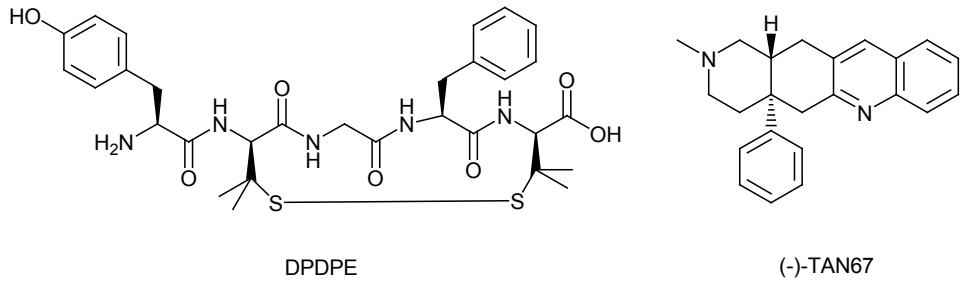

Figure 1.13: DOR agonists DPDPE and the non-peptide agonist (-)-TAN67.

The benzomorphan, ketocyclazocine (Figure 1.14), is the prototype for the κ-opioid receptor (KOR), although many κ- agonists also possess activity at either μ- or δ- receptors. In studies requiring a selective KOR agonist, U50,488H [61] or U69593 [62] are often used (Figure 1.14). Activation of the KORs has been reported to produce analgesia [63] without respiratory depression, however dysphoria [64] and sedation occur at lower doses than those needed for analgesic effects and this is also the case

with **1** [65]. The administration of KOR agonists has been reported to block or decrease the effects of cocaine in rodents [66] and squirrel monkeys [67] and findings suggest that this occurs by attenuating cocaine-induced increases in dopamine levels [68]. KOR agonists that are also partial MOR antagonists have been investigated as therapeutics for cocaine dependence [69]. The KOR participates in the symptoms of chronic morphine induced withdrawal [70] and mediates the adverse affects of Δ^9-tetrahydrocannabinol [71]. The most probable endogenous ligands for the KOR are dynorphins (Figure 1.11), and three receptor subclasses: κ_1, κ_2 and κ_3 are hypothesised to exist [49] but are still the topic of intense investigation.

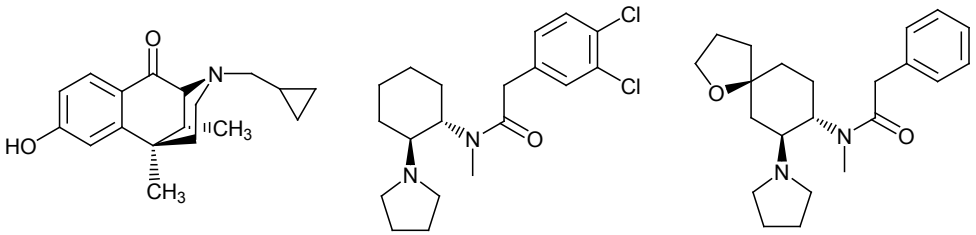

Ketocyclazocine U50,488H U69593

Figure 1.14: Prototypical KOR agonists ketocyclazocine U50,488H and U69593.

1.3.2 Studies on the Bioactivity of Salvinorin A

In comparison to the aforementioned opioid agonists, salvinorin A (**1**) is structurally unique since it lacks the characteristic aromatic rings and amine functionalities common of both synthetic and classical alkaloid agonists, previously believed essential for psychoactivity. It is the most potent natural product discovered to date and the only terpenoid structure that has demonstrated selective activity at opioid receptors. Gruber *et al.* report that the drug is barely active through ingestion, can be partially absorbed sublingually through the oral mucosa, and most effectively through vaporization and inhalation, whereby the active dose is 200 – 500 μg [72].

Other isolated products from the leaves of *S. divinorum* have since been screened for binding affinity and functional activity at opioid receptors. Salvinorin B is shown to posses much lower activity at the κ-receptor than **1** [73] and metabolism of the C(2) acetoxy substituent of **1** to give the inactive salvinorin B has been suggested as a major pathway for metabolic deactivation throughout the gastrointestinal tract [74, 75]. Salvinorin C, D and F have been tested for bioactivity by Munroe *et al.* and found to be barely active [76] at the KOR, Harding *et al.* [28] have reported partial KOR agonist activity for salvinicin A and low MOR antagonist activity for salvinicin B (Figure 1.3), revealing the first

diterpene with activity at the MOR. Bioassays by Simpson *et al.* [77] describe salvidivin A (Figure 1.3) as a KOR antagonist with some activity at MOR and DOR, further reaffirming the significance of the neoclerodane core as a new template for bioactive ligands.

Studies towards chemical transformations on salvinorin A are a subject of heavy investigation and over 100 salvinorin A analogues with measured biochemical activity are in the current literature, all of which have been prepared by semi-synthesis on the parent **1**. New analogues of **1** reported in chemical and pharmacological research literature are commonly analysed using binding assays at cloned receptors, and the accumulated data used to further insight into the structural requirements necessary for selectivity, binding efficacy and activity. Several research groups have concentrated on modification of the C(2) substituent and consistent findings show a general decrease in κ-agonist activity with larger ester groups. A number of semi-synthesised analogues containing C(2) propionate ester, carbamate and ethyl ether substituents have been prepared by Bégiun *et al.* [78] with reported KOR activity similar to **1** (Figure 1.15). Preparation of the methoxymethyl C(2) substituted analogue by Lee *et al.* [79] revealed a KOR agonist with approximately seven times greater potency than salvinorin A and is the first reported synthetic derivative of **1** with greater potency than the natural product. Some bioactive C(2) functional group analogues are listed in Figure 1.15 but is by no means extensive as the number of tested analogues continues to expand and most inactive analogues have been omitted.

R	k-K_i (nM)	EC_{50}(nM)	Efficacy (%)		
CH_3CO_2	1.3 ± 0.5	4.5 ± 1.2	99	(**1**)	[78]
OH	155 ± 23	371 ± 49	98	Salvinorin B	
$CH_3CH_2CO_2$	7.2 ± 0.5	20.4 ± 3.4	94	esters	[78]
$CH_3(CH_2)_2CO_2$	4.9 ± 0.6	9.9 ± 0.6	97		
NH_2CO_2	3.2 ± 0.2	6.2 ± 1.4	99	carbamates	
$CH_3N(H)CO_2$	83.0 ± 8.5	201 ± 10	81		[78]
$(CH_3)_2CHN(H)$	17.6 ± 3.1	18.9 ± 0.6	99	amine	[82]
$(CH_3)_2CHN(H)$	2.3 ± 0.6	7.2 ± 0.3	107	C(2)-epimer	
$(CH_3)_2N$	168 ± 10	240 ± 23	110		
CH_3CH_2O	7.9 ± 0.3	18.6 ± 2.6	103	ether	[78]
$PhCH_2O$	75.7 ± 5.9	161 ± 14	102		
CH_3OCH_2O	0.4 ± 0.02	0.6 ± 0.2	98		[79]
$CH_3CH_2C(O)N(CH_3)$	1.6 ± 0.1	0.75 ± 0.08	100	amide	[79]
CH_3COS	18.4 ± 7.9	4.77 ± 2.72	107	thioester	[80]
CH_3COS	151 ± 53	123 ± 30	106	C(2)-epimer	

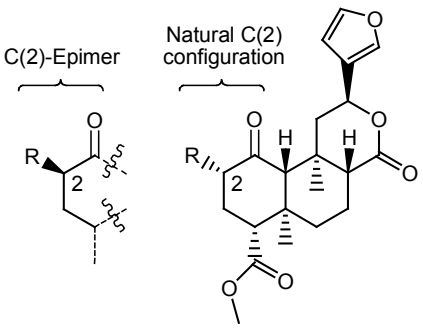

	R	μ- K_i (nM)	δ- K_i (nM)	κ- K_i (nM)
[83]	$PhCO_2$	12 ± 1	1170 ± 60	90 ± 2
	(Herkinorin)			
	$PhN(H)CO_2$	16 ± 1	230 ± 10	93 ± 3
	$MeSO_2$	6820 ± 660	>10000	2.3 ± 0.1
[84]	4-$BrPhCO_2$	10 ± 1	1410 ± 80	740 ± 40
	2-C_4H_3S	10 ± 2	1380 ± 130	260 ± 20

Figure 1.15: The measured binding affinity (K_i), functional activity (EC_{50}) and efficacy (%) values of C(2) modified Salvinorin A analogues [78-80, 82-84]. Efficacy determined as the percentage of maximal response produced by U50,488H [78-79, 82-84] and U69593 [83].

The C(2) thioester analogue of **1** has been prepared by Bikbulatov *et al.* [80] who report moderate KOR affinity with reduced activity for the C(2) epimer, a trend also reported for **1** [81]. Later studies by Béguin *et al.* [82] focus on the activity of C(2) epimers of a number of analogues and demonstrate diminished activity in all cases except the isopropyl amino product, which proved more active as the unnatural C(2)-epimer. Interestingly, the C(2) epimer of **1** has been reported to act as a DOR antagonist [81] and is the first synthesised diterpinoid derivative with DOR activity. Harding *et al.* [83] report the C(2) methanesulfonyloxy (Figure 1.15) derivative to possess similar KOR potency to **1** [83] and have demonstrated that analogues possessing aromatic C(2) ester substituents are only moderately active at KORs, but show increased affinity for MORs. The C(2) benzoate derivative *herkinorin* represents the first non-nitrogenous μ-agonist synthesised from **1** (Figure 1.15) and further studies by Tidgewell *et al.* [84] have shown that MOR/KOR selectivity decreases upon increased chain length or steric size of the C(2) ester group, with a large increase in MOR activity for the aromatic esters. The semi-synthesised 4-bromobenzoate and thiophene-2-carboxylate C(2) esters were reported to have high MOR activity with approximately two and five times MOR/KOR selectivity [84].

Lee *et al.* [85] have prepared a series of analogues containing various C(18) substituents were prepared and in general, longer or bulkier ester substituents decreased KOR binding affinity. Although potency was demonstrated to be lower for the C(8) epimer of **1** and its analogues, the C(18) carboxylic acid measured more potent as the C(8) epimer than in the natural configuration [85] (Figure 1.16). Studies addressing the KOR activity of the C(8) epimer of salvinorin B have also been published [86]. Further reports on the biological assessment for synthetic analogues of **1** have involved modified furan structures. Munroe *et al.* report that the reduction of the lactone ring to the pyran or the dihydropyran gave agonist compounds with high KOR affinity (Figure 1.16), inferring that the lactone carbonyl may not be crucial for receptor binding [86]. Remarkably, reduction of the ketone at C(1) gave a compound that retained considerable activity as a KOR agonist, whereas the C(1) alcohol and acetoxy compound produced no significant activity. Analogues prepared by hydrogenation of the furan ring gave compounds of lesser affinity and potency than the parent compound **1** [86].

Simpson *et al.* have recently reported on a semi-synthesis of salvinicin A and B from **1** [77] along with other selective modifications of the furan ring of **1**. Replacement of the 3-furyl group with a nitrogenous heterocycle was reported to decrease in KOR activity [77], as was removal of the furan altogether. The 2-bromofuran analogue was reported to be a potent KOR agonist and the incorporation of an oxadiazole group gave a synthetic analogue of **1** with KOR antagonist activity (Figure 1.16) [77]. Further work by the same group involved the preparation of a range of modified furan KOR agonists,

amongst which the *N*-sulfonylpyrrole derivative was mentioned to have low agonistic activity at KOR [87].

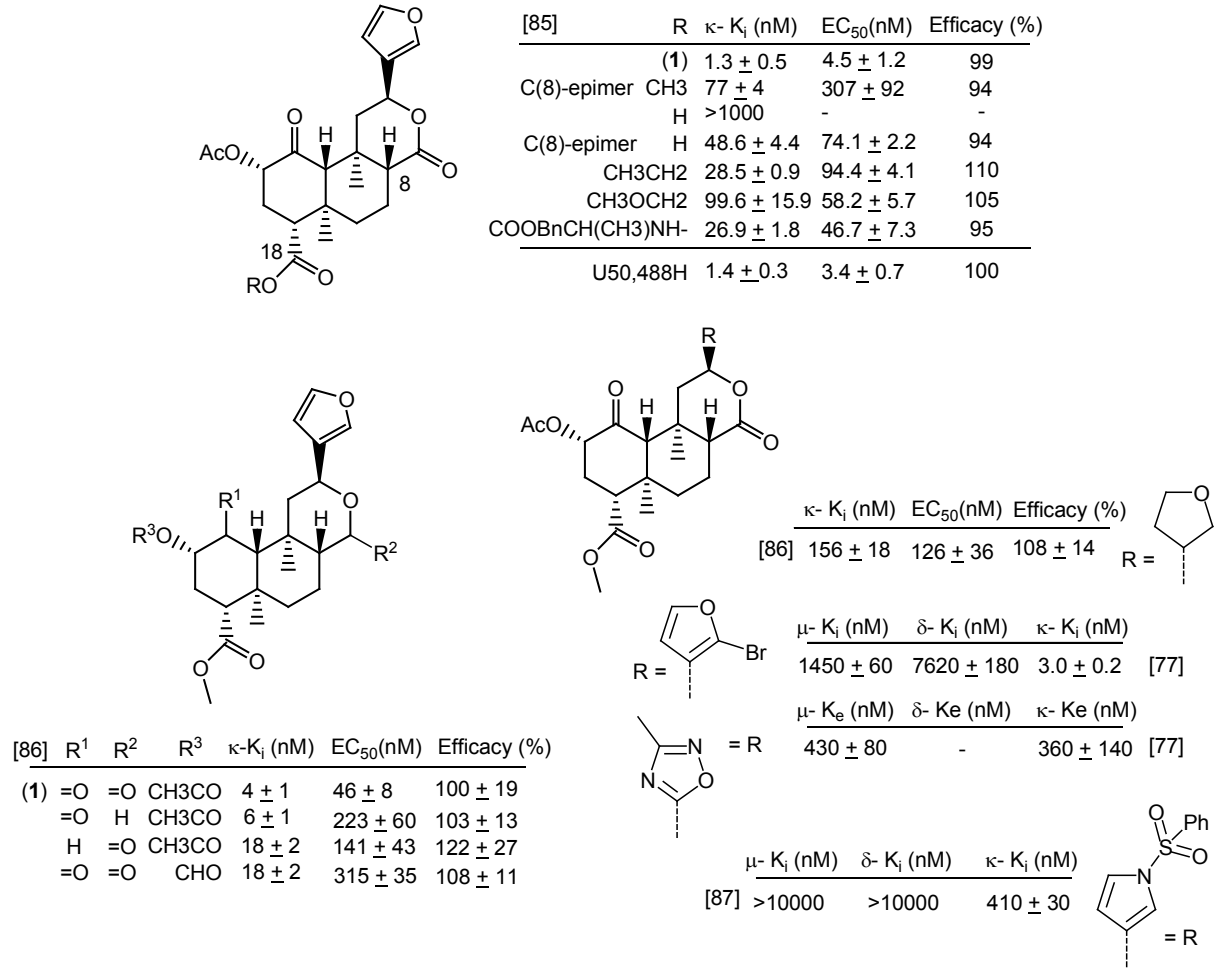

Figure 1.16: The measured binding affinity (K_i), functional activity (EC_{50}) and efficacy (%) values of C(18) modified Salvinorin A analogues reported by Lee *et al*. [85]. Furan modified bioactive analogues are also shown [86, 77, 87].

Prior to the publication of numerous salvinorin A analogues in the scientific literature with reported opioid receptor binding data, studies by Roth *et al.* [54] proposed a binding model for **1** based solely on hydrogen bonding interactions using an established model for the KOR bound to the agonist U69593, followed by atom overlap comparison with **1**. Computer modeled conformations for KOR docked salvinorin A predicted residues for H-bond acceptor interactions at the lactone (Tyr139), acetoxy (Tyr313) and ester (Tyr312) carbonyls and also at the furan oxygen (Gln115). A later model by Yan *et al.* [88] is based on a Rhodopsin template, and energy minimised by computer modeled docking with an ensemble of known agonists (bremazocaine, morphine, MPCB, U69593 and 6'-GNTI) according to

suggested structure activity relationships. Site-directed mutagenesis studies were performed to test their hypotheses via radioligand binding and functional assays, and suggest involvement from residues Tyr119 and Tyr320. New and more accurate models have since been proposed using the guidance of bioactivity measurements for known analogues and a refined qualitative model has been published by Kane *et al.* [60] and explores binding site interaction using wild-type and chimeric receptor studies to probe for changes in receptor function upon alteration of significant binding regions. Their results suggest that salvinorin A binds at transmembrane residues in TMII, TMVII and ELII of the KOR receptor protein and single point mutagenesis studies suggest involvement from Q115, Y119 (TMII) and Y312, Y313, Y320 (TMVII) residues, in near corroboration with studies by Roth *et al.* [54, 88]. A publication by Singh *et al.* [89] from the same laboratories has incorporated a combined ligand-based target-based approach for GPCR modeling using salvinorin A as a computational case study. The amino acid residues inferred necessary for KOR binding from earlier studies were considered in a computer docking simulation study to hypothesise an energy minimised binding mode for **1** (Figure 1.17, left).

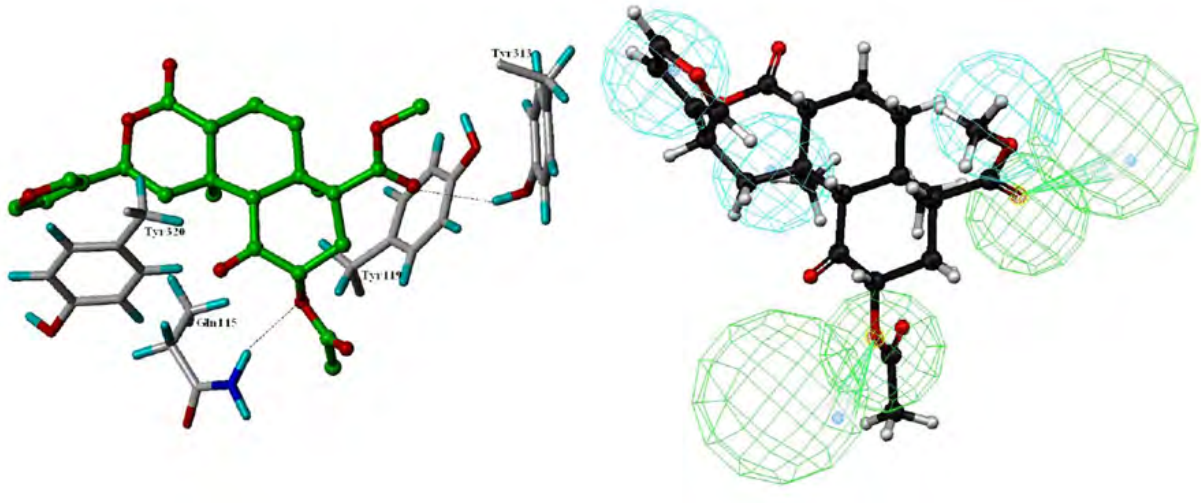

Figure 1.17: Left; Proposed binding mode with important amino acid residues [89] and Right; a current pharmacophore model for salvinorin A (**1**) reported by Singh *et al.* [89], constructed using 'Catalyst 4.8' computational software.

Compounds including **1** and analogues with reported potency as KOR agonists were used to construct a hypothetical computer generated pharmacophore model using 'Catalyst 4.8' software as shown in Figure 1.17 (right) [89]. The 'best-fit' pharmacophore was validated using an additional 12 analogues of **1** and also compared favorably in the prediction of known non-terpene KOR agonists. This approach aims to improve the identification of new lead compounds for the process of drug development based on the bioactive neoclerodane scaffold.

Studies by Vortherms *et al.* [90] follow a similar trend during studies to further the elucidation of the binding mechanisms through which **1** can act at the KORs and use the natural product to probe morphological differences between MOR, DOR and KOR opioid receptor classes. Using a combination of site-directed mutagenesis studies and computational modeling/dynamics analysis of the protein receptor, the authors support the current theory that differential helical orientations amongst GCPRs attribute ligand or neurotransmitter selectivity. The topology of binding amino acid residues at the extracellular segment in DOR and MOR receptors is suggested to disrupt binding of **1**, offering a rationale for KOR selectivity.

Further interest from the pharmacology and neuroscience community has led to a number of significant findings related to the activity of **1** and analogues with potential therapeutic value. Ansonoff *et al.* [91] have demonstrated using radioligand binding assays that **1** is a selective agonist at the κ_1 receptor subclass (Section 1.3.1) whereas the synthetic KOR agonists U50,488H and U69593 (Figure 1.14) show affinity for both κ_1 and κ_2 receptor subclasses. Groer *et al.* [92] have furthered characterization of the MOR bioactivity of herkinorin (Figure 1.15), the C(2) benzoate analogue of **1** and *in vivo* studies in mice have shown that the μ-activity of herkinorin does not involve interactions with β-arrestin proteins, which are currently accepted to play a role in mediating the side effects (tolerance, constipation, respiratory depression) associated with morphine based MOR agonists [92]. Studies by Rothman *et al.* [93] report allosteric modulation of μ-receptors upon interaction of **1** with KORs and Butelman *et al.* [94] have used **1** in a neuroendocrine biomarker assay. Braida *et al.* [95] have also reported the effect of **1** in zebrafish and tentitatively propose CB_1-cannabinoid receptor involvement based on known interactions between the KORs and cannabinoid system in self-administration studies.

1.4 Clerodane Diterpenes

The *trans*-neoclerodane structure of salvinorin A from *S. divinorum* contains a carbon skeleton common to the clerodane diterpene family of natural products, although it is the first diterpene to exhibit potent neuroactivity. Clerodane structures are commonly isolated metabolites from the *Salvia* species and attract significant interest due to their unique structures and bioactivity. The clerodane metabolites are often oxygenated and involve complex stereochemistry as a consequence of multiple metabolic steps. In order to further discuss the bioactivity and stereochemistry of clerodane compounds it is helpful to briefly describe the biogenesis through which terpenes are derived.

1.4.1 The Origin of Chirality in Terpenoid Natural Products

Biosynthesis and biotransformation processes within living organisms frequently produce complex organic structures, many of which contain intricate stereochemistry. The *in vivo* pathways by which these compounds are produced are of enormous interest to chemists and biochemists and over the past decade advances in this field have been very significant. Included in the terpene family are hormones, vitamins, drugs, as well as rubber. It was originally thought that all terpenes were biosynthesised via the 'mevalonate' pathway, however through ^{13}C labeling it has been uncovered that in plants a mevalonate independent pathway also exists, which is absent in mammals [96]. This non-mevalonate biosynthetic route is known as the methylerythritol phosphate (MEP) or 1-deoxy-D-xylulose-5-phosphate (DOXP) pathway. By either pathway, all terpenes are assembled from 'isoprene' (2-methyl-1,3-butadiene) units with two universal precursors, isopentenyl diphosphate and dimethylallyl pyrophosphate. Metabolites formed in the growth stage are referred to as primary metabolites and those formed thereafter are secondary metabolites. In some organisms, during various stages of growth, different pathways have been suggested to predominate. During these processes, one or more stereogenic centers are often introduced and transformations executed by enzymatic processes typically produce species in optically enhanced or optically pure form. A simple example of this is the production of (-)-limonene from geranyl diphosphate (GPP) [97] (Scheme 1.1).

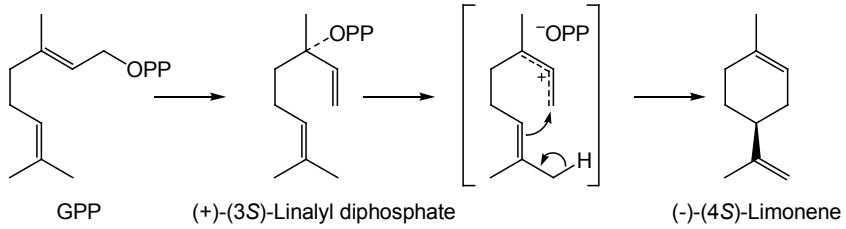

Scheme 1.1: The isomerization and cyclization of GPP to (-)-(4*S*)-limonene catalysed by limonene synthase [97].

Natural products contain substructures and stereogenic centers, which may be indicative of the biosynthetic pathways or even the subcellular location of its production. In higher plants and certain eubacteria, triterpenes are often made via the mevalonate pathway in the cytoplasmic compartment of a cell, whereas mono and diterpenes are biosynthesised in plant organelles (plastids) via the MEP pathway [97]. Metabolites have been known to switch pathways at intermediate stages of the metabolic process.

1.4.2 Biosynthesis and Nomenclature of Clerodane Diterpenes

Diterpenoids that feature the clerodane carbon skeleton are very common, the majority of which have been isolated from the *Lamiacae* and *Compositae* families. Clerodane diterpenoids have been shown to commonly occur via the MEP pathway, through the enzymatic cyclization of geranylgeranyl diphosphate (GGPP) [99] and appear to be related to labdane structures through a series of methyl and hydride shifts [100] (Scheme 1.2). The genes responsible for encoding terpene cyclase-like proteins involved in the biosynthesis of the antibiotic terpentecin (Section 1.6.1) have been isolated and the mechanism for the production of the *trans*-clerodane structure concluded by deuterium labeling in NMR studies [99]. The biogenic pathway for the synthesis of **1** in *S. divinorum* has been addressed in studies by Kutrzeba *et al.* [23] using the *in vitro* incorporation of [1-^{13}C]-glucose, [Me-^{13}C]-methionine and [1-^{13}C, 3,4-$^{2}H_2$]-1-deoxy-D-xyulose substrates followed by retro-biosynthetic NMR spectroscopic analysis. The authors suggest that the biosynthesis from clerodane pyrophosphate proceeds via the DOXP pathway based on ^{13}C NMR isotope patterns observed in the radiolabeled metabolic analogue of **1** (Scheme 1.2).

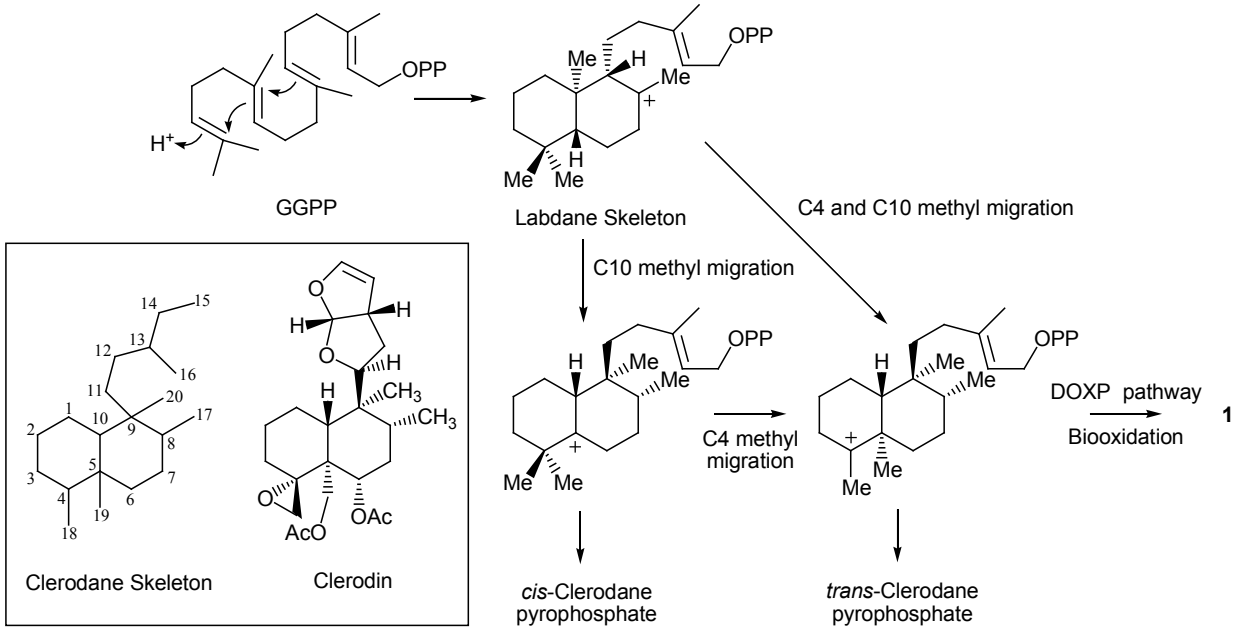

Scheme 1.2: The enzymatic cyclization of geranylgeranyl diphosphate (GGPP) to produce labdane and clerodane skeletons [100]. Biooxidation to give **1** has been reported to occur via the DOXP pathway [23].

The absolute stereochemistry of the insect antifeedant clerodin [101], the first member of the clerodane products to be isolated, has been revised [102] and is used as a template to describe stereochemistry in other clerodane metabolites. Those possessing identical absolute stereochemistry to clerodin are termed *neo*-clerodanes and those enantiomeric to clerodin are termed *ent-neo*-clerodanes. A

further *cis* and *trans* division of clerodanes based on the relationship of substituents at the C(5)/C(10) ring junction also exists. This system of naming clerodane diterpenes only describes the stereochemical aspects and ignores functionality and the connectivity of additional ring systems.

Based on the nomenclature described above, salvinorin A (**1**) is a *trans-neo*-clerodane structure and the three fused saturated six-membered ring systems will be referred to as rings **A**, **B**, and **C** (Figure 1.18) throughout the discussion section of this thesis. Ring **C** is a δ-lactone connected to a β-substituted furan and although common amongst clerodane terpenes only few examples exist of compounds which also possess the *trans-neo*- stereochemistry. The methyl and hydrogen bridge-head atoms at the **A**/**B** ring junction C(5)/C(10) are in the *trans*- configuration with respect to each other and the same relationship exists at the **B**/**C** ring junction C(8)/C(9) and along the adjoining **A**/**C** bond C(9)/C(10). Since the *trans* stereochemistry relationship exits between consecutive C(5)/C(10)/C(9)/C(8) bridge-head substituents, the tricyclic ring structure sits in a planar orientation and each fused saturated cyclohexane ring exists in the most stable chair conformation.

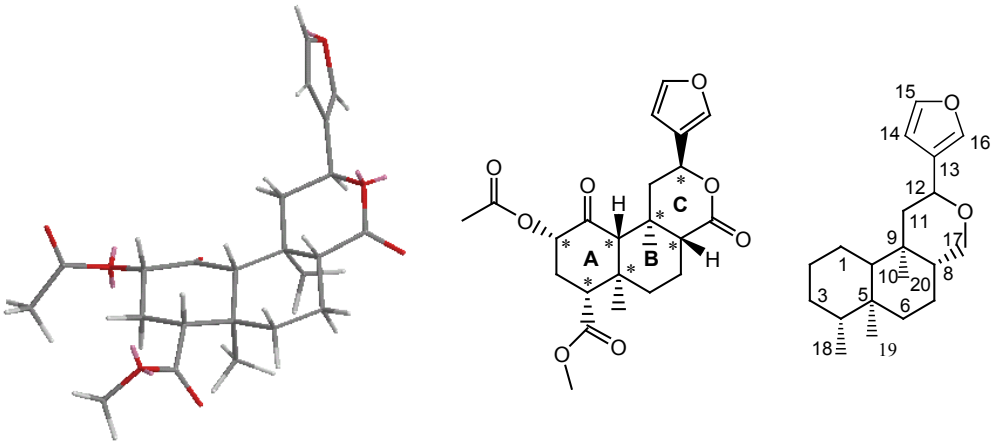

Figure 1.18: The Chem3D MM2 energy minimised structure of salvinorin A (left), the **ABC** ring system with stereocentres indicated* (middle) and the numbering system for the salvinorin A carbon framework (right).

Salvinorin A contains seven stereocentres as indicated in Figure 1.18. The number of possible stereoisomers is calculated by considering that each stereocentre has two possible configurations, hence a compound with seven stereocentres has: $(2)^7 = 128$ possible stereoisomers. The C(2)-epimer and C(8)-epimer of **1** have been prepared from the natural compound as discussed in Section 1.3.2, although the inversion of stereochemistry at C(4), C(5), C(9) might be more challenging, requiring the synthetic preparation of these diastereoisomers. It can be rationalised that inversion of stereochemistry at the

bridge-head atoms of **1** will change the stable *trans* chair conformation and a number of examples presented in section 1.4.3 demonstrate how the three-dimensional shape of the **ABC** ring system is determined by the stereocentres at the C(5)/C(10) and C(8)/C(9) ring junctions. Other clerodanes identified from biological plant extracts are also discussed in the following section.

1.4.3 Clerodane Diterpenes from Bioactive Plants

The clerodane diterpinoids are classified as secondary metabolites and are an important class of natural products due to their ubiquitous distribution and extensive structural variation [4]. Many clerodanes isolated from bioactive plant extracts have been comprehensively characterised, however bioassay data on the identified constituents is lacking. Existing bioassays on isolated terpenes from the clerodane family have revealed their unique biological activities.

The accumulation of secondary metabolites in plants may be the result of an evolutionary adaptation to defend against insects. Genus *Scutellaria* (Lamiacae) has provided some of the most potent neoclerodane insect antifeedants currently known. *trans*-Neoclerodanes Jodrellin A & B, isolated from *S. woronowii* [103] and Scutegalin B from *S. galericulata* [104] have been found to possess phagostimulant activity against larvae of lepidopteran *Spodoptera littoralis* (Egyptian cotton worm). Jodrellin B has also proven active against plant pathogenic fungi *Fusarium oxysporum* [105]. The significance of the Jodrellin structure as a means of chemical defence against botanical pests has made it an attractive target for total synthesis and to date there have been two successful total syntheses of Jodrellin A [106, 107] (Section 1.6.3).

As described in earlier discussion, clerodane diterpenoids identified from medicinal plants provide important new lead compound for furthering the understanding receptor systems in humans and the development of novel pharmaceuticals. Casearinol A (Figure 1.19), a *cis*-clerodane diterpene from the leaves of *Casearia guianensis* has been found to have immunomodulatory effects and may be useful in the search for immunosupressant compounds for the prevention of organ rejection in transplant patients [108]. The *trans*-neoclerodane lupulin A (Figure 1.19) from *Ajuga lupulina* has been shown to possess antibacterial activity against *Staphylococcus aureus*, *Pseudomonas aeruginosa* and *Escherichia coli*. [109]. *Saliva polystachya* has been traditionally used in Mexican folk medicine as an anti-gastralgic, anti-dysentric, purgative and emollient and Maldonado and Ortega have shown the aerial parts to be rich in clerodane diterpenoids [110]. One example is Polystachyne D [110] which contains similar connectivity and functionality to **1** however the *cis*- relationship at the **A**/**B** and **B**/**C** ring junctions creates a twisted u-shaped conformation in the skeleton (Figure 1.19).

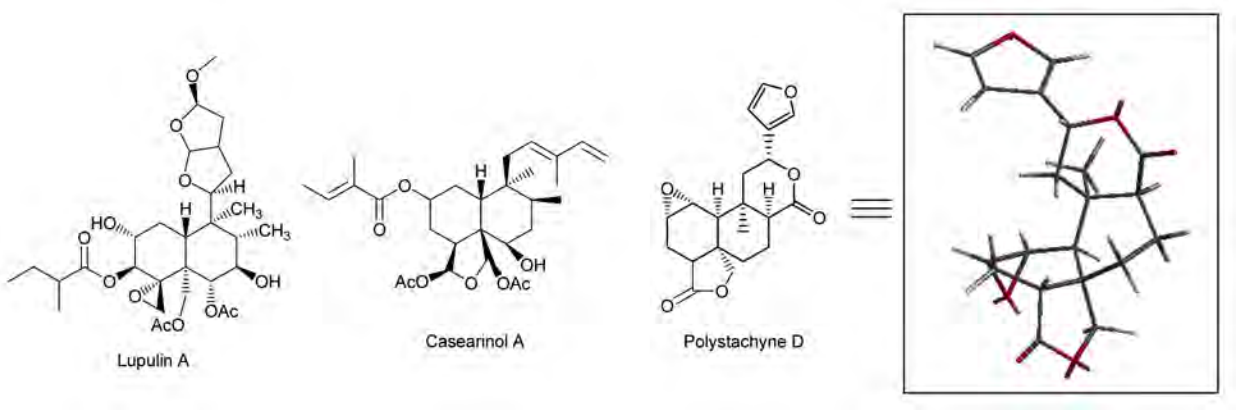

Figure 1.19: The antibacterial lupulin A and the immunomodulatory *cis*-clerodane casearinol A. The Chem3D MM2 energy minimised structure of polystachyne D is also shown.

cis-Clerodane diterpenes bearing similar chemical functionalities to salvinorin A have been isolated from bioactive fractions of the *Tinospora* genus (Menispermaceae family) (Figure 1.19). Leaf extracts from *Tinospora rumphii* are rich in clerodane diterpenes [111] and extracts are used medicinally in south-east Asia for the treatment of stomach disorders, ulcers and fevers with bioassays on methanolic stem extracts revealing significant stimulation glucose transport activity. Interestingly, isolated products from the stem extract have revealed several clerodane glycosides [112] similar to those found in stem extracts of *Tinospora cordifolia*, an Ayurvedic medicinal plant of India locally known as 'Guduchi', a herb is traditionally used for the treatment of urinary [113], liver and intestinal disorders [114] but also found to possesses immunostimulant activity [115]. Many isolated compounds from the *Tinospora* genus contain the fused δ–lactone ring at C(8)/C(9), incorporating the C(11)-C(16) side chain, and have *cis*-geometry at the **A**/**B** ring system. Highly oxygenated *cis*-*ent*-*neo*-clerodane diterpenes featuring the opposite stereochemistry to clerodin in the **B**/**C** ring junction, such as 6-hydroxyarcangelisin (Figure 1.20), have been isolated from the stem of *Tinospora cordifolia* [113] but no bioactivity studies on isolated compounds have been reported as yet.

A few other *trans*-neoclerodane metabolites of scientific interest include Bacchotricuneatin A [116] (Figure 1.20) isolated *Baccharis crispa*, that shows insect antifeedant activity against *Tenebrio molitor L.* larvae [117]. Structure-antifeedant activity relationships suggest that stereoelectronic factors are more important than hydrophobic effects [118] for antifeedant activity, which was significantly diminished upon hydrogenation of the furan substituent. Diterpenoids isolated from the genus *Lagochilus* (Lamiaceae) have provided *trans*-labdane diterpenes with strong bioactivity as hemostatic compounds. Lagochilin (Figure 1.20) from *Lagochilus inebrians* has been identified as the major bioactive

component and synthetic derivitization of the lagochilin structure has provided compounds of enhanced potency [119].

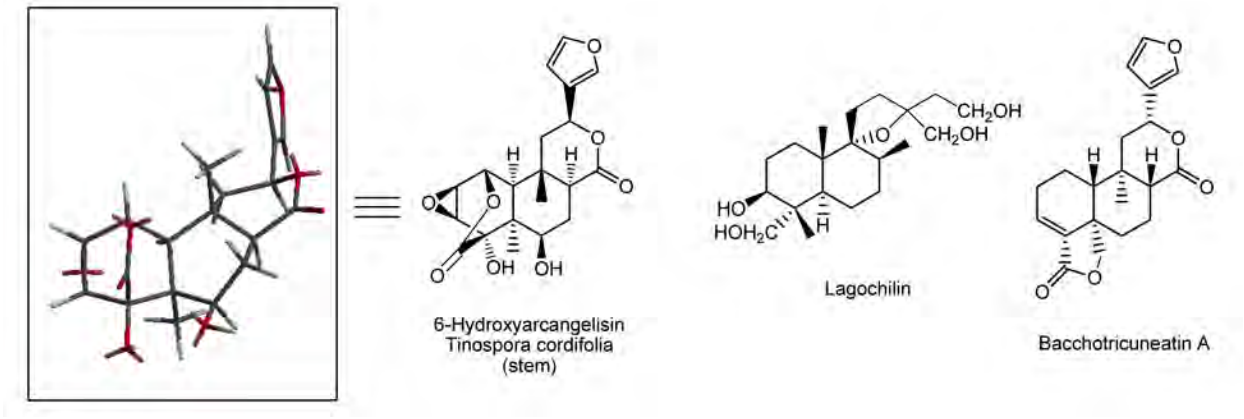

Figure 1.20: An MM2 minimised Chem3D structure of the *cis-ent*-neoclerodane diterpene 6-hydroxyarcangelisin. The *trans*-neoclerodane insect antifeedant Bacchotricuneatin A and hemostatic Lagochilin are also shown.

1.5 Introduction to Synthesis

Considerable research efforts from academic and industrial laboratories have resulted in the development of general methodologies for the preparation of chiral molecules with high enantiomeric purity. A number of these methods predominate in the area of natural product synthesis and will be explained.

1.5.1 The Chiral Pool

Both abundant and accessible, the chiral materials that are found in nature are referred to as the 'Chiral Pool'. Chiral pool materials have now been used as building blocks for chemists for over a century and include sugars, terpenes, amino acids and carbohydrates (Scheme 1.3, top). The oldest and most classic approach towards asymmetric synthesis is to design around chiral pool reagents, and many successful natural product syntheses have been accomplished in this manner [120].

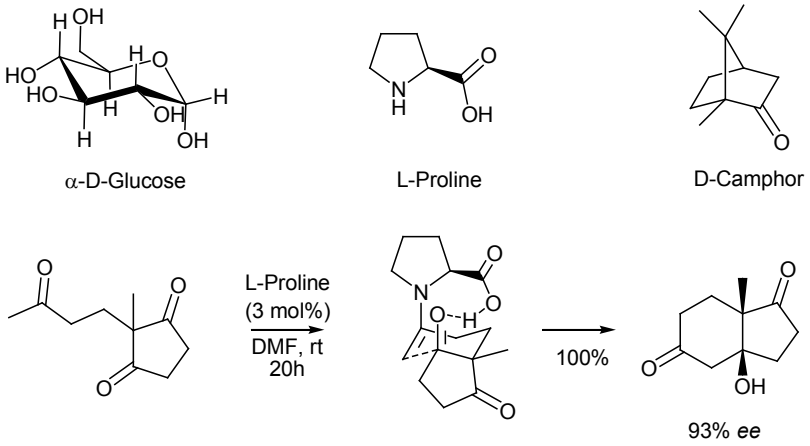

Scheme 1.3: Top; Chiral pool compounds α-D-glucose, L-proline and D-camphor. Bottom; L-Proline uses both acidic and basic functionalities to stereoselectively catalyse the Robinson annulation.

Optically pure amino acids and simple derivatives thereof have proven effective as chiral auxiliaries and ligands for metal complex based asymmetric catalysts. Proline itself has been used as an amphoteric chiral catalyst for aldol reactions, and Robinson annulations [121] (Scheme 1.3, bottom).

Chiral terpenes are isolated with varying degrees of enantioenrichment and monoterpenes such as pinenes, menthones, menthols, carvones, camphor and limonene (Scheme 1.4, top) are especially important and abundant compounds useful for synthetic manipulation. Monoterpenes are widely distributed in nature [122] and are obtained from plants in high yields. Terpenes are frequently used in asymmetric synthesis both as building blocks for the preparation of natural products and as ligands for stereoselective transformations.

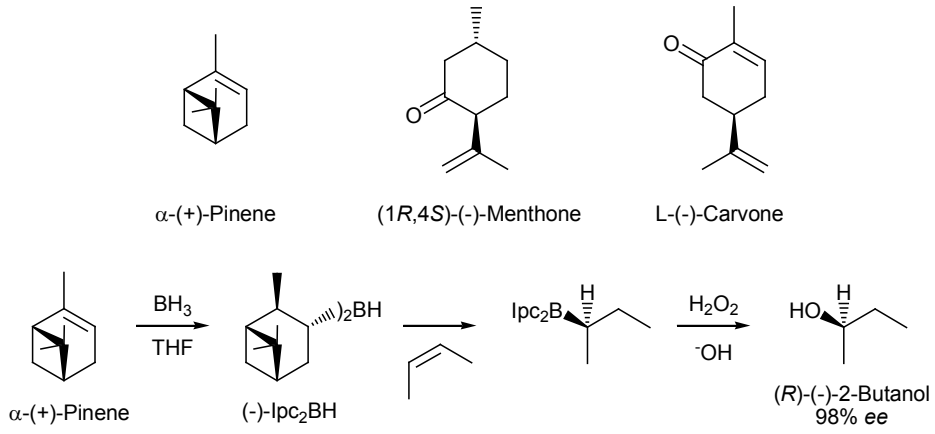

Scheme 1.4: Top; Chiral terpenes (+)-pinene, (-)-menthone and (-)-carvone from the chiral pool Bottom; (-)-Ipc_2BH prepared from (+)-pinene can be used in the asymmetric hydroboration of *cis*-but-2-ene to produce (*R*)-(-)-2-butanol in 98% *ee* [123].

Chiral reagents can be easily prepared through chemical or biological transformations of optically active terpenes. Hydroboration of α-pinene produces diisopinocampheylborane ((-)-Ipc_2BH), an effective reagent for the asymmetric hydroboration of *cis*-substituted alkenes [123]. Chiral reagents and ligands allow for the transfer of chirality into the desired target molecule, in this case, the product after hydrolysis is a chiral alcohol in high optical purity (Scheme 1.4, bottom). Unlike amino acids, which almost exclusively have the (*S*) configuration, many monoterpenes exist in Nature as both enantiomers variously distributed in different plant species. They are "scalemic" which means that both antipodes are produced by a single source, although one usually predominates [122].

Chiral pool reagents can be extremely useful if the diastereo- or enantio-selectivity is induced to give the desired isomer for synthesis. If the stereogenic center produced is the opposite to that wanted, asymmetric catalysis is often the most attractive alternative. Purification of a single enantiomer from a racemic mixture can provide both enantiomers in pure form. This process is known as racemic resolution and is almost always necessary when chiral products are obtained or formed in less than 100% optical purity.

1.5.2 Racemic Resolution

Racemic resolution is an approach that still dominates the pharmaceutical industry and many of the research institutions as the most reliable and economically attractive method of obtaining pure enantiomorphs [124]. Racemates can be resolved by two methods;

1. Formation of a diastereomeric derivative by reacting the racemate with an optically pure compound termed a 'resolving agent'.

The racemate can be reacted with a resolving agent to form a covalent bond, a diastereomeric complex, or a diastereomeric salt. The diastereomeric derivatives can then be purified by differences in chemical properties before the resolving agent is detached to yield a pure enantiomer. Typically, differences in solubility between diastereomeric pairs are used to separate enantiomers since the less soluble species tends to crystallise with increased optical purity. An example of this is shown in the resolution of racemic 2-chloro-3-phenyl-propionic acid using L-phenylalanine as the resolving reagent (Scheme 1.5). The racemic α-halo acid is recrystallised with L-phenylalanine to produce diastereomeric salts. The (*R*) salt of the α-halo acid has a lower solubility than its enantiomer and is separated as a solid, leaving the (*S*) salt in solution [124].

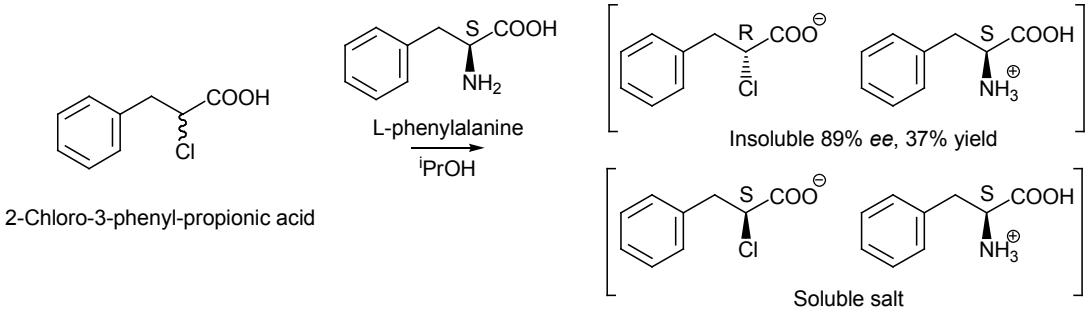

Scheme 1.5: Racemic resolution of 2-chloro-3-phenyl-propionic acid by formation of diastereomeric salts.

The number of resolutions achieved using diastereomeric salt formation alone is over 10,000 [124], however finding the most suitable resolving agent and crystallization conditions during development of chiral separation procedures for novel compounds often demands a high level of perseverance.

2. Chiral Separation by Chromatography.

Enantioselective separations based on the formation of transient diastereomer complexes are commonly rationalised using a three-point interaction model [125] that assumes a minimum of three simultaneous interactions between the optically pure 'chiral selector' and an enantiomer, where at least one interaction is stereochemically dependent. Enantioseparation by chromatography can be achieved by using either chiral mobile phase additives or a chiral stationary phase. A chiral stationary phase is composed of a chiral selector that is chemically bound or coated onto a polymer support. Chiral separation by Gas-Chromatography (GC) uses capillary columns with a stationary film of polysiloxanes bound to amino acid or β-cyclodextrin (Figure 1.21) derivatives and the chiral selector can constitute up to 30% of the stationary phase.

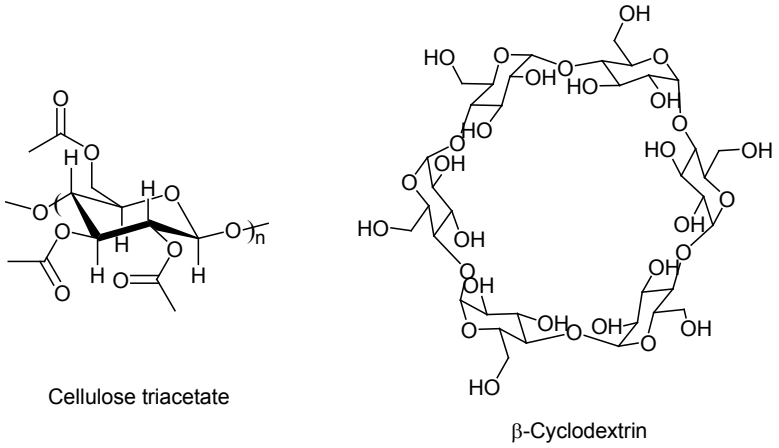

Figure 1.21: Chiral stationary phases cellulose triacetate and β-cyclodextrin.

Enantiomer separation by chromatography on a chiral GC column is an efficient method for analytical purposes and to separate small quantities of racemate, discussed in more detail in Section 3.3.2. Liquid chromatography using chiral stationary phases can successfully purifiy enantiomers on multigram scales, but it is expensive for larger scale production due to the price of solvents and consumables. Cellulose and modified cellulose columns such as cellulose triacetate (Figure 1.21) are an efficient stationary phase for liquid chromatography [126].

Chiral separation by capillary electrophoresis can be achieved by adding a chiral selector to the mobile phase and works by interacting with analytes in solution during the separation process [124]. β-Cyclodextrin works well for this process since it is water soluble and forms a bucket shape that can hold an organic molecule in the center. The retention differences due to variable interaction of each enantiomer with the cyclodextrin cavity discriminates each enantiomer during chromatography.

1.5.3 Asymmetric Synthesis

Asymmetric syntheses are designed to facilitate the synthesis of a single enantiomer as the major product, hence increasing the yield of the reaction and hopefully shortening the length of the synthetic route. Generally speaking, asymmetric synthesis involves the generation of chiral centers from prochiral materials during which process chirality is transferred from the reagent, catalyst, or auxiliary to the newly introduced asymmetric center. Often the degree of purity of the new enantiomer is less than 100% *ee* and further purification by racemic resolution is performed to provide the pure isomer. The differences entailed between the asymmetric techniques will be outlined under the categories asymmetric catalysis, chiral reagents, and chiral auxiliaries and discussed.

1.5.3.1 Chiral Auxiliaries

A chiral auxiliary modifies the substrate molecule by introducing a stereogenic center that will influence the reaction outcome in an asymmetric manner. After the key reaction steps, it must be removed unless it is to become part of the target compound. An efficient practice is to incorporate the chiral auxiliary as both a protecting group for sensitive functional groups as well as to transfer chirality to the substrate. If the auxiliary is removed intact after the asymmetric transformation it has the potential to be recycled.

The ephedrine derivatives serve as practical chiral auxiliaries for the preparation of most functional groups in highly enantioenriched forms including acids, alcohols, carbonyl and carboxylic

acids [127], amines [128] and sulfinates [129]. An asymmetric preparation of α-phenethylamine using a norephedrine chiral auxiliary is shown in Scheme 1.6. Hydrogenation of the imine prepared from acetophenone and (-)-norephedrine gives selectivity for the R_e face. The (-)-norephedrine auxiliary provides a chiral intermediate for the reduction to take place, then oxidative removal of the remaining auxiliary provides the (*R*)-α-phenethylamine and the nitrogen from the auxiliary is incorporated into the product [128] In this example, (-)-norephedrine acts as a self-immolative (non-recoverable) chiral auxiliary and ephedrine derivatives are often used in this manner since they are inexpensive and often not easily recovered.

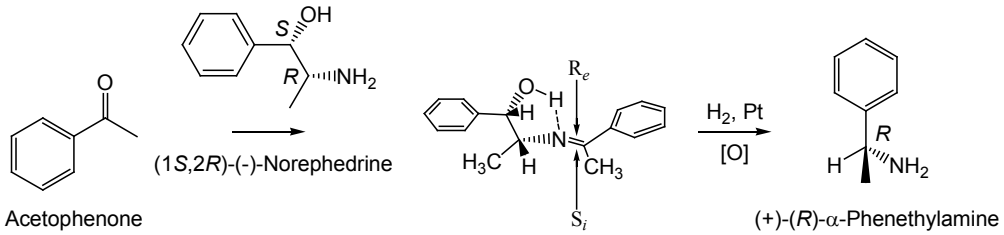

Scheme 1.6: Norephedrine as a chiral auxiliary in the preparation of (*R*)-α-phenethylamine from acetophenone [128].

1.5.3.2 Asymmetric Catalysis

An ionic complex prepared using an optically pure ligand with a reactive inorganic center can be used as a chiral reagent to prepare non-racemic compounds from planar sp^2 hybridised prochiral substrates. If the reactive complex can be reformed *in situ* or remains unchanged after the reaction, this is now referred to as an enantioselective catalyst. Chiral catalysis is one of the most popular and efficient methods for asymmetric synthesis and some commonly used reagents are described below.

Proline [130] and (-)-norephedrine [131] derived ligands that contain the 1,2-amino alcohol functional group system have been used to prepare asymmetric oxazaborolidine hydride complexes (Figure 1.22, top). The chiral borohydride complex facilitates enantioselective reduction of carbonyl, ketoxime [132] and imine [131] functionalities to give the corresponding alcohol or amine (Figure 1.22, top) products. A diastereomeric interaction takes place between the prochiral center being reduced and the ligand hydride complex, leading to optical enrichment of the reduced products.

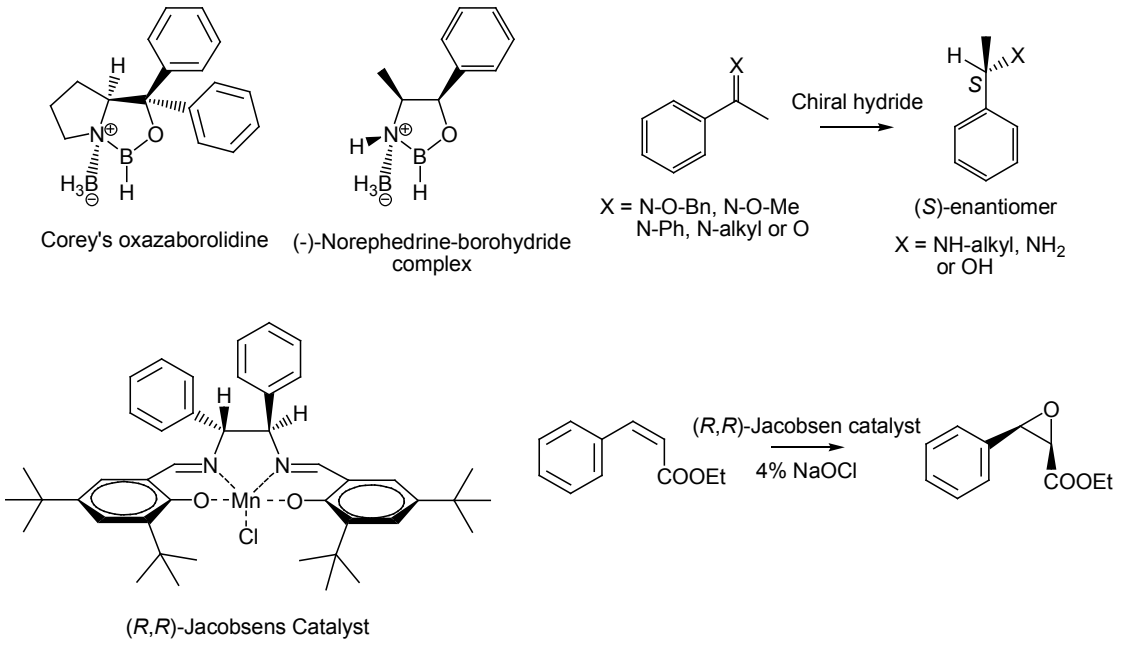

Figure 1.22: Top; The proline and (-)-norpehedrine borohydride complexes give enantioselective reduction of carbonyls and imines. Bottom; Jacobsens manganese(II)salen catalyst for enantioselective epoxidation of olefins [133].

Jacobsens catalyst, a manganene(II)salen complex, catalyses the stereoselective epoxidation of activated and unactivated double bonds using 4% hypochlorite solution [133] (Figure 1.22). The Jacobsens catalyst ligand is an imine dimer prepared by the reaction of a chiral diamine and two substituted salicylaldehyde molecules. Complexation to the redox active manganese cation provides a very efficient and scaleable chiral epoxidation catalyst. Sharpless catalytic asymmetric epoxidation conditions involve a Ti(IV) complex with the (+)-diisopropyl L-tartrate ligand to epoxidise a similar range of olefins as Jacobsens catalyst under mild conditions and has found use in the synthesis of complex natural products [134].

1.5.3.3 Biotransformation and Enzymatic Resolution

Asymmetric transformations using biological catalysts is an area often overlooked by synthetic research chemists, however the industrial synthesis of chiral amines relies on enzymatic processes for the production of commercial quantities of amino acids. The biological function of aminotransferase or transaminase enzymes is to take the amino groups of a donor amine and exchange it with a keto group of another molecule [135]. This consumed amine product of the enzymatic transformation is in a reversible equilibrium with the starting amine which is optically pure. The use of L-aspartic acid as an ‘amine

donor' allows the reaction to proceed to 90% completion due to the removal of oxaloacetic acid via further metabolism or decomposition to pyruvic acid (Scheme 1.7). Alternately, enzymatic resolution may be carried out on a racemic mixture of amides or esters through enantioselective hydrolysis. Purification of the unnatural D-isomer of amino acids is made accessible by this process. [124].

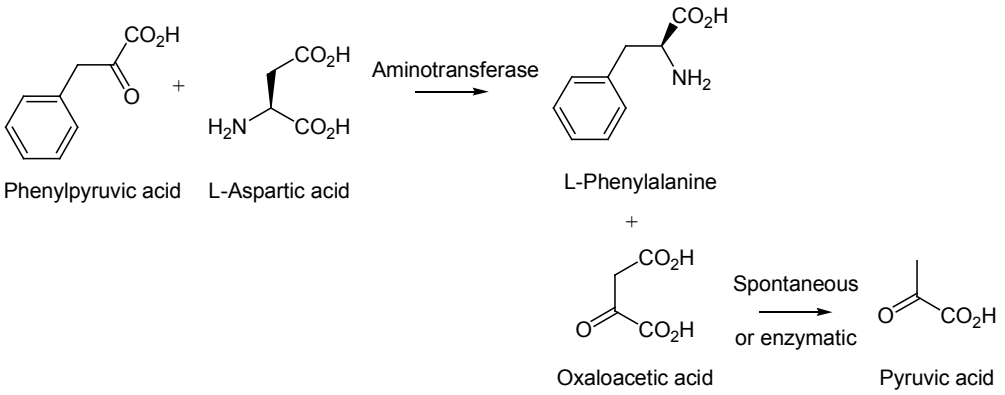

Scheme 1.7: Conversion of ketone to amine functionalities through the action of aminotransferase and the L-aspartic acid donor amine.

1.6 Asymmetric Approaches Towards Clerodane Natural Products

1.6.1 Synthesis via 'Wieland-Miescher' Ketone

Studies towards the synthesis of clerodane terpenes are not common in the literature. The most popular approach towards the diterpene backbone of clerodane and *neo*-clerodane structures is to synthesise the fused **A**/**B** ring system via a stereoselective Robinson annulation procedure.

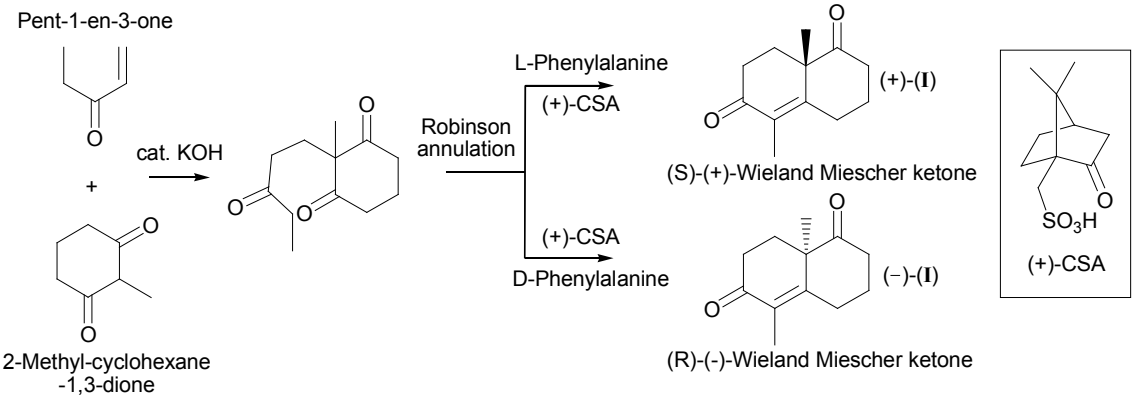

Scheme 1.8: Asymmetric Robinson annulation synthesis of the Wieland-Miescher ketone using (+)-CSA acid and phenylalanine [136].

The Michael-addition of 2-methyl-cyclohexane-1,3-dione to pent-1-en-3-one under basic conditions gives symmetrical triketone. Asymmetric cyclisation of the triketone in the presence of L or D-β-phenylalanine and D-10-camphorsulfonic acid ((+)-CSA) [136] provides optically active (*S*) and (*R*) isomers respectively of the bicyclic 1,4a-dimethyl-4,4a,7,8-tetrahydronaphthalene-2,5(3H,6H)-dione, known as the Wieland-Miescher ketone (**I**) (Scheme 1.8) [136].

A linear synthesis of the core of terpentecin has been reported by Ling *et al.* [137] using the (*S*)-(+)-Wieland-Miescher ketone Robinson annulation product (+)-(**I**) as a starting point for the bicyclic decalin ring system and provides a good example of the general synthetic methodology involved in creating additional stereocentres. Protection of the C(4) carbonyl as the cyclic acetal leaves the conjugated α,β-unsaturated carbonyl as the most reactive functionality. A stereoselective reductive alkylation reaction was then performed using lithium metal in ammonia, followed by heating with the alkylating agent vinyl bromide. This gives the 1,3-alkyl addition product with selectivity for the *trans*-C(5)/C(10) ring system relative to the starting ketone.

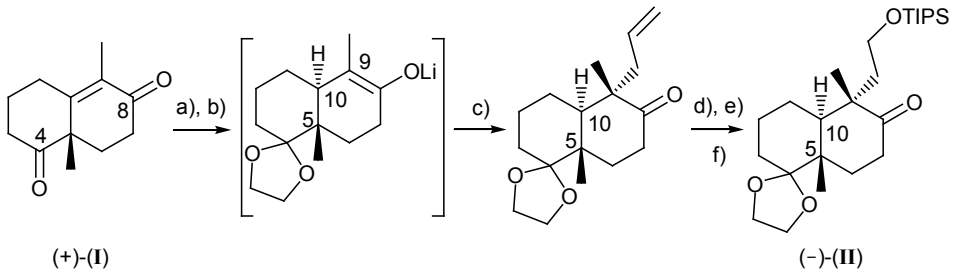

(+)-(**I**) (−)-(**II**)

a) 1.0 equiv. $(CH_2OH)_2$, 0.1 equiv. TsOH, 80°C, benzene, 12 h, 90% b) 5.0 equiv. $Li_{(0)}$, NH_3, −80 to −30°C, 1.0 equiv. H2O, c) 5.0 equiv. CH_2=$CHCH_2Br$, −80 to −30°C, 5 h, 78% d) O_3, CH_2 Cl_2, −78°C then 3.0 equiv. $LiAlH_4$, Et_2O, 0–25°C, 1 h, 65% e) 1.0 equiv. TIPSOTf, 1.3 equiv. 2,6-lutidine, DCM, −80°C, 0.5 h, 98% f) 1.4 equiv. Dess–Martin periodinane, DCM, 1h, 25°C, 87%.

Scheme 1.9: Reductive alkylation methodology of (*S*)-(+)-Wieland-Miescher ketone to give the trans-C(5)/C(10) bicyclic ketone (-)-(**II**) [137].

The C(9) alkyl substituent favors a *cis*- geometry with the adjacent C(10) bridge-head hydrogen, both of which are on the *exo*-face (Scheme 1.9). Ozonolysis of the terminal olefin, followed by reduction of the resulting aldehyde provides the C(5) hydroxy-ethyl side chain and protection as the trisopropylsilyl ether (TIPSO) allows access to the flexible clerodane starting material (-)-(**II**).

Oxidation of the C(6) carbon was achieved in a further 6 steps using literature procedures. Methylenation of the C(8) carbonyl using the Peterson olefination conditions involving trimethylsilylmethyl-magnesium chloride ($TMSCH_2MgCl$) [137] gave an *exo*-cyclic double bond that upon hydrogenation with Wilkinsons catalyst ($(Ph_3P)_3RhCl$) underwent face selective reduction of 20:1 in favour of the *cis*- orientation of substituents at C(8)/C(9) (Scheme 1.10).

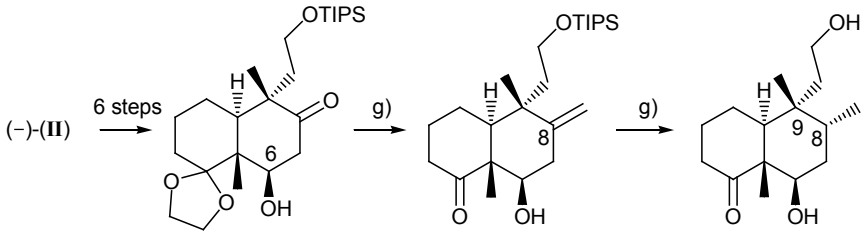

g) 1.1 equiv. $TMSCH_2MgCl$, Et_2O, 25°C, 2 h, then 1.0 equiv. HF·pyridine, Et_2O, 25°C, 6 h, 81% h) 0.01 equiv. $(Ph_3P)_3RhCl$, H2 (60 psi), benzene, 8 h, 92%;>20:1 *cis*:*trans*.

Scheme 1.10: Peterson olefination followed by hydrogenation with Wilkinsons catalyst [137].

Oxidation of the C(6) and C(7) positions was performed in 6 steps to provide the hydroxy ketone core of terpentecin as a single isomer in a total synthesis of 20 steps from (+)-(**I**) [137] (Scheme 1.11). Almstead *et al.* [138] have prepared the core of clerocidin (Scheme 1.11) using the same approach. Clerocidin and terpentecin have measured antibacterial and antitumor properties and have also been found to induce topoisomerase II-mediated DNA damage [139]. This mode of 'topoisomerase poisoning' has been suggested as a novel approach to new anticancer drugs [140].

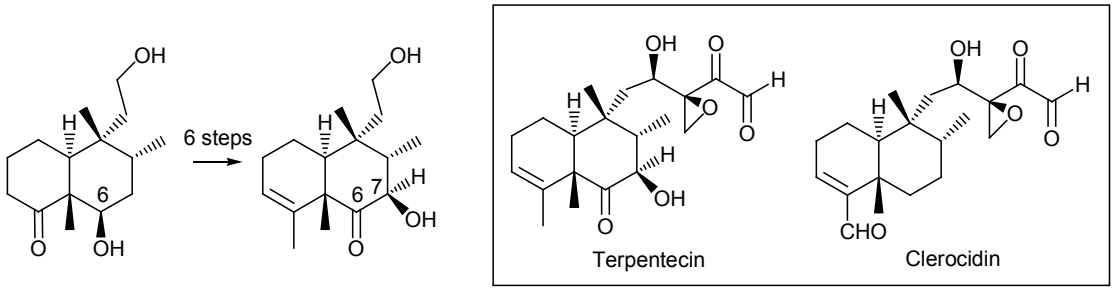

Scheme 1.11: Oxidation of C(6) and C(7) provides the core skeleton of terpentecin [137]. Both terpentecin and clerocidin have measured antibacterial and antitumor properties [139, 140].

A Japanese research group led by Hisahiro Hagiwara, have conducted a number of studies towards construction of the *trans*-*neo*-clerodane skeleton. In 1995, research towards the total synthesis of

an antibacterial clerodane from *Acritopappus longifolia* [141], 16-hydroxycleroda-3,13(14)Z-dien-15,16-olide was reported, starting from the (*R*)-(-)-Wieland-Miescher ketone (-)-(**I**). The C(10)/C(5) *trans*-selective reductive alkylation was used as in Scheme 1.9 to stereoselectively introduce the C(9) alkyl chain in six steps to produce (+)-(**II**). The conjugated α,β- unsaturated ketone was then introduced in five steps by functional group interconversion using known procedures [141] .

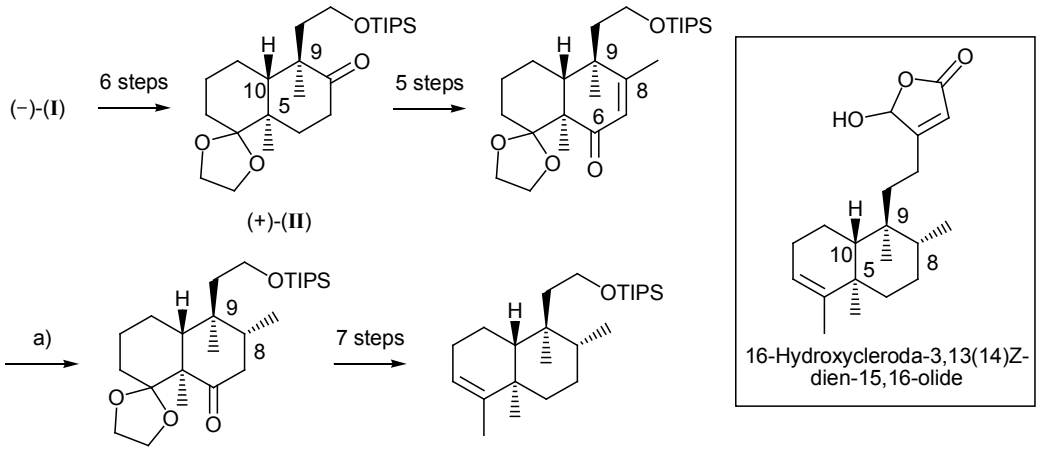

a) $Li_{(0)}$, liq. NH_3, THF, -78°C to reflux, 1 h, quenched in EtOH.

Scheme 1.12: Stereoselective construction of the *trans-neo*-clerodane skeleton from (-)-(**I**) as reported by Hagiwara *et al.* [141].

Reduction of the α,β-unsaturated olefin C(7)/C(8) using lithium metal in mixture of liquid ammonia and tetrahydrofuran (THF), followed by quenching in ethanol, was reported to produce the *trans*-neoclerodane stereochemistry [141]. A further seven steps were then required to produce the core of the target skeleton (Scheme 1.12).

The first total synthesis of (-)-methyl barbascoate [142], a natural product from the ethanol extract of *Croton californicus*, has been reported from the same research group in 2005. Traditionally, powdered leaves of this plant are used as a pain reliever for rheumatism and also used by fishermen to stun fish. The *trans*-neoclerodane was synthesised via a linear approach in 12 steps beginning with the chiral precursor (+)-(**II**) [136, 142, 143] (Schemes 1.13-1.15). Wittig olefination of the trans-decalone (+)-(**II**) produced the *exo*-cyclic olefin at C(8) which underwent hydroboration using borane-THF etherate (BH_3-THF), and oxidation with hydrogen peroxide (H_2O_2) to give a 3.8:1 ratio of 8α and 8β alcohols in favor of the undesired stereoisomer (Scheme 1.13).

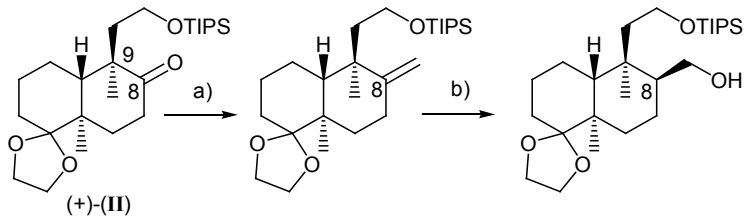

a) Ph_3PCH_3Br, NaHMDS, THF, reflux, 87% b) BH_3-THF, THF then NaOH, H_2O_2, 92%, 8α:8β, 3.8:1

Scheme 1.13: Wittig methylenation of C(8) in (+)-(**II**) carbonyl followed by hydroboration and oxidation to the primary alcohol [142].

The authors report oxidation with pyridinium dichromate (PDC) under basic conditions to produce the aldehyde substituent at C(8) in quantitative yield [142] without deprotection. This intermediate was easily epimerised at C(8) using sodium methoxide (NaOMe) in methanol to give the desired 8β diastereoisomer as the thermodynamically favoured epimer (Scheme 1.14).

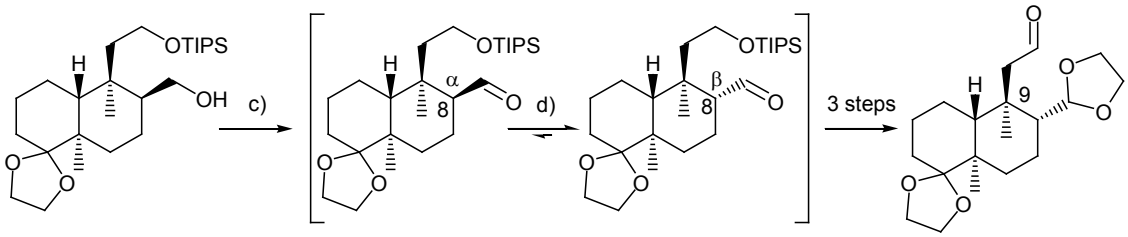

c) PDC, AcONa, MS-4Å, DCM, quant. d) MeONa, MeOH, rt, 95%

Scheme 1.14: Hagiwara *et al.* [142] report the C(8) aldehyde to epimerise to the desired isomer upon treatment with MeONa. Deprotection followed by oxidation of the C(9) chain to the aldehyde was achieved in three steps using known procedures [142].

Protection of the aldehyde as the acetal locked the C(8) stereocenter in the *trans-neo*-configuration by preventing further enolization, and subsequent desilylation followed by oxidation of the C(9) alkyl chain was reported to give the protected aldehyde in three steps using known reactions [142] (Scheme 1.14). The 3-furyl group was introduced by the nucleophilic reaction of 3-furyl lithium, prepared from the reaction between 3-bromofuran and n-butyl lithium, with the diacetal aldehyde to give the racemic C(12) furfurol in high yield (Scheme 1.15). Removal of the acetal protection groups, oxidation to the δ-lactone ring and introduction of C(4) conjugated ester was performed in four steps using known conditions to produce a 3:2 mixture of (-)-methyl barbascoate and its C(12) epimer [142].

Methyl barbascoate and salvinorin A (**1**) have many structural and functional group similarities as both share the same fused tricyclic skeletons, δ-lactone and 3-furanyl moieties. The 12-(*R*) stereochemistry of the 3-furyl moiety in (-)-methyl barbascoate forces the lactone ring into a boat conformation, however the 12-(*S*) isomer exists in the chair conformation as seen in **1**.

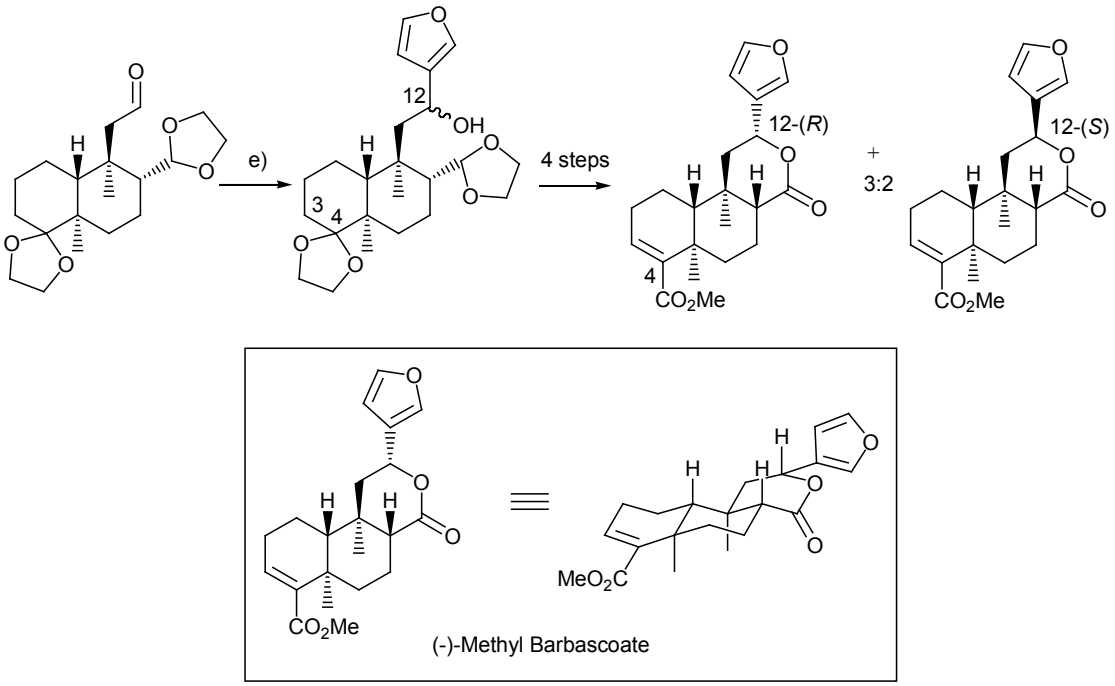

e) 3-Furyllithium, THF, -78°C, 86% yield, 12-(*R*):12-(*S*), 3:2

Scheme 1.15: Hagiwara *et al.* [142] report nucleophilic addition of the 3-furyl moiety followed by oxidation and functional group interconversion to provide (-)-methyl barbascoate in 18 steps overall from (+)-(**II**).

1.6.2 Synthesis from (-)-Verbenone

An approach by Kato *et al.* [144] provides the *trans*-decalone by Lewis-acid catalysed ring opening of a (-)-verbenone derivative. 1,4-Conjugate addition of vinyl Gilman reagent to the chiral terpene (-)-verbenone was performed in quantitative yield (Scheme 1.16). Methylation at the α-carbonyl position progressed regioselectively through deprotonation with lithium diisopropylamine (LDA) in the presence of 1-methyl-2-pyrrolidinone (NMP), followed by alkylation with iodomethane. The chemical transformation of the vinyl to a 2-acetoxy group was achieved in 3 steps by conventional reactions [144].

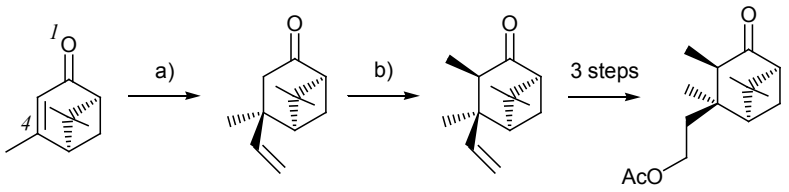

a) CH_2=CHMgBr, CuI, THF, quantitative b) LDA, MeI, NMP, THF

Scheme 1.16: Functionalization on the (-)-verbenone structure reported by Kato *et al.* [144].

Regioselective cleavage of the cyclobutane ring was achieved using a Lewis acid mixture of boron trifluoride diethyl etherate ($BF_3.OEt_2$), zinc(II)acetate ($Zn(OAc)_2$) and acetic anhydride (Ac_2O) to give the enol acetate (Scheme 1.17). Hydrolysis to the ketone was performed in potassium carbonate (K_2CO_3) solution and this was accompanied by concomitant epimerization of the α-methyl carbonyl group to give the *cis* methyl product in quantitative yield.

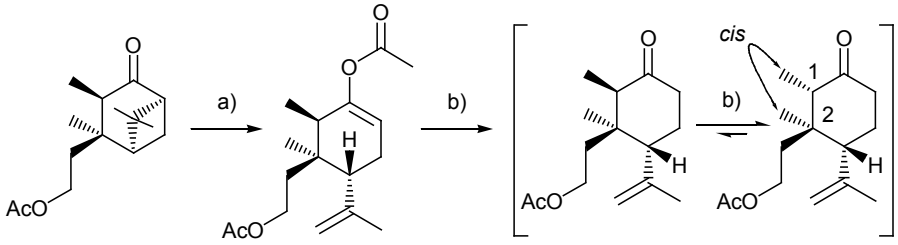

a) $BF_3.OEt_2$, $Zn(OAc)_2$, Ac_2O b) K_2CO_3/MeOH

Scheme 1.17: Regioselective lewis acid mediated ring opening of the (-)-verbenone derivative to provide a substituted cyclohexene structure followed by base assisted epimerization to the desired isomer.

Protection of the carbonyl and oxidation of the acetoxy substituent to the corresponding aldehyde was performed in 3 steps using literature methods [144]. Cyclization via an 'ene' reaction with diethyl aluminium chloride (Et_2AlCl) gave the *trans*-C(5)/C(10) decalin ring system and subsequent oxidation of the C(7) alcohol using Swern reaction conditions was reported to produced the α,β-usaturated carbonyl derivative in good yield (Scheme 1.18, step f). The 1,4-conjugate addition to C(9) using vinyl Gilman reagent gave the *cis* vinyl substituent relative to the adjacent bridgehead hydrogen C(10) in an analogous manner to the reductive alkylation product from the Wieland-Miescher ketone. α-Carbonyl methylation at C(8) progresses regioselectively through deprotonation with lithium hexamethyldisilazane (LHMDS), followed by alkylation with iodomethane to produce the *trans*-C(8)/C(9) dimethyl groups. Facile

epimerisation of the C(8) methyl group occurred using 5% KOH in methanol to provide the *trans*-neoclerodane skeleton in 17 steps from (-)-verbenone (Scheme 1.18, step i) [144].

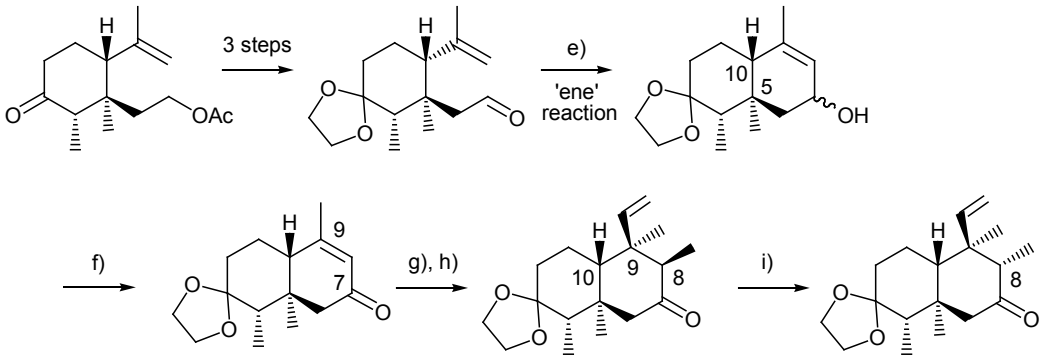

e) Et_2AlCl, DCM, 81% f) $(COCl)_2$, DMSO then Et_3N; DBU, DCM, 83% g) CH_2=CHMgBr, CuI, THF, 67% h) LHMDS, MeI, THF, 61% i) 5% KOH/MeOH, 95%.

Scheme 1.18: Ene-cyclization using Et_2AlCl to produce the *trans*-C(5)/C(10) decalin system followed by 1,4-Gilman addition, α-carbonyl methylation and finally C(8) epimerization to provide the *trans*-neoclerodane skeleteon [144].

1.6.3 Novel Clerodane Syntheses

As discussed in section 1.4.4, the potent insect antifeedant Jodrellin is an attractive target for total synthesis due to its potential as an antifeedant in farming and agriculture. Research by Ley *et al.* towards the synthesis of Jodrellin A and B [106, 107] have followed a linear synthetic approach to provide a successful pathway to the rigid epoxy diacetate decalin framework of the natural product (Scheme 1.19).

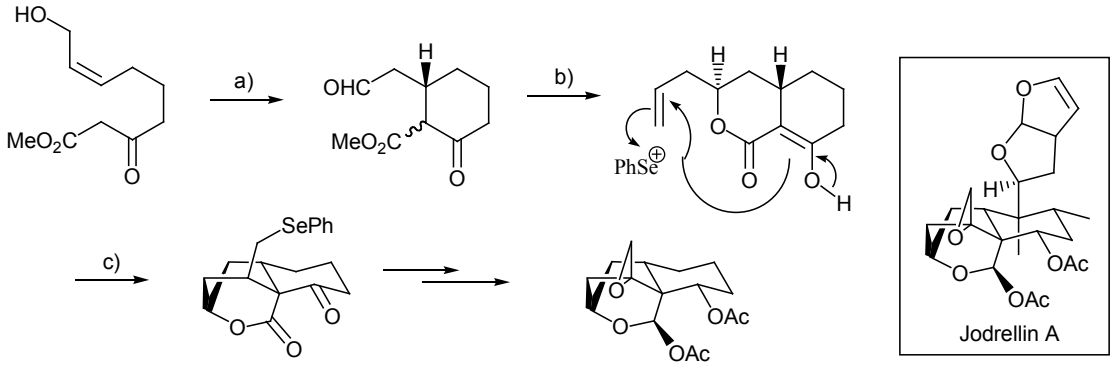

a) PDC, AcOH, 3Å molecular sieves, DCM b) NaH, THF, 0°C, $Li[Ti(allyl)(OPri)_4]$, -78°C c) NPSP, ZnI_2, DCM

Scheme 1.19: Synthesis of the Jodrellin A framework via a selenium mediated β-coupling [106, 107].

The key step in this methodology is the selenium mediated coupling of the β-ketoester to the alkene using *N*-phenylselenophthalimide (NPSP) to form the tricyclic Jodrellin skeleton. The Jodrellin framework was found to retain some of the insect antifeedant properties of the parent compound (Scheme 1.19).

A novel approach by Arns *et al.* [145] towards the *trans*-decalin core of Teucrolivin A was reported in 2006. A [4+2] cycloaddition reaction of 1,3-cyclohexadiene was performed using singlet oxygen, generated *in situ* from ozone gas under ultraviolet light in the presence of TPP, to produce the dioxabicyclic peroxide starting substructure. Reduction using methanolic thiourea to the *cis*-cyclohex-2-ene-1,4-diol provided a suitable building block for functionalization (Scheme 1.20). Olefination and incorporation of the 3-furyl moiety was conducted in eight steps and followed by a thermally induced tandem oxy-Cope/Claisen/ene reaction under microwave irradiation. This provided not only the *trans*-decalin clerodane core but also the neoclerodane geometry at C(8)/C(9). Ozonolysis of the olefins gave the hemiacetal system present in Teucrolivin A with relative stereochemistry identical to that in the natural product.

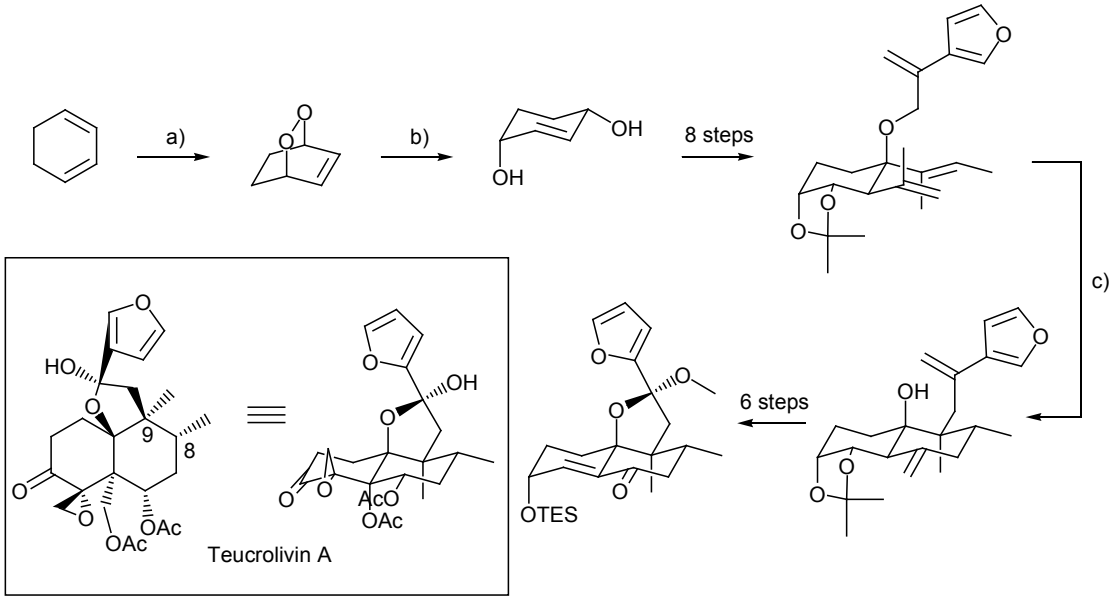

a) O_3, TPP, h*v*, DCM b) Thiourea, MeOH, c) Toluene/MW/120ºC

Scheme 1.20: Synthesis of Teucrolivin A starting from the [4π+2π] electron cycloadduct product of cyclohexadiene and singlet oxygen, published by Arns *et al.* [145].

1.6.4 Previously Reported Asymmetric Total Synthesis of Salvinorin A

At the time that the research presented in this manuscript was carried out, no successful or proposed strategies for the asymmetric total synthesis of **1** were reported in the literature. During the final manuscript preparation an asymmetric total synthesis of the target compound **1** was published by Scheerer *et al*. [31] who described the construction of the tricyclic *trans*-neoclerodane ring using a transannular Michael reaction cascade of an appropriate, highly substituted macrolactone. The required functionality for ring **A** was progressively introduced on an acyclic chain starting from 1-(2-thioxothiazolidin-3-yl)pent-4-en-1-one (Scheme 1.21). The stereochemistry at the C(4) ester of **1** was established by orthoester alkylation using Ni(II)-(*R*)-BINAP catalysis to give the β-ketoester in excellent enantioselectivity (94% *ee*) and interconversion to the α,β-unsaturated aldehyde was achieved in a further four steps using known methods. Selective aldol-type addition was reported in 9:1 d.r. using the acetate of the (*S*)-4-isopropyl-2-thioxothiazolidin-3-yl auxiliary in the presence of $Sn(OTf)_2$, followed by protection as the C(7) TBS ether. Mentioned by the authors as a footnote, the C(7) stereocenter was predicted to promote the convergence of macrocyclic precursors.

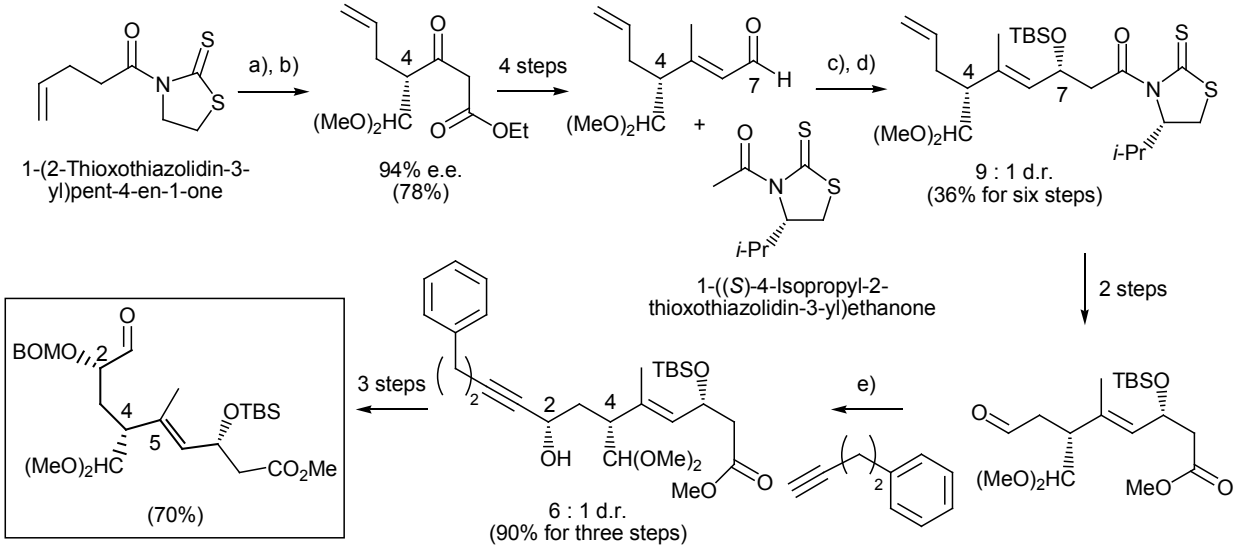

a) Ni-(*R*)-BINAP$(OTf)_2$, 2,6-lutadine, $BF_3.Et_2O$, $HC(OMe)_3$ b) $HO_2CCH_2CO_2Et$, *i*-PrMgCl, 65ºC c) $Sn(OTf)_2$, *N*-ethylpiperidine, -78ºC d) TBSOTf, 2,6-lutadine e) $Zn(OTf)_2$, (-)-*N*-Me-ephedrine, TEA.

Scheme 1.21: Scheerer *et al.* [31] have prepared the highly functionalised aldehyde using a combination of chiral catalysts and auxiliaries, as a major fragment for the convergent synthesis of **1**.

Transesterification to the methyl-ester followed by conversion to the terminal aldehyde was reported in two steps and (-)-*N*-methyl-ephedrine-mediated zinc acetylide addition was reported to give the propargylic alcohol in high yield with 6:1 preference for the desired stereochemistry in the corresponding C(2) acetoxy position in **1**. Protection of the alcohol and oxidative cleavage was carried out in three steps to provide the terminal aldehyde in 70% as a major convergent fragment to **1** [31] (Scheme 1.21).

Stereochemistry at the C(12) 3-furyl position was established using the (*R*)-B-Me-oxazaborolidene catalysed asymmetric reduction of 1-(furan-3-yl)but-2-yn-1-one and transformation to the vinyl iodide using known methods was reported to yield the second convergent fragment in three steps and high enantioselectivity (97% *ee*) [31] (Scheme 1.22).

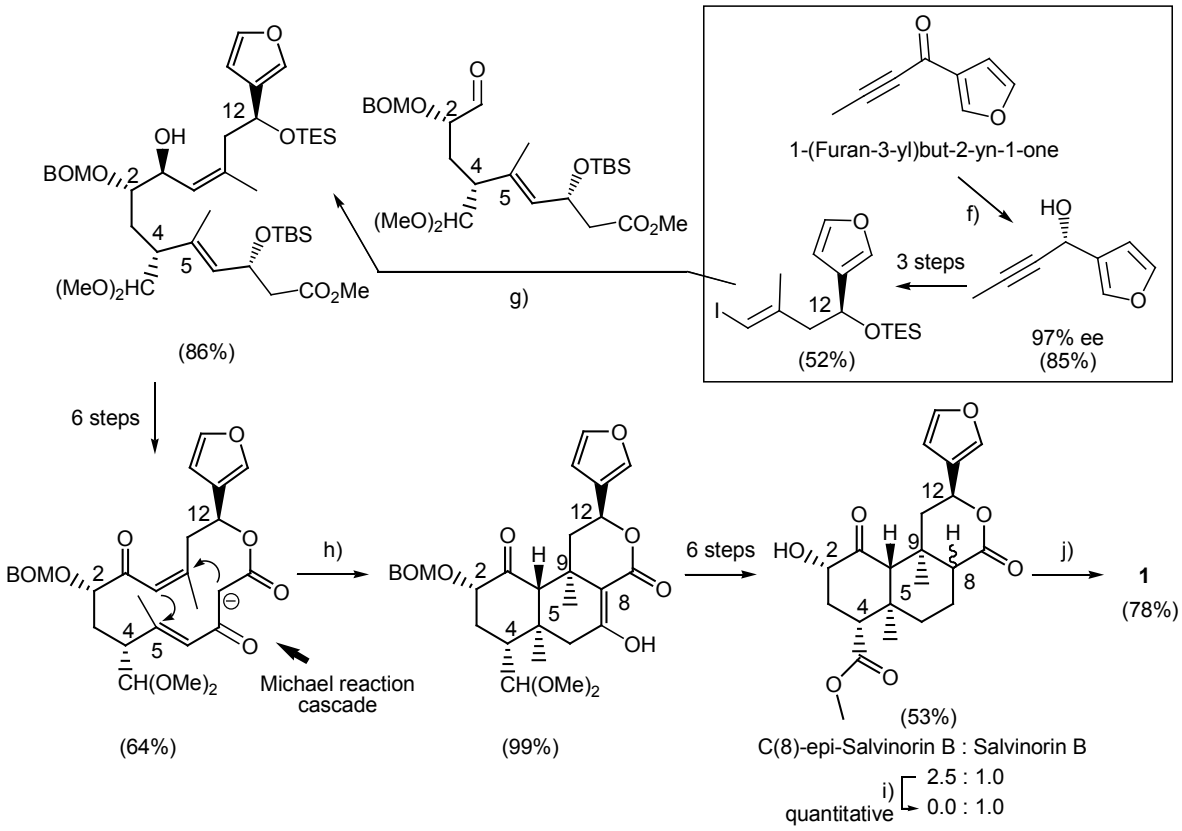

f) (*R*)- B-Me-oxazaborolidene, $BH_3.Me_2S$, -30ºC g) *n*-BuLi, $MgBr_2.OEt_2$, -78ºC, aldehyde, then $MgBr_2.OEt_2$, DCM, -78 to 0ºC h) TBAF, –78 to 5ºC i) K_2CO_3, MeOH, quantitative j) Ac_2O, Pyridine, DMAP.

Scheme 1.22: Scheerer *et al.* [31] report coupling of the furan fragment using the Grignard reaction of the vinyl iodide functionality with the aldehyde fragment in a convergent approach. Transformation to the bisenone followed by Michael reaction cascade gave the desired stereochemistry at C(5), C(9) and C(10) and as featured in **1**, which was obtained upon further synthetic manipulation.

The vinyl Grignard was generated using n-BuLi/$MgBr_2.OEt_2$ which was reacted with the aldehyde fragment, yielding the alcohol in 86%, and macrolactonization followed by oxidation to the bisenone system was reported in a further six steps (64%). The Michael reaction cascade was effected under very mild conditions (TBAF, -78 to 5ºC), resulting in a single tricyclic isomer in an impressive 99% yield. In this key step, diastereocontrol was achieved for the *cis*-oriented C(5) and C(9) methyl groups, both of which are positioned *trans* to the C(10) proton is in agreement with in the stereochemistry of **1**. The authors credit this result to the reinforcement from C(4) and C(12) stereocentres based on their experimental data on model compounds, and transformation to a mixture of C(8)-*epi*-salvinorin B and salvinorin B followed in a further five steps. C(8)-Epimerization followed by acetylation was accomplished (78%) to give **1** in thirty four steps overall from commercially available reagents.

This example represents the first reported synthesis of salvinorin A (**1**) and validates the significance of **1** as an important synthetic target. The synthesis described in this manuscript aims at achieving the same target product **1** and follows a different pathway to all examples described in section 1.6. The retrosynthetic analysis of **1** is outlined in section 1.7.

1.7 Retrosynthesis of Salvinorin A

The clerodane syntheses reviewed in section 1.6 all follow a linear synthetic methodology, starting from a chiral starting material and building on it in sequential sections to the original chiral core fragment. As has been hopefully observed from the examples shown, when choosing a chiral starting structure, the stereochemical outcomes required of the target product determine which products are most appropriate to initiate the synthesis. The starting material is required not only to possess as many chiral centers as possible in common with the desired target product, but also should direct sequential reactions in a stereoselectivly favourable manner. The highly oxygenated ketone ring present in salvinorin A appeared to have more functionality than could be introduced conveniently through linear modification of the Wieland-Miescher ketone (Section 1.6.1). Furthermore, studies by Hagiwara [142] (Figure 1.14) and chemical transformations on salvinorin A [86, 146] demonstrate that the carbon center C(8) is easily epimerised when adjacent to carbonyl functionalities. This led us to investigate a convergent synthesis and commence separate studies towards the synthesis of either end ring of the salvinorin A molecule and attempt to create the central ring during the junction of the two. An attractive feature of this synthesis is that both convergent halves contain definite pharmacophores that can be studied individually.

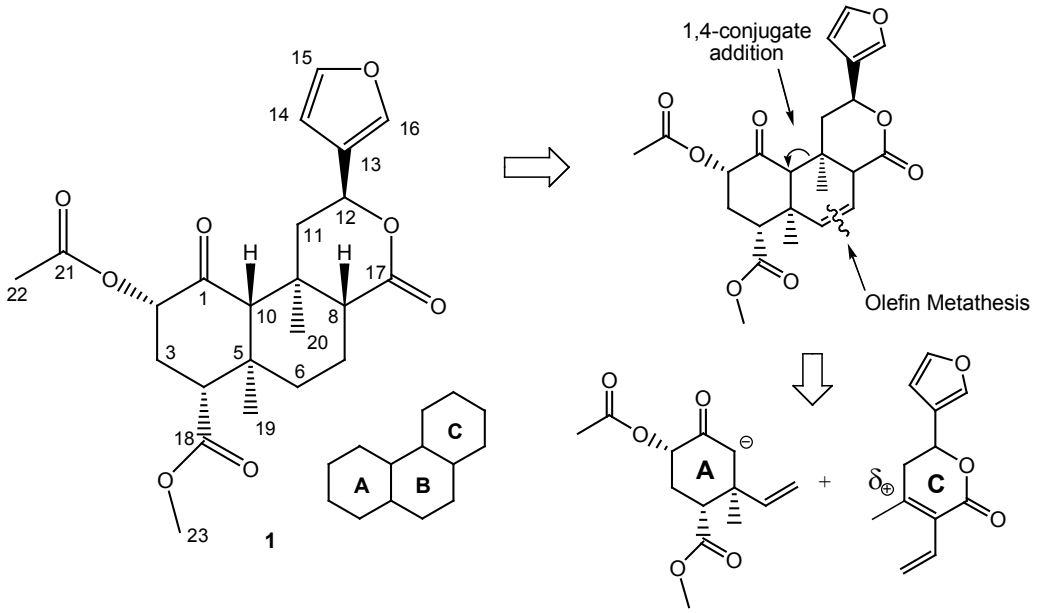

Scheme 1.23: Disconnection of salvinorin A (**1**) at ring **B** to produce convergent precursors rings **A** and **C**.

Ring **B** dissection of the tricyclic structure at C(9)/C(10) and C(6)/C(7) presents a functionalised cyclohexanone (ring **A**) and an α,β-unsaturated lactone (ring **C**) as precursors in a convergent synthesis (Scheme 1.23). Stereocentres adjacent to ketone and ester functionalities contain acidic protons and were identified as potential sites for racemization during preparation and purification.

Introduction of the vinyl substituent can be retrosynthetically derived from the reaction between a α,β-unsaturated ketone (**2**) and a vinyl Gilman nucleophile. Cleavage of the easily modified acetyl group leaves an α,β-unstaurated vinylogous acid (**3**) (Scheme 1.24). If this intermediate were prepared through rigorous reaction conditions involving heat or strongly acidic or basic conditions, dehydration of the alcohol would be likely and subsequent isomerization would produce an aromatic phenol.

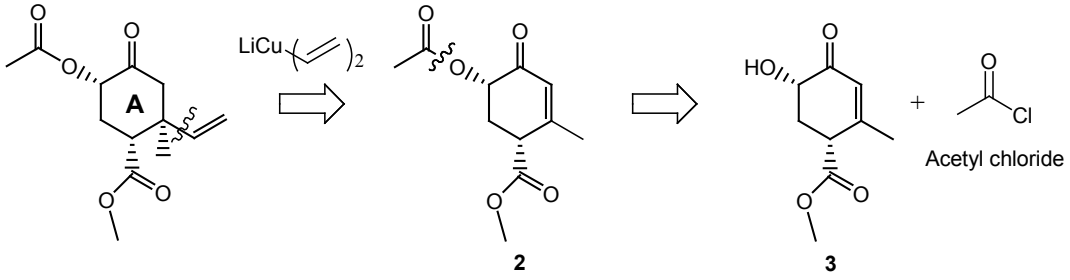

Scheme 1.24: Disconnection of ring **A** using a vinyl Gilman reagent and acetyl action using acetyl chloride.

For this reason we decided to prepare the alcohol (**3**) by the ether bridge cleavage of a 7-oxanorbornane or 7-oxabicyclo[2.2.1]heptane species (**4**). Ring opening of the bicyclic ether provides the stereochemistry of the ketone ring present in both salvinorin A and B. The enol of the ketone can then be retrosynthetically disconnected as the [4π+2π] electron Diels-Alder cycloaddition product between a substituted furan (**5**) and methyl acrylate (MAC) (Scheme 1.25).

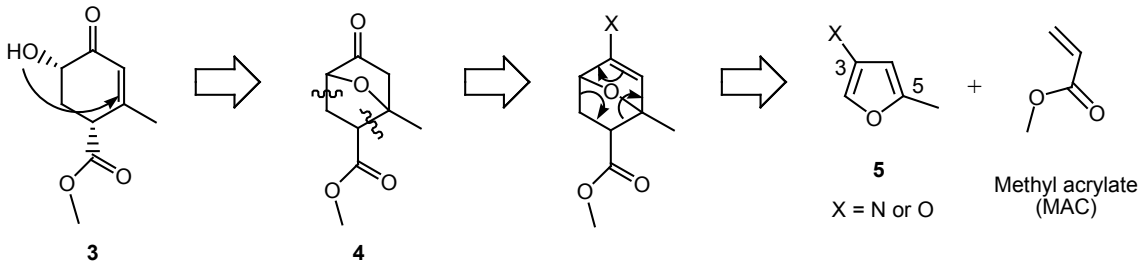

Scheme 1.25: The oxabicyclic ketone synthon (**4**) can be devised by a retro [4π+2π] electron cycloaddition reaction to produce a substituted furan starting material (**5**).

Heterosubstituted furans have been found useful as reactive dienes in the preparation of 7-oxa[2.2.1]bicycloheptane structures using Diels-Alder methodology. The compatible functional groups to incorporate as X in the 3-position of the furan starting material (Scheme 1.25) was narrowed to those labile to hydrolysis when connected to an isolated olefin. This allows for ether, ester, amide or amine substituents as the most accessible functionalities to include in this synthon. It was also decided at this point that if the C(3) substituent were to contain a chiral centre, it could act as a chiral auxiliary in the subsequent cycloaddition reaction to prepare a single enantiomer in excess. Amine-containing (X = *N*) chiral compounds are abundant and enamines are readily cleaved under aqueous acidic conditions, hence an amine substituent was chosen as the C(3) heteroatom. Literature research at this time revealed that little was known about the preparation or chemistry of 3-amino substituted furans and we were aware that the design of an expedient synthesis would be desirable.

Ring **C** was first disconnected by a retro Aldol or Reformatsky reaction to produce a substituted butanone attached to a vinyl acetic ester. Disconnection of the ester provides a 1,3-keto alcohol that can be rationalised as the retro aldol product between 3-furaldehyde and acetone (Scheme 1.26). Construction and connection of the vinyl acetic acid fragment will depend on the stability of the furfurol **8**. If an esterification procedure that preserves stereochemistry is required, α-halovinyl esters may be obtained directly through a deconjugation/esterification procedure using α-bromocrotonyl chloride in which case the activating substituent on the ester chain would be a halide. If stereochemistry at the alcohol is to be inverted during esterification, an activated vinyl acetic acid is then desired.

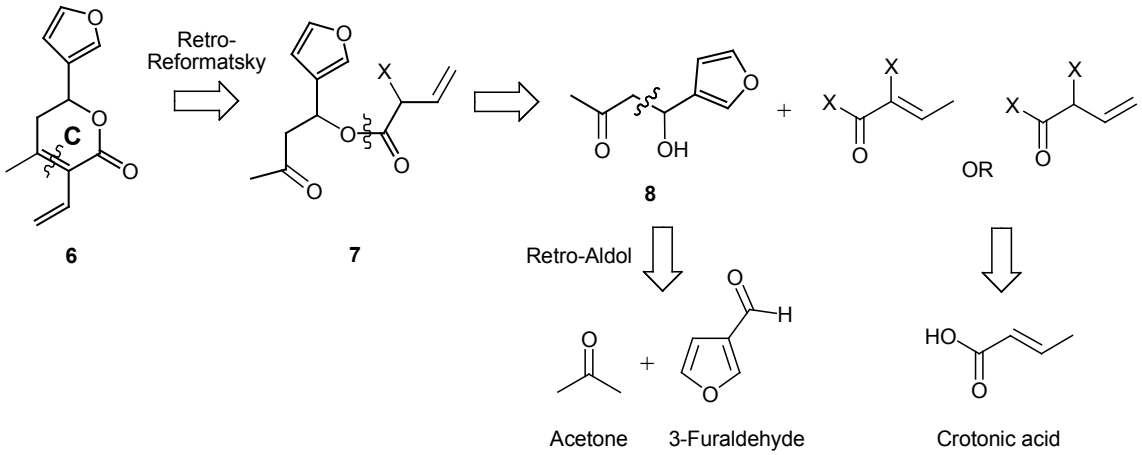

Scheme 1.26: Disconnection of ring **C** to the 3-furyl substituted butanone (**7**) followed by ester cleavage to the 3-furyl alcohol (**8**). The 1,3-ketoalcohol can be disconnected by a retro-Aldol reaction between 3-furaldehyde and acetone. The ester cleaved from **7** can be prepared from variety of acid chlorides accessible from crotonic acid.

Chapter 1
Introduction: References

[1] J. Ott. Psychoactive Card IV. "*Salvia divinorum* Epling et Játiva: Leaves of the Shepherdess Epling et Jativa", *Eleusis*, **1996**, *4*, 31-39. Reference obtained from http://www.sagewisdom.org/, 05/08/2007.

[2] D. J. Siebert, Personal communication.

[3] A. Reisfield. "The Botany of Salvia Divinorum (*Labiatae*)", *Sida, Contributions to Botany*, **1993**, *15*, 349-366.

[4] J. Ott. "Ethnopharmacognosy and Human Pharmacology of *Salvia divinorum* and Salvinorin A", *Curare*, **1995**, *18*, 103-129. Reference obtained from http://www.sagewisdom.org/reisfield.html 05/08/2007.

[5] R. G. Wasson. "A New Mexican Psychotropic from the Mint Family", *Botanical Museum Leaflets*, Harvard University, **1962**, *20*, 77-84. Reference obtained from http://www.sagewisdom.org/wasson1.html 05/08/2007.

[6] D. J. Siebert, Salvia Divinorum Research Center, www.sagewisdom.org. 05/08/2007.

[7] A. Shulgin, A. Shulgin. "TiKAL, The Continuation", Transform Press, Berkeley, **1997**, 645-727, ISBN 0-9630096-9-9.

[8] J. H. Halpern. "Hallucinogens and Dissociative Agents Naturally Growing in the United States", *Pharmacology and Therapeutics*, **2004**, *102*, 131-138.

[9] B. A. Clement, C. M. Goff, T. D. A. Forbes. "Toxic Amines and Alkaloids from *Acacia Rigidula*", *Phytochemistry*, **1998**, *49*, 1377-1380.

[10] S. A. Rovinsky. "*Salvia divinorum* Epling et Játiva-M. (*Labiatae*): An Ethnopharmacological Investigation", *The McNair Scholarly Review*. **1998**, *3*, 142-156; excerpts from J. B. Johnson. "The Elements of Mazatec Witchcraft", *Göteborgs Etnografiska Museum Etnologiska Studie*, **1939**, *9*, 119-149.

[11] For an historical account of Teonanácatl and Ololiuqui see; A. Hofmann. "Teonanácatl and Ololiuqui, two ancient magic drugs of Mexico". *Bulletin on Narcotics*, **1971**, *1*, 3-14.; Botanical Indentification in: Heim, R. and R. G. Wasson. 1958. "*Les Champignons* Hallucinogènes du Mexique: Etudes, ethnologiques, taxonomique, biologiques, physiologiques et chemiques". *Archives du Mus. Nat. d'Histoire Naturelle*, 7(VI).

[12] R. Heim, A. Hofmann. "Isolement de la psilocybine a partir du Stropharia cubensis Earle et d'autres esptkes de cham-pignons hallucinogenes mexicains appartenent au genre Psilocybe". *Revue de Mycologie*, **1959**, *23*, 347-351.

[13] H. Lindenblatt, E. Kraemer, P. Holzmann-Erens, E. Gouzoulis-Mayfrank, K. A. Kovar. "Quantitation of Psilocin in Human Plasma by High Performance Liquid Chromatography and

Electrochemical Detection: Comparison of Liquid-liquid Extraction with Automated On-line Solid-phase Extraction", *Journal of Chromatography, B: Analytical Technologies in the Biomedical and Life Sciences*, **1998**, *709*, 255-263.

[14] L. Rivier. "Ethnopharmacology of LSD and Related Compounds", Chapter 4, 43-46 in: "50 Years of LSD: Current Status and Perspectives of Hallucinogens: A Symposium of the Swiss Academy of Medical Sciences", **1994**, A. Pletscher (Ed.), D. Ladewig (Ed.). Taylor & Francis, ISBN 1850705690.

[15] C. Epling, C. D. Játiva-M. "A New Species of Salvia from Mexico", *Botanical Museum Leaflets*, Harvard University, **1962**, *20*, 75-76. Reference obtained from http://www.sagewisdom.org/epling&jativa.html 05/08/2007.

[16] L. J. Valdés III, J. L. Diaz, A. G. Paul. "Ethnopharmacology of Ska Maria Pastora *(Salvia divinorum,* Epling and Játiva-M.)", *Journal of Ethnopharmacology*, **1983**, 287-312.

[17] A. Ortega, J. F. Blount, P. D. Manchland. "Salvinorin, a New *trans*-Neoclerodane Diterpene from *Salvia divinorum* (Labiatae)", *Journal of the Chemical Society Perkins Transactions I,* **1982**, 2505-2508.

[18] L. J. Valdés III, W. M. Butler, G. M. Hatfield, A. G. Paul, M. Koreeda. "*Divinorin A*, a Psychotropic Terpenoid, and Divinorin B from the Hallucinogenic Mexican Mint *Salvia divinorum*", *Journal of Organic Chemistry*, **1984**, *49*, 4716-4720.

[19] J. W. Gruber, D. J. Siebert, A. H. Der Marderosian, R. S. Hock. "High Peformance Liquid Chromatographic Quantification of *Salvinorin A* from Tissues of *Salvia Divinorum* Epling & Játiva-M", *Phytochemical Analysis*, **1999**, *10*, 22-25.

[20] M. Koreeda, L. Brown, L. J. Valdés III. "The Absolute Stereochemistry of Salvinorins". *Chemistry Letters,* **1990**, 2015-2018.

[21] J.L. Giner, D. J. Kiemle, L. Kutrzeba, J. Zjawiony. "Unambiguous NMR Spectral Assignments of Salvinorin A". *Magnetic Resonance in Chemistry*, **2007**, *45*, 351-354.

[22] D. J. Siebert. "Localization of Salvinorin A and Related Compounds in Glandular Trichomes of the Psychoactive Sage, *Salvia divinorum*". *Annals of Botany*, **2004**, *93*, 763-771.

[23] L. Kutrzeba, F. E. Dayan, J. Howell, J. Feng, J.-L. Giner, J. K. Zjawiony. "Biosynthesis of Salvinorin A Proceeds via the Deoxyxylulose Phosphate Pathway". *Phytochemistry*, **2007**, *68*, 1872-1881.

[24] T. A. Munro, M. A. Rizzacasa. "*Salvinorins D-F*, New Newclerodane Diterpinoids from *Salvia Divinorum*, and an Improved Method for the Isolation of *Salvinorin A*", *Journal of Natural Products*, **2003**, *66*, 703-705.

[25] L. J. Valdès III, H-M. Chang, D. C. Visger, M. Koreeda. "*Salvinorin C*, a New Neoclerodane Diterpene from a Bioactive Fraction of the Hallucinogenic Mexican Mint *Salvia divinorum*", *Organic Letters*, **2001**, *3*, 3935-3937.

[26] D. Y. W. Lee, Z. Ma, L-Y. Liu-Chen, Y. Wang, Y. Chen, W. A. Carlezon Jr., B. Cohen. "New Neoclerodane Diterpenoids Isolated from the Leaves of *Salvia Divinorum* and their Binding Affinities for Human κ-Opioid Receptors", *Bioorganic & Medicinal Chemistry*, **2005**, *13,* 5635-5639.

[27] A. K. Bigham, T. A. Munro, M. A. Rizzacasa, R. M. Robins-Browne. "*Divinatorins A-C*, New Neoclerodane Diterpinoids from the Controlled Sage *Salvia divinorum*", *Journal of Natural Products*, **2003**, *66*, 1242-1244.

[28] W. W. Harding, K. Tidgewell, M. Schmidt, K. Shah, C. M. Dersch, J. Snyder, D. Parrish, J. R. Deschamps, R. B. Rothman, T. E. Prisinzano. "Salvinicins A and B, New Neoclerodane Diterpenes from *Salvia divinorum*", *Organic Letters*, **2005**, *7*, 3017-3020.

[29] O. Shirota, K. Nagamatsu, S. Sekita. "Neo-clerodane Diterpenes from the Hallucinogenic Sage *Salvia Divinorum*", *Journal of Natural Products*, **2006**, *69*, 1782-1786.

[30] L. J. Valdès III. "Loliolide from *Salvia Divinorum*", *Journal of Natural Products*, **1986**, *49*, 171.

[31] J. R. Scheerer, J. F. Lawrence, G. C. Wang, D. A. Evans. "Asymmetric Synthesis of Salvinorin A, A Potent K-Opioid Receptor Agonist". *Journal of the American Chemical Society*, **2007**, 129, 8968-8969.

[32] J. A. Le Bel. "Sur les relations qui existent entre les formulae atomiques des corps organiques et le pouvoir rotatoire de leurs dissolutions", *Bulletin de la Societe Chimique de France*, **1874**, *22*, 337-347; J. H. Van't Hoff. "Sur les formulas de structure dans l'espace", *Bulletin de la Societe Chimique de France*, **1875**, *23*, 295-301; P. J. Ramberg. "Chemical Structure, Spatial Arrangement: The Early History of Stereochemistry, 1874-1914". Ashgate Ltd., **2003**, 67-73, ISBN 0754603970.

[33] P. Y. Bruice, "Organic Chemistry", (2nd Ed.), Prentice-Hall, New Jersey, **1998**, 185.

[34] L. Pasteur. "Sur les relations qui peuvent exister entre la forme cristalline, la composition chimique et le sens de la polarisation rotatoire", *Annales de Chimie et de Physique*, **1848**, *24*, 442-459.

[35] G. Hallas. "Organic Stereochemistry", McGraw-Hill publishing Co. Ltd., England, **1965**, 40, 4, 53.

[36] J. McMurry. Organic Chemistry, Brooks/Cole Publishing, USA, **1996**, 300-307, 1014, ISBN 0-534-23832-7.

[37] J. Clayden, N. Greeves, S. Warren, P. Wothers, "Organic Chemistry", Springer-Verlag, New York, **2001**, 1222. ISBN 0 19 850346 6.

[38] B. Knoche, G. Blaschke, Investigations on the *in vivo* Racemization of Thalidomide by HPLC, *Journal of Chromatography A*, **1994**, *666*, 235-240.

[39] Emilien, G., Maloteaux, J. M., Emilion, G. Current Therapeutic Uses and Potential of β-Adrenoreceptor Agonists and Antagonists, *European Journal of Clinical Pharmacology*, **1998**, *53*, 389-404.

[40] M. Glewis. The Enantioselective Syntheses of Some Metabolites of Beta Blockers, Propranolol, Metoprolol and Alprenolol. PhD Thesis, RMIT University, **2002**.

[41] D. Hoyer, D. E. Clarke, J. R. Fozard, P. R. Hartig, G. R. Martin, E. J. Mylecharane, P. R. Saxena, P. P. A. Humphrey. "International Union of Pharmacoloogy Classification of Receptors for 5-Hydroxytryptamine (Serotonin)". *Pharmacological Reviews*, **1994**, *46*, 157-203.

[42] R. A. Webster (Ed.). "*Neurotransmitters, Drugs and Brain Function"*, John Wiley and Sons Ltd., **2001**, 251-264. ISBN:0471978191.

[43] A. Sidhu, M. Laruelle, P. Vernier. "Dopamine Receptors and Transporters", Marcel Dekker, ISBN: 0824708547.

[44] A. Shulgin, A. Shulgin, "PiHKAL, A Chemical Love Story ", Transform Press, Berkeley, **1991**, 633-637, ISBN 0-9630096-0-5.

[45] M. A. Parker, D. Marona-Lewicka, V. L. Lucaites, D. L. Nelson, D. E. Nichols. "A Novel (Benzodifuranyl)aminoalkane with Extremely Potent Activity at the 5-HT_{2A} Receptor". *Journal of Medicinal Chemistry*, **1998**, *41*, 5148-5149.

[46] D. M. Mottola, S. Laiter, V. J. Watts, A. Tropsha, S. D. Wyrick, D. E. Nichols, R. B. Mailman. Conformational Analysis of D1 Dopamine Receptor Agonists: Pharmacaphore Assessment and Receptor Mapping, *Journal of Medicinal Chemistry*, **1996**, *39*, 285-296.

[47] B. Hoffmann, S. J. Cho, W. Zheng, S. Wyrick, D. E. Nichols, R. B. Mailman, A. Tropsha. Quantitative Structure-Activity Relationship Modelling of Dopamine D1 Antagonists Using Comparative Molecular Field Analysis, Genetic Algorithms-Partial Least-Squares, and K Nearent Neighbor Methods, *Journal of Medicinal Chemistry*, **1999**, *42*, 3217-3226.

[48] N. A. Campbell. "Biology", (4^{th} Ed.) Benjamin/Cummings Publishing Company, Inc., California, **1996**, 1008-1009, ISBN 0-8053-1940-9.

[49] B. N. Dhawan, F. Cesselin, R. Raghubir, T. Reisine, P. B. Bradley, P. S. Portoghese, M. Hamon. "International Union of Pharmacology. XII. Classification of Opioid Receptors", *Pharmacological Reviews*, **1996**, *48*, 567-592.

[50] D. J. Siebert. "*Salvia Divinorum* and *Salvinorin A*: New Pharmacological Findings", *Journal of Ethnopharmacology*, **1994**, *43*, 53-56.

[51] D. J. Siebert, Salvia Divinorum Research Center, http://www.sagewisdom.org/novascreen.html, 05/08/2007

[52] R. A. Glennon, M. Titler, J. D. McKenney, "Evidence for 5-HT_2 involvement in the mechanism of action of hallucinogenic agent", *Life Sciences*, **1984**, *35*, 2505-2511.

[53] B. L. Roth, D. L. Willins, K. Kristiansen, W. K. Kroeze. "5-Hydroxytryptamine2-family receptors (5-hydroxytryptamine2A, 5-hydroxytryptamine2B, 5-hydroxytryptamine2C): where structure meets function", *Pharmacology & Therapeutics*, **1998**, *79*, 231-257.

[54] B. L. Roth, K. Baner, R. Westkaemper, D. Siebert, K. C. Rice, S. Steinberg, P. Ernsberger, R. B. Rothman. "*Salvinorin A*: A Potent Naturally Occurring Nonnitrogenous κ-Opioid Selective Agonist", *Proceeding of the National Academy of Sciences*, **2002**, *99*, 11934-11939.

[55] D. J. Sheffler, B. L. Roth. "Salvinorin A: the 'Magic Mint' Hallucinogen Finds a Molecular Target in the Kappa Opioid Receptor", *Trends in Pharmacological Sciences*, **2003**, *24*, 107-109.

[56] M. Waldhoer, S. E. Bartlett, J. L. Whistler. "Opioid Receptors", *Annual Review of Biochemistry*, **2004**, *73*, 953-990.

[57] J. McDonald, D. G. Lambert. "Opioid Receptors", *Critical Care and Pain*, **2005**, *5,* 22-25.

[58] R. J. Bodnar, M. M. Hadjimarkou. "Endogenous Opiates and Behaviour: 2002", *Peptides*, **2003**, *24*, 1241-1302.

[59] G. C. Rossi, G W Pasternak, R J Bodnar. "μ- and δ-Opioid Synergy Between the Periaqueductal Gray and the Rostro-Ventral Medulla", *Brain Research*, **1994**, *665*, 85-93.

[60] R. M. Quock, T. H. Burkey, E. Varga, Y. Hosohata, K. Hosohata, S. M. Cowell, C. A. Slate, F. J. Ehlert, W. R. Roeske, H. I. Yamamura. "The δ-Opioid Receptor: Molecular Pharmacology, Signal Transduction, and the Determination of Drug Efficacy", *Pharmacological Reviews*, **1999**, *51*, 503-532.

[61] P. F. VonVoigtlander, R. A. Lahti, J. H. Ludens. "U-50,488: A Selective and Structurally Novel non-μ (κ) Opioid Agonist", *Journal of Pharmacology and Experimental Therapeutics*, **1983**, *224*, 7-12.

[62] B. E. Kane, M. J. Nieto, C. R. McCurdy, D. M. Ferguson. "A Unique Binding Epitope for Salvinorin A, A Non-Nitrogenous Kappa Opioid Agonist". *The FEBS Journal*, **2006**, *273*, 1966-1974.

[63] L. A. Dykstra, D. E. Gmerek, G. Winger, J. H. Woods. "Kappa Opioids in Rhesus Monkeys: I. Diuresis, Sedation, Analgesia and Discriminative Stimulus Effects". *Journal of Pharmacology and Experimental Therapeutics*, **1987**, *242*, 413-420.

[64] A. Pfeiffer, V. Brantl, A. Herz, H. M. Emrich. "Psychotomimesis Mediated by κ-Opiate Receptors", *Science*, **1986**, *233*, 774-776.

[65] C. R. McCurdy, K. J. Sufka, G. H. Smith, J. E. Warnick, M. J. Nieto. "Antinociceptive Profile of Salvinorin A, A Structurally Unique Kappa Opioid Receptor Agonist". *Pharmacology, Biochemistry and Behavior*, **2006**, *83*, 109-113.

[66] C. A. Crawford, S. A. McDougall, C. A. Bolanos, S. Hall, S. P Berger. The Effects of the κ-Opioid Agonist U-50,488 on Cocaine Induced Conditioned and Unconditioned Behaviors and Fos Immunoreactivity, *Psychopharmacology*, **1995**, *120*, 392-399.

[67] R. D. Spealman, J. Bergman. Modulation of the Discriminative Stimulus Effects of Cocaine by μ- and κ-Opioids, *Journal of Pharmacology and Experimental Therapeutics*, **1992**, *261*, 607-615; R. D. Spealman, J. Bergman. Opioid Modulation of the Discriminative Stimulus Effects of Cocaine: Comparison of μ-, κ- and δ-Agonists in Squirrel Monkeys Discriminating Low Doses of Cocaine, *Behavioural Pharmacology*, **1994**, *5*, 21-31.

[68] I. M. Maisonneuve, S. Archer, S. D. Glick. "U50,488 a *κ*-Opioid Receptor Agonist, Attenuates Cocaine-Induced Increases in Extra-cellular Dopamine in the Nucleus Accumbens of Rats", *Neuroscience Letters*, **1994**, *181*, 57-60.

[69] J. L. Neumeyer, J. M. Bidlack, R. Zong, V. Bakthavachalam, P. Gao, D. J. Cohen, S. S. Negus, N. K. Mello. "Synthesis and Opioid Receptor Affinity of Morphinan and Benzomorphan Derivatives: Mixed κ Agonists and μ-Agonists/Antagonists as Potential Pharmacotherapeutics for Cocaine Dependence", *Journal of Medicinal Chemistry*, **2000**, *43*, 114-122.

[70] F. Simonin, O. Valverde, C. Smadja, S. Slowe, I. Kitchen, A. Dierich, M. Le Meur, B. P. Rodqes, R. Maldonado, B. L. Kieffer. "Disruption of the κ-Opioid Receptor Gene in Mice Enhances Sensitivity to Chemical Visceral Pain, Impairs Pharmacological Actions of the Selective κ-Agonist U-50,488H and Attenuates Morphine Withdrawal", *European Journal of Molecular Biology (EMBO)*, **1998**, *17*, 886-897.

[71] S. Ghozland, H. W. Matthes, F. Simonin, D. Filliol, B. L. Kieffer, R. Maldonado. "Motivational Effects of Cannabinoids are Mediated by μ-Opioid and κ-Opioid Receptors in Rats", *Journal of Neuroscience*, **2002**, *22*, 1146-1154.

[72] J. W. Gruber, D. J. Siebert, A. H. "Der Marderosian, R. S. Hock. High Peformance Liquid Chromatographic Quantification of Salvinorin A from Tissues of *Salvia Divinorum* Epling & Játiva-M", *Phytochemical Analysis*, **1999**, 10, 22-25.

[73] C. Chavkin, S. Sud, W. Jin, J. Stewart, J. K. Zjawiony, D. J. Siebert, B. A. Toth, S. J. Hufeisen, B. L. Roth. "*Salvinorin A*, an Active Component of the Hallucinogenic Sage *Salvia divinorum* is a Highly Efficacious κ-Opioid Receptor Agonist: Structural and Functional Considerations", *The Journal of Pharmacology and Experimental and Therapeutics*, **2004**, *308*, 1197-1203.

[74] M. D. Schmidt, M. S. Schmidt, E. R. Butelman, W. W. Harding, K. Tidgewell, D. J. Murry, M. J. Kreek, T. E. Prisinzano. "Pharmacokinetics of the Plant-Derived κ-Opioid Hallucinogen Salvinorin A in Nonhuman Primates", *Synapse*, **2005**, *58*, 208-210.

[75] M. S. Schmidt, T. E. Prisinzano, K. Tigdewell, W. Harding, E. R. Butelman, M. J. Kreek, D. J. Murry. "Determination of Salvinorin A in body fluids by high performance liquid

chromatography–atmospheric pressure chemical ionization", *Journal of Chromatography B. Analytical Technology and Biomedical Life Science*, **2005**, *818*, 221-225.

[76] T. A. Munro, M. A. Rizzacasa, B. L. Roth, B. A. Toth, F. Yan. "Studies Towards the Pharmacophore of *Salvinorin A*, a Potent κ-Opioid Receptor Agonist", *Journal of Medicinal Chemistry*, **2005**, *48*, 345-348.

[77] D. S. Simpson, P. L. Katavic, A. Lozama, W. W. Harding, D. Parrish, J. R. Deschamps, C. M. Dersch, J. S. Partilla, R. B. Rothman, H. Navarro, T. E. Prisinzano. "Synthetic Studies of Neoclerodane Diterpenes from Salvia divinorum: Preparation and Opioid Receptor Activity Salvinicin Analogues", *Journal of Medicinal Chemistry*, **2007**, *50*, 3596 - 3603.

[78] C. Béguin, M. R. Richards, Y. Wang, Y. Chen, L.-Y. Liu-Chen, Z. Ma, D. Y. W. Lee, W. A. Carlezon, Jr., B. M. Cohen. "Synthesis and *in vitro* Pharmacological Evaluation of *Salvinorin A* Analogues Modified at C(2)", *Bioorganic and Medicinal Chemistry Letters*, **2005**, *15*, 2761-2765.

[79] D. Y. W. Lee, V. V. R. Karnati, M. He, L-Y. Liu-Chen, L. Kondaveti, Z. Ma, Y. Wang, Y. Chen, C. Béguin, W. A. Carlezon Jr., B. Cohen. "Synthesis and *in vitro* Pharmacological Studies of New C(2) Modified *Salvinorin A* Analogues", *Bioorganic and Medicinal Chemistry Letters*, **2005**, *15*, 3744-3737.

[80] R. V. Bikbulatov, F. Yan, B. L. Roth, J. K. Zjawiony. "Convenient Synthesis and In Vitro Pharmacological Activity of 2-Thioanalogues of Salvinorins A and B", *Bioorganic and Medicinal Chemistry Letters*, **2007**, *17*, 2229-2232.

[81] W. W. Harding, M. Schmidt, K. Tidgewell, P. Kannan, K. G. Holden, B. Gilmour, H. Navarro, R. B. Rothman, T. E. Prisinzano. "Synthetic Studies of Neoclerodane Diterpenes from Salvia Divinorum: Semisynthesis of Salvinicins A and B and Other Chemical Transformations of Salvinorin A", *Journal of Natural Products*, **2006**, *69*, 107-112.

[82] C. Béguin, M. R. Richards J.-G. Li., Y. Wang, W. Xu, L.-Y. Liu-Chen, W. A. Carlezon Jr., B. M. Cohen. "Synthesis and *in vitro* Evaluation of *Salvinorin A* Analogues: Effect of Configuration at C(2) and Substitution at C(18)", *Bioorganic and Medicinal Chemistry Lett*ers, **2006**, *16*, 4679-4685.

[83] W. W. Harding, K. Tidgewell, N. Byrd, H. Cobb, C. M. Dersch, E. R. Butelman, R. B. Rothman, T. E. Prisinzano. "Neoclerodane Diterpenes as Novel Scaffold for μ-Opioid Receptor Ligands", *Journal of Medicinal Chemistry*, **2005**, *48*, 4765-4771.

[84] K. Tidgewell, W. W. Harding, A. Lozama, H. Cobb, K. Shah, P. Kannan, C. M. Dersch, D. Parrish, J. R. Deschamps, R. B. Rothman, T. E. Prisinzano. "Synthesis of Salvinorin A Analogues as Opioid Receptor Probes". *Journal of Natural Products*, **2006**, *69*, 914-918.

[85] D. Y. W. Lee, M. He, L. Kondaveti, L.-Y. Liu-Chen, Z. Ma, Y. Wang, Y. Chen, J-G. Li, C. Béguin, W. A. Carlezon Jr., B. Cohen. "Synthesis and *in vitro* Pharmacological Studies of C(4) Modified *Salvinorin A* Analogues", *Bioorganic and Medicinal Chemistry Letters*, **2006**, *16*, 5498-5502.

[86] T. A. Munro, K. K. Duncan, R. J. Staples, W. Xu, L. Y. Liu-Chen, C. Béguin, W. A. Carlezon Jr, B. M. Cohen. "8-*epi*-Salvinorin B: Crystal Structure and Affinity at the κ-Opioid Receptor". Beilstein Journal of Organic Chemistry, **2007**, *3,* 1.

[87] W. W. Harding, M. Schmidt, K. Tidgewell, P. Kannan, K. G. Holden, C. M. Dersch, R. B. Rothman, T. E. Prisinzano. "Synthetic Studies of Neoclerodane Diterpenes from *Salvia Divinorum*: Selective Modification of the Furan Ring". *Bioorganic and Medicinal Chemistry Letters*, **2006**, 16, 3170-3174.

[88] F. Yan, P. D. Mosier, R. B. Westkaemper, J. Stewart, J. K. Zjawiony, T. A. Vortherms, D. J. Sheffler, B. L. Roth. "Identification of the Molecular Mechanisms by Which the Diterpenoid Salvinorin A Binds to κ-Opioid Receptors", *Biochemistry*, **2005**, *44*, 8643-8651.

[89] N. Singh, G. Chevé, D. M. Ferguson, C. R. McCurdy. "A Combined Ligand-Based and Target-Based Drug Design Approach for G-Protein Coupled Receptors: Application to Salvinorin A, A Selective Kappa Opioid Receptor Agonist", *Journal of Computer Aided Molecular Design*, **2006**, *20*, 471-493.

[90] T. A. Vortherms, P. D. Mosier, R. B. Westkaemper, B. L. Roth. "Differential Helical Orientations Among Related G-Protein-Coupled Receptors Provide a Novel Mechanism for Selectivity: Studies with Salvinorin A and the κ-Opioid Receptor", *The Journal of Biological Chemistry*, **2007**, *282*, 3146-3156.

[91] M. A. Ansonoff, J. Zhang, T. Czyzyk, R. B. Rothman, J. Stewart, H. Xu, J. Zjwiony, D. J Siebert, F. Yang, B. L. Roth, J. E. Pintar. "Antinociceptive and Hypothermic Effects of Salvinorin A are Abolished in a Novel Strain of κ-Opioid Receptor-1 Knockout Mice", *The Journal of Pharmacology and Experimental Therapeutics,* **2006**, *318*, 641-648.

[92] C. E. Groer, K. Tidgewell, R. A. Moyer, W. W. Harding, R. B. Rothman, T. E. Prisinzano, L. M. Bohn. "An Opioid Agonist the Does Not Induce μ-Opioid Receptor-Arrestin Interaction or Receptor Internalization", *Molecular Pharmacology*, **2007**, *71*, 549-557.

[93] R. B. Rothman, D. L. Murphy, H. Xu, J. A. Godin, C. M. Dersch, J. S. Partilla, K. Tidgewell, M. Schmidt, T. E. Prisinzano. "Salvinorin A; Allosteric Interactions at the m-Opioid Receptor", *The Journal of Pharmacology and Experimental Therapeutics,* **2007**, *320*, 801-810.

[94] E. R. Butelman, M. Mandau, K. Tidgewell, T. E. Prisinzano, V. Yuferov, M. J. Kreek. "Effects of Salvinorin A, a κ-Opioid Hallucinogen, on a Neuroendocrine Biomarker Assay in Nonhuman

Primates with High κ-Receptor Homology to Humans", *The Journal of Pharmacology and Experimental Therapeutics*, **2007**, *320*, 300-306.

[95] D. Braida, V. Limonta, S. Pegorini, A. Zani, C. Guerini-Rocco, E. Gori, M. Sala. "Hallucinatory and Rewarding Effect of Salvinorin A in Zebrafish: κ-Opioid and CB_1-Cannabinoid Receptor Involvement", *Psychopharmacology*, **2007**, *190*, 441-448.

[96] F. Rohdich, S. Hecht, K. Gartner, P. Adam, C. Krieger, S. Amslinger, D. Arigoni, A. Bacher, W. Eisenreich. "Studies on the Nonmevalonate Role of IspH(LytB) Protein", *Proceedings of the National Academy of Sciences*, **2002**, *99*, 1158-1163.

[98] P. M. Dewick. "The Biosynthesis of C3-C25 Terpinoid Compounds", *Natural Product Reports*, **1999**, *16*, 97-130.

[99] E. Tadashi, D. Yasumasa, Y. Hamano, T. Dairi, H. Seto, K. Kakinuma. "A New Aroach for the Investigation of Isoprenoid Biosynthesis Featuring Pathway Switching, Deuterium Hyperlabeling, and 1H NMR Spectroscopy. The Reaction Mechanism of a Novel Streptomyces Diterpene Cyclase**"**, *Journal of Organic Chemistry*, **2003**, *68*, 5433-5438.

[100] A. T. Merritt, S. V. Ley. "Clerodane Diterpenoids", *Natural Product Reports*, **1992**, *9*, 243-287.

[101] S. V. Ley, P. S. Jones, N. S. Simpkins, A. J. Whittle, "Total Synthesis of the Insect Antifeedant Ajugarin I, and Degradation Studies of Related Clerodane Diterpenes", *Tetrahedron*, **1986**, *42*, 6519-6534.

[102] D. J. Rogers, G. G. Ünal, D. J. Williams, S. V. Ley. "The Crystal Structure of 3-Epicaryoptin and the Reversal of the Currently Accepted Absolute Configuration of Clerodin", *Journal of the Chemical Society, Chemical Communications*, **1979**, *3*, 97-99.

[103] J. C. Anderson, W. M. Blaney, M. D. Cole, L. L. Fellows, S. V. Ley, R. N. Sheppard, M. S. J. Simmonds. "The Structure of Two New Clerodane Diterpenoid Potent Insect Antifeedants from *Scutellaria woronowii* (Juz); Jodrellin A & B", *Tetrahedron Letters*, **1989**, *30*, 4737-4740.

[104] B. Rodríguez, M. C. de la Torre, B. Rodríguez, M. Bruno, F. Piozzi, G. Savona, M. S. J. Simmonds, W. M. Blaney and A. Perales. "Neo-clerodane insect antifeedants from *Scutellaria galericulata*". *Phytochemistry*, **1993**, *33*, 309-315.

[105] M. D. Cole, P. D. Bridge, J. E. Dellar, L. E. Fellows, M. C. Cornish, J. C. Anderson. "Antifungal activity of Neo-clerodane diterpenoids from *Scutellaria*". *Phytochemistry*, **1991**, *30*, 1125-1127.

[106] W. M. Blaney, A. C. Cuñat, S. V. Ley, F. J. Montgomery, S. J. Simmonds. "Model Studies Towards the Insect Antifeedant *Jodrellin A* using an Organosselenium Mediated Cyclization Reaction", *Tetrahedron Letters*, **1994**, *35*, 4861-4861.

[107] A. C. Cuñat, D. Díez-Martin, S. V. Ley, F. J. Montgomery. "Synthetic Studies Towards the Clerodane Insect Antifeedant *Jodrellin A*: Preparation of a Polycyclic Model Compound with Antifeedant Activity", *Journal of the Chemical Society Perkin Transactions 1*, **1996**, *7*, 611-620.

[108] M. S. Hunter, D. G. Corley, C. P. Carron, E. Rowold, B. F. Kilpatrick, R. C. Durley. "Four New Clerodane Diterpenes from the Leaves of *Casearia guianensis* which Inhibit the Interaction of Leukocyte Function Antigen 1 with Intercellular Adhesion Molecule 1", *Journal of Natural Products*, **1997**, *60*, 894-899.

[109] H. Chen, R. X. Tan, Z. L. Liu, Y. Zhang, L. Yang. "Antibacterial Neoclerodane Diterpenoids from *Ajuga lupulina*", *Journal of Natural Products*, **1996**, *59*, 668-670.

[110] E. Maldonado, A. Ortega. "*Polystachynes A-E*, Five *cis*-neo-Clerodane Diterpenoids from *Salvia ploystachya*", *Phytochemistry*, **2000**, *53*, 103-109.

[111] C. Y. Ragasa, M. C. Cruz, R. Gula, J. A. Rideout. "Clerodane Diterpenes from *Tinospora rumphii*", *Journal of Natural Products*, **2000**, *63*, 509-511.

[112] T. S. Martin, K. Ohtani, R. Kasai, K. Yamasaki. "Clerodane Diterpene Glucosides from *Tinospora Rumphii*", *Phytochemistry*, **1995**, *40*, 1729-1736.

[113] J. B. Hanuman, R. K. Bhatt, B. Sabata. "A Clerodane Furano-diterpene from *Tinospora Cordifolia*", *Journal of Natural Products*, **1988**, *51*, 197-201.

[114] R. Maurya, V. Wazir, A. Tyagi, R. S. Kapil. "Clerodane Diterpinoids from *Tinospora Cordifolia*", *Phytochemistry*, **1995**, *38*, 659-661.

[115] V. D. Gangan, P. Pradhan, A. T. Sipahimalani, A. Banerji. "Norditerpene Furan Glycosides from *Tinospora Cordifolia*", *Phytochemistry*, **1995**, *39*, 1139-1142.

[116] H. Wagner, R. Seitz, H. Lotter, "New Furanoid ent-Clerodanes from *Baccharis tricuneata"*, *Journal of Organic Chemistry*, **1978**, *43*), 3339-3345.

[117] R. D. Enriz, H. A. Baldoni, E. A. Jauregui, M. E. Sosa, C. E. Tonn, O. S. Giordano, "Structure-Activity Relationship of Clerodane Diterpenoids Acting as Antifeedant Agents", *Journal of Agricultural Food Chemistry*, **1994**, *42*, 2958-2963.

[118] R. D. Enriz, H. A. Baldoni, M. A. Zamora, E. A. Jáuregui, M. E. Sosa, C. E. Tonn, J. M. Luco, M. Gordaliza. "Structure-Antifeedant Activity Relationship of Clerodane Diterpenoids. Comparative Study with Withanolides and Azadirachtin", *Journal of Agricultural Food Chemistry*, **2000**, *48*, 1384-1392.

[119] O. S. Chizhov, A. V. Kessnikh, I. P. Yakovlev, B. M. Zoloterev, V. A. Petukhov. "Structure of *Lagochilin*", *Tetrehedron Letters*, **1969**, *10*, 1361-1364; U. N. Zainutdinov, R. Islamov, D. N. Dalimov, T. R. Abdurakhmanov, O. D. Matchanov, N. L. Vypova. "Structure-activity Relationship for Hemostatic Lagochilin Diterpenoids", *Chemistry of Natural Compounds*, **2002**, *38,* 161-163.

[120] K. Yang, B. Blackman, W. Diederich, P. T. Flaherty, C. J. Mossman, S. Roy, Y. M. Ahn, G. I. Georg. "Formal Total Synthesis of (+)-Salicylihalamides A and B: A Combined Chiral Pool and RCM Strategy", Journal of Organic Chemistry, **2003**, *68*, 10030-10039; C. V. Ramana, A. G.

Giri, S. B. Suryawanshi, R. G. Gonnade. "Total Synthesis of Pachastrissamine (Jaspine B) Enantiomers from D-Glucose", **2007**, *48*, 265-268.

[121] B. List. "Proline-catalysed Asymmetric Reactions". *Tetrahedron*, **2002**, *58*, 5573-5590.

[122] D. J. Ager. "Handbook of Chiral Chemicals", Marcel Dekker, New-York, **1999**, 83-100 ISBN: 0824710584.

[123] R. S. Ward. "Selectivity in Organic Synthesis", John Wiley and Sons, New York, **1999**, 72-74. ISBN: 0-471-98778-6.

[124] D. Kozma (Ed.), "CRC Handbook of Optical Resolutions via Diastereomeric Salt Formation", CRC Press, Florida, **2002**, 81, 61.

[125] C. F. Poole. "The Essence of Chromatography", Elsevier Science (Amsterdam), **2003**, 797-820, ISBN: 0-444-50198-3.

[126] E. R. Francotte. "Enantioselective Chromatography as a Powerful Alternative for the Preparation of Drug Enantiomers", *Journal of Chromatography A*, **2001**, *906*, 379-397.

[127] A. G. Meyers, B. H. Yang, H. Chen, L. McKinstry, D. J. Kopecky, J. L. Gleeson. "Pseudoephedrine as a Practical Chiral Auxiliary for the Synthesis of Highly Enantiomerically Enriched Carboxylic Acids, Alcohols, Aldehydes, and Ketones". *Journal of the American Chemical Society*, **1997**, *119*, 6496-6511.

[128] C. N. Pillai, R. Sreekvmore. "Asymmetric Synthesis of Amines by the Reductive Amination of Ketones Using (+) and (-)-Norephedrine Followed by Periodate Oxidation", *Tetrahedron Asymmetry*, **1993**, *9*, 2095-2100.

[129] J. Drabowicz, B. Bujnicki, P. Biscarini, M. Mikolajczyk. "Diastereomeric Sulfinates Derived from (L)-N-Methylephedrine: Synthesis, Applications and Rearrangements". *Tetrahedron: Asymmetry*, **1999**, *10*, 3177-3187.

[130] L. C. Xavier, J. J. Mohan, D. J. Mathre, A. S. Thompson, J. D. Carroll, E. G. Corley, R. Desmond, "(*S*)-Tetrahydro-1-methyl-3,3-diphenyl-1H,3H-pyrrolo-[1,2-c][1,3,2]oxazaborole-borane Complex". *Organic Synthesis*. **1996**, *74*, 50–71.

[131] B. T. Cho, Y. S. Chun. "Enantioselective Synthesis of Optically Active Secondary Amines via Asymmetric Reduction", *Tetrahedron Asymmerty*, **1992**, *3*, 1583-1590.

[132] M. P. Krzeminski, M. Zaidlewicz. "Asymmetric Reduction of Ketoxime Derivatives and N-alkylketimines with Borane-oxazaborolidine Adducts", *Tetrahedron Asymmetry*, **2003**, *14*, 1463-1466; Chen, C., Prasad, K., Repic, O. "A General Enantioselective Synthesis of α-Arylethylamines**"**, *Tetrahedron Letters,* **1991**, *32*, 7175-7178.

[133] W. Zhang, J. L. Loebach, S. R. Wilson, E. N. Jacobsen. "Enantioselective Epoxidation of Unfunctionalised Olefins Catalysed by (Salen)manganese Complexes", *Journal of the American Chemical Society*, **1992**, *112*, 2801-2803; M. S. Taylor, E. N. Jacobsen, "Asymmetric Catalysis

in Complex Target Synthesis", *Proceedings of the National Academy of Sciences*, **2004**, *101*, 5368-5373.

[134] D. L. Boger, M. A. Patane, J. Zhou. "Total Synthesis of Bouvardin, O-Methylbouvardin, and O-Methyl-N^9-desmethylbouvardin", *Journal of the American Chemical Society*, **1994**, *116*, 8544-8556.

[135] D. I. Stirling, A. L. Zeitlin, G. W. Matcham, J. D. Roswell Jr., "Enantiomeric Enrichment and stereoselective Synthesis of Chiral Amines", Celgene Corporation, Jan 1 **1992**, US Patent 5169780. AN 549830.

[136] H. Hagiwara, H. Uda. "Optically Pure (4a*S*)-(+)- or (4a*R*)-(-)-1,4a-Dimethyl-4,4a,7,8-tetrahydronaphthalene-2,5(3*H*,6*H*)-dione and Its Use in the Synthesis of an Inhibitor of Steroid Biosynthesis", *Journal of Organic Chemistry*, **1988**, *53*, 2308-2311.

[137] T. Ling, F. Rivas, E. A. Theodorakis. "Stereoselective Synthesis of the Fully Functionalised Core Fragment of Terpentecin", *Tetrahedron Letters*, **2002**, *43*, 9019-9022.

[138] J.-I. K. Almstead, T. P. Demuth Jr., B. Ledoussal. "An Investigation into the Total Synthesis of Clerocidin: Stereoselective Synthesis of a Clerodane Intermediate", *Tetrahedron Asymmetry*, **1998**, *9*, 3179-3183.

[139] C. Jamora, M. Theodoraki, V. Malhotra, E. A. Theodorakis. "Investigation of the Biological Mode of Action of Clerocidin Using Whole Cell Assays", *Bioorganic & Medicinal Chemistry,* **2001**, *9*, 1365–1370.

[140] B. S. Glisson, W. E. Ross. "DNA Topoisomerase II: a Primer on the Enzyme and its Unique Role as a Multidrug Target in Cancer Chemotherapy", *Pharmacology & Therapeutics,* **1987**, *32*, 89–106.

[141] H. Hagiwara, K. Inome, H. Uda. "A Total Synthesis of an Antibacterial Clerodane, 16-Hydroxycleroda-3,13(14)*Z*-dien-15,16-olide", *Journal of the Chemical Society Perkin Transactions 1*, **1995**, 757-764.

[142] H. Hagiwara, K. Hamano, M. Nozawa, T. Hoshi, T. Suzuki, F. Kido. "The First Total Synthesis of (-)-Methyl Barbascoate", *Journal of Organic Chemistry*, **2005**, *70*, 2250-2255.

[143] H. Hagiwara, K. Inome, H. Uda. "A Total Synthesis of an Antibacterial Clerodane, 16-Hydroxycleroda-3,13(14)*Z*-dien-15,16-olide", *Journal of the Chemical Society Perkin Transactions 1*, **1995**, 757-764.

[144] M. Kato, H. Kosugi, A. Kodaira, H. Hagiwara, B. Vogler. "Stereocontrolled Synthesis of the Key Intermediate for the Enantioselective Synthesis of Clerodane Natural Products", *Tetrahedron Letters*, **1997**, *38*, 6845-6848; M. Kato, M. Watanabe, B. Vogler, B. Z. Awen, Y. Masuda, Y. Tooyama, A. Yoshikoshi. "The Use of 4,4-Disubstituted Nopinones for Natural-

Product Synthesis. Synthesis of Elemanoid Sesquiterpenes", *Journal of Organic Chemistry*, **1991**, *56*, 7071-7076.

[145] S. Arns, L. Barriault. "Concise Synthesis of the neo-Clerodane Skeleton of *Teucrolivin A* Using a Pericyclic Reaction Cascade", *Journal of Organic Chemistry*, **2006**, *71*, 1809-1816.

[146] K. Tidgewell, W. W. Harding, M. Schmidt, K. G. Holden, D. J. Murry, T. E. Prisinzano. "A Facile Method for the Preparation of Deuterium Labeled *Salvinorin A*: Synthesis of [2,2,2-$^{2}H_{3}$]-Salvinorin A", *Bioorganic and Medicinal Chemistry Letters*, **2004**, *14*, 5099-5102.

Chapter 2

Synthesis of 3-Furylamines

Furans serve as versatile building blocks in synthetic chemistry [1,2] and many biologically active molecules [3] and natural products [4] incorporate the furan moiety. This has resulted in the continued development of many routes to furan derivatives [5]. Although the chemistry of furans permits ready functionalisation at the C(2) and C(5) positions, similar operations at the C(3) or C(4) positions are difficult to achieve. The C(3) and C(4) substituted furans are typically produced by ring closing reactions, rather than by direct substitution of furan itself. The aromaticity and reactivity of furan will be discussed in the context of the preparation of nitrogen or 'aza' substituted furans, and strategies for the incorporation of nitrogen substituents at the C(3) position will be outlined.

2.1 Conjugation and Aromaticity

The increased stability of conjugated compared to isolated double bonds has been demonstrated experimentally from the partial hydrogenation of 1,3-butadiene [6] (Scheme 2.1).

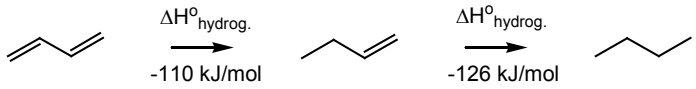

Scheme 2.1: Stepwise energies for the partial hydrogenation of 1,3-butadiene [6].

In a conjugated carbon chain, the extra stability can be partially attributed to the shortened bond distances in σ bonds formed from overlap of sp^2 orbitals, compared to σ bonding involving only sp^3 orbitals [6] as in ethane. According to molecular orbital theory, the π bond is created by a combination of two *p* orbitals. The π orbital results from combining two 2p molecular orbitals (MOs) of separate carbon atoms and the in-phase combination (lower energy) accounts for the bonding orbital (π MO), whilst the out-of-phase combination (higher energy) accounts for the antibonding molecular orbital (π* MO). This is shown using a simple molecular orbital diagram for the example ethylene (Figure 2.1) where electrons occupy the lowest energy bonding orbitals. The π orbital is the highest occupied molecular orbital (HOMO) and these electrons are the most available for chemical reactions. Each sp^2 hybridised orbital forms a framework of unpolarizable σ bonds, with one unhybridised π-orbital perpendicular to the trigonal hybrid orbitals. In the conjugated 1,3-butadiene example, the interaction between π bonding

orbitals of each double bond provides additional stabilization energy due to a greater delocalisation of π electrons.

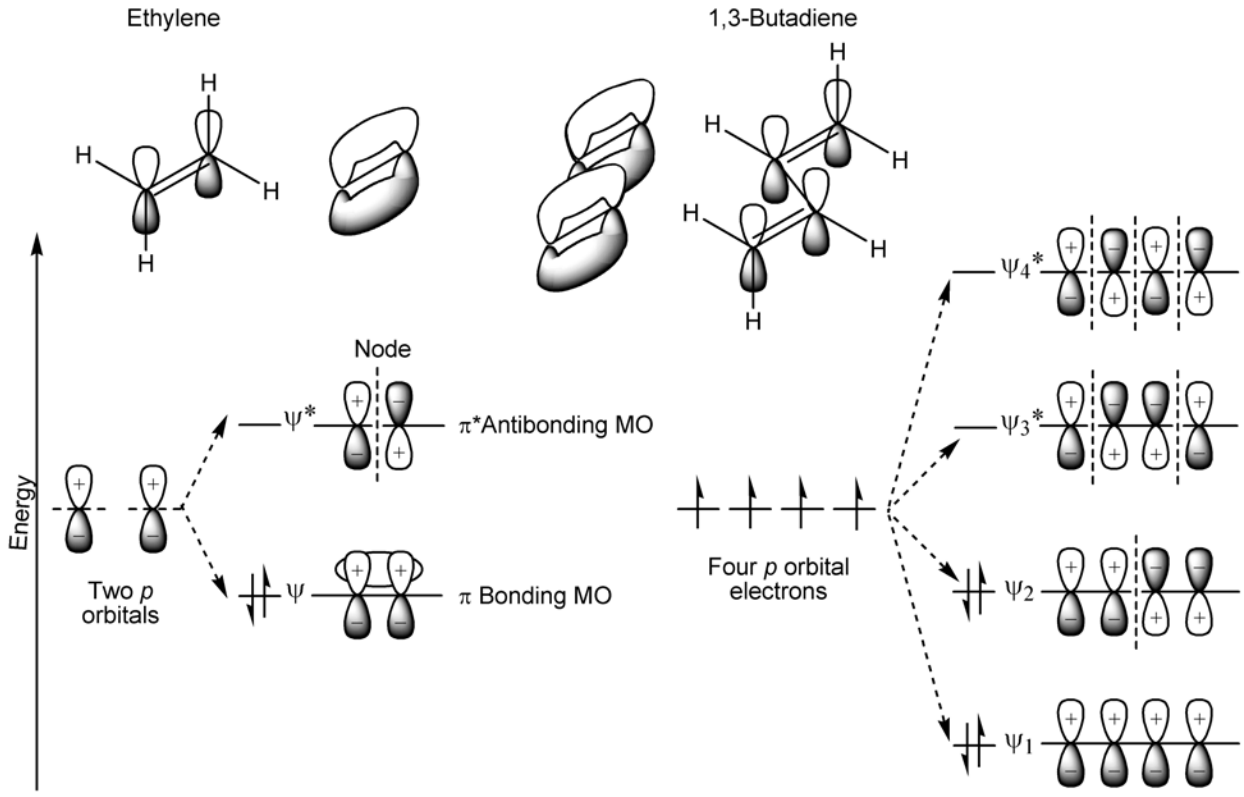

Figure 2.1: Energy level diagram demonstrating the molecular orbitals resulting from the combination of *p*- atomic orbitals in ethylene and 1,3-butadiene.

The energy of the highest occupied molecular orbital (HOMO) ψ_2 is a good approximation to the lowest ionization potential of the molecule and represents the least tightly held electrons. The lowest unoccupied molecular orbital (LUMO) ψ_3* describes the easiest pathway for the addition of more electrons to the system.

In cyclic unsaturated compounds, the possibility of resonance-hybrid structures can contribute an additional degree of stability such that π bonds do not posses the typical reactivity observed in acyclic conjugated olefins. This phenomenon was first observed in benzene and benzene-containing compounds and associated with an enhanced aroma. Hence the term now used to describe this extra stability is aromaticity. The experimental heat of hydrogenation of benzene demonstrates an aromatic stability, or resonance energy, of 152 kJ/mol compared to the calculated value for cyclohexatriene [7]. The

delocalised *p* electrons in the lowest energy bonding orbital of benzene are best described as doughnut-shaped clouds above and below the benzene ring (Figure 2.2).

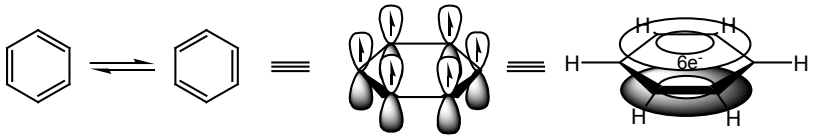

Figure 2.2: Canonical forms of benzene and a Chemdraw representation of the π- cloud in the benzene ring.

In 1931, Erich Hückel noticed that all compounds demonstrating aromaticity are conjugated, planar, monocyclic compounds with 6 *p*-orbital systems containing (4n + 2) π electrons. The Hückel rule can be applied to unsaturated ring systems of all sizes to predict aromaticity and is of relevance to the five membered furan heterocycle under investigation. Heterocyclic compounds such as thiophene, pyrrole and furan, obey the Hückel aromaticity rule and contain four *p*-orbital electrons contributed by double bonds, and two *p*-orbital electrons from the heteroatom. Resonance energies contributed by aromaticity are 121, 88 and 67 kJ/mol respectively [7], and the furan ring possesses a lesser degree of aromaticity than the other heterocycles mentioned. Unlike benzene, these aromatic heterocycles have nonequivalent positions and are more reactive at the 2-position, in close proximity to the heteroatom. The canonical forms of furan are shown in Figure 2.3.

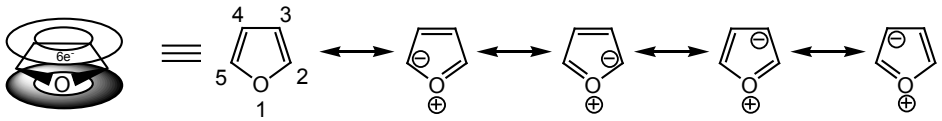

Figure 2.3: Canonical forms of furan and a Chemdraw representation of the π- cloud in the furan ring.

Syntheses of the furan ring commonly involve an intramolecular cyclization of a 1,4-diketone system. An established method for the preparation of 2,5-disubstituted furans is the *Paal-Knorr* synthesis, which can be modified to also prepare pyrrole and thiophene compounds [8]. Mild heating in the presence of the Lewis acid catalyst zinc chloride ($ZnCl_2$) is sufficient to cyclize hexane-2,5-dione to 2,5-dimethylfuran, which is reversible to the 1,4-diketone system under strongly acidic conditions (Scheme 2.2). The furan product acquires an additional portion of resonance energy upon formation of the aromatic conjugated π system. In this example, aromaticity is a crucial factor in the formation of the furan system and favorably moves the dehydration of the hemi-ketal intermediate towards the complete formation of the stabilized furan product.

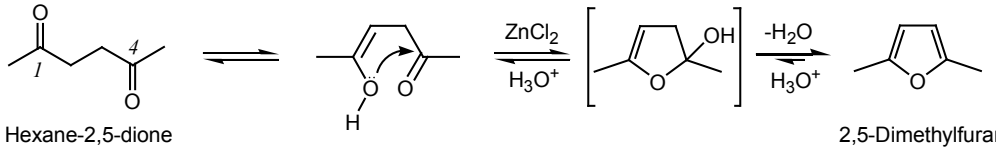

Scheme 2.2: *Paal-Knorr* synthesis; Lewis acid promoted cyclization of hexane-2,5-dione to produce 2,5-dimethylfuran [8].

The Feist-Benaig synthesis involves a condensation between chloroacetone and ethyl acetoacetate using pyridine as a base to create the 1,4-diketone system (Scheme 2.3). The intermediate ketone undergoes dehydration to yield the 2,5-dimethyl furan with an ethyl carboxylate substituent at the C(3) position [9].

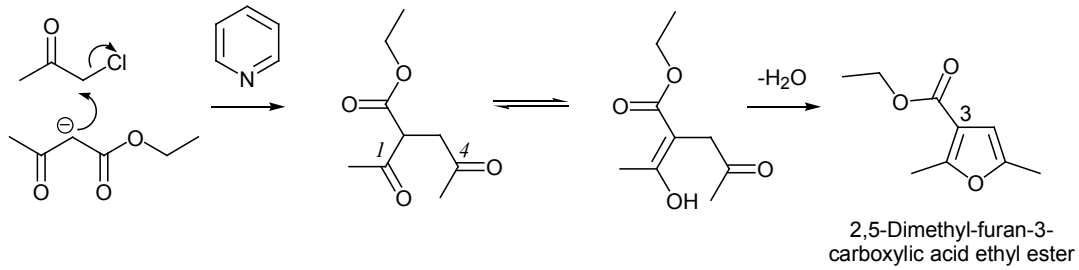

Scheme 2.3: Feist-Benaig synthesis; Base mediated condensation to produce the 1,4-diketone and subsequent cyclization to produce 2,5-dimethyl-furan-3-carboxylic acid ethyl ester [9].

2.1.1 Stability Considerations of Heterosubstituted Furans

The amine containing furan compounds are properly named as furylamines attributing nomenclature to the highest ranking amine group, however the name 3-aminofuran has more often appeared in the literature and both are used interchangeably. Although the primary furan-3-ylamine has not been reported in the literature, some attention has been shown towards the predicted instability associated with this compound. In particular, C(3)-amino and hydroxy substituted furans have been modeled by Bodor, Dewar and Harget [10] using semi-empirical SCF MO theory with Hückel σ, π approximation in ideal, gas phase conditions. Heats of atomization (ΔH_a) were calculated for the furan-3-ylamine and the non-aromatic furan-3-ylidene-ammonium tautomer and the difference value used as an indicator of the enthalpy of tautomerisation. The aromatic form was predicted to be more stable than the imino compound, although its enthalpy of tautomerization is remarkably low (0.061 eV)[10] (Scheme 2.4) and in solution may exist in equilibrium and provide a facile pathway for unwanted side reactions. In

contrast, the C(3) hydroxy derivative is predicted to exist predominately as the furan-3-one ketone tautomer indicated by a negative enthalpy of tautomerisation (Scheme 2.4).

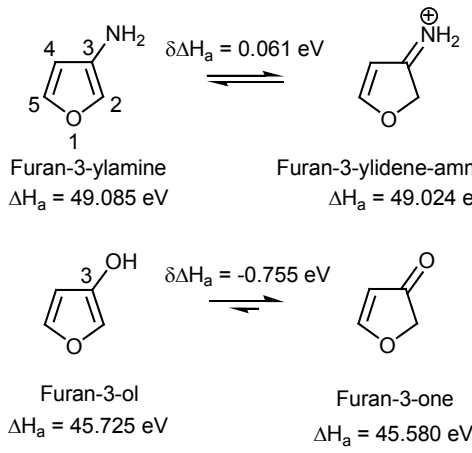

π electron population

C(3) group	NH_2	OH	OMe	Furan(H)
O(1)	1.720	1.718	1.721	1.710
C(2)	1.166	1.154	1.165	1.078
C(3)	1.030	1.049	1.048	1.067
C(4)	1.100	1.107	1.093	1.067
C(5)	1.061	1.057	1.061	1.078

Scheme 2.4: Enthalpy of tautomerization for furan-3-ylamine and furan-3-ol [10] and a listing of π-electron population density values for C(3) amine, hydroxy and methoxy substituted furans in comparison to the unsubstituted furan [11].

Aromatic stabilization energies for furans possessing electron withdrawing groups (EWG) and electron donating groups (EDG) have been approximated by John *et al.* [11] using standard LCAO SCF MO theory, and the geometry of the furan nucleus taken from the STO-3G basis set. Substituent effects were measured by comparison of stabilizing influence on furan compared to the benzene nucleus. Their findings suggest that, relative to a phenyl group, the furyl group acts as a π-electron donor and σ-electron acceptor. Inductive σ-electron withdrawal by the ring oxygen is more pronounced at the C(2)-position and π-electron density is enhanced from overlap with oxygen π-orbitals, resulting in higher C(2) HOMO energy values relative to C(3).

In general, a π-EWG at C(2) or C(3) stabilises the aromaticity of the furan nucleus. A π-EWG at C(2) stabilises the furan system by participating in conjugative π-interaction and π-EWG at C(3) enhance stabilisation by resonance delocalisation of charge onto the oxygen ring (Scheme 2.5). The charge distribution for a range of C(3) oxa and aza substituted furans indicates an increased π electron density on the ring oxygen and at the C(2) position relative to the unsubstituted furan (Scheme 2.4). This effectively suppresses electron delocalization from the oxygen. Stabilization energies for amine, hydroxy and methoxy substituents were calculated by John *et al.* [11] to be –11.6, -14.9 and –2.5 kJ/mol, respectively. The negative values indicate a destabilised system and this is not surprising considering the

π-electron donor, σ-electron accepting nature of the heteroatom substituents is opposing the same electronic trend inherent in the furan moiety.

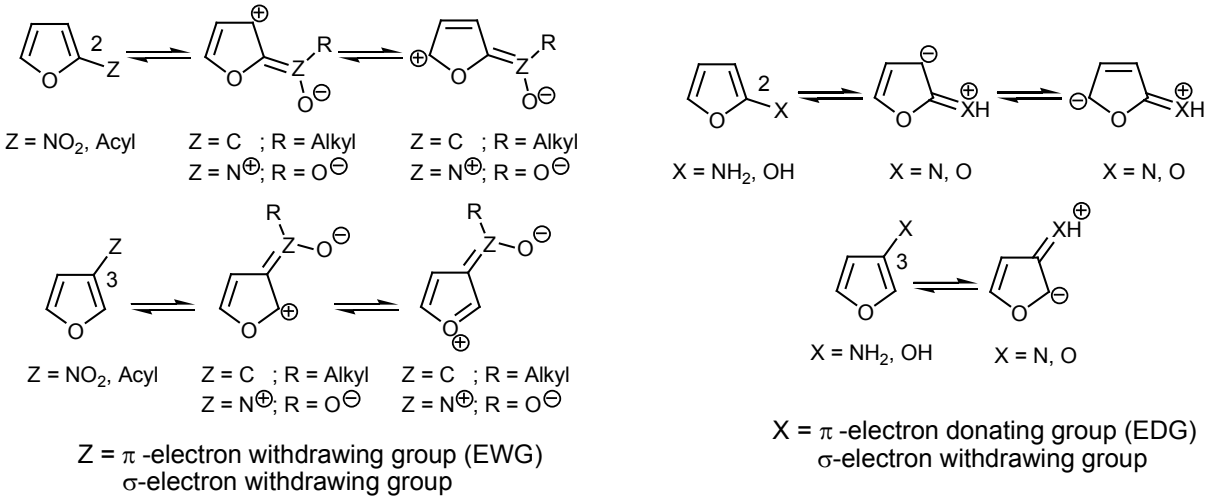

Scheme 2.5: Resonance stabilised structures of C(2) and C(3) substituted furans attached to π-EWG (Z) and π-EDG (X).

The C(2) heterosubstituted structures are predicted to be more stable due to resonance considerations (Scheme 2.5) and this is in agreement with theoretical findings by both John [11] and Bodor [10]. Theoretical studies by Shokhen *et al.* [12] suggest that proton affinity for the C(3) amine is higher than the C(2) amine derivative, however hydrolysis of the quaternary ammonium salt is likely in both cases.

The synthesis of aza substituted five membered heterocycles can be carried out by functional group interconversions on the aromatic ring or by synthesis from acyclic precursors and both approaches will be discussed in the following sections. Given the inherent instability of the unsubstituted 3-aminofuran, approaches to the preparation of mono and bis *N*-substituted 3-aminofurans were investigated.

2.2 Syntheses of Aza-substituted Furans by Modifications on the Furan Ring

Early efforts towards introducing an aza group to the furan ring proceeded via functional group rearrangement of a C(3) carboxylic acid or ester substituent. Preparation of 3-furoyl azide from commercially available 3-furoic acid [13, 14] has allowed access to the isocyanate using a thermally induced Curtius rearrangement [7] (Scheme 2.6). The methodology described by Prugh *et al.* [15]

towards the 3-furylamine involved reaction of the isocyanate with methanol (MeOH) to provide methyl *N*-(3-furyl)carbamate, followed by alkylation with iodomethane (CH_3I). Reduction of the carbamate with lithium aluminium hydride ($LiAlH_4$) gave furan-3-yl-dimethyl amine (Scheme 2.6) and ^1H NMR data for this compound was reported. The authors report that upon workup of the reaction, the free base amine was only stable under inert atmosphere at 0ºC and isolation was conducted using preparative-scale gas chromatography. The stable trimethylammonium salt was formed by reaction of the amine with CH_3I at 0ºC and biological studies found these materials to be toxic in cats and rodents [15].

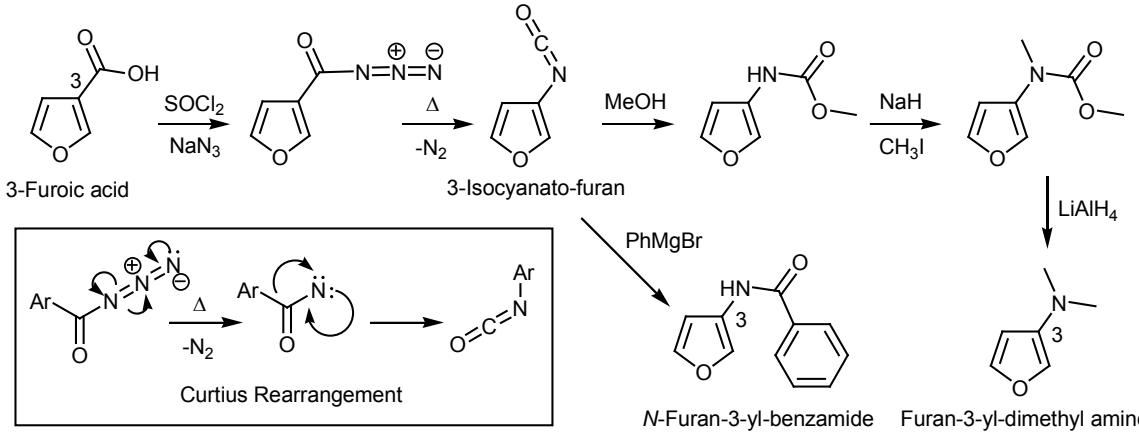

Scheme 2.6: The nitrogen heteroatom can be introduced at the C(3) position via the *Curtius Rearrangement* and the 3-isocyanato-furan product has been reacted to prepare *N*-furan-3-yl-benzamide [14] and furan-3-yl-dimethyl amine [15].

No other literature examples could be found featuring the 2,4,5-unsubstituted-3-aminofurans, although the 3-acetaminofuran has been studied by a number of researchers [13, 14, 16]. *N*-Furan-3-yl-benzamide has been prepared by Burtner [14] from the isocyanate by reaction with phenyl magnesium bromide and found to be a stable white crystalline solid (Scheme 2.6). Kuhn *et al.* [16] prepared a range of C(5)-ethylene-diol substituted *N*-furan-3-yl-acetamines *via* the Curtius rearrangement protocol and derivatization of the amide with CH_3I was reported to produce the trimethylammonium salt. Although this general methodology provided the aza substituent at the desired C(3) position on the furan ring, the rearrangement strategy appeared inflexible for the easy incorporation of a range of amine substituents.

The interconversion of 2-furoic acid to the corresponding carbamate was later reported by Ninomiya *et al.* [17] using diphenylphosphoryl azide ($N_3PO(OPh)_2$) in the presence of triethylamine and ^{t}BuOH. Synthesis of the 3-alkoxycarbonylaminofurans was more recently improved upon by Campbell *et al.* [18] using the one step methodology to provide the 3-(^{t}butoxy-carbonylamino)furan in moderate yields (Scheme 2.7). The authors mention that repeated attempts to isolate 3-aminofuran by removal of

the carbamyl group under a range of conditions led to decomposition and confirmed the material to be unisolable.

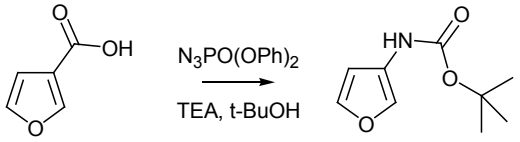

Scheme 2.7: The interconversion of 3-furoic acid to 3-(*t*butoxycarbonylamino)furan has been reported by Campbell *et al.* [18] using $N_3PO(OPh)_2$.

The introduction of substituents directly at C(3)/C(4) on the unsubstituted furan ring is complicated since the most reactive positions are those closest to the heteroatom at the C(2)/C(5) positions. Protons H(2)/H(5) are acidic and can be removed to form the stable organo-lithium nucleophile, allowing substitution by means of reaction with alkyl halides and acid anhydrides or chlorides. Furan is the least aromatic of the heterocycles mentioned in Section 2.1, however this is conducive for functional group interconversion by electrophilic aromatic substitution. Resonance structures for intermediates resulting from electrophilic attack at the C(2) position; exemplified by the nitration of furan (Scheme 2.8), indicate greater delocalisation of positive charge around the furan ring compared with reactions at the C(3) position [19]. This permits furan to readily undergo electrophilic aromatic substitution at the C(2)/C(5) positions in preference to the C(3)/C(4) positions.

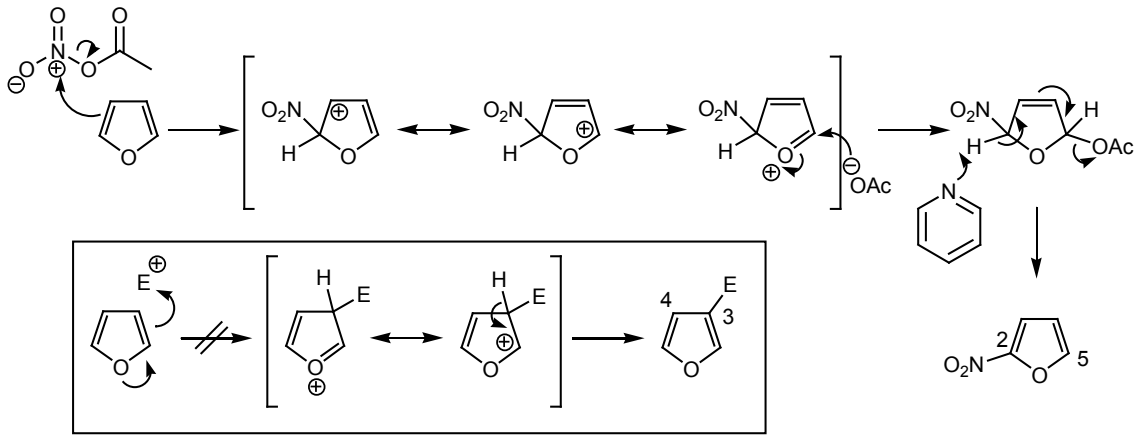

Scheme 2.8: The nitration of furan is an example of typical electrophilic substitution at the C(2) position and is stabilised by enhanced delocalization of positive charge, in contrast to the unfavoured substitution at C(3) [19].

In some furan systems, the nitro group leads to the amino furan via catalytic reduction using palladium on calcium carbonate ($CaCO_3$) under a hydrogen atmosphere. An appropriate example is the preparation of 5-amino-furan-2-carboxylic acid methyl ester by Freure *et al.* [20] (Scheme 2.9, top), and

Padwa *et al.* [21] have more recently found use of this furan as a diene in Diels-Alder reactions to preparing substituted anilines. An alternate method for introduction of the amine substituent at the C(2) position is the direct nucleophilic displacement on 2,5-dinitrofuran [17] to produce 1-(5-nitro-furan-2-yl)-piperidine (Scheme 2.9, bottom), although no reports could be found involving similar methodology at the C(3) position.

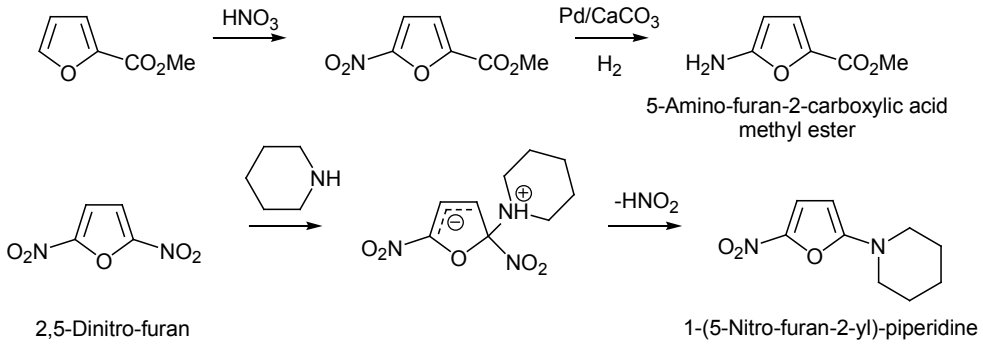

Scheme 2.9: Top; Introduction of the amine substituent by nitro reduction with $Pd/CaCO_3$ /H_2 [20, 21] to produce 5-amino-furan-2-carboxylic acid methyl ester. Bottom: Nucleophilic displacement of 2,5-dinitrofuran with piperidine to produce 1-(5-nitro-furan-2-yl)-piperidine [17].

EWG substituents in benzene systems have a meta-directing effect on subsequent electrophilic substitution reactions. In five membered heterocycles, EWG at the C(3)/ C(4) positions have a strong meta-directing influence and the directed position is the already favoured C(2)/C(5) position. In the example given in Scheme 2.10, the C(3) acetyl EWG in 1-furan-3-yl-ethanone directs nitration toward the C(5) position. EWG in the C(2)/C(5) positions generally do not have enough influence over the resonance stabilised intermediates to give C(3) or C(4) electrophilic substitution products unless a Lewis acid is used. The acetylation of 2-nitro-1H-pyrrole in the presence of boron trifluoride etherate ($BF_3.Et_2O$) Lewis acid, gives the C(3) acetyl product almost exclusively (Scheme 2.10).

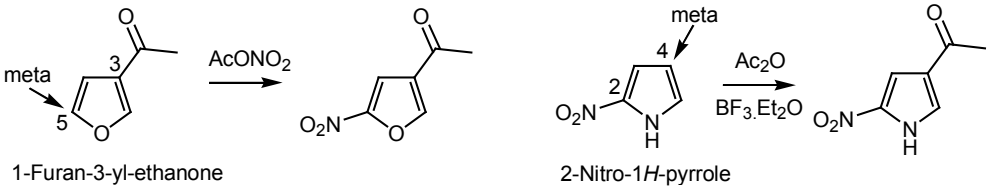

Scheme 2.10: EWG at the C(3) position of 1-furan-3-yl-ethanone directs nitration to the *meta*- position C(2). With the incorporation of $BF_3.Et_2O$, the acetylation of 2-nitro-1H-pyrrole has been reported to occur predominately at the *meta*- position C(4) [19].

The electrophilic bromination of furan systems containing a carbonyl EWG in the 2- position produce polybrominated compounds at low temperature as the result of multiple additions of bromine. At –15ºC 2-furoic acid reacts with bromine to give the saturated tetrabromo-compound [22] (Scheme 2.11). At higher temperatures the bromofuran is formed as the HBr elimination product to give 5-bromo-furan-2-carboxylic acid predominately [23]. In the case of 2-furaldehyde, Gol'dfarb *et al*. report the use the Lewis acid aluminium chloride ($AlCl_3$) and two equivalents of bromine to produce the unstable 4,5-dibromo-furan-2-carbaldehyde (**7**) exclusively at temperatures above 60ºC [24]. Studies by Chadwick *et al.* [25] applied this reaction protocol at 50ºC in 1,2-dichloroethane (DCE) and identified brominated intermediates by GLC analysis, reporting the *meta*-substituted product 4-bromo-furan-2-carbaldehyde (**8**) in 20% yield as a mixture with **7** (40%) and the unreacted aldehyde (30%) (Scheme 2.11). Reactions conducted without $AlCl_3$ have been reported to provide the 5-bromo-furan-2-carbaldehyde (**9**) as a single product [26]. Although the aldehyde EWG has an enhanced *meta*-directing influence in the presence of a Lewis acid, stabilizing effects from C(2) EWG are still not adequate to give the C(4)-substituted **8** furan exclusively.

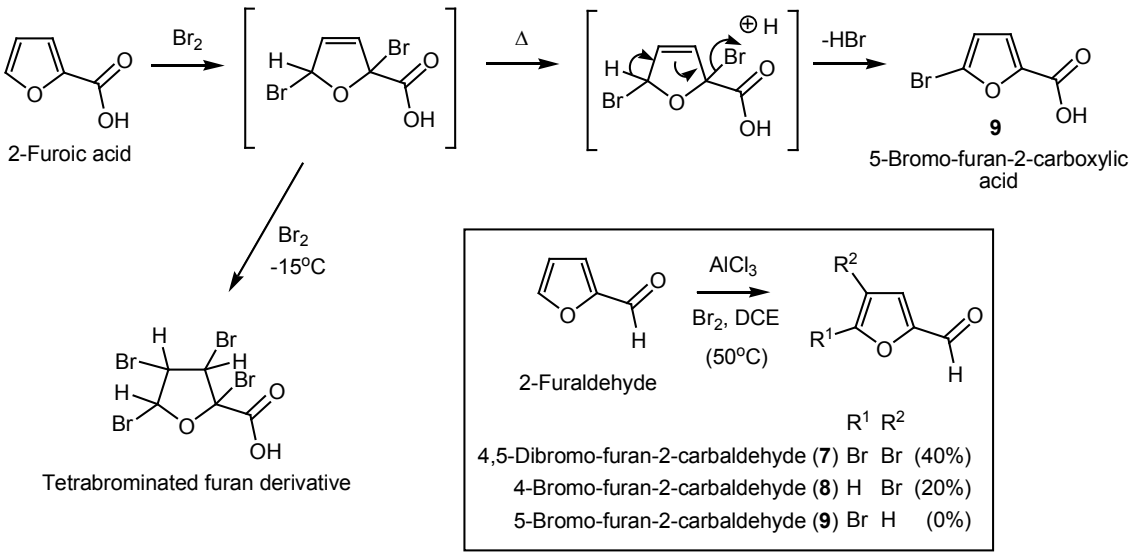

Scheme 2.11: Bromination of 2-furoic acid produces the tetrabrominated product at low temperature and 5-bromo-furan-2-carboxylic acid at higher temperatures. The reactivity of 2-furaldehyde is similar, although bromination in the presence of $AlCl_3$ can provide the 4-bromo-furan-2-carbaldehyde **8** in low yields at 50ºC [25] or **7** as a major product above 50ºC [24].

3-Bromofuran and 3-chlorofuran have been prepared by Shepard *et al.* [27] and reported as distillable, acid sensitive liquids. These aromatic halogen substituents can be interconverted to the amine functionality using palladium coupling reactions. It is not the aim of this thesis to review the vast scope and flexibility of palladium coupling reactions in organic synthesis [28], however the research relevant to

3-halofuran coupling will be mentioned. Recent progress in palladium coupling of aryl halides by Tomori *et al.* [29] has involved the investigation of suitable electron rich phosphine ligands to sufficiently catalyse a wide range of Suzuki coupling and amination reactions. Reports by Wolfe *et al.* [30] have described the efficient coupling of diarylamines to aryl halides using the newly developed ligands and high yields of 3-bromofuran-coupled triarylamine products have been reported by Harris *et al*. [31] (Scheme 2.12). This prompted the investigation in this work of an expedient pathway to 4-bromo-2-methyl-furan (**10**) to explore the potential of the palladium coupling system as a flexible methodology for the preparation 3-furylamines (Scheme 2.12).

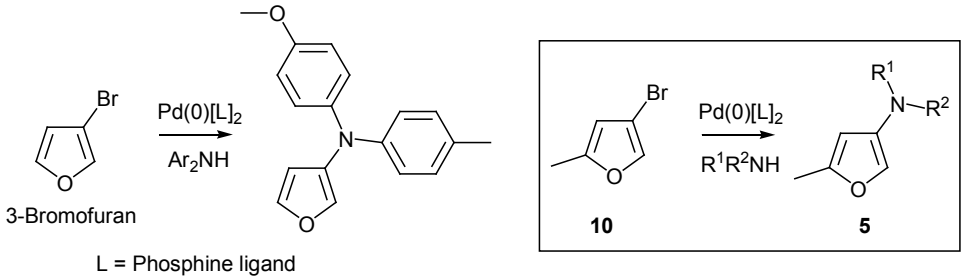

Scheme 2.12: The *N*,*N*-diaryl 3-furylamine has been prepared by palladium coupling of 3-bromofuran to an aromatic 2° amine using an approriate phosphine ligand [31]. This methodology could be applied to the preparation of **5** from **10**.

2.2.1 Synthesis of 3-Bromo-5-methylfuran

Bromination of 2-furaldehyde was undertaken according to the procedure of Chadwick *et al.* [9]. Two and one half equivalents of $AlCl_3$ reacted exothermically with the aldehyde in DCE to form a solid complex and required cooling to prevent decomposition. Two molar equivalents of Br_2 were added and the solution heated at 50ºC for 3.5 hr to produce a mixture of brominated products, with complete reaction of the starting furaldehyde contrary to the reported outcome. Formation of **8** (20%) and **9** (40%) was confirmed by molecular ions in GC-MS analysis (Figure 2.4, top left) in a mixture of polyhalogenated products, all of which show a characteristic $[M-1]^+$ peak corresponding to a β-unsaturated aldehyde. Polychlorinated tetrahydrofurans and acid chlorides were formed as a major by-product at low temperatures and the ratio of halogens was determined by isotopic ratios (Appendix 2.1)

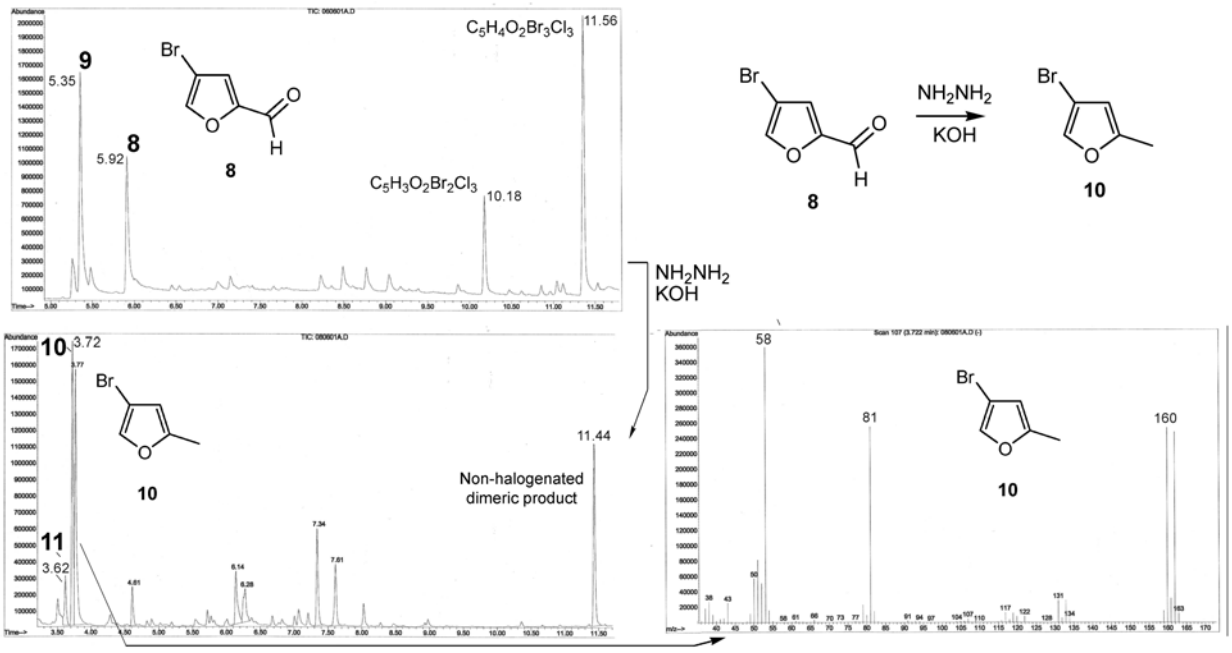

Figure 2.4: Top left; GC-MS of the reaction mixture for the bromination of 2-furaldehyde at 50°C in the presence of $AlCl_3$ to form **8** in 20% yield. Bottom: GC-MS of the crude Wolff-Kishner reduction product indicating the successful formation of **10** in low yields.

Isolation of the monobrominated furans was achieved by rapid elution of the crude material with diethyl ether (Et_2O) on silica gel using flash column chromatography to produce the unstable products as an inseparable mixture indicated by GC-MS analysis. The 5-bromo-furan-2-carbaldehyde **9** was distinguished from the isomer **8** in GC analysis by comparison with a pure sample of **9** (t_R = 5.35), prepared by bromination in the absence of $AlCl_3$ [32]. The dibrominated furaldehyde **7** formed in 85% upon performing the bromination at 60ºC and found stable to distillation whereas the monobrominated species **8** and **9** were prone to decomposition. Gol'dfarb *et al.* [33] report good yields of the 4-bromo-2-ethylfuran *via* Wolff-Kishner reduction of the corresponding 4-bromo-2-acetylfuran and this strategy was applied to the mixture of aldehydes **7-9**. Wolff-Kishner reduction of the brominated aldehydes was conducted with the Huang-Minlon conditions [34], using hydrazine (NH_2NH_2) and potassium hydroxide (KOH) in diethylene glycol. Direct distillation from the reaction vessel gave small amounts of the C(2)/C(5) methylated products **10** (0.5%) and **11** (4%) as identified by GC-MS analysis (Figure 2.4, bottom) and the dibrominated furan **7** could not be reduced under the same conditions (Scheme 2.13), instead undergoing decomposition to a black tar. The 2-bromo compound **11** is suspected to have undergone displacement by hydrazine followed by hydrolysis during reaction work-up to produce a major impurity at t_R = 3.77 min with a molecular ion at *m/z* 98, equal to the 2-hydroxy-5-methyl product (Appendix 2.2).

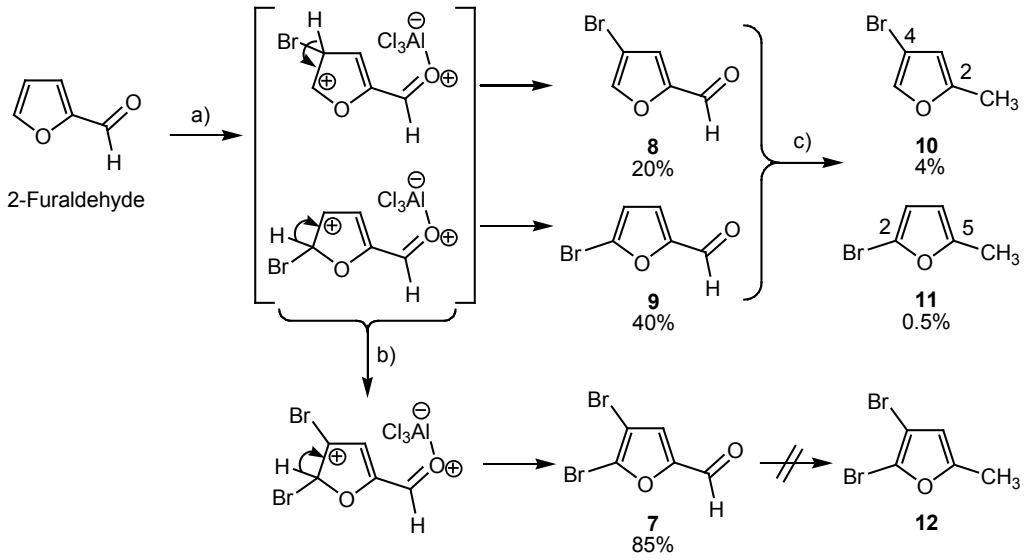

a) 2.5 Equivalents of $AlCl_3$, 1.5 equivalents of Br_2, DCE, 50ºC, 3.5 h b) Performed at 60ºC c) NH_2NH_2, KOH, diethylene glycol, 195ºC.

Scheme 2.13: Formation of an $AlCl_3$ complex with 2-furaldehyde enhances the electron withdrawing effect of the carbonyl substituent and provided a mixture of the dibrominated furan **7**, and monobrominated compounds **8** and **9**. The latter are stable to reduction using the Wolff-Kishner reaction to provide 5-methyl products **10** and **11** in poor yields.

The 4-bromo-2-methyl furan product **10** was more stable to the reduction conditions, however reaction mixtures contained many by-products of similar boiling point. Decomposition at room temperature, accompanied by darkening of the small amount of material obtained, prevented the products from being used for further reactions. Shepard and coworkers describe the halogenated furans as colourless oils that darken upon standing and eventually change to insoluble resins, and suggest storage in sealed ampules over alkaline hydroquinone [28]. Alkaline hydroquinone was effective in minimising decomposition at room temperature, however dicolouration was also reduced when stored in a dark environment, indicating that sensitivity to UV light may be a contributing factor towards decomposition. This observation is consistent with the reported photochemical reactivity of bromofurans [26].

A more selective approach to **10** was pursued starting from methyl 2-furoate **13**. Conditions described in the patent literature [35] were optimised to prepare 2,3-dibromofuran **16** (Scheme 2.14), followed by methylation and debromination using conditions based on literature by Katsumura *et al.* [36] to give **10.** Although this approach appeared straightforward, reproducing the patent literature proved time consuming and required optimization of most procedures. The optimized experimental methods are described in Section 6.1.

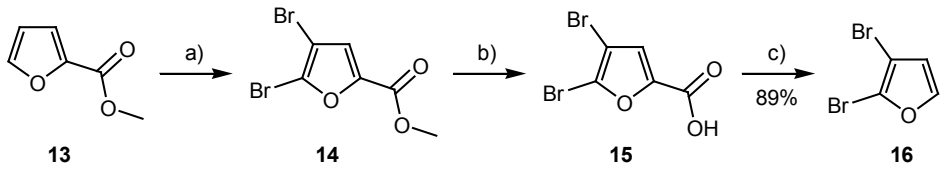

a) 2 Equivalents Br_2, $CHCl_3$, 70ºC, 98% b) 4M NaOH, 70ºC, 2.5 h, 98% c) $Cu_{(0)}$ powder, quinoline, 180ºC, 89%

Scheme 2.14: Dibromination of methyl-2-furoate **13**, followed by saponification and subsequent decarboxylation using copper in quinoline to produce 2,3-dibromofuran **16**.

Initial bromination conditions in carbon tetrachloride (CCl_4) at 80ºC gave good yields of 4,5-dibromo-furan-2-carboxylic acid methyl ester **14**, although over-brominated products were identified by GCMS analysis, indicating a range of high molecular weight compounds containing the characteristic tetrabrominated isotope pattern (Figure 2.5). When performed in chloroform ($CHCl_3$) overnight at 70ºC the reaction was 96% selective for **14** (Scheme 2.14) owing to the decreased efficiency of $CHCl_3$ as a bromination solvent. The progress of this reaction could be monitored by the evolution of HBr gas from the boiling solution and **14** was stable upon storage at 0ºC in a dark environment.

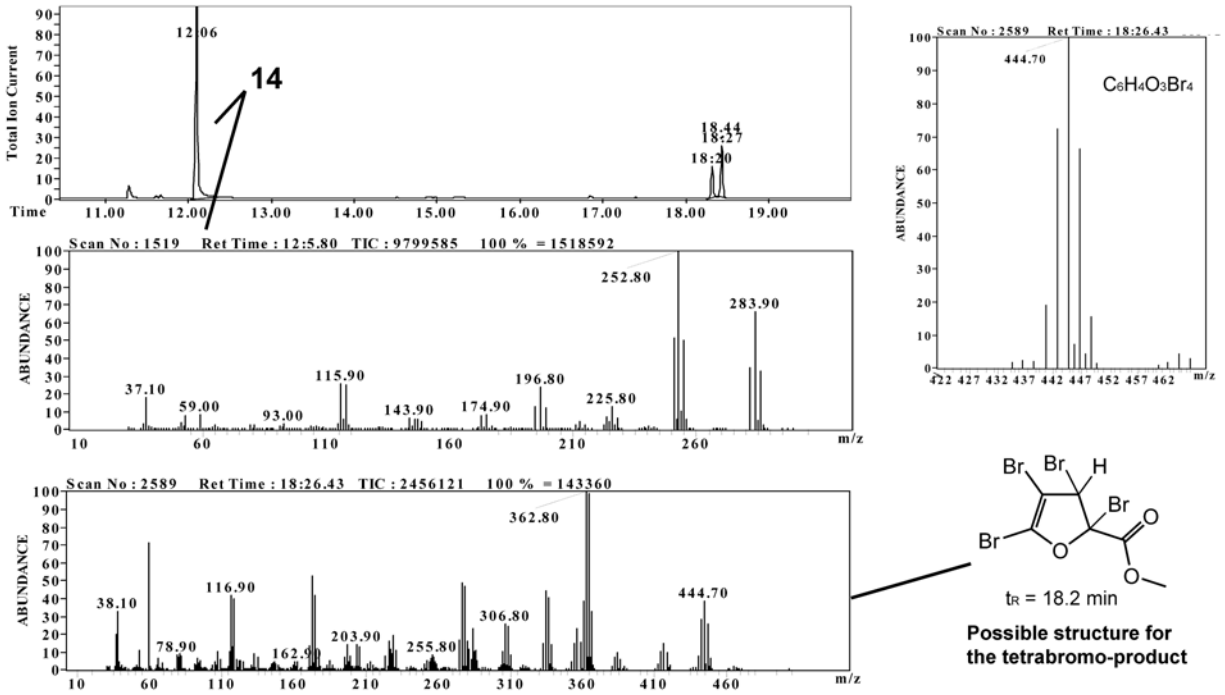

Figure 2.5: GC-MS analysis for the bromination of **13** in CCl_4. Tetrabrominated peaks at t_R = 18 min have the characteristic isotope pattern for four bromine atoms.

Saponification of the ester in 4 M sodium hydroxide (NaOH) solution provided quantitative conversion to 4,5-dibromo-furan-2-carboxylic acid (**15**) which could be purified in only moderate size batches by recrystallization from boiling water, since solubility was found to be ~10 g/L. Decarboxylation was achieved using copper bronze powder in quinoline at 180ºC to produce 2,3-dibromofuran (**16**) as a distillable light blue liquid that underwent decomposition upon exposure to UV light. Optimization was realised when reproducible high yields of **16** were obtained upon performing the reaction without agitation. With magnetic stirring the yield was reduced to 30%; this can be explained by considering that the decarboxylation relies on the presence of the copper(I) species [37], which upon exposure to air oxidise to copper(II). The use of copper(I) halides directly in the reaction gave disappointing results as did the use of mercury salts, also known to mediate decarboxylation [38] *via* the furan mercurial.

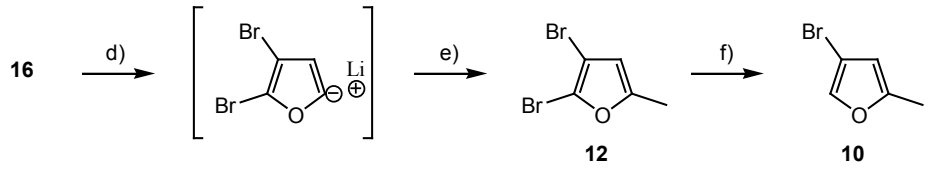

d) LDA, THF, -15ºC e) CH_3I, 90% f) ^tBuLi, -78ºC, H_2O, 90%

Scheme 2.15: Preparation of the 5-furyl lithium intermediate from **16** and LDA, followed by methylation (CH_3I) at the C(5) position and debromination (^tBuLi) at the C(2) position to provide **10**.

After removal of the C(5) proton using the hindered base lithium diisopropylamine (LDA) to produce the 5-lithiofuran intermediate, methylation of the furan was achieved by the addition of iodomethane (CH_3I) to give 2,3-dibromo-5-methyl-furan (**12**) in quantitative yield (Scheme 2.15). Mono-debromination could be performed in the same reaction mixture using *tertiary*-butyl lithium (^tBuLi) in THF at -78ºC to give excellent yields of **10** provided temperature conditions were closely controlled. The identity of **10** was confirmed by a molecular ion in GC-MS and was characterised by ^1H and ^{13}C NMR analysis. The product was found to be a colourless, sweet smelling oil that was UV sensitive and required storage at –18ºC in a dark environment.

2.2.2 Palladium Coupling of Secondary Amines to 3-Bromo-5-methylfuran

Palladium (Pd(0)) catalysed amination of aryl bromides has become a promising synthetic method for halide to amine functional group interconversions (see Section 2.2) and recently applied to

the coupling of 3-bromofuran in a sequential one pot synthesis of triarylamines (Scheme 2.16). The catalytic palladium species, Pd(0) is generated *in situ* from a Pd(II) source as the diacetate $Pd(OAc)_2$ or the dibenzylidene acetone (dba) complex $Pd(dba)_2$ or $Pd_2(dba)_3$ are often used since the complexing ligands are labile. High yields of coupling products with aryl halides have been reported using both aryl and alkyl amines provided a phosphine ligand is incorporated into the catalytic cycle. Mechanistic studies on this system show that the mixture of amine and sodium tertiary-butoxide (NaO^tBu) base are responsible for the reduction of the Pd(II) precatalyst to the Pd(0) species which is in turn stabilised by the phosphine ligand [39]. The success of the coupling system is not only reliant on the phosphine ligand for stabilization of the reactive Pd(0) species, but it has also been suggested that the phosphine acts to inhibit the formation of the catalytically inactive palladium bis(amine)arylhalide complex [39]. As a result many phosphines have been trialed in palladium coupling systems and the bidentate 2,2'-bis-diphenylphosphanyl-[1,1']binaphthalenyl (BINAP) [39], DPPF [40] and monodentate di-*t*-butyl-*ortho*-biphenylphosphine ($P(^tBu)_2$-*o*-biphenyl) [30] (Scheme 2.16) have been successfully applied.

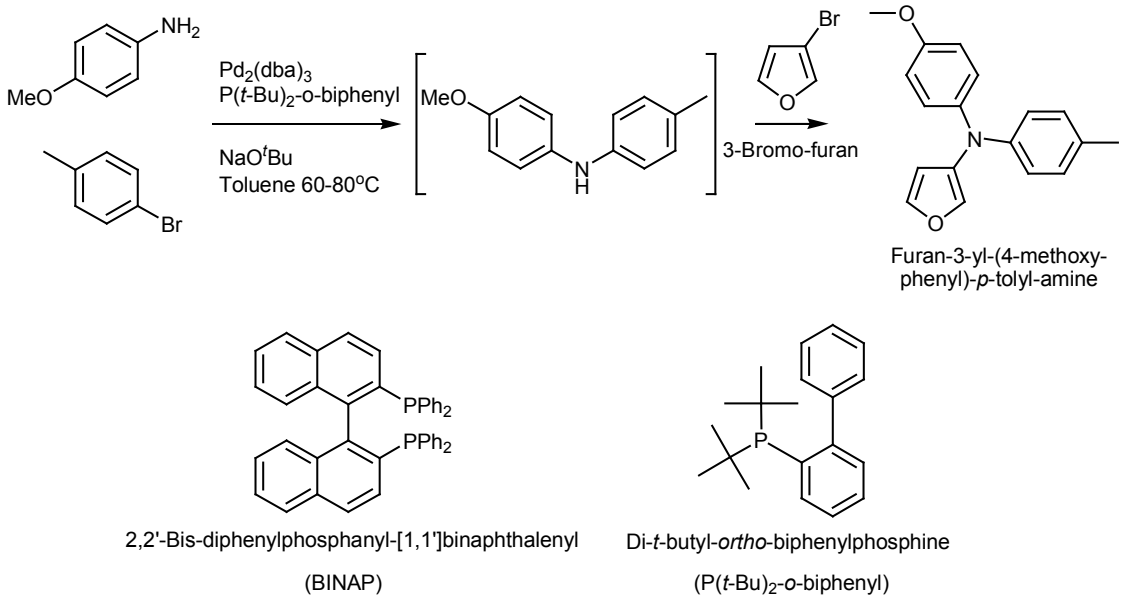

Scheme 2.16: One-pot Pd(0) catalysed amination of 1-bromo-4-methylbenzene with 4-methoxyphenylamine, followed by 3-bromofuran to produce the triarylamine product furan-3-yl-(4-methoxyphenyl)-*p*-tolyl-amine. Ligands used in palladium coupling reactions include the electron rich phosphines BINAP and P-($^tBu)_2$-*o*-biphenyl [32].

The catalytic Pd(0) coupling cycle begins with 'oxidative addition' of the aryl halide to the palladium complex to form an intermediate which can co-ordinate with the amine (Scheme 2.17). Deprotonation of the amine followed by 'reductive elimination' produces the aryl-amine product and regeneration of the Pd(0) catalyst. The catalytic cycle is shown for the Pd(BINAP) catalyst system,

which has been thoroughly investigated [41]. The Pd(P(^{t}Bu)$_2$-*o*-biphenyl)$_2$ system proceeds by a similar mechanism, however the phosphine is now a mono-dentate ligand and requires at least two equivalents to form the active catalyst.

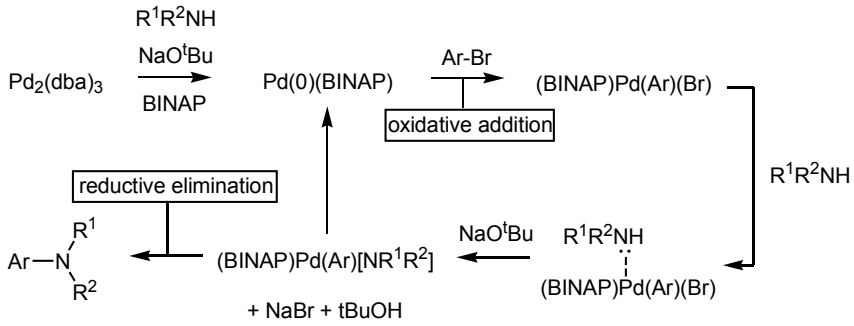

Scheme 2.17: The palladium coupling cycle involves oxidative addition across the Pd(0)(BINAP) catalyst, followed by complexation of the amine and reductive elimination under basic conditions to produce the arylated amine Ar-NR^{1}R^2.

4-Bromo-2-methylfuran **10** contains two EWG's, namely bromine and oxygen, with one EDG, methyl, and overall is considered as an electron poor aromatic system. Although this system is unfavourable for palladium coupling reactions, phosphine ligands prepared by Tomori *et al.* [29] have facilitated coupling of electron poor aryl halides and triflates with dialkyl- and diaryl- secondary amines. The coupling of 3-bromofuran to diarylamines has been reported by Harris *et al.* [31] to proceed in excellent yields using the Pd(P(^{t}Bu)$_2$-*o*-biphenyl)$_2$ ligand [30], however the coupling of dialkyl amines with the halofuran was not mentioned.

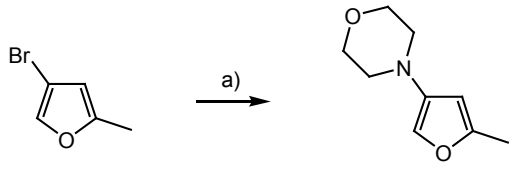

10 **5a**

4-(5-Methylfuran-3-yl)morpholine

a) Pd$_2$(dba)$_3$, P(^{t}Bu)$_2$-*o*-biphenyl, NaO^{t}Bu, morpholine, toluene, 70ºC, 4 hr, 30%

Scheme 2.18: Palladium coupling of **10** with morpholine under conditions described by Harris *et al.* [31] provided 4-(5-methylfuran-3-yl)morpholine (**5a**) in 30% yield.

Coupling of pyrrolidine and diisopropylamine to the furylhalide **10** under conditions described by Harris *et al.* [31] gave clean mixtures of starting materials with no detectable formation of coupled product by GC-MS analysis. GC-MS monitoring of the reaction of **10** with morpholine (Section 6.2) indicated a maximum yield of 30% for the coupled product 4-(5-methylfuran-3-yl)morpholine (**5a**) after 4 h at 70ºC (Scheme 2.18) and longer times gave slow decomposition of the aminofuran. Higher temperatures and increased quantities of palladium complex or base did not improve yields proportionately and made isolation of **5a** increasingly difficult. The amine **5a** was not stable to distillation from the crude mixture, which required refrigeration soon after workup to avoid decomposition. Purification by extraction into aqueous acid led to fast decomposition of **5a** and the furan also proved unstable to chromatographic separation on deactivated silica.

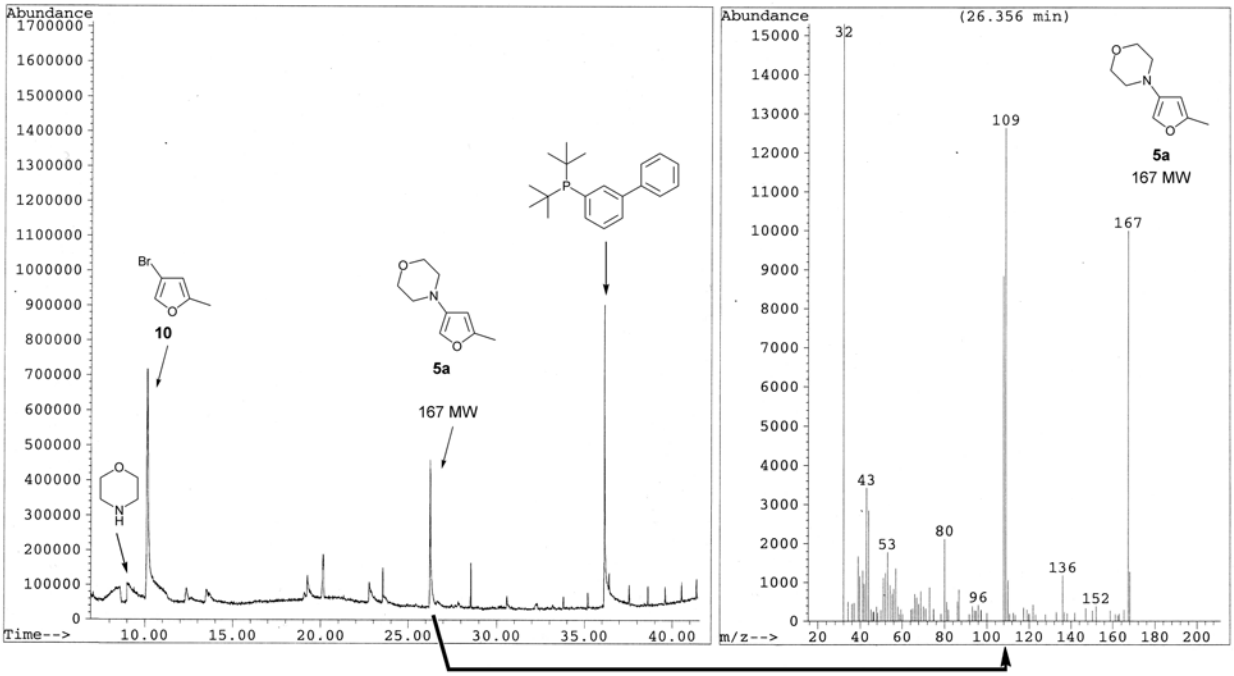

Figure 2.6: GC-MS of the Pd(0)[P(^{t}Bu)$_2$-*o*-biphenyl]$_2$ coupling of **10** to morpholine to produce **5a** in 30% yield relative to **10**.

Rapid elution with Et_2O through a small fluorosil column resulted in an improvement in product purity but decomposition continued to accompany chromatographic separation techniques. At this point the coupling strategy seemed problematic. It was suspected that the coupling system was effective but the inherent instability of the 3-furylamine system was not conducive to preparations involving elevated temperatures above 70ºC. Optimization of this particular Pd(0) coupling reaction may involve the preparation of suitable phosphine ligands and is far beyond the scope of this work. Rather than reconsider the synthetic strategy for ring **A** the scarce mention of 3-aminofurans in the published

literature and the largely unexplored chemical properties of these compounds encouraged the persistence of research. Synthetic methodologies from acyclic precursors were investigated as an alternative approach and will be presented in the following section.

2.3 Synthesis from Acyclic Precursors

Literature searches revealed numerous syntheses towards C(3) aza substituted furans from acyclic precursors. However in many instances product intermediates required the incorporation of substituents at the C(2) and C(5) positions. Recent publications towards 3-furylamines include a procedure developed by Redman *et al*. [42] involving the condensation of ethyl glycolate with α-cyanoketones under Mitsunobu conditions (Scheme 2.19, top). Deprotonation adjacent to the ester using NaH in THF led to cyclization from nucleophilic attack at the nitrile and subsequent tautomerisation to the furan. In this instance the primary aminofuran is formed and the furan ring is stabilised by the ester EWG, which also contains π–orbitals that contribute to the conjugated aromatic system.

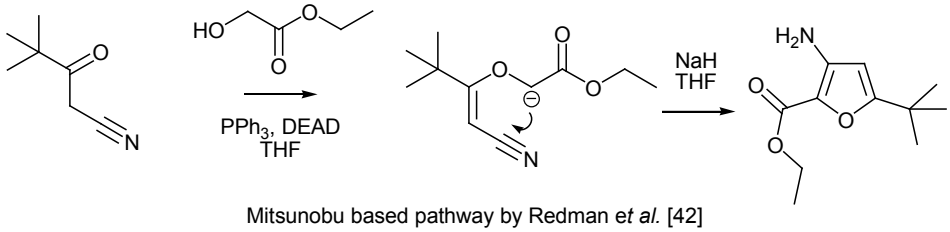

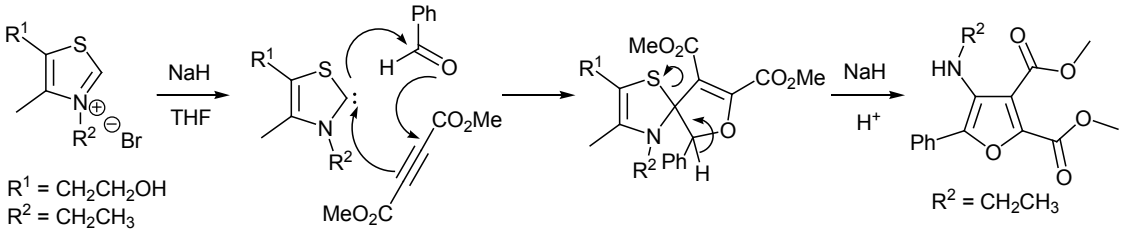

Scheme 2.19: Pathways towards carboxylate substituted 3-aminofurans.

The multicomponent reaction described by Ma *et al.* [43] uses a thiazole carbene as an umpolung to react with benzaldehyde and dimethylacetylene dicarboxylate (DMAD) giving the tetrasubstituted 3-aminofuran diester in moderate yields (Scheme 2.19, bottom). Both pathways necessitate the introduction of ester substituents in the furan product since the reaction mechanisms rely on the properties of the ester EWG to facilitate the formation of reaction intermediates.

The aryl substituted 3-aminofuran ring has been prepared by a number of methods and there are three syntheses in the literature for the preparation of dialkyl-(5-methyl-2,4-diphenyl-furan-3-yl)-amines. Mageswaran *et al.* [44] have reported the base catalysed [3,2]-sigmatropic rearrangement of a phenyl-(prop-2-ynyl) ammonium ylide in protic solvent. Upon heating, cyclization via intramolecular nucleophilic addition of the enol oxygen to the allene intermediate gives the dimethyl-(5-methyl-2,4-diphenyl-furan-3-yl)-amine (Scheme 2.20, top; R = Me). The authors report this compound to be rather unstable and prone to rapid decomposition upon exposure to light and air. This is not surprising since, in contrast to the stabilizing effect of the electron withdrawing ester substituent, the phenyl substituents are EDG and destabilise the aromatic system.

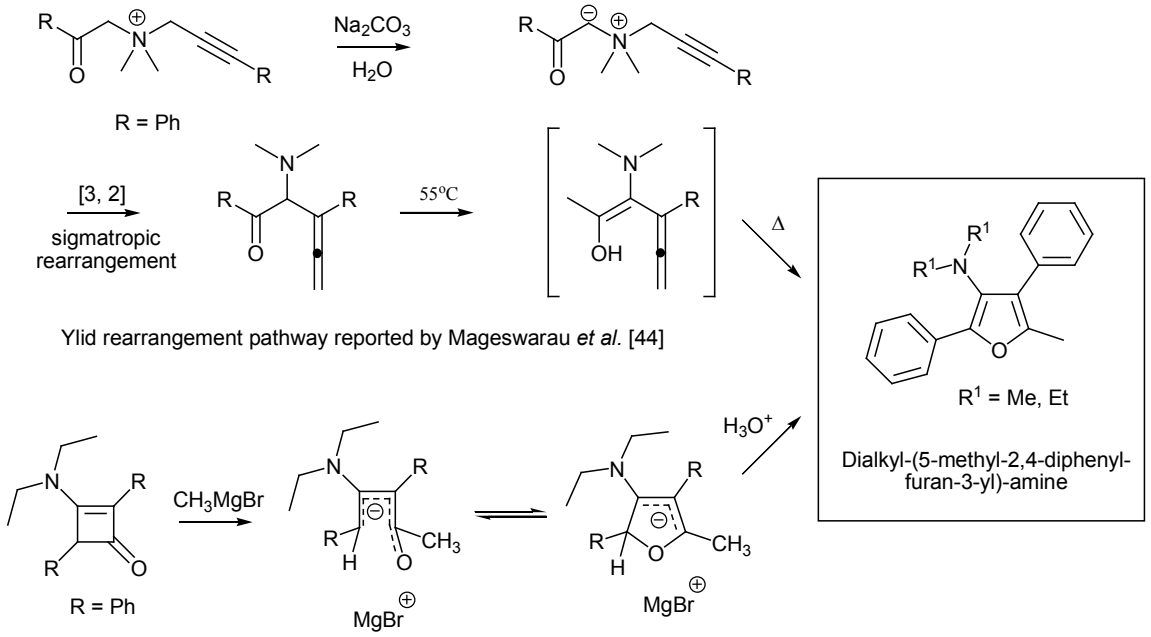

Scheme 2.20: Novel pathways towards the 2,4-diphenyl substituted 3-aminofurans.

Ficini *et al.* have prepared dimethyl-(5-methyl-2,4-diphenyl-furan-3-yl)-amine using the Feist-Benaig synthesis shown in Scheme 2.3, followed by interconversion of the ester substituent to the amine *via* the Curtius rearrangement as seen in Scheme 2.6 [45]. A novel methodology was also reported, involving the reaction of 3-diethylamino-2,4-diphenyl-cyclobut-2-enone with methyl Grignard reagent (Scheme 2.20, bottom). Rearrangement of the Grignard intermediate results in ring expansion to the five-membered heterocyclic benzylic anion, stabilised by the magnesium bromide cation [45]. This reaction proceeds via a ring expansion/rearrangement process to provide diethyl-(5-methyl-2,4-diphenyl-furan-3-yl)-amine in one step from the amine substituted cyclobutenone (Scheme 2.20; R^1 = Et).

Mageswaran *et al.* [44] described the hydrolysis of dimethyl-(5-methyl-2,4-diphenyl-furan-3-yl)-amine under aqueous acidic conditions to give 5-methyl-2,4-diphenyl-furan-3-one (Scheme 2.21). A brief investigation was conducted in this work into the preparation of the 4-methyl-3(2H)-furanone (**16**) as a potential precursor via condensation of the ketone with an amine, ie: pyrrolidine, to give the furan **5a** as the imine tautomer.

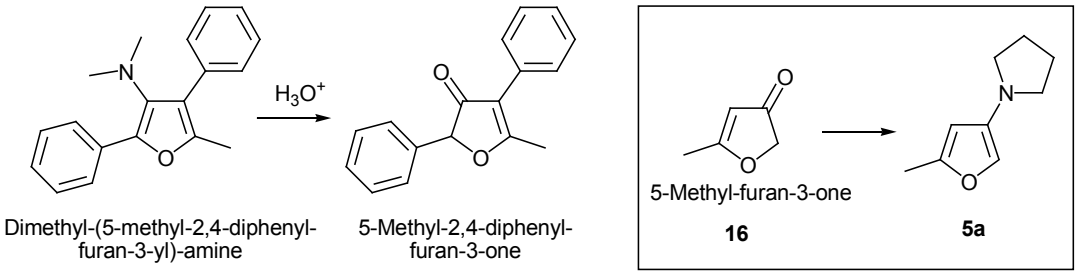

Scheme 2.21: The hydrolysis of dimethyl-(5-methyl-2,4-diphenyl-furan-3-yl)-amine was reported under aqueous acidic conditions [44] to the produce corresponding 5-methyl-2,4-diphenyl-furan-3-one. Conversely, the 5-methyl-furan-3-one **16** may provide **5a** by a condensation reaction with pyrrolidine.

Following a procedure reported by Cui *et al.* [46], the Claisen condensation between acetone and ethyl 2-chloroacetate was used in an attempt to prepare 1-chloropentane-2,4-dione. The lithium enolate of acetone was prepared by the reaction of a stoichiometric ratio of LDA and acetone at –30ºC. The reaction was cooled to –50ºC and the enolate reacted with one half equivalent of ethyl 2-chloroacetate to allow for the acidity of protons at the α-position to the ester. Upon aqueous workup the 1-chloro-pentane-2,4-dione product was not observed and GC-MS analysis revealed a molecular ion for **16** in a low yield as a result of base mediated cyclization to the furanone (Scheme 2.22). At room temperature, the cyclic product **16** has a reported half-life of 60 minutes in the presence of base [47] and polymerises as it forms to give a low 10% yield (Section 6.3).

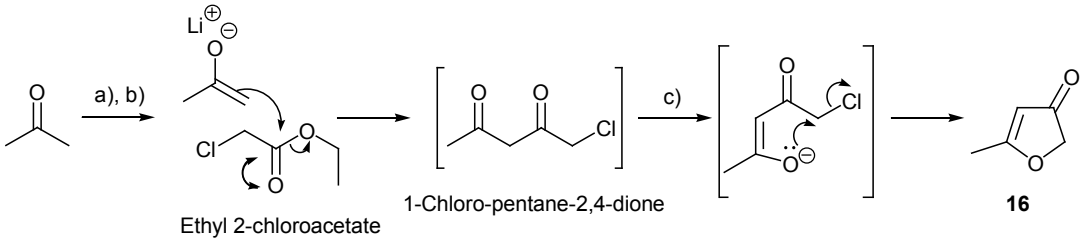

a) LDA, -30ºC, THF b) Chloroacetic acid ethyl ester, -50ºC c) Aqueous base, 10%

Scheme 2.22: Preparation of 4-methyl-3(2H)-furanone **16** from the Claisen reaction between acetone and chloroacetic acid ethyl ester, followed by base catalysed cyclization.

The ketone **16** was easily isolated by column chromatography on silica using a hexane:EtOAc gradient elution to give a clear oil and ^{1}H NMR data was in agreement with that reported by Hofmann *et al.* [48]. Although the compound was stable in solution, the neat compound required refrigeration to prevent polymerization. The condensation between **16** and pyrrolidine was trialed in benzene using a Dean-Stark trap to remove the water formed from dehydration (Scheme 2.22). The 1,4-addition product could be expected to form under these conditions as a possible byproduct, but this was not observed and instead **16** underwent slow polymerization and the amine reagent remained unchanged and was observed in high concentration in GC-MS analysis after the polymerization of **16** was complete. *p*-Toluene sulphonic acid (*p*-TsOH) was added to aid dehydration by protonation of the amine, in an attempt to prevent base catalysed polymerization and perhaps aid in the dehydration of cyclization intermediates. Unfortunately, the same results were obtained as for the neutral conditions and condensation trials with morpholine indicated no improvement.

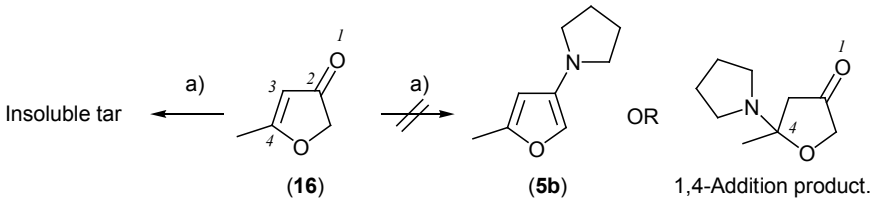

a) Benzene, Dean-Stark trap, Pyrrolidine, 90ºC

Scheme 2.23: The condensation of **16** and pyrrolidine failed to give the furan **5a** or the 1,4-addition product and instead led to decomposition products.

Despite failed attempts to condense **16** with secondary amines, the tendency for cyclization of the 1,3-diketone system containing labile or reactive substituents at the terminal γ-position was duly noted. The possibility of incorporating the amine into the 1,3-diketone backbone as an enamine functionality was investigated as a consequence of these observations. Literature research into the preparation of γ-hydroxy-β-aminoethylenic ketones revealed two references, both of which mentioned the isolation of an aminofuran rather than the enamine intermediate. Gusev *et al.* [49] propose that the reaction of diacetylenic glycols with 30% diethylamine solution under aqueous conditions produces the β-aminoethylenic ketone or 'enaminone' system by di-addition of the amine to the alkynes, followed by hydration of one enamine group. Continued heating facilitated a retro-aldol reaction of the α-hydroxy carbonyl chain and subsequent cyclization to give diethyl-(5-methyl-2-propyl-furan-3-yl)-amine in moderate yields (56%) (Scheme 2.24). The product was characterised by UV, IR and ^{1}H NMR spectroscopy, as well as by elemental analysis. This approach provided furans containing additional

substitution at C(2) and removal or modification of alkyl substituents while following the same synthetic methodology may be quite difficult.

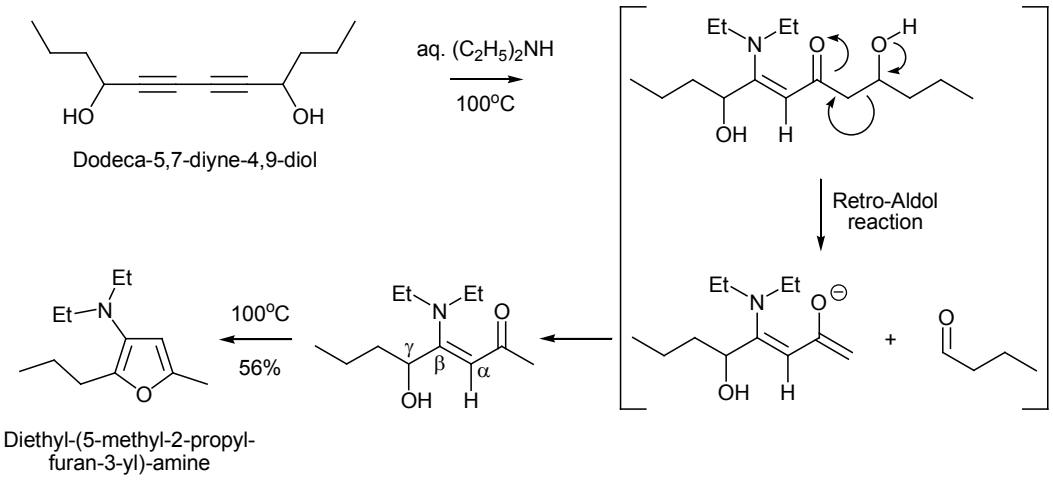

Scheme 2.24: Reaction of dodeca-5,7-diyne-4,9-diol with aqueous diethylamine at 100ºC provides moderate yields of dimethyl-(5-methyl-2-propyl-furan-3-yl)-amine *via* a retro-aldol pathway [49].

Research conducted by Bowden *et al.* [50] on the addition of amines to conjugated ethynyl ketones describes the preparation of stable enaminones using primary and secondary amines, occurring by 1,4-addition at the β-position to the carbonyl group (Scheme 2.25, top). This reaction is commonly referred to as a Michael-type 1,4-conjugate addition reaction [7].

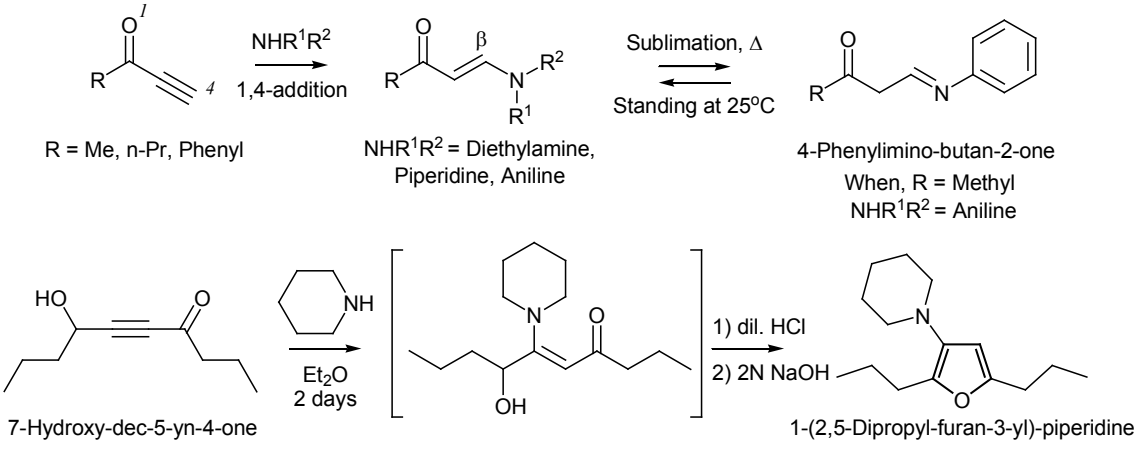

Scheme 2.25: Top; Addition of amines to ethynyl ketones provides stable β-enaminones [50]. Upon purification by sublimation, the imine tautomer 4-phenylimino-butan-2-one was formed for the aniline addition product. Bottom; the Michael addition of piperidine to 7-hydroxy-dec-5-yn-4-one resulted in the formation of the 1-(2,5-dipropyl-furan-3-yl)-piperidine via the enaminone intermediate [50].

Both acyl and benzoyl enaminone products were found to possess strong near UV absorption characteristics similar to butadiene and the values for maximum wavelength of light absorption (λ_{max}) are given in comparison to the non-aminated derivatives, demonstrating the powerful auxochromic effect of the amine substituent in this conjugated system. The authors report that the Michael-type addition of piperidine to 7-hydroxy-dec-5-yn-4-one resulted in the formation of the 1-(2,5-dipropyl-furan-3-yl)-piperidine upon standing in Et_2O for 2 days. Workup involved extraction of the aminated intermediates into aqueous acid, followed by basifying the solution with 2 N NaOH and extraction to yield the furan product. The enaminone intermediate was not isolated during this process and it is likely that the furan product is prepared in the workup procedure rather than upon standing in the ethereal mixture (Scheme 2.25, bottom).

Although reference to the mechanism for the 3-aminofuran formation was not found, cyclization of γ-hydroxy-α,β-unsaturated systems has been mentioned by the same group [51] during the hydration of the hex-3-en-5-yn-2-ol using mercuric sulphate ($HgSO_4$) and sulfuric acid under steam distillation conditions. In this instance hydro-oxo-biaddition at the alkyne [6] following the Markovnikov rule and subsequent acid hydrolysis gives the α,β-unsaturated ketone, which undergoes thermal cyclization and dehydration to yield the furan (Scheme 2.26). Intermediates in the cyclization process are unknown, although an anionotropic rearrangement has been reported in these systems as a possible source for the production of hexane-2,5-dione [51], the furan precursor in Scheme 2.2.

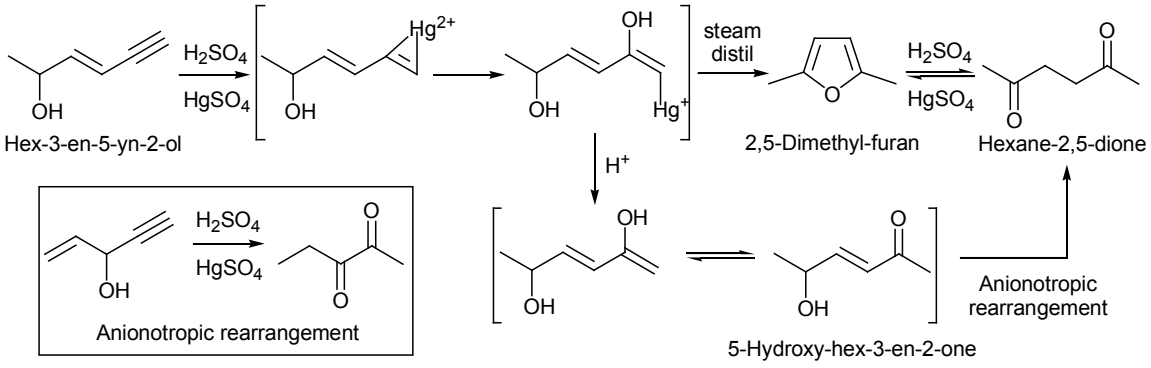

Scheme 2.26: Studies by Heilbron on the preparation of 2,5-dimethyl-furan via an anionotropic rearrangement of 5-hydroxy-hex-3-en-2-one [52].

This isomerization may occur more easily in the β-aminated compounds by tautomerisation involving the nitrogen. The imine isomer 4-phenylimino-butan-2-one has been isolated from sublimation of the aniline addition product (Scheme 2.25, top) and was reported to isomerise back to the α,β-unsaturated tautomer upon standing at 25ºC [50].

The cited literature references containing details on the preparation of the 3-aminofurans are general publications addressing the reactivity of acetylinic alcohols. No studies have been conducted concentrating on the utility or flexibility of this approach towards 3-furylamines for use in synthetic chemistry. The next section will detail a study on the preparation of the 3-furylamine compounds from an acyclic enaminone, prepared using a Michael-type addition to the appropriate alkynone backbone.

2.3.1 Preparation of Protected Ketoalkynols

From the studies presented in Section 2.3, the substituted furylamine **5** can be retrosynthetically derived *via* the enaminone, from the ketoalkynol **18** (Scheme 2.27). The alcohol 5-hydroxy-pent-3-yn-2-one has been reported in the literature by Duranti *et al.* [52] and characterised to be a reactive oil, sensitive to light, heat and air, and stores poorly even in a dark environment at –20ºC. It was therefore more desirable to use the hydroxy protected derivative **18** and literature procedures describe a short synthesis from prop-2-yn-1-ol, incorporating the tetrahydropyran-2-yl (THP) protecting group [52].

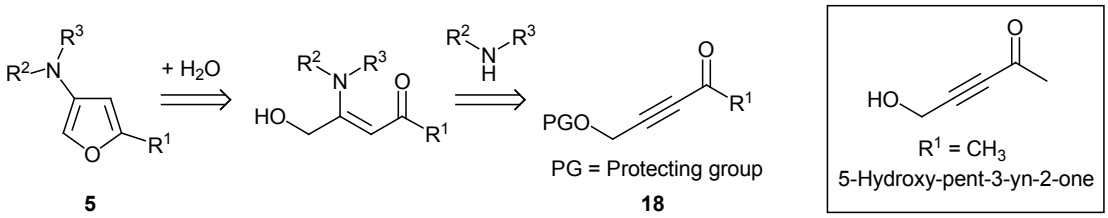

Scheme 2.27: Retrosynthesis for the preparation of 3-aminofuran heterocycles **5** from the hydroxy protected alkynone **18** *via* the enaminone.

Prop-2-yn-1-ol was first protected as the tetrahydropyran-2-yl (THP) derivative in neat 3,4-dihydro-2H-pyran using a catalytic amount of phosphoryl chloride ($POCl_3$) following methodology by Henbest *et al.* [53] (Scheme 2.27). The THP protection proceeds by acid catalysis, and once derivatised is extremely stable under strong basic conditions even in the presence of water. Addition of a KOH pellet to the neat mixture was sufficient in neutralizing the catalyst and the crude material was distilled directly to give a 90% yield of 3-(tetrahydropyran-2-yloxy)prop-1-yne **17**. The acetylinic proton was removed using sodamide ($NaNH_2$) in boiling Et_2O under inert conditions following methodology reported by Duranti *et al.* [52] to provide a suspension of the sodium acetylide salt. The tetramethylsilyl (TMS) and tetraethylsilyl (TES) protected derivatives of **17** were found to undergo silyl rearrangement to the terminal acetylinic position upon deprotonation using sodamide or LDA.

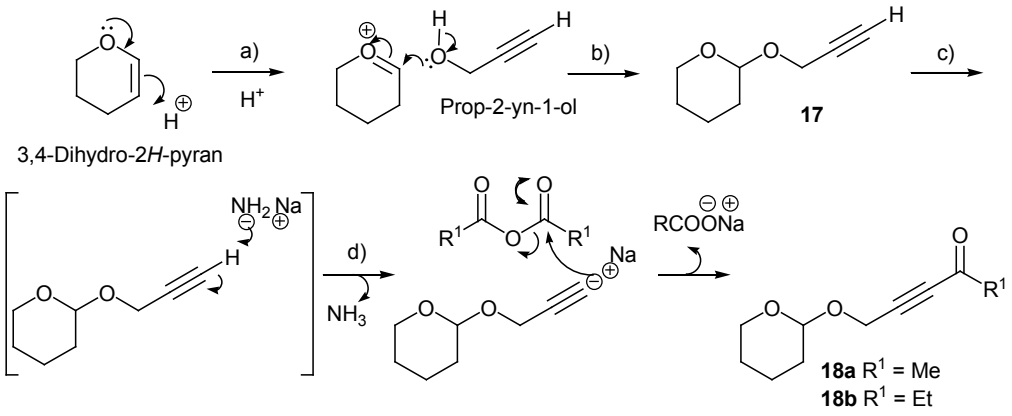

a) 3,4-Dihydro-2H-pyran, prop-2-yn-1-ol, cat. $POCl_3$ b) KOH, distil, 90% c) $NaNH_2$, Et_2O, reflux 5 h d) $(R^1CO)_2O$, –5ºC to –10ºC, R^1 = Me, 70%; R^1 = Et, 70%

Scheme 2.28: Acid catalysed THP protection of prop-2-yn-1-ol in 3,4-dihydro-2H-pyran to produce **17**. The sodium acetylide salt of **17** was acylated with Ac_2O (R^1 = Me) to provide **18a** and propanoic anhydride (R^1 = Et) to produce **18b**.

Reaction of the sodium acetylide suspension of **17** with acetic anhydride (Ac_2O) at –10ºC (Scheme 2.28; R^1 = Me) gave the 5-(tetrahydro-2-yloxy)pent-3-yn-2-one **18a** and the structure was confirmed by ^1H and ^{13}C NMR and GC-MS analysis (Figure 2.7). The methyl singlet at δ 2.3 ppm in ^1H NMR and the carbonyl ^{13}C signal at δ 184 positively confirmed the presence an acetyl group and THP signals at δ 4.8 and δ 1.8 - 1.5 signify that the protecting group was still attached to the molecule. $H(6'_A)$ and $H(6'_B)$ are locked in axial and equatorial configurations on the pyran ring and appear as separate signals at δ 3.8 and 2.6. Weak signals are present for the quaternary C(4) and C(3) acetylinic carbons at δ 88 and 85 respectively and these chemical shifts are in the agreement predicted values generated using Chemdraw. A small $[M-1]^+$ ion can be seen at *m/z* 181 in the GC mass spectrum and this is characteristic of conjugated ketones [54]. The *m/z* 85 fragment ion is the base peak in the MS of **18a** and this fragment is characteristic of a THP group and is generated from heterolysis at the acetal carbon.

If the crude mixture of **18a** was kept cool and under inert atmosphere during workup, the unreacted acetylene **17** was effectively removed under high vacuum and the remaining alkynone was often used without further purification. Otherwise, **18a** was purified by vacuum distillation (93ºC/1mm Hg) as a clear viscous oil. The 6-(tetrahydropyran-2-yloxy)hex-4-yn-3-one **18b** was prepared in good yields by reacting the sodium acetylide suspension with propanoic anhydride (R^1 = Et) following the same procedure.

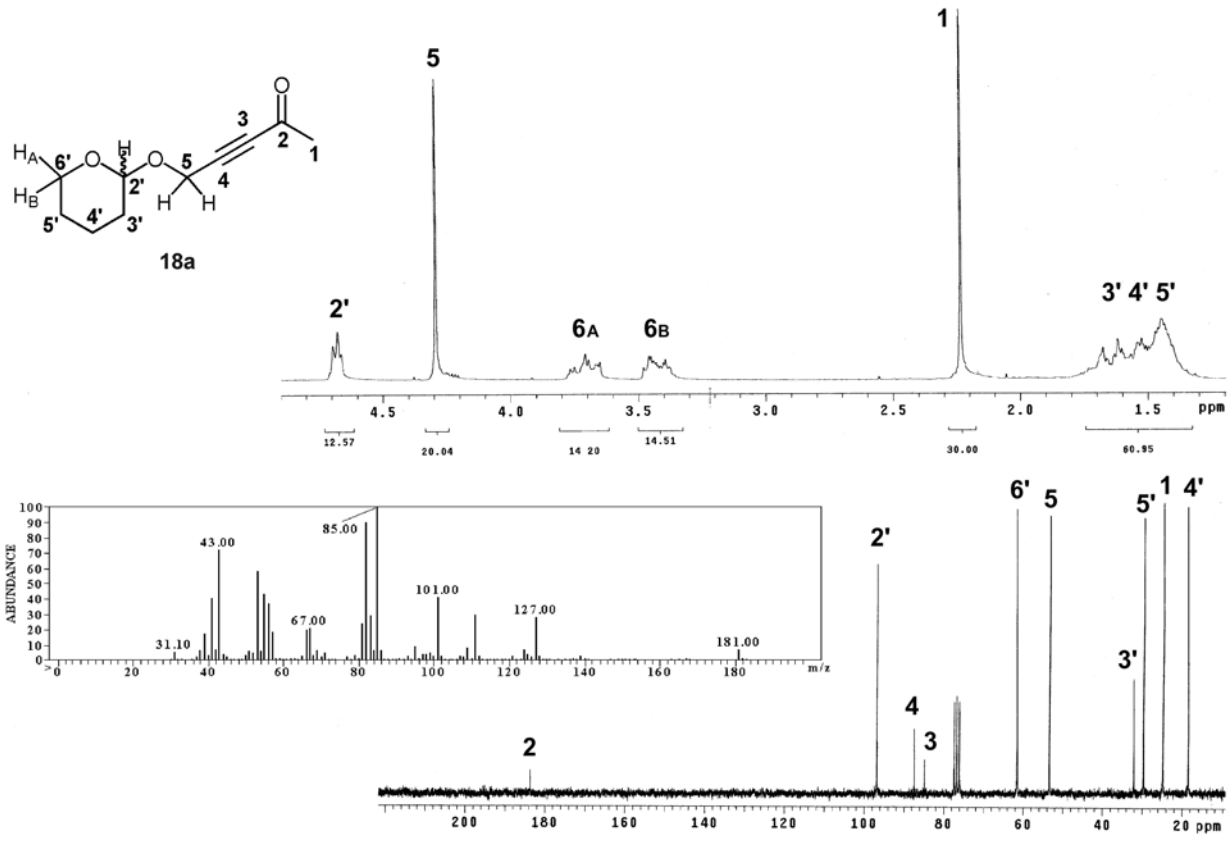

Figure 2.7: 200 MHz ^{1}H and 50 MHz ^{13}C NMR analysis of **18a** and EIMS fragmentation.

The 4-(tetrahydropyran-2-yloxy)but-2-ynal **18c** (R^1 = H) was prepared from **17** using conditions described by Journet *et al.* [55] (Scheme 2.29).

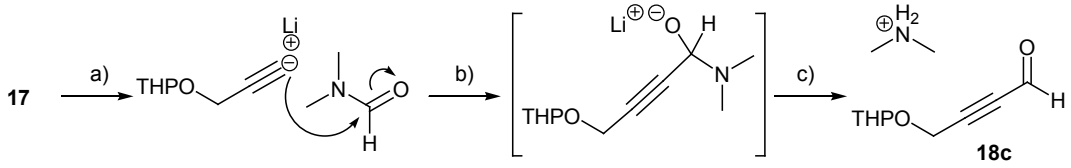

a) *n*-BuLi, THF, -40°C b) DMF c) Aq. KH_2PO_4, 84%

Scheme 2.29: Formylation of the terminal acetylene of **17** using DMF with acidic quenching to provide **18c**.

Deprotonation of **17** with *n*-butyl lithium (*n*-BuLi) at –40ºC produced the lithium acetylide, which was subsequently formylated with *N*,*N*-dimethylformamide (DMF). Quenching in an aqueous solution of potassium dihydrogen orthophosphate (KH_2PO_4) as an acidic buffer (pH 4.1 – 6.7) gave the aldehyde by hydrolysis of the lithio intermediate. Acidic quenching conditions are necessary since dimethylamine is liberated during hydrolysis and must be protonated in order to prevent Michael-type

addition to the newly formed 4-(tetrahydro-pyran-2-yloxy)-but-2-ynal **18c**. The THP protecting group was found to be stable in the aqueous acidic buffer and **18c** was prepared in high yield (84%). The procedures for synthesis of **18a-c** are included in Section 6.4.1 with characterization data.

2.3.2 1,4-Conjugate Addition to Alkynones

The 1,4-addition product from the reaction between **18** and a nucleophile produces a substituted ethylenic system that can exist in either the *E*- or *Z*- isomeric forms (Scheme 2.30). Bowden *et al.* [50] mention that the reaction of **18a** produces the enaminone product as a single isomer and Michael *et al.* [56] report that the *E*-isomer is formed when R^1 = Me and the *Z*-isomer predominates is cases where R^1 = H due to intra-molecular hydrogen bonding with the nitrogen.

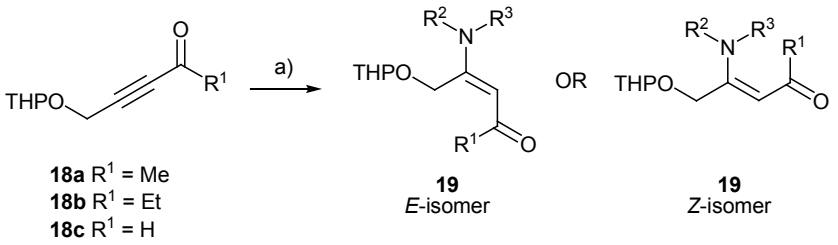

18a R^1 = Me
18b R^1 = Et
18c R^1 = H

19
E-isomer

19
Z-isomer

a) NHR^2R^3 neat or in dry THF.

Scheme 2.30: Nucleophilic addition to **18** can result in *E*- or *Z*- isomers dependant on the acyl substituent R^1.

Michael-type addition reactions when R^1 = Me, Et gave quantitative yields when performed under solventless conditions by the addition of equimolar amounts of the amine to the stirred oil **18a** or **18b**. Smaller alkyl amines react exothermically during the addition and decomposition was minimised by initial cooling in a 10ºC water bath followed by stirring at room temperature for two hours. The more sterically hindered amines diisopropylamine and dibenzylamine required mild heating (60ºC) and prolonged stirring in order to achieve optimal yields. GC and ^{1}H NMR analysis of the crude products indicated complete reaction of the alkyne in clean mixtures using the primary and secondary amines (Table 2.1) to produce enaminones **19a-k**. In the case of ethylene diamine, one half equivalent of the amine was used to produce a quantitative yield of di-addition product **19f**. The addition of amines might proceed *via* the nucleophilic mechanism for addition to α,β-unsaturated carbonyls, followed by proton abstraction from the enaminium ion and enolization [7] (Scheme 2.31).

	R^1	R^2R^3NH	% yield (**19**)
a)	Me	Morpholine	> 97[A]
b)	Me	Diethylamine	> 97[A]
c)	Me	Diisopropylamine	> 97[B]
d)	Me	Pyrrolidine	> 97[A]
e)	Me	Dibenzylamine	> 97[B]
f)	Me	Ethylenediamine	> 97[A]
g)	Me	*n*-Butylamine	> 97[A]
h)	Me	Cyclohexylamine	> 97[A]
i)	Et	Morpholine	> 97[A]
j)	Et	Diethylamine	> 97[A]
k)	Et	*n*-Butylamine	> 97[A]

Table 2.1: Yields of **19a-k**. [A]Performed neat at 10ºC-25ºC. [B]Performed neat at 60°C

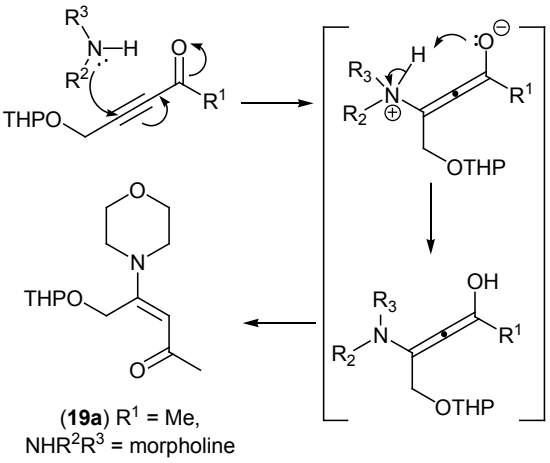

Scheme 2.31: Possible mechanism for the Michael addition to the alkynone. The morpholine addition product of **18a** (R^1 = Me) provides **19a** as the *E*-isomer.

Energy minimised (MM2) Chem 3D models of the addition product 4-morpholino-5-(tetrahydropyran-2-yloxy)pent-3-en-2-one **19a** indicate the *E*-isomer to be more stable than the *Z*-isomer (Figure 2.8). The carbonyl in the *Z*-isomer is slightly out of plane with the olefin due to steric interference with the amine substituent, disrupting the planar geometry favorable for resonance stabilization of π-electrons [57]. The 3D model of the *E*-isomer shows a planar conjugated system as the amine and carbonyl substituents are in a geometrically distant spatial arrangement. It should also be noted that H(2') on the THP protecting group is a chiral center and has a diastereotopic relationship to H(5).

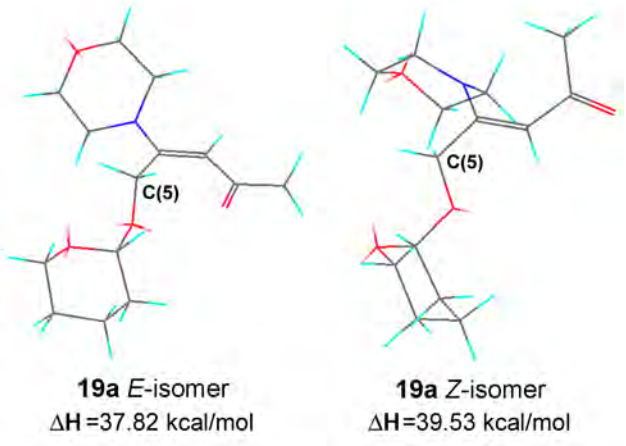

Figure 2.8: Energy minimised (MM2) Chem3D models of *E*- and *Z*- geometric isomers of **19a**. The proximity of the carbonyl in the *E*-isomer has an influence on the C(5) hydrogens in ^{1}H NMR studies.

^{1}H and ^{13}C NMR characterization of **19a** revealed the addition product had formed as a single isomer (Figure 2.9). An AB quartet ^{1}H NMR signal for the C(5) methylene group at δ 5.29 and 4.71 (J = 11.9 Hz) indicates non-equivalent chemical environments for the attached H(5_A) and H(5_B) protons and restricted rotation of the tetrahydropyran-2-yloxy group. This is in agreement with the 3D model for the *E*-isomer, whereby the proximity of the carbonyl to the *cis*- oriented methylene group is not equidistant to both C(5) protons. A new signal at δ 5.2 with an integral area equal to one proton is in agreement with Chemdraw predictions for the α-proton H(3) and suggests successful formation of the enaminone. Reaction of the triple bond is confirmed by the absence of ^{13}C quaternary acetylinic signals at δ 88 and 85 for C(4) and C(3) as seen in **18a**, and the presence of a protonated olefinic carbon at δ 98 corresponding to C(3) and a quaternary β-enamine signal for C(4) at δ 159. Mass spectrometry fragmentation indicates a molecular ion at *m/z* 269 in agreement with the molecular weight of **19a** and fragments *m/z* 85 and 84 correspond to fragmentation of the THP and morpholine rings, respectively. General trends observed in EI fragmentation of the enaminones **19a-n** include ions as a result of THP cleavage, observed in **19a** as a major fragment *m/z* 185, and subsequent homolysis of the acetyl group to give a base peak at *m/z* 142 in **19a** (Appendix 2.3).

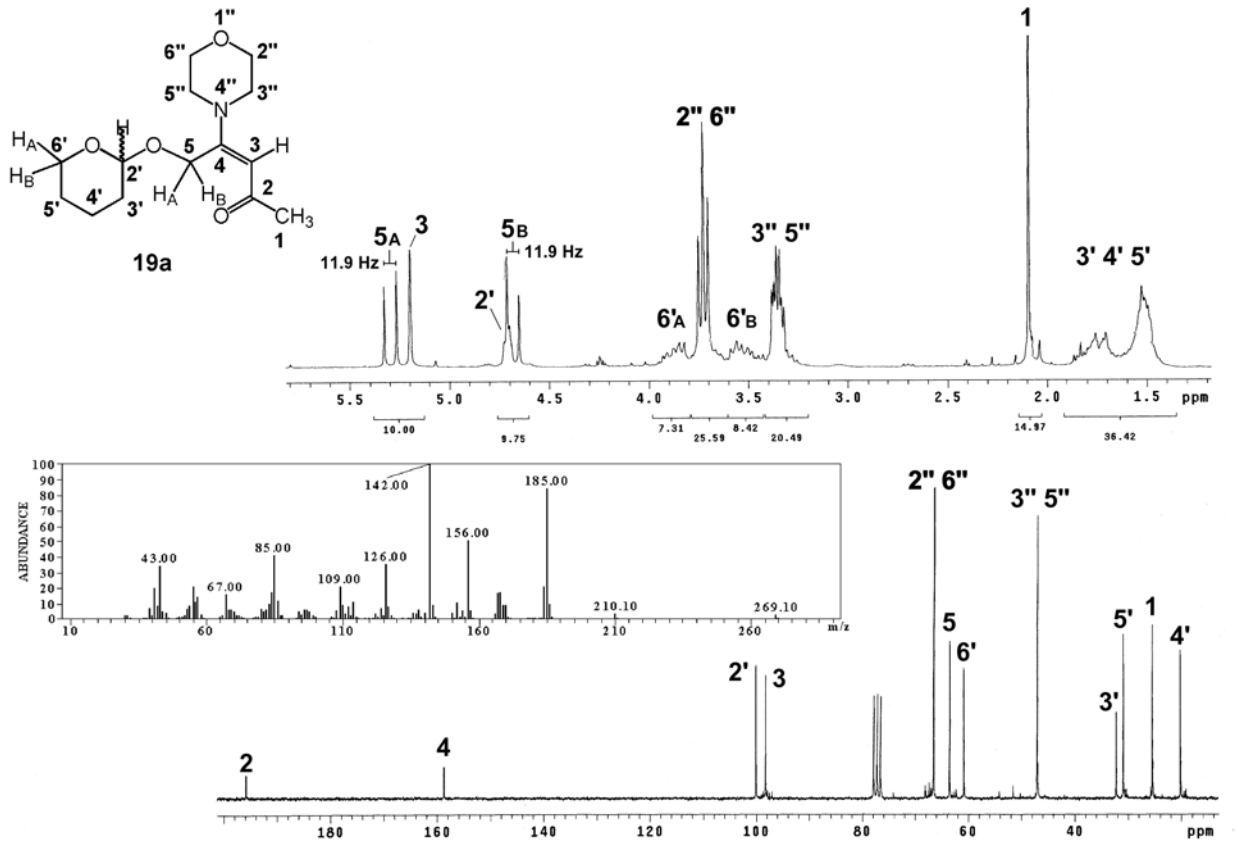

Figure 2.9: 200 MHz ^{1}H and 50 MHz ^{13}C NMR analysis of **19a** and EIMS fragmentation.

Extended studies on the addition of nucleophiles to the alkynone **18a** gave interesting results (Table 2.2). This study was used to gain insight into the reactivity of the alkynone and reveal limitations in nucleophiles that can successfully be used in addition reactions. Aniline underwent 1,4-addition in good yields upon heating the neat mixture at 50ºC for 24 hr, however diphenylamine did not react under solvent-less conditions or in THF at 60ºC and is perhaps limited by steric crowding of the nitrogen atom. *N*-methylaniline showed only 15% addition product by GC-MS using solventless conditions, however yields improved to 90% upon heating in THF at 60ºC for 2 days. Imidazole behaved similarly indicating 95% yield by GC-MS after 24 hr at 60ºC. Pyrrole failed to provide any addition product, even after heating for prolonged periods (7 days) and this can be explained by the low nucleophilicity of the aromatic heterocycle. Similarly, formamide, acetamide and *N*-methyl formamide were inert to addition reaction due to the low nucleophilcity of amides. Sodium azide and the sulphur nucleophile, ethanethiol anion, underwent facile addition to the alkynone at room temperature and provided clean reaction mixtures. Sodium ethoxide failed to react as a nucleophile, resulting in an unidentified mixture of by-products, presumably since it can act as a base due to the acidity of the α-carbonyl hydrogens in **18a**. The successful formation of the α,β-unsaturated addition products was confirmed by molecular mass fragment ions in GC-MS studies and integrals of characteristic $H(5_A)/H(5_B)$ ^{1}H NMR signals. The products listed below are not fully characterised and are beyond the scope of this synthetic study.

R^1	Nucleophile (Nu:)	% yield (**19**) (GC-MS)
Me	Aniline	91^A
Me	*N*-Methyl aniline	90^B
Me	Pyrrole	-
Me	Diphenylamine	-
Me	Formamide	-
Me	Acetamide	-
Me	*N*-Methylacetamide	-
Me	Imidazole	95^B
Me	Indole	15^B
Me	DIMCARB $(CH_3)_2NH^+CO_2^-$	$> 97^A$
Me	$CH_3CH_2S^-Na^+$	$> 97^C$
Me	$CH_3CH_2O^-Na^+$	-
Me	$CH_3COO^-Na^+$	-
Me	$Na^+N_3^-$	$> 97^C$

Table 2.2: Extended studies on the addition of nucleophiles to **18a**. Yields are measured by GC-MS and products not fully characterised. ^{A}Performed neat. ^{B}Performed in THF at 60ºC. ^{C}Performed in THF at room temperature.

The aldehyde **18c** (R^1 = H) was reacted in quantitative yields by slow addition to a solution of the amine in dry THF at 5°C (Scheme 2.32). The morpholine, diethylamine and *n*-butylamine addition products were prepared and the reactivity of the aldehyde toward nucleophiles appeared comparable to the ketones **18a-b**.

	R^1	R^2R^3NH	% yield (**19**)
l)	H	Morpholine	> 97
m)	H	Diethylamine	> 97
n)	H	*n*-Butylamine	> 97

Table 2.3: Yields of **19l-n**.

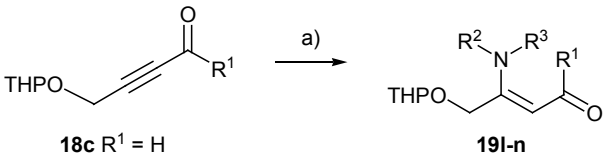

18c R^1 = H **19l-n**

a) NHR^2R^3, dry THF, -5°C, quantitative

Scheme 2.32: 1,4 Addition to **18c t**o prepare **19l-n**.

^{1}H and ^{13}C NMR analysis of product **19l** showed a second order AB quartet for the methyene protons H(4_A) and H(4_B) at δ 4.6 and the expected 8.1 Hz coupling between the aldehyde H(1) and olefinic α-proton H(2) (Figure 2.10). The H(4) AB quartet system in **19l** was closer to a second order signal compared with the methylene AB system for H(5) in **19a**. This is concordant with the *Z*-isomer whereby the carbonyl substituent is *trans*- to the C(4) pyranyl ether and no longer exerts shielding effects to influence the chemical and magnetic environments of H(4) protons. The smaller diethylamine analogue **19m** showed a singlet for the H(4) signal, indicating that geometrical hindrance to rotation about the C(3)/C(4) bond due to the amine size may also be responsible for the second order nature of the diastereotopic methylene signals. Product **19n** gave a 2:1 mixture of *E- and Z-* isomers as indicated from the integral areas of the H(1) or H(2) protons and individual signals for each isomer were confirmed by ^{1}H COSY 2D NMR (Appendix 2.4). ^{1}H Frequency differences for H(4_A) and H(4_B) were measured for the *E*- and *Z*- isomers of **19n** using the formula $\Delta\upsilon_{AB} = (4C^2 - J^2)^{0.5}$ [58] and found to be 108.9 and 23.8 times the respective coupling constants. As chemical shift differences $\Delta\upsilon / J$ approach 10, the peaks appear with second order splitting as shown in Figure 2.10. Upon removal of residual THF under strong vacuum, decomposition products began to appear in product mixtures of **19l-n** suggesting that THF solvation was essential for stabilizing the aldehyde. The apparent quartet signals in the ^{1}H spectrum of **19n** at δ 3.17 and 3.10 correlate to the H(1'') protons for *E*- and *Z*- isomers and ^{1}H COSY NMR show these peaks to be second order AB quartets. The H(1)/H(2) protons in the E-isomer of **19n** are in a *cis*-arrangement and have a smaller coupling constant of 2.6 Hz.

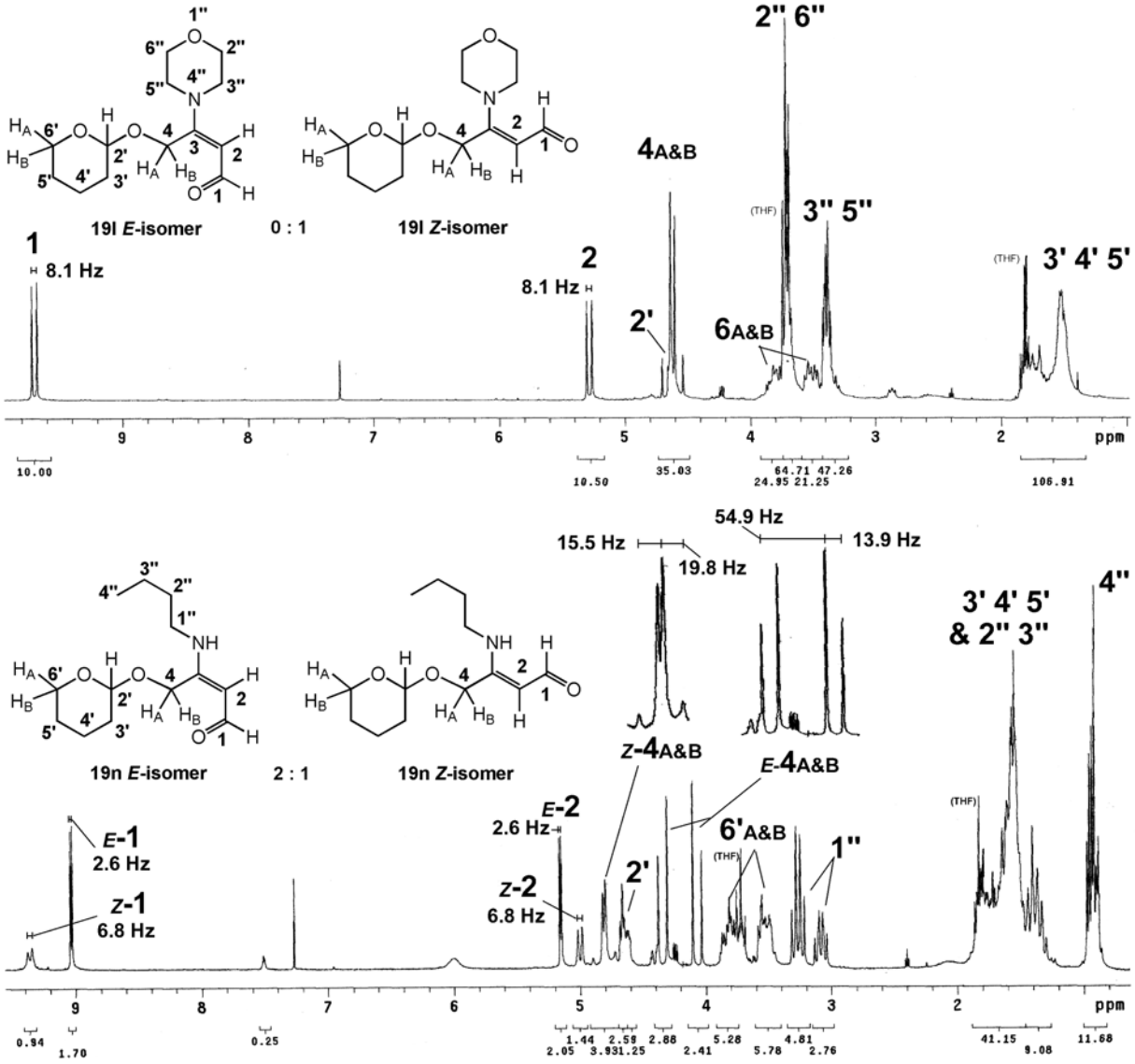

Figure 2.10: 200 MHz ^{1}H NMR for the *Z*-isomer of **19l** and the mixture of *E*- and *Z*- isomers of **19n**.

2.3.3 Preparation of 3-Aminofurans from Enaminones

In the presence of acid, deprotection of the THP protecting group (Scheme 2.33) follows the reverse mechanism to that shown in the protection Scheme 2.28. The enamine nitrogen is protonated under these conditions; however reports suggest the β-acyl enaminium ion is stable to hydrolysis in dilute aqueous acid [50].

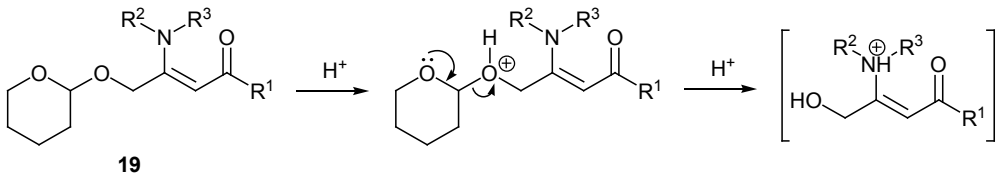

19

Scheme 2.33: Acid catalysed THP deprotection to form the β-acyl enaminium ion.

Acids trialed for the deprotection step included hydrochloric acid (HCl), sulphuric acid (H_2SO_4), nitric acid (HNO_3), and *p*-TsOH in chlorinated aprotic solvents ($CHCl_3$, DCM) and protic solvents (MeOH, EtOH, H_2O) to give multicomponent mixtures containing no detectable product by GC-MS and ^{1}H NMR analysis. One exception is the reaction of **19a** with *p*-TsOH in methanol at 70ºC, which provided clean conversion to the cyclised hydrolysis product **16** in 40 min as confirmed by ^{1}H and ^{13}C NMR data of the known compound. Orthophosphoric acid (H_3PO_4) in DCM gave promising results and during reaction monitoring by GC-MS analysis the furan was observed as the major product with a molecular ion of *m/z* 167 matching the mass of the furan target **5a**. The workup procedure reported by Bowden *et al.* [50] involving extraction of the hydrolysis product into aqueous acid led to multicomponent mixtures and without detectable formation of the furan product. Material obtained upon workup by neutralization with sodium bicarbonate ($NaHCO_3$) showed no ^{1}H NMR furan signals in the expected aromatic δ 6 – 7 region. Re-analysis of the isolated material by GC-MS analysis showed no material matching the retention time and fragmentation of the product observed in the crude reaction in progress. Upon extraction of the enaminium salt from the H_3PO_4/DCM reaction solution into distilled water, the protonated intermediate was stable for a short period of time (ca. 15min). After immediate basification (pH 14) of the aqueous extract, the freebase amines were extracted from the cloudy yellow mixture with Et_2O. GC-MS analysis revealed a 20% yield of **5a** and decomposition products were reduced considerably by using 1,2-dichloroethane (DCE) rather than DCM. Further improvements involved the use of anhydrous trifluoroacetic acid (TFA), and color changes from green-blue to red were often observed in association with the progress of the reaction. An optimal reaction time of 40 min was found experimentally for the deprotection to reach completion and longer reaction times encouraged the formation of by-products. When basification and extraction procedures were performed at 0ºC-5ºC,

excellent yields of **5a** were obtained in >98% purity by GC-MS. The tertiary substituted 3-aminofurans were stable as the free bases and could be stored for long periods at -18°C.

(**19**)	R^1	R_2R_3NH	% yield (**5**)
a)	Me	Morpholine	96
b)	Me	Diethylamine	90
c)	Me	diisopropylamine	95
d)	Me	Pyrrolidine	84
e)	Me	dibenzylamine	73
i)	Et	Morpholine	91
j)	Et	Diethylamine	88
l)	H	Morpholine	67
m)	H	Diethylamine	64

Table 2.4: Yields of furans **5a-e, i-j, l-m**.

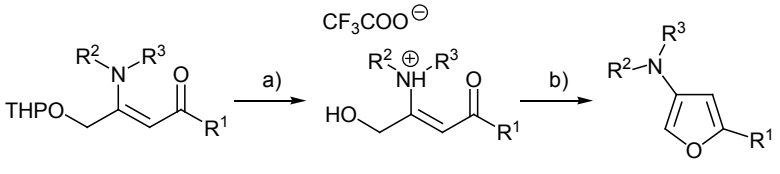

19 **5**

a) CF_3COOH, DCE b) 4 M NaOH

Scheme 2.34: Preparation of tertiary 3-aminofurans **5a-e**, **i-j**, **l-m** from the corresponding enaminones in Table 2.4.

The morpholine substituted furan **5a** was reproducibly prepared on multigram scales in almost quantitative yield. 2D HETCOR analysis of **5a** is shown in Figure 2.11 with DEPT 135 spectrum. Furan signals at δ 6.82 and δ 5.86 each integrate as one proton and are in the predicted region for aromatic proton signals H(2') and H(4') respectively. The protonated aromatic signals showed ^{13}C NMR correlation to C(2') at δ 123.9 and C(4') at δ 100.2 and both signals were confirmed as C-H groups by DEPT 135 data, as deduced from the positive signal orientation. The highest frequency protonated signals in the HETCOR spectrum are assigned to H(2')/C(2') and occur at lower frequency than observed in the unsubstituted furan ring. The (5')-position is closest to both σ-electron withdrawing heteroatoms and deshielded with respect to diamagnetic anisotropy resulting in typically high frequency shift for H(2'). High π-electron density at C(2') creates in a decrease in paramagnetic shielding due to repulsion of electrons away from the nucleus. This results in an ~20 ppm upfield shift for C(2') in ^{13}C NMR and a small 0.5 ppm upfield shift for H(2') in ^{1}H NMR with respect to that observed in furan. The chemical shift of the H(4') proton is in close agreement with that reported by Gusev *et al.* [49] for diethyl-(5-methyl-2-propyl-furan-3-yl)-amine (Scheme 2.24) of δ 5.72. The methyl group H(6') at δ 2.22 is correlated to a positively oriented CH_3 signal at δ 14.0 and the quaternary aromatics carbons C(3') and C(5') are absent from the DEPT spectra, but appear in the ^{13}C NMR as weak signals at δ 152.5 and 141.7. The higher frequency quaternary signal can be assigned as C(5') since it is attached to the more electronegative ring oxygen and has electron movement from the oxygen lone pair into the π-system in its resonance forms. The ^{1}H NMR multiplet at δ 3.81 with an integral area of four protons is assigned to the H(6) and H(2) methylenes, adjacent to the ether oxygen of the morpholine ring and this signal correlates to a single negatively oriented CH_2 peak at δ 66.6 in ^{13}C DEPT 135 NMR analysis. Similarly, a ^{1}H NMR multiplet at δ 2.87 corresponding to four protons is assigned to the H(5) and H(3) methylene

protons adjacent to the amine and correlates to a single CH_2 peak at δ 50.8 in DEPT 135 data. The chemical formula of **5a** was confirmed by electrospray ionization high-resolution mass spectrometry analysis (ESI-HRMS) and provided an accurate mass for the protonated amine $C_9H_{14}NO_2$ in agreement to three decimal places of the theoretical value (168.1025 calc., *m/z* 168.1019 found). ESI-HRMS were obtained for all new furan compounds in Table 2.4 and are listed in Appendix 6.1. EIMS analysis of furans **5a-n** gave a molecular ion and often an $[M+1]^{+\cdot}$ from proton abstraction. Typical furan losses include heterolytic cleavage of the amine substituents to give the $C_5H_5O^{+\cdot}$ ion (*m/z* 81), and loss of $CH_3^{\cdot}$ to give the *m/z* 152 ion, followed by cleavage of CO to give the *m/z* 124 ion in a two-step reaction [15] (Appendix 2.5).

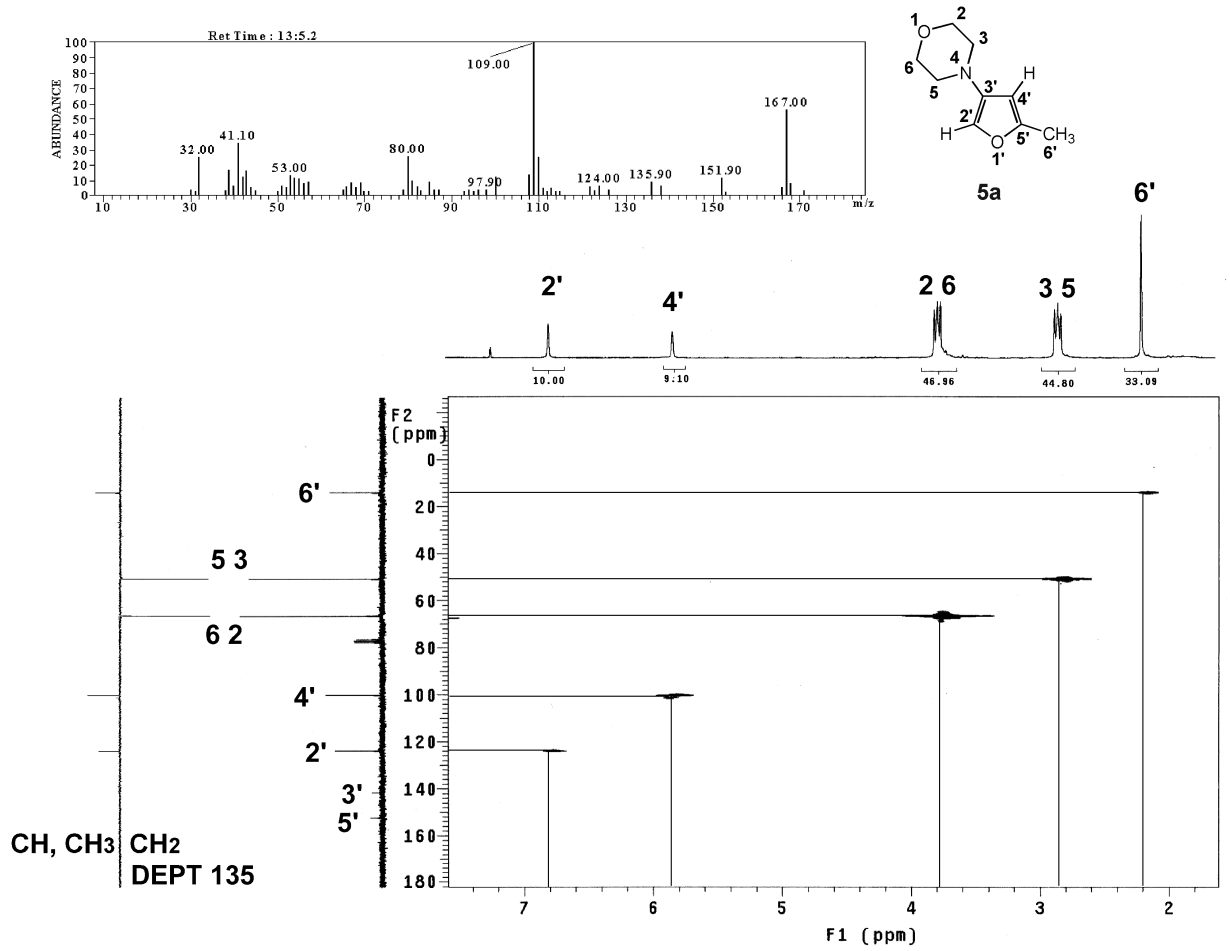

Figure 2.11: EIMS and 200 MHz ^{1}H/50 MHz ^{13}C HETCOR NMR analysis of **5a**. ^{13}C DEPT 135 NMR data is on the right margin. CH and CH_3 groups are positive, CH_2 groups are negative.

^{1}H and ^{13}C NMR chemical shifts for the aromatic furylamine ring C(2')/C(3')/C(4')/C(5') were very similar for all analogues of **5** where R^1 = Me or Et. Aromatic furan ^{1}H NMR signals were usually

broad singlets, however $J_{3',5'}$ = 1.1 Hz coupling was observed for **5i**. In analogues **5l-m** where R^1 = H, chemical shifts reported were close to those of the only literature example reported, furan-3-yl-dimethylamine [15]. Coupling constants for **5l** are $J_{2',4'}$ = 1.1 Hz, $J_{2',5'}$ = 1.6 Hz and $J_{4',5'}$ = 1.8 Hz (Appendix 2.6) in close agreement with the dimethyl analogue quoted as $J_{2',4'}$ = 1.1 Hz, $J_{2',5'}$ = 1.8 Hz and $J_{4',5'}$ = 1.8 Hz [15].

Deprotection and cyclization of secondary alkyl enaminones performed better in chloroform than DCE. 3-*N*-Alkyl substituted furans **5f-h**, **k** and **n** (R^3=H) were stable in solution at 0°C and gave molecular ions in GC-MS analysis, but required conversion to the *N*-acetyl derivatives **21** for isolation and characterization (Scheme 2.35). Confirmation of the amide derivative was established using ^{13}C NMR by the presence of an amide carbonyl at δ 171.0. ^{13}C NMR signals for the furan ring suggest that the aromatic system is no longer π-electron rich as the C(5) carbon has shifted by δ 16 toward higher frequency compared to the dialkylated amines in Table 2.4, due to decreases paramagnetic shielding. The amide group has an electron withdrawing effect on the nitrogen atom and the quaternary C(4) proton has shifted to a δ 10 lower frequency due to corresponding decreases in substituent electronegativity. The chemical formulae of 3-furylamides **21f-h**, **k**, **n** were confirmed by ESI-HRMS and provided masses accurate to three decimal places for each compound. Spectral characterization for **21g** is shown in Appendix 2.7. The experimental procedures for the syntheses of **5**, **19** and **21** are included in Section 6.4.

(**19**)	R^1	R_2R_3NH	% yield (**21**)
f)	Me	ethylenediamine	73[A]
g)	Me	n-butylamine	90[A]
h)	Me	cyclohexylamine	86[A]
k)	Et	n-butylamine	84[A]
n)	H	n-butylamine	65[A]

Table 2.5: [A] The secondary C(3)-amines were isolated as *N*-acetyl derivatives.

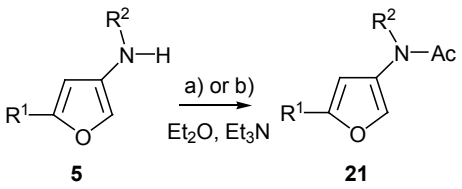

5 **21**

a) Ac_2O, when R^2 = n-butyl, ethylene diamine

b) AcCl, when R^2 = cyclohexylamine.

Scheme 2.35: Preparation of 3-furylamides **21**.

When R^1 = Me or Et, higher product yields were obtained than for the unsubstituted R^1 = H compounds. The amine substituents containing more hydrophilic groups gave higher yields of cyclised product compared to *N*,*N*-dibenzyl-5-methylfuran-3-amine **5e**, which contains bulky aromatic substituents and this may indicate that the aqueous workup is less efficient for more hydrophobic amines.

It is worth noting that **5e** was the only furan product that was stable at room temperature and did not require storage at –20ºC. The aniline conjugate addition product successfully cyclised to the furan **5** however an efficient derivatization method for the *N*-(furan-3-yl)aniline has not yet been found and the free amine is only stable for 1-2 h in ethereal solution at room temperature.

In the series of aminofurans discussed, aromatics unsubstituted at the 2, 4 and 5 positions were less stable upon storage and preliminary studies towards the preparation of the 5-arylaminofuran (R^1 = Ar) resulted in compounds that underwent decomposition within a few minutes after workup and in $CDCl_3$ while trying numerous attempts to collect NMR data.

Products **19a-n** and **5a-n** discussed in Section 2.3.2 and 2.3.3 were characterised by ^{1}H NMR, ^{13}C NMR, GC-MS analysis. Products **5a-n** were also characterised by FTIR and data is listed in Appendix 6.1.

2.3.4 ^{1}H NMR Studies on Cyclization Intermediates

The cyclization procedure described in Section 2.3.3 has been flexibly applied to the preparation of a range of 3-furylamines, however no cyclization intermediates could be identified in the crude furan mixtures. A small investigation was undertaken to examine intermediates in the cyclization scheme indicative of acid or base mediated cyclization, and perhaps elucidate a mechanism for the formation of the furan.

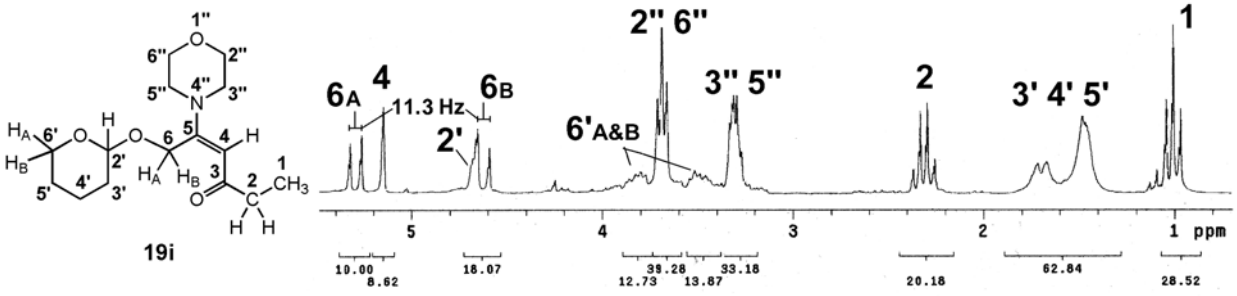

Figure 2.12: 200 MHz ^{1}H NMR spectrum of **19i** with peak assignments.

The morpholine addition product **19i** (Figure 2.12) was dissolved in $CDCl_3$ and mixed with 100µl of TFA in an NMR tube. The protonated enaminone was analysed by ^{1}H NMR and the successful THP deprotection was indicated from the collapse of the AB quartet from H(6_A) and H(6_B) to form a singlet at δ 5.50 (Figure 2.13, top) with an integral area of two protons. The olefinic C(4) proton has a decrease in shielding due to protonation of the conjugated nitrogen in **19i-int** and can be seen as a broad

down-field signal at δ 6.24 in agreement with Chemdraw predictions. The CH_2 groups H(3') and H(5') are closest to the morpholine nitrogen and appear as two separate downfield signals at δ 3.72 and δ 3.60 when the nitrogen group is protonated. The THP group appears to have reacted with TFA as indicated by a methine singlet at δ 6.04. Olefinic signals from 2,3-dihydro-2*H*-pyran were not observed and instead a sharp single proton corresponding to the predicted shift for the H(2') signal in trifluoroacetic acid tetrahydropyran-2-yl ester ring was present.

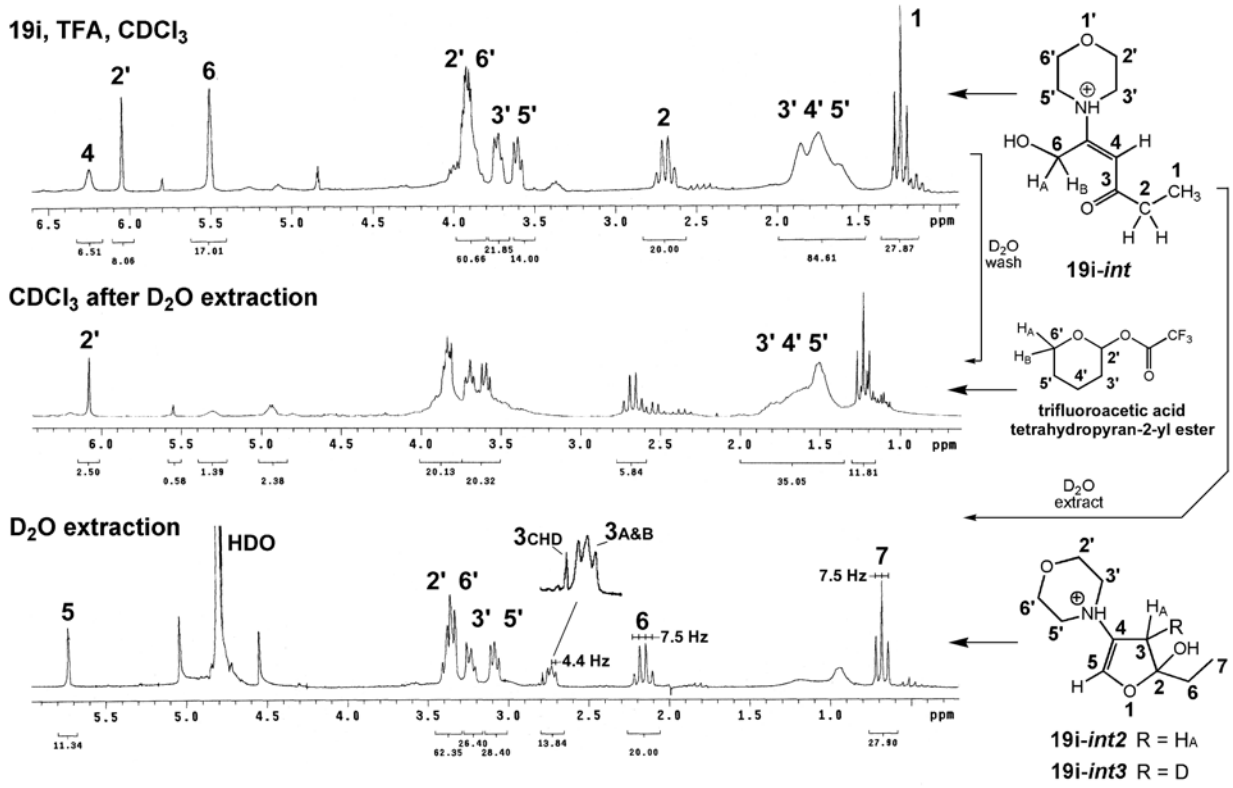

Figure 2.13: Top; 200 MHz ^{1}H NMR spectrum of **19i** with TFA in $CDCl_3$ to give the proposed compound **19i-int**. Middle; $CDCl_3$ solution after extraction with D_2O. Bottom; ^{1}H NMR of the D_2O extract and assignments for the proposed intermediates **19i-int2** and **19i-int3**.

The amine products were removed by extraction with D_2O and subsequent ^{1}H NMR analysis of the remaining $CDCl_3$ solution indicated persistence of the proposed trifluoroacetic acid tetrahydropyran-2-yl ester H(2') singlet at δ 6.04 and THP signals at δ 1.30-1.80 as a major component (Figure 2.13, middle). The D_2O extract mixture required multiple attempts to obtain a clean spectrum (Figure 2.13, bottom). The highest frequency ^{1}H NMR signal is a singlet at δ 5.73 with an integral area of one proton and can be assigned to a olefinic enamine hydrogen. Resonance due to the ethyl chain appears as a quartet H(6) and triplet H(7) at δ 2.15 and δ 0.68 ($J_{6,7}$ = 7.5 Hz) but both signals have shifted upfield (lower frequency) in comparison to the previous spectrum shown (Figure 2.13; Figure 2.12, top),

indicating that the ethyl substituent is no longer adjacent to carbonyl or enol functionalities. This finding suggests that the protonated intermediate formed upon extraction into D_2O is in the cyclic hemiketal form. If the enamine double bond was present between C(3) and C(4), a methylene CH_2 signal would be expected at approximately δ 4.4 and this was not the case. Two new signals are observed at δ 2.7 and integrate as one proton, indicating that a portion of this signal may have been deuterated from the D_2O solvent whilst undergoing tautomerizarion. The chemical shift of this signal also indicates that it is not attached to the same carbon as a heteroatom. The larger signal at δ 2.72 appears as an AB quartet (J = 4.4 Hz) whereas the smaller one, perhaps due to the mono-deuterated compound is a singlet at δ 2.79. The AB quartet suggests that these protons are in a locked conformation and the chemical shift most likely corresponds to the H(3) protons in the structure **19i-int2** and the deuterated compound **19int-3** (Figure 2.13). Attempts at longer 2D experiments on this intermediate failed due to changing signal shifts and intensities, and since assignments are only based on ^{1}H NMR data the structural assignments proposed are only tentative.

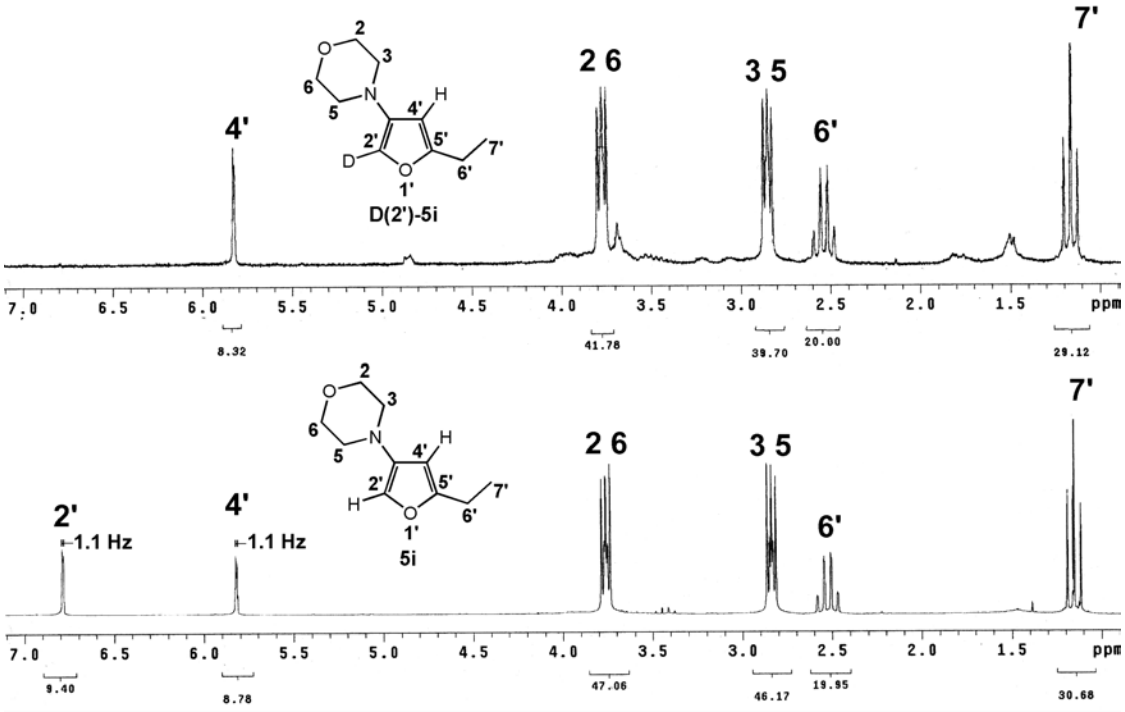

Figure 2.14: Top; 200 MHz ^{1}H NMR of the C(2')-deuterated furan **D(2')-5i** in $CDCl_3$ obtained from basification of the D_2O extract with NaOD and extraction into $CDCl_3$. Bottom; 200 MHz ^{1}H NMR spectrum of the non-deuterated furan **5i**.

The cyclization procedure gave extremely low yields when conducted in deuterated solvents and needed to be performed rapidly in order to obtain enough material to obtain a spectrum of the furan product. Basification of the aqueous D_2O NMR solution with NaOD and extraction into $CDCl_3$ gave a

clean ^{1}H NMR spectrum of the deuterated furan structure 4-(2-deutero-5-ethyl-furan-3-yl)-morpholine **D(2')-5i** (Figure 2.14). Preparation of the non-deuterated furan derivative **5i** followed by treatment with D_2O showed the disappearance of the aromatic H(2) signal at δ 6.83 indicating that the deuterium exchange did not take place as part of the mechanism and instead the C(2) proton is acidic and labile to ^{2}H isotope exchange. This observation is consistent with results published by Campbell *et al.* [18] who mention C(2) deuterium exchange during ^{1}H NMR experiments of 3-(^{t}butoxy-carbonylamino)furan in D_2O, indicating a degree of enamine character in the C(3) aza furan derivatives. The aromatic H(4') in **D(2')-5i** has an integral area of one proton and no decrease in intensity due to deuteration via the **19int-3** intermediate. This observation suggests heavy isotope effects [7] in the cyclization as a primary reason for the large decrease in product yield in D_2O, whereby the final aromatization under basic conditions proceeds much more slowly for **19int-4** or **19int-3** than **19int-2** and results in decomposition.

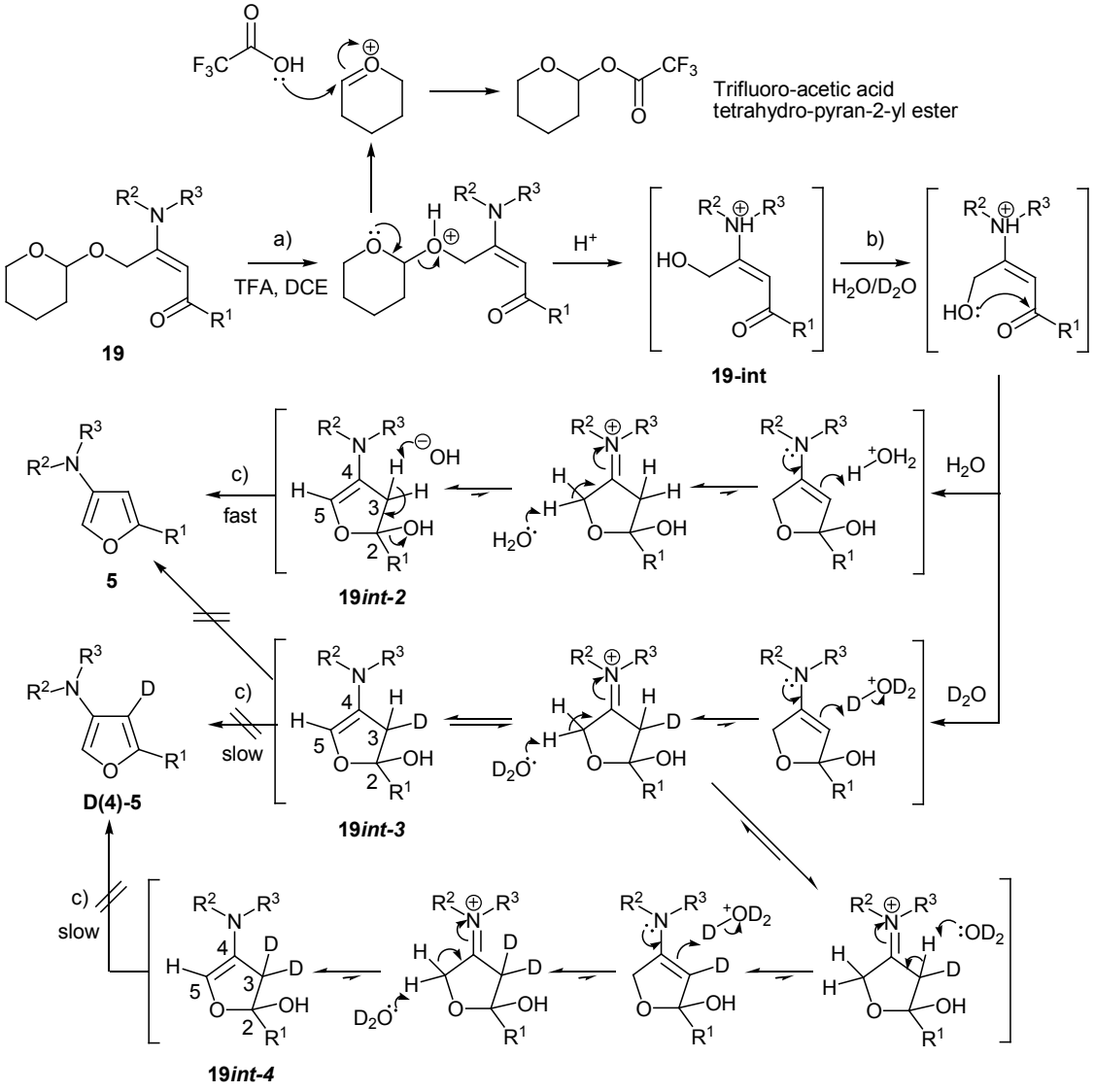

Scheme 2.36: Proposed reaction pathway for the cyclization of the enaminone **19** to the furan **5**.

Based on the above study, a proposed cyclization mechanism for the formation of 3-furylamines is shown in Scheme 2.36. The key steps in the proposed sequence are as follows;

1. The THP deprotection proceeds in DCE and reacts with TFA to produce trifluoroacetic acid tetrahydropyran-2-yl ester and the deprotected enaminium ion **19i-int**.

2. Cyclization to the hemi-ketal **19int-2** occurs upon extraction into water and the enamine double bond is free to tautomerise via the imine to the C(5)/C(4) position. In doing this, deuteration can occur at the C(3) position to produce **19int-3** or **19int-4**.

3. Dehydration occurs via a base mediated mechanism using aqueous NaOH to provide the furan product.

2.4 Preparation of Chiral 3-Furylamines

The preparation of a chiral 3-furylamine derivative has been reported by Schlessinger *et al.* for use in a Diels-Alder approach towards the construction of (+)-cyclophellitol [59, 60]. In this case, synthesis of the 3-furylamine involved progressively building the furan around the amine structure, starting with (*S*)-2-(1-methyl-1-methoxypropyl)-pyrrolidine (Scheme 2.37), a L-proline derived chiral secondary amine. Alkylation of the nitrogen atom with methyl 2-bromoacetate provided the tertiary amine, that was subsequently deprotonated at the α-position to the ester using potassium hexamethyldisilazane (KHMDS) and reacted with (*tert*-butyl-dimethylsilanyloxy)acetaldehyde to produce 3-[(*S*)-2-(1-methyl-1-methoxypropyl)-pyrrolidin-1-yl]-5*H*-furan-2-one. Treatment with an additional portion of KHMDS gave the furan via enolization of the carbonyl under basic conditions and subsequent reaction with triisopropylsilylchloride (TIPSCl) produced the 2-triisopropylsiloxy ether substituted furan in 56% overall yield from the starting amine.

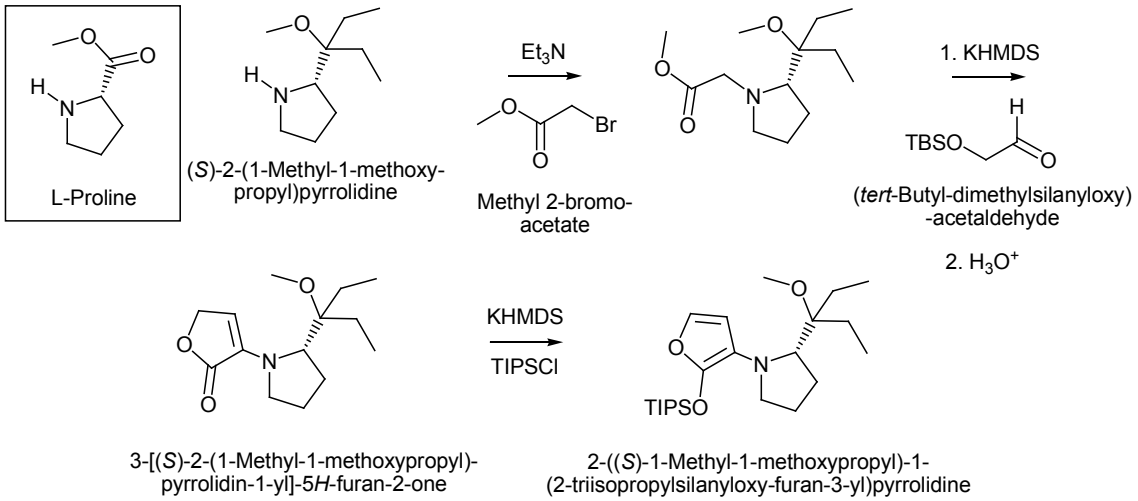

Scheme 2.37: Synthesis of 2-((*S*)-1-methyl-1-methoxypropyl)-1-(2-triisopropylsilanyloxy-furan-3-yl)pyrrolidine from the L-proline derivative (*S*)-2-(1-methyl-1-methoxypropyl)pyrrolidine.

The authors report this furan to be highly reactive in pericyclic reactions and provide excellent face selectivity of <97:3 upon Diels-Alder reaction with methyl acrylate in DCM at 22ºC [59]. The authors also mention that the isolation of the furan product is cumbersome and reactions are carried out by preparation of the furan *in situ* from the furanone. `The reports by Schlessinger *et al.* motivated the synthesis of a proline derived auxiliary for use in the furylamine synthesis. Reduction of L-proline to (+)-(*S*)-2-(hydroxymethyl)pyrrolidine with $LiAlH_4$ following a procedure described by Enders *et al.* [61] failed to produce clean reduction mixtures and 10-15% recovery of a mixture of L-prolinol and L-proline was common. (Scheme 2.38) This was most likely due to the effective complexation of prolinol with the Al^{3+} reducing agent and small amounts of material could be recovered from heating the $Al(OH)_3$ workup residue in 1 M/HCl.

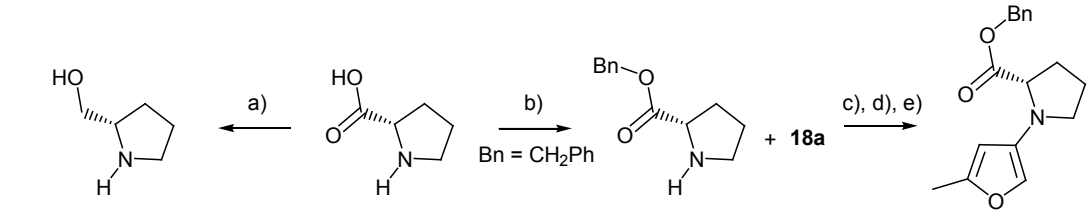

a) $LiAlH_4$, THF, 10% b) $SOCl_2$, BnOH >97% c) **18a**, neat >97% d) TFA, DCE, r.t. e) 4 M NaOH, 35%

Scheme 2.38: Low yields of (+)-(*S*)-2-(hydroxymethyl)-pyrrolidine were obtained from the reduction of L-proline. Preparation of **5o** was achieved in low yields using the L-proline benzyl ester **22**.

The reduction of L-proline seemed problematic and a proline ester was prepared and trialed as an indicator of the stability of proline derived 3-aminofurans. L-Proline benzyl ester **22** was prepared by reaction of L-proline with $SOCl_2$ in benzyl alcohol (BnOH) by modified procedures to those described in the literature [61]. The 1,4-conjugate addition of **22** to the alkynone proceeded in quantitative yields, however the ester-containing substituent led to a large decrease in yield for the cyclization reaction to provide the furan **5o** in low yields (35%) (Scheme 2.38). The product was also prone to decomposition, requiring protection from air and storage below –20ºC and the experimental details are included in Section 6.5.1.

Many of the furans prepared in Section 2.3.3 had a similar tendency to decompose and required frequent distillation, although compounds containing larger alkyl and arylamine substituents demonstrated increased stability. The *N*,*N*-dibenzyl-5-methylfuran-3-amine **5e** was a stable white solid at room temperature, indicating that chiral secondary amines containing aromatic substituents may be more suitable for the preparation of stable chiral 3-furylamines. The ephedrine diastereomers (1*S*,2*S*)-(+)-pseudoephedrine **23** and (1*R*,2*S*)-(-)-ephedrine **24** differ in stereochemistry at the C(1) hydroxy group and were chosen as cheap chiral pool auxiliaries to be attached to the furan ring (Figure 2.15).

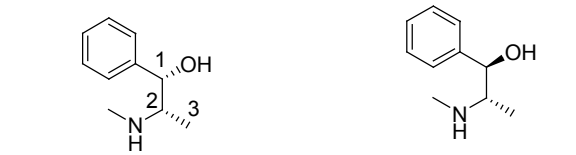

(1*S*,2*S*)-(+)-Pseudoephedrine **23**

(1*R*,2*S*)-(-)-Ephedrine **24**

Figure 2.15: Structures of (1*S*,2*S*)-(+)-pseudoephedrine **23** and (1*R*,2*S*)-(-)-ephedrine **24** differ in stereochemistry at the C(1) carbon.

1,4-Addition reactions of **23** and **24** with the alkynone **18a** were conducted in dry THF and GC-MS analysis indicated the complete reaction of starting materials after 4 hr to produce a mixture of isomers (Figure 2.16, bottom) with identical mass spectrum and no molecular mass ion. Thermal interconversion between isomers was noticed during chromatographic separation as indicated by tailing on the leading edge of the analyte peak, even at low concentrations. GC-MS traces of the addition product of **23** indicated the formation of **19p** as two major isomers (Figure 2.16, top left), however the addition product of **24** produced **19q** as three or more major isomers (Figure 2.16, top right) and complete GC resolution of intermediates **19p-q** was not achieved.

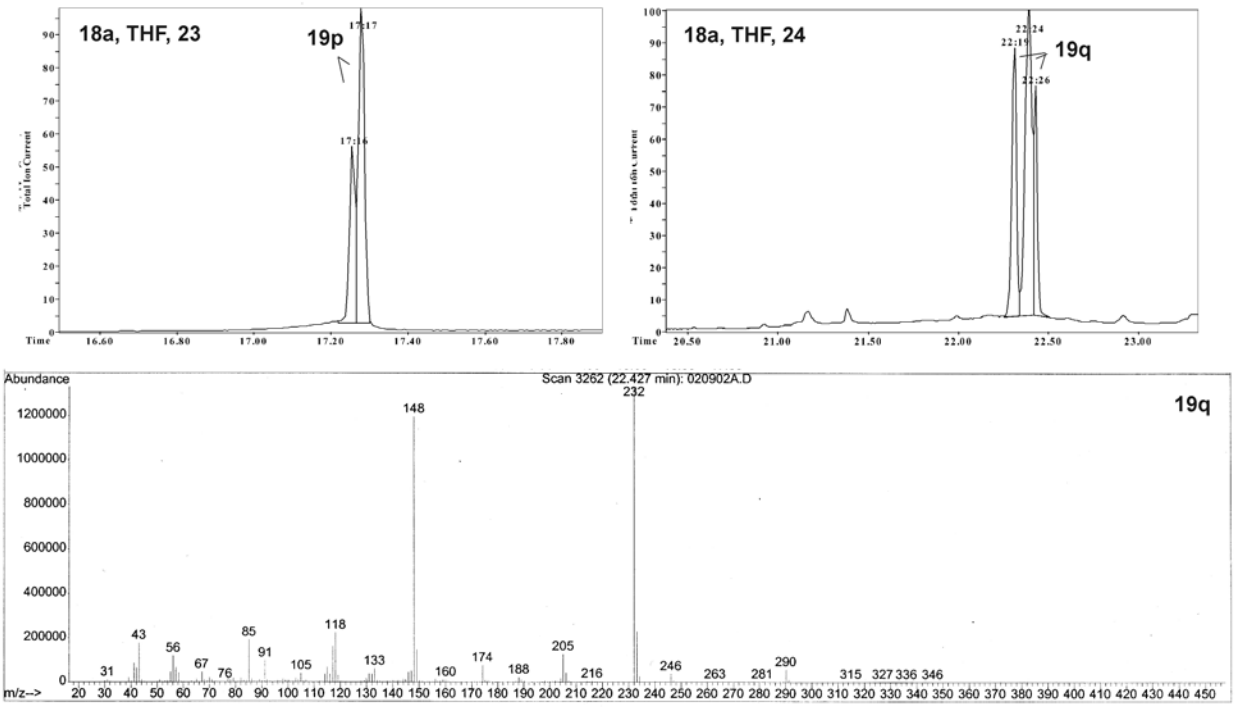

Figure 2.16: Left; GC trace of product mixture **19p** starting at 70ºC followed by 10ºC/min temperature ramp. Right; GC trace of product mixture **19q** starting at 50ºC followed by 10ºC/min temperature ramp. Bottom; The electron impact mass spectrum for **19p** and **19q** contain the same major mass fragment ions and a spectrum of **19q** is shown.

^{13}C NMR analysis of the addition product **19p** (Appendix 2.8) revealed a mixture of two major isomers and two minor isomers. Two strong carbonyl signals are apparent at δ 207 and indicate a loss of the α,β-unsaturated system in comparison to addition products **19a-n**, exemplified by **19b** (Figure 2.9), in which case the carbonyl can be observed upfield at δ 195.9. The absence of quaternary enamine signals at δ 158.8 and olefinic proton signals at ~δ 5.2 in ^{1}H NMR also support this finding. 2D HMQC NMR analysis (Figure 2.17) indicates ^{13}C NMR signals at δ 95.5 – 96.9 are due to non-protonated carbons and the chemical shift is indicative of attachment to two heteroatoms. This observation suggests that the hydroxy group on the phenyl-propanol chain had reacted with the quaternary enamine carbon to form the five membered cyclic oxazolidine ring. Studies by Walker *et al.* [62] on the mass spectrum of ephedrine and pseudoephedrine derived oxazolidines identify characteristic fragment mass ions *m/z* 148, 118 and 91. All of these fragment ions are present in the mass spectrum of **19p** (Appendix 2.8) and **19q** (Figure 2.16, bottom) supporting the five-membered heterocyclic structure 1-(3',4'-dimethyl-5'-phenyl-2'-((tetrahydro-2H-pyran-2''-yloxy)methyl)oxazolidin-2-yl)propan-2-one (Scheme 2.39) that can exist as erythro or threo isomers at the C(2') carbon.

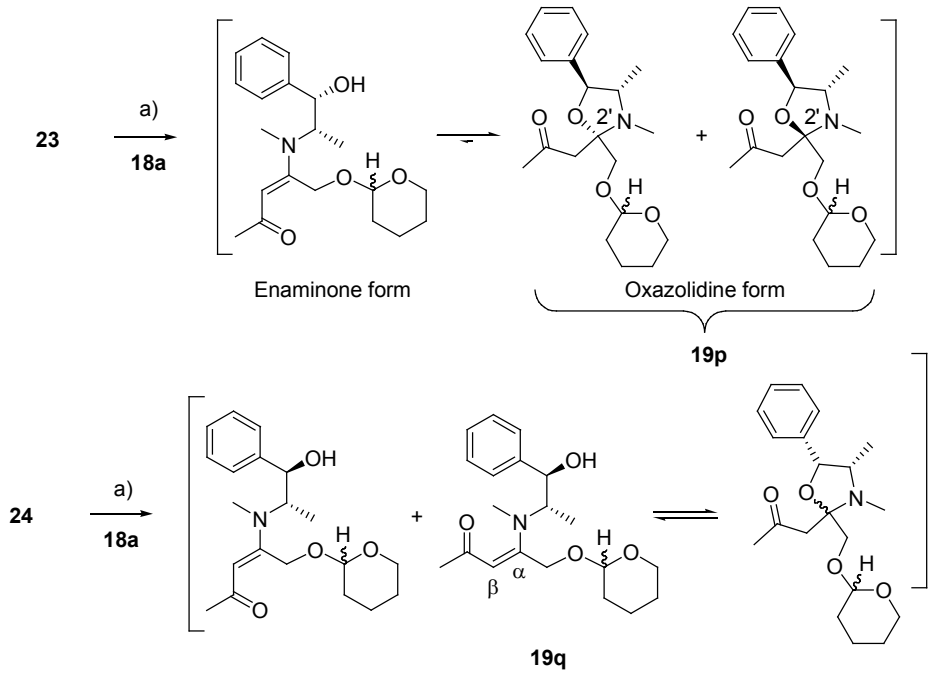

a) THF, 40ºC to r.t., 2 h

Scheme 2.39: Addition products of **23** and **24** with **18a** produce the enaminone intermediate that rapidly undergo isomerization to the five membered oxazolidine structures **19p** and **19q**.

NMR assignments were made for the major isomeric structures of **19p** using HMQC NMR data (Figure 2.17). Non-protonated ^{13}C NMR signals at δ 96.8 and 96.2 are assigned to the C(2') heterocyclic quaternary oxazolidine carbon. Two separate sets of AB quartet signals between δ 4.06 – 3.44 are assigned to H(7'') and correlate to C(7'') carbon signals at δ 70.4 and 69.8. Two ^{1}H NMR signals at δ 2.82 appear as second order peak splitting and correlate to the C(1) carbon signals at δ 49.5 and 49.6. Correlations between H(4'), H(5') and H(6') on the ephedrine chain were confirmed by COSY analysis (Appendix 2.9) and revealed that H(1) methylene signals are overlapped with the H(4') methine signal. The ephedrine analogue **19q** was characterised by ^{1}H and ^{13}C NMR, although the increased number of isomers led to broad indistinguishable ^{1}H NMR peak shapes (Appendix 2.10) and low signal to noise for distinguishing quaternary carbons. Differences in ^{1}H NMR chemical shifts for H(4'), H(5') and H(6') due to anisotropic effects of the benzene ring were consistent with that observed by Hyne [63], and multiple broad singlets for the N-CH_3 H(7') suggest that **19q** is in equilibrium with the enaminone form (Scheme 2.39, bottom). A broad uncorrelated singlet at δ 5.19 in the COSY NMR analysis also supports this hypothesis and is most likely the β-olefinic hydrogen (Appendix 2.10).

The hydrolysis kinetics of ephedrine derived oxazolidines has been well studied [64] and complete hydrolysis has been achieved at pH 1-11 at 37ºC under aqueous conditions. It was thus

assumed that hydrolysis of the oxazolidine would be facile and occur during aqueous workup procedures. Cyclization of **19p-q** using the workup procedure described in Section 2.3.3 resulted in a messy mixture of products and attempts to extract the protonated enaminone into distilled water were ineffective due to the bulky hydrophobic ephedrine group.

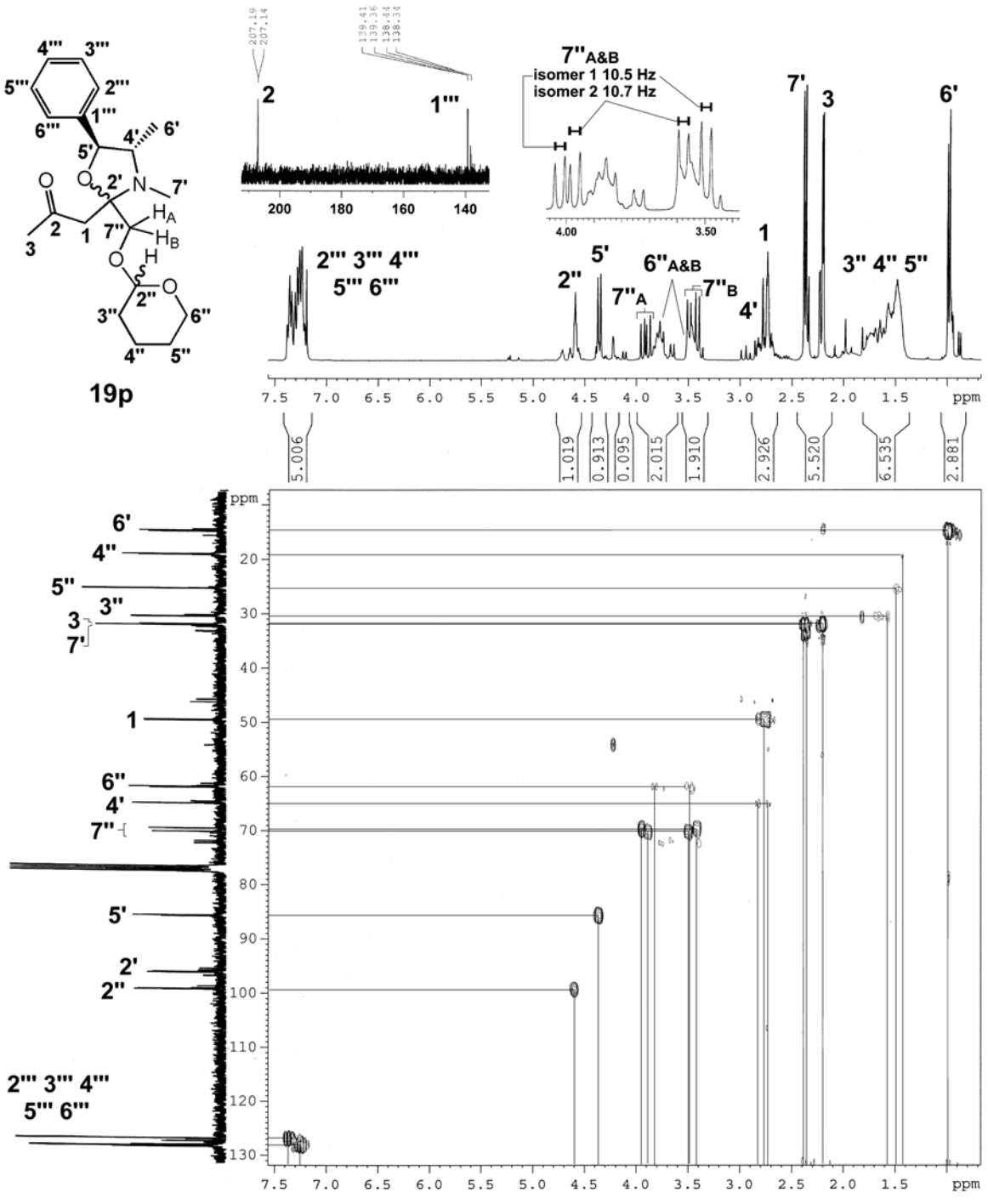

Figure 2.17: 300 MHz ^{1}H/75 MHz ^{13}C HMQC NMR of **19p**. ^{1}H and ^{13}C NMR correlations are shown for the major oxazolidine isomer.

A significant portion of the enaminones **19p-q** underwent hydrolysis to the ketone in aqueous acid at 0ºC, as evidenced by the identification of **23** and **24** in product mixtures by mass spectrum library match (Wiley 6 library, 92%). Aromatic ^{1}H NMR signals at δ 6.73 and 5.82 and a molecular ion *m/z* 245 in GC-MS spectrum confirmed the presence of the furan structure (1*R*,2*S*)-2-(*N*-methyl-*N*-(5-methylfuran-3-yl)amino)-1-phenylpropan-1-ol (**5q**) (Appendix 2.10) and separation of the ephedrine impurity by rapid flash column chromatography using Et_2O on silica was successful, although always accompanied by some decomposition of the furan. Decomposition was indicated by a bright red colour and was noticed when the column was run too slowly, or at temperatures higher than STP. The workup procedure was modified by quenching the TFA/DCE deprotection mixture with ice-cold 5 M NaOH solution, directly in a separating funnel followed by vigorous mixing. The solution changed from a deep red colour when initially agitated, to a very pale yellow colour when the cyclization was complete. This led to quantitative recovery of cyclised product **5q**, however under conditions required for cyclization, some THP- group migration to the benzylic oxygen occured to produce **5q-THP** (Scheme 2.40) as indicated by the characteristic H(2''') methine signal at δ 4.41 and broad aliphatic signals at δ 1.66 - 1.44 in ^{1}H NMR, and *m/z* 85 fragment ion in GCMS analysis (Appendix 2.10).

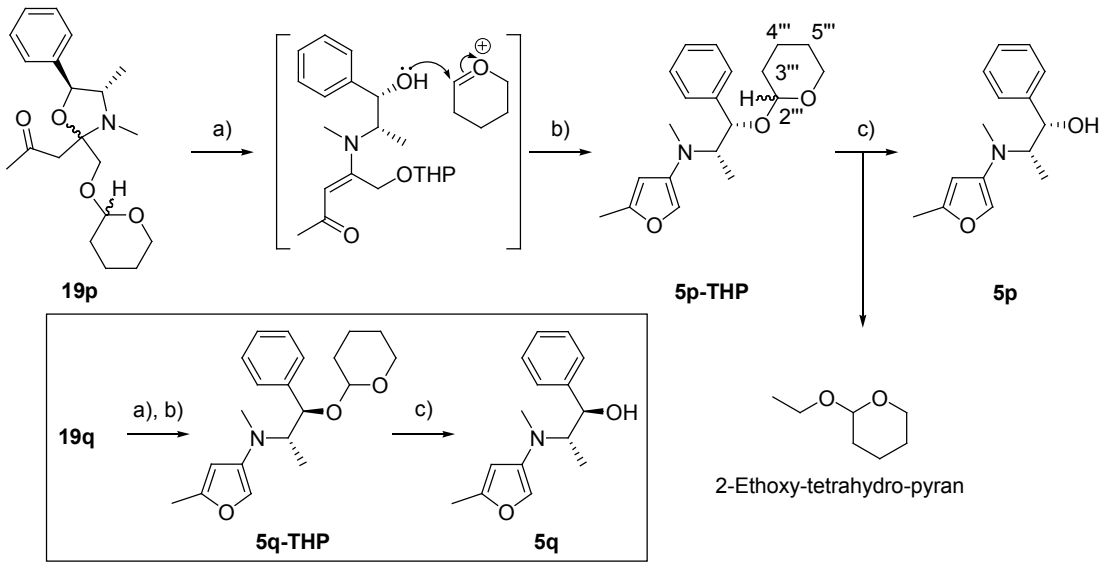

a) TFA, DCE b) Aq. 5 M NaOH, 0ºC c) *p*-TsOH, EtOH, 60^{o}C, >97%

Scheme 2.40: Cyclization of the oxazolidines **19p-q** using TFA, followed by THP deprotection in EtOH provided the ephedrine and pseudoephedrine substituted furans **5p** and **5q** in high yields.

On treatment with TFA the ephedrine derived furan **19p** gave complete migration of the THP group to form <97% **5p-THP** (Scheme 2.40) according to GC-MS signal integration although molecular ions were absent for both **5p-THP** and **5q-THP**. Complete THP deprotection was achieved by heating at

60ºC with *p*-toluenesulphonic acid in ethanol. Furan products **5p-5q** were stable in aqueous acid at 0ºC and purified by extraction into cold ice-cold 2 M HCl, washing the aqueous solution with DCM to remove the 2-ethoxytetrahydropyran, then basification to pH 14 with ice-cold 3 M NaOH (Scheme 2.40). Extraction with DCM provided 96% isolated yield of **5p** and **5q** in >98% purity by ^{1}H NMR and GC-MS analysis and the products were stable for long periods upon storage at -18°C. ^{1}H and ^{13}C NMR data is presented in Figure 2.18 for the furan **5p** along with mass fragmentation data.

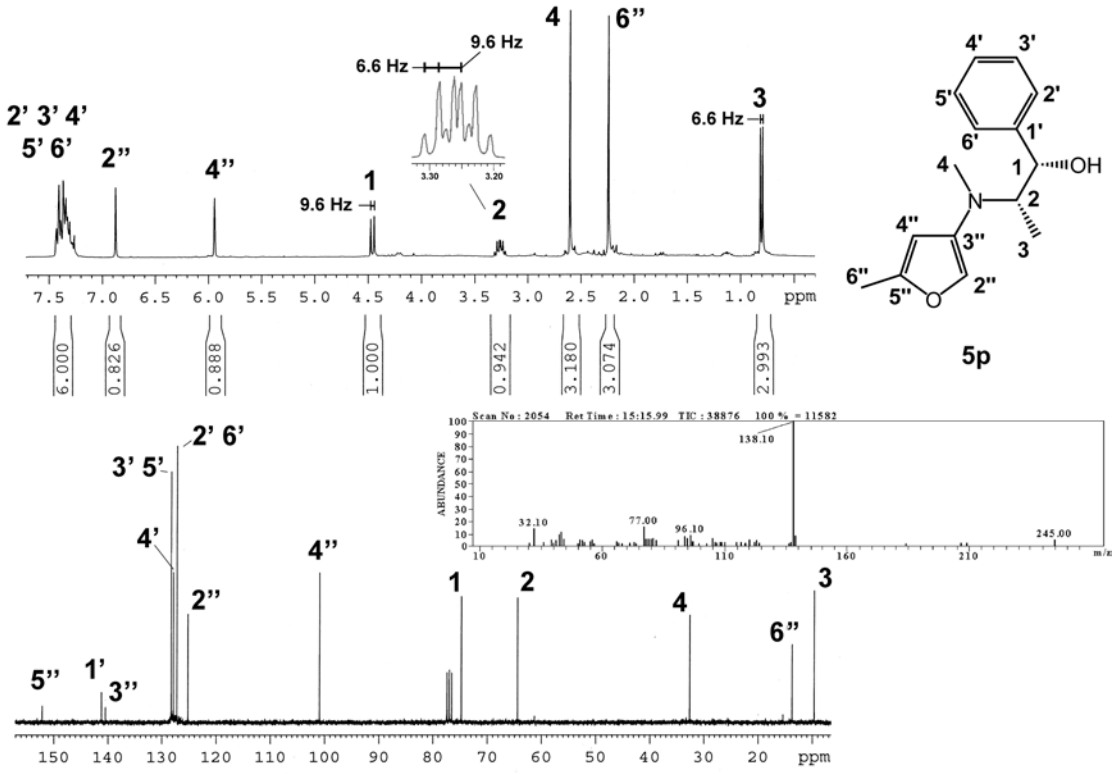

Figure 2.18: 300 MHz ^{1}H and 75 MHz ^{13}C NMR data for (1*S*,2*S*)-2-(*N*-methyl-*N*-(5-methylfuran-3-yl)amino)-1-phenylpropan-1-ol **5p** showing. The mass spectrum of **5p** shows a molecular ion at *m/z* 245.

In the ^{1}H NMR of **5p** (Figure 2.18) a double quartet is observed for the H(2) proton at δ 3.26 ($J_{2,3}$ = 9.6 Hz, $J_{2,1}$ = 6.6 Hz) with coupling to doublets at δ 4.46 and 0.80 corresponding to the H(1) ($J_{1,2}$ = 9.6 Hz) and H(3) ($J_{1,3}$ = 6.6 Hz) doublets at respectively. Aromatic ^{1}H NMR furan signals are seen at δ 6.87 for H(2'') and δ 5.94 for H(4'') and are at typical chemical shifts for the 5-methyl-3-aminofuran substitution pattern. The low intensity C(5'') and C(3'') ^{13}C NMR quaternary signal are observed at δ 152.5 and 140.8 respectively and the aromatic methyl C(6'') at δ 14.1 is accompanied by an expected ^{1}H NMR singlet H(6'') at δ 2.25. The three protons from the nitrogen methyl H(4) appear as a singlet at δ 2.60 and the C(4) signal can be assigned to the ^{13}C NMR peak at at δ 33.0 in close agreement with Chemdraw predictions. The experimental protocol for the preparation of **5p-q** is included in Section 6.5.2 with a listing of NMR characterization data.

Chapter 2

Synthesis of 3-Furylamines: References

[1] W. Eberbach, In *Houben-Weyl Methoden der Organischem Chemie*, (5th Ed.), Vol. E6a, Thieme: Stuttgart, **1994**, 16.

[2] Y. Kobayashi, M. Nakano, C. Biju Kumer, K. Kishihara. "Efficient Conditions for Conversion of 2-Substituted Furans into 4-Oxygenated 2-Enoic Acids and Its Application to Synthesis of (+)-Aspicilin, (+)-Patulolide A, and (-)-Pyrenophorin", *Journal of Organic Chemistry*, **1998**, *63*, 7505-7515.

[3] T. H. Brown, M. A. Armitage, R. C. Blackmore, P. Blurton, G. J. Durant, C. R. Ganellin, R. G. Ife, M. E. Parsons, D. A. Rawlings, B. P. Slingsby, *European Journal of Medicinal Chemistry*, **1990**, *25*, 217-226.

[4] D. K. Barma, A. Kundu, R. Baati, C. Mioskowski, J. R. Falck, "A Convenient Preparation of 3-Substituted Furans: Synthesis of Perillene and Dendrolasin", *Organic Letters*, **2002**, *4*, 1387-1389.

[5] S. Ma, L. Li. "Palladium-Catalyzed Cyclization Reaction of Allylic Bromides with 1,2-Dienyl Ketones. An Efficient Synthesis of 3-Allylic Polysubstituted Furans", *Organic Letters*, **2000**, *2*, 941-944; C-C. Pai, R-S. Liu, "Enantiocontrolled Construction of Tricyclic Furan Derivatives via an Asymmetric Diels-Alder Reaction", *Organic Letters*, **2001**, *3*, 1295-1298; F. Stauffer, R. Neier, "Synthesis of Tri- and Tetrasubstituted Furans Catalyzed by Trifluoroacetic Acid", *Orgamic Letters*, **2000**, *2*, 3535-3537.

[6] J. McMurry. "Organic Chemistry", (4th Ed.), Brooks and Cole publishing, U.S.A., **1996**, 500-501, 762. ISBN 0-534-23832-7.

[7] J. March. "Advanced Organic Chemistry: Reactions, Mechanisms and Structure", (4th Ed.), John Wiley and Sons, N.Y., **1992**, 30, 45, 228, 1091-1093, 795-796, 741-742. ISBN 0-471-58148-8.

[8] B. S. Furniss, A. J. Hannaford, P. W. G. Smith, A. R. Tatchell. "Vogel's Textbook of Practical Organic Chemistry", (5th Ed.), Longman Group, U.K. Ltd., **1989**, 1146-1148. ISBN 0-582-46236-3.

[9] J. D. Roberts, M. C. Caserio. "Basic Principles of Organic Chemistry", W. A. Benjamin Inc., New-York, **1964**, 998.

[10] N. Bodor, M. J. S. Dewar, A. J. Harget. "Ground States of Conjugated Molecules. XIX. Tautomerism of Heteraromatic Hydroxy and Amino Derivatives and Nucleotide Bases", *Journal of the American Chemical Society*, **1970**, *92*, 2929-2936.

[11] I. G. John, L. Radom. "Conformations, Stabilities, and Charge Distributions in 2- and 3-Monosubstituted Furans. An ab initio Molecular Orbital Study", *Journal of the American Chemical Society*, **1978**, *100*, 3981-3991.

[12] M. A. Shokhen, V. G. Andrianov, A. V. Eremeev, S. V. Barmina. "Dependence of the reactivity of five membered aromatic heterocycles on their structure. 2: Effect of aza substitution on the proton affinity of aminofurans", *Khimiya Geterotsiklicheskikh Soedinenii*, **1987**, *2*, 175-178.

[13] R. Kuhn, G. Krüger. "Das Chromogen III Der Morgan-Elson-Reaktion", *Chemie Berichte*, **1957**, *90*, 264-277.

[14] R. R. Burtner. "Orientation in the Furan Nucleus. VIII. β-Acylaminofurans", *Journal of the American Chemical Society*, **1934**, *56*, 666-667; H. M. Singleton, W. R. Edwards. "Preparation and Properties of Some Derivatives of 2-Aminofuran". *Journal of the American Chemical Society*, **1938**, *60*, 540-544.

[15] J. D. Prugh, W. C. McCarthy. "Heterocyclic Amines III. 3-Dimethylaminofuran", *Journal of Medicinal Chemistry*, **1966**, *9*, 254-255.

[16] R. Kuhn, G. Krüger. "3-Acetamino-furan aus *N*-Acetyl-D-glucosamin; ein Beirag zur Theorie der Morgan-Elson-Reaktion", *Chemie Berichte*, **1956**, *6*, 1473-1486 and references therein; S. F. Mason. "The Tautomerization of *N*-Heterocyclic Hydroxy-Compounds. Part II. Ultraviolet spectra", *Journal of the Chemical Society*, **1957**, 5010-5017.

[17] T. Shioiri, K. Ninomiya, S. Yamada. "Diphenylphosphoryl azide. New convenient reagent for a modified Curtius reaction and for peptide synthesis", *Journal of the American Chemical Society*, **1972**, *94*, 6203-6205.

[18] M. M. Campbell, A. D. Kaye, M. Sainsbury, "3-Acylamino Furan", *Tetrahedron*, **1982**, *38*, 2783-2786.

[19] D. T. Davies. "Aromatic Heterocyclic Chemistry", Oxford University Press, N.Y., **1997**, 14-17. ISBN: 0-19-855660-8.

[20] B. T. Freure, J. R. Johnson. "The Structure of Nitrofuran and the Mechanism of Nitration in the Furan Series", *Journal of the American Chemical Society*, **1931**, *53*, 1142-1147.

[21] A. Padwa, M. Dimitroff, A. G. Waterson, T. Wu. "Diels-Alder Reaction of 2-Amino-Substituted Furans as a Method for Preparing Substituted Anilines", *Journal of Organic Chemistry*, **1997**, *62*, 4088-4096.

[22] J. M. Tedder, A. Nechvatal, A. W. Murray, J. Carnduff. "Basic Organic Chemistry: Part 3", John Wiley and Sons Ltd., London, **1970**, 96-97. ISBN: 0-471-85013-6.

[23] L. C. Raiford, W. G. Huey, "Reduction of the 2-nitrophenyl esters of certain acids", *Journal of Organic Chemistry*, **1941**, *6*, 858-866.

[24] Y. L. Gol'dfarb, Y. B. Vol'kenshtein, B. V. Lopatin. "Bromination and Chloromethylation of Thiophen-2-aldehyde In the Presence of an Excess of Aluminium Chloride", *Zhurnal Obshchei Khimii*, **1964**, *34*, 969-977.

[25] D. J. Chadwick, J. Chambers, D. Meakins, R. L. Snowden. "Esters of Furan-, Thiophen- and *N*-Methylpyrrole-2-carboxylic Acids, Bromination of Methyl Furan-2-carboxylate, Furan-2-carbaldehyde, and Thiophen-2-carbaldehyde in the Presence of Aluminium Chloride", *Journal Chemical Society Perkin Transactions I*, **1973**, 1766-1773.

[26] R. Antonioletti, M. D'Auria, A. De Mico, G. Piancatelli, A. Scettri. "Photochemical Synthesis of 3- and 5-Aryl-2-furyl Derivatives", *Journal of the Chemical Society, Perkins Transactions I*, **1985**, 1285-1288.

[27] A. F. Shepard, N. R. Winslow, J. R. Johnson. "The Simple Halogen Derivatives of Furan", *Journal of the American Chemical Society*, **1930**, *52*, 2083-2090.

[28] A. Togni, H. Grützmacher. "Catalytic Heterofunctionalization", Wiley-VCH Verlag., **2001**, ISBN: 3-527-30234-4.

[29] H. Tomori, J. M. Fox, S. L. Buchwald. "An Improved Synthesis of Functionalized Biphenyl-Based Phosphine Ligands", *Journal of Organic Chemistry*, **2000**, *65*, 5334-5341.

[30] J. P. Wolfe, H. Tomori, J. P. Sadighi, J. Yin, S. L. Buchwald. "Simple, Efficient Catalyst System for the Palladium-Catalyzed Amination of Aryl Chlorides, Bromides and Triflates", *Journal of Organic Chemistry*, **2000**, *65*, 1158-1174.

[31] M. C. Harris, S. L. Buchwald. "One-Pot Synthesis of Unsymmetrical Triarylamines from Aniline Precursors", *Journal of Organic Chemistry*, **2000**, *65*, 5327-5333.

[32] R. Antonioletti, M. D'Auria, A. De Mico, G. Piancatelli, A. Scettri. "Photochemical Synthesis of 3- and 5-Aryl-2-furyl Derivatives", *Journal of the Chemical Society, Perkins Transactions I*, **1985**, 1285-1288. **find paper specifically for 5-bromofuraldehyde.

[33] Y. L. Gol'dfarb, L. D. Tarasova. "Synthesis of 2,4-Disubstituted Furans", *Doklady Akademii Nauk SSSR*, **1965**, *163*, 1393-1396.

[34] D. Todd. "The Wolff-Kishner Reduction, *Organic Reactions*, **1948**, *4*, 378-422; Huang-Minlon. "A Simple Modification of the Wolff-Kishner Reduction", *Journal of the American Chemical Society*, **1946**, *68*, 2487-2488.

[35] B. Majoie. "2,3-Dibromofuran by Bromination of Furancarboxaldehydes", Societe de Recherches Industrielles ("SORI"), Patent U.S. 3,714,197, (**1971**), CAN: 74:76318, AN: 1971:76318.

[36] Katsumura, S., Ichikawa, K., Mori, H. "Synthesis of Tetrasubstituted Butenolide, Bromobeckerelide by Regioselective Lithiation of Furan Followed by Photosensitized Oxygenation of α-Silylfuran", *Chemistry Letters*, **1993**, *9*, 1525-1528.

[37] T. Cohen, R. A. Schambach. "Copper-quinoline decarboxylation", *Journal of the American Chemical Society*, **1970**, *92*, 3189-3190.

[38] H. Gilman, G. F. Wright. "Furan Mercurials". *Journal of the American Chemical Society*, **1933**, *55*, 3302-3313.

[39] J. P. Wolfe, S. L. Buchwald. "Scope and Limitations of the Pd/BINAP catalyzed amination of aryl bromides". *Journal of Organic Chemistry*, **2000**, *65*, 1144-1157.

[40] F. E. Goodson, S. I. Hauck, J. F. Hartwig. "Palladium-Catalyzed Synthesis of Pure, Regiodefined Polymeric Triarylamines". *Journal of the American Chemical Society*, **1999**, *121*, 7527-7539 and references therein.

[41] V. Farina. "Comprehensive Organometallic Chemistry", (2nd Ed.), Pergamon Press, Oxford, **1995**, *Vol. 12*, 160-240.

[42] A. M. Redman, J. Dumas, W. J. Scott. "Preparation of 5-Substituted 3-Aminofuran-2-Carboxylate Esters", *Organic Letters*, **2000**, *2*, 2061-2063.

[43] C. Ma, H. Ding, G. Wu, Y. Yang. "Facile Synthesis of Highly Substituted 3-Aminofurans from thiazolium Salts, Aldehydes and Dimethyl Acetylene Dicarboxylate", *Journal of Organic Chemistry*, **2005**, *70*, 8919-8923.

[44] S. Mageswaran, W. D. Ollis, D. A. Southam, I. O. Sutherland, Y. J. Thebtaranonth. "Base Catalysed Rearrangements Involving Ylide Intermediates. Part 11. Rearrangements of 3-Phenylprop-2-ylnylammonium Ylides", *Journal of the Chemical Society Perkin Transactions 1*, **1981**, 1969-1980.

[45] J. Ficini, M. Claeys, J. C. Depezau. "Sur une synthese inattendue d'amino-3 furannes", *Tetrahedron Letters*, **1973**, 14, 3353-3355.

[46] J.-N. Cui, T. Ema, T. Sakai, M. Utaka. "Control of Enantioselectivity in the Bakers Yeast Asymmetric Reduction of γ-Chloro-β-diketones to γ-Chloro-(*S*)-β-hydroxy ketones", *Tetrahedron: Asymmetry*, **1998**, *9*, 2681-2692.

[47] J.K. Seydel, E.R. Garrett, W. Diller, K.J. Schaper. "5-Methyl-3(2H)furanone from Acid Catalyzed Solvolysis of 2-Deoxy-D-Ribose", *Journal of Pharmaceutical Sciences*, **1967**, *56*, 858-862.

[48] A. Hofmann, W. v. Philipsborn, C. H. Eugster. NMR. "Untersuchungen an einfachen Furenidon system. Synthese des unsubstituierten Δ^2-Furenidons-(4) (β-Hydroxyfuran)", *Helvetica Chimica Acta*, **1965**, *48*, 1322-1331.

[49] B. P. Gusev, V. F. Kucherov. "Reaction of Diacetylenic Glycols with Amines", *Izvestiya Akademii Nauk SSSR, Seriya Khimicheskaya,* **1974**, *1*, 206-208.

[50] K. Bowden, E. A. Braude, E. R. H. Jones, B. C. L. Weedon. "Research on Acetylenic Compounds. Part II. (A) The Addition of Amines to Ethynyl Ketones. (B) Auxochromic

Properties and Conjugating Power of the Amino Group", *Journal of the Chemical Society*, **1946**, 45-52.

[51] I. M. Heilbron, E. R. H. Jones, P. Smith, B. C. L. Weedon. "Researches on Acetylenic Compounds. Part IV. The Hydration of Some Acetylentlcarbinols Derived from α,β-Unsaturated Aldehydes", *Journal of the Chemical Society*, **1946**, 54-58.

[52] E. Duranti, C. Balsamini. "Synthesis of 4-Oxo-2-alkyn-1-ols", *Synthesis*, **1974**, 357-358.

[53] H. B. Henbest, E. R. H. Jones, I. M. S. Walls. "Researches on Acetylenic Compounds. Part XXVI. Further Reformatsky Reactions with Propargyl Bromides", *Journal of the Chemical Society*, **1950**, 3646-3650.

[54] E. Pretsch, P. Bühlmann, C. Affolter. "Structure Determination of Organic Compounds: Tables of Spectral Data", Springer-Verlag, New York, **2000**, 358-360, 323-324. ISBN: 3-540-67815-8.

[55] M. Journet, D. Cai, L. M. di Michele, R. D. Larsen. "Highly Efficient Synthesis of α,β-Acetylenic Aldehydes From Terminal Alkynes Using DMF As the Formylating Reagent", *Tetrahedron Letters*, **1998**, *39*, 6427-6428.

[56] J. P. Michael, C. B. de Koning, D. Gravestock, G. D. Hosken, A. S. Howard, C. M. Jungmann, R. W. M. Krause, A. S. Parsons, S. C. Pelly, T. V. Stanbury. "Enaminones: Versatile Intermediates for Natural Product Synthesis", *Pure and Applied Chemistry*, **1999**, *71*, 979-988.

[57] R. Bruckner. "Advanced Organic Chemistry: Reaction Mechanisms". Hardcourt Press, California, **2002**, 415. ISBN: 0-12-138110-2.

[58] J. B. Lambert, E. P. Mazzola. Nuclear Magnetic Resonance Spectroscopy: An Introduction to Principles, Applications and Experimental Methods, Prentice Hall publishing, New Jersey, **2003**, 115. ISBN 0130890669.

[59] R. H. Schlessinger, T. R. R. Pettus, J. P. Springer, K. Hoogsteen. "Diastereoselective Diels-Alder reactions Using Furan Substituted with a Nonracemic Amine", *Journal of Organic Chemistry*, **1994**, *59*, 3246-3247.

[60] R. H. Schlessinger, C. P. Bergstrom. "Enantioselective Synthesis of (+)-Cyclophellitol", *Journal of Organic Chemistry*, **1995**, *60*, 16-17.

[61] D. Enders, H. Eichenauer. "Assymetrische Synthesen via metallierte chirale Hydrazone. Enantioselective Alkylierung von cyclischen Ketonen und Aldehyden", *Chemie Berichte*, **1979**, *112*, 2933-2960.

[62] R. B. Walker, D. S. Moore, M. D. Massey. "Mass Spectra of Some Oxazolidines Formed by Reaction of Ephedrine and Pseudoephedrine with Aliphatic Ketones", *Organic Mass Spectrometry*, **1989**, *24*, 345-346.

[63] J. B. Hyne. "Nuclear Magnetic Resonance Spectra and Configuration. The N.M.R. Spectra of Diastereoisomeric Heterocyclic Derivatives of the Ephedrines", *Journal of the American Chemical Society*, **1959**, *81*, 6058-6061.

[64] M. Johansen, H. Bundgaard. "Prodrugs as Delivery Systems. XXV: Hydrolysis of Oxazolidines - A Potential New Prodrug Type", *Journal of Pharmaceutical Sciences*, **1983**, *72*, 1294-1298; S. A. Soliman. "Estimation of the Dissociation Constants of Some Unstable Diastereomeric Oxazolidines of Ephedrine and Pseudoephedrine", *Canadian Journal of Pharmaceutical Sciences*. **1973**, *8*, 132-135.

Chapter 3

Diels-Alder Reactions of 3-Furylamines

3.1 The Diels-Alder Reaction

Otto Diels and Kurt Alder were the first two scientists to offer theoretical grounding for the [4π +2π] electron cycloaddition reaction, first mentioned in synthetic literature by Zincke in 1892-1912 [1] and later identified by von Euler in 1923 [2], nowdays called the "diene synthesis" or the Diels-Alder (D-A) reaction. Publication by Diels and Alder [3] on the theoretical considerations of the mechanism allowed the basic understanding necessary for organic chemists to apply D-A chemistry to synthesis. The D-A reaction has since become a versatile tool in organic chemistry for the preparation of functionalised six-membered rings and the principal researchers were awarded a Nobel Prize in 1950 for their contributions.

Mechanistically, the D-A reaction is considered to be a concerted pericyclic reaction with an aromatic transition state and the driving force is the formation of two new σ-bonds. The *classical* D-A reaction involves the formation of a six-membered ring by reaction of a conjugated 4π-electron system, called the 'diene' and a 2π-electron system called the 'dienophile'. No intermediate is involved in the bond making and breaking process, thus proceeding in a concerted fashion during which up to four stereogenic centres can be introduced simultaneously (Figure 3.1).

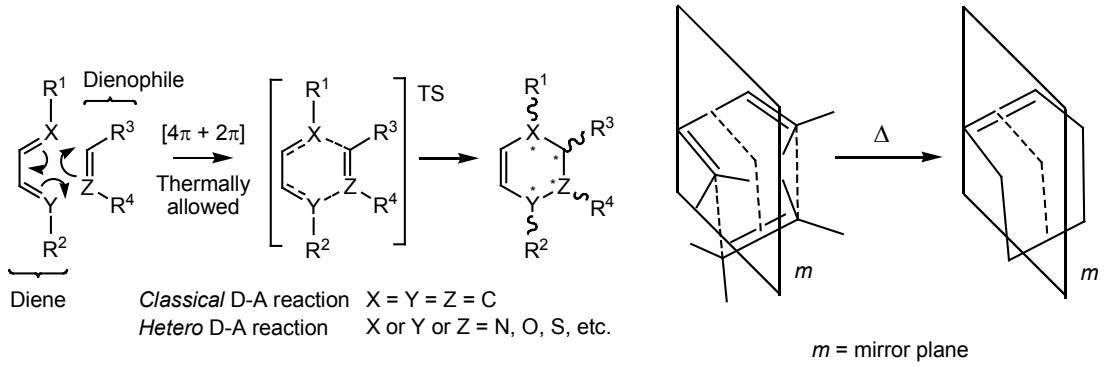

Figure 3.1: Diene and dienophile undergo a [4π + 2π] electron cycloaddition reaction, during which orbital symmetry is conserved with respect to the mirror plane *m*.

When either the diene or the dienophile contains sp^2 heteroatoms at the reactive positions in the conjugated system, labeled X, Y and Z in Figure 3.1, the cycloaddition reaction can proceed to give the

six membered heterocycle. In this way, the D-A reaction can also be used to form carbon-heteroatom or heteroatom-heteroatom bonds and in either case the reaction is called a *hetero* Diels-Alder reaction.

The understanding of pericyclic reactions was revolutionised in 1965 after Woodward and Hoffmann published a number of preliminary publications on the theoretical and experimental examination of concerted processes [4]. The authors inferred that concerted processes occur readily when frontier orbital symmetry of the reactants and products is conserved with respect to the mirror plane *m* (Figure 3.1). A thorough explanation of the conservation of orbital symmetry using a frontier molecular orbital (FMO) approach to explain thermally allowed [4π + 2π] concerted processes was published in 1969 [5] and has formed the basis for organic chemists to rationalise the production of isomers from D-A reactions. The versatility of D-A chemistry was greatly enhanced by the predictive capability of the orbital symmetry approach and is now one of the most widely used synthetic methods in organic chemistry, providing a direct route to highly functionalised ring systems such as those found in carbohydrate and terpenoid structures [6]. In Section 3.1.1 a short discussion on the use of simple Hückel molecular orbital theory (SHMO) in the quantitative prediction of regiochemical outcomes is presented, highlighting the role of FMOs in determining the reactivity of dienes and dienophiles. A short review is also given on the popular methods for rate and regioselectivity enhancement in D-A chemistry followed by a description of strategies for enantioselectivity in D-A chemistry.

3.1.1 Application of MO-Theory to the Prediction of Regiochemical Outcomes

Simple Hückel molecular orbital theory (SHMO) is a reliable method to describe the reactivity between planar conjugated π-systems. Reactive dienes must be able to form a *cis* or quasi *cis* conformation of the diene system [7] and participating MOs can be formed from the linear combination of atomic orbitals (LCAO) and must be symmetric or antisymmetric with respect to the mirror plane [5]. Basic assumptions for the use of MO theory have been outlined by Gimarc [8] and suggest that only the unhybridised valence electrons need to be considered in the analysis of the olefinic reagents. Contributions by Fukui [9] and Houk [10] have established that the FMO HOMO and LUMO determine the reactivity of the Diels-Alder system. The reaction between π-electron systems is determined by the magnitude of constructive HOMO/LUMO orbital overlap and is most efficient for reagent orbitals that are closest in energy.

Analysis of solutions to the electronic Schrödinger equation provides a description of the distribution of electrons and the discrete energy of electrons with that distribution. The time independent

Schrödinger equation for the electronic wave function using the Born Oppenheimer approximation is shown in Equation 3.1,

$$\hat{H}\Psi = E\Psi \tag{3.1}$$

where $\hat{H}$ is the Hamiltonian operator and describes the motion of N electrons, Ψ is the electronic wave-function and E is the electronic energy expressed as an eigenvalue. Qualitative molecular orbital theory can be applied using the Hückel approximations to provide π-system eigenvalues and π-orbital coefficients. The total energy of the molecule is taken as the sum of individual valence electron orbital energies and the Fock operator (F) is approximated to the effective Hamiltonian (h^{eff}). The Hückel independent electron assumption (IEA) is used to describe the unhybridised π-orbitals where N_N = the number of orbitals (Equation 3.2) and electron-electron interactions are ignored.

$$F(1) \approx h^{eff}(1) \qquad h^{eff}(1)\phi_a(1) = \varepsilon_a\phi_a(1) \qquad E_{IEA} = 2\sum_{a=1}^{M}\varepsilon_a \tag{3.2}$$

$$\phi(1) = \sum_{A=1}^{N_N} C_A\chi_A(1) \qquad \int \chi_A(1)\chi_B(1)d\tau_1 = \delta_{AB} \tag{3.3}$$

Since only the unhybridised orbitals are considered, overlap between adjacent π orbitals is approximated to zero. Using computational software [11] the calculated energy is expressed as an expectation value of the MO (Equation 3.3), the effective Hamiltonian is differentiated with respect to the coefficient C_A to give Equation 3.4 and the matrix elements are diagonalised as shown in Equation 3.5. Derivations of the Equations 3.2 to 3.5 are described in Rauk [7] and the number of matrix elements in the determinant goes up quadratically as the number of basis orbitals increases.

$$(h_{AA} - \varepsilon)C_A + \sum_{B\neq A}^{N_N} h_{BA}C_B = 0 \quad \text{for each A} = \{1,\ldots,N_N\} \tag{3.4}$$

$$\begin{vmatrix} h_{11}-\varepsilon & h_{12} & h_{1N_N} \\ h_{21} & h_{22}-\varepsilon & h_{2N_N} \\ h_{N_N1} & h_{N_N2} & h_{N_NN_N}-\varepsilon \end{vmatrix} = 0 \tag{3.5}$$

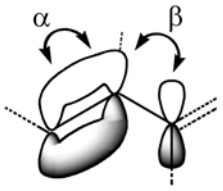

The diagonal matrix elements h_{AA} are designated the term α and describe the energy of an electron in the 2p orbital of an sp^2 hybridised carbon atom. The off-diagonal matrix elements h_{AB} are

designated the term β and represent the energy of interaction between two 2p orbitals of sp^2 carbon atoms which are attached by a σ bond. Energy levels of bonding and antibonding orbitals are expressed relative to α in energy scale in units of $|\beta|$. Interaction diagrams are presented by representing π orbitals of SHMO theory on the same energy scale as σ, σ* and non-bonding orbitals to visually represent the mixing of orbitals to form the product. Although this approach is not strictly theoretically accurate, molecular orbital energy diagrams can be used to gain an understanding of the interacting orbitals during the formation of new sp^3 σ bonds.

The conservation of orbital symmetry in pericyclic reactions is best summarised by the paraphrase from Woodward and Hoffmann, "The characteristic of concerted processes is that it is possible to transform continuously the molecular orbitals of reactants into products in such a way as to preserve the bonding character of all occupied orbitals at all stages of the reaction." [10]. This is exemplified by the simplest reaction between 1,3-butadiene and ethylene presented in the interaction diagram (Figure 3.2) using SHMO energy levels. In this symmetry allowed process, no bonding energy level moves to a higher energy level that crosses the energy gap E_0, to correlate to an antibonding level. The [4π+2π] cycloaddition reaction is under thermal control and is photochemically forbidden [5].

The D-A reaction of 1,3-butadiene and ethane is difficult, requiring high temperatures and pressures (185ºC, 125 bars, 36 h) [12] but has been shown experimentally to proceed in a concerted fashion [11]. The HOMO of butadiene and LUMO of ethylene are antisymmetric (A) and orbital overlap via a boat-like transition state leads to the formation of a new σ bond between these orbitals. The ease of electron delocalisation between these orbitals determines the reactivity of the system. The HOMO of ethylene and LUMO of butadiene also stabilise the interactive overlap and are both symmetric (S) with respect to *m*, with symmetry being retained throughout the reaction to give constructive overlap in the new bond. FMO considerations for two such interacting systems have been discussed by Fukui [13] using second order perturbation theory and indicate that the larger the orbital overlap and smaller the energy level separation ($\Delta E_{HOMO/LUMO}$) of the two overlapping HOMO/LUMO orbitals, the larger the contribution of the orbital pair to stabilization of the system.

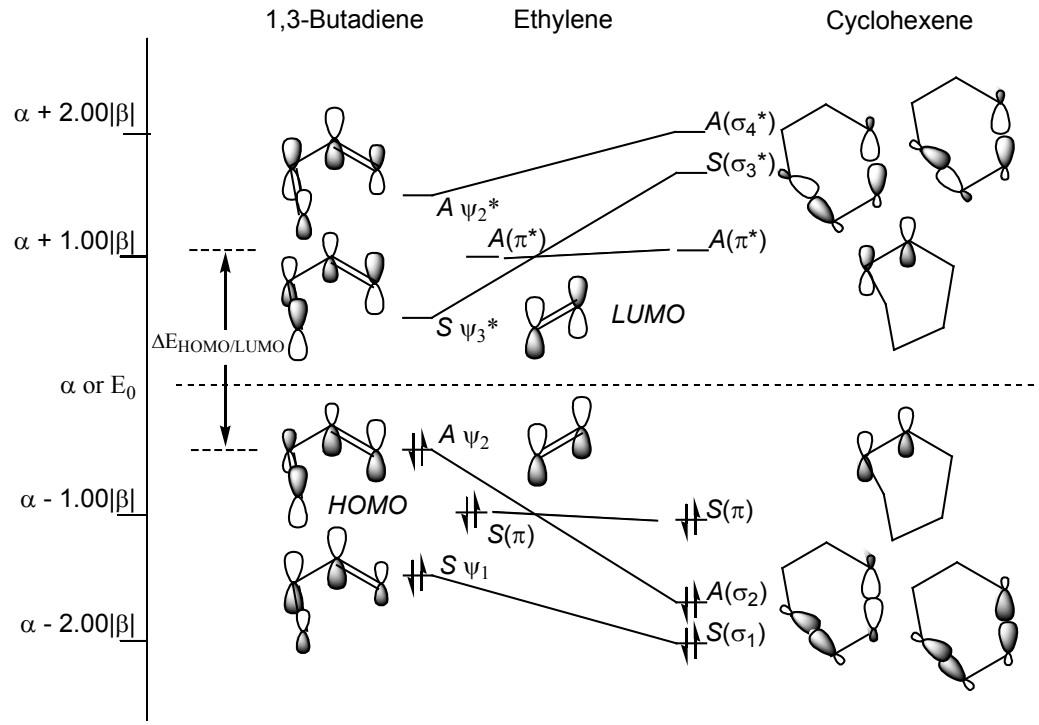

Figure 3.2: Interaction diagram of ethylene and 1,3-butadiene to form cyclohexene using SHMO energy level approximations.

Decreases in the energy gap are hence accompanied by increases in reaction rate or changes in isomeric composition. The incorporation of EWG or EDG into D-A reactants causes polarization of the frontier orbitals and corresponding changes in energy levels and orbital coefficients at the reactive olefin centers. Reagents containing EDG or EWG are sometimes called 'activated' dienes and dienophiles. Theoretical studies on the polarization effect of substituents has been documented by Gleiter *et al.* [14] who emphasise that interaction between two large and two small MOs is more efficient than the interaction of four FMOs of the same size.

When the FMO gap between reactants is large, side reactions can predominate in progressive attempts to force the reaction towards completion. A decrease in the energy gap can be achieved by the incorporation of one or more EDG in the diene, thus leading to an increase in HOMO energy levels, and the incorporation of one or more EWG in the dienophile to produce a corresponding decrease in LUMO energy. This is referred to as a *normal* electron demand activation. The effect of an amine as an example of an EDG at C(1) or C(2) of the 1,3-butadiene chain can be modeled using SHMO approximations and the relative coefficient magnitude and symmetry of the frontier HOMO orbitals are represented using shaded and un-shaded circles, generated using software written by Cannings [11]. Similarly the effect of a carboxyl EWG on the dienophile LUMO energy can be shown on the same scale, demonstrating the role of activating groups in decreasing the frontier orbital energy gap (Figure 3.3, left).

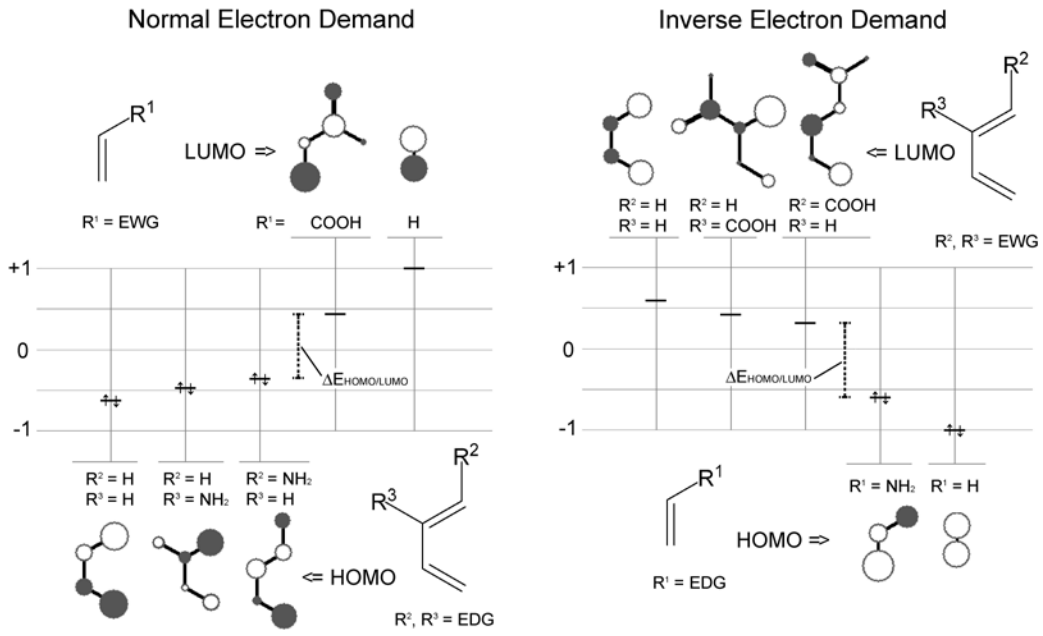

Figure 3.3: Differences in FMO energy levels between neutral and activated dienes and dienophiles are exemplified by SHMO energy diagrams of reactants incorporating an amine EDG ($R^x = NH_2$) and carboxyl EWG ($R^x = COOH$). Magnitudes of orbital coefficients are represented by the shaded and un-shaded circles.

Inverse electron demand D-A reactions involve the LUMO of the diene and the HOMO of the dienophile, therefore the incorporation of an EDG in the diene and EWG in the dienophile is necessary to provide a decreased activation energy for the concerted process. This is also illustrated in Figure 3.3, right, using the same activating substituents. Reactions between reactants without activating substituents, e.g. ethylene and butadiene, are called neutral D-A reactions.

FMO magnitudes of furan and 1,3-butadiene are symmetrical with respect to *m* in contrast to the C(1) and C(2) substituted examples shown in Figure 3.3 and the 3-furylamine dienes. The incorporation of substituents into the D-A reagents provides two possible regioisomeric products, and approaches towards the prediction of regioselectivity have involved the use of FMO Hückel coefficients with some success [15, 16]. Analysis of constructive overlap of HOMO and LUMO lobes for symmetry allowed MOs indicates preferential overlap for coefficients that are closest in energy [9]. The greater the difference between orbital coefficients of the reactive olefin carbons, the more regio-selective the cycloaddition will be. Polarization of the frontier orbitals in activated dienes and dienophiles of both inverse and normal demand (Figure 3.4) provide *ortho*/*para* substitution in the final product for monosubstituted reactants.

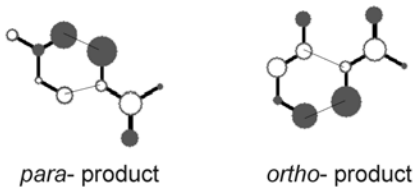

Figure 3.4: Magnitudes of FMO coefficients indicate that the *para* product is favored in the reaction between the C(2) aminobuta-1,3-diene and acrylic acid. The *ortho* product is favored in the reaction between C(1) aminobuta-1,3-diene and acrylic acid.

In this study, appropriate reagents were chosen to model the D-A reaction between the 3-furylamines **5** and methyl acrylate (MAC) by considering only the core skeletons of the reacting species, namely 3-aminofuran and acrylic acid. 3-Aminofuran is an activated furan as observed from a calculated increase in HOMO energy level, represented in the SHMO diagram in Figure 3.5. Additional increases in reactivity can be expected from the π-donor effect of the amine contributing towards a decrease in aromatic stabilization, as discussed in Section 2.1.1 Symmetry allowed orbital diagrams were constructed and computationally derived Hückel energies [11] are shown in Figure 3.5 for the interacting HOMO/LUMO orbitals.

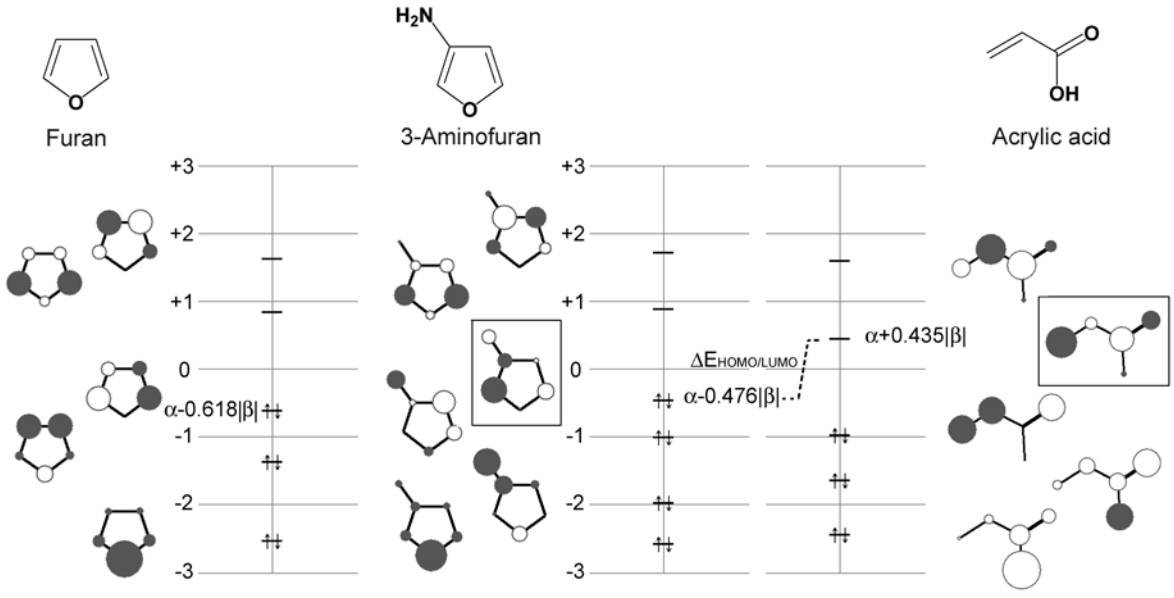

Figure 3.5: Simple Hückel orbital diagram for furan, and model reagents 3-aminofuran and acrylic acid. The energy gap between FMOs involved in the concerted pericyclic D-A pathway is indicated.

In the [4π+2π] transition state involving activated reactants, overlap between lobes possessing the largest coefficients contribute a larger degree of σ bond formation [15], demonstrating a degree of asynchronicity in the reaction of activated adducts. During the asynchronous process, the σ bonds are simultaneously but dissymmetrically formed and bond formation is dependent on the ability of the substituents to stabilise the charge on each reactant at the transition state [17]. Although a small $\Delta E_{HOMO/LUMO}$ leads to enhanced reactivity and thermodynamically stable products, reagents and intermediates may be chemically amphoteric and self-reactive. Prediction of regiochemical outcome in the D-A product between 3-aminofuran and acrylic acid using frontier orbital coefficients indicates constructive overlap and closely matched coefficient values when substituents are in the *para* orientation (Figure 3.6). This provides antisymmetric overlap with respect to *m*, whereas the *meta* orientation does not conserve orbital symmetry in the product and has non-constructive overlap indicated by large differences in coefficients.

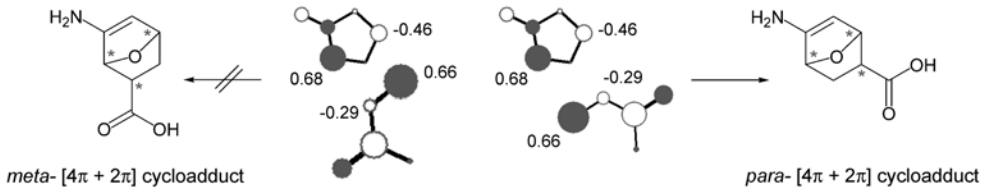

Figure 3.6: Regioprediction by comparison of FMO orbital overlap using simple Hückel coefficients indicates the *para* isomer as the favored product for the reaction between 3-aminofuran and methyl acrylate.

Sucessful regiochemical predictions have also been proposed based on matching electrophilicity of the diene and nucleophilicity of the dienophile [18]. MAC is considered a strong electrophile and has a larger LUMO coefficient at the β-position. In general, the terminus β to an alkyl or conjugating substituent has a larger HOMO coefficient, in which case the reactive portion of the furan provides the same regiochemistry as observed in the Hückel model. A review covering qualitative and quantitative theories that have successfully been used to model the D-A reaction are in literature by Ess *et al.* [17].

Bond formation in the D-A reaction is a suprafacial process that preserves the *cis* or *trans* conformation of the dienophile. Substituents in both diene and dienophile rotate in a disrotatory motion relative to each other to maintain orbital overlap symmetry and reactions can proceed *via* two possible suprafacial arrangements, named *endo* and *exo*, to provide a mixture of diastereomeric products. This concept is exemplified in Scheme 3.1 by the reaction between 3-aminofuran and acrylic acid. In the *endo* arrangement the bulkier sides of the reactants lie next to each other, and in the *exo* arrangement the dienophile substituents are geometrically distant from the diene system. The *endo* isomer is usually

formed in excess and this observation was originally justified by Alder and Stein [19] as a tendency of maximum accumulation of unsaturation, then later explained by Woodward and Katz [20] as the consequence of additional stabilization from secondary π-orbital interactions between the diene and carbonyl orbital. The *endo* compound has the substituent on the inside concave face of the bicyclic ring, however in most cases the *exo* isomer is the thermodynamically favored product as the substituent is pointed towards the convex face which is geometrically distant to the ring and contributes less steric energy. Salts and solvents can heavily influence D-A reaction kinetics and is discussed in the following section.

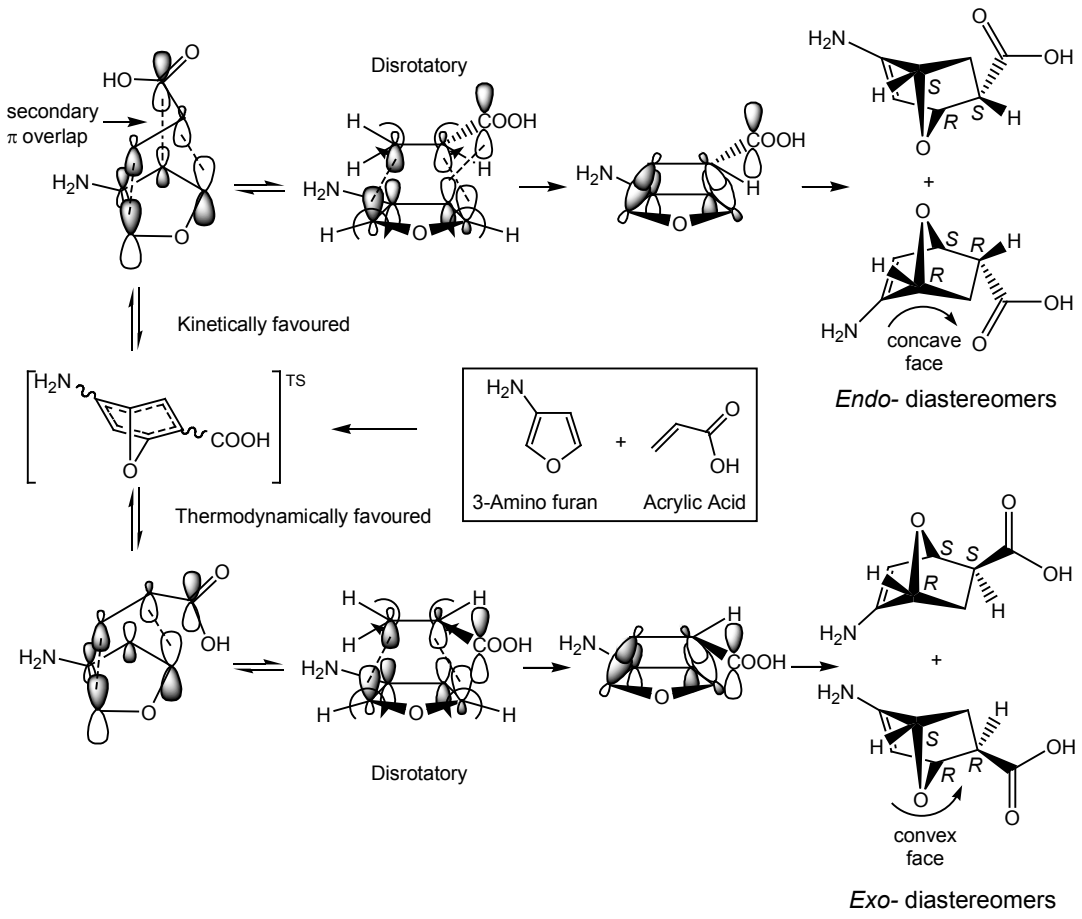

Scheme 3.1: The [4π+2π] electron cycloaddition is reversible and proceeds in a disrotatory manner with respect to substituents on the reactive carbons. Often the kinetically favoured *endo* diastereomer predominates due to secondary π-orbital interactions in which case the *exo* form is thermodynamically more stable due to steric considerations.

In most instances the Diels-Alder reaction is reversible with the retro Diels-Alder process leading to an equilibrium involving regeneration of the original reactants. This has been demonstrated experimentally by the interconversion of pure D-A regioisomers upon heating [21]. *Endo-exo*

isomerization of D-A adducts has been documented by Berson *et al.* [21,22] and is commonly observed in reactions involving stabilised transition states that have only small differences in free energy (~12 kJ/mol) [14]. Studies of the temperature dependence on diastereomeric ratios in reactions between cyclopentadiene and a range of acrylates [21] have been shown to closely fit the Arrhenius equation

$$\log(k_{endo}/k_{exo}) = \log(A_{endo}/A_{exo}) + (E_{exo} - E_{endo})/2.303RT \qquad (1.6)$$

where the product ratio *endo*/*exo* is equal to the specific rate coefficients k_{endo}/k_{exo}, A is the frequency factor and E is the activation energy [21]. Although not all reactants fit the Alder rule for the preference of *endo* isomer, Berson *et al.* demonstrated using linear free energy relationships a strong linear correlation between empirical solvent polarity and $\log(k_{endo}/k_{exo})$ [22]. The non-polar D-A diene, cyclopentadiene showed preference towards the *endo* cycloadduct with increasing solvent polarity in reactions with MAC, methyl methacrylate, and methyl *trans*-crotonate. The authors attribute the changes in reactivity to the occurrence of a greater permanent electric dipole in the *endo* transition state, which is stabilised by polar reaction media. More recent theoretical work by Schlachter *et al.* [23] supports these experimental findings, demonstrating that in the gas phase the *exo* product is favored and preference for the *endo* adduct is a result of solvation at the transition state.

D-A reactions with activated dienophiles containing conjugated EWG can undergo reactivity and regioselectivity improvement upon co-ordination of the carbonyl oxygen lone pair. Protonation or Lewis-acid complexation at the oxygen of an α,β-unsaturated carbonyl system increases the electron-withdrawing effect of the carbonyl group on the carbon-carbon double bond, resulting in lower MO energies and an enlarged terminal LUMO lobe [24]. Rate and selectivity enhancement in D-A chemistry has been heavily researched and approaches toward improvement in reaction efficacy are described in Section 3.1.2 along with a discussion addressing changes in diastereoselectivity with solvent polarity and the use of this concept in synthesis.

3.1.2 Rate and Selectivity Enhancements in Diels-Alder Reactions

D-A reactions that are slow or produce a number of isomers have been enhanced by ultrasonic irradiation, catalysis and increased pressures. The application of these techniques in synthesis have been reviewed by Pindur *et al.* [25]. Reactions performed under increased pressure proceed due to an accompanying negative volume of activation, although a pressure of 1500 atm (1.5 kbar) are required to create rate enhancement approximately 10 times that observed at 1 atm [26]. The reaction between 2-methylfuran and a range of α,β-unsaturated ketones has been investigated by Rimmelin *et al.* [27] and

sucessfully carried out under very high pressures in DCM (13.5 kbar, 37ºC, 23-25 h). Both mono and di-activated dieonphiles were reported to give excellent yields of cycloadduct under increased pressure, and mono activated dienophiles gave the *ortho* oriented products, exemplified by the adduct obtained from 2-methylfuran and MAC which is reported to proceed in quantitative yield (48:52 *endo*:*exo*) [27] (Scheme 3.2). The heteroatom in furan does not contribute towards activation of the diene since it is involved in stabilizing the aromatic system and the low reactivity of furan dienes towards D-A addition with monoactivated dienophiles at atmospheric temperature and pressure is partially due to aromaticity.

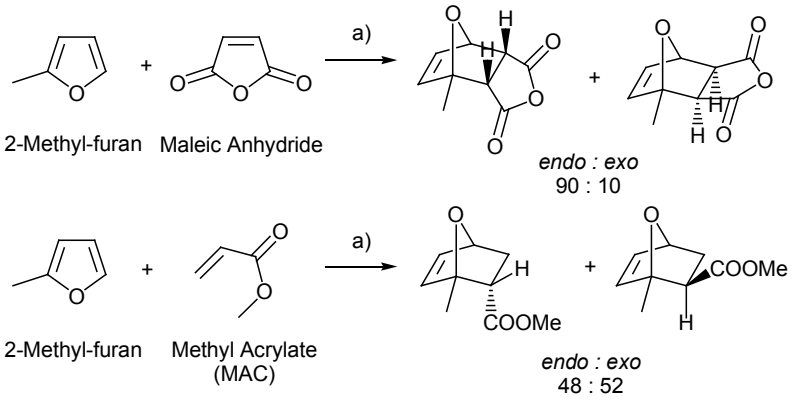

a) DCM, 13.5 kbar, 37ºC, 23-25 h, >98%.

Scheme 3.2: 2-Methyl furan undergoes facile cycloaddition in DCM at 13.5 kbar and mono activated dienophiles provide *ortho*- orientation of substituents in the cycloadduct [27].

Ultrasound irradiation has been reported to influence D-A reaction kinetics in heterogenous mixtures and improvements have been ascribed to more efficient mixing of reactants, although increases in yield and *exo* selectivity have also been achieved in the reaction between cyclopentadiene and methyl vinyl ketone upon sonication in halogenated solvents [28].

As mentioned earlier in Section 3.1.1, Lewis-acids increase the rate of D-A reactions by coordination of the lone pair of electrons on one of the reactants to produce a corresponding decrease in MO energy levels. For example, $AlCl_3$ can coordinate to the oxygen lone pair of an α,β-unsaturated carbonyl system with η^1 σ-character to increase the electron-withdrawing effect of the carbonyl group, resulting in lower LUMO energy at the β olefinic carbon. Inuka *et al.* have researched the catalytic effect of $AlCl_3$ on the cycloaddition reaction between butadiene and MAC, demonstrating a rate enhancement at 20ºC by a factor as large as 10^5 [29]. The authors attributed a reduction in enthalpy of activation to the effect of Lewis acids on the rate of D-A reactions, leaving entropy almost unaffected [29]. $AlCl_3$ has been used as a D-A catalyst by Hosomi *et al.* [30] to accelerate the cycloaddition of the relatively

unactivated 2-trimethylsilylmethyl-1,3-butadiene with a range of α,β-unsaturated carbonyls to provide excellent regioselectivity (>93%) for the *para* products for use in terpene syntheses. $BF_3.Et_2O$ has been used to catalyse D-A reactions involving activated dienes under very mild conditions [31] and the catalysed reaction of furan with methyl vinyl ketone has been modeled using DFT calculations [32] demonstrating the role of $BF_3.Et_2O$ to bring the reactants together for interaction. The application of lithium perchlorate diethyl ether clatherate $Li^+(OEt_2)_2ClO_4^-$ in D-A catalysis has been included in a review by Kumar [33] who suggests the action of a combination of catalytic effects attributed by the Li^+ Lewis acid and polar conditions. Lewis-acid catalysis using transition metal (Fe^{3+}, Cr^{3+}) exchanged montmorillonite and bentonite clays has been reported by Adams [34] to facilitate the D-A reaction of furan and pyrrole with α,β-unsaturated carbonyls in low yields at room temperature and under heterogeneous conditions, achieving an increase in rate by as much as a factor of 10^6 (Scheme 3.3).

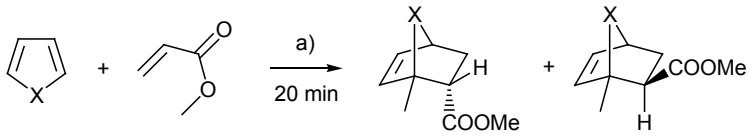

X=	Yield (%)	*endo : exo*
O	14	3.0 : 1.0
NH	35	4.0 : 1.0

a) Cr^{3+} exchanged Tonsil 13 catalyst, DCM, 25ºC

Scheme 3.3: Cr^{3+} exchanged clays prepared by Adams [34] catalyse the room temperature D-A reaction of furan and pyrrole with MAC in low yield.

Substituents can be influenced by electron donation or withdrawal by the solvent to induce corresponding changes in FMO coefficients. In normal electron demand reactions, the LUMO energy of dienophiles with π-accepting groups is lowered by hydrogen bonding, similar to Lewis-acid catalysis, leading to enhanced mixing with the HOMO of the diene. Water has found a novel place as a D-A solvent due to the special effects observed from strong hydrogen bonding interactions on non-polar solutes and the mechanism of rate enhancement has been reviewed by a number of authors [34, 35]. The use of aqueous reaction media for D-A reactions was reported in 1931 by Diels and Alder [3] who demonstrated the reaction of furan with the doubly activated dienophile maleic acid in water at 20ºC. The novel applications for water as a versatile D-A reaction medium was not properly recognised until the 1980s by Rideout *et al.* [36] who demonstrated that the rate of the D-A reaction between cyclopentadiene and methyl vinyl ketone in water was 740 times the rate observed in isooctane. Further rate enhancement of was reported upon reaction in an aqueous solution of 4.86 M lithium chloride (LiCl) and kinetics studies showed a rate 1818 times that in isooctane, in contrast to MeOH which gave only a 12 times

increase. The second order rate constants reported by Breslow *et al.* [36] are tabulated in Scheme 3.4 for reactions at 20°C.

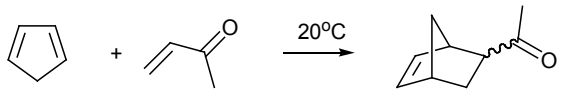

Solvent	*endo : exo*
Neat	3.8 : 1.0
EtOH	8.5 : 1.0
Water	21.4 : 1.0

Solvent	Additive	k_2 X 10^5, M^{-1} s^{-1}
Isooctane		5.9
MeOH		75.5
H_2O		4400
H_2O	LiCl (4.86M)	10800
H_2O	β-cyclodextrin	10900

Scheme 3.4: Second order rate constants reported by Breslow *et al.* indicates an increase in reaction kinetics in aqueous media and in the presence of antichaotropic salt (LiCl) [36]. Increases in selectivity for the *endo* product are reported upon increase in solvent polarity [37].

Preference for the *endo* diastereoisomer upon increases in solvent polarity has also been measured by Breslow *et al.* [37] (Scheme 3.4) and improvement in rate and selectivity were attributed to enhanced hydrophobic interactions between non-polar reigons in aqueous solvent. Hydrophobic interaction is the term used to describe the tendency of non-polar molecules to aggregate in aqueous media and the hydrophobic effects between the non-polar reigons of organic molecules are suggested to be important in protein folding and molecular recognition including enzyme-substrate binding [38]. Neutron scattering studies by Jancsó *et al.* have shown the presence of short range hydration shells on non-polar solutes to aid the dissolution process [39] and this has been reviewed by Finney *et al.* [40]. The hydration shell is involved in micelle behavior at high dilution, which can occur before the occurrence of phase separation. Theoretical studies using Monte Carlo simulations by Jorgensen [41] have indicated a decrease in calculated transition energy barriers for *endo:exo* regioisomers with the inclusion of 500 water molecules, suggesting stabilization of the transition state due to solvation. Breslow *et al.* support the role of hydrophobic interactions experimentally by the addition of LiCl as an 'anti-chaotropic' salting-out agent [42], which diminishes the hydration shells and hence solute solvation to result in an increase in reaction kinetics. The 'chaotropic' salt guanidinium chloride (GnCl, 4.86M) was later investigated and shown to increase solvation and decrease noticeable non-polar effects in the reaction between *N*-ethylmaleimide and anthracene compared to pure water [43].

The utility of polar effects in D-A chemistry has been implemented in the synthesis of quassinone natural products by Grieco *et al.* during the diasteroselective preparation of the fused tricyclic ring [44] (Scheme 3.5). Cycloadducts from the reaction between functionalised bicyclic dienophiles and the ester, acid and sodium salt of a diene carboxylate (Scheme 3.5, top) gave regioselective addition in

polar and organic solvents to provide the tricyclic quassinone skeleton. The newly fused cyclohexene ring has a *cis*- conformation with respect to the cyclohexanone ring and the tricyclic structure is produced as mixture of H(14)-α and H(14)-β diastereoisomers. Increases in rate and considerable improvements in yield were reported for reactions performed in water when R = Et, H demonstrating preference for the H(14)-β isomer in polar reaction conditions and when the reaction was performed neat. Aggregation effects were suggested on the basis of experimental data showing further increases in rate and selectivity for the β product (Scheme 3.5, top; R = Na) when diene concentrations were progressively increased in a rapidly stirred aqueous mixture [44].

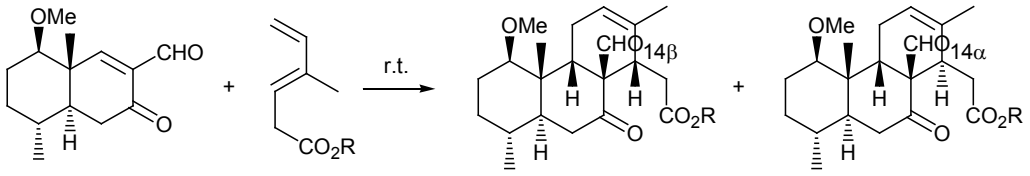

Diene Concentration [M]	Solvent	R =	Time (h)	Yield (%)	**H(14)-β : H(14)-α**
1	Benzene	Et	288	52	1.0:1.2
1	Toluene	H	168	46	1.0:1.4
-	Neat	Et	144	69	1.3:1.0
1	H_2O	Et	168	82	1.3:1.0
1	H_2O	H	17	85	1.5:1.0
0.1	H_2O	Na	120	46	1.1:1.0
1	H_2O	Na	8	8	2.0:1.0
2	H_2O	Na	5	5	3.0:1.0

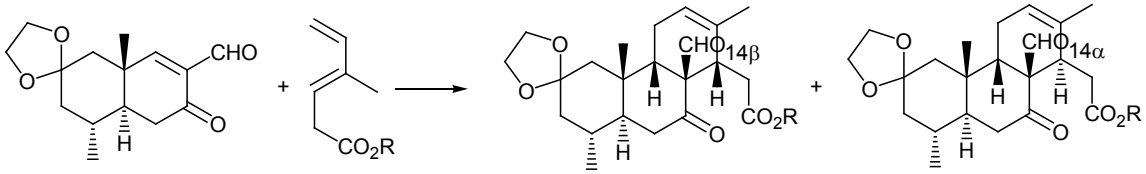

1.0 M Diene
0.2 M Dienophile

Solvent	R =	Temp (°C)	Time (h)	Yield (%)	**H(14)-β : H(14)-α**
Toluene	Et	100	36	97	1.0:1.1
Water	Na	r.t.	4.5	90	3.0:1.0
5.0 M $LiClO_4/Et_2O$	H	r.t.	5	85	2.3:1.0

Scheme 3.5: D-A methodology towards quassinoid natural products by Greco et al. [44, 45] involves the preparation of a functionalised tricyclic skeleton as a mixture of C(14) diastereoisomers. Changes in proportions of α and β isomers where observed upon changes in solvent polarity.

Studies by Grieco *et al.* on the catalytic effects of water and 5 M $LiClO_4/Et_2O$ for the reaction between functionalised α,β-unsaturated bicyclic ketones and carboxyl diene derivatives (Scheme 3.5, bottom) [45] indicate similar catalytic effects for both ionic solvents, with selectivity for the β isomer. A small degree of selectivity for the α isomer was reported for reactions in non-polar aromatic solvents. The examples discussed show a reversal of selectivity from the α isomer in nonpolar solvents, to the β isomer in ionic reaction media.

The methods for introducing chirality in the synthesis of simple chiral molecules has been described in Section 1.5 and approaches towards diastereoselectivity in D-A reactions is discussed in Section 3.1.3.

3.1.3 Diastereoselectivity in Diels-Alder Reactions

Diastereoselectivity in D-A reactions can be achived by the incorporation of chiral auxiliaries in either diene or dienophile reagents, although optically active dienophiles are employed more frequently for D-A selectivity since they are more conveniently prepared. The individual diastereomeric products, once separated from each other, are generally isolated in enantioenriched form (high *ee*). A relevant example of this is the chiral dienophile (-)-1-cyanovinyl camphanate prepared from the incorporation of the (-)-camphanoyl auxiliary by condensation of (-)-camphonyl chloride with 2-oxopropiononitrile [46]. Research by Vogel *et al.* [46] has involved the zinc iodide (ZnI_2) catalysed cycloaddition of furan to (-)-1-cyanovinyl camphanate to prepare a mixture of diastereomeric bicyclic cyanohydrins (Scheme 3.6).

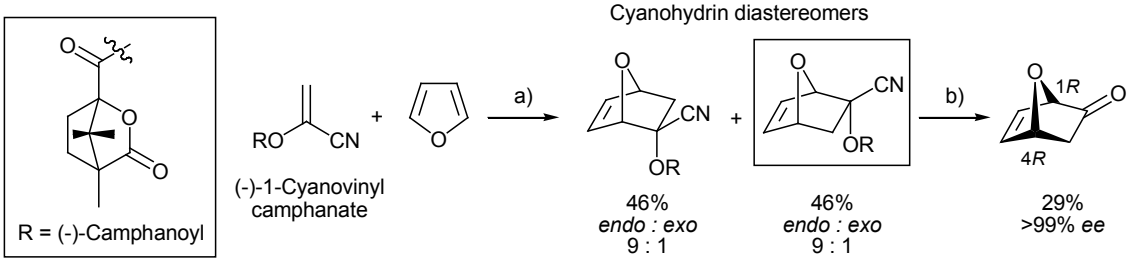

a) ZnI_2, 20ºC, 4 days, 92% b) Recryst. from hexane, THF/H_2O, 1 N KOH, formaldehyde, 29%

Scheme 3.6: Vogel *et al.* [46] have used the (-)-camphoryl auxiliary in the optical pure dienophile (-)-1-cyanovinyl camphanate to provide the optically pure (1*R*, 4*R*)-7-oxabicyclo[2.2.1]hept-5-en-2-one via the separation and hydrolysis of the cyanohydrin intermediate.

Recrystallization to >98% *ee* was achieved for a single isomer from hexane, before hydrolysis to the optically pure (+)-(1*R*,4*R*)-7-oxabicyclo[2.2.1]hept-5-en-2-one in 29% yield overall. Resolution of the bicyclic ketone from a racemic mixture was later reported using successive recrystallizations of the cyanohydrin-brucine complex from MeOH followed by hydrolysis to provide the optically pure (+)-(1*R*, 4*R*)-isomer in 20% yield [47]. The pure bicyclic enantiomer has since proven to be a flexible starting material for the preparation of a range of optically pure sugars [48], myo-inositol derivatives [49] and subunits for macrotetrolide [50] and aminoglycoside [51] antibiotics. Enzymatic resolution of the

cyanohydrin ester with *Aspergillus lipase* has been reported by Sef *et al.* [52] to provide the ketone in 20% *ee* and stereospecific functionalization with *Candida cylindracea* was also mentioned to provide products in >97% *ee* and in moderate yields.

High diastereoselectivities have been accomplished in the reaction between 5-benzyloxymethyl-1,3-cyclopentadiene and the chiral dienophile (-)-(*R*)-menthyl acrylate by the addition of aluminium chloride as catalyst [53]. The aluminium complex of the (*S*,*S*)-stilbenediamine derived sulfonamide has been used by Corey [54] as a chiral catalyst for the D-A reaction between acrylyloxazolidinone and 5-benzyloxymethyl-1,3-cyclopentadiene and proposed that the action of the catalyst is via coordination of the acrylyl carbonyl (Scheme 3.7). Chiral D-A catalysts have been heavily investigated and bis(oxazoline) copper complexes [55] as well as Jacobsen-type complexes formed with chromium and cobalt [56] are reported to successfully catalyse face selective cycloadditions.

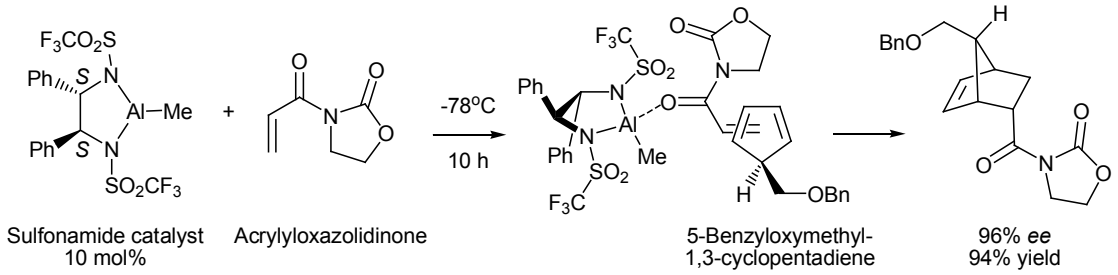

Scheme 3.7: D-A reaction of the complex prepared from acrylyloxazolidinone and a chiral sulfonamide catalyst with 5-benzyloxymethyl-1,3-cyclopentadiene has been reported by Corey [54] to proceed in excellent yield and selectivity at low temperatures.

Chiral dienes are typically prepared by the incorporation of a chiral auxiliary into the appropriately substituted diene backbone. Barluenga *et al.* [57] have incorporated the proline derived (+)-(*S*)-2(methoxymethyl)pyrrolidine as a chiral auxiliary into 2-amino-1,3-butadienes to produce highly functionalised cyclohexanones using D-A chemistry (Scheme 3.8). D-A reactions of (*E*)-dienes with a range of nitroalkenes in MeOH at –80ºC were reported to produce the *endo* cycloadducts in moderate yields with exclusive *para* regioselectivity relative to the nitro and amine substituents. Excellent diastereoselectivity was reported for dienes containing the *tert*-butyldimethylsiloxy (R^1 = TBDMS) group and a decrease in enantiomeric excesses for the methyl derivative (R^1 = Me) was accompanied by an increase in yield, perhaps indicating the role of steric influence of the oxygen substituent (R^1) towards the rate and diastereoselectivity of the cycloaddition. Hydrolysis of the chiral auxiliary at pH 4.6 using a CH_3COOH/CH_3COONa buffer in THF provides a useful methodology for the preparation of functionalised cyclohexanones as chiral synthetic building blocks (Scheme 3.8, top). Reaction of 1-

nitropropene with the corresponding (*Z*)-dienes produced the open chain Michael addition products, which were reported to cyclise to the chiral 2-substituted furan upon stirring in aqueous acid (Scheme 3.8, bottom).

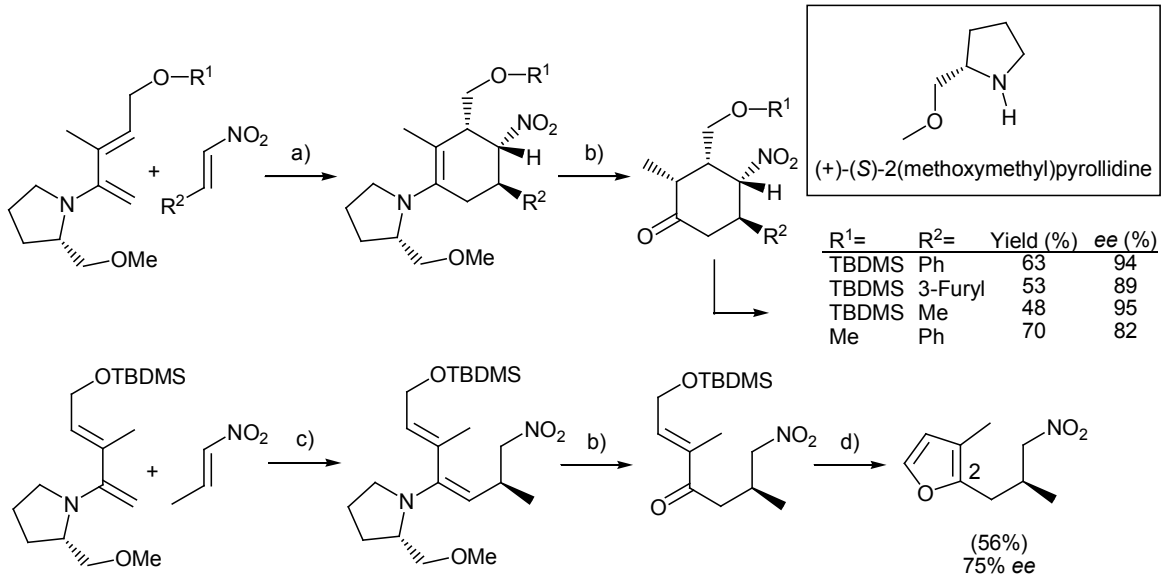

a) MeOH, -80ºC to r.t. b) Aq. CH_3COOH/CH_3COONa, pH = 4.6, THF, r.t. c) Et_2O, -80ºC to r.t. d) 3.0 M HCl, THF, r.t.

Scheme 3.8: Top; D-A reactions with (+)-(*S*)-2(methoxymethyl)pyrrolidine substituted (*E*)-dienes have been reported by Barluenga *et al.* [57] to give *endo* cycloadducts in high diastereoselectivity and hydrolysis in mildly acidic (pH = 4.6) buffer provided the functionalised cyclohexanone. Bottom; Reaction of (*Z*)-dienes are reported to give the Michael addition product and hydrolysis in acid gave the chiral C(2) substituted furan [57].

Although chiral dienes are effective at directing the stereochemical outcome of the newly formed D-A adducts, appropriate methodology must firstly be available for the incorporation of auxiliaries into dienes containing the desired substitution. The activated diene 1-methoxy-3-(trimethylsiloxy)-butadiene, named Danishefsky's diene after the principal researcher, has provided not only a reactive diene for D-A studies but a reliable protocol for the incorporation of heterosubstitutents on the 1,3-butadiene chain [58]. 1-Amino-3-siloxy-1,3-butadienes have been obtained using similar methodology [59] and the C_2-symmetric (+)-*trans*-diphenylamine, (2*R*,5*R*)-2,5-diphenylpyrrolidine has been used by Kozmin *et al.* [60] as an effective chiral D-A auxiliary for the total synthesis of (-)-α-elemene (Scheme 3.9). Cycloaddition reaction of the chiral 1-amino-3-siloxy-1,3-butadiene with methacrolein are reported to give the *ortho*/*para* product with respect to the amine and siloxy substituents with exclusive selectivity for the *endo* diastereomer. Wittig methylenation followed by hydrolysis in aqueous acidic THF allowed

the preparation of the chiral vinyl-cyclohexenone in good enantiomeric purity (85% *ee*) and interconversion of the α,β-unsaturated ketone was performed in four steps to provide (-)-α-elemene in seven steps from the chiral diene.

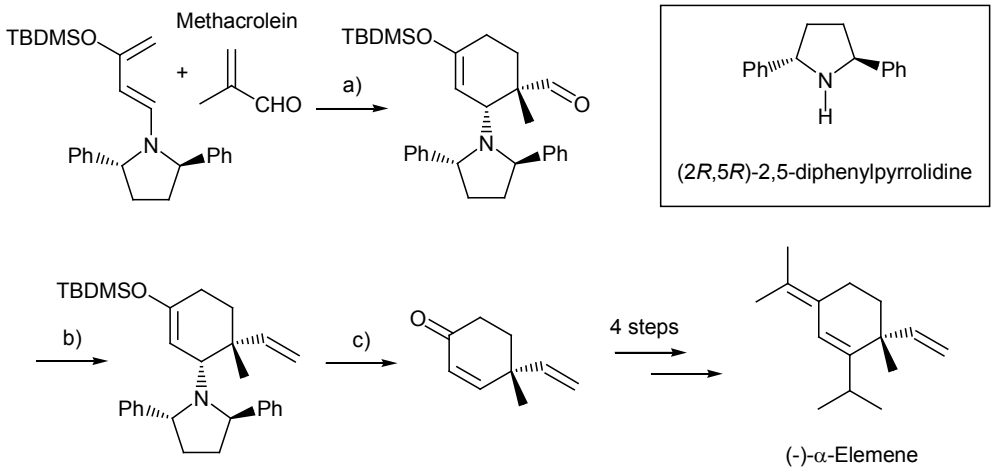

a) 0ºC to r.t., toluene, 94%, 85% *ee* b) Ph_3PCH_3Br, *n*-BuLi, THF, 99% c) aq. HCl, THF, 82%

Scheme 3.9: Kozmin *et al.* [59] have incorporated the (2*R*,5*R*)-2,5-diphenylpyrrolidine auxiliary into 1-amino-3-siloxy-1,3-butadiene to achieve good enantioselectivity in D-A reactions with methacrolein. This provides a direct pathway to the functionalised cyclohexenone in high yield which was transformed in four steps to (-)-α-elemene.

Petrzilka *et al.* have comprehensively reviewed the preparation and D-A reaction of heterosubstituted 1,3-dienes for the chemical literature to 1981 [31], however no literature review specifically addressing the D-A reactions of heterosubstituted furan dienes was found. The role of furan in D-A chemistry will be briefly discussed and the reactivity of C(3) heterosubstituted furans reviewed with focus on achieving enantioselectivity in D-A reactions involving C(3) hetersubstituted furan dienes.

In summary for Section 3.1, the synthetic value of the D-A cycloaddition can be attributed by the following features:

- It can potentially set four stereocenters in one step.

- If unsymmetrical dienes and dienophiles combine it is highly selective and gives ‘ortho’ and ‘para’ products as the predominant regioisomers, and the endo cycloadduct as the predominant diastereomer.

- If a disubstituted (*Z*)-alkene is used, the orientation of the two substituents in the product will be *cis*, alternately an (*E*)-alkene will give *trans* geometry in the product. The (*E*/*Z*) information from the diene is also retained in the cycloadduct.

- Stereochemical information in either diene or dienophile is also transferred to the D-A product in varying degrees. By using the appropriate chiral catalyst or auxiliary the cycloaddition can be made diastereoselective leading to enantiomerically enriched products. Multiple rings can be created in the same step with defined stereochemistry.

3.2 The Role of Furan in Diels-Alder Chemistry

The Diels-Alder reaction of furan is one of the most direct methodologies for preparing 7-oxabicyclo[2.2.1]heptanes, also called 7-oxanorbornanes. As mentioned in Section 3.1.2, furan is considered to be a poor diene due to its aromaticity [61] and is often not compatible as a D-A diene at high temperatures due to facile reversion by retro-Diels-Alder reaction to the stable aromatic furan system. The heat of reaction of furan with ethylene has been reported to be 32 kJ/mol lower that the reaction between cyclopentadiene and ethylene due to aromaticity and differences in ring strain [62]. The retro D-A process is a useful synthetic strategy and has been applied to the synthesis of 3-bromofuran and 4-bromo-2-methylfuran (**10**) via the D-A reaction of furan with maleic anhydride. Bromination of the cycloadduct intermediate has been reported to provide the *trans*-dibromo product, and thermally mediated dehydrohalogenation and retro-D-A reaction in the presence of quinoline provides the furan products (Scheme 3.10) [63]. The *exo* face of the 7-oxanorbornane structure is less hindered and more reactive towards synthetic transformations. This is exemplified in the selective dehydrohalogenation of the *exo* bromine of the dibromoadduct during heating in quinoline, prior to retro D-A reaction to the bromofuran (Scheme 3.10) [63].

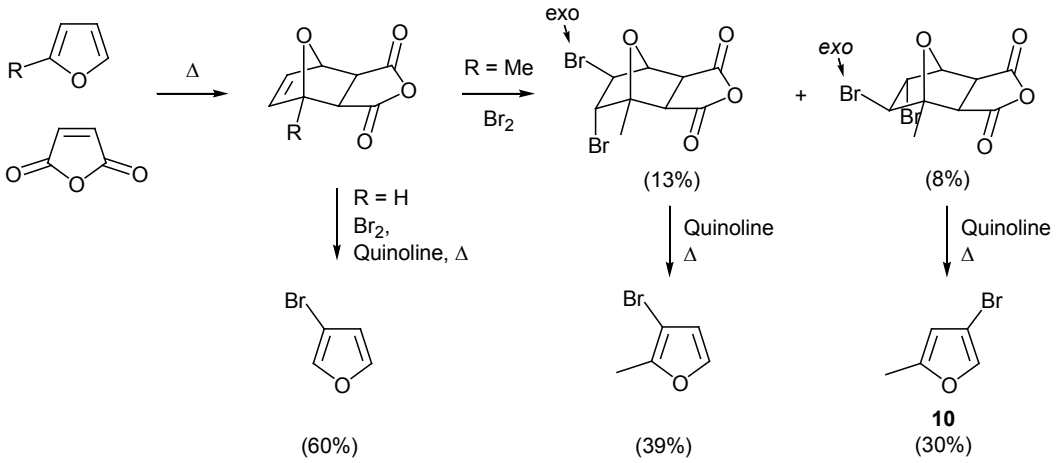

Scheme 3.10: The 7-oxanorbornanes prepared via the D-A reaction of furan and 2-methyl furan with maleic anhydride, undergo facile bromination across the olefin and dehydrohalogenation followed by retro-D-A reaction to the furan has been reported upon heating in quinoline [63].

Access to substituted furan derivatives allows for the preparation of specifically functionalised 7-oxanorbornanes using D-A chemistry, that may have required a more lengthy process and a greater number of steps to prepare by other means. Cycloadducts prepared using activated furans are most convenient when the activating substituent or substituents are readily interconverted to useful or relevant functionality for the formation of the target molecule. CBS-QB3 computational studies discussed by Pieniazek *et al*. [64] have involved the calculation of activation and reaction enthalpies for the D-A reactions of C(2) and C(3) methyl, methoxy and halogenated furans with ethylene. Their results indicate that the inverse demand reaction using EWG substituted halofurans is more facile than reactions with furan or EDG substituted furans. A significant increase in exothermicity was indicated for the reaction with 2-fluorofuran and calculations indicate that all halogen substituents at the C(3) position produced a similar decrease in activation enthalpy, but to a lesser extent than to the C(2) analogue. Incorporation of EDGs at C(3) were calculated to produce a more significant influence on enthalpy values than at C(2) and the methoxy substituent was shown to have a larger effect than the methyl substituent due to π-donor effects.

Although the role of C(3) heteroatom activating substituents on the furan ring is the primary research topic involved in the synthetic pathway under investigation, the successful D-A reactions of C(2) heterosubstituted furans and their practical application should briefly be mentioned. Furans containing C(2) oxygen heterosubstituents have been prepared by Cella [65] and used in D-A chemistry for the preparation of substituted aryl ethers via acid catalysed aromatization of the 7-oxanorbornane cycloadduct (Scheme 3.11, top).

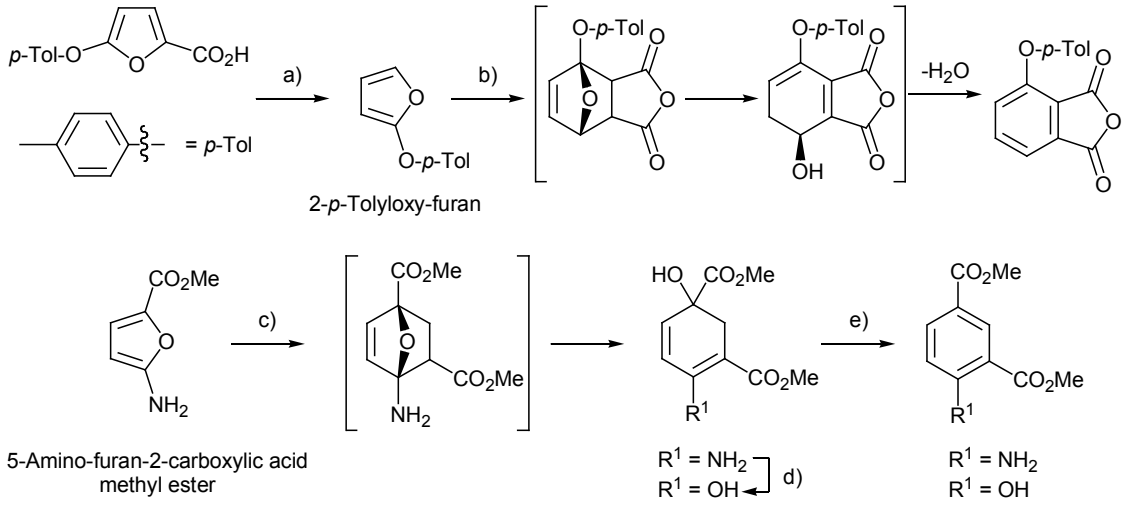

a) 10 mol % TFA, $CDCl_3$, 100ºC b) Maleic Anhydride c) MAC, benzene, 80ºC, 12 h, 92 % d) Aq. THF, p-TsOH, 84%, 25ºC, 30 min e) $BF_3.Et_2O$, >94% for R^1=NH_2 or OH.

Scheme 3.11: Top; Cella [65] has prepared 2-*p*-tolyloxy-furan for D-A reaction with maleic anhydride and reports hydrolysis of the ketal ether bridge and aromatization. Bottom; D-A reaction between MAC and 5-aminofuran-2-carboxylic acid methyl ester followed by aromatization using $BF_3.Et_2O$ has been reported to give the substituted amine and phenol products in high yields [65].

Similarly, Cochran *et al.* [66] and Padwa *et al.* [67] have carried out the D-A reaction between the 5-aminofuran-2-carboxylic acid methyl ester diene (Section 2.2) and MAC to give the cycloadduct in high yield in benzene at 80ºC (Scheme 3.11, bottom). D-A reactions of both C(2)-oxa and C(2)-aza substituted furans involve the formation of acetal and hemi-aminoacetal type functionality in the cycloadduct which undergoes acid mediated or even spontaneous cleavage of the bicyclic ether ring. Smooth dehydration of the alcohol intermediate was reported using $BF_3.OEt_2$ to provide the aniline product in high yields [67].

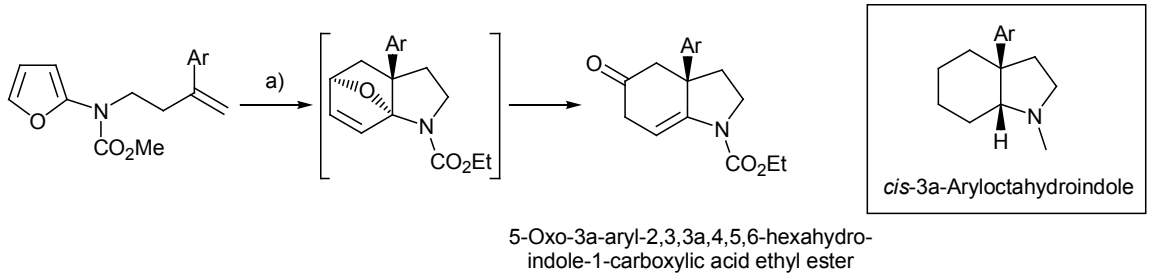

a) Toluene, 155ºC, 20 h, 78% for Ar = 3,4-Dimethoxybenzene.

Scheme 3.12: Intramolecular D-A reaction of 2-furylamides has been reported by Padwa *et al.* [67] to proceed in good yield to produce the functionalised hexahydroindolinone skeleton for use in natural product synthesis.

Intramolecular D-A reactions using C(2) amide substituted furans has been conducted by Padwa *et al.* [67] and applied to the synthesis of key intermediates for the preparation of the hexahydroindolinone structure as precursors to the *cis*-3a-aryloctahydroindole skeleton, observed in the *Sceletium* alkaloids [68] (Scheme 3.12). Literature on the D-A reactions of both C(2) and C(3) heterosubstituted furans is relatively scarce and relevant publications involving cycloaddition of C(3) heterosubstituted furans is reviewed in the following section.

3.2.1 Diels-Alder Reactions of C(3) Heterosubstituted Furans

The incorporation of π-electron donor substituents on the furan ring has a destabilizing effect on the aromatic system as discussed in Section 2.1, and hence decreases the tendency for retro D-A reactions, although the potential for Michael-type side reactions with electrophiles is increased when the C(2) and C(5) positions of the activated furan are unsubstituted. Comparison between the room temperature D-A reaction of furan and the diactivated 3,4-dimethoxyfuran with 1,4-benzoquinone under high pressure have been discussed by Jurczak *et al.* [69], who demonstrate furan to react at 22 kbar in Et_2O, whereas 3,4-dimethoxyfuran required only 9 kbar in toluene. D-A reactions between 3,4-dimethoxyfuran and maleic anhydride derivatives have been published by Matsumoto *et al.* [70] and are reported to proceed under high pressure (10 kbar) at room temperature in THF.

Studies towards the D-A reaction of 3,4-dimethoxyfuran (Scheme 3.13; R = Me) and 3,4-bis-benzyloxyfuran (Scheme 3.13; R = Bn) at atmospheric pressure have been conducted by Koreeda *et al.* [71], who report successful D-A reactions with acyclic α,β-unsaturated ketones in benzene at 80ºC and upon catalysis with ZnI_2 at ambient temperature. Reaction of 3,4-dimethoxyfuran with 10 equivalents of cyclohex-2-enone using ZnI_2 catalysis in benzene was reported to occur at the C(2) and C(5) furan positions to give the di-1,4-addition product (Figure 3.13, top). The cycloaddition between 3,4-bis–benzyloxyfuran with MAC was reported to proceed in excellent yields and has been utilised by Koreeda *et al.* [71] for the preparation of (±)-methyl triacetylshikimate (Scheme 3.13, bottom). Cycloadducts prepared in benzene at 80ºC gave 2:1 selectivity for the *endo* product and quantitative yields were reported for neat reactions carried out with ZnI_2 catalyst to give an improved 15.3:1 *endo:exo* ratio. Olefin reduction with PtO_2 catalyst was reported to be selective for the less hindered *exo* face of the bicyclic ring and base mediated ether cleavage with LiHMDS provided the racemic cyclic oxygenated core of (±)-methyl triacetylshikimate in a further two steps.

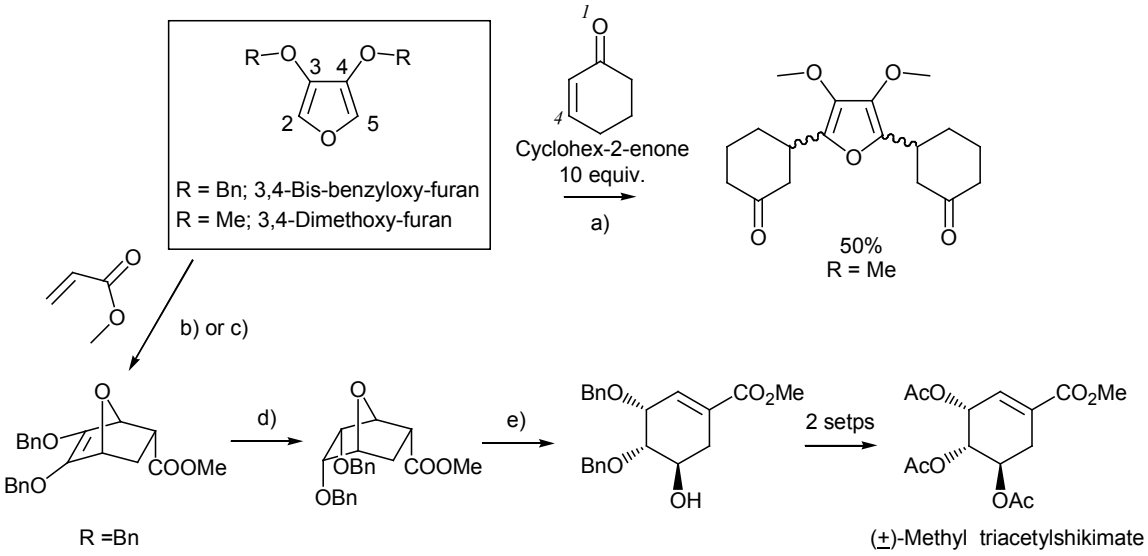

a) 0.1 equiv. ZnI_2, benzene, 80ºC, 1 h b) Benzene, 80ºC, 24 h, 88%, *endo:exo* 2:1 c) Neat, ZnI_2, (0.1 equiv.), 1 h, r.t., 98%, *endo:exo* 15.3:1 d) PtO_2, EtOAc, r.t., 1 h, 93% e) LiHMDS, THF, -42ºC, 9 h, 78%.

Scheme 3.13: Koreeda *et al.* have investigated the reactivity of the diactivated 3,4-dimethoxyfuran (R = Me) and 3,4-bis-benzyloxyfuran (R = Bn) at atmospheric pressure [71]. Top; When R = Me, reaction with an excess of cyclohex-2-enone in benzene with ZnI_2 catalysis was reported to give the di-1,4-addition product in moderate yield. Bottom; When R = Bn, neat reaction with ZnI_2 catalysis was reported to proceed in qualitative yield in 15.3:1 selectivity for the *endo* product and the product was transformed to the racemic oxygenated core of (±)-methyl triacetylshikimate.

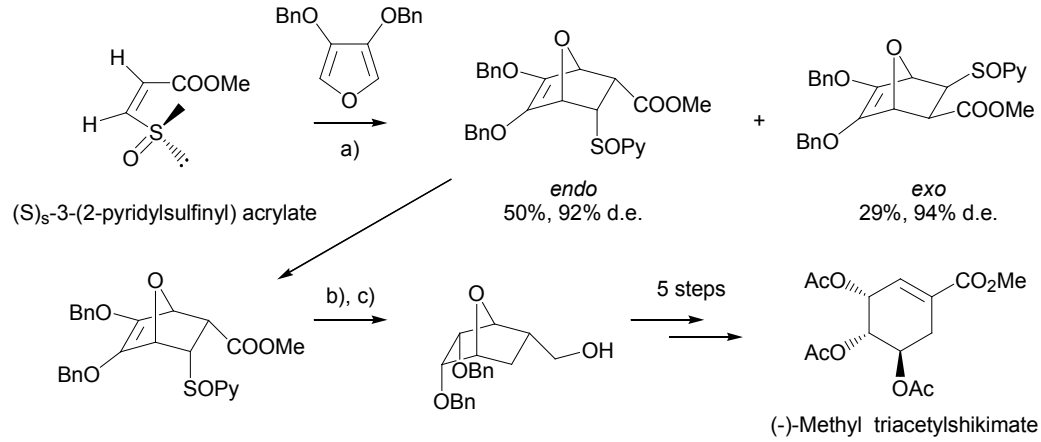

a) Et_2AlCl, DCM, -20ºC, 5 days b) PBr_3, DMF, 0ºC c) $LiAlH_4$, Et_2O, r.t.

Scheme 3.14: High selectivity has been reported by Takahashi *et al.* [72] in the D-A reaction between the chiral dienophile $(S)_s$-3-(2-pyridylsulfinyl)acrylate and 3,4-bis-benzyloxyfuran. The optically enriched cycloadducts provided the key precursor for a steroselective synthesis of (-)-methyl triacetylshikimate in five steps.

A diastereoselective approach towards the D-A reaction of 3,4-dibenzyloxyfuran has been published by Takahashi *et al.* [72] using the sulphoxide $(S)_s$-3-(2-pyridylsulfinyl)acrylate as a chiral dienophile (Scheme 3.14). Reaction of the sulphoxide in the presence of diethyl aluminium chloride at –20ºC was reported to produce a mixture of *endo* and *exo* products in high diastereoselectivity. The chiral sulphoxide group was removed from the major *endo* product by reduction with PBr_3 to give the sulfide, which was cleaved by further reduction with $LiAlH_4$ with concurrent reduction of the olefin at the *exo* face. (-)-Methyl triacetylshikimate was prepared in 5 steps from the alcohol by known reactions [72].

The D-A reactivity of *N*-3'-furylbenzamide has been investigated by Bridson [73] and was the only example involving 3-furylamide cycloadducts that could be found in the literature. The reaction of maleic anhydride in a concentrated ethereal solution of *N*-3'-furylbenzamide was reported to give the exo cycloadduct at room temperature, which crystallised from solution after 24 h (Scheme 3.15). The author mentions that the enamide cycloadduct was idenitifed by ^{1}H NMR in solution but decomposed upon heating during recrystallization and reverted to the furylamide upon attempted isolation. The D-A reaction of *N*-3'-furylbenzamide with dimethyl maleate at reflux in isopropanol (^{i}PrOH) was reported to give clean conversion to the cycloadduct in good yield (Scheme 3.15) [73]. Clean but reversible addition of the alcohol to the enamide was reported to produce the alkoxamide as deduced by ^{1}H NMR studies and the isopropoxyl group underwent facile hydrolysis upon contact with traces of moisture. Bridson reports that hydrolysis of the alkoxamide was successful in water to give the exo ketone product in quantitative yield.

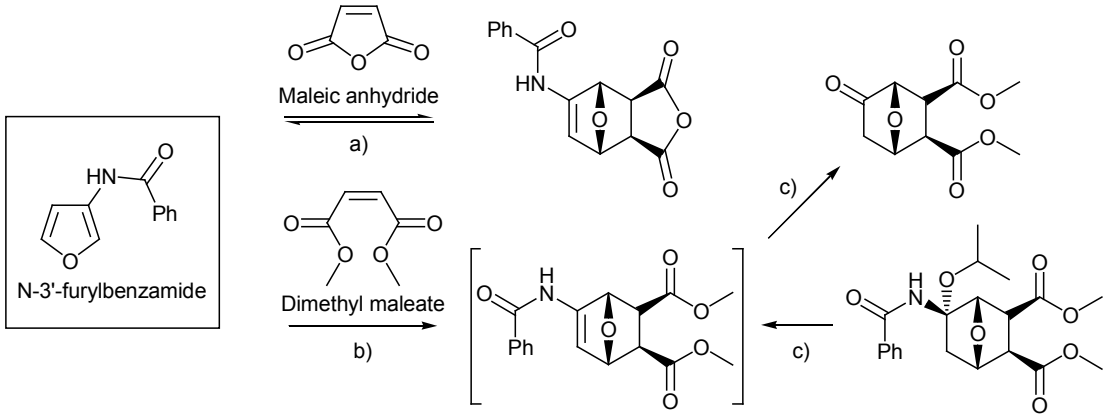

a) Et_2O, r.t., 24 h, 76% b) ^{i}PrOH, reflux, 4 days 85% c) H_2O

Scheme 3.15: Studies by Bridson [73] on the D-A reactivity of *N*-3'-furylbenzamide with maleic acid in Et_2O and dimethyl maleate in ^{i}PrOH revealed good yields of D-A cycloadduct and hydrolysis of the enamide was reported to be successful by stirring in water.

The *endo* product was obtained by conducting the D-A reaction in MeOH and the hydroxyamide intermediate was suggested as the identity of the isolated product on the basis of ^{1}H NMR, IR and elemental analysis, and is stabilised by intramolecular hydrogen bonding to the carbonyl [73] (Scheme 3.16, top). Bridson reports that the reaction of a 2:1 mixture of *N*-3'-furylbenzamide and MAC in a solution of toluene at 111ºC gave the D-A cycloadduct, followed by substitution at the C(5) olefin with a second equivalent of furan via the C(2') aromatic carbon. The acrylate and amide activating substituents react with *para* regioselectivity in the D-A adduct as indicated from the relative orientation of substituents in the final adduct (Scheme 3.16, bottom).

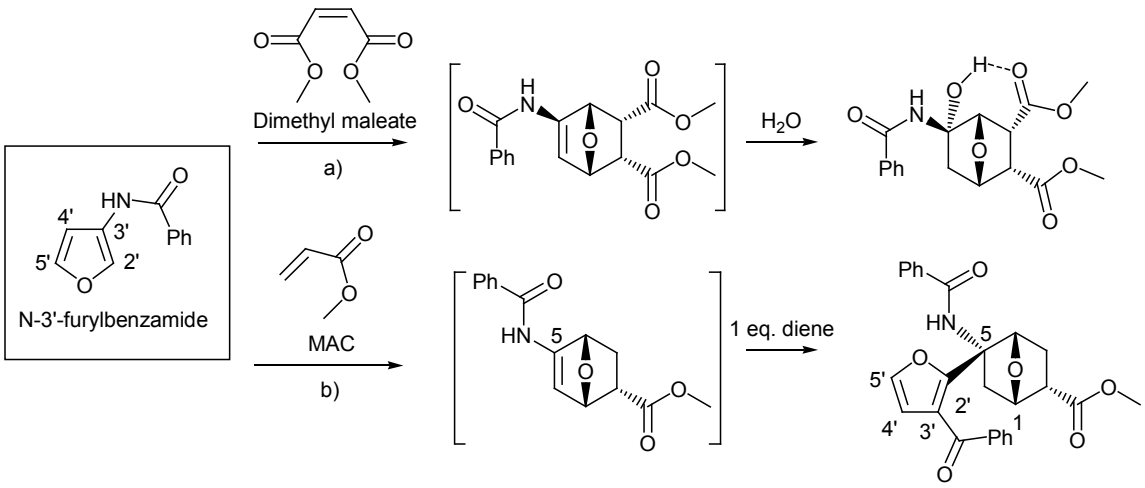

a) 1:1 Ratio of diene:dienophile, MeOH, reflux, 4 days, 5.7% b) 2:1 Ratio of diene:dienophile, toluene, 111ºC, 10 h, 55%.

Scheme 3.16: Top; Bridson [73] reports that D-A reaction of *N*-3'furylbenzamide with dimethyl maleate in MeOH proceeds in low yield followed by the addition of water to give the *endo* hydrogen bond stabilised hydroxylamine cycloadduct. Bottom; D-A of a 2:1 mixture of *N*-3'-furylbenzamide with MAC in toluene was reported to produce the C(5) furan adduct [73] of the D-A product in a non-reversible reaction.

Campbell *et al.* [74] have found that 3-(^{t}butoxycarbonylamino)furan provides a low yield of the hydroxycarbamate cycloadduct via D-A reaction with dimethylacetylenedicarboxylate (DMAD) in toluene followed by reaction with traces of water (Scheme 3.17). The enamine was not observed and subsequent hydrolysis in aqueous acid was reported to give the 7-oxanorbornane ketone in moderate yields. Reaction of the 3-furylcarbamate with methyl 3-nitroacrylate in Et_2O for 2 days was reported to give a low yield of the Michael-type α,β-addition product and a small amount of a stable enamine cycloadduct (3%) assigned as the *endo* configuration at the ester substituent on the basis of ^{1}H NMR.

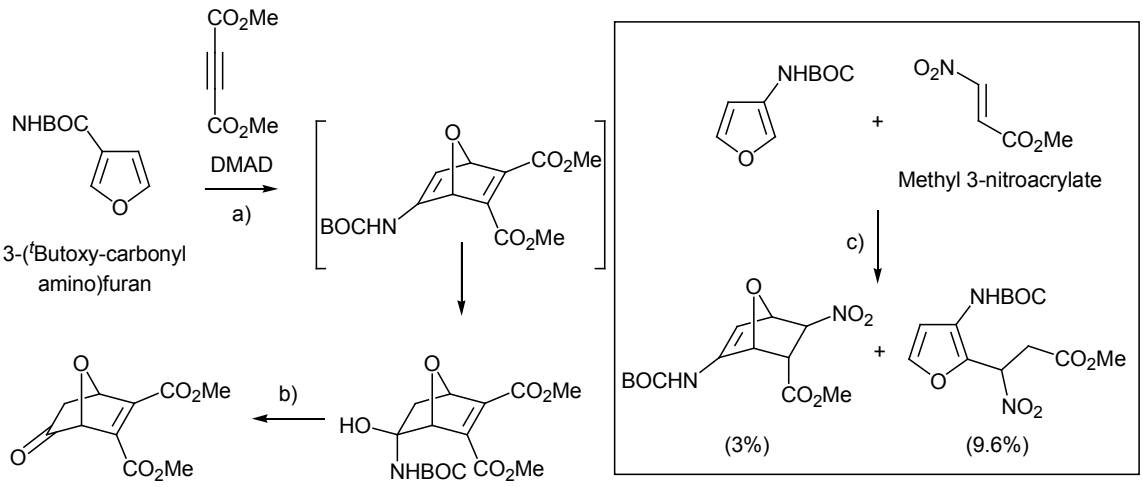

a) Toluene, 110ºC, 3 h, 24%, b) Et_2O, 1.0 M HCl, 24 hr, 53%, c) Et_2O, r.t., 2 days.

Scheme 3.17: Campbell *et al.* [74] have reported the D-A reaction of 3-(ᵗbutoxycarbonylamino)furan with DMAD to proceed in 24% yield, however reaction with methyl 3-nitroacrylate predominately formed the Michael-type addition product in 9.6% yield, as well as the D-A cycloadduct in small amounts (3%).

The D-A reaction of 3-methylthiofuran with a selection of mono activated dienophiles has been reported by Yamamoto *et al.* [75] and cycloadducts were obtained with exclusive regiochemistry and in good yields by stirring the reagents at room temperature in Et_2O or neat for a number of days. D-A reaction with dimethyl maleate was mentioned to be successful in aqueous methanol and provided 81% conversion over 10 days.

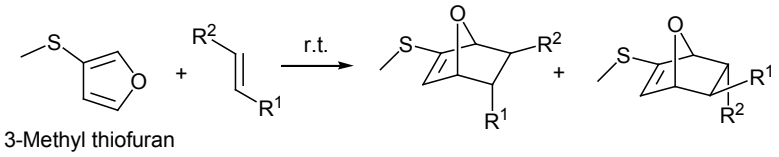

R^1 =	R^2 =	Solvent	Time (days)	Yield (%)	*endo : exo*
CO_2Me	H	Neat	3	74	85 : 15
COMe	H	Et_2O	2	89	90 : 10
CO_2Me	CO_2Me	H_2O-MeOH	3	67	57 : 43
CO_2Me	CO_2Me	H_2O-MeOH	10	81	58 : 42

Scheme 3.18: Yamamoto *et al.* [75] have reported on the D-A reactivity of 3-methylthiofuran with a range of mono and di-activated dienophiles and good yields of cycloadduct were prepared upon prolonged stirring at ambient temperature.

Enantioselectivity was accomplished in the D-A reaction of 3-methylthiofuran using a chiral catalyst in a similar manner to Corey [54] as discussed in Section 3.1.3. 3-Acryloyl-1,3-oxazolidine-2-

one was used as a dienophile in the presence of a catalytic portion of a chiral titanium complex prepared from dichlorodiisopropyl titanium ($TiCl_2(OiPr)_2$) (0.1 mol equiv.) and a tartaric acid derived 1,4-dialcohol to give 85:15 selectivity for the *endo* product in 87% *ee* (Scheme 3.19). The authors mention that 3-methoxyfuran was also reacted in the presence of the titanium catalyst system to form the D-A cycloadduct in good yields with a small degree of chiral selectivity, although no data was included for these experiments [75].

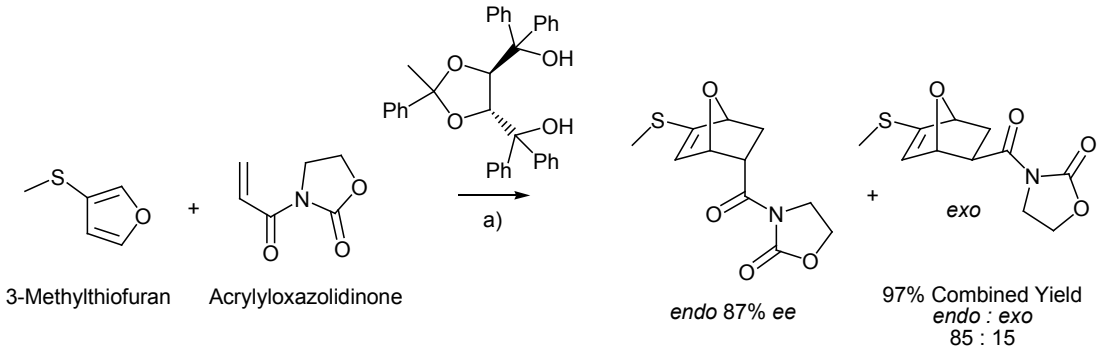

a) $TiCl_2(O\text{-}^iPr)_2$ (0.1 mol equiv.), MS 4Å, toluene:petroleum ether (1:1), -10ºC to –5ºC, 2.5 h

Scheme 3.19: Yamamoto *et al.* [75] have reported the enantioselective D-A reaction of 3-methyl thiofuran using a tartaric acid derived titanium catalyst to provide the *endo* isomer as the major product in 87% *ee*.

The preparation of 2-((*S*)-1-ethyl-1-methoxy-propyl)-1-(2-triisopropylsilanyloxyfuran-3-yl)-pyrrolidine by Schlessinger *et al.* [68] has been described in Section 2.3 and the same group has investigated the D-A reactivity of this chiral 3-furylamine diene. Reaction with MAC in toluene at –20ºC to was reported to provide the D-A adduct with exclusive ortho/para regioselectivity and the favoured *endo* diastereomer was prepared in a 19:1 *endo*:*exo* ratio with an impressive >99% *ee* [76] (Scheme 3.20, top). The D-A cycloadduct prepared by the reaction between MAC and 1-(4-bromo-2-methyl-5-triisopropylsilanyloxy-furan-3-yl)-2-((S)-1-methyl-1-methoxy-ethyl)-pyrrolidine diene (Scheme 3.20, bottom) was reported to form in high yield [68] with the same *para* regiochemistry for amine and carboxyl substituents as observed for reactions involving the 2,3-diheterosubstituted furan. The authors report a 10:1 ratio of diastereomers with preference for the *endo* product in greater than 99% *ee*, and the inclusion of chlorotitanium triisopropoxide ($[(CH_3)_2CHO]_3TiCl$) was observed to enhance the diastereomeric ratio to 15:1 [68].

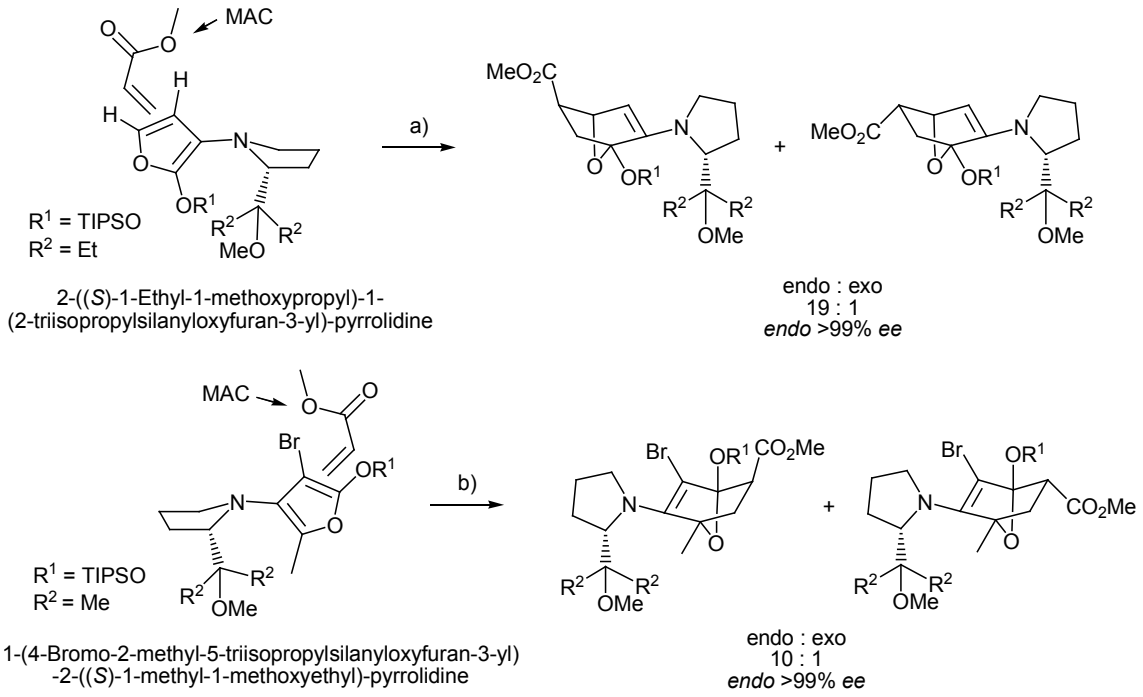

a) Toluene, -20ºC, 12 h, 94% b) DCM, 22ºC, 12 h, 93%

Scheme 3.20: Top; Schlessinger *et al.* have reported the D-A reaction between 2-((*S*)-1-ethyl-1-methoxy-propyl)-1-(2-triisopropylsilanyloxy-furan-3-yl)-pyrrolidine and MAC to yield the *endo* product as the major isomer in >99% *ee* [76]. Bottom; D-A reaction of MAC with 1-(4-bromo-2-methyl-5-triisopropylsilanyloxy-furan-3-yl)-2-((*S*)-1-methyl-1-methoxy-ethyl)-pyrrolidine has been reported to produce the *endo* cycloadduct in 99% *ee* in DCM at 22ºC [68].

A similar proline derived 3-furylamine has been utilised by Schlessinger *et al.* [77] for the stereoselective construction of the β-glucosidase inhibitor (+)-cyclophellitol via the D-A reaction with dimethyl 2,3-pentadienedioate at –100ºC (Scheme 3.21). Stereoselective transformations were effectively performed on the bicyclic D-A adduct before cleavage of the oxygen bridge to create the same stereochemistry as observed in the natural product. Hydrolysis of the enamine in aqueous acid followed by reduction of the ketone using sodium borohydride ($NaBH_4$) provided reaction at the *exo* face to give the *endo* alcohol with respect to the bridge. Subsequent isomerization and ozonolysis produced the correct relative stereochemistry of substituents on the cyclohexane ring and the oxygenated core of the natural product was prepared by reduction in a further four steps. Epoxide ring closure was performed in an additional two steps to provide (+)-cyclophellitol in thirteen steps from the chiral 3-furylamine.

Schlessinger *et al.* [78] have also reported that the aforementioned nonracemic C(3) and C(4) aminofurans can prepared bound to a solid polymer-substrate, facilitated by reaction of the oxygen

enolate with a silyl derived polymer. The polymer-bound aminofurans have been reported to provide cycloadducts in excellent yield and stereoselectivity (>99% *ee*) and the advantages of this approach have been mentioned to include a simplified work-up procedure and clean recovery of the chiral auxiliary.

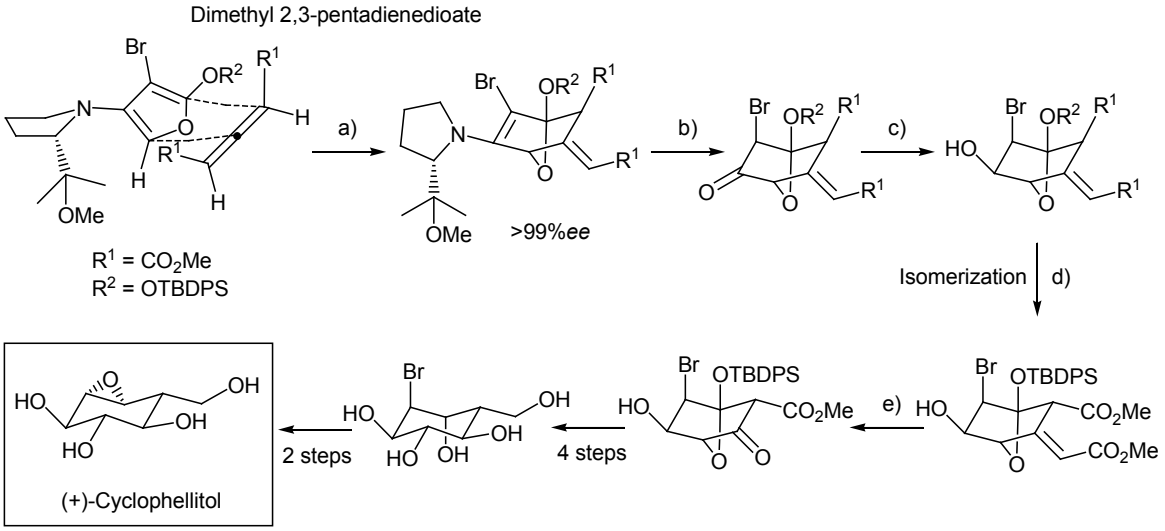

a) THF, -100ºC, 91% b) 2.0 M HCl, MeCN, 0ºC, 93% c) $NaBH_4$, EtOH, -78ºC, 94% d) DMAP, THF, 22ºC, 48 h, 79%, e) O_3, DCM, -78ºC, 4 h; DMS, -78ºC, 1 h, 22ºC, 1 h, 86%

Scheme 3.21: Schlessinger *et al.* [77] have used the D-A reaction of the proline derived 3-furylamine with dimethyl 2,3-pentadiendioate allene to produce the *endo* cycloadduct in >99% *ee*. Hydrolysis in aqueous acidic acetonitrile (MeCN) gave clean hydrolysis to the ketone that was reduced using $NaBH_4$, followed by isomerization using DMAP and ozolonysis. Stereoselective transformation to (+)-Cyclophellitol was achieved in a further 6 steps.

3.3 Diels-Alder Reactions of 3-Furylamines

The literature review of experimental publications and theoretical considerations presented in Sections 3.1 and 3.2 predict the activated 3-furylamines to be reactive dienes in D-A chemistry. *Ab initio* molecular-orbital studies suggest that the presence of an amino group on the furan ring has a destabilizing effect on the aromaticity of furan [79], as well as producing an increase in HOMO energy levels [80]. Both effects contribute to an increase in reactivity towards pericyclic reactions and promote exclusive selectivity in regiochemical outcomes. SHMO overlap indicates that *para* regiochemistry can be expected with respect to the orientation of activating groups in the reactants and 3-amino-5-methyl derivatives should prefer the *ortho*/*para* regiochemistry desired for the target natural product. The literature described in Section 3.1.2 indicates that to some extent, the rate and diastereoselectivity can be appropriately modified utilizing solvent polarity or catalysis and enantioselectivity can be controlled

using chiral C(3) heterosubstituents. The following section describes the D-A reactions of the appropriate non-chiral 3-furylamines prepared in Section 2.3, along with an investigation of face selectivity using optically pure 3-aza-5-methylfurans prepared in Section 2.4.

3.3.1 Investigation of Diels-Alder Reaction Conditions

Preparation of 3-furylamines from tetrahydropyran-2-yloxy (THP) protected alkynols has allowed for the incorporation of a variety of amine substituents in these Diels-Alder substrates (Chapter 2). The mixture of products expected from the D-A reaction between the achiral 5-methyl-3-aza-furans and MAC consists of *endo* and *exo* diastereomers of methyl 5-(dialkylamino)-1-methyl-7-oxa-bicyclo[2.2.1]hept-5-ene-2-carboxylate (**25**) as equal amounts of (1*S*,4*S*) and (1*R*,4*R*) enantiomers (Scheme 3.22).

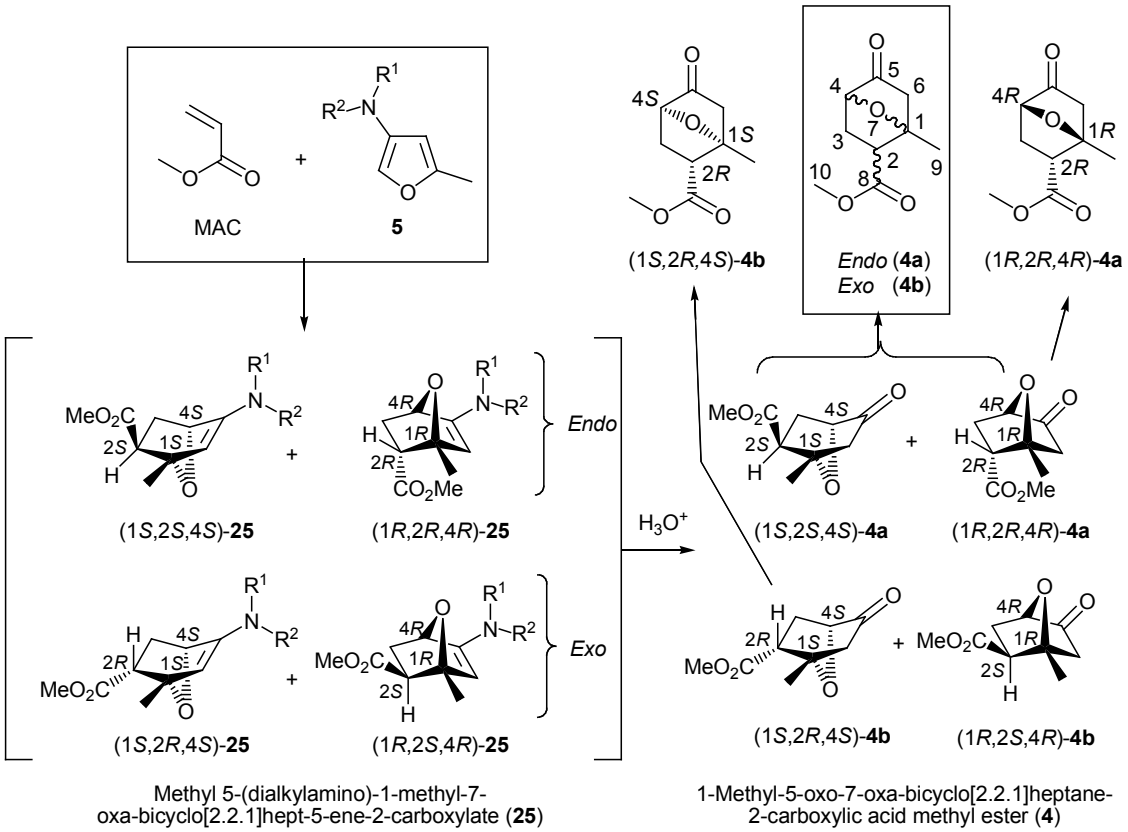

Scheme 3.22: D-A reaction of non-chiral 3-aza-5-methylfurans with MAC should produce a racemic mixture of *endo* and *exo* enamines **25** which can undergo hydrolysis in aqueous acidic conditions to form *endo* (**4a**) and *exo* (**4b**) diastereoisomers of 1-methyl-5-oxo-7-oxa-bicyclo[2.2.1]heptane-2-carboxylic acid methyl ester. The (1*S*,2*R*,4*S*)-**4b** and (1*R*,2*R*,4*R*)-**4a** antipodes can be used in the synthesis of the natural product **1**.

The respective diastereomers of 1-methyl-5-oxo-7-oxa-bicyclo[2.2.1]heptane-2-carboxylic acid methyl ester (**4a-4b**) can then be obtained by hydrolysis of the enamine to provide the functionalised 7-oxanorbornane intermediates. The *exo* ketone (1*S*,2*R*,4*S*)-**4b** has both methyl ester and oxygen bridge in the correct stereochemical orientation to that observed in the target **1**, although the *endo* ketone (1*R*,2*R*,4*R*)-**4a** may also be used by means of stereochemical inversion at the C(4) position subsequent to transformations involving ether ring cleavage.

Preliminary D-A reactions were performed by reacting 4-(5-methylfuran-3-yl)morpholine (**5a**) with MAC in *n*-hexane (Scheme 3.23) at a range of temperatures with monitoring by GCMS analysis. Reaction in hexane at 40ºC was very slow, however two small peaks at t_R = 12:27 and 12:33 min with molecular ions corresponding to the 7-oxanorbornane diastereoisomers (**4**) (*m/z* 184) appeared after 8 h, indicating that the hydrolysis of **25** may occur in the presence of atmospheric moisture (Figure 3.7). Reactions conducted at 50ºC and 70ºC had improved yields of **4**, however notable decomposition occurred with increasing temperatures along with the accumulation of a major by-product at t_R = 16:17 min that showed no observed molecular ion in MS analysis but a characteristic high mass fragment ion at *m/z* 247. At temperatures above 50ºC, GC-MS analysis Figure 3.7 indicated the formation of a small amount of aminated product (*m/z* 173) at t_R = 12:06 min featuring a morpholine fragment ion (*m/z* 84) and this molecular weight corresponds to the 1,4-addition product of the hydrolysed morpholine group to MAC. As such D-A reactions under conditions involving the hydrolysis of **25** required at least 2 equivalents of dienophile to account for the reaction of the amine with MAC (Scheme 3.23). A molecular ion for the enamine was not observed and reactions conducted in sodium dried hexane did not improve yield or allow for better GC detection of either isomer of **25**. Diastereoisomeric ratios and yields of **4** prepared using **5a** in hexane are shown in Table 3.1.

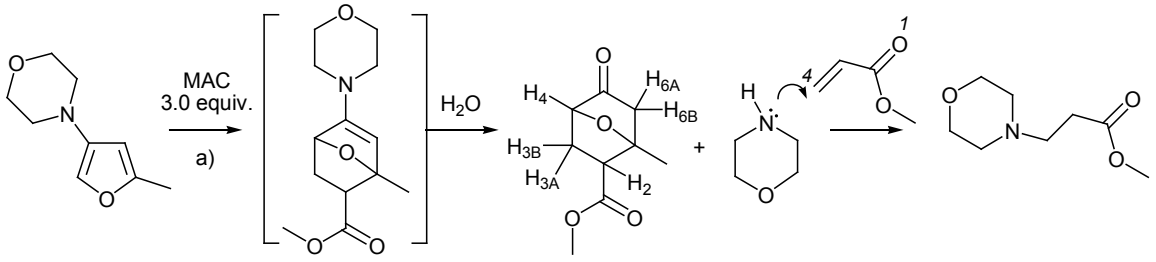

a) *n*-Hexane, 40ºC, 50ºC and 70ºC, 8 h

Scheme 3.23: D-A reaction of **5a** with MAC in *n*-hexane produced increasing yield of **4** at higher temperatures. The facile 1,4-addition reaction of morpholine to MAC occurred at 70ºC, indicated by a parent ion at *m/z* 173 in GC-MS analysis.

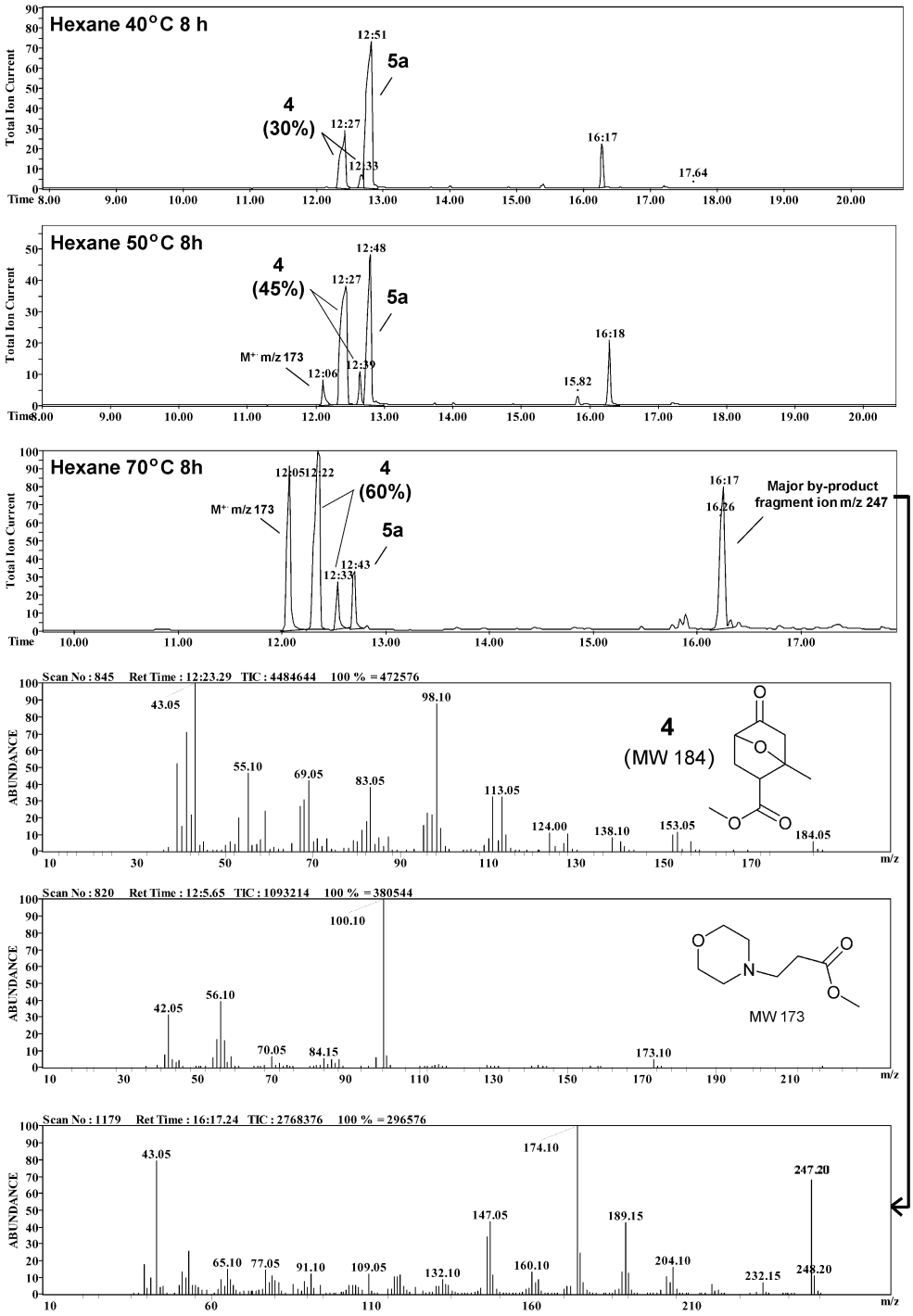

Figure 3.7: GC-MS spectrum for the reaction of **5a** with MAC at 40, 50 and 70ºC show increasing yields for **4** ($M^{+\cdot}$ *m/z* 184) and the hydrolysed morpholine group was observed to react with the dienophile *via* 1,4-addition to give the amine by-product ($M^{+\cdot}$ *m/z* 173) observed as an earlier eluting component than **4** at t_R = 12:06. A major by-product is formed at high temperatures with a fragment ion of *m/z* 247. GC analysis conditions are listed in Section 6.10, Instrument 1.

Extraction of the D-A reaction mixtures with 0.5 M HCl facilitated the removal of aminated biproducts and the diastereoisomers of **4** were separated by column chromatography on silica gel (10:1 pentane:EtOAc). A pale yellow oil with TLC retention of R_f = 0.38 was isolated in >99% purity as confirmed by GC-MS analysis. ^{1}H NMR analysis of the pure isomer confirmed the presence of a methyl substituent H(9) at δ 1.70 and a methyl ester substituent H(10) at δ 3.72 as two large singlets, each with an integral area equivalent to three protons (Figure 3.8). ^{13}C NMR analysis showed the expected C(5) ketone and C(8) ester carbonyl peaks at δ 210.3 and 172.2 respectively (Figure 3.8). The bridgehead proton H(4) adjacent to the electron withdrawing ether and carbonyl functionalities can be assigned to the broad downfield doublet (J = 6.6 Hz) at δ 4.37 with an integral region equal to one proton. The COSY NMR analysis indicates that the H(4) signal is correlated with two proton signals at δ 2.33 and δ 2.16, assigned as H(3_A) and H(3_B) resonances respectively. The H(3) peaks are confirmed by HMQC and DEPT 135 analysis to be attached to the C(3) methylene carbon at δ 30.9 (Figure 3.9), thus confirming that the cycloaddition proceeded with *para* selective regiochemistry with respect to the ester and amine substituents. The downfield negatively oriented DEPT 135 NMR signal at δ 46.0 can be assigned to the C(6) methylene adjacent to the carbonyl group and HMQC data shows correlation to protons H(6_A) and H(6_B) at δ 2.39 and 2.17, respectively. The H(6) protons show strong coupling to each other in COSY analysis and appear as second order doublets almost overlapped with the diastereotopic signals from H(3). Coupling constants between H(6) methylene protons $J_{6A,\ 6B}$ = 17.8 Hz, $J_{6B,\ 6A}$ = 18.4 Hz were not identical, indicating that H(6_B) is split by an additional proton signal. The H(2) proton is assigned to the signal at δ 2.88 in good agreement with Chemdraw predictions and COSY analysis indicated correlations to H(3_A) and H(3_B) in agreement with the proposed structure. ^{1}H NMR analysis conducted using 300 MHz spectrometry did not sufficiently resolve the overlapping second order H(6) methylene signals and 500 MHz experiments were required to provide adequate resolution to measure ^{1}H coupling constants for H(3_A)/H(3_B). The methylene protons on C(3) exhibit first order AX splitting ($J_{3A,\ 3B}$ = 13.4 Hz) and H(3_A) was observed to be a doublet of doublet of doublets ($J_{3A,\ 3B}$ = 13.4 Hz, $J_{3A,\ 4}$ = 6.6 Hz, $J_{3A,\ 2}$ = 11.4 Hz) and the H(3_B) signal appeared as a double doublet ($J_{3B,\ 3A}$ = 13.4 Hz, $J_{3B,\ 2}$ = 5.4 Hz). The ^{1}H coupling constant between H(3_B) and H(4) is ~0 Hz, and principles described by the Karplus equation suggest that these protons are locked in almost orthogonal positions on the 7-oxanorbornane moiety [81]. The H(2) signal appears as a doublet of doublet of doublets ($J_{2,\ 3A}$ = 11.4 Hz, $J_{2,\ 3B}$ = 5.4 Hz, $J_{2,\ 6B}$ = 2.1 Hz) and although no COSY correlation was apparent for the four-bond-w-coupling between H(2) and H(6_B), ^{1}H homo-decoupling NMR experiments demonstrated the collapse of H(2) to form a doublet of doublets upon decoupling at the H(6_B) frequency (Appendix 3.1). These observations indicate that the isolated diastereomer is 1-methyl-5-oxo-7-oxa-bicyclo[2.2.1]heptane-2-carboxylic acid methyl ester (**4a**) and is in the *endo* configuration whereby H(2) is coupled to H(6_B) ($J_{2,\ 6B}$ = 2.1 Hz) and H(3_A) has an equatorial *cis* relationship with H(2) and H(4), however H(3_B) and H(4) are at a 90º angle as indicated by $J_{3B,\ 4}$ = ~0

Hz. Confirmation of the connectivity of the bicyclic ether was established from the strong correlation between C(1) at δ 86.0 and C(4) at δ 81.4 in heteronuclear multiple bond correlation (HMBC) analysis (Appendix 3.2) and ^{1}H homo-decoupling experiments conducted at 200 MHz are shown in Appendix 3.1 and confirm the structure proposed for **4a**.

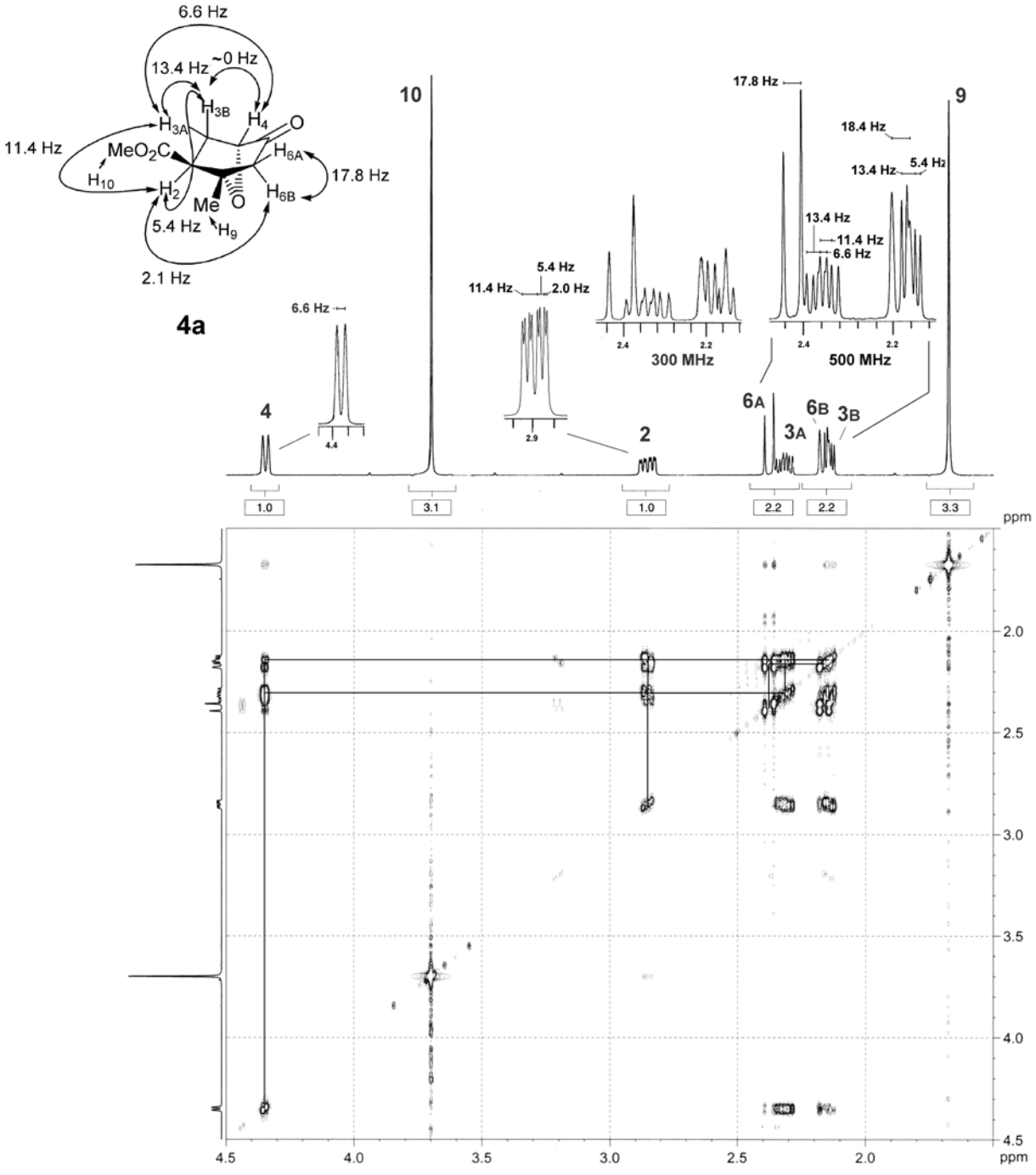

Figure 3.8: 500 MHz ^{1}H and COSY NMR analysis of *endo* 1-methyl-5-oxo-7-oxa-bicyclo[2.2.1]heptane-2-carboxylic acid methyl ester (**4a**). The 300 MHz ^{1}H NMR for the overlapping H(3_A)/H(3_B) and H(6_A)/H(6_B) signals is shown on the same scale.

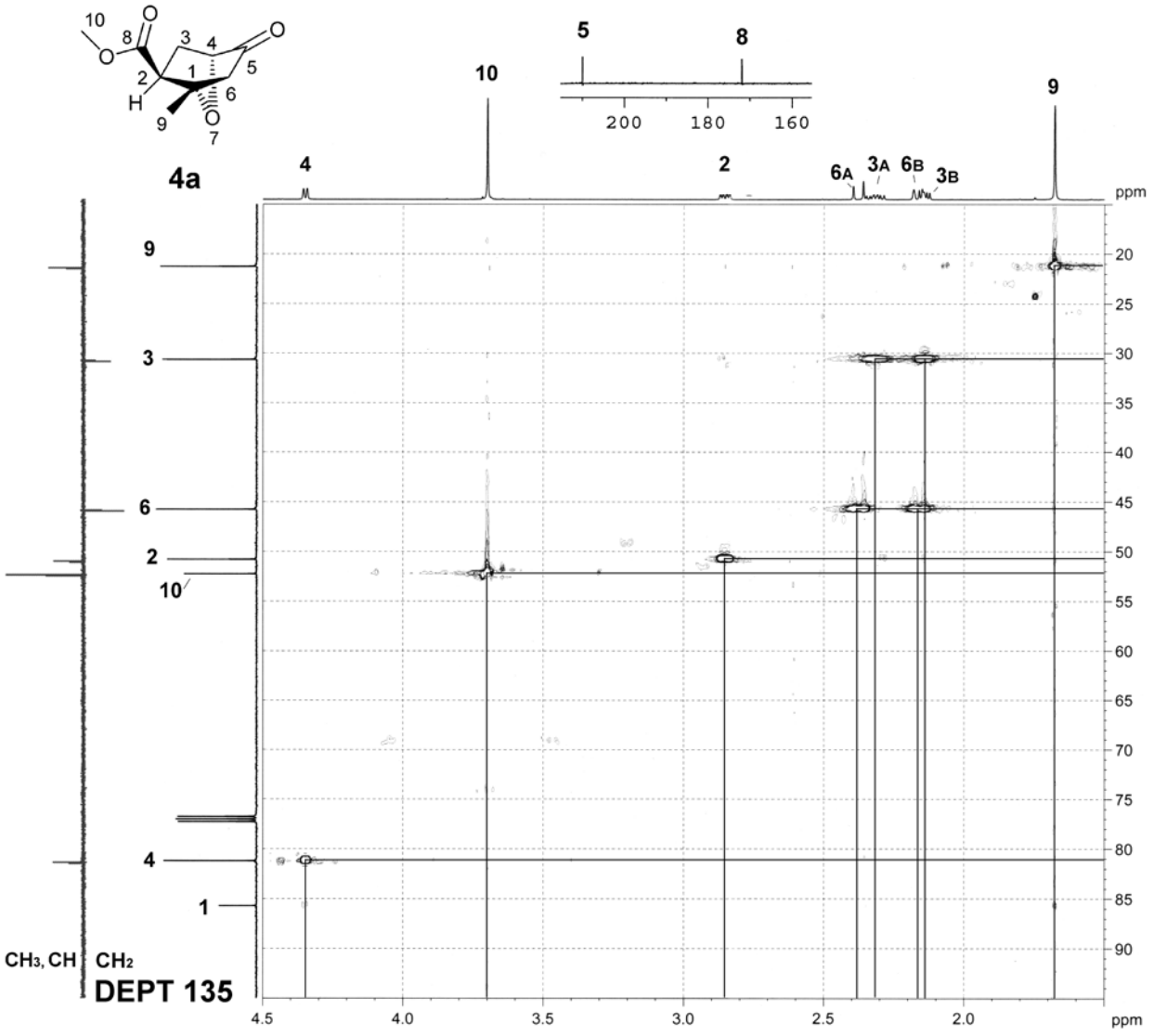

Figure 3.9: 500 MHz HMQC spectrum of **4a**, 125 MHz ^{13}C and DEPT 135 NMR analysis is also shown with structural assignments. ^{13}C NMR data for **4a** is also included in Appendix 3.2.

The *exo* diastereomer of 1-methyl-5-oxo-7-oxa-bicyclo[2.2.1]heptane-2-carboxylic acid methyl ester (**4b**) was produced in low concentration during the reaction of **5a** in hexane and was not isolated from the product mixtures in suitable purity for characterization. Further D-A reactions between **5a** and MAC were conducted in DCM to successfully yield a mixture of **4** and **25** as indicated by GC-MS (Figure 3.10), and no change of diastereomeric ratio was observed over time suggesting that the cycloaddition is under kinetic control. Reactions performed at 25ºC (Figure 3.10) and 45ºC gave identical product mixtures and in both cases a large GC peak with a molecular ion corresponding to the enamine intermediate **25** (*m/z* 253) was observed at t_R = 14:18 min.

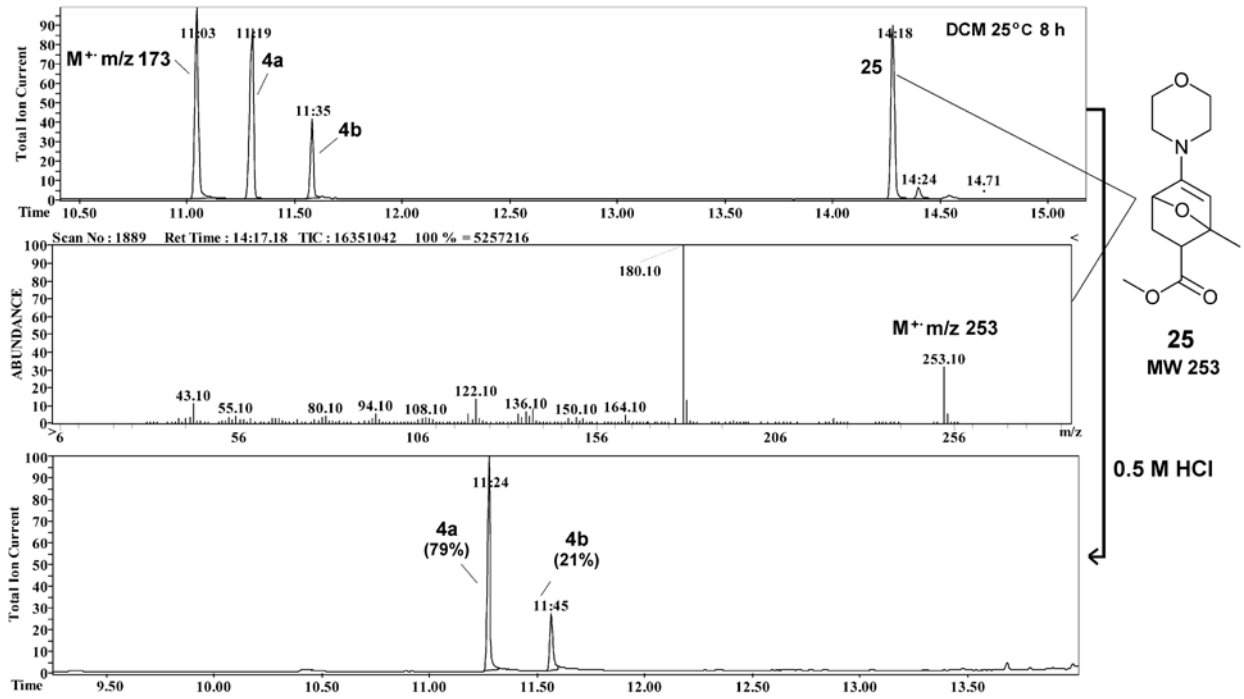

Figure 3.10: GC-MS analysis of the crude D-A reaction of **5a** with MAC in DCM at 25ºC indicates clean conversion to the cycloadduct **25** with significant *in situ* hydrolysis to 4 due to atmospheric moisture. Hydrolysis in 0.5 M HCl gave **4a** and **4b** in a 4:1 ratio.

During D-A reactions of **5a** in DCM, decomposition accompanied reaction times longer than 12 h. The enamine **25** was labile to hydrolysis from traces of moisture and crude mixtures typically contained both **4** and **25**. Attempts to isolate **25** were unsuccessful and a retro D-A reaction to reform **5a** occurred during distillation and column chromatography on silica gel. Hydrolysis of the crude material in 0.5 M HCl and extraction with DCM provided an isolated 93% combined yield of **4** in an *endo*:*exo* ratio of 4:1 as determined by GC integral regions (Figure 3.10). Cycloadditions conducted at sub-ambient temperatures were also successful and as expected returned a mixture of unreacted **5a** and **4** due to decreases in reaction rates at lower temperatures (Appendix 3.3). Reactions conducted in DCM progressed with the formation of much less by-product than reactions in hexane and purification by column chromatography on silica gel (10:1 pentane:EtOAc) provided **4b** in 19% yield (TLC, $R_f = 0.12$) as a pure white crystalline solid with similar GC-MS fragmentation to the *endo* isomer (Appendix 3.4).

300 MHz ^{1}H NMR experiments on **4b** (Figure 3.11) showed a doublet for H(4) at δ 4.47 and the COSY spectrum indicates correlation to H(3_A) ($J_{4,\,3A}$ = 6.4 Hz) but not H(3_B), suggesting a similar 90º dihedral angle for H(3_A) and H(4) as observed in **4a**. The H(2) proton at δ 2.80 appears as a double doublet with coupling to H(3_A) and H(3_B) ($J_{2,\,3A}$ = 5.1 Hz, $J_{2,\,3B}$ = 8.7 Hz) as corroborated by COSY data

and four-bond-w-coupling to the H(6) AB quartet at δ 2.25 is not observed, as expected for the *exo* configuration. The H(3) methylene signals demonstrate AX coupling ($J_{3A,\ 3B}$ = 13.4 Hz) and H(3_A) (δ 2.52) shows COSY correlations to H(2), H(4) and H(3_B), appearing in ^{1}H NMR data as an apparent doublet of triplets. H(3_B) (δ 1.94) appears as a double doublet with the expected coupling to H(3_A) (J = 13.4 Hz) and H(2) (J = 8.7 Hz). Although ^{13}C NMR spectrum of **4b** was similar to **4a**, HMQC analysis (Appendix 3.4) revealed that the C(2) carbon in **4b** is present at δ 49.4 and appears at lower frequency than the C(6) methylene carbon at δ 50.5, whereas these signals are in the reverse order in **4a** (C(2) δ 51.1, C(6) δ 46.0, Figure 3.9). The structure of **4b** was also consistent with HMBC data (Figure 3.11) and the ether bridge was confirmed by strong correlation of the methine bridge doublet H(4) to C(1) and C(2). Signals from H(3) correlate to C(2) and the C(5) carbonyl shifts and H(3_A) correlates to C(4) whereas H(3_B) correlates to C(1). The H(6) AB quartet signal correlates to the expected C(9), C(2), C(1) and C(5) carbon shifts.

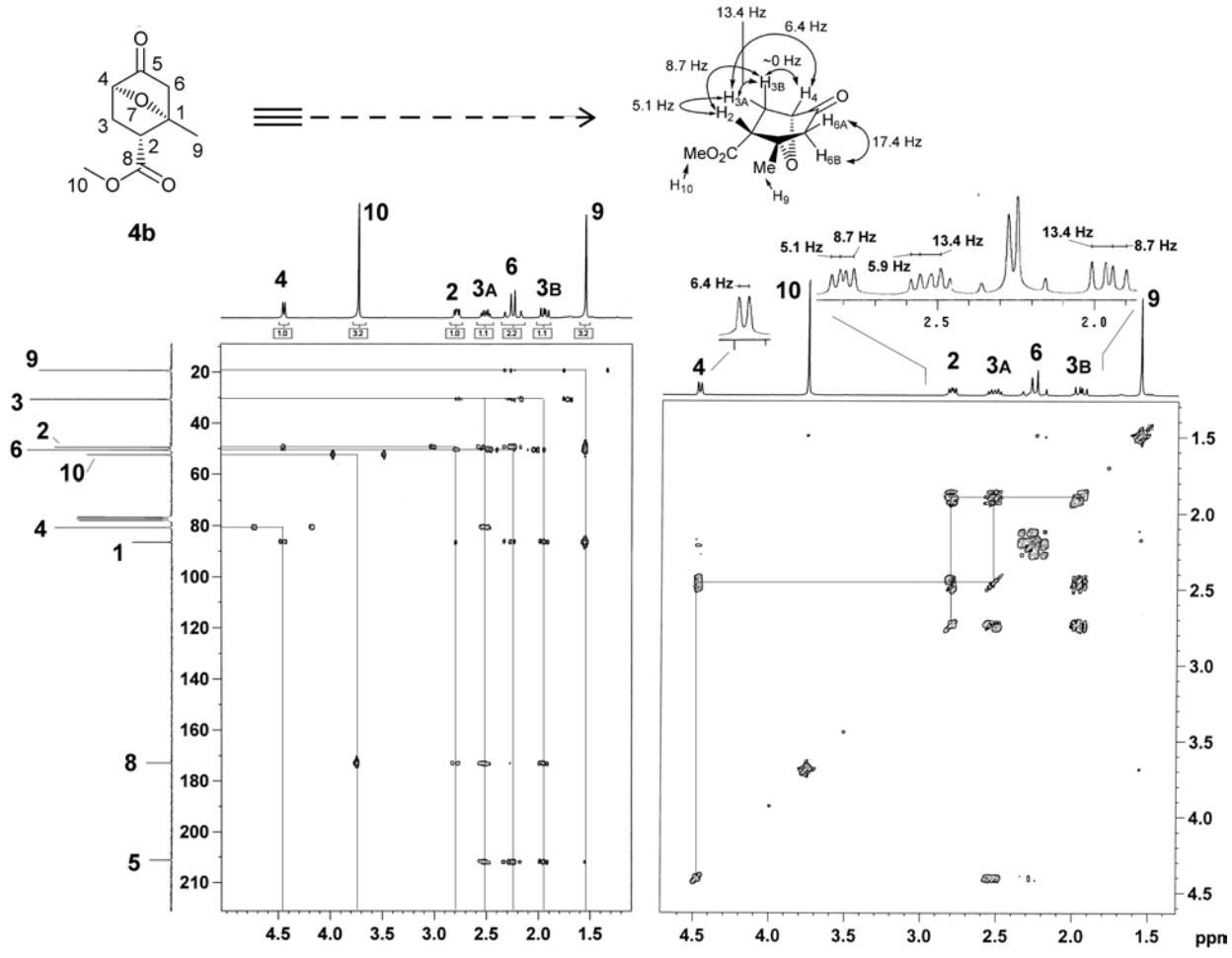

Figure 3.11: ^{1}H 300 MHz/^{13}C 75 MHz HMBC NMR and 300 MHz COSY NMR spectrum of **4b** with correlations.

A simple procedure for the separation of **4b** from a mixture of diastereomers of **4** was realised upon the addition of Et_2O to D-A hydrolysis mixtures, after which the *exo* diastereomer **4b** crystallised in high purity whereas the *endo* diastereomer **4a** is completely soluble. Recrystallization of **4b** in Et_2O allowed for the preparation of suitable material for X-ray crystal structure analysis and crystal data determined conclusively the identity of **4b** as the *exo* product (Figure 3.12). The X-ray crystal CIF file and a summary of bond distances for C-C bonds is included in Appendix 3.5, and comparison with figures quoted by Allen *et al.* [82] indicate that distances are close to the expected values.

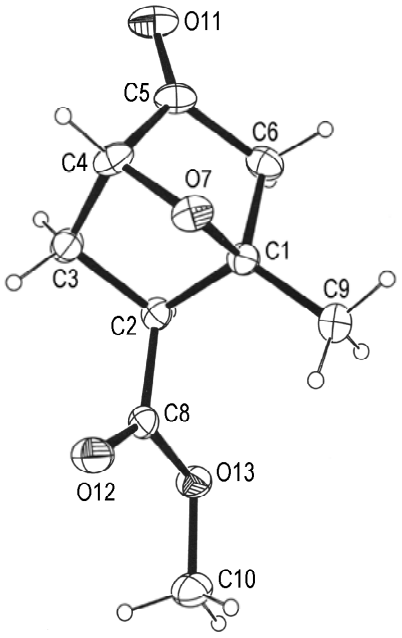

Figure 3.12: ORTEP drawing of *exo*-methyl 1-methyl-5-oxo-7-oxa-bicyclo[2.2.1]heptane-2-carboxylate **4b**. Crystal Data. $C_9H_{12}O_4$, MW = 184.19, T = 293(2) K, λ = 0.71073 Å, triclinic, space group *P*-1, a = 7.2235(10), b = 8.1158(11), c = 8.3058(12) Å, α = 75.273(2)°, β = 74.540(3)°, γ = 86.114(2)°, V = 453.89(11) Å^3, Z = 2, D_c = 1.348 Mg/m^3, μ(Mo Kα) = 0.106 mm^{-1}, F(000) = 196, crystal size 0.50 x 0.15 x 0.10 mm^3, 2428 reflections measured, 1583 independent reflections (R_{int} = 0.0587); the final wR(F^2) was 0.1414 (all data) and final R was 0.0529 for 1311 unique data [$I > 2\sigma(I)$]. Goodness of fit on F^2 = 1.029. Crystallographic data for the structure reported has been deposited with the Cambridge Crystallographic Data Centre as deposition No. 288600.

The diene **5a** was not reactive with MAC in Et_2O or dioxane however reactions performed with heating in the aromatic solvents benzene and toluene led to the exclusive formation of a by-product at t_R = 16:17 min featuring a predominant *m/z* 247 fragment in GC-MS analysis (Appendix 3.6). This compound was observed to have an identical mass spectrum to the major product formed in hexane at 70ºC (Figure 3.7) and product mixtures obtained from toluene at 111ºC provided suitably pure material

for NMR analysis (Appendix 3.6). ^{1}H and ^{13}C NMR analysis features signals for the 7-oxabicyclo[2.2.1]heptane moiety indicating that the D-A cycloaddition was successful. However the absence of a ketone or enamine signals in ^{13}C NMR analysis suggests that the side reaction has occurred at the C(5) carbon. ^{1}H NMR integral regions indicate the presence of two morpholine moieties in different chemical environments and ^{13}C NMR aromatic signals characteristic of a 2,3,5-trisubstituted furan point toward the nucleophilic addition product involving the C(2') position of **5a** with **25** to provide **26** (Scheme 3.24). Similar structures have been reported by Bridson [73] during the D-A reaction of *N*-3'-furylbenzamide (Section 3.2.1) and tentative NMR assignments for **26** are included in Appendix 3.6 based on previously assigned structures and Chemdraw predictions.

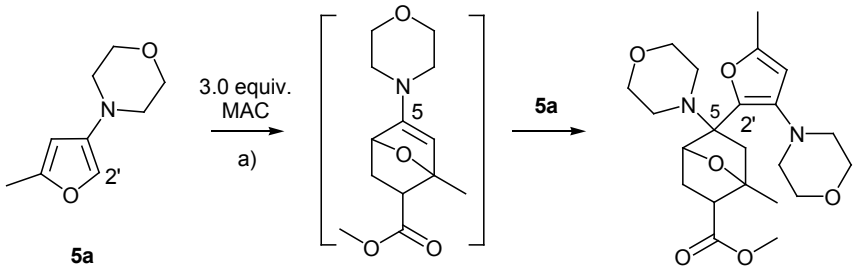

a) Toluene, 111ºC, 8 h.

Scheme 3.24: Reaction of **5a** with MAC in toluene at 111ºC gave **26** via formation of the D-A cycloadduct **25** followed by addition to the C(5) enamine olefin with a second equivalent of **5a** which reacts at the C(2') furan carbon.

The neat reaction between **5a** and MAC also produced **26** in high yield and GC-MS analysis did not indicate the reproducible formation of cycloadducts **4** or **25** although yields >5% of **4** were encountered on one occasion.

D-A reactions of **5a** with two equivalents of MAC in aqueous media were undertaken at room temperature to produce excellent yields of **4** in short reaction times (Scheme 3.25). Upon rapid stirring, small droplets of **5a** distributed throughout the aqueous heterogenous solution and after successful cycloaddition to form **25** the crude material slowly aggregated and formed a film on top of the water which partially hydrolysed to **4** with continued stirring. Attempts at progressive ^{1}H NMR experiments in D_2O indicated that the cycloaddition was almost spontaneous in aqueous media since the disappearance of furans signals was complete before the time required for ^{1}H NMR acquisition (~1:30 min). Cycloadditions conducted in aqueous solution gave the cleanest product mixtures when conducted at low

concentrations (5.4 x 10^{-4} [M]) and the analysis of changes in diastereomeric ratio with temperature demonstrated a preference for the *endo* product **4a** at low temperatures (Table 3.1). GC-MS analysis of the crude D-A extracts indicated that the intermediate **25** was present in large quantities at 2ºC and that the hydrolysis of **25-*exo*** occurs rapidly whereas **25-*endo*** is in equilibrium with **4a** and is predominately hydrolysed in reactions conducted at 45ºC (Appendix 3.7). Complete hydrolysis of both diastereoisomers of **4** was achieved in aqueous acidic acid and best results were obtained by allowing 2 h reaction time for partial hydrolysis followed by extraction into DCM and vigorous shaking with 0.5 M HCl. In all cases the cycloaddition proceeds in >99% yield and the *m/z* 167 molecular ion for **5a** was observed, even in the presence of 4.0 equivalents excess of MAC, and can be detected in the tailing edge of the **4b** peak (Figure 3.13).

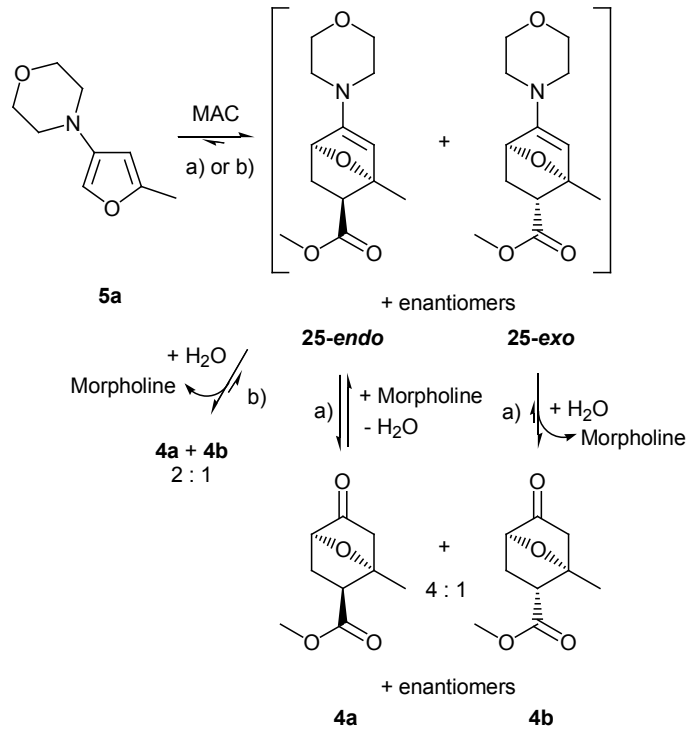

a) H_2O, 25ºC, 2 h b) H_2O, 45ºC, 2 h.

Scheme 3.25: D-A reaction of **5a** with MAC in water (25ºC) gave rapid conversion to **25** and the hydrolysis of **25-*exo*** to **4b** appeared to be more facile than the hydrolysis of **25-*endo*** to **4a** (Appendix 3.7). Aqueous reaction at 45ºC gave a predominately hydrolysed 2:1 mixture of **4a** and **4b** whereas reaction at 25ºC gave a 4:1 mixture.

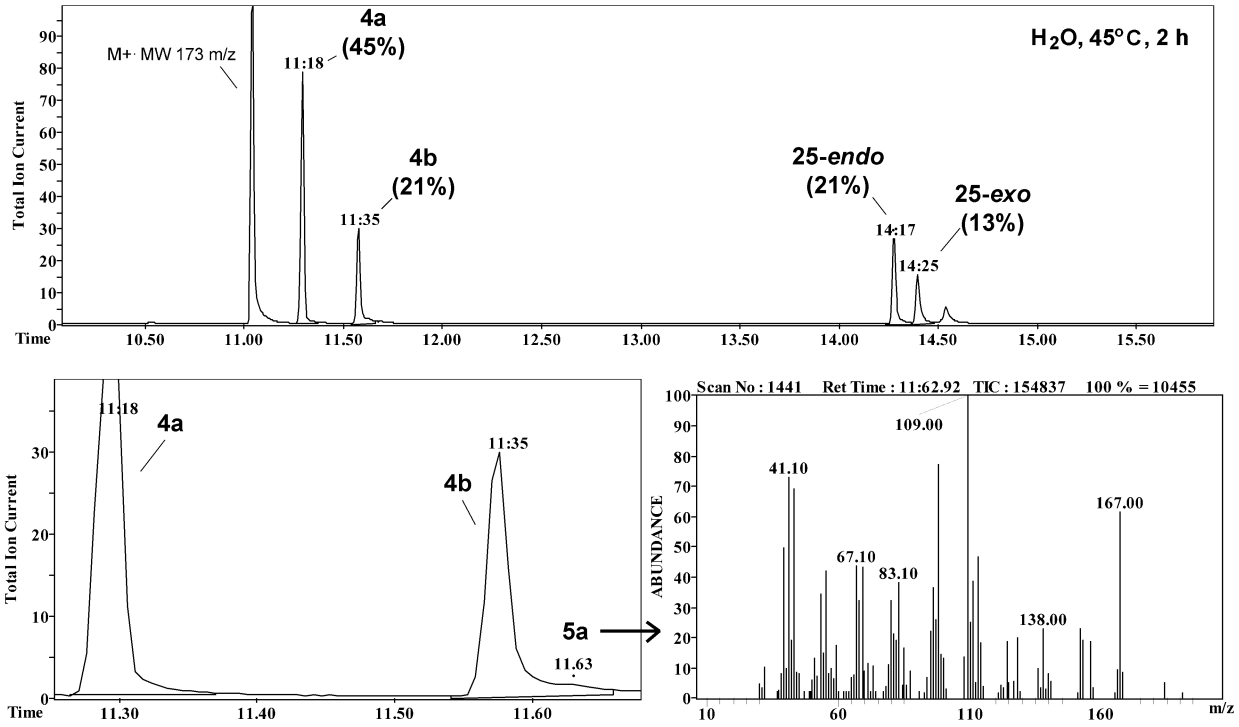

Figure 3.13: GC-MS analysis of the crude extract from the D-A reaction between **5a** with MAC in water at 45ºC indicated the clean formation of cycloadducts **25** and **4** and the enamine **25** was predominately hydrolysed to **4** after a 2 h reaction time. The MS of the starting furan **5a** could be detected in the tailing edge of **4b**, suggesting the D-A reaction is in equilibrium with **5a** with strong preference for the cycloadduct.

These results indicate that the cycloadduct **25** is in equilibrium with **5a** in aqueous reactions and suggest that formation of the enamine of the kinetically favoured *endo* product (**25-*endo***, Figure 3.25) involves a lower transition state energy. A predominance of **4a** may thus be obtained by conducting the D-A cycloaddition at low temperatures with sufficiently active dienes. Reactions at temperatures above 45ºC encouraged the formation of by-products and this complicated repeated attempts to form a predominance of the *exo* diastereoisomer via D-A equilibration to the thermodynamic product **25-*exo***. It should also be mentioned that measurements of changing diastereoisomeric ratio over time was made difficult due to the facile hydrolysis to **4**.

5-Methyl-3-amino furans of various amine size were trialed to study the steric effect of C(3) amine substituents on reactivity and changes in *endo:exo* selectivity. Reactions of *N*,*N*-diisopropyl-5-methylfuran-3-amine **5c** with MAC in toluene was successful at 70ºC in moderate yield (8 h, 42% yield **4**) and reactions in DCM proceeded upon prolonged stirring at room temperature (120 h, 30% yield **4**). In both solvents a diastereomeric ratio of 1:1 was observed with significant decomposition (Table 3.1), leading to difficulties in purification. D-A reaction of **5c** with MAC in water was observed to provide

excellent yields of **4** (>95%) in clean reaction mixtures with 1:2 selectivity for the *exo* product **4b** (Table 3.1) as indicated by GC-MS analysis (Appendix 3.8). The enamine intermediate **27** (Scheme 3.26) was not isolated and mostly hydrolysed after 4 h reaction times at ambient temperature, followed by complete hydrolysis upon aqueous acidic workup. The cycloaddition of **5c** in aqueous LiCl solutions was conducted in order to observe the effect of increases in ionic strength and reactions in 3.0 M LiCl had no effect on diasteroselectivity although complete hydrolysis to **4** was achieved in high yield (91%) under neutral conditions in 1 h (Table 3.1). The salting-out effect of LiCl was apparent in reacting solutions and **5c** immediately formed a biphasic solution without a period of visible micellar suspension.

5	MAC (eq.)	Solvent	Temp. (°C)	Time (h)	% Yield **4**[A]	d.r.[C]
a	3.0	Toluene	111	12	0	-
a	3.0	Hexane	40	8	30	5:1
a	3.0	Hexane	50	8	45	7:1
a	3.0	Hexane	70	8	60[B]	9:1
a	3.0	Benzene	80	12	0[B]	-
a	3.0	Dioxane	100	24	0[B]	-
a	2.0	DCM	-78 to 0	8	4	2:1
a	2.0	DCM	4	8	69	2:1
a	2.0	DCM	r.t.	8	93	4:1
a	2.0	Water	1	2	>95	5:1
a	2.0	Water	r.t.	2	>95	4:1
a	2.0	Water	45	2	>95	2:1
c	2.0	Toluene	60	8	0	-
c	2.0	Toluene	70	8	42[B]	1:1
c	1.5	DCM	r.t.	120	30[B]	1:1
c	1.5	Water	r.t.	4	>95	1:2
c	1.5	3.0 M LiCl	r.t.	1	91	1:2
c	1.5	0.1 M CH_3COOH	r.t.	1	87	1:1
c	1.0	DIMCARB	r.t.	1	>95	3:7
b	1.5	Water	r.t.	2	>95	3:2
b	1.5	3.0 M LiCl	r.t.	1	>95	1:1
e	2.5	DCM	r.t.	8	0	-
e	2.0	Water	r.t.	8	>95	4:1

Table 3.1: Diels-Alder reactions of 3-furylamines **5a**, **5b**, **5c** and **5e**. [A]Combined yields of **4** as determined by GC-MS. [B]Significant decomposition. [C]Ratio of diastereoisomers **4a**:**4b**. Reactions in organic media performed using 1.2 mmol of **5** in 10 mL solvent. Reactions in ionic media performed using 0.6 mmol of **5** in 20 mL solvent.

The ionic liquid *N*',*N*'-dimethylamino-*N*,*N*-dimethylcarbamate (dimethylamine-CO_2 adduct, DIMCARB) [83] provided a polar reaction media with similar hydrogen bond donating and accepting properties to that seen in water, in which the D-A reagents are completely soluble. Reactions of **5c** in DIMCARB were complete in 1 h using an equi-molar quantity of MAC and produced the cycloadduct **4** with 3:7 selectivity for **4b**. These results strongly suggest that the hydrogen bond donor properties of the solvent are predominantly responsible for increases in reaction rate of the 3-furylamine dienes whereas hydrophobic interactions as discussed in Section 3.1.2 may contribute to a lesser extent.

D-A reactions of *N*,*N*-diethyl-5-methylfuran-3-amine **5b** with MAC in water and 3.0 M LiCl were equally successful (>95% **4**, Table 3.1) and the enamine D-A product was not observed in GC studies indicating complete hydrolysis to the ketone **4** after 1-2 h at room temperature. *N*,*N*-Dibenzyl-5-methylfuran-3-amine **5e** did not react with MAC in DCM but was successful in water and progressed slowly over 8 h to provide **4** in 4:1 *endo:exo* ratio. The slow reaction rate was suspected to be due to a decrease in solubility attributed by the larger aromatic substituents on the amine, and reaction times could be reduced to 1 h when ultrasonic irradiation was employed as a means of dispersing the furan in aqueous media.

The influence of the C(5) amine group on diastereoselectivity is apparent for reactions involving **5c** whereby the steric effect of the isopropyl substituents towards crowding the furan face leads to the *exo* compound predominating due to repulsion of the ester substituent (Scheme 3.26) and the disruption of secondary π-orbital overlap. The ethyl substituted furan **5b** produces a small excess of the *endo* compound **4a** in water and an equal ratio of **4a** and **4b** was observed in 3.0 M LiCl solution, possibly due increases in reaction rate corresponding with decreases in transition state energies as suggested by Jorgensen [41]. Although hydrophobic effects are typically observed to encourage increases in *endo* product [36], a strong trend towards *endo* selectivity was not observed with increases in solvent polarity potentially due to the polar nature of the amine substituent. At ambient temperature furan, **5e** possessing dibenzylamine substituents provided D-A cycloadducts in the same diastereomeric ratio as reactions involving the morpholine substituted furan **5a**, indicating that the aromatic substituents may be oriented too far away from the reactive carbons to influence diastereoselectivity or alternately contribute a small degree of π-orbital overlap with the incoming dienophile.

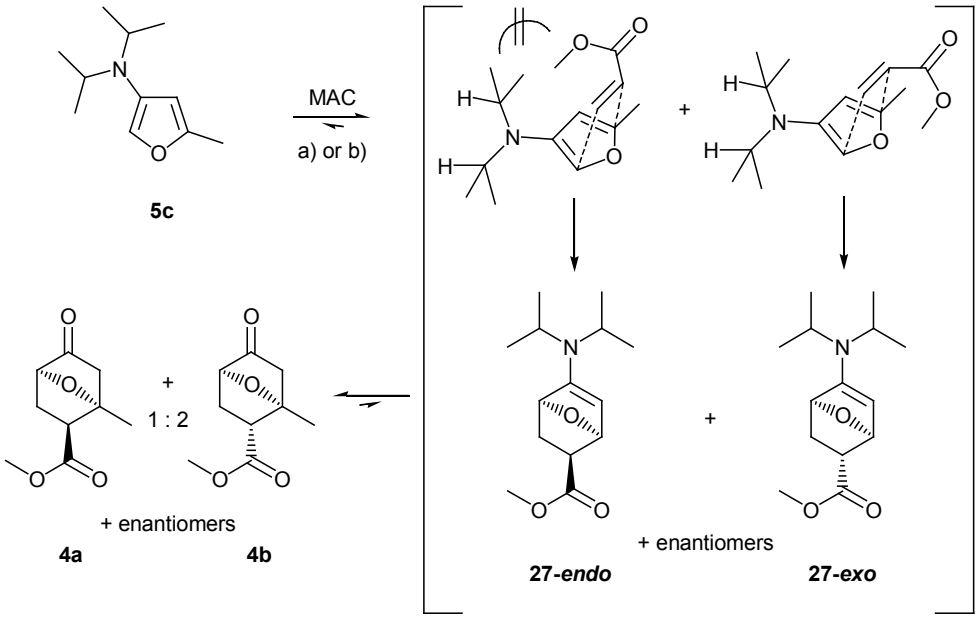

a) H_2O, 25ºC, 4 h b) 3.0 M LiCl 1 h

Scheme 3.26: The D-A reaction of **5c** with MAC in H_2O or 3.0 M LiCl produced the cycloadduct **27** in quantitative yield followed by hydrolysis upon continued stirring to produce the ketone in a 1:2 ratio of **4a**:**4b**.

Reaction of **5c** with MAC in 0.1 M CH_3COOH was observed to produce an increase in diene reactivity compared to neutral conditions and the enamine cycloadduct was hydrolysed *in situ* to produce a 1:1 mixture of **4a**:**4b** accompanied by a small amount of decomposition as indicated by GC-MS analysis (Appendix 8). Increases in the reactivity of 3-furylamines are expected upon protonation of the amine, leading to an increase in HOMO energy of the furan system (Figure 3.14). Increases in reactivity of the protonated **5c** species may account for a decrease in *exo* selectivity although conformational changes in the protonated compound may also contribute as well as hydrogen bonding of the dienophile to the amine hydrogen.

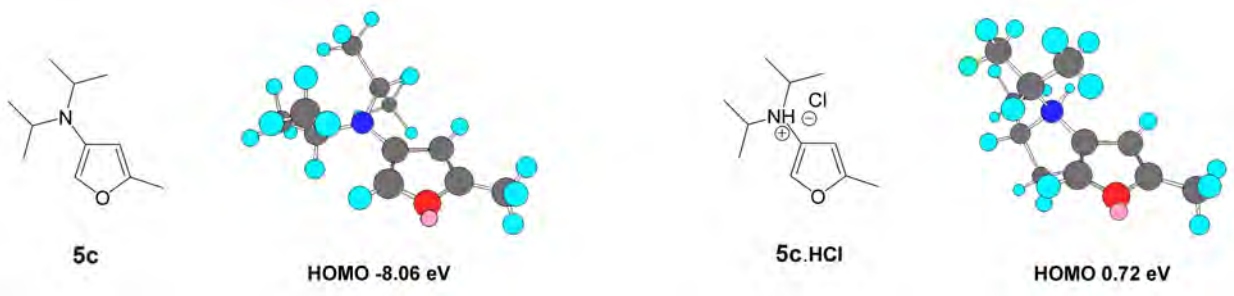

Figure 3.14: Chem3D generated MM2 energy minimised structures of **5c** and calculated HOMO energy levels are shown, indicating changes in conformation of the isopropyl substituent and an increase in HOMO energy levels.

Although more hindered amines **5c** and **5e** gave poor yields in DCM, all furans studied were successfully transformed into D-A products in water, highlighting the unique properties of polar reaction media towards increasing D-A reaction rate. The rate enhancement observed in aqueous reaction media is in agreement with the findings of Breslow *et al.* [36] as discussed in Section 3.1.2, and in the research presented the advantage of an aqueous environment extends to the hydrolysis of the enamine D-A adduct thereby minimizing side reactions of the enamine. The use of water as a reaction medium for organic synthesis is also considered an environmentally benign or "green" alternative to the use of toxic or non-biodegradable solvents, and the ionic liquid DIMCARB proved equally useful as a benign reaction media for expedient cycloadditions of **5** since the solvent can be dissociated under gentle vacuum or heating then recondensed as the addition product for reuse [83]. D-A reactions in ionic solvents progressed without decomposition provided all materials were freshly distilled whereas trials performed in organic solvents were not significantly affected by small impurities or adventitious moisture. In aqueous media gram quantities of racemic products **4a** and **4b** were made accessible using the furylamines **5a** and **5c** and the racemates were used for subsequent preliminary studies involving ether cleavage of the 7-oxanorbornane ring. Face selective D-A studies using the chiral amines **5p** and **5q** were pursued with the aim of producing a pure enantiomer of **4** with suitable absolute stereochemistry for use in the natural product synthesis. The general reaction conditions for the D-A reaction of **5a-e** in organic and aqueous reaction media are included in Sections 6.6.1-6.6.3.

3.3.2 Chiral Separation of Diels-Alder Products by Gas Chromatography

In order to determine the extent of chiral induction due to the influence of optically pure auxiliaries, a simple method was required to determine the ratio of enantiomers of **4a** and **4b**. Enantiomeric purity can easily be determined by comparison with the optical rotation of the pure enantiomer, however at the time of this research these values had not been reported in the literature. Capillary GC using chiral columns was investigated as a direct method of determining enantiomeric ratios and has the advantage that enantiomeric excesses of both diastereomers can be measured simultaneously without the physical isolation of **4a** from **4b**.

GC columns containing a percentage of β-cyclodextrin (Chapter 1, Figure 1.24) derivatives in the stationary phase are useful for the chiral separation of oxygenated monoterpenes [84] and have also been used for comprehensive two-dimensional gas chromatography (GC x GC) for the enantioselective analysis of essential oils [85]. The separation and elution order of enantiomers is strongly influenced by temperature and optimal separation is typically achieved by using low starting temperatures and a slow

temperature ramp. Inversion in elution order is occasionally observed at temperatures either side of the isoelution temperature [86].

Preliminary studies were performed on the racemate of **4** using a CP-Chiralsil-dex CB GC column (Varian) which contains β-cyclodextrin as a chiral selector bonded to dimethylpolysiloxane, to achieve partial resolution of **4b** with total co-elution of **4a** (50ºC, 3ºC/min to 200ºC). The same temperature program was used chiral separation studies with a J&W Cyclosil-β (Agilent) column consisting of 30% heptakis(2,3-di-O-methyl-6-O-*t*-butyl dimethylsilyl)-β-cyclodextrin (in stationary phase DB-170) to provide good separation of **4b** although **4a** remained unresolved (Figure 3.15, left). The Et-TBS-β-CD column (MeGA, Legnano, Italy) composed of 30% diethyl-*t*-butylsilyl-β-cyclodextrin in the relatively non-polar polymethylsiloxane (PS086) stationary phase provided excellent chiral separation for enantiomers of **4a** and **4b** and optimal separation was achieved using temperature program conditions from 60ºC to 180ºC at 2ºC /min. The crystalline *exo* product **4b** was isolated by precipitation from Et_2O at -18ºC and GC analysis on the Et-TBS-β-CD stationary phase (Figure 3.15, middle) gave complete resolution of enantiomers. GC analysis of the crystallization mother liquor shows a 11:1 ratio of **4a**:**4b** (Figure 3.5, right) clearly differentiating the retention times for enantiomers of **4**.

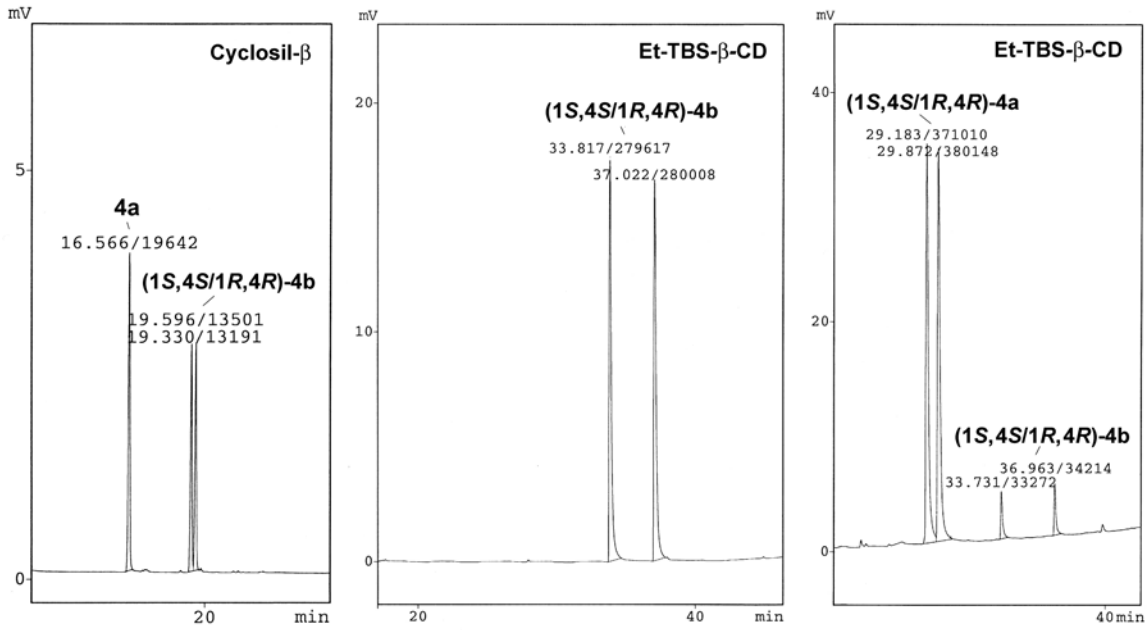

Figure 3.15: Left; Chromatogram of a mixture of **4a** and **4b** on J&W Cyclosil-β column showing the separation of (1*R*/1*S*)-**4b** only. Midddle; Chromatogram of **4b** after crystallization from Et_2O using a Et-TBS-β-CD stationary phase. Right; Chromatogram of Et_2O crystallization mother liquor consisting of **4a:4b** (11:1).

Small changes in the retention time of analytes were observed with changes in relative peak heights and minor differences in column head pressure. Column dimensions and GC conditions for the chiral separation of **4** are included in Section 6.10.

3.3.3 Enantioselective Diels-Alder Reactions

D-A reactions involving non-chiral 5-methyl-3-furylamines with MAC (Section 3.3.1) demonstrated both DCM and water to be suitable reaction media and these conditions were subsequently used for enantioselective D-A studies of chiral 3-furylamines. Reaction of **5p** with MAC in DCM at 0ºC revealed that the (+)-pseudoephedrine-derived 5-methyl-3-furylamine diene was very reactive towards [4π+2π] electron cycloadditon and GC-MS monitoring indicated the formation of a major and minor product featuring a molecular ion at *m/z* 331 in agreement with the mass of the cycloadduct (Appendix 3.9). Fragment ions characteristic of the pseudoephedrine derived oxazolidine (*m/z* 91, 118, 148) as observed for **19p** (Section 2.4, Figure 2.16) suggested that the enamine **28-int** preferentially exists as the five membered heterocycle **28-*endo***. Reactions conditions were optimised by reacting **5p** at –50ºC with slow warming to ambient temperature over 8 h to achieve **28-*endo*** (>95% yield, GC-MS) in high purity and the identity of the enamine diastereoisomer was confirmed by partial hydrolysis in HCl to reveal **4a** (Scheme 3.27). Distillation, column chromatography on deactivated silica and gas chromatography in the presence of chemically active GC injector liners or columns led to an appreciable retro-D-A reaction of **28**, indicating that the oxazolidine form of the cycloadduct may act to prevent a facile retro [4π+2π] reaction from occurring.

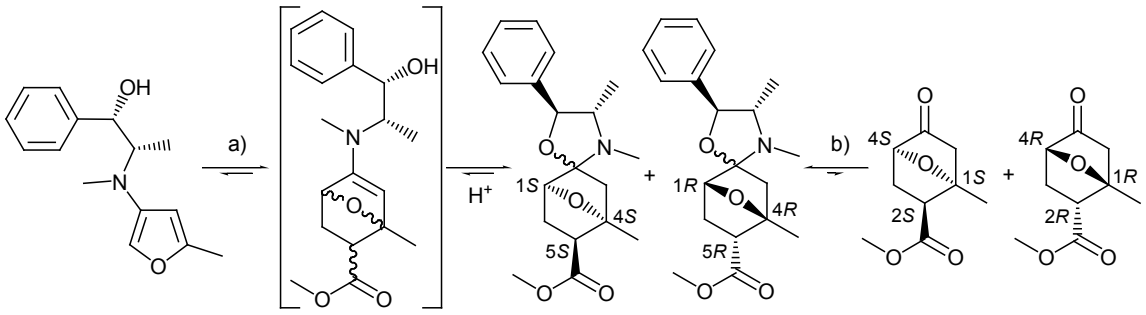

a) MAC, DCM, -50ºC to 25ºC over 8h, 95% b) 0.5 M HCl, 20%

Scheme 3.27: D-A reaction of **5p** with MAC in cold DCM with warming to ambient temperature gave the enamine cycloadduct **28-int** as a single isomer in >95% which spontaneously underwent intramolecular cyclization to the spiro oxazolidine heterocycle **28-*endo***. Partial hydrolysis in 0.5 M HCl gave the *endo* 7-oxanorbornane **4a**.

^{13}C NMR analysis of the crude D-A mixture indicated a highly enriched mixture of (1*S*,4*S*,5*S*) and (1*R*,4*R*,5*R*)-methyl 3',4,4'S-trimethyl-5'S-phenylspiro[7-oxa-bicyclo[2.2.1]heptane-2,2'-[1,3]oxazolidine]-5-carboxylate diastereomers **28** and chemical shifts of the major isomer are assigned in the HMQC NMR shown in Figure 3.16. The bicyclic structure of **28-*endo*** was confirmed by COSY NMR indicating correlation between the bridgehead H(1) at δ 4.60 and methylene signals from H(6_B) at δ 2.04, and correlation between H(5) at δ 2.70 with H(6_A) at δ 2.55 and H(6_B) (Appendix 3.10). HMQC and DEPT 135 analysis (Figure 3.16) agree with conclusions drawn from MS fragmentation data, showing the product to exist as the oxazolidine as indicated from the quaternary C(2/2') spiro signal at δ 108.8 and the C(3) methylene signal at δ 41.7 correlated to H(3_A) and H(3_B) at δ 2.43 and 1.85, respectively.

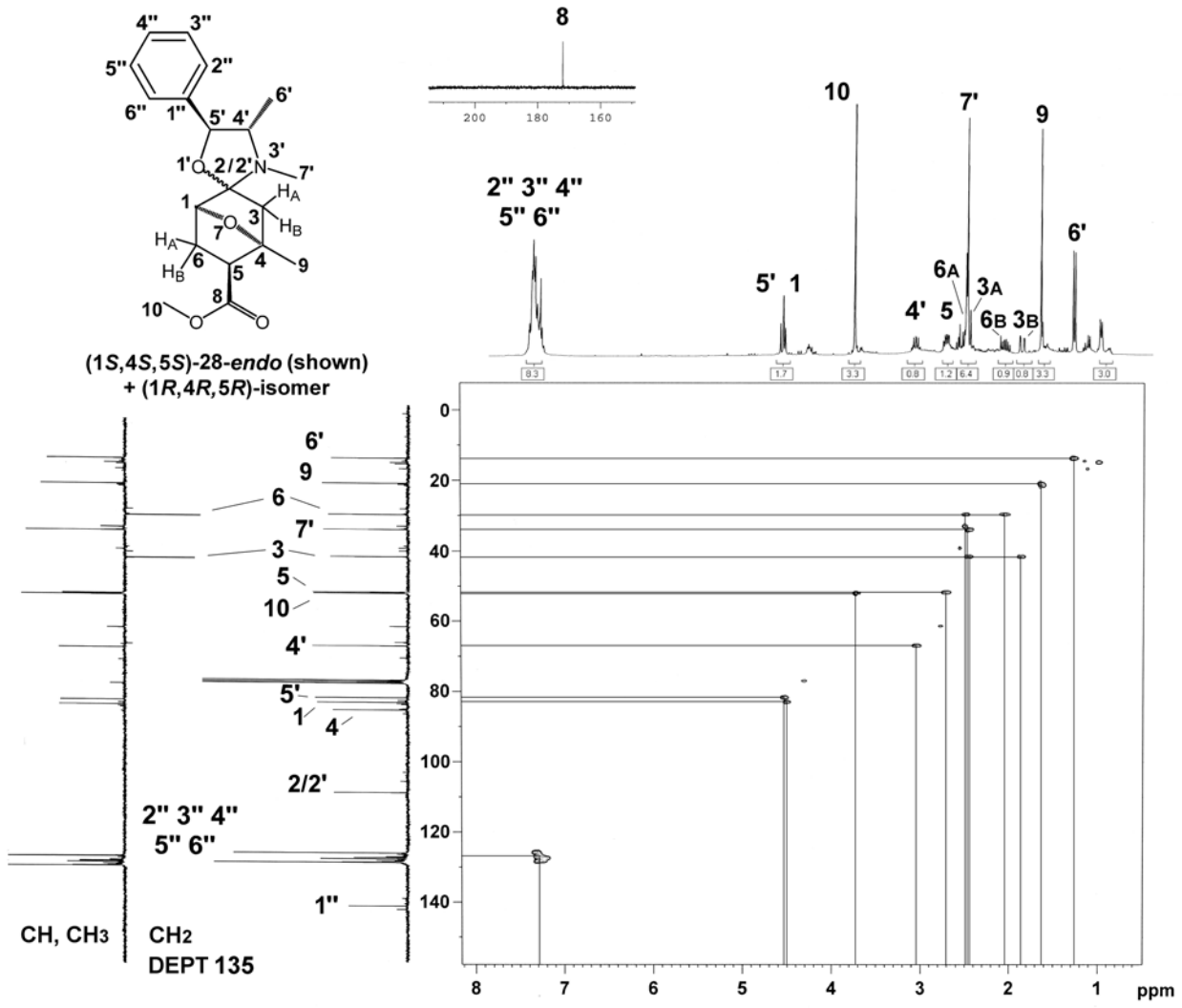

Figure 3.16: 300 MHz ^{1}H/75 MHz ^{13}C HMQC NMR of **28-*endo*** with structure assignments is shown and the quaternary C(2')/(2) carbon is confirmed by DEPT 135 NMR.

The disappearance of both the C(2/2') spiro and C(3) methylene carbon signals at δ 108.8 and 41.5 in acidic D_2O suggests facile reversion to the enamine **28-int** upon protonation (Appendix 3.10) although full characterisation on this intermediate could not be obtained. Connectivity of the ephedrine and bicyclic moieties was confirmed by HMBC correlations and four-bond-w-coupling was observed in ^{1}H NMR consistent with the *endo* diatereoisomer (Appendix 11). The general experimental procedure for the reaction of **5p-q** in DCM is included in Section 6.6.4.

At this stage an attempt was made to purify by crystallization the mixture of (+)-pseudoephedrine derived 7-oxanorbornanes shown in Figure 3.16 in order to obtain a single isomer for the determination absolute stereochemistry. The **28-*endo*** mixture was a low melting semi-solid and crystallization was unsuccessful in hexane:ether mixtures at low temperatures (–20-0ºC). As well, the oxazolidine salt could not be crystallised due to facile reversion to **28-int**. The oxazolidine **28-*endo*** was unreactive towards reduction by $NaBH_4$ in EtOH and $LiAlH_4$ in Et_2O and required acidic reduction conditions to effect interconversion to the enamine **28-int** allowing reduction of the olefin to produce the amine product **29** (Scheme 3.28).

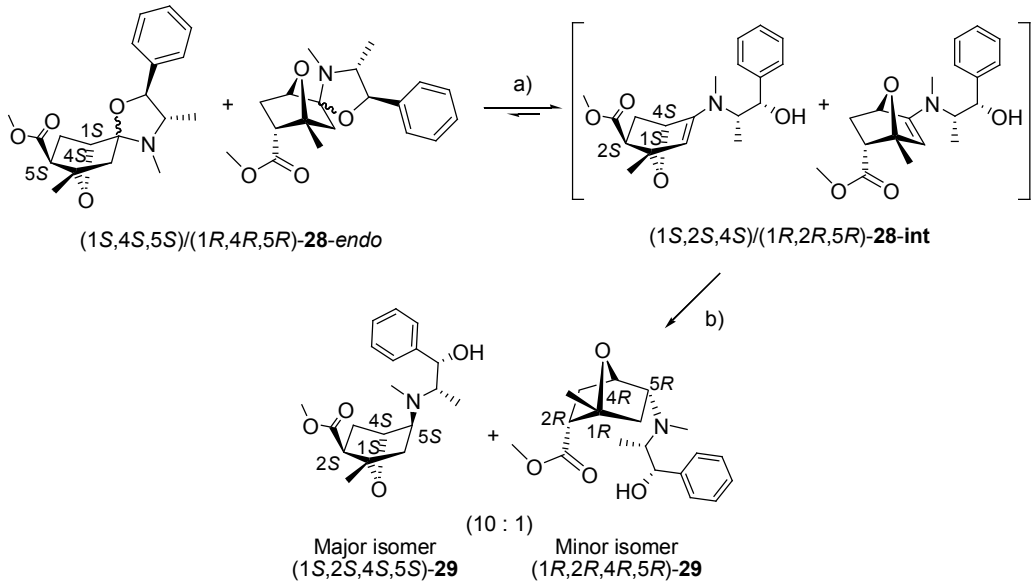

a) Glacial CH_3COOH b) $NaBH(OAc)_3$ preformed from $NaBH_4$ in CH_3COOH, 25ºC, 70%

Scheme 3.28: The oxazolidine **28-*endo*** was equilibrated with the enamine **28-int** in glacial acetic acid followed by reduction to the tertiary amine using $NaBH(OAc)_3$ to produce a 10:1 mixture of diastereoisomers of **29**.

These conditions were satisfied by performing the reduction in glacial acetic acid using sodium triacetoxyborohydride ($NaBH(OAc)_3$), preformed from $NaBH_4$ in acetic acid according to a procedure

described by Hutchins *et al.* [87]. Clean reduction of **28-*endo*** was achieved to give a single peak in GC-MS analysis with no molecular ion and a base peak at *m/z* 226 corresponding to fragmentation of the pseudoephedrine chain of **29** (Appendix 3.12). The amine was easily purified by bulb-to-bulb distillation to provide 70% yield of **29** as a colourless resin and the structure of the reduced compound was confirmed by COSY correlations of H(5) at δ 3.12 to H(6) at δ 1.64 and H(4) at δ 4.40 (Appendix 3.12).

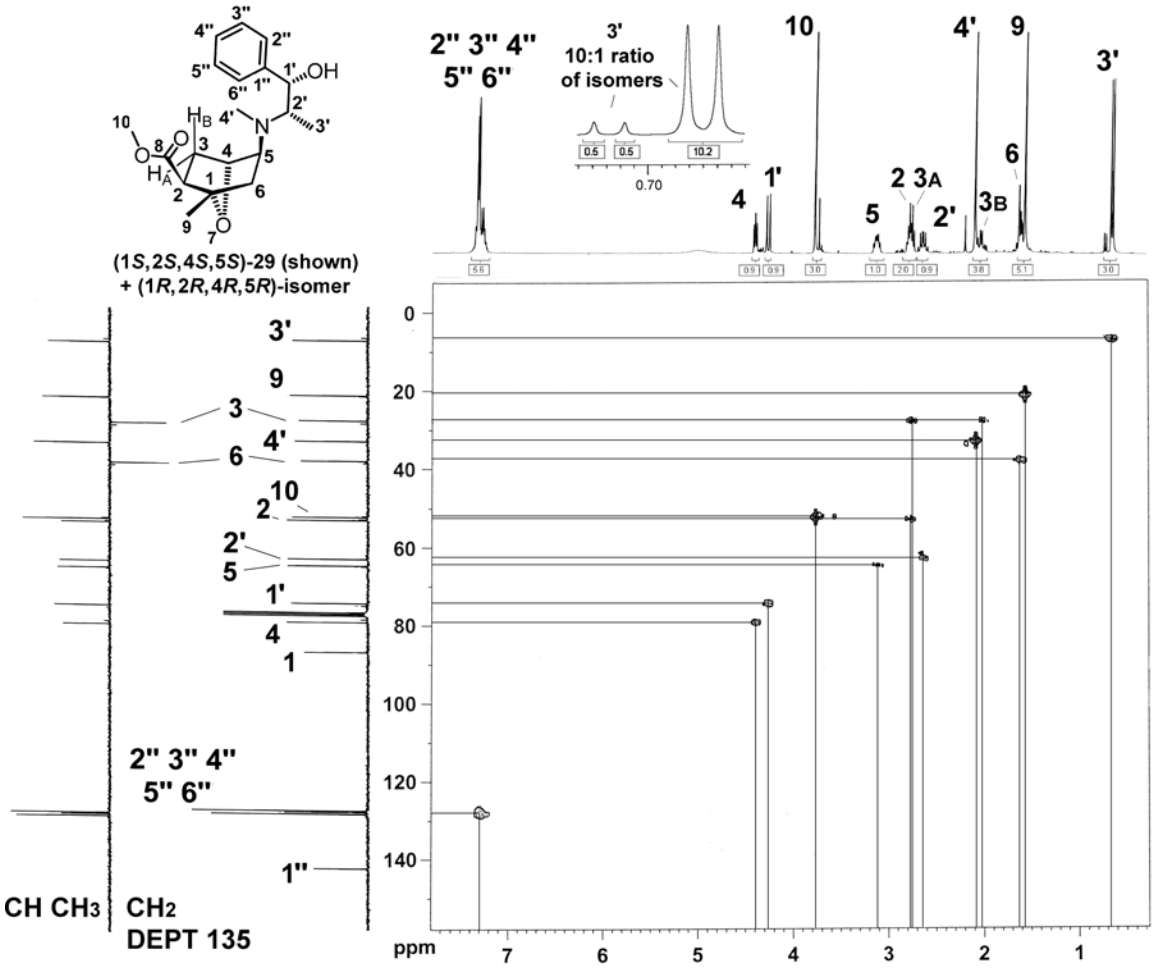

Figure 3.17: 300 MHz ^{1}H/75 MHz ^{13}C HMQC NMR spectrum of a mixture of (1*S*,2*S*,4*S*,5*S*)-**29** and (1*R*,2*R*,4*R*,5*R*)-**29** and DEPT 135 NMR data.

The *exo* face of the 7-oxanorbornane ring is less hindered and more accessible for reduction to the give *cis-endo* product, as exemplified in work by Koreeda *et al.* [71] and Takahashi *et al.* [72] (Section 3.2.1), therefore **29** is assigned as the *endo* C(5) amine although confirmation could not be obtained via coupling constants to the H(5) signal which appeared as a broad multiplet. Two diastereoisomers were observed in ^{13}C NMR spectrum (Appendix 3.13) and ^{1}H NMR integral regions of C(3') indicates a 10:1 a mixture of diastereoisomers (Figure 3.17). ^{13}C and ^{1}H NMR assignments for the major isomer of **29** were made based on HMQC data (Figure 3.16) and methylene carbon signals for

C(6) at δ 38.3 and C(3) at δ 28.0 are confirmed by DEPT 135 analysis (Figure 3.16). HMBC analysis also corroborated the structure of **29** and is included in Appendix 3.13.

Although the amine **29** was very stable, crystallization as the protonated amine salt produced hydroscopic solids with many counter-ions (Cl^-, picrate, $AuBr_4^-$) that were unsuitable for X-ray crystal analysis. Crystallization in Et_2O using $HCl_{(g)}$ (Section 6.6.5) produced a white amorphous hydrochloride salt that was filtered under a dry N_2 atmosphere and redissolved in MeCN followed with counter-ion exchange by the addition of silver perchlorate ($AgClO_4$) to yield a solution of the perchlorate salt **29.HClO$_4$** (Scheme 3.29). The AgCl precipitate was filtered from the MeCN solution after cooling to 0ºC and **29.HClO$_4$** was carefully crystallised in MeCN by vapour diffusion with Et_2O. ^1H and ^{13}C NMR analysis of **29.HClO$_4$** indicated that the recrystallised material consisted of a single isomer (Figure 3.18) and NMR assignments were made based on COSY and HMQC analysis (Appendix 3.14). In comparison to ^1H NMR data of **29**, the expected downfield shifts for H(5), H(2') and H(4') signals were observed for protons situated closest to the quaternary amine in **29.HClO$_4$** and the $H(3_A)/(3_B)$ methylene signals appear as a second order multiplet at δ 2.30. The crude material could also be recrystallised from EtOH to provide a pure isomer however ethanolic solutions of the perchlorate salt were observed to decompose upon heating above 45ºC. X-ray crystal structure data on the major isomer of **29.HClO$_4$** (Figure 3.19) revealed that the (+)-pseudoephedrine auxiliary had promoted facial selectivity in the [4π+2π] cycloaddition for the (1*S*,4*S*) isomer. In this methodology, the optically pure auxiliary **23** has allowed for diastereoselectivity in the D-A reaction and incorporation into subsequent bicyclic derivatives provides diasteroisomeric differentiation of the enriched mixture of bicyclic antipode moieties.

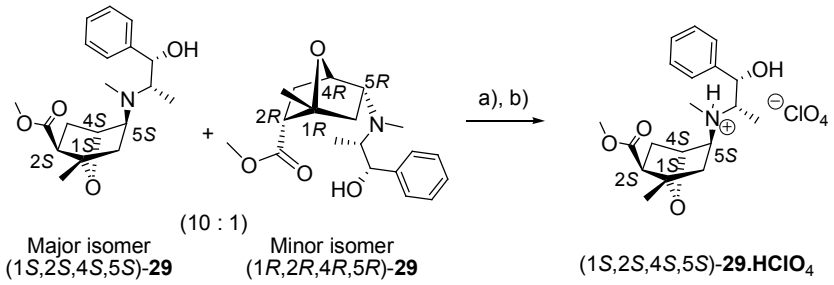

a) $HCl_{(g)}$, Et_2O b) MeCN, $AgClO_4$, Et_2O.

Scheme 3.29: Precipitation of **29** as the hydrochloride salt followed by counter-ion exchange using $AgClO_4$ in MeCN allowed the purification of (1*S*,2*S*,4*S*,5*S*)-**29.HClO$_4$** by crystallization using vapour diffusion with Et_2O.

The X-ray crystal structure of (1*S*,2*S*,4*S*,5*S*)-**29.HClO$_4$** also provides confirmation that the reduction of **28-*endo*** had selectively occurred at the less hindered *exo*- face. The X-ray crystal CIF file

and a summary of bond distances for C-C bonds are included in Appendix 3.15, along with a comparison of bond lengths with literature values.

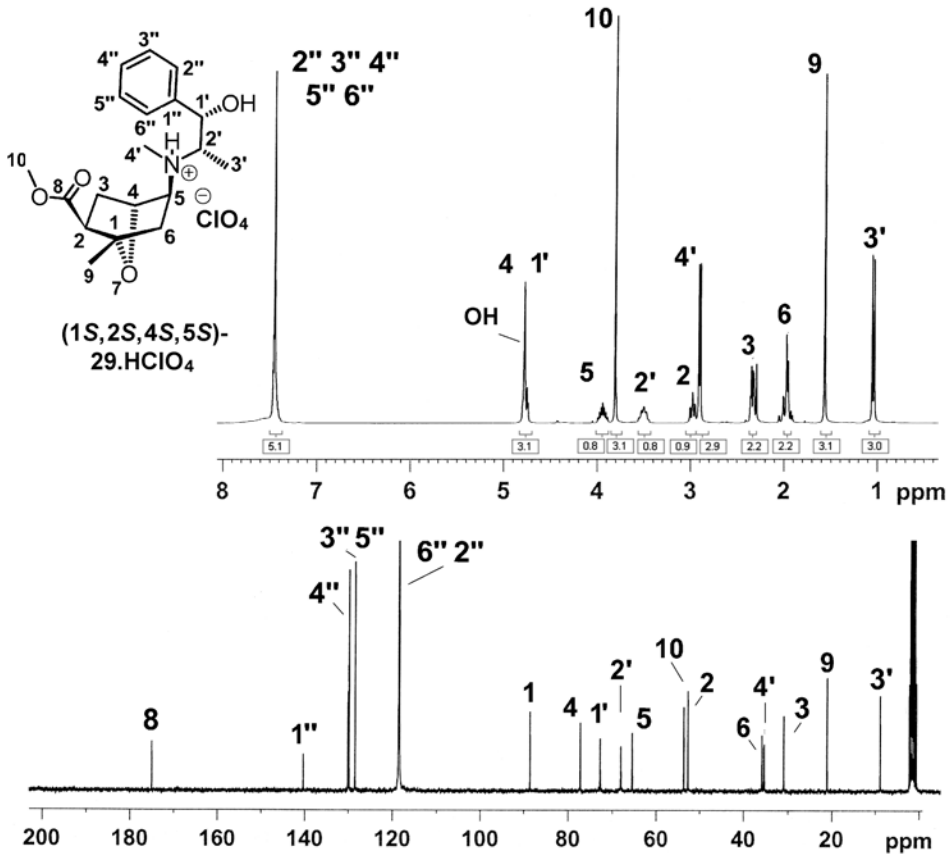

Figure 3.18: 300 MHz ^{1}H NMR and 75 MHz ^{13}C NMR spectrum of (1*S*,2*S*,4*S*,5*S*)-**29.HClO$_4$**, obtained by crystallization from MeCN using vapour diffusion with Et_2O, indicates a single diasteroisomer.

The oxazolidine **28-*endo*** was stable to hydrolysis in aqueous environments and efficient hydrolysis conditions were required to facilitate clean conversion to **4a** for a reliable calculation of enantiomeric excess. Upon heating in strongly acidic solutions (pH = 1; H_2O, MeCN/H_2O and EtOH/H_2O), **28-*endo*** underwent a retro Diels-Alder reaction via **28-int** rather than hydrolysis, as indicated from increasing concentration of **5p** in GC-MS analysis, leading to a loss in enantio- and diastereomeric excesses along with slow decomposition as indicated by chiral GC analysis. After many attempts effective hydrolysis was achieved by gentle heating in a buffer solution of NaOAc/CH_3COOH (pH = 5.5) to give the optically enriched ketone **4a** in 90% isolated yield (Scheme 3.30). Enantiomeric excess (*ee*) of **4a** was measured by chiral-GC on a Et-TBS-β-CD column (MeGA, Italy) to provide baseline resolution of the enantiomers and indicating 85% *ee* of the (1*S*,2*S*,4*S*)-**4a** product (Figure 3.20, top left; Table 3.2) on reactions at $\leq$ 1.0 mmol scales ($\leq$ 0.25g). Reactions at multigram scales performed comparably well to give (1*S*,2*S*,4*S*)-**4a** in 80% *ee* and this measurement for enantiomeric purity is

consistent with ^{1}H NMR integral regions of H(3') in the mixture of diastereomers of **29** (Figure 3.17). Hydrolysis in strong acidic conditions typically gave the *endo* product in ~65% *ee* with a small amount of *exo* product, demonstrating that the equilibrating D-A reaction under aqueous acidic environments has a detrimental effect on stereoselectivity in the ketone product. The general procedure for the hydrolysis of oxazolidines **28** and **30** is included in Section 6.6.6.

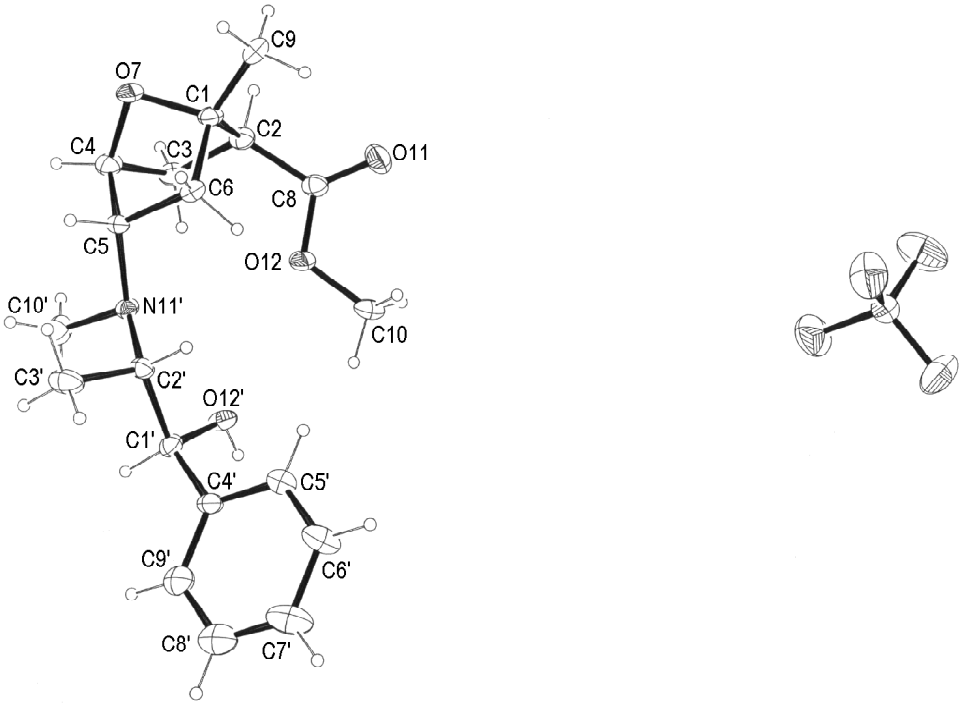

Figure 3.19: ORTEP drawing of (1*S*,2*S*,4*S*,5*S*)-methyl 5-(*N*-((1*S*,2*S*)-1-hydroxy-1-phenylpropan-2-yl)-*N*-methylamino)-1-methyl-7-oxa-bicyclo[2.2.1]heptane-2-carboxylate perchlorate salt (1*S*,2*S*,4*S*,5*S*)-**29.HClO$_4$**. Crystal Data. $C_{19}H_{28}ClNO_8$, MW = 433.87, T = 293(2) K, λ = 1.54180 Å, orthorhombic, space group *P*-$2_12_12_1$, *a* = 8.511(2), *b* = 15.356(5), *c* = 15.839(3) Å, $\alpha = 90.00^o$, $\beta = 90.00^o$, $\gamma = 90.00^o$, *V* = 2070.1(9) Å^3, Z = 4, D_c = 1.392 Mg/m^3, μ(Cu Kα) = 2.025 mm^{-1}, F(000) = 920, crystal size 0.20 x 0.10 x 0.02, 2462 reflections measured, 2365 independent reflections (R_{int} = 0.0230); the final *w*R(F^2) was 0.1371 (all data) and final R was 0.0496 for 2006 unique data [$I > 2\sigma(I)$]. Goodness of fit on F^2 = 1.071. Crystallographic data for the structure reported has been deposited with the Cambridge Crystallographic Data Centre as deposition No. 288601.

Reaction of the (-)-ephedrine derived 3-aminofuran **5q** with MAC in DCM at –50ºC to 25ºC over 8 h (Scheme 3.30) gave quantitative conversion to the oxazolidine **30** as indicated by GC-MS and fragmentation was almost identical to that observed in **28**-*endo* (Appendix 3.16). Hydrolysis in NaOAc/CH_3COOH buffer provided a 3:1 ratio of **4a**:**4b** in 56 and 47% *ee* respectively as determined by chiral GC analysis (Figure 3.20, bottom left). Comparison of chiral GC analyses of D-A adducts prepared from **5p** and **5q** revealed both ephedrine isomers to direct face selectivity in the same manner, whereas

the diastereomeric outcome was quite different between the auxiliaries. The ephedrine isomers **23** and **24** (Section 2.4, Figure 2.15) have a diasteromeric relationship and differ in stereochemistry at the benzylic C(1') alcohol, suggesting that the preferential face for D-A cycloaddition was determined by the stereochemistry at the C(2') amine group. The decrease in *endo* selectivity observed when using the (-)-ephedrine derived furan **5q** may indicate a closer proximity of the benzene ring to the furan face in the transition state, hindering the exclusive formation of the *endo* isomer. The *exo* isomer **4b** can reasonably be expected to have formed with preference for the same face of the furan diene as observed in the *endo* compound and the major enantiomer can be assigned as (1*S*,2*R*,4*S*)-**4b**.

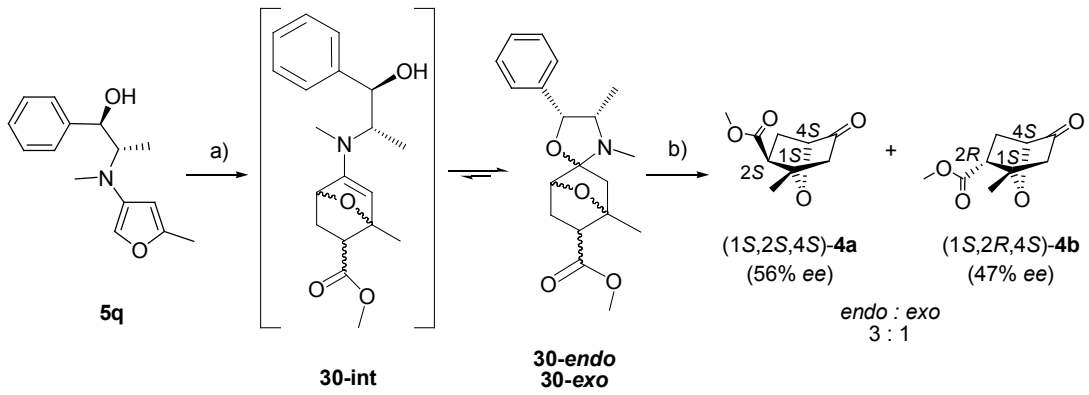

a) DCM, MAC, -50 to 25ºC b) NaOAc/CH_3COOH, H_2O, 70ºC, 2h, 87%.

Scheme 3.30: D-A reaction of **5q** with MAC in cold DCM with warming to ambient temperature gave the enamine cycloadduct **30-int** which underwent intramolecular cyclization to the spiro oxazolidine heterocycle **30**. Hydrolysis in NaOAc/CH_3COOH solution produced an optically enriched 3:1 mixture of **4a** and **4b**.

Heterogeneous D-A reactions of **5p** and **5q** with MAC in water were very slow with stirring at room temperature but progressed in excellent yields and in short reaction times when performed with the aid of ultrasonic irradiation (>80% yield, 1.5 h). 3-Furylamine **5e** containing aromatic substituents has been shown to react to completion without sonication, suggesting that the sonication in this case is simply a means of suspending the furan in solution, rather than a rate enhancing phenomenon. Small scale reactions ($\leq$ 1.0 mmol) carried out using **5p** in aqueous media gave a mixture of **28** and **4** as identified by GC-MS (Appendix 3.17) and the extent of hydrolysis to **4** was varied depending on the location of the reaction vessel in the ultrasonic bath. The excess dienophile was removed under vacuum to prevent the D-A reaction from occurring with unreacted portions of **5p** during extraction into DCM, and following work-up the crude cycloadduct was heated under hydrolysis conditions for 2 h. Chiral GC analysis indicated good enantiomer purity (75% *ee*, Table 3.2) for both diastereoisomers of **4** that were prepared in a 9:1 *endo:exo* ratio (Figure 3.20, top right).

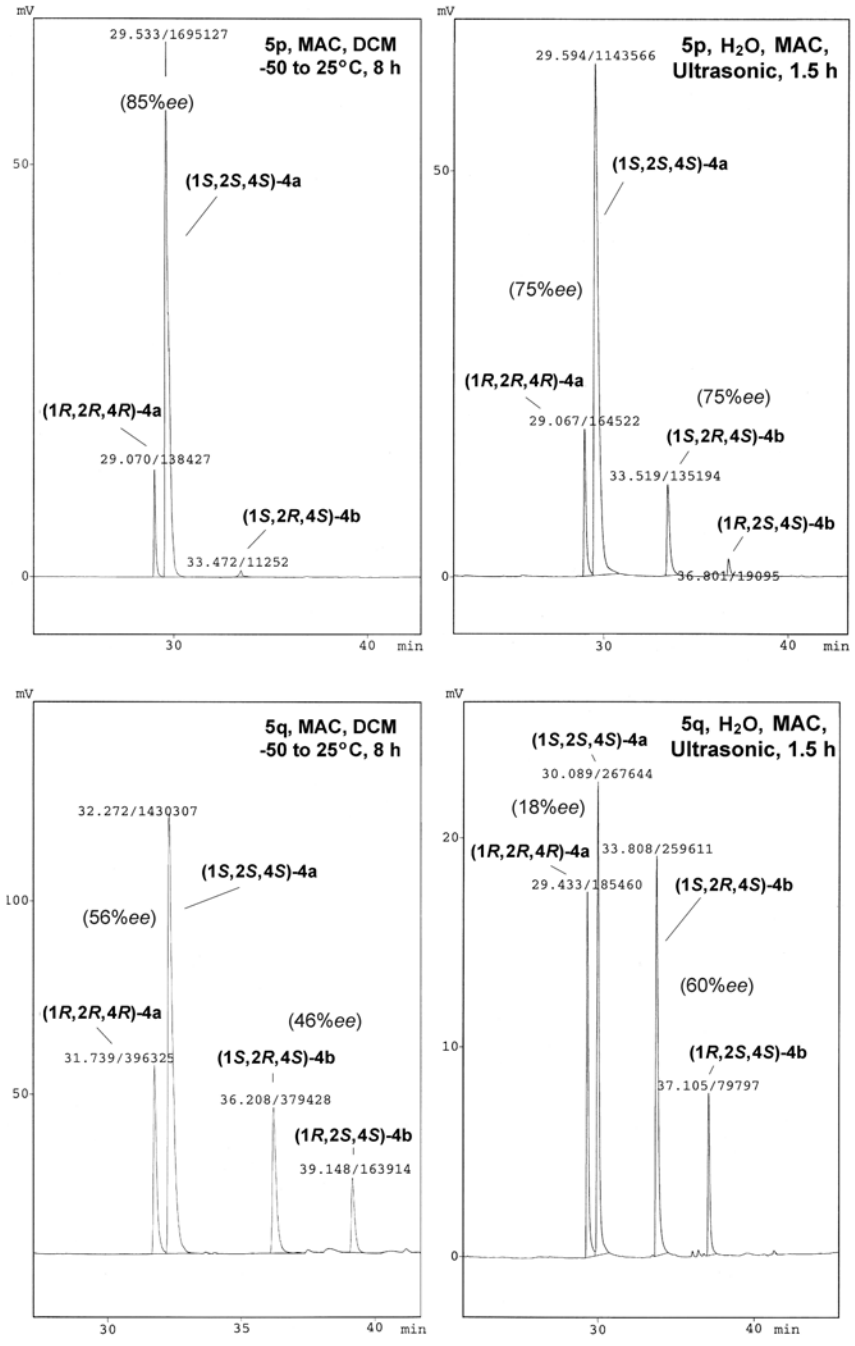

Figure 3.20: Chiral GC analysis using Et-TBS-β-CD stationary phase, showing optically enriched mixtures of **4** prepared using the chiral dienes **5p** and **5q** by the D-A reaction with MAC. Calculated enantioselectivities for **4a** and **4b** are listed in Table 3.2 and represent the average reproducible values. Top left; The 7-oxanorbornane **4a** is prepared in >99% diastereoselectivity using **5p** in DCM, starting at –50ºC with warming to –10ºC for 2 h and reaching 25ºC over an 8 h period. Bottom left; Reaction of **5q** in DCM under the same conditions as for **5p** produced a 1:3 ratio of **4a**:**4b**. Top right; Reaction of **5p** in H_2O produced a 9:1 ratio of **4a**:**4b** after 1.5 h at temperatures between 10 to 20ºC under ultrasonic irradiation. Bottom right; Reaction of **5q** in H_2O produced ratio of **4a**:**4b** varying between 1.3:1 to 1:1 after 1.5 h at temperatures between 10 to 20ºC under ultrasonic irradiation.

During ultrasonic irradiation of **5q** in aqueous media, observation of the reaction in progress indicated that **5q** was more soluble than **5p** under the same conditions and reactions with MAC gave *endo*:*exo* ratios ranging from 1.3:1 to 1:1 depending on the efficiency of irradiation and reaction temperature. GC-MS analysis showed that the enamine cycloadduct **30-int** predominately underwent hydrolysis *in situ* (Appendix 3.18) likely due to enhanced solubility, and the crude material was heated in NaOAc/CH_3COOH buffer to hydrolyse the remaining oxazolidine **30**. Reasonable diastereoselectivity was observed for (1*S*,2*R*,4*S*)-**4b** achieving 60% *ee* (Table 3.2) and providing a 1:1 ratio of diastereoisomers when bath temperature was maintained between 10 and 20°C (Figure 3.20, bottom right). Poor selectivity was achieved for (1*S*,2*S*,4*S*)-**4a** (18% *ee*) and this lack of face discrimination can be expected with increases in reaction rates in hydrogen bond donating solvents.

The D-A reaction of **5q** with MAC in 3.0 M LiCl was observed to behave as a heterogeneous mixture due to 'salting-out' effects (Section 3.1.2) and GC-MS analysis indicated that decreases in solubility with increasing in ionic strength prevents the facile *in situ* hydrolysis of **30-int** (Appendix 3.18). No change in stereoselectivity was detected between reactions in water and 3.0 M LiCl, although a slight increase in **4a** was noticed and can be explained by hydrophobic effects. Aqueous reactions using **5q** on multigram scales required 3 equivalents of acrylate to ensure the consumption of all starting material, but did not perform as well and a loss of 12 to 15% *ee* was typically encountered.

5	MAC (eq.)	Solvent	Temp (°C)	Time (h)	*endo:exo*[A]	%*ee* (**4a**)	%*ee* (**4b**)	% Yield[B]
p	3.0	DCM	-50 to 25	8.0	99:1	85	n.d.	90
p	3.0	DCM	25	8.0	9:1	79	66	90
p	1.5	Water	10 - 20	1.5	9:1	75	75	83
p	1.5	MeOH:Water (1:10)	25	3.0	7:3	32	15	69
p	1.5	Dioxane:Water (1:10)	25	3.0	3:1	32	15	52
q	3.0	DCM	-50 to 25	8.0	3:1	56	46	87
q	1.5	Water	10 - 20	1.5	1:1	18	60	81
q	1.5	Water, 0.5 eq. TBAI	11 - 20	2.0	3:2	-	56	64
q	1.5	3 M LiCl	10 - 20	1.5	3:2	18	60	79

Table 3.2: Enantioselective Diels-Alder reactions using ephedrine auxiliaries. [A]Ratio of diastereoisomers (**4a**:**4b**) [B]Combined yield of *endo* and *exo* products. Results produced on ≤ 1.0 mmol scales. Reactions in water performed with ultrasonic irradiation.

The addition of miscible co-solvents (dioxane, MeOH) to aid in the aqueous solubility of **5p** led to a large decrease in diastereoselectivity (Table 3.2) for both diastereomers of **4**, indicating the importance of hydrogen bonding to the optical induction in aqueous media. The addition of one half molar equivalent of tetrabutyl ammonium iodide (TBAI) surfactant to **5q** in MAC also produced a

noticeable decrease in selectivity for **4b** and results for the most successful D-A trials are included in Table 3.2. A general procedure for the reaction of **5p-q** in aqueous media is included in Section 6.6.7.

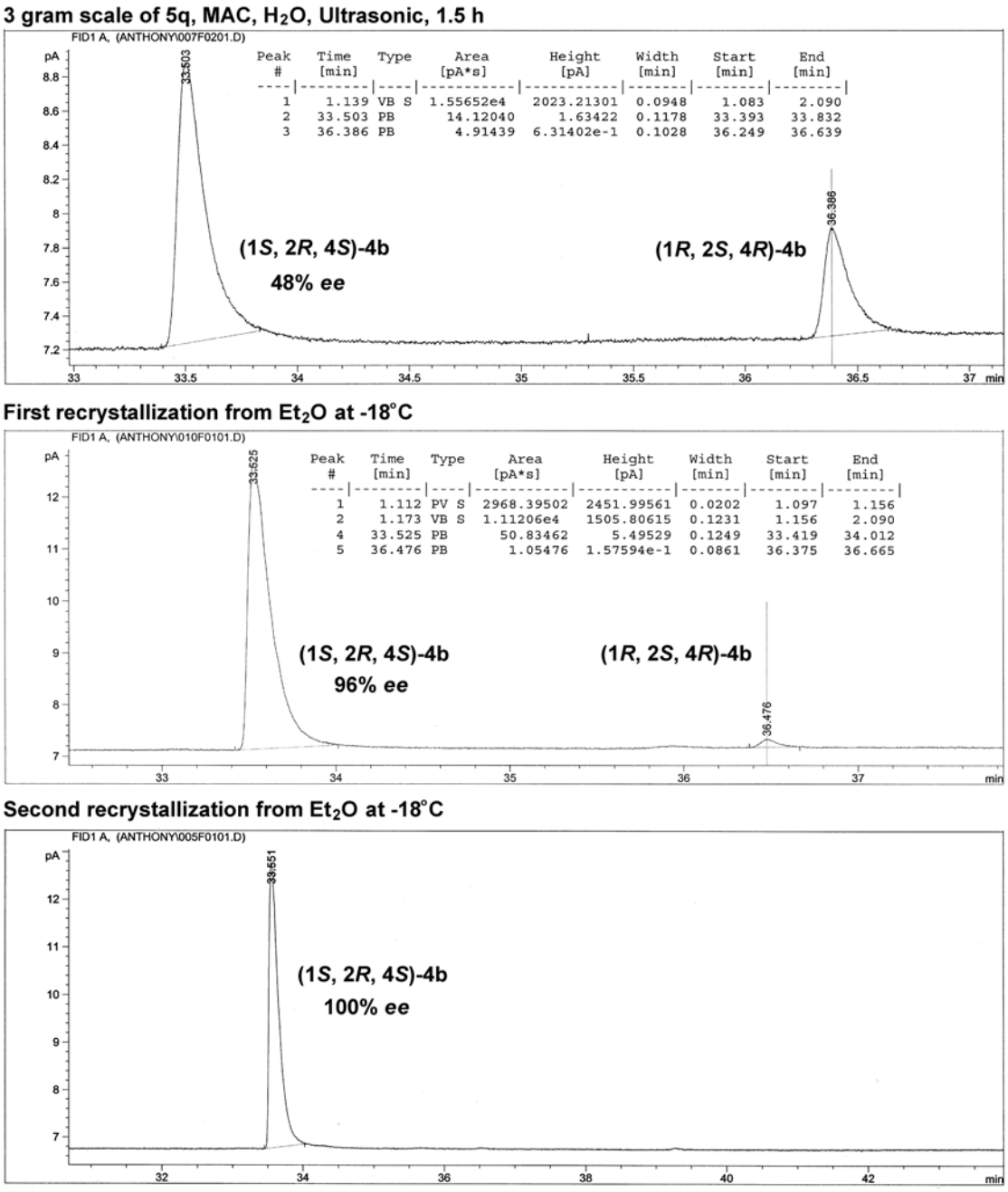

Figure 3.21: Chiral GC analyses conducted using a Et-TBS-β-CD stationary phase. Top; An enantioenriched mixture of the *exo* isomer was prepared on a 2 g (8.2 mmol) scale from the reaction between **5q** and MAC in H_2O to provide **4b** in 48% *ee* as determined by chiral GC analysis. Middle and Bottom; Two recrystallization from Et_2O at –18ºC provided the single (1*S*,2*R*,4*S*)-**4b** enantiomer in optical purity as indicated by chiral GC analyses.

Attempts to obtain an optical rotation reading for samples of **4a**, prepared in 85% *ee* from **5p** in DCM, did not give a reliable reading or even an indication of the sign of rotation and this observation suggested that the 7-oxanorbornanes **4a** and **4b** do not have strong optical activity as a pure enantiomer. Multiple recrystallizations of an enantioenriched mixture of **4b** from ether at –18ºC allowed the isolation of the (1*S*,2*R*,4*S*)-**4b** enantiomer in optical purity after two crystallizations, as indicated by chiral GC analysis (Figure 3.21). (1*S*,2*R*,4*S*)-**4b** was found to be a colourless resin at room temperature and enriched in the supernatant as the racemic precipitate was removed. This indicates that the **4b** material has more efficient crystal packing as the racemate and that the maximum achievable isolated yield of (1*S*,2*R*,4*S*)-**4b** using this purification method is equal to the enantiomeric excess in the original D-A mixture. Two optical rotation measurements were performed on the (1*S*,2*R*,4*S*)-**4b** enantiomer, and were obtained at λ = 690 nm at two different concentrations (Section 6.6.8). The product was identified to be dextrorotatory with an absolute optical rotation of $[a]_D^{25} = +1.72°$ (c = 1.45, $CHCl_3$) and can be assigned as (+)-(1*S*,2*R*,4*S*)-**4b**.

The product (+)-(1*S*,2*R*,4*S*)-**4b** has the same absolute stereochemistry at the (2*R*) ester and (4*S*) ether functionalities as featured in Ring **A** of the natural product **1** (Figure 3.22). Subsequent studies were directed towards the synthetic modification of the *exo*- product **4b** involving ether cleavage and derivitization and are detailed in Chapter 4. The development of a direct methodology for the preparation of ring **C** is also discussed along with studies towards the introduction of diastereoselectivity at the C(12) chiral center adjacent to the 3-furyl moiety (Figure 3.22).

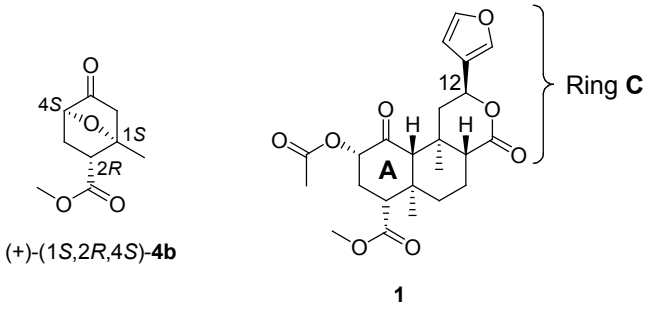

Figure 3.22: The (+)-(1*S*,2*R*,4*S*)-**4b** enantiomer has the same absolute stereochemistry as observed in ring **A** of the natural product **1**.

Chapter 3

Diels-Alder Reactions of 3-Furylamines: References

[1] T. Zincke. H. Günther. "Ueberführung von Pentenderivaten in Indenderivate", *Justus Liebigs Annalen der Chemie*, **1893**, *272*, 243-270.

[2] H. von Euler, K. O. Josephson. "Uber Kondensationen an Doppelbindungen. I: Uber die Kondensation von Isopres mit Benzochinon", *Berichte der Deutschen Chemischen Gesellschaft*, **1920**, *53*, 822-826.

[3] O. Diels, K. Alder. "Synthesen in der Hydroaromatischen Reihe". *Justus Liebigs Annalen der Chemie*, **1928**, *460*, 98-122; O. Diels, K. Alder, **"**Synthesen in der hydroaromatischen Reihe. XII. Mitteilung. („Dien-Synthesen" sauerstoffhaltiger Heteroringe. 2. Dien-Synthesen des Furans)". *Justus Liebigs Annalen der Chemie*, **1931**, 490, 243-257. For an historical review see: J. A. Berson. "Discoveries Missed, Discoveries Made: Creativity, Influence, and Fame in Chemistry", *Tetrahedron*, **1992**, *48*, 3-17.

[4] R. B. Woodward, R. Hoffmann. "Stereochemistry of Electrocyclic Reactions", *Journal of the American Chemical Society*, **1965**, *87*, 395-397; R. B. Woodward, R. Hoffmann. "Selection Rules for Sigmatropic Reactions", *ibid*, **1965**, *87*, 2511-25121; R. B. Woodward, R. Hoffmann. "Selection Rules for Concerted Cycloaddition Reactions", *ibid*, **1965**, *87*, 2046-2048.

[5] R. B. Woodward, R. Hoffmann. "Conservation of Orbital Symmetry". *Angewandte Chemie International Edition* (*Eng*), **1969**, *8*, 781-932; R. Hoffmann, R. B. Woodward. "The Conservation of Orbital Symmetry", *Accounts of Chemical Research*, **1968**, *1*, 17-22.

[6] K. C. Nicolaou, S. A. Snyder, T. Montagnon, G. Vassilikogiannakis. "The Diels-Alder Reaction in Total Synthesis". *Angewandte Chemie International Edition English*, **2002**, 41, 1668-1698.

[7] A. Rauk. Orbital Interaction Theory of Organic Chemistry (2nd Ed.), John Wiley and Sons Inc., New-York, **2000**, 169-170, 196-200. ISBN 978-0-471-35833-6

[8] B. M. Gimarc. "Applications of Qualitative Molecular Orbital Theory", *Accounts of Chemical Research*, **1974**, *7*, 384-392.

[9] K. Fukui. "Recognition of Stereochemical Paths by Orbital Interaction". *Journal of Chemical Research*, **1971**, *4*, 57-64.

[10] K. N. Houk. "The Frontier Molecular Orbital Theory of Cycloaddition Reactions", *Accounts of Chemical Research*, **1975**, *8*, 361-369.

[11] A. Rauk, R. Cannings. "SHMO, A Simple Huckel Molecular Orbital Theory Calculator", http://www.chem.ucalgary.ca/SHMO/. Reference last accessed 07/08/2007.

[12] K. N. Houk, Y.-T. Lin, F. K. Brown. "Evidence for the Concerted Mechanism of the Diels-Alder Reaction of Butadiene with Ethylene. *Journal of the American Chemical Society*, **1986**, *108*(3), 554-556.

[13] K. Fukui. "The Role of Frontier Orbitals in Chemical Reactions". *Angewandte Chemie* **1982**, *21*, 801-809 and references therein.

[14] R. Gleiter, M. C. Bŏhm. "Regio- and Stereoselectivity in Diels-Alder Reactions. Theoretical Considerations". *Pure and Applied Chemistry*. **1983**, *55*, 237-244.

[15] O. Eisenstein, J. M. Lefour, N. T. Anh, R. F. Hudson. "Simple Prediction of Cycloaddition Orientation, 1. Diels-Alder Reactions", *Tetrahedron*, **1977**, ***33,*** 523-531.

[16] P. V. Alston, R. M. Ottenbrite, O. F. Guner, D. D. Shillady. "A Transition State FMO Approach for Prediction of the Regioselectivity of the Diels-Alder Reaction". *Tetrahedron*, **1986**, *42*, 4403-4408.

[17] D. H. Ess, G. O. Jones, K. N. Houk. "Conceptual, Qualitative and Quantitative Theories of 1,3-Dipolar and Diels-Alder Cycloadditions Used in Synthesis". *Advanced Synthesis and Catalysis*, **2006**, *348*, 2337-2361.

[18] S. D. Kahn, C. F. Pau, W. J. Hehre. "Modeling Chemical Reactivity. 1. Regioselectivity of Diels-Alder Cycloadditions of Electron Rich Dienes with Electron Deficient Dienophiles". *Journal of the American Chemical Society*, **1986**, *108*, 7381-7396.

[19] K. Alder, G. Stein. "Untersuchungen uber den Verlauf der Diensynthese", *Angewandte Chemie*, **1937**, *50*, 510-519.

[20] R. B. Woodward, T. J. Katz. "The Mechanism of the Diels-Alder Reaction", *Tetrahedron*, **1959**, *5*, 70-89.

[21] J. A. Berson, A. Remanick. "The Mechanism of the Diels-Alder Reaction. The Stereochemistry of the *endo-exo* Isomerization of the Adducts of Cyclopentadiene with Acrylic and Methacrylic Esters", *Journal of the American Chemical Society*, **1961**, *83*, 4947-4956.

[22] J. A. Berson, Z. Hamlet, W. A. Mueller. "The Correlation of Solvent Effects on the Stereoselectivities of Diels-Alder Reactions by Means of Linear Free Energy Relationships. A New Empirical Measure of Solvent Polarity", *Journal of the American Chemical Society*, **1962**, *84*, 297-304.

[23] I. Schlachter, Y. Mattay, J. Suer, U. Howeler, G. Wurthwein, E. Wurthwein. "Combined Quantum Chemical and MM-Approach to the *endolexo* Selectivity of Diels-Alder Reactions in Polar Media". *Tetrahedron*, **1997**, *53*, 119

[24] K. N. Houk. "On the Lewis-Acid Catalysis of Diels-Alder Reactions". *Journal of the American Chemical Society*, **1973**, *95*, 4094-4096.

[25] U. Pindur, G. Lutz, C. Otto. "Acceleration and Selectivity Enhancement of Diels-Alder Reactions by Special and Catalytic Methods", *Chemical Reviews*, **1993**, *93*, 741-761.

[26] J. R. McCabe, C. A. Eckert. "Role of high-pressure kinetics in studies of the transition states of Diels-Alder reactions", *Accounts of Chemical Research,* **1974**, *7*, 251-257.

[27] J. Rimmelin, G. Jenner, P. Rimmelin. "Influence de la pression dans la synthèse diénique du système oxa-7 bicyclo[2.2.1]heptane, ã partir du méthyl-2 furanne. Caracyerisation spectrale des adduits of cinétique de reaction", *Bulletin de la Societe Chimique de France*, **1978**, *9-10*, 461-464.

[28] T. P. Caulier, J. Reisse. "On Sonochemical Effects on the Diels-Alder Reaction", *Journal Of Organic Chemistry*, **1996**, *61*, 2547-2548.

[29] T. Inukai, T. Kojima. "Aluminium Chloride Catalyzed Diene Condensation. IV. Kinetic Study of Butadiene-Methyl Acrylate Reaction", *Journal of Organic Chemistry*, **1967**, *32*, 872-875.

[30] A. Hosomi, H. Iguchi, J. Sasaki, H. Sakurai. "Highly Regioselective Diels-Alder Reactions of 2-Trimethylsilylmethyl-1,3-butadiene Catalyzed by a Lewis Acid and Applications to Synthesis of Terpenes", *Tetrahedron Letters*, **1982**, *23*, 551-554.

[31] M. Petrzilka, J. I. Grayson. "Preparation and Diels-Alder Reactions of Hetero-Substituted 1,3-Dienes", *Synthesis*, **1981**, 753-786.

[32] M. Avalos, R. Babiano, J. L. Bravo, P. Cintas, J. L. Jiménez, J. C. Palacios, M. A. Silva. "Computational Studies on the BF_3-Catalyzed Cycloaddition of Furan with Methyl Vinyl Ketone: A New Look at Lewis Acid Catalysis", *Journal of Organic Chemistry*, **2000**, 65, 6613-6619.

[33] A. Kumar. "Salt Effects in Diels-Alder Reaction Kinetics", *Chemical Reviews*, **2001**, *101*, 1-19.

[34] J. M. Adams, S. Dyer, K. Martin, W. A. Matear, R. W. McCabe. "Diels-Alder Reactions Catalysed by Cation-exchanges Clay Minerals", *Journal of the Chemical Society Perkin Transactions 1*, **1994**, *6*, 761-765.

[35] S. Otto, J. B. F. N. Engberts. "Diels-Alder Reactions in Water", *Pure and Applied Chemistry*, **2000**, *72*, 1365-1372.

[36] D. C. Rideout, R. Breslow. "Hydrophobic Acceleration of Diels-Alder Reactions", *Journal of the American Chemical Society*, **1980**, *102*, 7816-7817.

[37] R. Breslow, U. Maitra, D. Rideout. "Selective Diels-Alder Reactions in Aqueous Solutions and Suspensions", *Tetrahedron Letters*, **1983**, *24*, 1901-1904.

[38] R. S. Spolar, J-H. Ha, M. T. Record. "Hydrophobic Effect in Protein Folding and Other Noncovalent Processes Involving Proteins", *Proceeding of the National Academy of Science*, **1989**, *86*, 8382-8385.

[39] G. Jancsó, L. Cser, T. Grósz, Y. M. Ostanevich. "Hydrophobic Interaction and Small-Angle Neutron Scattering in Aqueous Solutions", *Pure and Applied Chemistry*, **1994**, *66*, 515-520.

[40] J. L. Finney, A. K. Soper. "Solvent structure and perturbations in solutions of chemical and biological importance", *Chemical Society Reviews*. **1994**, *23*, 1-10.

[41] W. L. Jorgensen, J. F. Blake, D. C. Lim, D. L. Severance. "Investigation of solvent effects on pericyclic reactions by computer simulations", *Journal of the Chemical Society, Faraday Transactions*, **1994**, *90*, 1727-1732; J. Chandrasekhar, S. Shariffskul, W. L. Jorgensen. "QM/MM Simulations for Diels-Alder Reactions in Water: Contribution of Enhanced Hydrogen Bonding at the Transition State to the Solvent Effect", *Journal of Physical Chemistry B*, **2002**, *106*(33), 8078-8085.

[42] R. Breslow, C. J. Rizzo. "Chaotropic Salt Effects in a Hydrophobically Accelerated Diels-Alder Reaction", *Journal of the American Chemical Society*, **1991**, *113*, 4340-4341.

[43] R. Breslow, T. Guo. "Diels-Alder Reactions in Nonaqueous Polar Solvents. Kinetic Effects of Chaotropic and Antichaotropic Agents and of β-Cyclodextrin", *Journal of the American Chemical Society*, **1988**, *110*, 5613-5617.

[44] P. A. Grieco, P. Garner, Z. He. "'Micellar' Catalysis in the aqueous intermolecular Diels-Alder Reaction: Rate Acceleration and Enhanced Selectivity", *Tetrahedron Letters*, **1983**, *24*, 1897-1900.

[45] P. A. Grieco, J. J. Nunes, M. D. Gaul. "Dramatic Rate Accelerations of Diels-Alder Reactions in 5 M Lithium Perchlorate-Diethyl Ether: The Cantharidin Problem Reexamined", *Journal of the American Chemical Society*, **1990**, *112*, 4595-4596.

[46] E. Vieira, P. Vogel. "The Preparation of Optically Pure 7-Oxabicyclo[2.2.1]hept-2-ene Derivatives. The CD Spectrum of (+)-(1*R*)-7-Oxabicyclo[2.2.1]hept-5-en-2-one", *Helvetica Chimica Acta*, **1983**, *66*, 1865-1871.

[47] K. A. Black, P. Vogel. "Optical Resolution of 7-Oxabicyclo[2.2.1]hept-2-ene Derivatives. Diastereoselectivity in the Formation of Cyanohydrine-Brucine Complexes". *Helvetica Chimica Acta*, **1984**, *67*, 1612-1615.

[48] P. Vogel, D. Fattori, F. Gasparini, C. Le Drain. "Optically Pure 7-Oxabicyclo[2.2.1]hept-5-en-2-yl Derivatives ("Naked Sugars") as New Chirons". *Synlett*, **1990**, 173-185.

[49] O. Arjona, A. de Dios, R. F. de la Pradilla, J. Plumet. "Highly Diastereoselective Bis-Hydroxylation of a Protected Conduritol B: A Short Route to myo-Inositol Derivatives", *Tetrahedron Letters*, **1991**, *32*, 7309-7312; O. Arjona, A. Candilejo, A. de Dios, R. F. de la Pradilla, J. Plumet. "Osmium-Mediated Asymmetric Synthesis of Glycosyl-myo-inositols from Oxanorbornanes", *Journal of Organic Chemistry*, **1992**, *57*, 6097-6099.

[50] A. Warm, P. Vogel. "Synthesis of (+)- and (-)- Methyl 8-Epinonactate and (+)- and (-)-Methyl Nonactate", *Helvetica Chimica Acta*, **1987**, *70*, 690-700.

[51] E. Reynard, J-L. Reymond, P. Vogel. "Highly Stereoselective Synthesis of (±)-Aminobromocyclitol Derivatives from Furan", *Synlett*, **1991**, 469-471.

[52] R. Saf, K. Faber, G. Penn, H. Griengl. "Enzymatic Preparation of Optically Active 7-Oxabicyclo[2.2.1]heptane derivatives", *Tetrahedron*, **1988**, *44*, 389-392.

[53] E. J. Corey, H. E. Ensley. "Preparation of an Optically Active Prostaglandin Intermediate via Asymmetric Induction", *Journal of the American Chemical Society*, **1975**, *97*, 6908-6909.

[54] E. J. Corey. "New enantioselective routes to biologically interesting compounds", *Pure and Applied Chemistry*, **1990**, *62*, 1209-1216.

[55] J. S. Johnson, D. A. Evans. "Chiral Bis(oxazoline) Copper(II) Complexes: Versatile Catalysts for Enantioselective Cycloaddition, Aldol, Michael, and Carbonyl Ene Reactions", *Accounts of Chemical Research*, **2000**, *33*, 325-335.

[56] Y. Huang, T. Iwama, V. H. Rawal. "Design and Development of Highly Effective Lewis Acid Catalysts for Enantioselective Diels-Alder Reactions", *Journal of the American Chemical Society*, **2000**, *124*, 5950-5951.

[57] J. Barluenga, F. Aznar, C. Ribas, C. Valdés. "Cycloaddition Reactions of Chiral 2-Amino-1,3-butadienes with Nitroalkenes: Synthesis of Enantiomerically Pure 4-Nitrocyclohexanones", *Journal of Organic Chemistry*, **1997**, *62*, 6746-6753.

[58] S. Danishefsky, T. Kitahara, "Useful diene for the Diels-Alder reaction", *Journal of the American Chemical Society*, **1974**, *96*, 7807-7808; S. Danishefsky, "Siloxy dienes in total synthesis". *Accounts of Chemical Research*, **1981**, *14*, 400-406.

[59] S. A. Kozmin, J. M. Janey, V. H. Rawal. "1-Amino-3-siloxy-1,3-butadienes: Highly Reactive Dienes for the Diels-Alder Reaction", *Journal of Organic Chemistry*, **1999**, *64*, 3039-3052.

[60] S. A. Kozmin, V. H. Rawal. "Asymmetric Diels-Alder Reactions of Chiral 1-Amino-3-siloxy-1,3-butadiene: Application to the Enantioselective Synthesis of (-)-α-Elemene", *Journal of the American Chemical Society*, **1997**, *119*, 7165-7166.

[61] W. G. Dauben, H. O. Krabbenhoft. "Organic reactions at high pressure. Cycloadditions with furans", *Journal of the American Chemical Society*, **1976**, 98, 1992-1993.

[62] P. Vogel, J. Cossy, J. Plumet, O. Arjona. "Derivatives of 7-Oxabicyclo[2.2.1]heptane in Nature and as Useful Synthetic Intermediates", *Tetrahedron*, **1999**, *55*, 13521-13642.

[63] J. Šrogl, M. Janda, I. Stibor. "Experiments in the Furan Series. XII. Preparation of 3-Furyl Ketones", *Collection of the Czechoslovakian Chemical Communication*, **1970**, *35*, 3478-3480; J. Koyanagi, K. Yamamoto, K. Nakayama, A. Tanaka. "Preparation of 3-Bromo-2-methylfuran and 4-Bromo-2-methylfuran", *Journal of Heterocyclic Chemistry*, **1994**, *31*, 1093-1095.

[64] S. N. Pieniazek, K. N. Houk. "The Origin of the Halogen Effect on Reactivity and Reversibility of Diels-Alder Cycloadditions Involving Furan", *Angewandte Chemie*, **2006**, *118*, 1470-1473.

[65] J. A. Cella. "3-Substituted-2-furoic Acids as Latent Dienes for the Preparation of Aryl Ethers and Thioethers via the Diels-Alder Reaction", *Journal of Organic Chemistry*, **1988**, *53*, 2099-2103.

[66] J. E. Cochran, T. Wu, A. Padwa. "Synthesis of Polysubstituted Anilines Using the Diels-Alder Reaction of Methyl 5-Aminofuroate", *Tetrahedron Letters*, **1996**, *37*, 2903-2906.

[67] A. Padwa, M. Dimitroff, A. G. Waterson, T. Wu. "Diels-Alder Reaction of 2-Amino-Substituted Furans as a Method for Preparing Substituted Anilines", *Journal of Organic Chemistry*, **1997**, *62*, 4088-4096.

[68] R. H. Schlessinger, T. R. R. Pettus, J. P. Springer, K. Hoogsteen. "Diastereoselective Diels-Alder Reactions Using Furan Substituted with a Nonracemic amine", *Journal of Organic Chemistry*, **1994**, 59, 3246-3247.

[69] J. Jurczak, A. L. Kawczyński, T. Koźluk. "Stability of Cycloadducts Obtained by High Pressure Diels-Alder Reactions between 3,4-Dimethoxyfuran and 1,4-Benzoquinones: Kinetic Studies of Retro-Diels-Alder Reaction", *Journal of Organic Chemistry*, **1985**, *50*, 1106-1107.

[70] K. Matsumoto, Y. Ikemo, S. Hashimoto, H. S. Lee, Y. Okamoto. "High Pressure [4+2] Cycloaddition Reactions of 3,4-Dimethoxyfuran with Dichloromaleic Anhydride and with Cyclopropane Derivatives", *Journal of Organic Chemistry*, **1986**, *51*, 3729-3730.

[71] M. Koreeda, K-Y. Jung, J. Ichita. "Diels-Alder reactions of 3,4-Dialkoxyfurans: an Application to the Highly Efficient Synthesis of (+)-Methyl Triacetylshikimate". *Journal of the Chemical Society Perkin Transcations 1*. **1989**, 2129-2131.

[72] T. Takahashi, T. Namiki, Y. Takeuchi, T. Koizumi. "A New Synthetic Route to Methyl (-)-Shikimate by Asymmetric Diels-Alder Reaction of $(S)_s$-3-(2-Pyridylsulfinyl)acrylate", *Chemical and Pharmaceutical Bulletin*, **1998**, *36*, 3213-3215.

[73] J. N. Bridson. "Reactions of *N*-3'furylbenzamide with Some Dienophiles", *Canadian Journal of Chemistry*, **1979**, *57*, 314-317.

[74] M. M. Campbell, A. D. Kaye, M. Sainsbury. "3-Acylamino Furan", *Tetrahedron* **1982**, *38*, 2783-2786.

[75] I. Yamamoto, K. Narasaka. "Diels-Alder Reaction of 3-Methylthiofuran and Transformation of the Cycloadducts to Substituted Cyclohexenols", *Chemistry Letters*, **1995**, 1129-1130.

[76] R. H. Schlessinger, X.-H. Wu, T. R. R. Pettus. "Diastereoselective Diels-Alder reactions Using Furan Substituted with a Proline Derived Auxiliary", *Synlett*, **1995**, 536-538.

[77] R. H. Schlessinger, C. P. Bergstrom. "Enantioselective Synthesis of (+)-Cyclophellitol", *Journal of Organic Chemistry*, **1995**, *60*, 16-17.

[78] R. H. Schlessinger, C. P. Bergstrom. "Diastereoselective Diels-Alder Reactions of Nonracemic 3- and 4-Amino Furans Bound to Polystyrene. A Comparison of These Reactions to their Solution State Analogues", *Tetrahedron Letters*, **1996**, *37*, 2133-2136.

[79] I. G. John, L. Radom. "Conformations, Stabilities, and Charge Distributions in 2- and 3-Monosubstituted Furans. An ab initio Molecular Orbital Study". *Journal of the American Chemical Society*, **1978**, *100*, 3981-3991.

[80] A. Padwa, M. Dimitroff, A. G. Waterson, T. Wu. "Diels-Alder Reaction of 2-Amino-Substituted Furans as a Method for Preparing Substituted Anilines". *Journal of Organic Chemistry*, **1997**, *62*, 4088-4096

[81] J. Clayden, N. Greeves, S. Warren, P. Wothers, "Organic Chemistry", Springer-Verlag, New York, **2001**, 824. ISBN 0 19 850346 6.

[82] F. H. Allen, O. Kennard, D. G. Watson, L. Brammer, A. G. Orpen, R. Taylor. "Tables of Bond Lengths determined by X-ray and Neutron Difftraction. Part 1. Bond Lengths of Organic Compounds", *Journal of the Chemical Society Perkin Transactions 2*, **1987**, *12*, S1-S19.

[83] C.-P. Maschmeier, J. Krahnstover, H. Matschineer, U. Hess. "Electrochemical Study of a Dimethylamine-CO_2 Addition Compound- A New Electrolyte". *Electrochimica Acta*. **1990**, *35*(4), 769-770; U. P. Kreher, A. E. Rosamilia, C. L. Raston, J. L. Scott, C. R. Strauss. "Self-associated, distillable ionic media", *Molecules*. **2004**, 9, 387-393.

[84] C. Bicchi, A. D'Amato, P. Rubiolo. "Cyclodextrin Derivatives as Chiral Selectors for Direct Gas Chromarographic Separation of Enantiomers in the Essential Oil, Aroma and Flavor Fields", *Journal of Chromatography A*, **1999**, *843*, 99-121.

[85] R. Shellie, P. Marriott, C. Cornwell. "Application of Comprehensive Two-Dimensional Gas Chromatography (GC x GC) to the Enantioselective Analysis of Essential Oils". *Journal of Separation Science*, **2001**, *24*, 823-830.

[86] C. F. Poole. "The Essence of Chromatography", Elsevier, Amsterdam, **2003**, 797-820. ISBN: 0-444-50198-3.

[87] R. O. Hutchins, W.-Y. Su, R. Sivakumar, F. Cistone, Y. P. Stercho. "Stereoselective Reductions of Substituted Cyclohexyl and Cyclopentyl Carbon-Nitrogen π Systems with Hydride Reagents". *Journal of Organic Chemistry*, **1983**, *48*, 3412-3422.

Chapter 4

Studies Toward the Synthesis of Ring A

4.1 Investigation of 7-Oxanorbornane Ether Ring Cleavage

As discussed in Chapter 3, the 7-oxanorbornane skeleton can be conveniently prepared using the Diels-Alder reaction with furan to access the 7-oxa-bicyclo[2.2.1]hept-2-ene 7-(oxanorbornene) moiety as a precursor to molecules containing the saturated oxanorbornane bicyclic ether. The 7-oxanorbornane ring is present in carotenoids, cantharidin, cineole as well as a range of terpenoids. Synthetic strategies towards these naturally occurring bicyclic structures have been reviewed by Vogel *et al.* [1]. 7-Oxanorbornanes have been termed molecular 'LEGO'® due to their flexibility as a functional unit towards the preparation of macrocyclic molecules and polymers containing cyclic units [1]. Functionalised 7-oxanorbornanes and 7-oxanorbornenes are versatile synthetic intermediates for the preparation of sugar and carbohydrate type polyoxygenated structures and as such, many methodologies exist for rearrangement of the bicyclic ring and cleavage of the ether bridge. Lautens *et al.* [2] have reviewed the regio- and enantio-selective nucleophilic ring opening of 7-oxabicyclo[2.2.1]hept-2-enes using transition metal catalysts. The authors also report on the efficient cleavage of 5,6-bis(methoxymethyl)-7-oxa-bicyclo[2.2.1]hept-2-ene using $Ni(COD)_2$/(*R*)-BINAP with the hydride nucleophile DIBAL-H [2] (Scheme 4.1, top) to yield the cyclohexenol in excellent yield and stereoselectivity (97% yield, 92-97% *ee*).

Raney nickel hydrogenolysis has been used by Forsey *et al.* [3] for the cleavage of the benzylic oxabicyclic ether rings, resulting in stereo- and chemo-selectivity at C(1) during the preparation of a range of *Podophyllium* lignan skeletons (Scheme 4.1, middle). 7-Oxabicyclo[2.2.1]hept-2-ene ether opening with alkyl nucleophiles has been reported to occur using alkyl halides and $Ni(PPh_3)_2Cl_2$/Zn catalysis [4] and similar results have been obtained with Grignard reagents [5] and organolithium nucleophiles [6]. In these cases, the carbon nucleophile reacts at the C(3) olefin as demonstrated in the reaction of *n*-BuLi with 5,6-bis(trisopropylsiloxymethyl)-7-oxa-bicyclo[2.2.1]hept-2-ene (Scheme 4.1, bottom), to yield the cyclohexenol in high yield (96%) at ambient temperature [6, 7].

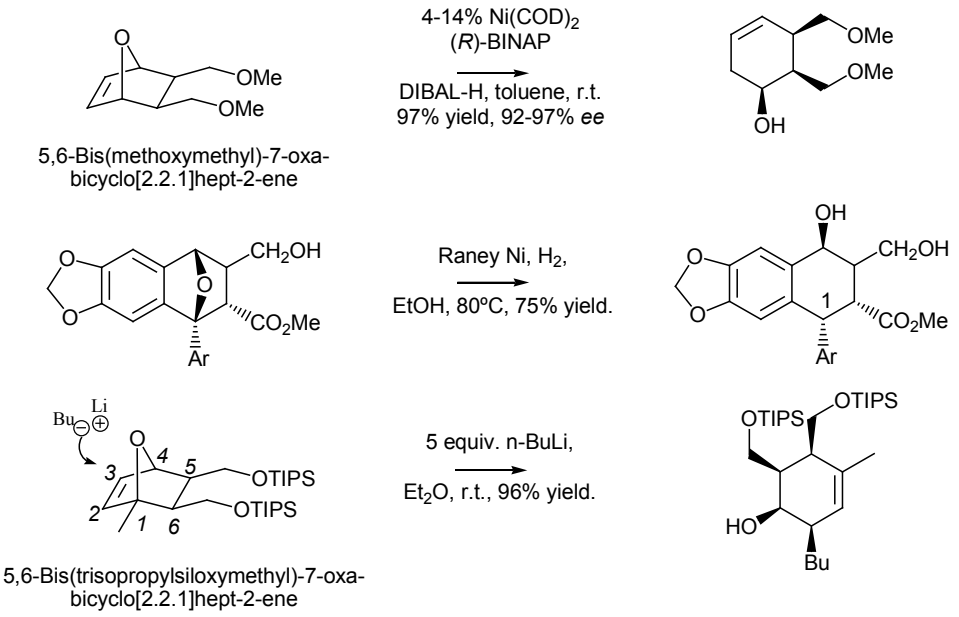

Scheme 4.1: Ether ring openings of 7-oxabicyclo[2.2.1]hept-2-enes. Top; Lautens *et al.* have reported the $Ni(COD)_2$/(*R*)-BINAP catalysed stereoselective hydrogenation of 5,6-bis(methoxymethyl)-7-oxa-bicyclo[2.2.1]hept-2-ene using DIBAL-H [2]. Middle; Forsey *et al.* [3] have used Raney nickel hydrogenolysis for the cleavage of aryl substituted cyclic ether rings in the preparation of *Podophyllum* lignans. Bottom; Ring cleavage with organolithium nucleophiles has also been used by Lautens *et al.* [6] to prepare the functionalised cyclohexenol in excellent yield.

Ring opening reactions of the saturated the 7-oxa-bicyclo[2.2.1]heptane ring can be facilitated by sufficiently acidic or basic reagents and the base mediated 7-oxanorbornane ring opening using LHMDS has been reported by Koreeda *et al.* [8] as shown in Scheme 3.13 (Section 3.2.1) in the synthesis of (±)-methyl triacetylshikimate. A general strategy for the acid mediated ring opening of cyclic ethers has been reported by Tanoue *et al.* [9], using H_2SO_4 /Ac_2O at room temperature to give the diacetoxy hydrolysis products. Similar conditions have been applied to the cleavage of 7-oxanorbornane bicyclic ethers by Ogawa *et al.* [10] who report excellent yields of 1,4-diacetylated product (94%) using sealed reaction vessels at 80ºC (Scheme 4.2, top) and the acetolysis product was obtained as a 1:1 mixture of isomers as a consequence of nucleophilic attack at both C(1) and C(4).

Acid mediated cleavage of **4b** under conditions reported by Ogawa *et al.* [10] gave the aromatized ester methyl 4-acetoxy-2-methylbenzoate as indicated by GC-MS library matching (Section 6.7.1), suggesting that more mild acidic conditions are essential to prevent aromatization.

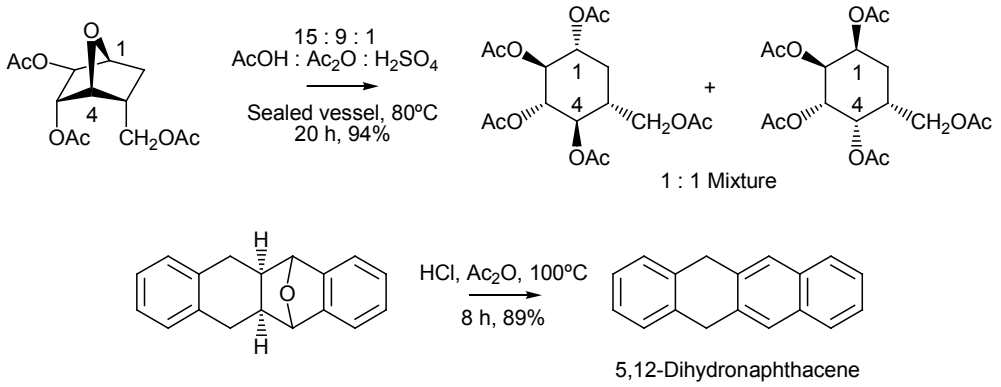

Scheme 4.2: Top; Ogawa *et al.* [10] have reported the acid mediated hydrolysis of the 7-oxanorbornane ring using $AcOH/Ac_2O/H_2SO_4$ to produce the 1,4-diacetoxy isomers in a 1:1 mixture. Bottom; Luo *et al.* [11] report the acid mediated dehydration of aryl bicyclic ethers using HCl/Ac_2O to yield the aromatised product, as shown in the preparation of 5,12-dihydronapthacene.

Luo *et al.* [11] report the acidic cleavage of aryl bicyclic ethers using HCl/Ac_2O to also facilitate dehydration to the conjugated aromatic system in high yield, as shown in the preparation of 5,12-dihydronaphthacene (Scheme 4.2, bottom). This example suggests that even weaker acidic conditions may be unfavourable for the preparation of dioxa- ether cleavage products of **4** and the ring opened alcohol, if formed, is likely to dehydrate to the stable aromatic product.

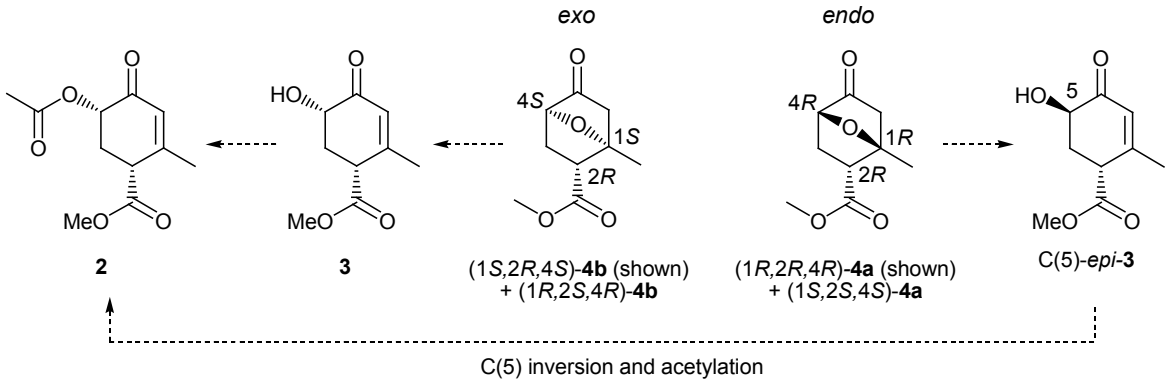

Scheme 4.3: Ether cleavage pathways for the transformation of **4a** and **4b** to **2**.

As mentioned in Section 3.3.1 the *exo* ketone (1*S*,2*R*,4*S*)-**4b** can be used directly in the asymmetric synthesis of the target **1** *via* the ether ring opening/rearrangement to **3**, followed by acetylation to the convergent precursor **2**. The *endo* ketone (1*R*,2*R*,4*R*)-**4a** may also be used but can be expected to produce the alcohol C(5)-*epi*-**3** upon ether cleavage which would require acetoxy inversion at C(5) to yield **2** (Scheme 4.3). The racemic ethers (1*R*,2*R*,4*R*)/(1*S*,2*S*,4*S*)-**4a** and (1*S*,2*R*,4*S*)/(1*R*,2*S*,4*R*)-

4b were used to explore ether cleavage/rearrangement reactions and the pathway presented has not yet been completed using the optically pure ketone (1*S*,2*R*,4*S*)-**4b**.

The ethers **4a-b** are new compounds and as such, no conditions had been reported for functional group modification of the skeleton of **4**. Studies towards ether cleavage under acidic and basic conditions are presented in Section 4.1.1 and the identification of cleavage products are accompanied by a number of proposed mechanisms. Lewis-acid mediated ether cleavage of 7-oxabicyclo[2.2.1]heptanes are reviewed in Section 4.1.2 and products from the reaction of **4** in the presence of Lewis-acids are identified.

4.1.1 Acid/Base Mediated Ether Cleavage of 7-Oxanorbornanes

Functional group transformations on the optically pure 7-oxa-bicyclo[2.2.1]heptan-2-one derivatives mentioned in Section 3.1.3 (Scheme 3.6) have led to the successful preparation of a range of optically active sugars [12] and the oxygenated cyclohex-5-ene-1,2,3,4-tetrol core of Corduritol natural products [13, 14]. Base mediated rearrangement of the 7-oxa-bicyclo[2.2.1]heptan-2-one ring in the presence of *tert*-butyl-dimethylsilyl triflate (TBDMSOTf) has been reported by Vogel *et al.* to facilitate C-O cleavage with retention of stereochemistry at the carbonyl α-siloxy C(6) stereocentre [12, 13] (Scheme 4.4, top), to the give the 6-siloxy-cyclohex-2-en-1-one in high yield (89%).

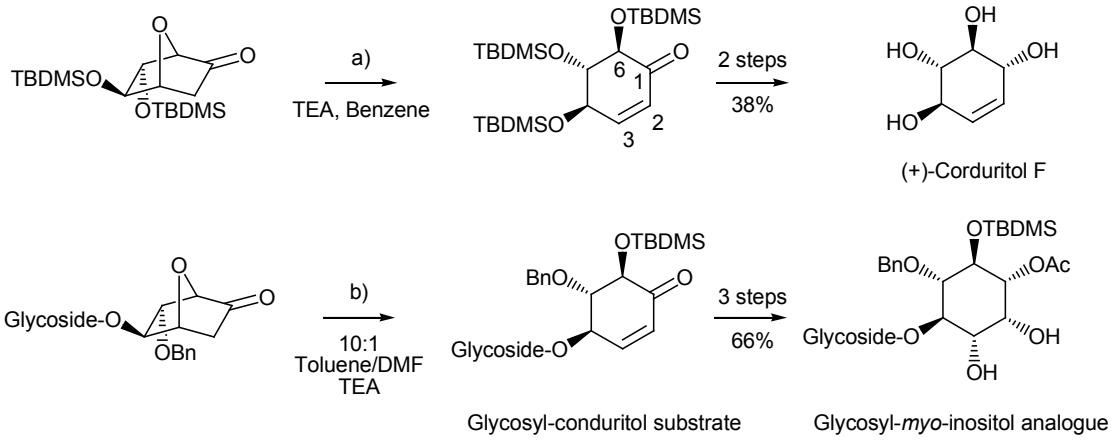

a) TBDMSOTf, Benzene, 25ºC, 4 h; TBDMSOTf, TEA, Benzene, 25ºC, 1 h, 89% b) TBDMSOTf, -23ºC, 2 h; TBDMSOTf, TEA, Benzene, 25ºC, 5 h, 88%.

Scheme 4.4: Top; The facile base mediated rearrangement of the 7-oxa-bicyclo[2.2.1]heptan-2-one ring using TBDMSOTf/TEA has been used by Vogel *et al.* [13] to prepare the natural product (+)-Corduritol F in moderate yield. Bottom; Arjorna *et al.* [15] have prepared the glycoside containing cyclohex-5-ene-1,2,3,4-tetrol using similar conditions, allowing access to the glycosyl-*myo*-inositol analogues in a further three steps.

Vogel's conditions involve the slow addition of TBDMSOTf to a solution of the bicyclic ether and TEA in benzene and have been used by Arjona *et al.* [14, 15] for the preparation of glycoside containing *myo*-inositol derivatives *via* the α,β-unsaturated Glycosyl-cordutitol substrate intermediate (Scheme 4.4, bottom).

The conditions described above were applied to the ether cleavage of racemic **4a** at room temperature using multiple additions of TEA and TBDMSOTf over a period of 6 h to ensure a high degree of conversion of the starting 7-oxanorbornane (Section 6.7.2). GC-MS monitoring revealed the formation of two major products at t_R=13:46 min and t_R=15:32 min (Figure 4.1) in 69% and 30% yields respectively, both of which contain the TBDMS group as indicated by the loss of a *t*-butyl group (*m/z* 57). Omitting TEA in this procedure gave no reaction, returning **4a** without decomposition.

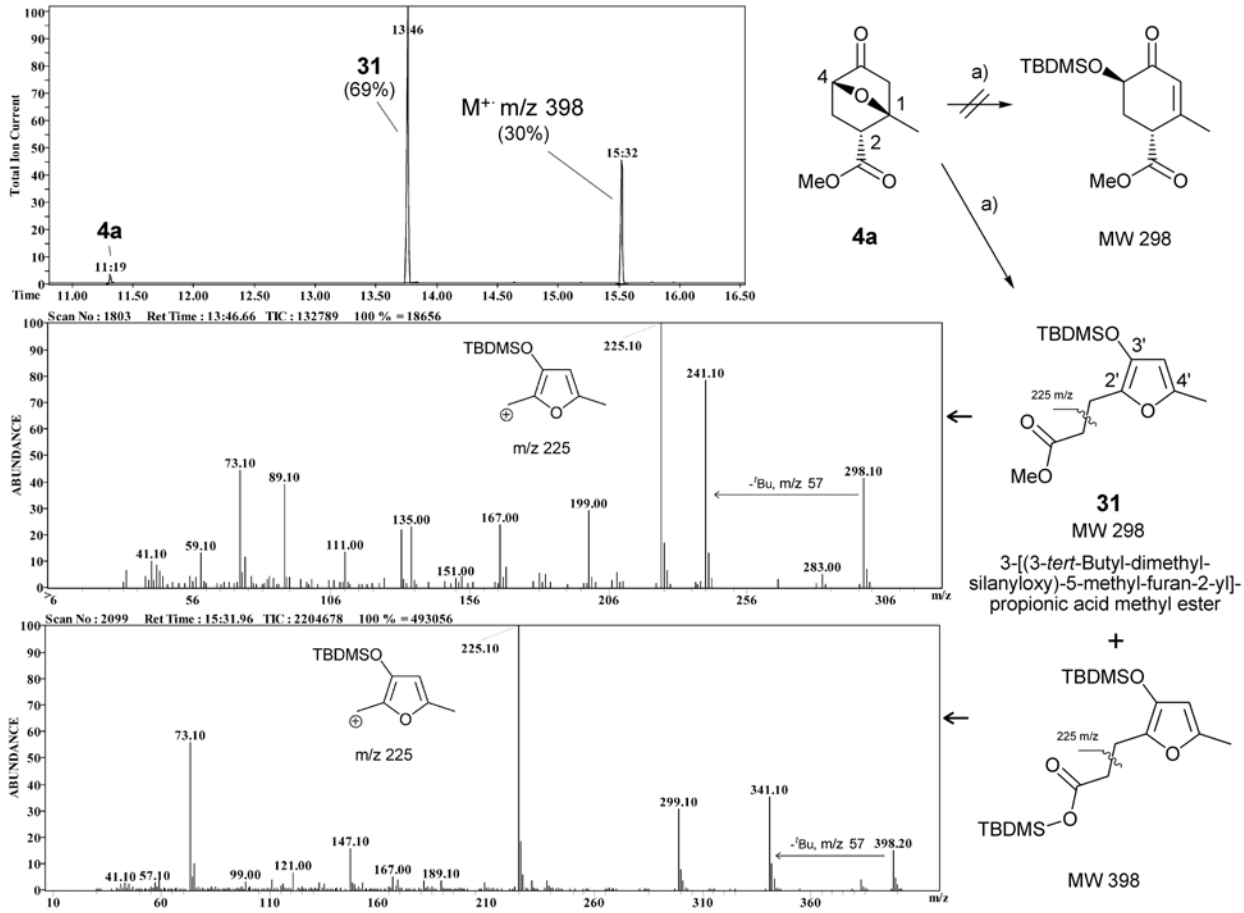

a) TBDMSOTf, Benzene, 25ºC, 4 h; TBDMSOTf, TEA, Benzene, 25ºC, 2 h.

Figure 4.1: The crude GC-MS analysis for the reaction of **4a** with TBDMSOTf/TEA is shown with EI-MS spectrum. Base peak ions for the 3'-siloxy-2',5'-dimethylfuran fragment at *m/z* 225 indicate major product as 3-[(3-*tert*-butyl-dimethyl-silanyloxy)-5-methyl-furan-2-yl]-propionic acid methyl ester **31**, corroborated by a *m/z* 298 molecular ion.

The MS fragmentation for the earlier eluting compound shows a molecular ion at *m/z* 298 in agreement with the desired C-O cleavage product and the second component has a molecular ion at *m/z* 398 in agreement with a TBDMS transesterified cleavage product (Figure 4.1). Disappointingly, the notable absence of *m/z* 97 fragment ion [16] inferred that neither product contained the desired methyl cyclohexanone structure. The major product **31** was purified by column chromatography in SiO_2 (5:1 Hexane:EtOAc) and ^{13}C NMR analysis (Figure 4.2) indicated four signals in the aromatic region at δ 148.2, 138.4, 136.9, 103.2 suggesting the formation of a furan ring to produce 3-[(3-*tert*-butyl-dimethyl-silanyloxy)-5-methyl-furan-2-yl]-propionic acid methyl ester. This conclusion was supported by a common base peak at *m/z* 225 present in MS analyses for both silylated products, corresponding to the 3'-siloxy-2',5'-dimethylfuran fragment ion (Figure 4.1) produced from homolytic cleavage of the ester.

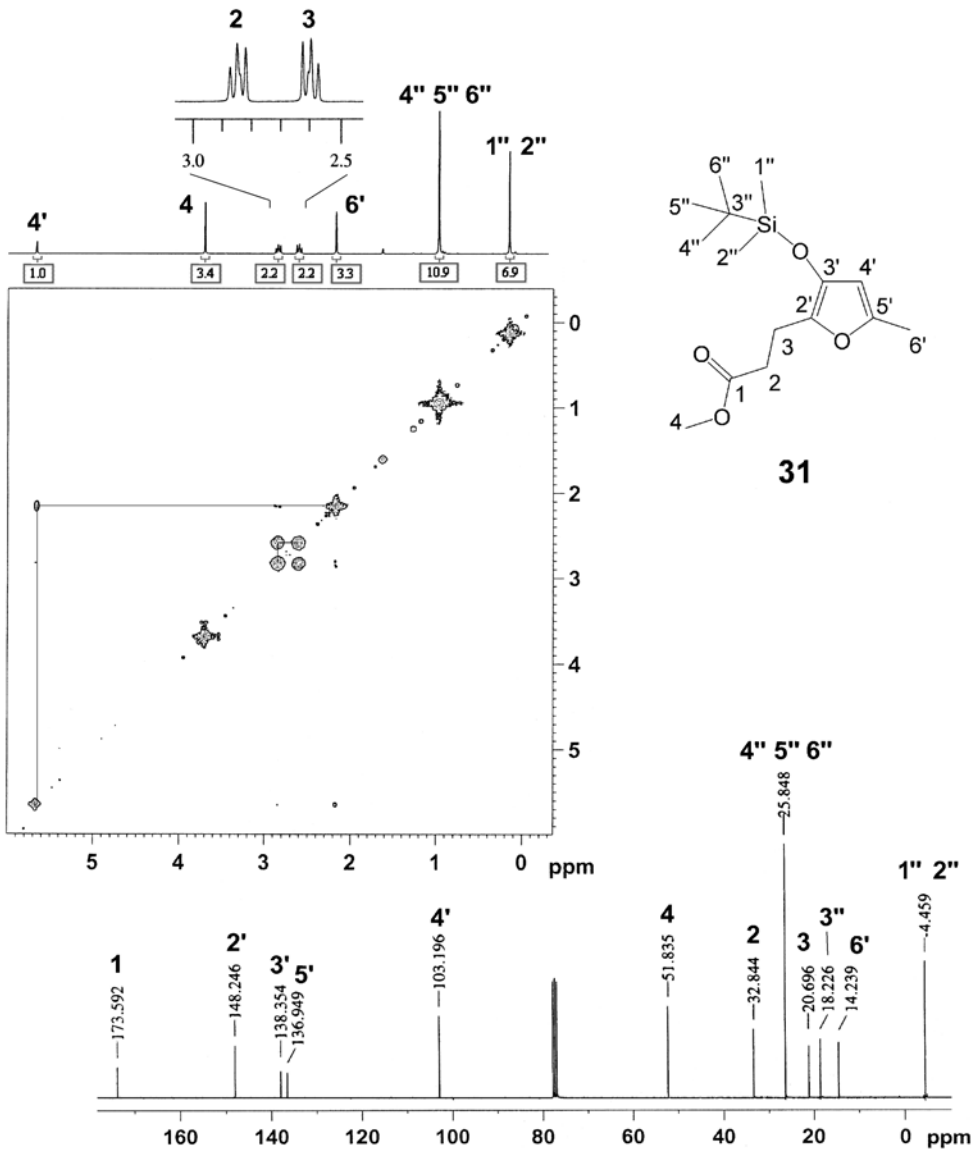

Figure 4.2: 300 MHz ^{1}H COSY NMR and ^{13}C NMR spectrum of **31**.

COSY NMR analysis (Figure 4.2) indicates correlations between H(2) and H(3) methylene signals at δ 2.85 and 2.60 corroborating that cleavage of the carbon-carbon bond between the ester C(2) and tertiary bridgehead C(1) had proceeded in preference to the opening of the bicyclic C(1)-O-C(4) ether bridge. Vinylic coupling of the H(6') methyl signal at δ 5.66 to the furan proton H(4') at δ 2.16 is also observed in agreement with the proposed structure of **31**. ^{13}C NMR signals were assigned using HMQC and DEPT 135 analysis (Appendix 4.1). The aromatic signals at δ 148.2, 138.4 and 136.9 are absent in DEPT 135 data in agreement with non-protonated C(2'), C(3') and C(5') furan carbon signals. Negatively oriented DEPT 135 signals are present at δ 20.7 and 32.8 and correspond to the C(2) and C(3) methylene carbons respectively in the propionate chain of **31**.

At this point it occurred that the adverse C-C cleavage pathway might be assisted by ether oxygen protonation due to traces of trifluoromethanesulphonic acid (TfOH), formed from the hydrolysis of TBDMSOTf. The reaction of **4a** with TfOH gave no reaction in benzene, MeCN and Et_2O, although a number of literature examples were found that report sulphonic acid derivatives mediate 7-oxanorbornane rearrangements to the C-C and C-O cleavage products. The ether ring opening of C-glycoside containing 6-chloro-7-oxa-bicyclo[2.2.1]hept-5-ene derviatives using TfOH in anhydrous MeCN has been discussed by Pasquarello *et al.* [17], who theorise the cleavage of the ether bridge to proceed *via* a vinylic carbocation intermediate followed by Ritter reaction with MeCN (Scheme 4.5, top).

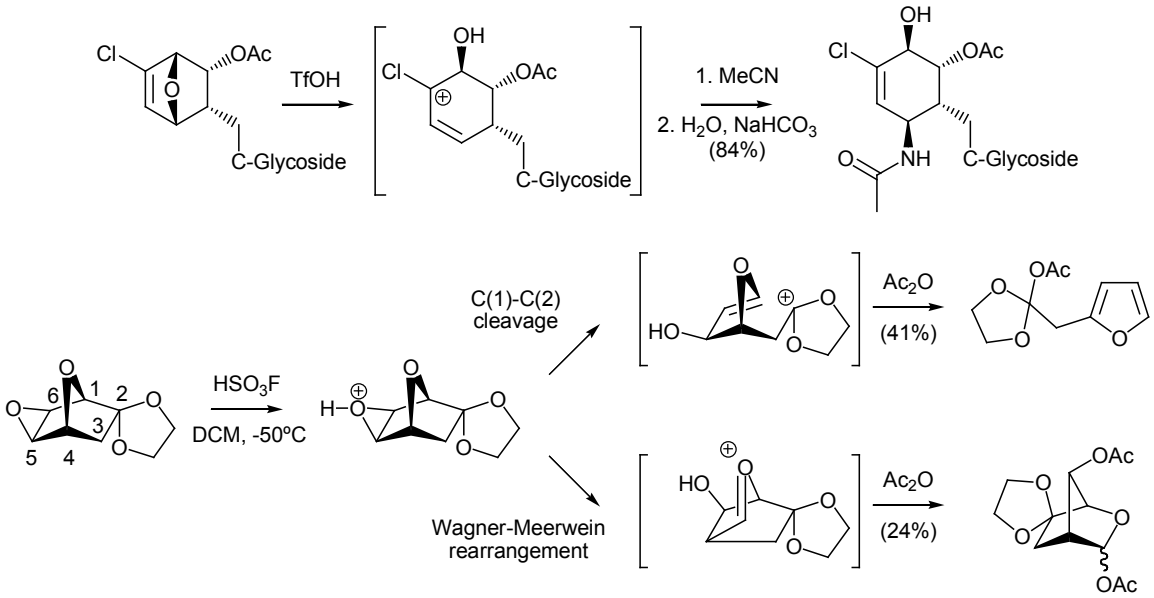

Scheme 4.5: Top; The TfOH catalysed C-O opening reported by Pasquarello *et al.* [17] who theorise the reaction to proceed via the vinylic carbocation intermediate followed by Ritter reaction with MeCN. Bottom; Vogel *et al.* [12, 18] report the cleavage of substituted epoxy-7-oxa-norbonyl derivatives with HSO_3F/ Ac_2O to produce the furan product (41%) as a result of C(1)-C(2) cleavage, as well as the Wagner-Meerwein rearrangement product (24%).

Vogel *et al.* have discussed a number of acid catalysed Wagner-Meerwein type rearrangements [18] of 5-*exo*-6-*exo*-epoxy-7-oxa-2-norbonyl derivatives (Scheme 4.5, bottom). The authors mention an accompanying C(1)-C(2) bond cleavage pathway upon reaction of the ethylene acetal substituted epoxy-7-oxa-norbonyl with fluorosulphonic acid (HSO_3F) and Ac_2O at –50ºC to provide the furan in moderate yield (41%) [12]. The described literature on the sulphonic acid mediated oxa-bicyclo cleavage suggest that an additional epoxy or olefin functionality may be required on the saturated 7-oxa-bicyclo[2.2.1]heptane system to effect ether cleavage using TfOH. The ketone **4** does not satisfy these structural requirements and is inert to reaction with TfOH, and the TBDMS protected enolate is the most likely intermediate in the formation of the furan **31** but was not observed in GC-MS analyses.

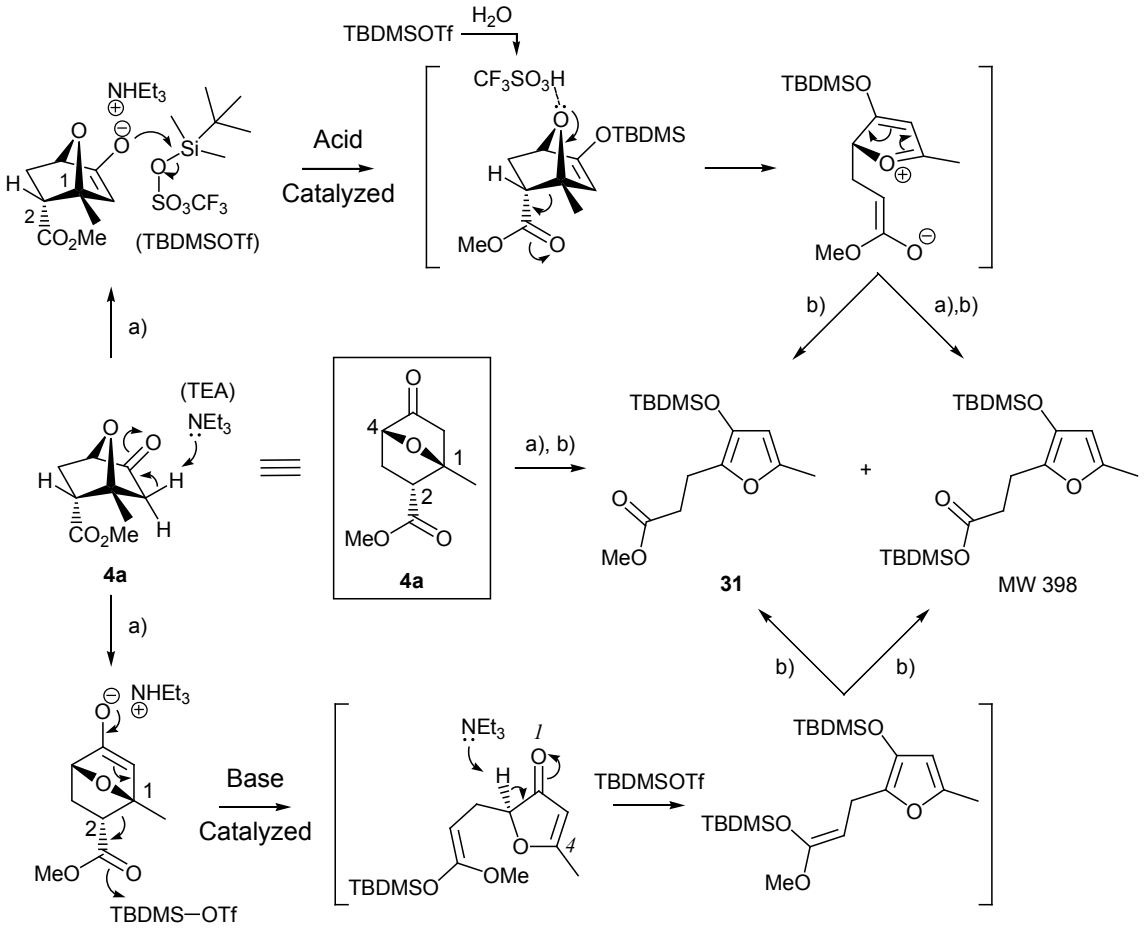

a) 1.4 equiv. TBDMSOTf, 1.9 equiv. TEA, benzene, 25ºC, 4 h; 1.6 equiv. TBDMSOTf, 2.1 equiv. TEA, benzene, 25ºC, 2 h b) Et_2O, 1 M HCl, **31** (69%).

Scheme 4.6: Proposed mechanisms for the reaction between **4a** and TBDMSOTf in the presence of TEA to give the furan **31**. Top; The acid catalysed pathway can proceed via silylation of the enolate followed by protonation of the ether oxygen. Bottom; The base catalysed pathway can proceed from the enolate ion *via* a retro 1,4-conjugate addition followed by ester enolate trapping with TBDMSOTf.

A proposed mechanism for the formation of **31** is shown in Scheme 4.6 (top) and can involve silylation of the enolate tautomer, followed by protonation of the bicyclic oxygen and C(1)-C(2) cleavage to the ester enolate. Silylation of the ester enolate by an additional equivalent of TBDMSOTf can occur at this stage to produce a mixture of **31** and the transesterified TBDMS ester ($M^{+\cdot}$ *m/z* 398) upon workup with 1 M HCl, as observed in the crude product mixtures (Figure 4.1).

A base catalysed mechanism (Scheme 4.6, bottom) may also occur whereby the enolate of **4a** undergoes a retro 1,4-conjugate addition, during which the cleavage at C(1)-C(2) occurs and the ester enolate is trapped by TBDMSOTf to form the conjugated furanone intermediate. The aromatic furan system is subsequently formed upon base mediated enolization and reaction with an additional equivalent of TBDMSOTf to give a mixture of **31** and the TBDMS ester upon workup with 1 M HCl. The ring cleavage of **4a** did not occur in the presence of TEA without the incorporation of TBDMSOTf and the unexpected C-C bond cleavage prompted further investigation into base mediated ring opening reactions to reveal whether the C-O bond could be preferentially cleaved in the absence of the silylating agent.

Experimental work published by McMorris *et al.* [19] describes the ether ring openings of 7-oxanorbornanes with K_2CO_3 in $^{i}PrOH/H_2O$ (Scheme 4.7, top) to give the α,β-unsaturated ketone as desired in the cleavage of **4**. Takahashi *et al.* [20] have achieved similar results using LHMDS in THF to produce α,β-unsaturated carbonyl compounds in moderate yield (Scheme 4.7, bottom).

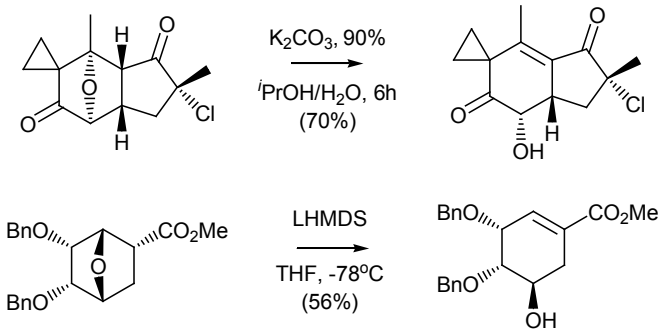

Scheme 4.7: Top; Base mediated bicyclic ether cleavage has been reported by Morris *et al.* [19] to proceed in good yields using K_2CO_3 to give the α,β-unsaturated ketone. Bottom; Takahashi *et al.* [20] have utilised $LiN(TMS)_2$ at low temperatures to facilitate the base mediated ether cleavage of the oxygenated bicyclic ether to produce the α,β-unsaturated ester.

Reaction of **4a** with LHMDS in THF at low temperature (–78°C to –50°C, Section 6.7.2) gave a single product **32** at t_R = 12:21 min in GC-MS analysis (Appendix 4.2), featuring a molecular ion at *m/z* 184 and no noticeable *m/z* 97 fragment ion suggesting that the product does not contain the methyl cyclohexenone skeleton. Purification was achieved by FCC in SiO_2 (5:3 pentane:EtOAc) and ^{1}H NMR analysis revealed an olefinic singlet H(4') at δ 5.44 ppm with an integral area of one proton, which shows attachment to a ^{13}C NMR peak at δ 104.6 in HMBC NMR analysis (Figure 4.3). Strong HMBC correlations between H(4') and a quaternary carbon signal at δ 190.5 (C(5')), carbonyl signal at δ 204.3 (C(3')) and methine signal at δ 85.0 (C(2')) are evident, indicating that these functionalities are in close proximity. These ^{13}C NMR chemical shifts observed in **32** closely match the ^{13}C NMR spectrum of the α,β-unsaturated furanone **16** (Chapter 2, Section 2.3) and ^{1}H COSY NMR analysis (Appendix 4.2) shows signals indicative of a propionic ester chain coupled to the H(2') methine signal, to confirm **32** as methyl 3-(2,3-dihydro-5-methyl-3-oxofuran-2-yl)propanoate (Scheme 4.8). The ketone **32** was positively identified in low yield by GC-MS analysis (Appendix 4.3) as a desilylation product upon treatment of **31** with tetrabutyl ammonium fluoride (TBAF) (Scheme 4.7) and verifies that **31** and **32** are structurally related tautomers. The expected α-ketol product (1*R*,5*R*)/(1*S*,5*S*)-methyl 1-methyl-5-oxo-7-oxa-bicyclo[2.2.1]heptane-2-carboxylate (C(5)-*epi*-**3**), shown as the (1*R*,2*R*)-enantiomer in Figure 4.8, was not observed and reactions involving **4b** with base revealed identical reactivity to **4a**. Studies addressing the stereochemistry at C(2') were not undertaken and it was assumed that **32** is racemic as tautomerisation to the furan can occur under basic conditions.

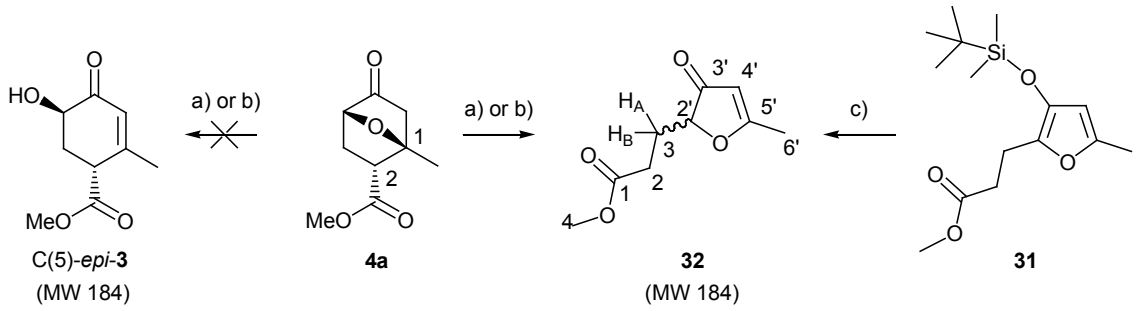

a) LHMDS, THF, -78°C to -45°C over 2 h, 56% b) K_2CO_3, ^{i}PrOH, 12 h, 12% c) **31**, TBAF, DCM, 25°C, 1.5 h.

Scheme 4.8: Treatment of **4a** with LHMDS or K_2CO_3 did not give the expected α-ketol product and instead underwent C(1)-C(2) cleavage to produce methyl 3-(2,3-dihydro-5-methyl-3-oxofuran-2-yl)propanoate **32**. The structure of **32** was also confirmed by desilylation of **31** with TBAF.

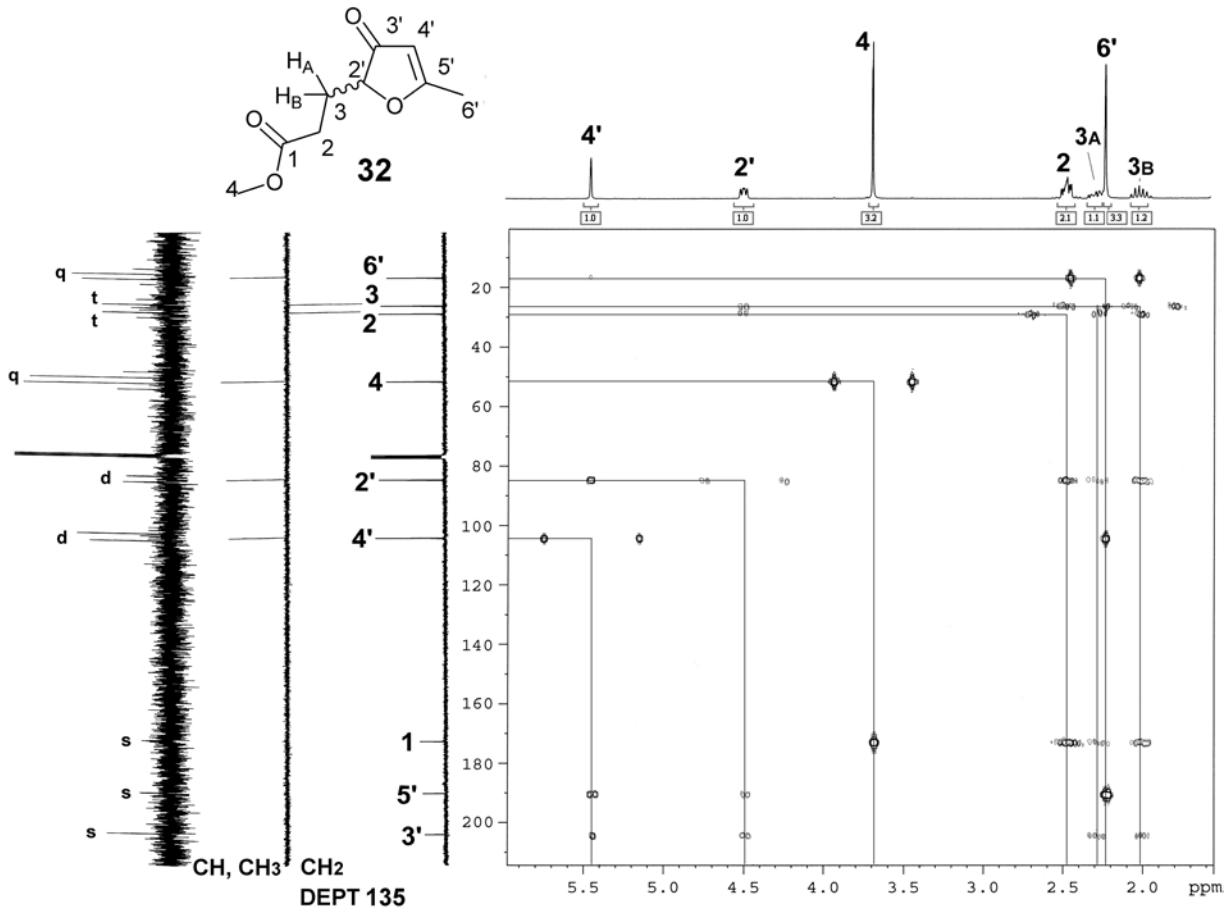

Figure 4.3: ^{1}H 300 MHz/^{13}C 75 MHz HMBC NMR analysis of **32** with DEPT 135 NMR and heteronuclear ^{13}C-^{1}H coupled NMR data also shown.

DEPT 135 analysis clearly shows the negatively oriented H(3) and H(4) methylene signals which appear as triplets in heteronuclear ^{13}C coupled NMR data and these observations support the proposed structure of **32**. Reaction of **4a** with K_2CO_3 under conditions described by McMorris *et al.* [19] gave similar results to reaction with LHMDS to produce a 12% yield of **32** after stirring at ambient temperature for 12 h. These observations confirm that the C(1)-C(2) cleavage between the ester and the tertiary bridgehead occurs as the result of a base mediated mechanism (Scheme 4.5, bottom) and is likely to proceed *via* the enol ketone tautomer of **4a** followed by rearrangement of the enolate anion.

No similar examples could be found in the literature that involve base mediated C-C bond cleavage chemistry of 7-oxa-bicyclo[2.2.1]heptan-2-one derivatives and this may be owing to the scarcity of available preparations for these structures. Selectivity in the formation of the five membered products **31** and **32** may be solely due to the positioning of the C(2) ester substituent, allowing the stabilization of the negative charge onto the carboxyl oxygen. A single publication by Rainer *et al.* [21] was found involving

C-C cleavage of the substituted 7-oxanorbornanone (Scheme 4.9, top) and norbornanone (Scheme 4.9, bottom) skeletons to provide the substituted five membered rings. The authors mention the scarcity of this type of ring cleavage and suggest a mechanism involving a four membered hemiacetal intermediate, formed between the ketone and alcohol functionalities [21].

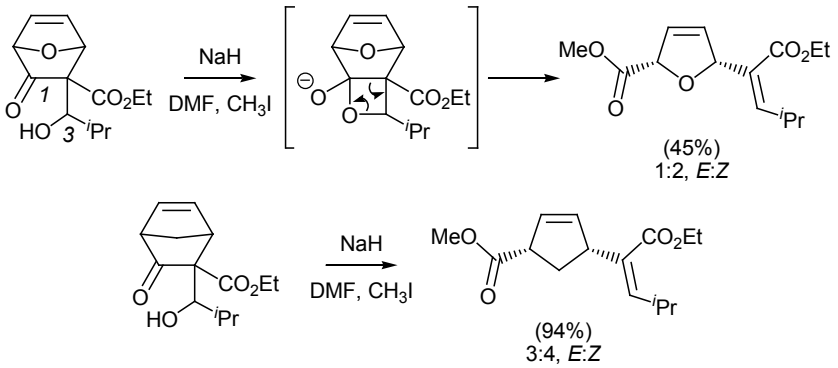

Scheme 4.9: Rainer *et al.* [21] describe the C-C cleavage in some bicyclic structures using NaH and suggest a four-membered hemiacetal intermediate formed from the 1,3-keto-alcohol system. The 7-oxanorbornanone (top) and norbornanone (bottom) skeletons behaved similarly to produce the five membered cyclic olefins.

Although the same mechanism would not be possible for the formation of **31** and **32** from **4a** due to the absence of the necessary substitutents, this example highlights that the substitution on the bicyclic structure has an important role in the C-C bond breaking reactions discussed in Section 4.1.2. This consideration suggests that the reaction of **4a** with Lowry-Brönsted bases leads to the five membered heterocyclic products, however the same conditions may not be able to be applied to even closely related structures without obtaining unpredictable results. This outcome initiated a re-direction in studies toward the 7-oxa-bicyclo[2.2.1]heptan-2-one ether cleavage to focus on Lewis-acids in an attempts to effect C-O cleavage *via* an alternate mechanism.

4.1.2 Lewis-Acid Facilitated Ring Cleavage of 7-Oxanorbornanes

Due to the unforseen side reaction of **4a** under basic conditions to give the five membered heterocycle, Lewis-acid catalysed ether cleavage was investigated and was expected to proceed by co-ordination of the lone pair electrons on the bicyclic ether oxygen bridge. A review of Lewis-acid mediated 7-oxanorbornanone ether cleavages was undertaken to find suitable conditions for the reaction of **4**.

Vidari *et al.* [22] have reported on the stereoselective rearrangement reactions of geraniol epoxide using Fe(III) and Zr(IV) Lewis-acids to yield the substituted cyclohexenol structures as chiral intermediates in terpene synthesis. The action of ferric(III) chloride hexahydrate ($FeCl_3.6H_2O$) on geraniol epoxide was reported to form a 1:1 mixture of (1*S*,5*R*)-5-(hydroxymethyl)-4,6,6-trimethylcyclohex-3-enol and the 7-oxanorbornane in modest yield (40%) (Scheme 4.10, top). The authors suspected that the bicyclic product was an intermediate in the formation of the dialcohol, and this conclusion was supported by the reaction of the isolated bicyclic product with an additional portion of $FeCl_3.6H_2O$ to give a small yield of the dialcohol (37%). Vidari *et al.* [22] also report on an improved ether cleavage reaction using $ZrCl_4$ under anhydrous conditions to produce (1*S*,5*R*)-5-(hydroxymethyl)-4,6,6-trimethylcyclohex-3-enol in quantitative yield from the 7-oxanorbornane intermediate, and in moderate yield (52%) from geraniol epoxide (Scheme 4.10, bottom).

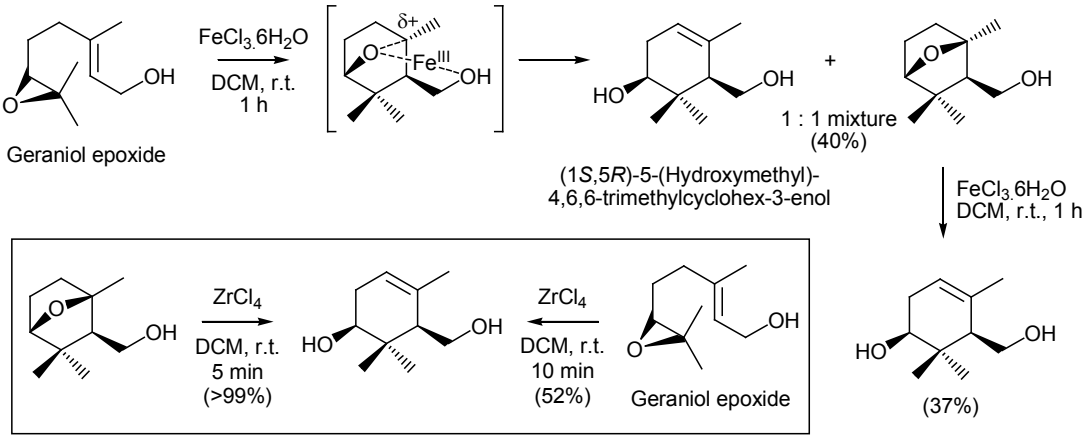

Scheme 4.10: Research conducted by Vidari *et al.* [17] involves the Lewis-acid mediated rearrangement of geraniol epoxide. Top; $FeCl_3.6H_2O$ was reported to produce the cyclohexenol via the 7-oxanorbornane intermediate. Bottom; $ZrCl_4$ was reported to give improved results for both the 7-oxanorbornane and geraniol epoxide rearrangements.

No reaction was observed upon treatment of **4a** with $FeCl_3.6H_2O$ or $ZrCl_4$ under conditions described by Vidari *et al.* [22] and reactions at higher temperature also returned only starting material. Reaction of **4a** with $TiCl_4$ under anhydrous conditions as described by Arjona *et al.* [23] was also unsuccessful and returned **4a** without decomposition.

Boron trifluoride etherate ($BF_3.(Et_2O)$) Lewis-acid in the presence of the iodide ion has been discussed by Mandal *et al.* [24] as a mild and selective reagent for the cleavage of alkyl and aryl ethers. The $BF_3.(Et_2O)$/iodide system has also been used for 7-oxanorbornane ether cleavage by Mehta *et al.* [25] in the synthesis of novel inositols. Tetrabutylammonium iodide (TBAI) was used as the iodide

source and results in nucleophilic attack by the iodide ion with inversion of stereochemistry to provide the ring opened tertiary alcohol. The iodinated compound was modified in two steps to produce the novel *neo*-inositol derivative containing the octahydroxydecalin core [25] (Scheme 4.11, top).

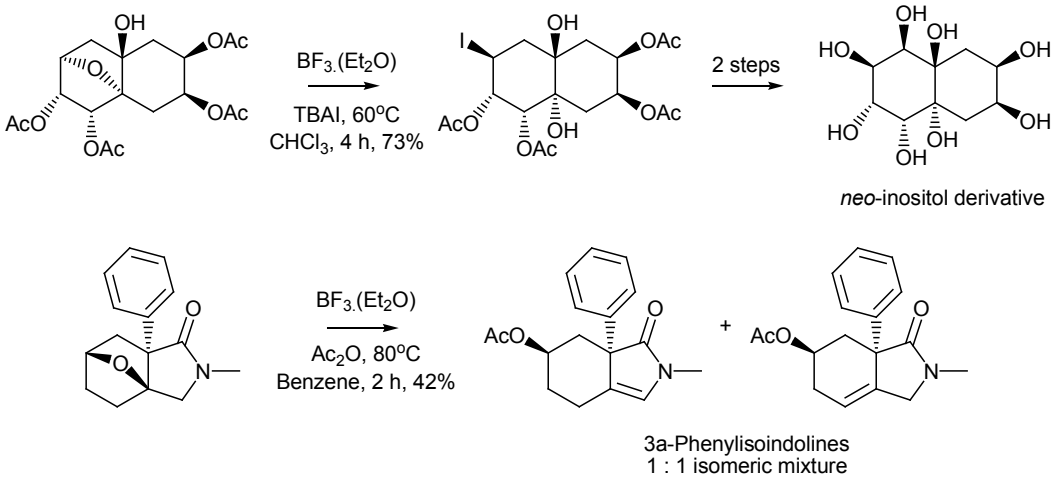

Scheme 4.11: Top; Research conducted by Mehta *et al.* [25] involves 7-oxanorbornane cleavage using $BF_3.(Et_2O)$/TBAI to produce the iodinated product with inversion of stereochemistry, followed by conversion to the *neo*-inositol derivative in two steps. Bottom; Research conducted by Gschwend *et al.* [26] involved 7-oxanorbornane ether cleavage using $BF_3.(Et_2O)/Ac_2O$ to produce the acetoxy substituted product as a 1:1 mixture of olefin isomers.

Gschwend *et al.* [26] have reported the successful 7-oxanorbornane ether cleavage using $BF_3.(Et_2O)$ in the presence of Ac_2O during the preparation of 3a-phenylisoindolines, to produce the acetoxy derived product with retention of stereochemistry as a 1:1 mixture of olefin isomers (Scheme 4.11, bottom).

No reaction occurred between **4b** and $BF_3.(Et_2O)$ in DCM at a range of temperatures (-78-25ºC). Reaction of **4b** with $BF_3.(Et_2O)$ in the presence of TBAI performed according to procedures described by Mehta *et al.* [25] and Mandal *et al.* [24] was also unsuccessful, returning only the starting ether as indicated by GC-MS monitoring. Reaction of **4b** with $BF_3.(Et_2O)/Ac_2O$ (Section 6.7.3) under conditions described by Gschwend *et al.* [26] gave one major product **33** (Scheme 4.12) at t_R = 13:49 min in 68% according to GC-MS analysis (Figure 4.4), showing a large *m/z* 43 base peak indicative of an acylated product [16] and a *m/z* 243 fragment ion, although no molecular ion was observed.

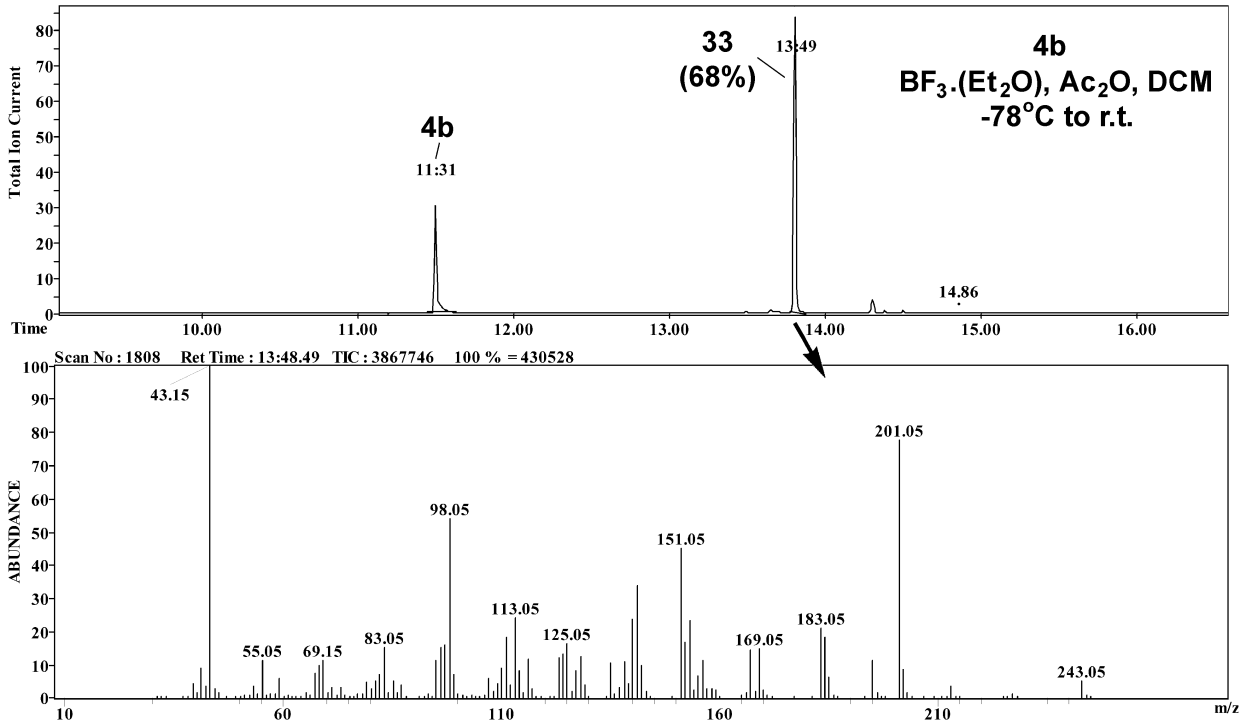

Figure 4.4: GC-MS of the crude ether cleavage reaction of **4b** with $BF_3.(Et_2O)$ in the presence of Ac_2O to give 68% conversion to the acylal derivative **33**. The molecular ion $M^{+\cdot}$ *m/z* 286 is not seen and the largest fragment ion *m/z* 243 and corresponds to the loss of an acetyl group (*m/z* 43).

Separation of **33** from the unreacted **4b** using column chromatography (pentane:EtOAc 4:1) provided suitable material for $^{1}H/^{13}C$ HMQC NMR and DEPT 135 NMR analysis (Appendix 4.4). NMR data shows signals characteristic for a substituted 7-oxa-bicyclo[2.2.1]heptane of similar structure to **4b** including a methine bridgehead doublet at δ 5.10 corresponding to H(4). A notable absence of the carbonyl signal at δ 211.0 inferred that derivatization of the ketone of **4b** had occurred upon reaction with $BF_3.(Et_2O)/Ac_2O$. Two ^{1}H NMR signals at δ 2.05 with an integral area equivalent to 6 protons, and ^{13}C NMR ester carbonyl signals δ 169.0 and 168.7 (Appendix 4.4) indicate two acetoxy substituents to identify **33** as the 5,5-diacetate derivative methyl 5,5-diacetoxy-1-methyl-7-oxa-bicyclo[2.2.1]heptane-2-carboxylate (Scheme 4.12). This conclusion is supported by the appearance of a quaternary aliphatic signal at δ 107.9 in close agreement with Chemdraw predictions for the C(5) resonance. The largest fragment ion (*m/z* 243) observed in EIMS analysis (Figure 4.4) can be rationalised by the facile cleavage of an acetyl substituent (*m/z* 43) from the acylal **33** (MW 286).

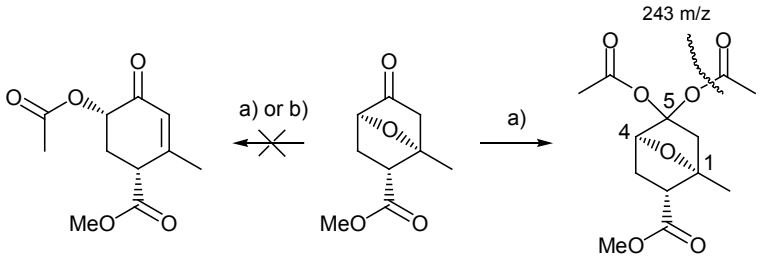

2
(MW 226)
(1*R*, 5*S*)/(1*S*, 5*R*)-Methyl 5-acetoxy-2-methyl-4-oxocyclohex-2-enecarboxylate

4b

33
(MW 286)
Methyl 5,5-diacetoxy-1-methyl-7-oxa-bicyclo[2.2.1]heptane-2-carboxylate

a) DCM, Ac_2O, $BF_3.(Et_2O)$, -78 to 25ºC, 12 h, 68% b) DCM, TBAI, $BF_3.(Et_2O)$, -78 to 25ºC then Ac_2O

Scheme 4.12: Reaction of **4b** with $BF_3.(Et_2O)$ produced the C(5) acylal derivative methyl 5,5-diacetoxy-1-methyl-7-oxa-bicyclo[2.2.1]heptane-2-carboxylate **33** in moderate yield (68%). The desired methyl 5-acetoxy-2-methyl-4-oxocyclohex-2-enecarboxylate **2** was not seen.

$BF_3.(Et_2O)$ [27] and other Lewis-acids [28] in the presence of acid anhydrides have been reported to convert a range of aldehydes to the 1,1-diacetate or 'acylal' derivatives. Although this transformation is typically poor when applied to ketones, Curini *et al.* [28] report the formation of the acylal of cyclohexanone in low yields using the heterogenous catalyst zirconium sulfophenyl phosphonate [27]. Unfortunately, the ketone **4b** showed a strong preference for acylal formation rather than undergoing ring cleavage to (1*R*,5*S*)/(1*S*,5*R*)-methyl 5-acetoxy-2-methyl-4-oxocyclohex-2-enecarboxylate **2**, shown as the (1*R*,5*S*) isomer in (Scheme 4.12). This result suggests that BF_3 has a more predominant Lewis-acid interaction with the lone pair electrons on the carbonyl oxygen, rather than the bicyclic ether oxygen. A likely reason for this is that BF_3 was used as the commercially available Et_2O complex (Sigma-Alrich) and it occurred that a boron reagent in non-ethereal solvent could be more appropriate for the ether cleavage of **4**. Boron tribromide (BBr_3) obtained as a 1M solution in DCM (Sigma-Alrich) was used in subsequent studies and the larger size of the bromine halogen substitutents was thought more likely to stabilise tertiary carbocation formation upon C-O cleavage at C(1).

Literature relevant to the BBr_3-mediated ether cleavage of 7-oxa-bicyclo[2.2.1]heptanes was reviewed, paying particular attention to suggested mechanistic pathways. The stereo- and regio-selective ether bridge cleavage of 1,2,3,4-tetrahydro-1β,4β-epoxy-2α,3α-carbonyldioxyl arenes using BBr_3 has been studied by Koreeda *et al.* [29, 30] who used AM1 calculations to correlate the observed regioselectivity to the stabilization of the benzylic carbocation in the bay region of the arene system. The authors later rationalised that the BBr_3 Lewis-acid forms a complex with the ether oxygen lone pair, resulting in polarization of the C-O bond followed by cleavage to a benzylic carbocation that reacts in a

face-selective manner with the bromine ion from the bromoborane ether intermediate [31] (Scheme 4.13).

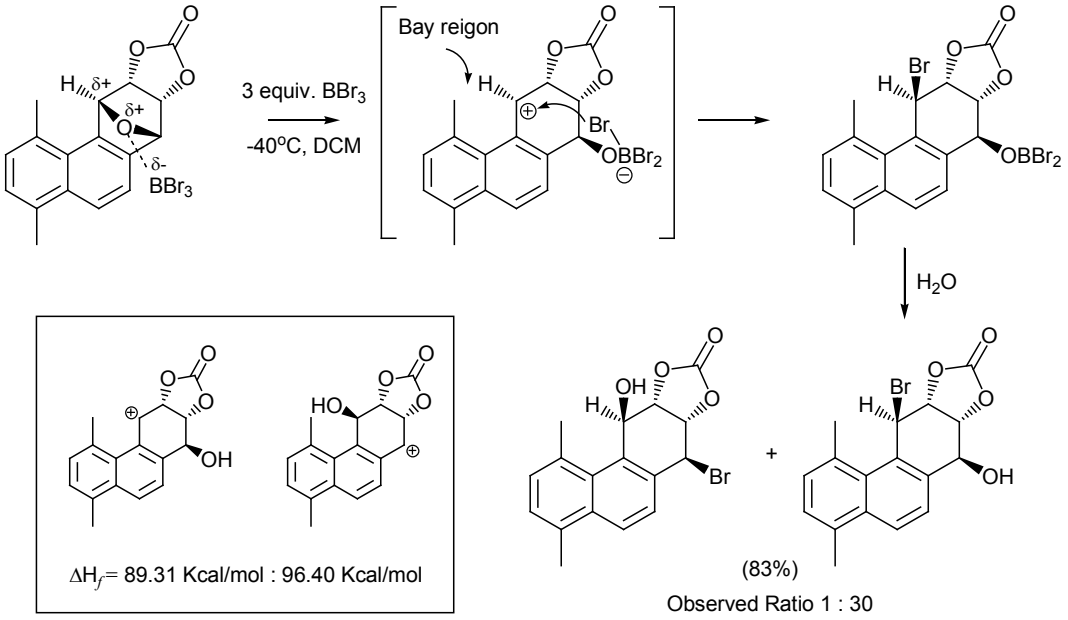

Scheme 4.13: Koreeda *et al.* [29] have conducted studies on the stereo- and regioselective ether opening of 1,2,3,4-tetrahydro-1β,4β-epoxy-2α,3α-carbonyldioxyl arenes using BBr_3. The authors have rationalised the reaction to proceed *via* a stabilised carbocation intermediate based on AM1 calculations in support of experimental findings [31].

Mosimann *et al.* [32] have described a number of BBr_3-mediated ring openings of 7-oxabicyclo[2.2.1]heptanes during the stereoselective preparation of tetradecahydrophenanthrene type diterpenes. Reaction of acetoxy substituted 7-oxanorbornanes with HBr in AcOH was reported to give the brominated product in good yield (80%) as the result of S_N2 type acid mediated hydrolysis (Scheme 4.14, top), with stereochemical inversion at C(4) but retention of stereochemistry at the C(1) acetoxy position. Reaction of the same compound with BBr_3 was reported to provide the ether cleavage product in 69% yield without the incorporation of bromine. The authors propose an intermediate incorporating the adjacent *endo* acetoxy moiety based on migration of the C(2) acetoxy group to the C(1) position with inversion of stereochemistry upon quenching in aqueous $NaHCO_3$, whereas stereochemistry of the C(4) hydroxyl group is preserved with respect to the ether bridge [32]. Mosimann *et al.* also report chemoselectivity in the BBr_3 facilitated cleavage of C(1)/C(12) and C(4)/C(7) bicyclic ether moieties (Scheme 4.14, bottom) contained on an anisoate (An) substituted tetra-decahydrophenanthrene backbone [32]. Carefully controlled reaction temperatures gave selective cleavage of the C(1)/C(12) ether in 84% yield at –50°C and both ethers in 50% yield upon reaction at –18°C. The authors report stereochemical inversion at both C(7) and C(12) in the ether cleavage products and suggest similar involvement from the

anisoate group in the ring opening mechanism to that shown for the acetoxy products but without acyl migration. In all examples shown in Figure 4.14 the crude reaction was quenched in $NaHCO_3$ and in the bottom scheme the alcohol products were subsequently acetylated with Ac_2O and DMAP in pyridine.

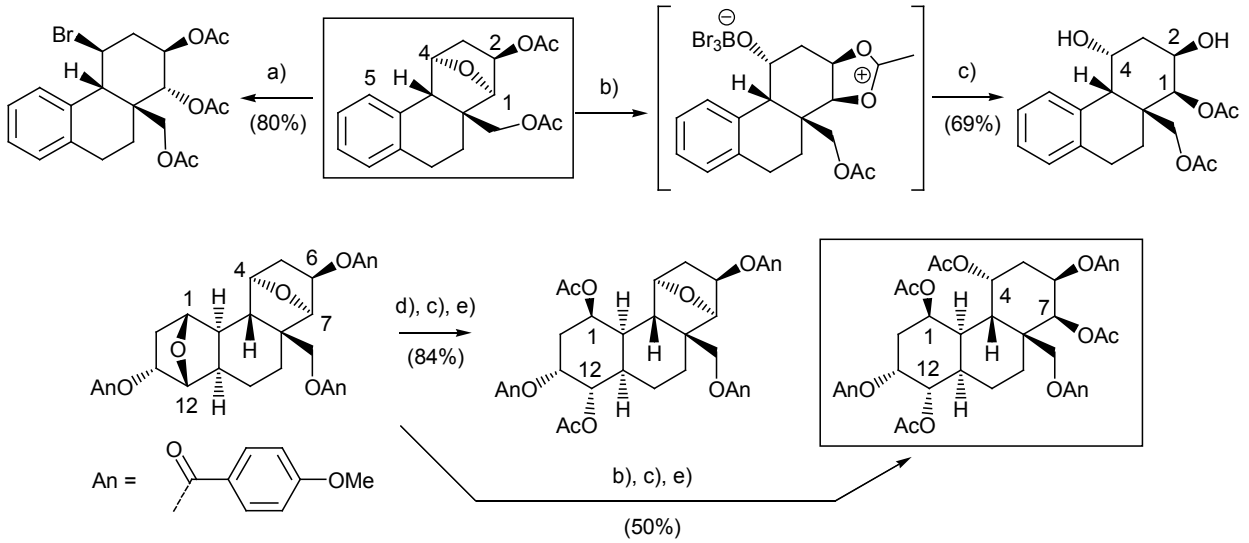

a) HBr/AcOH, 55ºC, 18 h b) BBr_3, DCM, -18ºC, 45 min c) Aq. $NaHCO_3$, 0ºC, 5 min d) BBr_3, DCM, -50ºC, 15 min e) Ac_2O, Pyridine DMAP

Scheme 4.14: Mosimann *et al*. [32] have described the stereo- and chemo-selective cleavage of the 7-oxanorbornane ether ring. Top; Reaction with HBr was reported to undergo an S_N-2 type inversion with the bromide ion. Cleavage with BBr_3 provided retention of stereochemistry at C(4) but inversion at C(1) via an intermediate involving the adjacent C(2) acetoxy group. Bottom; The chemoselective BBr_3 cleavage of carbocycles containing two 7-oxanorbornane functionalities using controlled temperatures to produce the anisoate (An) substituted tetradecahydrophenanthrene structures.

Further studies towards the BBr_3 ether cleavage of 7-oxabicyclo[2.2.1]heptanes have been presented in research by Jotterand *et al.* [33] during the total asymmetric synthesis of carba-hexopyranoses. Short reaction times (10 min) were used to cleave the ether bridge of the pentapivaloate substituted 7-oxanorbornanes (Scheme 4.15) and the authors mention that both alcohol groups which are formed as a result of ether cleavage are oriented on the same face of the cyclohexane skeleton. An intermolecular S_N-2 type inversion with H_2O at the quaternary C(1) position is suggested to be unlikely due to steric constraints. A plausible mechanism offered by Jotterand and co-workers [33] involves the formation of a cationic intermediate with the adjacent pivaloate (Piv) substituents, followed by intramolecular equilibration and subsequent hydrolysis upon workup in aqueous $NaHCO_3$ solution to

provide the 1,4-diol in high yield (88%). Both hydroxyl groups are situated on the same face with retention of stereochemistry with respect to the bicyclic ether bridge in the reactant.

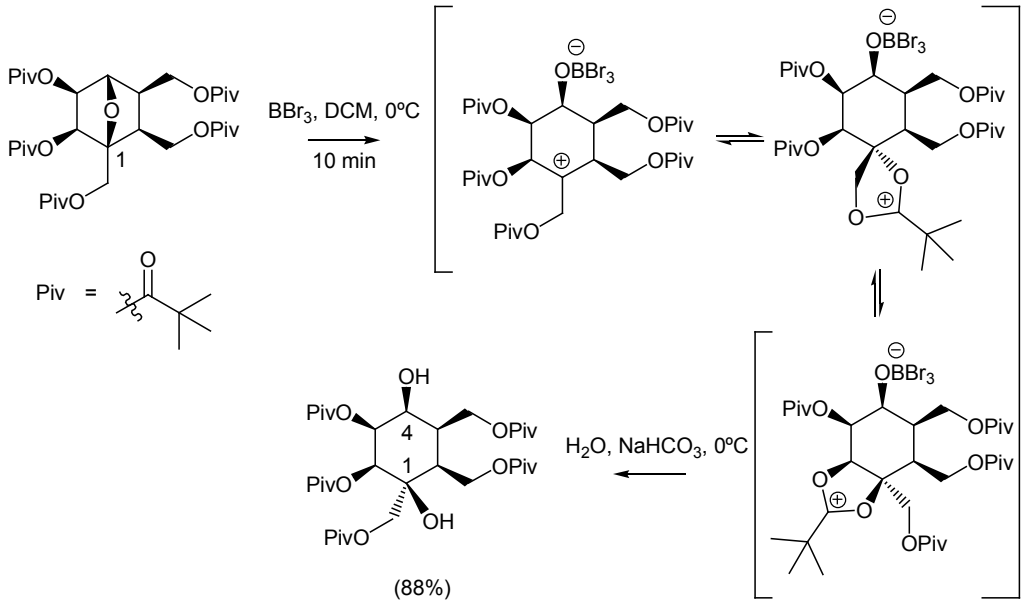

Scheme 4.15: Jotterand *et al.* [33] report the BBr_3-mediated cleavage of the pentapivaloate derived 7-oxanorbornanes to yield the 1,4-dihydroxy hydrolysis products with retention of stereochemistry. The authors propose that the reaction intermediates the pivaloate group and equilibration followed by quenching in $NaHCO_3$ leads to *cis*-oriented hydroxyl groups in the cleavage product.

Pasquarello *et al.* [17] have reported the BBr_3-mediated ether cleavage of glycoside substituted 7-oxanorbornenes (Scheme 4.16) and suggest a vinylic carbocation intermediate, similar to that observed for the acid mediated ring opening with TfOH (Section 4.1.1, Scheme 4.5). Quenching in aqueous $NaHCO_3$ was reported to form the C(2) hydroxy product in good yield (72%) with the incorporation of bromine at C(5) on the same face as the hydroxyl group. The authors suggest that the brominated product results from the reaction of a bromide ion from the bromo-borane with a cationic reaction intermediate onto the least sterically hindered face [13]. The relationship between the equatorial C(5) bromine and axial C(2) hydroxy was deduced from NMR studies and a half-chair confirmation suggested for the cyclohexene ring based on coupling constants.

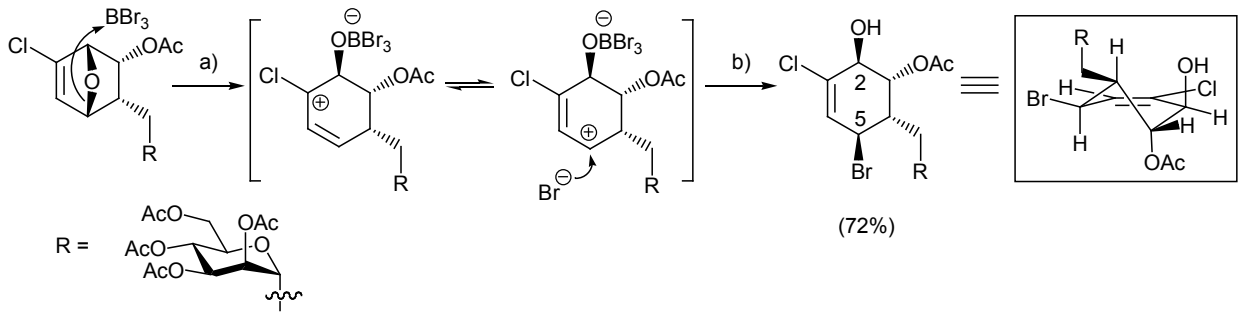

a) BBr_3, DCM, 0ºC, 15 min b) Aq. $NaHCO_3$

Scheme 4.16: Research presented by Pasquarello *et al.* [17] involves BBr_3-mediated ether cleavage of the 7-oxanorbornenes and the authors suggest a vinylic carbocation intermediate followed by reaction with the bromide ion at C(5) on the same face as the bromoborane ether, followed by quenching in saturated $NaHCO_3$ to give the C(2) alcohol in good yield (72%) with retention of stereochemistry.

Studies by Barrero *et al.* [34] have focused on the synthesis of oxygenated monocarbocyclic sesquiterpenoids and incorporate the BBr_3-mediated 7-oxanorbornane cleavage of (2',5'-epoxy-2',6',6'-trimethyl)cyclohexyl-methyl acetate (Scheme 4.17; Top). Quenching in a solution of 1M collidine/DCM was reported to give the rearranged cleavage product with retention of stereochemistry at the C(1) hydroxyl group in a mixture of exocyclic and endocyclic olefin regioisomers (72%). Later studies by Barrero *et al.* [35] involve similar conditions with 4-(2',5'-epoxy-2',6',6'-trimethyl)cyclohexyl-2-butylacetate to produce the rearranged C(1) hydroxyl derivative 3-(3'-acetoxybutyl)-2,2,4-trimethylcyclohex-3-enol in high yield (89%) with retention of stereochemistry (Scheme 4.17; Bottom). Chemoselectivity was reported for the ring opened endocyclic C(3)/C(4) olefin and the less substituted olefin isomers were not mentioned as isolable side-products [35].

The reaction of **4b** with BBr_3 in dry DCM was performed at 0ºC followed by quenching in $NaHCO_3$ solution according to methodology described by Jotterand *et al.* [34] and GC-MS analysis of the product mixtures revealed that no reaction had occurred (Scheme 4.18). Similar results were obtained upon quenching in H_2O using methodology described by Koreeda *et al.* [29] and procedures that avoid aqueous quenching mixtures were subsequently investigated.

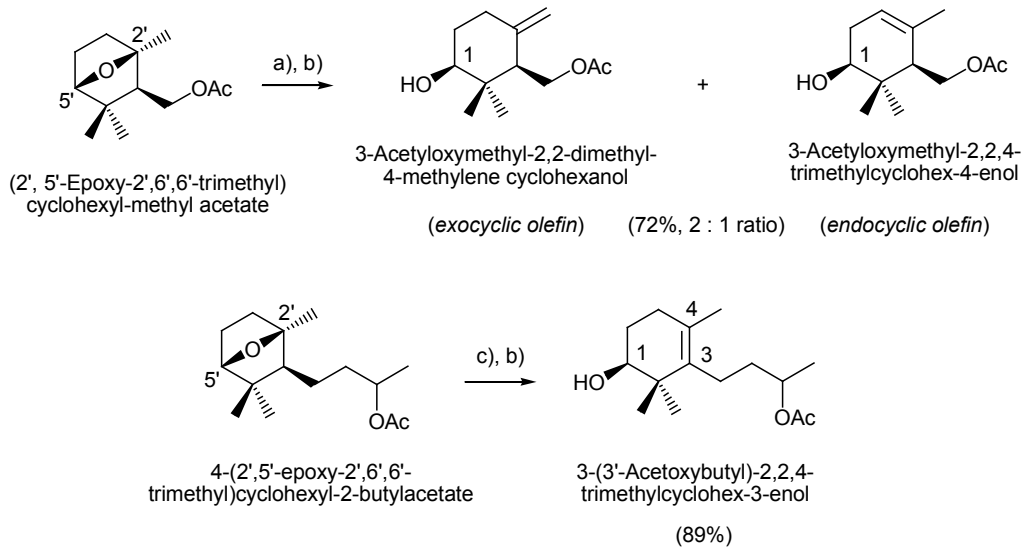

a) BBr_3, DCM, r.t., 10 min b) 1 M Collidine in DCM c) BBr_3, DCM, r.t., 15 min

Scheme 4.17: Research presented by Barrero *et al.* [34, 35] describes the ether cleavage of 7-oxanorbornanes using BBr_3 followed by quenching in 1 M collidine. Top; 4-(2',5'-Epoxy-2',6',6'-trimethyl)cyclohexyl-2-butylacetate undergoes rearrangement to give a mixture of olefin isomers with retention of stereochemistry at the C(1) hydroxyl group [34]. Bottom; Treatment of 4-(2',5'-Epoxy-2',6',6'-trimethyl)cyclohexyl-2-butylacetate with BBr_3/collidine was reported to give chemoselective cleavage to 3-(3'-Acetoxybutyl)-2,2,4-trimethylcyclohex-3-enol in 89% yield [35].

Conditions described by Barrero *et al.* [34, 35] appeared to be suitable for the transformation of **4b** directly to **3** as formation of the olefin accompanies ether cleavage and is likely to form in conjugation with the ketone. Procedures reported by Barrero *et al.* [35] were trialed and the reaction of **4b** in dry DCM with BBr_3 at ambient temperature followed by quenching in 1 M collidine/DCM solution gave a complex mixture of by-products. Optimization procedures revealed the reaction of BBr_3 with **4b** to be very temperature sensitive and upon decreasing reaction temperatures to 5ºC a small number of major products were formed selectively as indicated GC-MS analysis (Figure 4.5, top). EI-MS for peaks at t_R = 13:06 and t_R = 13:08 min feature molecular ions *m/z* 264, 266 in agreement with the molecular weight for the C(2) brominated isomers (1*S*,2*RS*,5*S*)/(1*R*,2*RS*,5*R*)-methyl 2-bromo-5-hydroxy-2-methyl-4-oxocyclohexanecarboxylate **34** (15%) (Scheme 4.18) and a $[M - Br]^{+\cdot}$ ion at *m/z* 185 and *m/z* 97 ion characteristic of the methyl cyclohexanone fragment [16] support the ring opened structure.

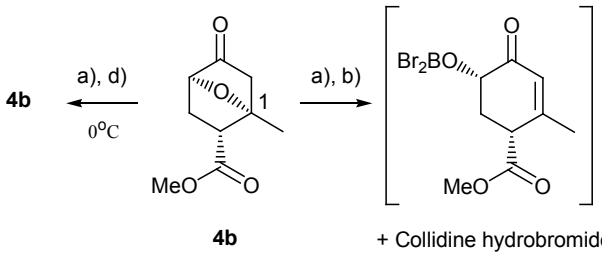

Temp of a)	**3** (%)	**34** (%)
5°C	6	15
0°C	35	5
-1°C	61	0

Table 4.1: Yields of **3** and **34** by GC-MS at a range of temperatures

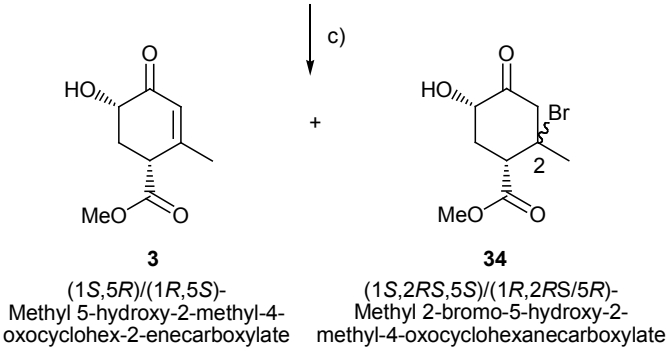

3
(1*S*,5*R*)/(1*R*,5*S*)-Methyl 5-hydroxy-2-methyl-4-oxocyclohex-2-enecarboxylate

34
(1*S*,2*RS*,5*S*)/(1*R*,2*RS*/5*R*)-Methyl 2-bromo-5-hydroxy-2-methyl-4-oxocyclohexanecarboxylate

a) BBr_3 in DCM, 10 min b) 1 M Collidine in DCM, 25-30ºC to r.t., 35 min c) 1 M HCl, d) Aq. $NaHCO_3$, r.t.

Scheme 4.18: Reaction of **4b** with BBr_3 followed by quenching in aqueous $NaHCO_3$ returned the starting ether with no detectable formation of **3**. Reactions involving quenching in 1M collidine/DCM gave the desired α,β-unsaturated ketone (1*S*,5*R*)/(1*R*,5*S*)-methyl 5-hydroxy-2-methyl-4-oxocyclohex-2-enecarboxylate **3** and small quantities of the C(2) bromo isomers (1*S*,2*RS*,5*S*)/(1*R*,2*RS*,5*R*)-methyl 2-bromo-5-hydroxy-2-methyl-4-oxocyclohexanecarboxylate **34**.

In the same mixture, an ether cleavage product at t_R = 12:15 min featuring a *m/z* 184 molecular ion in agreement with the structure of (1*S*,5*R*)/(1*R*,5*S*)-methyl 5-hydroxy-2-methyl-4-oxocyclohex-2-enecarboxylate **3** was observed as a minor component (6%). Reactions conducted at –1ºC (Figure 4.5) gave significantly improved selectivity to return **3** as the major ether cleavage product (61%) and EI-MS fragmentation features a large *m/z* 97 ion and *m/z* 41, 55 fragments as expected for the cyclic ketone **3** [16]. Reactions with BBr_3 conducted below –5ºC demonstrated extremely low reactivity and returned only the starting compound. GC-MS analysis of either the crude reaction in progress or the DCM quenching mixture gave poor and irreproducible data. Distinguishable and reproducible GC signals were only observed after conducting the workup procedure, involving multiple extractions with 1 M HCl and this observation strongly suggests the formation of a bromoborane ether intermediate (Scheme 4.18).

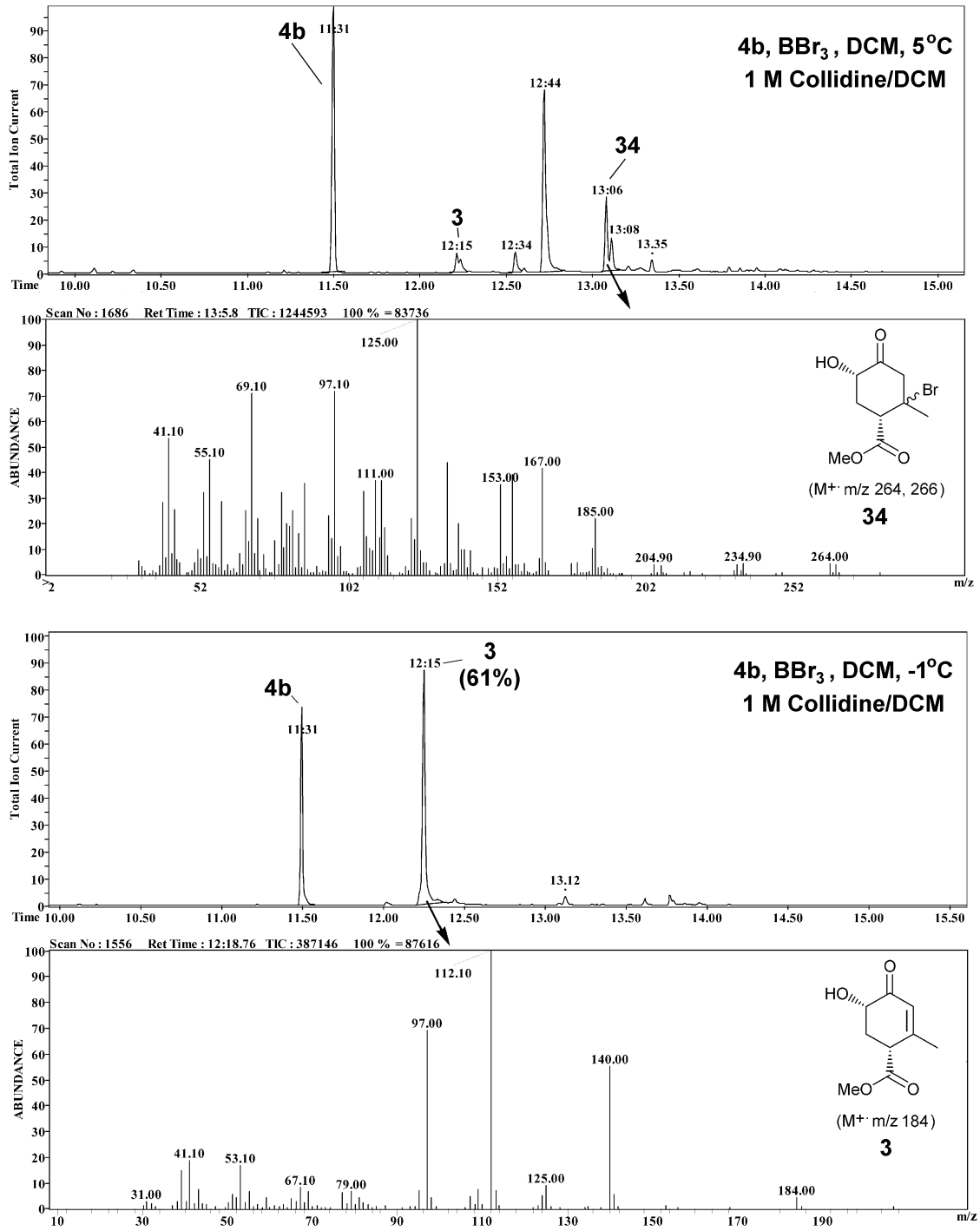

Figure 4.5: Top; GC-MS analysis of the BBr_3 ether cleavage of **4b** conducted at 5ºC, followed by quenching and workup using the described procedures gave a mixture of products amongst which the peaks at t_R = 13:06 min and t_R = 13:08 min show a molecular ion corresponding to the ring opened brominated product **34**. Bottom; GC-MS of the ether cleavage of **4b** conducted at –1ºC shows a single major product at t_R = 12:15 min in 61% with fragments *m/z* 97, 55, 41 characteristic of a cyclic ketone [16] and a molecular ion at *m/z* 184 in agreement with the structure of **3**.

The fortuitous occurrence of quenching at 30ºC in a 1 M collidine solution prepared using LR grade DCM revealed optimal conditions to provide **3** in 61% yield with respect to **4b**, without side-reactions or decomposition as indicated by GC-MS analysis (Figure 4.5, bottom). Further studies using dry DCM as the quenching diluent returned more complex reaction mixtures than experienced with LR grade reagents and repeated trials suggested that a small amount of moisture in the quenching solution may be advantageous for the clean formation of **3**. Studies involving the addition of stoichiometric equivalents of water to the quenching solution were not undertaken but may have indicated more clearly the role of water in this reaction process. The broad differences in reactivity observed between reactions quenched in aqueous $NaHCO_3$ and 1M collidine in DCM suggests that the BBr_3 complexation may occur with selectivity at low temperatures and the ether cleavage proceeds upon mixing with the appropriate base during quenching. Trials were conducted using TEA, *N*,*N*-diisopropylethylamine (Hünigs base), 2,6-lutadine and pyridine in DCM quenching mixtures with poor results and no further improvements could be found for this process. Typical ether cleavage reactions were performed using 75 mg (0.41 mmol) of **4b** in 100 ml of dry DCM and limitations to the BBr_3-mediated process were experienced upon a two-fold increase the concentration of **4b**, resulting in decomposed reaction mixtures. The ether cleavage performed more satisfactorily when BBr_3 was used as the limiting reagent (0.30 mmol, 0.73 mol equivalents) and the yield of conversion to **3** based on BBr_3 was calculated at a desirable 84%, assuming the reaction with **4b** proceeds in a stoichiometric fashion. Larger scales (300 mg **4b**/400 ml DCM) did not perform as well and a 20 to 25% decrease in yield was observed but without decomposition. Disappointingly, reactions involving quantities of **4** larger than 500 mg were ineffective and trials using increased temperature or BBr_3 could not be optimised to provide **3** in >5% yield.

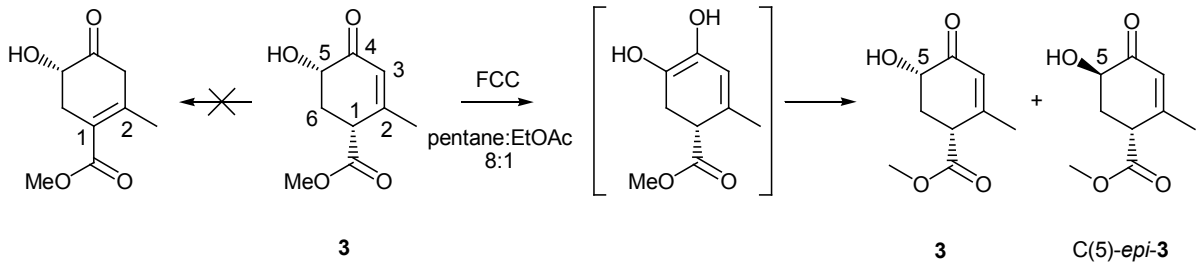

Scheme 4.19: The purification of **3** by FCC methods led to C(5) racemization likely *via* the conjugated enol tautmer to provide a mixture of **3** and C(5)-*epi*-**3**.

Attempts to purify the ring opened product **3** by FCC on SiO_2, alumina (neutral) and fluorocil using pentane:EtOAc in various ratios (1:1-8:1) all led to the isolation of a mixture of **3** and the α-ketol epimer C(5)-*epi*-**3** (Figure 4.6, left) presumably due to keto-enol tautomerisation during retention on the stationary phase (Scheme 4.19). The α,β-unsaturated ester containing the 1,2-olefin was not observed in

GC-MS or NMR analyses of the crude ring cleavage mixtures or FCC purified products establishing that the 2,3-olefin is stable in conjugation with the ketone. GC-MS analysis of column fractions obtained from FCC purification on SiO_2 indicated mixtures of **3** and C(5)-*epi*-**3** ranging from 9:1 to 1:2 with later eluting fractions containing higher amounts of C(5)-*epi*-**3** which displays slightly greater retention on the stationary phase. Attempts to prevent tautomerization involved deactivation of the SiO_2 by stirring with TEA/pentane, but gave little improvement in TLC and FCC separation. Disappointingly, column chromatography on cellulose acetate using EtOH/water mixtures [36] also resulted in slow C(5) epimerization but to a lesser extent than the previously mentioned stationary phases.

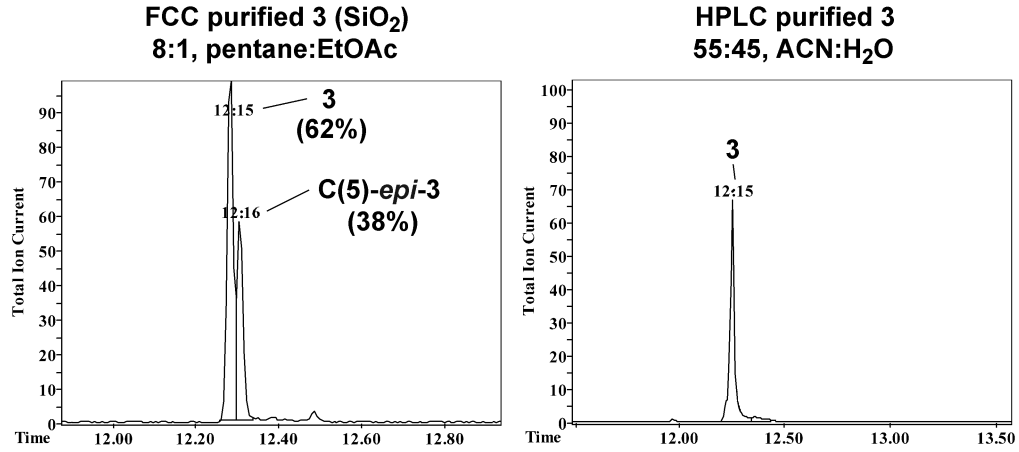

Figure 4.6: GC traces for the purification of crude BBr_3/collidine ether cleavage mixtures. Left; Isolation by FCC on silica gel shows a mixture of the ether cleavage product **3** and the C(5) diastereoisomer C(5)-*epi*-**3** as a result of on-column keto-enol tautomerisation of the carbonyl. Right; Purification of **3** by semi-preparative HPLC separation shows the isolated product in >99% purity without epimerization.

The successful isolation of **3** was eventually achieved by semi-preparative HPLC on a Phenomenex C-18 stationary phase. On the C-18 column, retention times for **3** exceeding 12 minutes led to gradual epimerisation at the C(5) hydroxyl stereocenter as indicated by GC-MS analysis of the purified fractions. Optimal resolution was achieved using 55:45 MeCN:H_2O ratio as the mobile phase to provide separation of **3** in 5:04 min using a maximum loading of 33 mg of crude material per injection. HPLC results for optimised separation conditions are presented in Section 4.4. Extraction from the LC solvent revealed **3** as a colourless oil and analysis by GC-MS (Figure 4.6, right) indicated a single compound with no detectable epimerisation at C(5). The structures of both epimers of **3** were characterised by ^{13}C and ^{1}H NMR and the relative stereochemistry of substituents were verified by COSY and NOESY 2D analysis as presented in Section 4.2.

The chemo- and stereo-selective preparation of the C(5) hydroxy substituted cyclohex-2-enone **3** is not reported in the literature and few synthetic methodologies towards this type of functionalised skeleton exist. The lack of known syntheses of enantiomerically enriched α'-acetoxy- and α'-hydroxy-α,β-unsaturated cyclic ketones has been addressed in studies by Tanyeli *et al.* [37] (Scheme 4.20) who accessed the racemic (*R*/*S*)-2-oxocyclohex-3-enyl acetate (72%) by means of the manganese(III) acetate ($Mn(OAc)_3$) oxidation of cyclohex-2-enone in benzene using a Dean–Stark trap. Chiral resolution of the racemic α'-acetoxylated product was reported by the same group [38] utilizing chemo-enzymatic hydrolysis with Pig Liver Esterase in a pH = 7.00 phosphate buffer to selectively hydrolyse the (*R*)-isoform to the alcohol (*R*)-6-hydroxycyclohex-2-enone.

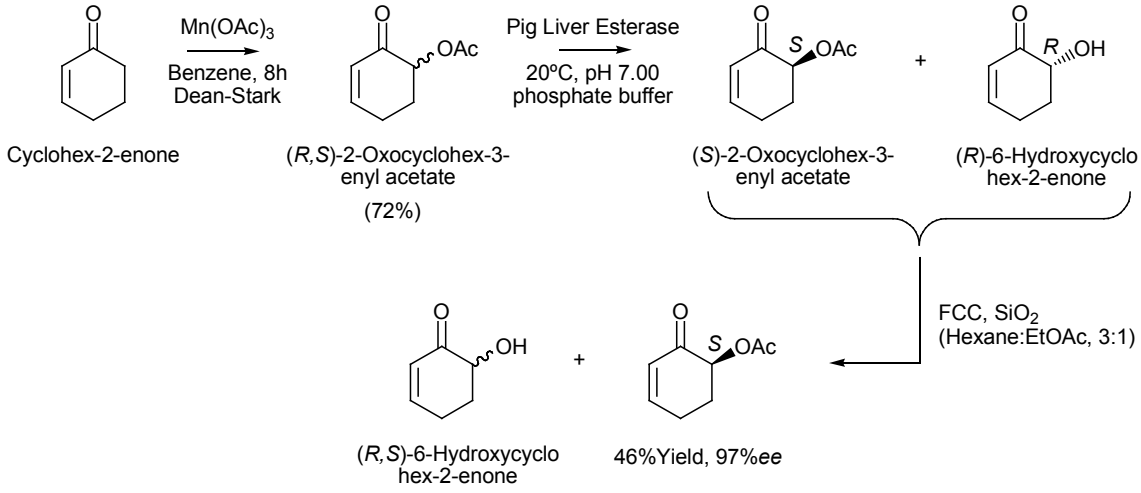

Scheme 4.20: Tanyeli *et al.* have reported the preparation of racemic (*R*,*S*)-2-oxocyclohex-3-enyl acetate *via* the $Mn(OAc)_3$ oxidation of cyclohex-2-enone [37]. Chemo-enzymatic resolution of (*S*)-2-oxocyclohex-3-enyl acetate was achieved using Pig Liver Esterase [38] and the α'-acetoxylated compound was purified by FCC, also providing the racemic alcohol (*R*,*S*)-6-hydroxycyclohex-2-enone.

The authors report successful purification by FCC on SiO_2 (Hexane:EtOAc, 3:1) to isolate the (*S*)-2-oxocyclohex-3-enyl acetate enantiomer in 46% and 97% *ee* (Scheme 4.20), but also mention that 6-hydroxycyclohex-2-enone was not isolated in an enantiomerically enriched form and attribute this to the fast racemization and/or rearrangement of α'-hydroxylated cyclic enones [38]. This is a similar finding to the results presented in Section 4.1.2 and suggests that FCC is inappropriate for the separation of α'-hydroxylated cyclic enones, but might be effective for the purification of the α'-acetoxy derivatives.

4.2 NMR Characterisation of Methyl-5-hydroxy-2-methyl-4-oxocyclohex-2-enecarboxylate (3 and C(5)-*epi*-3)

The α,β-unsaturated ketol **3** is a new compound and an important intermediate in the natural product synthesis of **1**, so NMR characterization data was carefully examined to confirm the structure and relative stereochemistry in both C(5) isomers of **3**. ^{1}H COSY NMR (Figure 4.7) of the HPLC purified alcohol **3** indicated a single compound confirming that no detectable epimerisation at C(5) had occurred in agreement with GC-MS data.

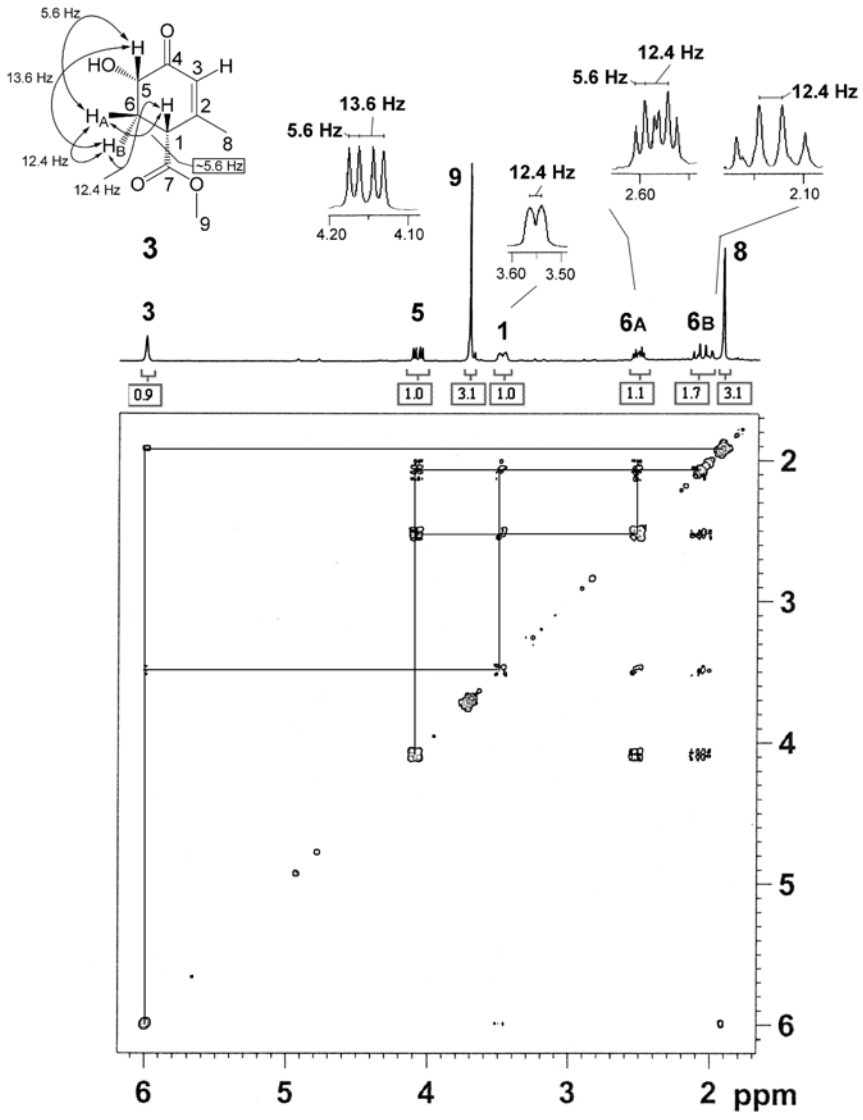

Figure 4.7: 300 MHz ^{1}H COSY NMR of **3** with structural correlations and coupling constants shown.

The structure of **3** was confirmed by ^{1}H COSY NMR cross-peaks (Figure 4.7) which show correlation between the H(6) methylene protons and the H(1) α-ester proton at δ 3.55, corroborating with the C-O cleavage of the ether bridge, rather than C-C bond breakage as observed in basic reaction media. The downfield α'-carbonyl proton H(5) appears as a double doublet at δ 4.15 and shows ^{1}H COSY NMR correlations to the diastereotopic methylene protons H(6_A) ($J_{5,6A}$ = 5.6 Hz) at δ 2.59 and H(6_B) ($J_{5,6B}$ = 13.6 Hz) at δ 2.14, confirming that the six-membered ring is intact in agreement with the structure of **3**. The H(6_A) proton shows geminal coupling ($J_{6A,6B}$ = 12.4 Hz) and appears as a doublet of triplets at higher frequency than H(6_B), suggesting an equatorial position for H(6_A) on the carbocyclic ring. The H(6_B) signal shows COSY cross-peaks with the geminal proton ($J_{6A,6B}$ = 12.4 Hz), H(1) ($J_{1,6B}$ = 12.4 Hz) at δ 3.55 and H(5) ($J_{5,6B}$ = 13.6 Hz) appearing as a broad apparent quartet (J = 12.4 Hz) in ^{1}H NMR data. The olefinic H(3) signal at δ 6.05 integrates as one proton and confirms that the position of the endocyclic α,β-unsaturated bond is in conjugation with the ketone. Weak ^{1}H COSY NMR correlations are observed between H(3) and the vinylic protons of the methyl group H(8) at δ 1.98 and also H(1) at δ 3.55. Although vinylic coupling between H(3) and the methyl signals H(8) is not resolved in the 300 MHz ^{1}H NMR spectrum, vinylic coupling between H(3) and H(1) is apparent and results in a poorly resolved signal for the expected H(1) doublet of double doublets, also split by H(6_A) and H(6_B).

^{13}C NMR signals were assigned using HMQC data (Figure 4.8) and support the structure **3**. The diastereotopic H(6_A) and H(6_B) methylene signals show correlation to the same carbon signal C(6) at δ 34.2, and the olefinic signal H(3) correlates to a positively oriented DEPT 135 signal at δ 127.7 (C(3)) in the ^{13}C NMR olefinic region. The ketone C(4) and ester C(7) carbonyl signals are observed at δ 199.1 and 171.4 respectively, also the C(2) quaternary olefin signal is assigned to the weak ^{13}C NMR resonance at δ 158.7 in close agreement with Chemdraw predictions. The connectivity of **3** was verified by HMBC analysis (Appendix 4.5) and the chemical formula of **3** was confirmed by ESI-HRMS to provide an accurate mass for the $[M + Na]^{+\cdot}$ ion $C_9H_{12}O_4Na$ in agreement to three decimal places of the theoretical value (207.0633 calc., *m/z* 207.0627 found).

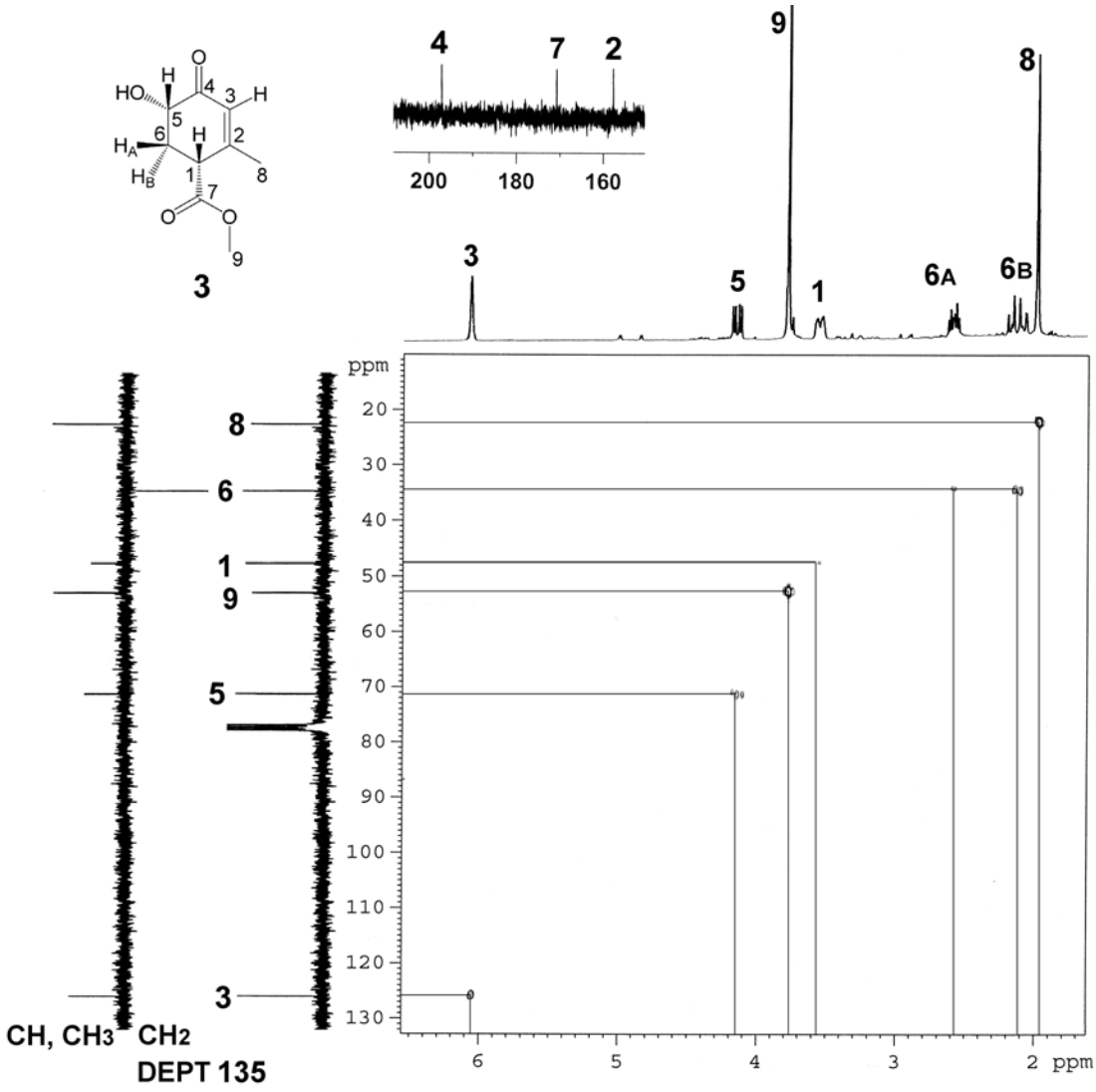

Figure 4.8: 300 MHz ^{1}H/ 75 MHz ^{13}C HMQC NMR of **3** with structural assignments and DEPT 135 NMR data.

Although the α,β-unsaturated backbone of **3** is a rigid system of sp^2 hybridised orbitals, the saturated portion of the ring incorporating C(6), C(5) and C(1) can adopt pseudo-boat and pseudo-chair conformations. Semi-empirical MO calculations with Chem3D using an MM2 Hamiltonian were carried out for the pseudo-chair and pseudo-boat conformers of **3** and the estimated heats of formations reveal only a small difference in ΔH values (Figure 4.9, left) suggesting that facile inversion between the two conformers might be possible, however NMR data shows signals for only one conformer at 20ºC. The large coupling constants (~12 - 13 Hz) observed between H(5)/H(6_B) and H(1)/H(6_B) indicate that these vicinal protons have a *trans* diaxial relationship (180° dihedral angle) to H(6_A), in agreement with the pseudo-chair conformation for the cyclohexenone ring of **3**. The energy minimised model for the pseudo-boat conformer of **3** (Figure 4.9, left) shows a gauche geometry between H(1), H(6) and H(5) protons on

the saturated section of the ring, with characteristically smaller dihedral angles by comparison with the pseudo-chair conformer.

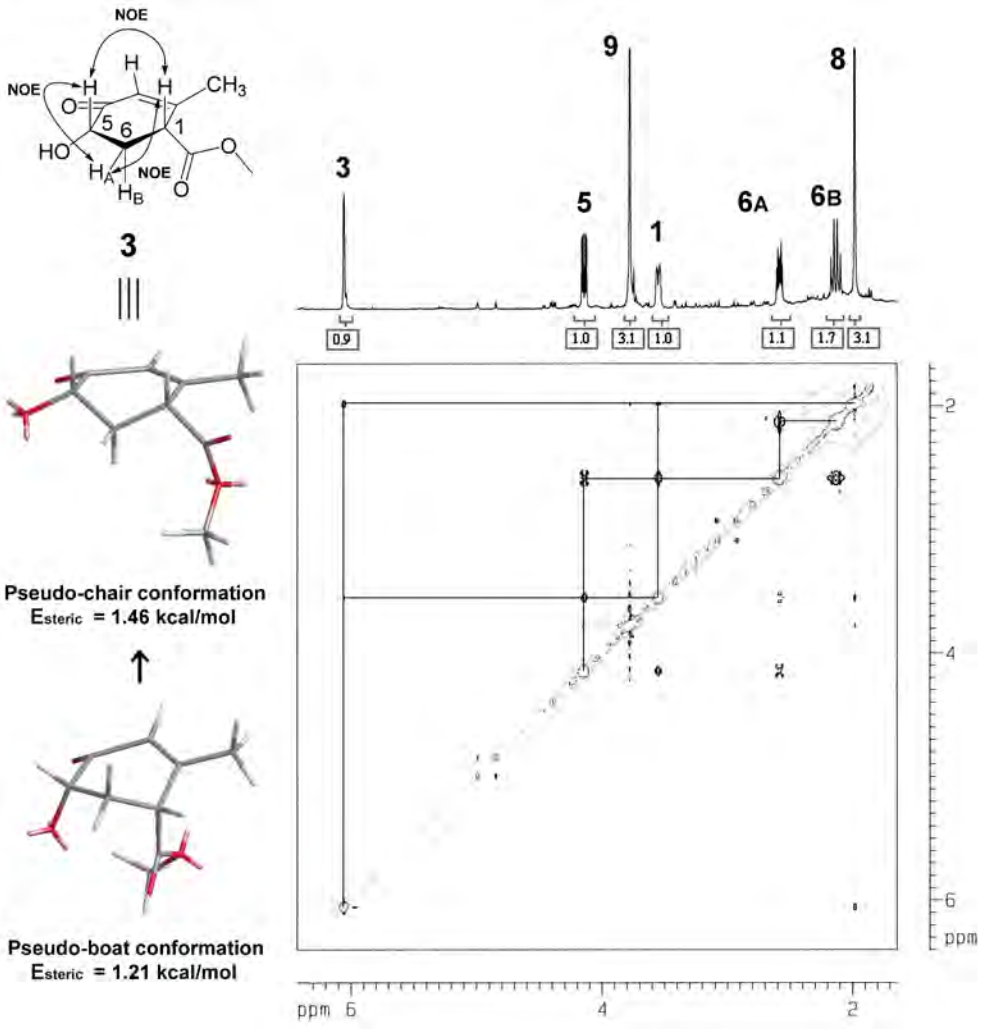

Figure 4.9: Left; Energy minimised models of the pseudo-chair and pseudo-boat conformers for 3 calculated using Chem3D (MM2). Right; 500 MHz ^{1}H-^{1}H NOESY NMR analysis of **3** with cross-peaks shown.

500 MHz ^{1}H-^{1}H NOESY NMR analysis of **3** shows NOE correlation between H(1)/H(5) (Figure 4.9, Right) indicating that both protons are most likely positioned on the same face of the cyclohexenone ring. Strong NOE correlations are also observed between H(5)/H(6_A) and H(1)/H(6_A), but NOE correlations between H(6_B) with both H(1) and H(5) are very weak. This observation supports ^{1}H-^{1}H coupling data and conclusively establishes the pseudo-chair conformation for **3** whereby H(6_B) has a *trans* diaxial relationship with the adjacent methine protons.

The pseudo-boat conformation is calculated to be slightly more sterically favoured and this is contrary to the structure deduced from NMR data. Discrepancy in the calculated model are overcome upon considering that in the pseudo-chair conformation, the periplanar relationship between the carbonyl oxygen and hydroxy substituent may allow for additional energies of stabilization such as weak hydrogen bonding interaction and π-orbital overlap. A more advanced modelling approach is required to refine the structural parameters responsible for the observed conformer and was left as a topic for future studies.

The C(5) hydroxyl epimer (C(5)-*epi*-**3**) also required characterization before the structure of **3** could be assigned unambiguously. A number of samples containing mixtures of both **3** and C(5)-*epi*-**3** were isolated during attempts at purification by FCC on SiO_2 and GC-MS data for a typical FCC purified mixture is shown in Figure 4.6, although epimeric ratio was varied depending on the time spent on the stationary phase. ^{1}H NMR signals due to C(5)-*epi*-**3** were identified using COSY NMR analysis, conducted on a 2:1 mixture with the epimer **3** and is included in Appendix 4.6 along with ^{13}C NMR data. 500 MHz NOESY analysis was performed on a 1:1 mixture of **3** and C(5)-*epi*-**3** (Figure 4.10) to enable a direct comparison in NOE strength for each epimer and ^{1}H NMR structure assignments for C(5)-*epi*-**3** are indicated by numbering with the *epi*- prefix. The notable absence of NOE between *epi*-H(1)/*epi*-H(5) conclusively verifies the *cis* relative stereochemistry between H(1)/H(5) in **3** and confirms that the BBr_3-mediated ether cleavage proceeds with retention of stereochemistry at the C(5) hydroxyl group.

Assignments for *epi*-H(6_A)/*epi*-H(6_B) methylene signals were established using NOESY data and ^{1}H NMR coupling constants. ^{1}H NMR data shows the *epi*-H(5) signal as a doublet of doublets at δ 4.39 (dd, $J_{epi\text{-}5,epi\text{-}6A}$ = 13.3 Hz, $J_{epi\text{-}5,epi\text{-}6B}$ = 5.5 Hz) with almost identical coupling constants to the downfield H(5) signal for **3** at δ 4.15, suggesting coupling to a *trans* diaxial oriented vicinal proton assigned as *epi*-H(6_A). In corroboration with ^{1}H NMR coupling data, the *epi*-H(5) signal shows no NOE correlation with the vicinal axial proton *epi*-H(6_A) which appears as a doublet of triplets (dt, $J_{epi\text{-}5,epi\text{-}6A}$ = 13.3 Hz, $J_{epi\text{-}6B,epi\text{-}6A}$ = 13.3 Hz, $J_{epi\text{-}1,epi\text{-}6A}$ = 6.0 Hz) at δ 2.12 overlapped with signals from H(6_A). NOE is observed between *epi*-H(5) and the adjacent equatorial proton *epi*-H(6_B) at δ 2.69, which appears as a doublet of doublet of doublets ($J_{epi\text{-}6A,epi\text{-}6B}$ = 13.3 Hz, $J_{epi\text{-}5,epi\text{-}6B}$ = 5.5 Hz, $J_{epi\text{-}1,epi\text{-}6B}$ = 1.8 Hz). The *epi*-H(1) signal appears as a broad doublet (J = ~6.0 Hz) at δ 3.41 and is upfield from the equivalent H(1) signal due to **3**, but in both cases this signal is poorly resolved due to additional vinylic coupling. Both *epi*-H(6_A) and *epi*-H(6_B) show NOE with *epi*-H(1), indicating a gauche relationship between H(1) and H(6) methylene protons.

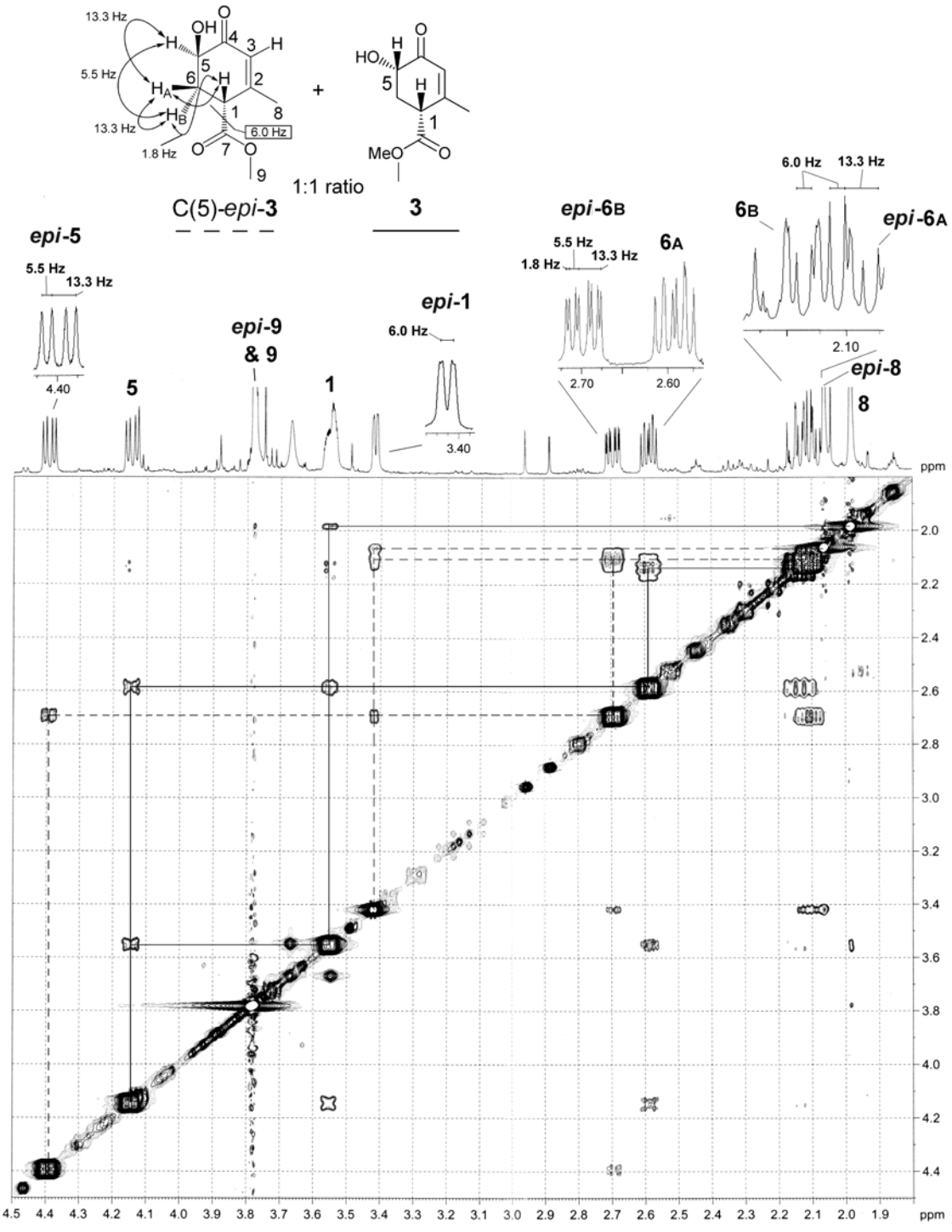

Figure 4.10: 500 MHz ^{1}H-^{1}H NOESY NMR analysis of a 1:1 mixture of **3** and C(5)-*epi*-**3** with ^{1}H NMR assignments for the C(5)-*epi*-**3**. The absence of NOE between *epi*-H(5)/*epi*-H(1) in C(5)-*epi*-3 unambiguously confirms the relative stereochemistry of H(1)/H(5) for **3**.

The observed ^{1}H-^{1}H NMR coupling constants and NOE correlations suggest that C(5)-*epi*-**3** exists in the pseudo-boat conformation. Comparison of the heats of formation estimated from the MM2 energy minimised Chem3D models for the pseudo-chair and pseudo-boat conformers are shown in Figure 4.11 and indicate the latter conformer to be favoured, in agreement with the structure deduced by NMR observations.

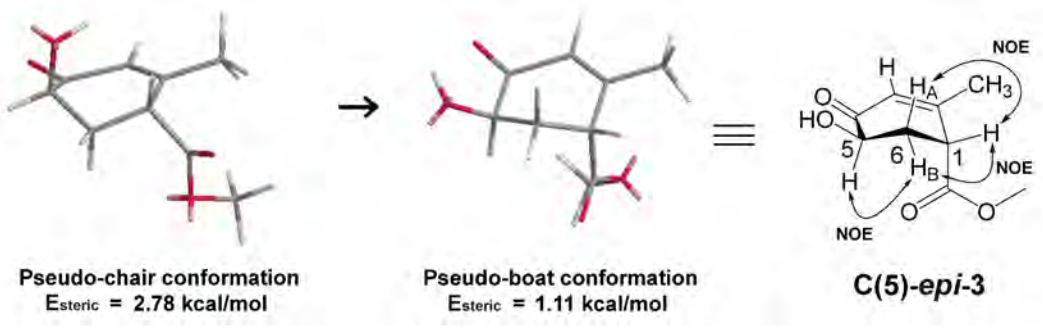

Figure 4.11: Energy minimised models of the pseudo-chair and pseudo-boat conformers for C(5)-*epi*-**3** calculated using Chem3D (MM2) are shown and comparison of estimated heat of formation suggests C(5)-*epi*-**3** to exist as the pseudo-boat conformer in support of NOESY NMR data.

The geometry of protons in the pseudo-chair conformer (Figure 4.11) would be expected to show similar coupling values to those observed in **3**. This considered, NMR characterization clearly identifies C(5)-*epi*-**3** to exist as the pseudo-boat conformer and is easily identified in a mixture with **3**. The confirmation of relative stereochemistry in the C(5)-epimer conclusively proves that the stereochemistry of **3** is retained throughout the oxabicyclo[2.2.1]heptane cleavage of **4b** to provide the H(1)/H(5) *cis* relative stereochemistry as desired in the natural product **1**.

4.2.1 BBr_3 Cleavage of 4a and Mechanistic Considerations

The optimised conditions for the BBr_3/collidine ether cleavage were applied to the ether cleavage of the *endo* isomer **4a** (Scheme 4.21) in order to gain insight into the utility of this system as a general protocol for the ether cleavage of **4**. Reaction of **4a** with BBr_3 in DCM at –1ºC for 10 min followed by quenching in 1 M collidine at 30ºC provided ether cleavage without decomposition as indicated by GC-MS analysis (Figure 4.12), to yield the desired α'-hydroxy enone as a mixture of C(5) epimers.

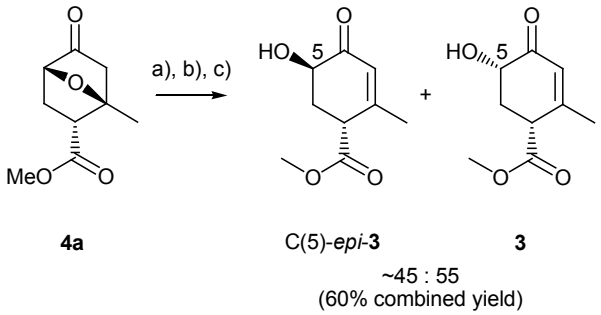

a) BBr_3, DCM, -1ºC, 10 min b) 1 M Collidine in DCM 25-30ºC c) 1 M HCl.

Scheme 4.21: The ether cleavage of **4a** using BBr_3 formed a mixture of **3** and C(5)-*epi*-**3** in 55:45 ratio, indicating racemization during the ring opening process to yield a small excess of **3** as the C(5) stereochemically inverted product.

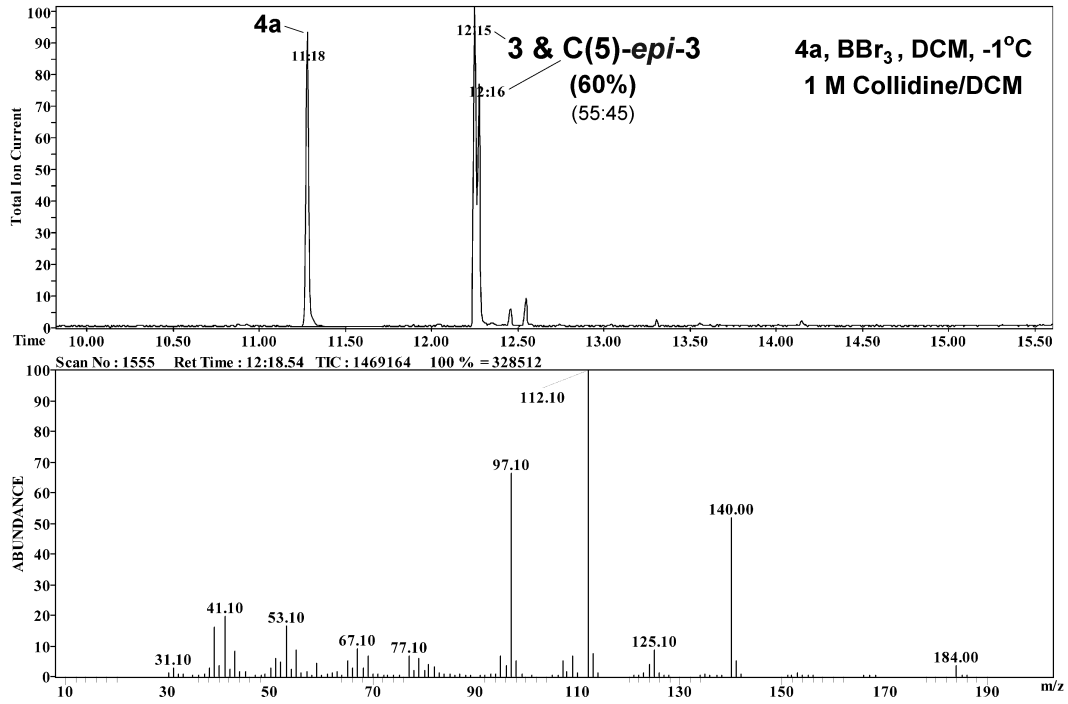

Figure 4.12: GC-MS analysis of the BBr_3 cleavage of **4a** conducted under optimised conditions shows a 55:45 mixture of **3**:C(5)-*epi*-**3** and the products were verified by comparison of GC retention times and MS fragmentation.

This observation reveals that the BBr_3/collidine ether cleavage system can be applied to the ring opening of **4a**, although stereochemistry at C(5) is not retained and the epimer **3** predominates, presumably as the result of a stabilised intermediate in the ring opening mechanism. The α,β-unsaturated cyclic enone is able to tautomerise to the conjugated diene and the resulting 1,2-dioxy system might be encouraged by Lewis-acid attraction of the C(5) boron enolate to the lone pair electrons of the C(4) enol

oxygen (Scheme 4.22). Equilibration to the C(4) boron enolate is also possible although more detailed characterization of these intermediates was not feasible. The tendency of **4b** towards yielding **3** as a single ether cleavage product, as compared to **4a** which unavoidably forms a mixture of C(5) isomers but enriched in the inverted epimer **3**, is strong evidence for anchimeric influence from the carboxylic ester. The Lewis-acid properties of the borane ether intermediate may allow for interaction with the ester carbonyl *via* a seven-membered dioxy type complex as shown in Scheme 4.22, leading to an excess of **3** upon workup with aqueous acid.

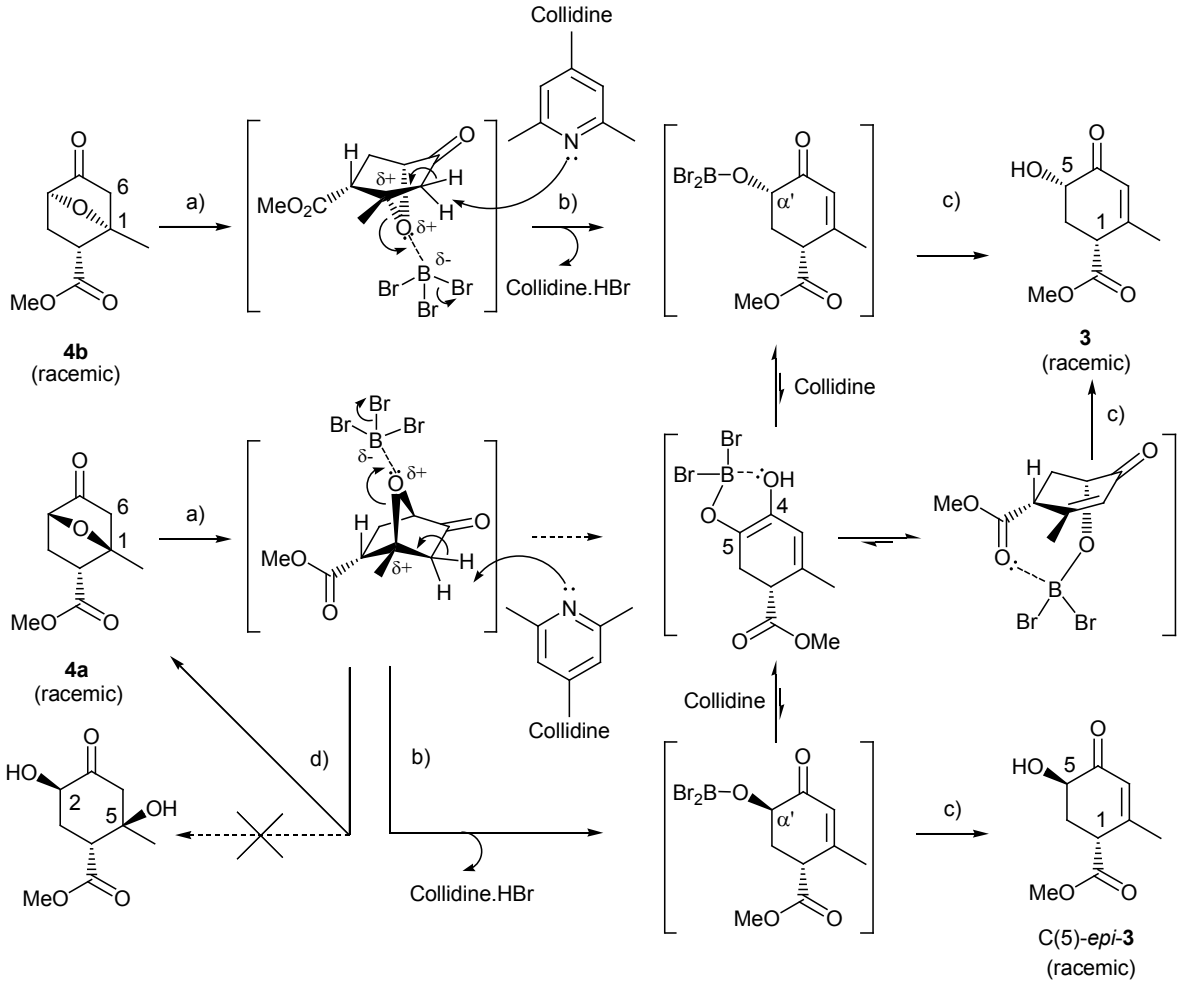

a) BBr_3 in DCM, –1°C, 10 min b) 1 M Collidine in DCM 25-30ºC c) 1 M HCl d) sat. $NaHCO_3$, r.t.

Scheme 4.22: The proposed mechanism for the BBr_3/collidine ether cleavage of **4a** and **4b** is based on ratios of **3**:C(5)-*epi*-**3** obtained from reaction at –1ºC, and involves co-ordination of BBr_3 with the ether oxygen as described by Gopalaswamy *et al.* [31] followed by abstraction of H(6) during quenching in collidine. The observed C(5) epimerization during the cleavage of **4a** can be rationalised as the result of enolization and intramolecular interaction with the ester carbonyl leading to equilibration to give **3** in a small excess upon work-up. The 2,5-diol was not formed upon quenching in aqueous media, indicating that a carbocation intermediate is unlikely.

During reaction of **4a** or **4b** at –1ºC, co-ordination of BBr_3 with the oxygen bridge might be primarily responsible for facilitating the ether cleavage due to weakening of the C(1)-O bond as suggested by Gopalaswamy *et al.* [31], allowing deconjugation by abstraction of an α-carbonyl proton followed by rearrangement. As such, the mechanism proposed in Scheme 4.20 for the formation of **3** proceeds *via* complexation of the ether oxygen without tertiary carbocation formation. This conclusion was supported by experiments involving quenching of the BBr_3 coordination complex of **4a** and **4b** in saturated $NaHCO_3$ solution, that were shown by GC-MS to return the starting ethers **4,** rather than the C(2)-hydroxy compound as reported in research by Mosimann *et al.* [32] (Scheme 4.12) and Jotterand *et al.* [33] (Scheme 4.14). Treatment of the co-ordinated intermediate prepared at –1ºC with the hindered base collidine facilitates removal of the α-keto proton to produce the α,β-unsaturated borane ether which is hydrolysed in 1M HCl (Scheme 4.22). Chirality at the C(5) hydroxy stereocenter is removed upon tautomerisation of the carbonyl to the diene sp^2 system, which is encouraged by boron complexation of the enolate oxygen. The *cis* H(1)/H(5) relative stereochemistry may equilibrate as the stabilised keto-form the due to intramolecular Lewis-acid attraction between the α'-bromoborane ether intermediate and the ester carbonyl oxygen. This proposed pathway is supported by the experimental outcomes described in Section 4.1.4 and provides a plausible explanation for the observed predominance of **3** in the BBr_3 ether cleavage reaction of **4a** and **4b**.

4.3 Preparation and Characterisation of (1R,5S)/(1S,5R)-Methyl 5-acetoxy-2-methyl-4-oxocyclohex-2-enecarboxylate (2)

Acetylation of the alcohol **3** was achieved using a large excess of acetyl chloride (AcCl) in the presence of a tertiary amine base to produce **2** (t_R = 13:39 min) as confirmed by a *m/z* 226 molecular ion in GC-MS analysis (Figure 4.13) and a *m/z* 97 fragment consistent with the methyl cyclohexanone backbone. Acetylation of a purified sample of **3** was successful in the presence of TEA and pyridine bases to give excellent conversion to **2** (*ca.* 95%) with a small amount of decomposition but unfortunately these mixtures also demanded the HPLC purification of **2**. An optimised one-pot methodology was realised upon carrying out the acetylation of **3** with a large excess of AcCl, added directly to the 1 M collidine/DCM quenching solution (Scheme 4.23) at 22ºC. This approach was convenient from a preparative perspective and complete consumption of **3** was achieved in 35 min to give a two component mixture of **4b** and **2** with minimal decomposition and no epimerization at C(5) as indicated by GC-MS analysis (Figure 4.13).

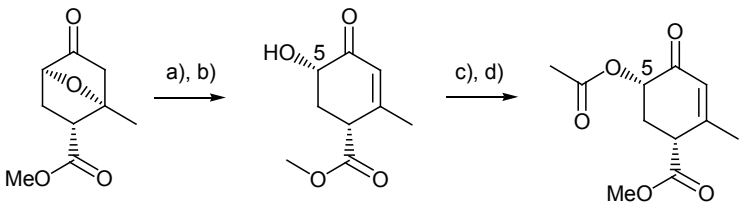

a) BBr_3, DCM, -1ºC, 10 min b) 1 M Collidine in DCM 25-30ºC, 35 min c) 2 ml AcCl, 22ºC, 35 min d) 1 M HCl.

Scheme 4.23: Acetoxylation of the C(5) hydroxyl group was most conveniently achieved by the addition of AcCl to **3** in the 1 M collidine/DCM quenching mixture and led to the complete consumption of **3** in 35 min as indicated by GC-MS monitoring. The separation of **2** was achieved by semi-preparative HPLC to give **2** in 40% isolated yield.

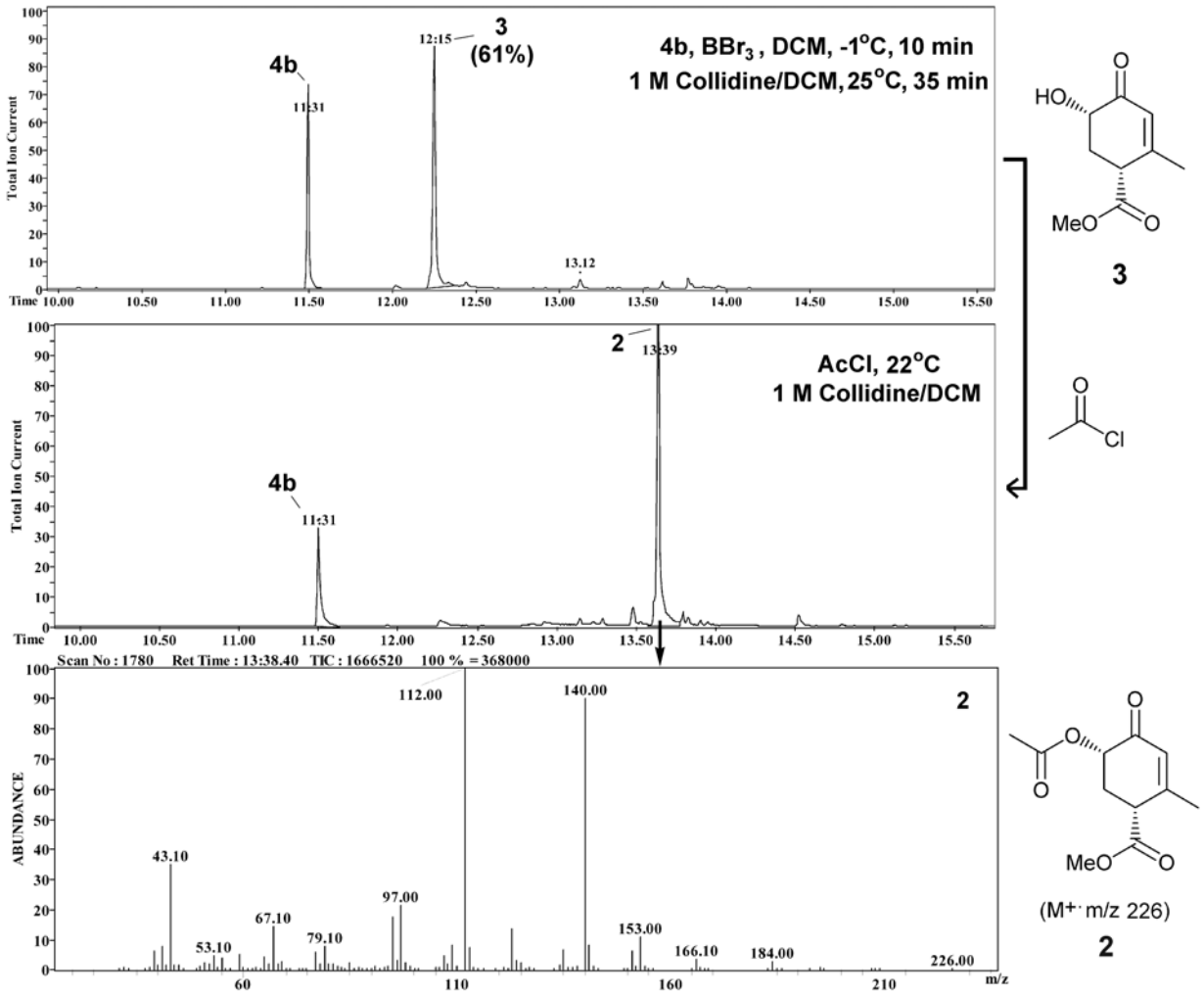

Figure 4.13: Top; Middle; GC-MS analysis of the crude acetylation mixture indicating the complete acetylation of the alcohol **3** in 35 min to produce a high yield of **2** with a small amount of by-product. Bottom; EI-MS of the acetylated product shows an $M^{+\cdot}$ ion at *m/z* 226 in agreement with **2**.

In a similar manner to the alcohol **3**, the C(5) acetoxy epimer of **2** was formed during FCC purification attempts, as indicated in the GC-MS analysis of chromatography fractions (Appendix 4.7). The isolation of **2** was achieved by semi-preparative HPLC separation using an MeCN:H_2O (55:45) mobile phase to provide baseline LC separation of **2** in a short retention time (t_R = 7.24) min (Section 4.4) and under favourable conditions to prevent epimerisation at the C(5) chiral center. HPLC separation of the crude acetylation mixture shown in Figure 4.13 (Middle) provided the acetoxy product **2** in 40% isolated yield.

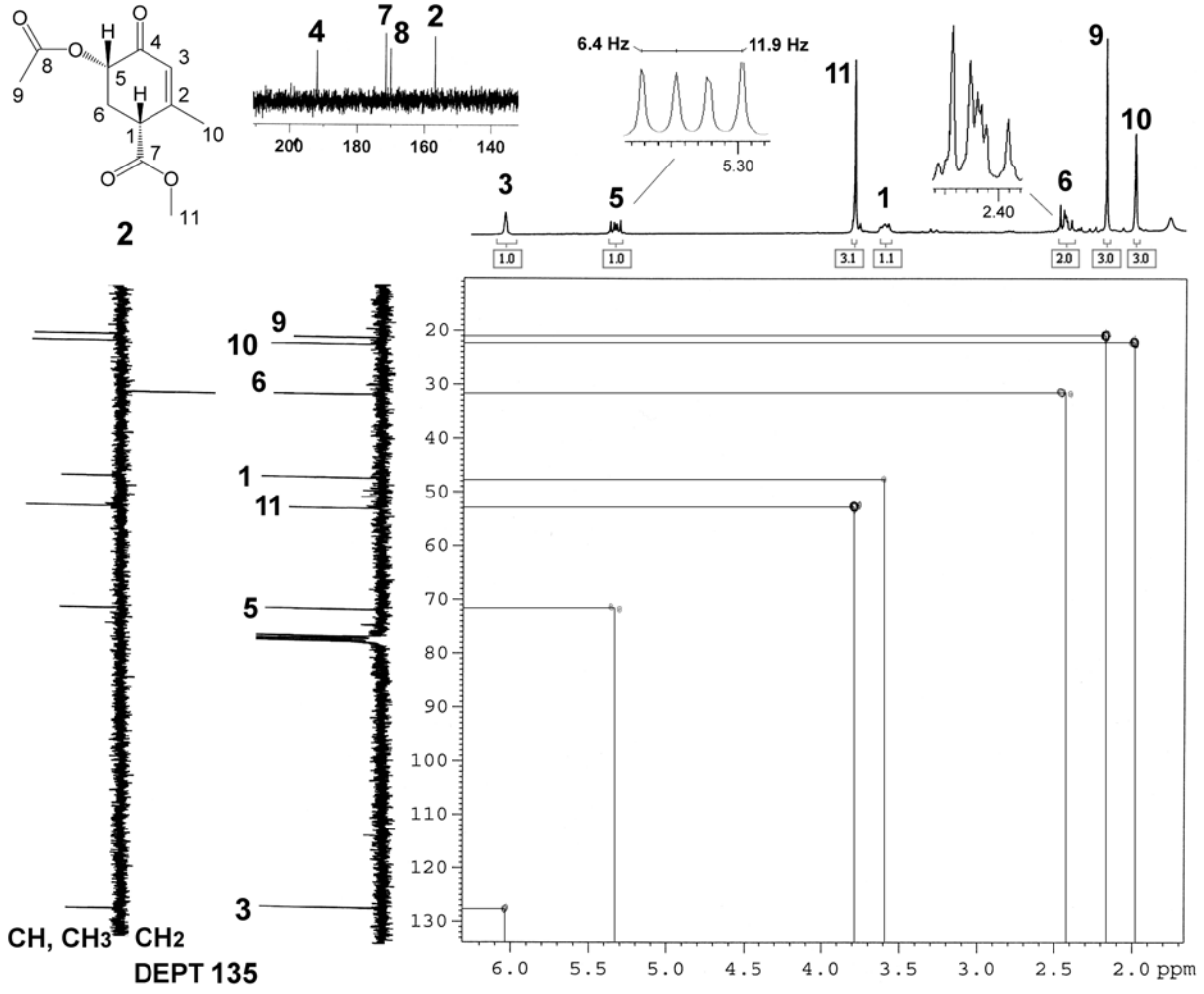

Figure 4.14: 300 MHz ^{1}H/75 MHz ^{13}C HMQC NMR and DEPT 135 NMR of **2** with structural assignments.

^{1}H COSY NMR analysis (Appendix 4.8) confirmed the isolated product to be a single compound and showed the expected correlations between the downfield H(5) doublet of doublets ($J_{5,\,6A}$ = 11.9 Hz, $J_{5,\,6B}$ = 6.4 Hz) at δ 5.32 and H(6) methylene protons at δ 2.44 which appear as an overlapped multiplet with an integral area of two protons as shown in Figure 4.14. Strong correlation exists between H(6) and

the broad, highly split H(1) signal at δ 3.58 and weak correlation between H(3) and the vinylic H(1) and H(10) methyl singlet at δ 1.98 is also observed and correlations are indicated in Appendix 4.8. The acetoxy H(9) methyl singlet is apparent at δ 2.17 with an integral area equal to three protons as anticipated in the acylated product **2**.

Structural assignments for ^{13}C NMR signals were confirmed by HMQC correlations (Figure 4.14) and are in close agreement with the predicted Chemdraw values. The presence of an acetoxy carbonyl signal C(8) at δ 170.3 and methyl signal C(9) at δ 21.0 are in agreement with the structure of **2**, and olefinic signals at δ 157.1 and 127.7 are assigned as C(2) and C(3) respectively in agreement with the α,β-unsaturated ketone. DEPT 135 NMR data (Figure 4.14) shows a negatively oriented C(6) methylene signal at δ 31.7 correlated to the H(6) multiplet at δ 2.44 consistent with the structure of **2**. Connectivity of the cyclohexenone ring was verified by HMBC data and is included in Appendix 4.9.

4.4 HPLC Separation Studies and Characterisation of Significant By-products

HPLC separation studies were conducted using a Phenomenex C-18 (250 mm × 10 mm) stationary phase with a maximum loading of 33 mg of crude product mixture per injection, followed by detection using UV-Vis spectroscopy, monitored at 254 nm (Section 6.10.3). HPLC studies on a range of different reaction mixtures indicated the possible interference from the brominated by-products **34**, that were found to increase in concentration upon prolonged stirring (>50 min) of **3** in the quenching mixture. This result strongly suggests that the C(2)-bromo products are produced due to the olefin addition reaction between **3** and HBr as discussed in Section 4.1.2, which is gradually released by BBr_3 upon contact with atmospheric moisture during the experimental protocol. The clean and expedient acetylation of **3** required a large excess of AcCl (>120 mol equiv.) and preliminary studies using lesser quantities of AcCl showed only partial conversion to **2** as indicated by GC-MS analysis (Figure 4.15), along with the formation **34** showing a minor and major brominated isomer at t_R = 13:06 min and t_R = 13:08 min with characteristic *m/z* 264, 266 molecular ions. The mixture shown was used to optimise the mobile phase for HPLC separation to avoid the co-elution of **34** with **3** or **2**. The EI-MS fragmentation of the later eluting C(2)-isomer of **34** (t_R = 13:08 min) is shown in Figure 4.15 and as expected is very similar to the earlier eluting C(2)-isomer at t_R = 13:06 min shown in Figure 4.5 (Section 4.1.2) which was prepared as the major isomer from the reaction of **4b** with BBr_3 at 5ºC.

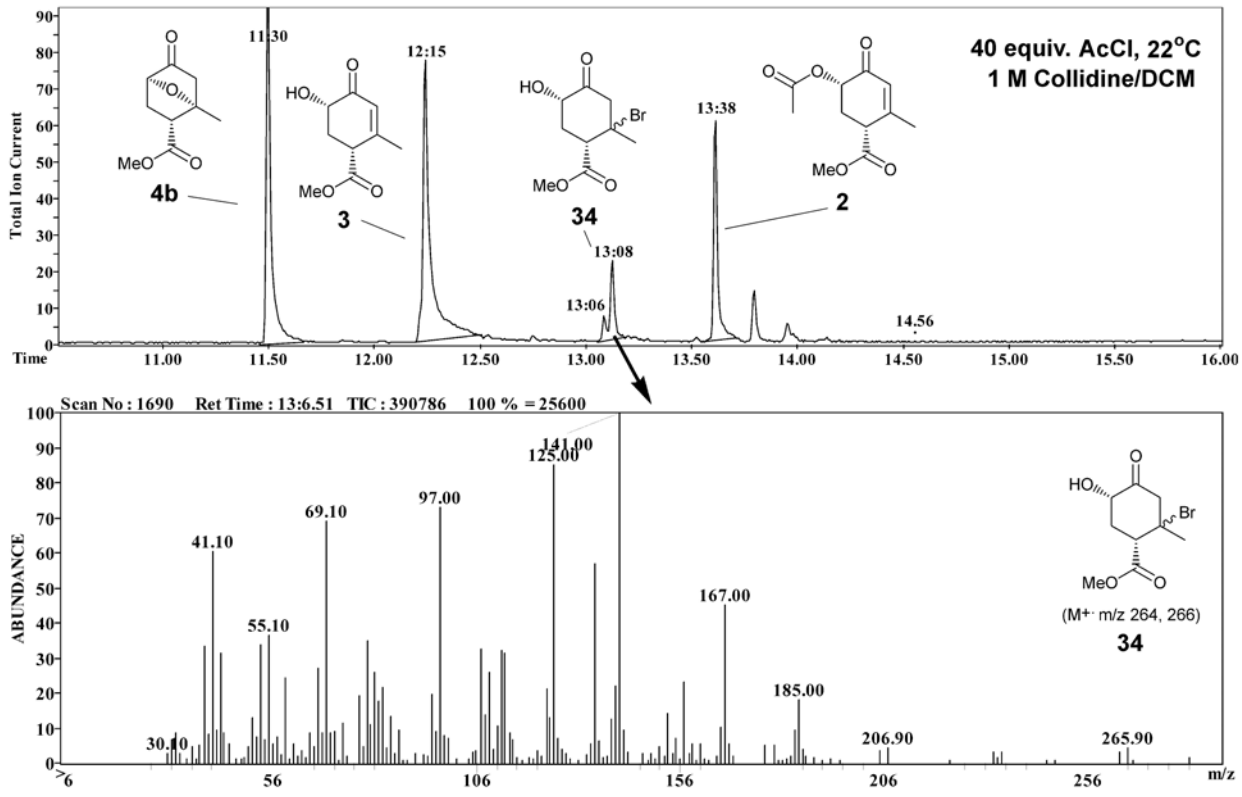

Figure 4.15: GC-MS spectrum for the partial acetylation of **3** prepared using 40 equivalents of AcCl to produce a mixture of **4b**, **3**, **2** and **34**. The mixture shown was used to optimise the mobile phase for HPLC separation to avoid the co-elution of **34** with **2** or **3**.

Optimization of the mobile phase for HPLC separation of the ring cleavage products revealed 55:45 MeCN:H_2O to provide baseline separation of **3** at t_R = 5:04 min and **2** at t_R = 7.24 min from **34** which appears at t_R = 6.24 min between the two α,β-unsaturated compounds (Figure 4.16, Left). The UV spectrum of **2** and **3** (Figure 4.16, Right) show a similar shape and identical UV absorbance maxima at λmax = 235 nm due to the strong absorbance of the α,β-unsaturated carbonyl chromaphore [39]. The 7-oxanorbornane **4b** does not have a strongly absorbing UV-Vis chromaphore and was not observed during monitoring at 254 nm, although NMR analysis of the HPLC fractions revealed that the components were isolated without interference from the co-elution of **4b**.

The UV spectrum of the brominated compound **34** shows a broadened range of absorption and a shifted absorption maximum at λ_{max} = 225 nm towards a shorter wavelength compared to **2**/**3** (235 nm) and the observed hypsochromic shift is due to the removal of the conjugated system. The HPLC purified fraction collected at t_R = 6.24 min gave **34** as a yellow resin in >3% yield and ^{1}H NMR characterization

revealed that the single LC peak labelled **34** in Figure 4.16 (Left) contained a mixture of co-eluting isomers in 1.0:0.3 ratio, consistent with GC-MS data (Figure 4.15).

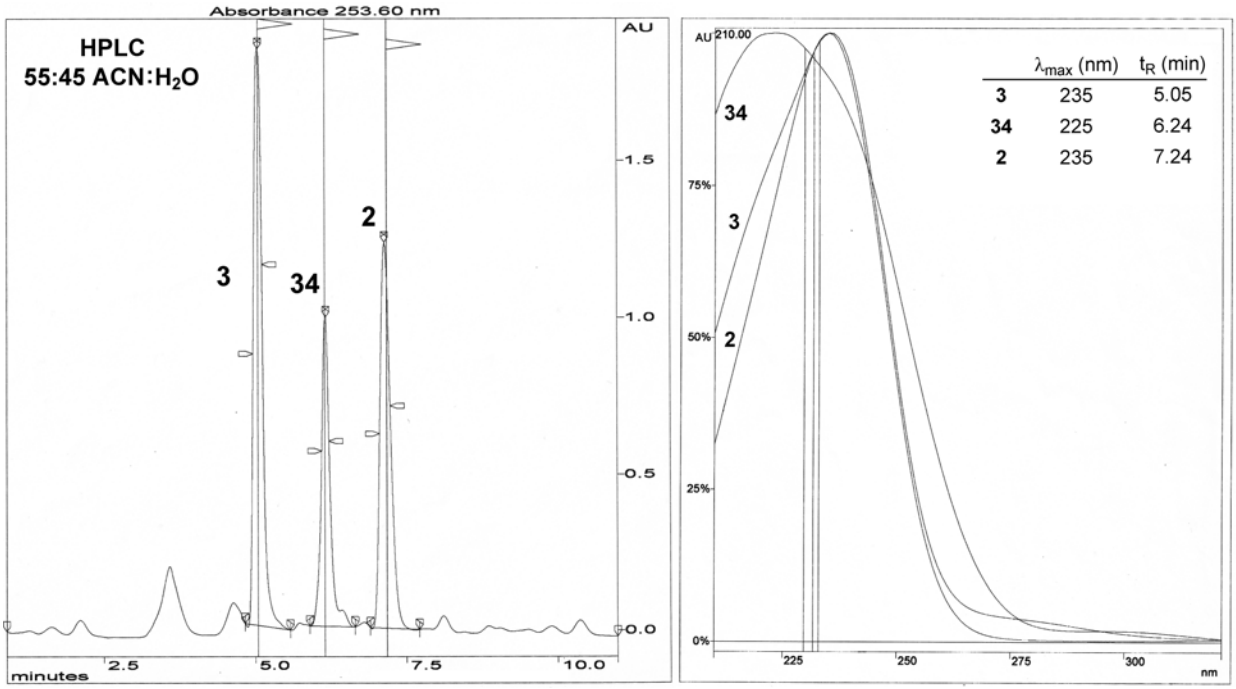

Figure 4.16: Left; The HPLC UV-Vis trace (254 nm) for the separation of the ether cleavage mixture shown in Figure 4.15, using the optimised mobile phase 55:45 MeCN:H_2O. Baseline separation of **3** at t_R = 5:04 and **2** at t_R = 7.24 min from **34** at t_R 6.24 min was achieved as shown. Right; UV-Vis spectrum (200 to 325 nm) for **3** and **2** are similar since both contain the α,β-unsaturated enone chromaphore and a common λ_{max} = 235 nm. The C(2)-bromo compound **34** shows a broad absorbance with λ_{max} = 225 nm.

^{1}H NMR signals for the major isomer of **34** were assigned using COSY correlations and ^{1}H-^{1}H NMR coupling constants (Figure 4.17). The H(3) methylene signal appears as an AB quartet ($J_{3A,3B}$ = 17.3 Hz) at δ 2.26 with an integral area equivalent to two protons, confirming the absence of the olefin. The equatorial H(6_A) signal at δ 2.52 appears as an overlapping doublet of doublet of doublets ($J_{6A,6B}$ = 13.4 Hz, $J_{6A,5}$ = 6.2 Hz, $J_{6A,1}$ = 5.3 Hz) and shows COSY correlation to the H(6_B) doublet of doublets ($J_{6B,6A}$ = 13.4 Hz, $J_{6A,1}$ = 8.7 Hz) at δ 1.95. Both H(6_A) and H(6_B) show correlation to the H(1) doublet of doublets ($J_{1,6B}$ = 6.2 Hz, $J_{1,6A}$ = 5.3 Hz) at δ 2.80, however the H(5) doublet ($J_{5,6A}$ = 6.2 Hz) at δ 4.47 only shows coupling to the H(6_A) signal indicating an approximate 90° dihedral angle between H(5) and the axial H(6_B) signal. ^{1}H COSY NMR correlations for the major isomer are consistent with the cyclohexanone ring present in **34** and vicinal coupling constants between 5 - 9 Hz observed for H(5)/H(6) and H(6)/H(1) suggests a gauche relationship for the ring protons.

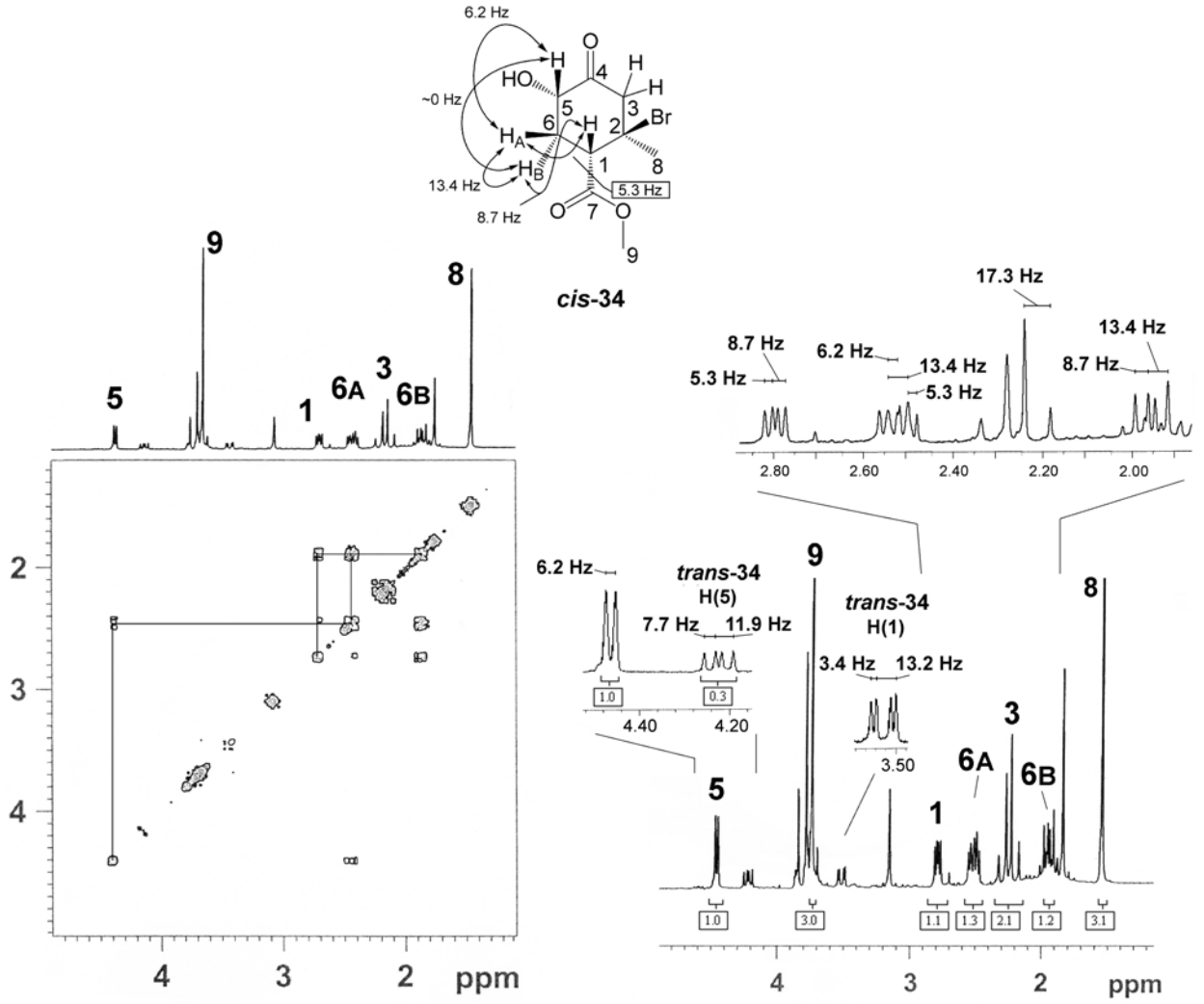

Figure 4.17: 300 MHz COSY analysis of the isolated HPLC peak at 6:24 min (Figure 4.16) shows a 1.0:0.3 mixture of *cis*-**34** and *trans*-**34** isomers and the structure of *cis*-**34** was confirmed using ^{1}H-^{1}H NMR coupling constants.

The Markovnikov addition of HBr to the olefin of **3** is expected to proceed more readily at the least sterically hindered face to produce **34** with C(1) methyl ester and C(2) methyl substituents in the *cis*- relative stereochemistry (*cis*-**34**). An MM2 energy minimised model of *cis*-**34** was constructed using Chem3D and the chair conformer shown in Figure 4.18 was calculated as the sterically favoured product, featuring H(1) and H(5) protons in the equatorial configuration with dihedral angles $\geq$90° with respect to the H(6) protons. This model is consistent with the observed vicinal coupling constants in the major isomer, confirming that signals assigned in Figure 4.17 are due to the *cis*-**34** C(2)-epimer which appears at t_R = 13:08 min in GC-MS analyses. The H(6_A)/H(6_B) protons of *cis*-**34** are partially overlapping with H(6) signals due to the minor component *trans*-**34**, as indicated by the respective integral areas. Resolved ^{1}H NMR signals due to *trans*-**34** shown in Figure 4.17 include the H(5) double-doublet ($J_{5,\,6B}$ = 11.9 Hz, $J_{5,\,6A}$ = 7.7 Hz) at δ 4.23 and H(1) double-doublet ($J_{1,6B}$ = 13.2 Hz, $J_{1,6A}$ = 3.4 Hz) at δ 3.52, both of

which feature large coupling constants indicative of an anti relationship with the vicinal axial H(6_B) proton. Ring cleavage procedures conducted at 1ºC gave a 1.0:0.7 ratio of *cis*:*trans* **34** and the structure of the *trans*-**34** C(2)-epimer was confirmed using ^{1}H COSY NMR correlations (Appendix 4.10). MM2 energy minimised models constructed using Chem3D show a low steric energy conformer for the H(1)/H(5) axial configuration (Figure 4.18), consistent with the observed NMR coupling data. ^{13}C NMR characterization for *cis*-**34** was achieved with the aid of DEPT 135 data (Appendix 4.11) and negative oriented signals for C(3) at δ 49.5 and C(6) at δ 29.5 were observed in agreement with the *cis*-**34** structure.

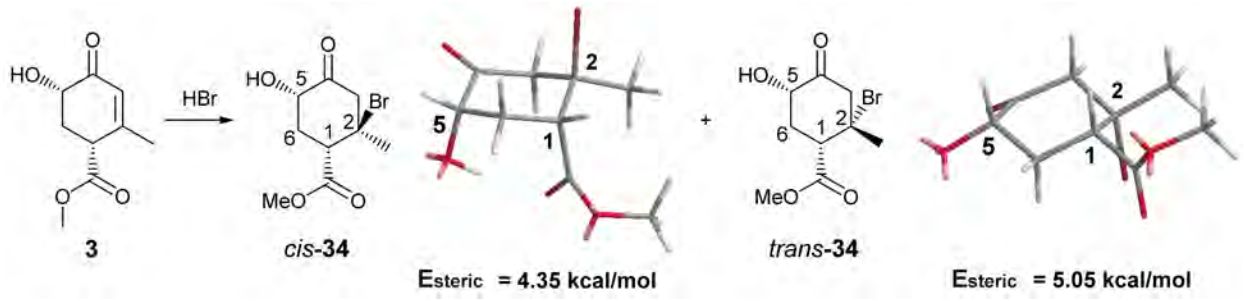

Figure 4.18: The addition of HBr to **3** forms a mixture of *cis*- and *tras*-**34**. Energy minimised models of the chair conformations for both isomers calculated using Chem3D (MM2) are shown with estimated heats of formation.

The *cis*-**34** isomer was not separated from the *trans*-**34** isomer using LC separation techniques and conditions conducive to the preparation of either C(2) brominated isomer exclusively would provide access highly functionalised molecules that might also be used as intermediates in the synthesis of **1** or related structures. Changes in the epimeric ratio of *cis*- and *trans*-**34** in BBr_3/collidine cleavage mixtures was found to be heavily depending on reaction temperature. The implication of reaction temperature on the ether cleavage mechanism was considered and is outlined in Section 4.4.1 along with possible directions for further study. The NMR characterisation of *cis*/*trans*-**34** are included in Section 6.8.

4.4.1 Mechanistic Rationale for the Formation of Brominated Isomers 34

When the BBr_3/collidine cleavage reactions were conducted at 0 to 1ºC, or allowed to stand for prolonged periods at ambient temperature after quenching, small amounts of the brominated isomers **34** were observed in GC-MS analyses (Figure 4.19; top right) and indicated the predominance of the *cis*-**34** product in these cases. The formation of **34** as a product of *in situ* HBr olefin addition was verified by the addition of 48% HBr to a solution of the isolated alcohol **3** in 1M DCM/collidine to give *cis*-**34** as the major isomer (Figure 4.19, top left) as a result of HBr addition across the less hindered olefin face in a Markovnikov fashion. GC-MS analysis of reaction mixtures after treatment with 48% HBr also shows a

by-product in 16% at t_R = 12.49 min, featuring a *m/z* 166 molecular ion and *m/z* 77 fragment ion (Figure 4.19, bottom right) in agreement with the aromatised product, formed due to dehydration of the α'-hydroxy enone **3**.

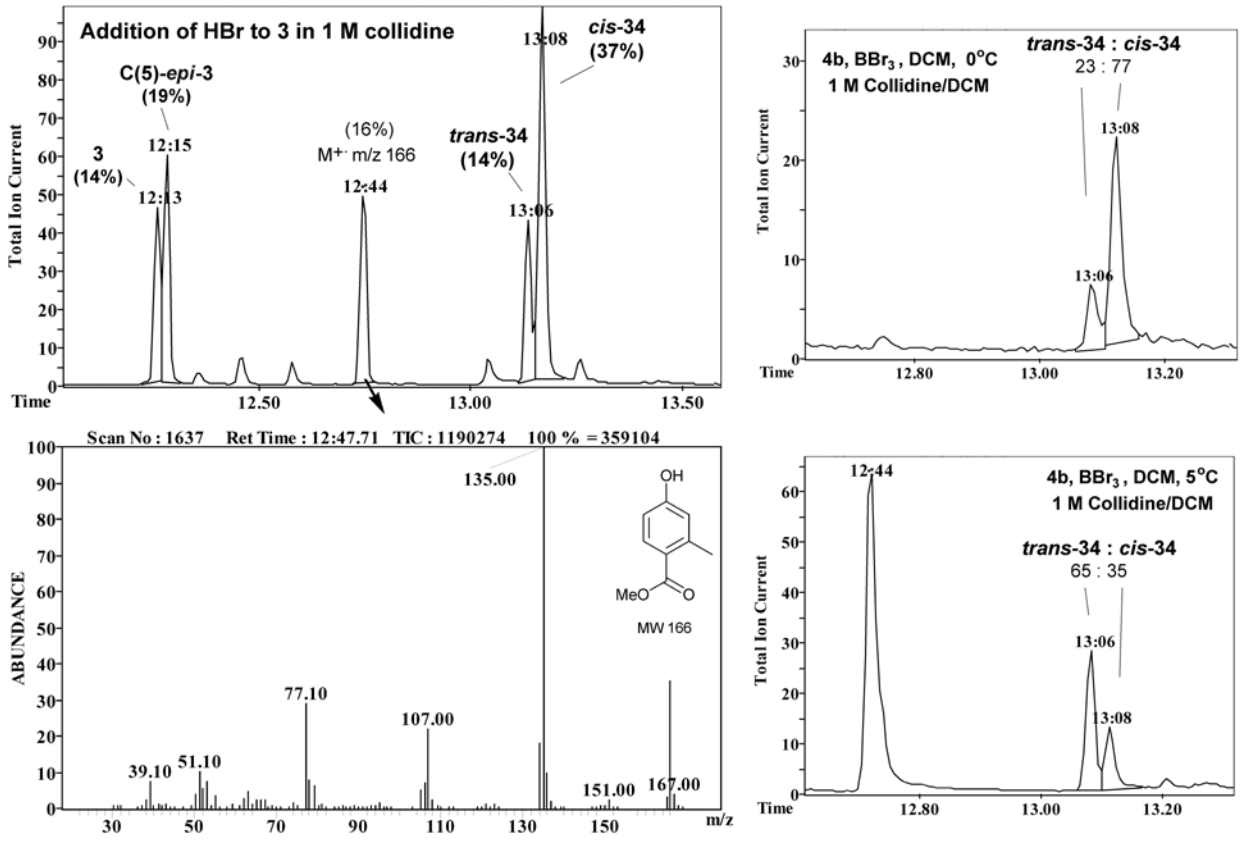

Figure 4.19: Top left; The addition of 48% HBr (10 equiv.) to **3** followed by stirring at 22ºC for 10 min led to the formation of **34** in 51% yield in a 14:37 *cis*:*trans* ratio. Bottom left; An aromatised product was identified at t_R = 12:44, showing a molecular ion $M^{+\cdot}$ *m/z* 166 corresponding to the substituted phenol and a *m/z* 77 fragment ion characteristic of a benzene ring. Top right; Isomers of **34** formed during the reaction of **4b** with BBr_3/collidine at 0ºC shows a 77:23 *cis*:*trans* ratio with a predominance of *cis*-**34** (t_R = 13:08 min). Bottom right; Isomers of **34** formed upon reaction of **4b** with BBr_3/collidine at 5ºC shows a 35:65 *cis*:*trans* ratio with a predominance of the *trans*-**34** isomer (t_R = 13:06 min).

The action of BBr_3 on **4b** at 5ºC gave more complex reaction mixtures, also shown in Figure 4.5 (Section 4.1.2), featuring **34** in 15% yield with a predominance of *trans*-**34** as the major isomer (t_R = 13:06 min) in a 35:65 *cis*:*trans* ratio (Figure 4.19, bottom right). The aromatised product at t_R = 12:44 min was also seen to increase at higher temperatures than 0ºC. A significant finding in this study is that the ring cleavage and bromination to form *trans*-**34** at temperatures ≤ 5ºC proceed with retention of stereochemistry with respect to the ether ring of **4b**. A proposed mechanism for the observed face

selectivity in the cleavage of **4b** at 5ºC is rationalised as due to an intramolecular S_N1 reaction between the boron ether intermediate and the tertiary carbocation formed as the result of C-O cleavage at C(1) in **4b**, during which the bromide ion reacts at the same face as the borate group (Scheme 4.24). The face selective BBr_3 cleavage of **4b** is consistent with studies by Koreeda *et al.* [29, 30] and Gopalaswamy *et al.* [31] in support of a ring opening mechanism involving the stable tertiary carbocation intermediate.

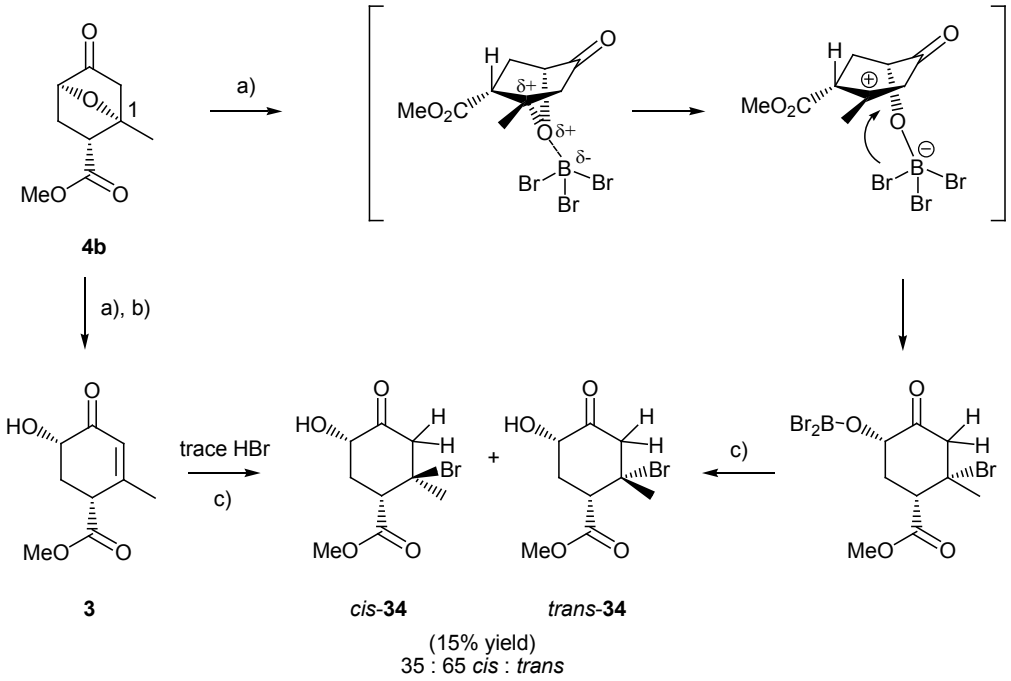

a) BBr_3, DCM, 5ºC, 10 min b) 1 M Collidine in DCM 25-30ºC, 35 min c) 1 M HCl.

Scheme 4.24: The BBr_3 ether cleavage of **4b** at 5ºC was found to give a 15% yield of the brominated isomers **34** in a 35:65 *cis*:*trans* ratio. A proposed mechanism to account for the predominace of *trans*-**34** involves the formation of a carbocation intermediate at C(1) followed by reaction of the bromide ion at the same face as the boron ether intermediate. At the same time a mixture of *cis*- and *trans*-**34** can form due to the *in situ* reaction of **3** with HBr.

The *cis*-**34** product may arise in the same product mixture *via* deconjugation to the α,β-unsaturated borane ether upon treatment with collidine followed by HBr olefin addition, or alternately by the intermolecular reaction of the carbocation with a bromide anion contributed by a second borane intermediate to result in stereochemical inversion at C(2). Attempts to form *trans*-**34** as the exclusive C(2)-bromo isomer at temperatures as high as 25ºC led to extensive decomposition and the *trans*-**34** isomer was unable to be isolated in sufficient purity by FCC to achieve characterisation by ^{13}C NMR analysis without slow epimerization at C(5).

During the synthesis of **2** and **3**, the brominated by-products **34** are avoidable by closely controlled reaction conditions. In this study, the ratio of *cis*:*trans* isomers of **34** prepared under a range of conditions has proven to give valuable information about the reaction mechanism. Factors preventing this methodology from being applied at reaction scales larger than 100 mg remain unknown and a better understanding of reactive intermediates is essential for further optimisation of this synthetic methodology toward ring **A**. Future studies may include BCl_3 mediated ether cleavage of **4** (Scheme 4.25), which has been reported by Koreeda *et al.* [30] to produce the *cis*- chlorinated alcohol in high yield and following the same mechanism as suggested for BBr_3.

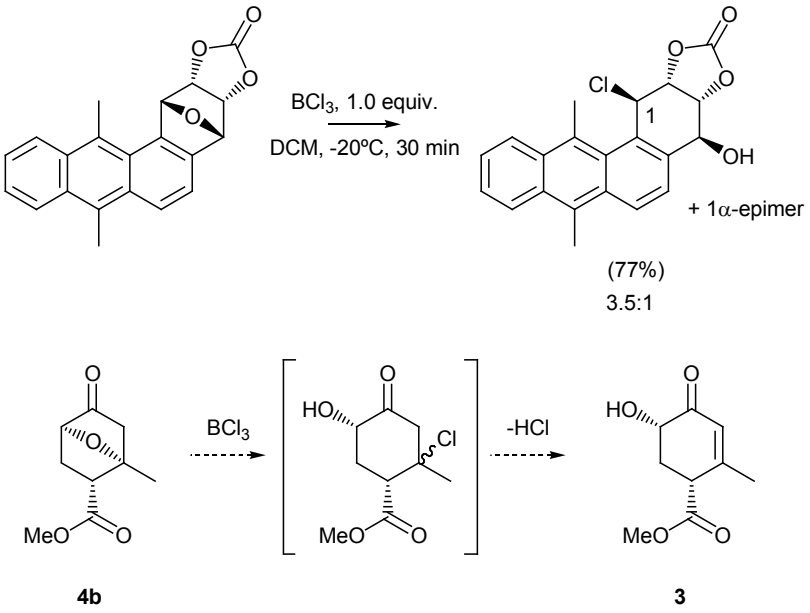

Scheme 4.25: Top; Koreeda *et al.* [30] have discussed the BCl_3 mediated cleavage of the 7-oxanorbornante moiety in high yield and mild under conditions (-20ºC) to produce the *cis*-chloro alcohol in a 3.5:1 ratio with the 1α-epimer. Bottom; Further work towards the ether cleavage of **4** may involve reaction with BCl_3 to produce either the chloro-alcohol or α,β-unsaturated alcohol **3**.

The authors report the chlorinated products to be more stable to isomerization than the brominated equivalents, suggesting that BCl_3 cleavage of **4b** may be a viable pathway to **3** but requiring dehydrohalogenation of the chloro-intermediate.

4.5 Preliminary Studies Towards 1,4-Gilman Reactions with (1R, 5S)/(1S,5R)-Methyl 5-acetoxy-2-methyl-4-oxocyclohex-2-enecarboxylate (2) and Further Work

The final step in the synthesis of ring **A** involves the 1,4-conjugate addition to **2** as a means of introducing the vinyl group at C(2) to be used as a functionalised substituent for the attachment of ring **C**. The steric influence of the C(1) ester and C(5) acetoxy substituents, which occupy the same face of the cyclic enone **2**, are likely to provide stereochemical control in the 1,4-conjugate addition with preference for the S_i face (Scheme 4.26). This would result in the *trans*- oriented C(2) vinyl group with respect to C(1) and C(5) substituents, yielding C(2) in the *S*- configuration in agreement with the natural product **1**. Transformation of **2** by reaction at the β-olefinic carbon requires a reactant that can act as suitable Michael donor to achieve selectivity for β-attack at the enone, without reacting at the electrophilic C(4) carbonyl. The proposed pathway uses organocopper reagents to achieve this process.

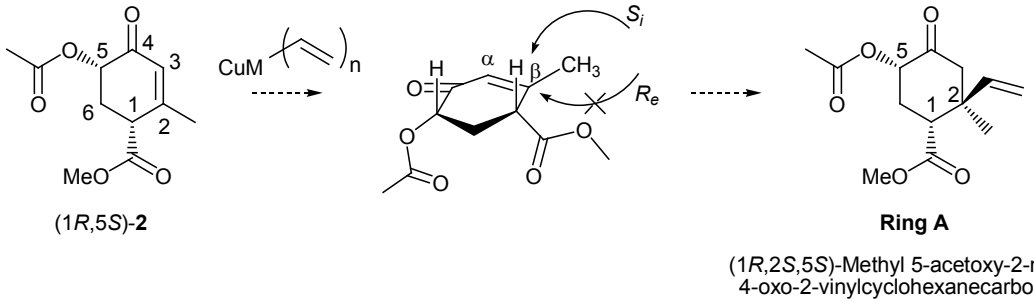

Scheme 4.26: The final transformation in the synthesis of Ring **A** involves the Michael-type addition reaction of a vinyl copper reagent to the β-olefinic carbon of (1*R*,5*S*)-**2**. The *S*- configuration can be expected at C(2) as a result of 1,4-addition to the least S_i hindered face.

Organocopper reagents have found a central role in natural product synthesis and are utilised in the examples of clerodane syntheses shown in Section 1.6.2. They are highly chemo-, regio- and stereo-selective, reacting as a soft nucleophile with a range of Michael acceptors as well as aldehydes and alkyl halides under very mild conditions [40]. Organo-copper nucleophiles show selectivity for the soft electrophilic β-carbon of α,β-unsaturated Michael acceptors, in contrast to hard organometallic nucleophiles such as Grignard and organolithium reagents that preferentially react at the hard carbonyl centre.

Early research on the preparation and chemistry of mono- and di-alkylcopper (homocuprate) compounds was published by Gilman and co-workers between 1936-1952, who successfully differentiated the ether insoluble mono-alkyl derivative from the soluble di-alkylcopper species during reactions between methyllithium and copper (I) salts [41] Scheme 4.27, left). These organocuprate compounds are nowdays called 'Gilman' reagents. The synthetic utility of Gilman reagents was later recognised by House *et al.* [42] in 1966 who discuss changes in the 1,2-regioselective reaction of MeMgBr with *trans*-3-penten-2-one upon catalysis by copper (I) iodide (1.2 mol %), to form the 1,4-conjugate addition product exclusively. This observation was rationalised to proceed by transmetalation to the mono-organocopper intermediate prior to conjugate addition [42]. Modern techniques more commonly involve homocuprate reagents (R_2CuLi or R_2CuMgX) due to the enhanced nucleophilicity, stability and homogeneity compared to their mono-organocopper counterparts, and a good description of the reported organocopper reagent types can be found in literature by Taylor [40].

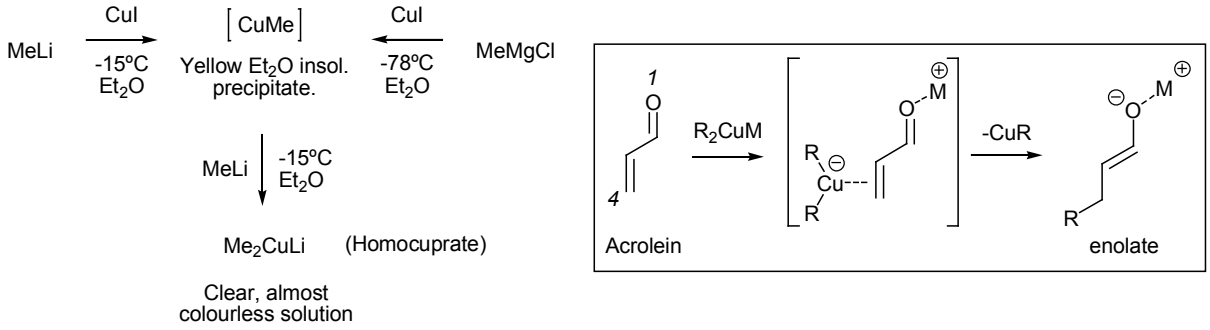

Scheme 4.27: Left; The reaction of one equivalent of MeLi or MeMgCl with cuprous iodide (CuI) in Et_2O was reported by Gilman *et al.* [41] to give the mono-organocopper compound as a yellow precipitate. Reaction with a second equivalent of MeLi gives the homocuprate, which is soluble in Et_2O and gives a clear solution. Right; The mechanism for the 1,4-cuprate addition to enones has been reviewed by Woodward [43] and is shown using acrolein as an example. Complexation of the π-system followed by alkylation to produce the enolate, and can be 'trapped' at this stage by reaction with TMSCl, accompanied by enhanced reaction rate and yields.

The mechanism by which the organocuprate reacts with the enone system has attracted some interest from the scientific community owing to the synthetic usefulness of this transformation. A comprehensive review was not undertaken as part of this work and the literature addressing theoretical and experimental data on reaction intermediates is best summarised in a review by Woodward [43] and includes material published up to the year 2000. The currently accepted mechanism, shown using the example acrolein (Scheme 4.27, right), involves an intermediate complex featuring co-ordination between the soft homocuprate anion with the π-cloud of the olefin. The Gilman counter-ion M^+ is usually a charged Lewis-acid (eg. Li^+, MgX^+) and is able to co-ordinate with the lone pair electrons of the carbonyl oxygen in a hard-hard interaction which is essential for the 1,4-addition to occur [43].

Transformation of the complex to the enolate occurs by reaction of only one of the two carbocuprate groups at the C(4) olefin. Although the transition states for this process are still uncertain, Corey *et al.* [44] have suggested a copper (III) β-adduct involving reversible π-complexation and more recent studies by Woodward [43] support this hypothesis.

The vinyl Gilman reagent was prepared in THF at -30ºC (Scheme 4.28, top) following a modification of the procedure described by Kato *et al.* [44] using copper(I) iodide (0.5 equiv.) and the commercially available Grignard reagent vinyl magnesium bromide (2.5 equiv.). The formation of the intermediate mono-vinyl cuprate was apparent during the addition of Grignard reagent by the initial formation of a precipitate, which gradually disappeared to leave an opaque yellow solution of the homocuprate following the completion of Grignard addition. The homocuprate divinyl Gilman reagent was cooled to -50ºC after which the enone **2**, shown as the (1*R*,5*S*)-enantiomer (Scheme 4.28, bottom) was slowly added over 2 h followed by quenching with aqueous NH_4Cl at -50ºC.

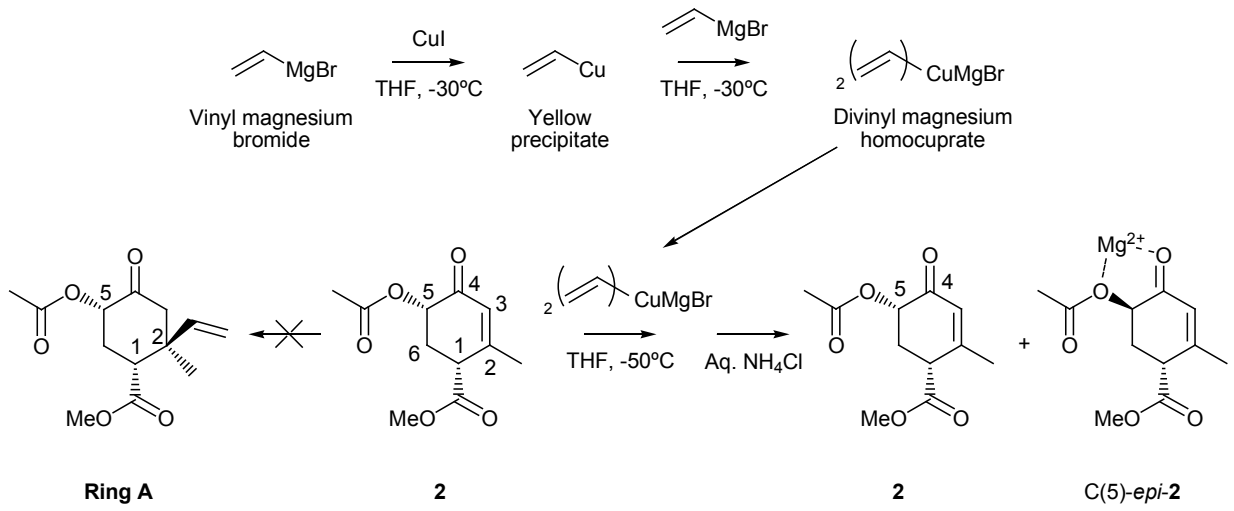

Scheme 4.28: Top; Formation of the divinyl homocuprate was achieved by the reaction of vinyl magnesium bromide with Cu(I)I in THF at –30ºC. Bottom; Reaction of **2** with the divinyl homocuprate was conducted at –50ºC but alkylation at C(2) did not occur. The product mixture returned a mixture of **2** and C(5)-*epi*-**2** due resulting from C(5) racemization.

Analysis of the product mixture revealed that the enone **2** was stable to the Gilman reaction conditions but did not form the desired 1,4-addition product as shown by GC-MS analysis (Figure 4.20). Instead, epimerization at C(5) occurred to give a mixture of **2** and C(5)-*epi*-**2** and this observation suggests that the Mg^{2+} ion shows strong Lewis-acid affinity for the α-acetoxy carbonyl functionality.

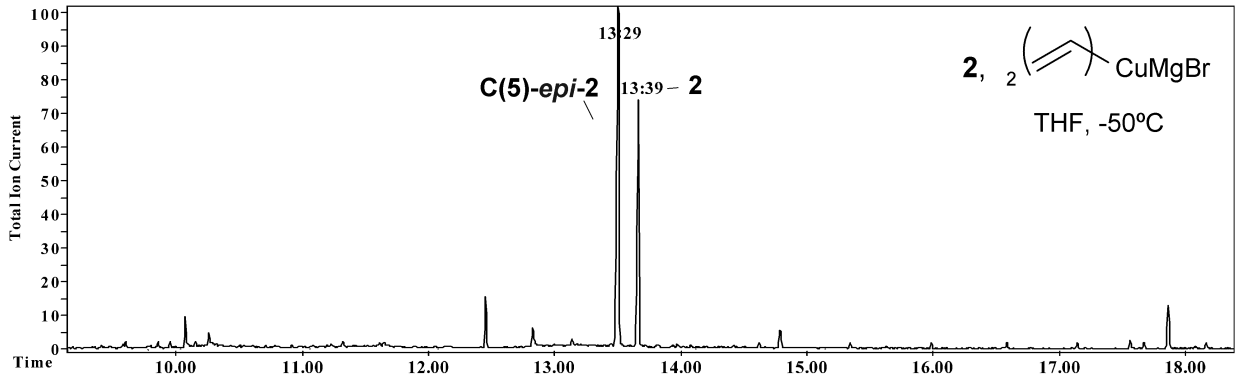

Figure 4.20: GC trace of the product mixture obtained from the reaction of **2** with the divinyl homocuprate in THF at –50ºC showing a mixture of **2** and C(5)-*epi*-**2**.

Attempts at increased temperatures (-78 to 25ºC) according to methodology described by Trauner *et al.* [45] also failed to form the desired structure Ring **A**. Disappointingly, trials involving the divinyllithium homocuprate, prepared from vinyl lithium in place of the vinyl Grignard, were not attempted due to time and financial constraints. Reaction of **2** with the mono-vinylcopper intermediate was also attempted without success. Limited scale quantity and purification capacity leading to time consuming isolation of only small quantities of **2** and **3** ($\geq$50 mg) were major hindrances in a speedy conclusion to this final step. Ideas and comments on further work are included in the following section along with general conclusions for Chapter 4.

4.6 Conclusion and Further Work

Although improvements in the 1,4-conjugate addition to the enone of **2** might be found upon utilizing the divinyllithium organocuprate, vast improvement is more likely to be realised by using rate enhancing additives. A large number of techniques are available to alter the reactivity of organocuprates and relevant examples will be briefly outlined. Improvements in the reaction of mono-organocopper Gilman reagents in the presence of Lewis-acids has been reviewed by Yamamoto [46], who highlights catalysis of a range of organocuprates with $BF_3.Et_2O$ as a means of improving the 1,4-addition to β,β-disubstituted acrylates. Lipshutz *et al.* [47] have described significant rate enhancement for the addition of divinyl Gilman to the trimethylated cyclohex-2-enone structure using $BF_3.Et_2O$ catalysis (Scheme 4.29). The effects of $BF_3.Et_2O$ on Gilman organocuprates has also attracted some research and Lipshutz *et al.* [47] have identified modified cuprates in NMR experiments upon reaction in THF. The authors suggest that both the formation of reactive cuprate intermediates and co-ordiation of the carbonyl lone pair electrons can contribute to changes in reactivity.

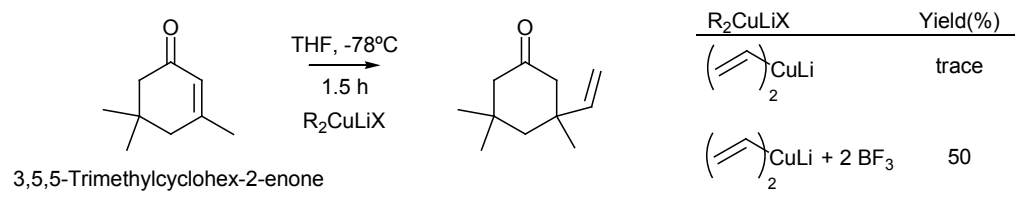

Scheme 4.29: Improvements in the 1,4-addition of vinyl Gilman organocuprates to 3,5,5-trimethylcyclohex-2-enone have been reported by Lipshutz *et al.* [47] using $BF_3.Et_2O$ catalysis.

Corey *et al.* [44] have discussed the compatibility of TMSCl with Gilman reagents at –78ºC and report enhancement in reaction rate to yield the 'trapped' TMS-enolate (Scheme 4.30, top). Gilman reaction involving the γ-ether substituted cyclohexenone and lithium divinylcuprate was reported to show excellent *trans*- selectivity in the presence of TMSCl. The authors propose that silylation occurs during the reversible π-conjugate addition transition state [44] and describe reaction times of less than two minutes in the presence of five equivalents of TMSCl.

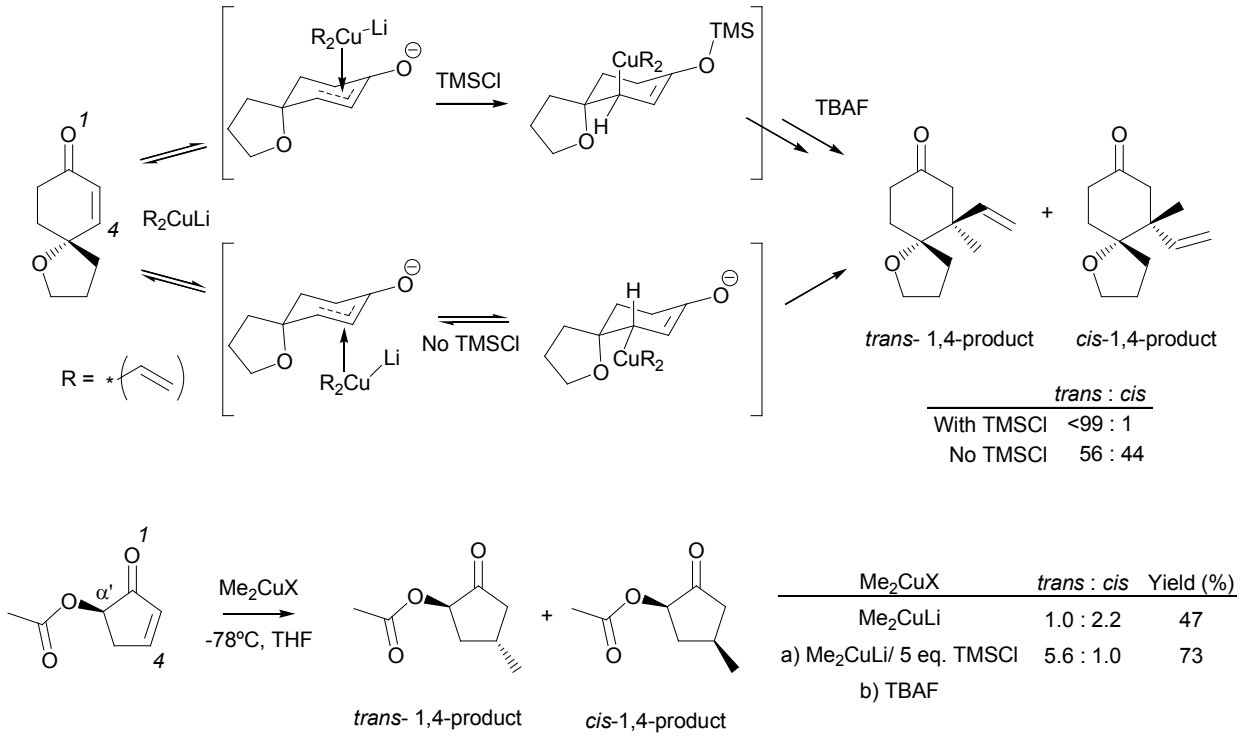

Scheme 4.30: Top; Corey *et al.* [44] have published the 1,4-addition of lithium divinylcuprate to a γ-ether substituted cyclohexenone and report enhanced rate and selectivity in the presence of TMSCl. The authors propose silylation to occur in the transition state. Bottom; Smith *et al.* [48] describe yield and selectivity improvements in the conjugate addition of Gilman reagents to α'-acetoxy substituted cyclopentenones upon the addition of TMSCl.

Smith *et al.* [48] have studied the effect of TMSCl on Gilman reactions involving the 1,4-congugate addition to α-oxa substituted cyclopentenones. The α'-acetoxy substituted cyclopentenone was reported to show diastereofacial selectivity for the *trans*- product and improved in yield in the presence of TMSCl, whereas in the absence of silylating agent the *cis*- isomer predominately forms (Scheme 4.30, bottom). Reactions in the presence of TMSCl were reported to give the TMS enol-ethers as Gilman products that were subsequently deprotected using TBAF. The authors attribute selectivity in this reaction to electronic effects involving polarization of the enone π-system rather than steric effects and support this hypothesis with computational studies [49].

Further work towards the divinylcuprate conjugate addition to **2** could possibly utilise rate enhancement using $BF_3.Et_2O$ Lewis-acid catalysis or reaction in the presence of TMSCl. Selectivity for the *trans*- conjugate addition product, as expected in the latter methodology, is in favour of the desired stereochemistry for the natural product **1**. Examples involving the conjugate addition of Gilman reagents to structures containing similar functionality to **2** are shown in Scheme 4.26 and Scheme 4.27 and strongly encourage that the desired transformation of **2** can be achieved and without racemization at C(5).

In conclusion, ether cleavage of the Diels-Alder adduct **4** was much more complicated than expected. As shown throughout Chapter 4, ether cleavage of the 7-oxabicyclo[2.2.1]heptane moiety can follow a number of hydrolysis and rearrangement pathways, and the necessary methodology for ether modification is predominately dependent on the position and functionality of substituents on the bicyclic core. In this chapter, both the Lewis-acid and base mediated ether cleavage pathways have been investigated for the new compounds **4a** and **4b**. An unreported base mediated C-C cleavage of **4** has been identified and presents itself as a unique pathway to specifically substituted furans and furanones **31** and **32**. The successful BBr_3 mediated ether cleavage of **4** to yield the desired cyclohexenone **3** also revealed that the Lewis-acid facilitated ether cleavage of **4b** proceeds with retention of stereochemistry at C(5) whereas the cleavage of **4a** does not. A mechanism for the BBr_3 ether cleavage has been proposed based on the ratio of brominated epimers **34** and is consistent with the existing literature. D-A face-selectivity in the preparation of the (1*S*,2*R*,4*S*)-enantiomer of **4b** using **5q** has been achieved as described in Chapter 3, and the optimised BBr_3 ether cleavage as reported establishes a stereoselective pathway from **24** to (1*R*,2*S*)-**2** in 60% *ee* as a chiral precursor to the natural product **1** (Scheme 4.31). The syntheses presented in this chapter were conducted using the racemic 7-oxanorbornanes (1*S*,2*R*,4*S*)/(1*R*,2*S*,4*R*)-**4b** and (1*R*,2*R*,4*R*)/(1*S*,2*S*,4*S*)-**4a**, and optical rotation data for the non-racemic ether cleavage products (1*R*,2*S*)-**3** and (1*R*,2*S*)-**2** are yet to be recorded.

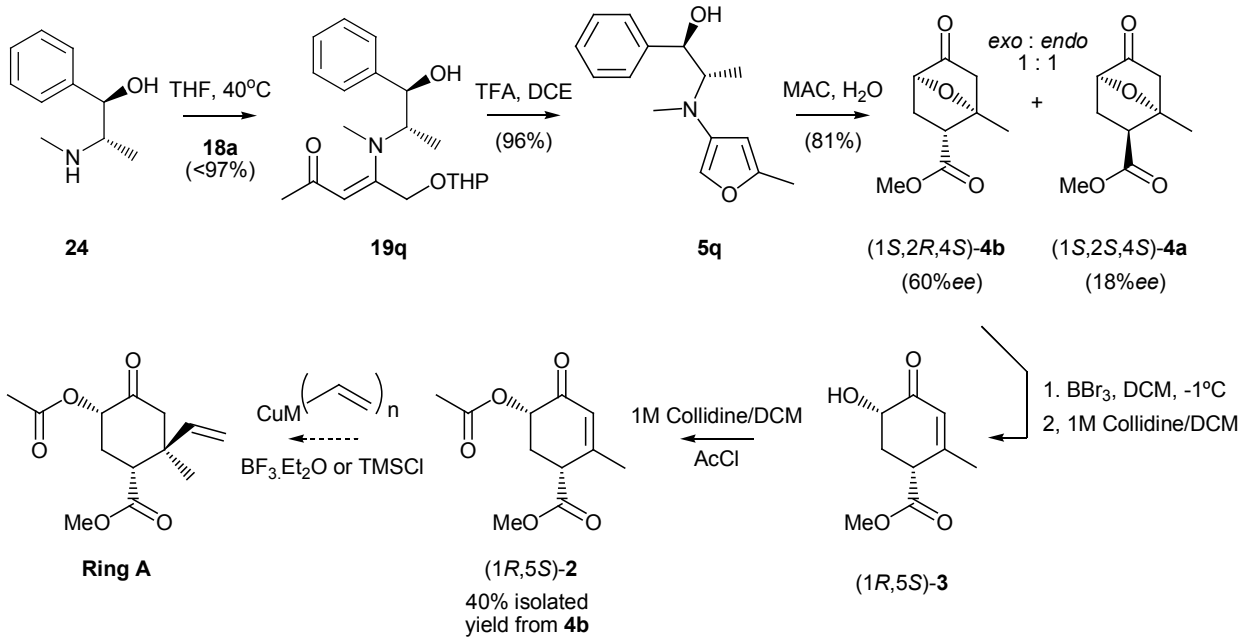

Scheme 4.31: The chiral furylamine **5q** prepared from the commercially available **24** has been shown to undergo D-A reaction with MAC in H_2O to give the *exo*-cycloadduct (1*S*,2*R*,4*S*)-**4b** in 60% *ee* as a 1:1 mixture with the *endo* isomer. Ether cleavage using BBr_3 at -1ºC followed by quenching in collidine provides (1*R*,2*S*)-**3** with retention of stereochemistry and *in situ* acetyl with AcCl provides (1*R*,2*S*)-**2** in 40% overall from (1*S*,2*R*,4*S*)-**4b**. Ring **A** can be accessed in a stereoselective manner by reaction of (1*R*,2*S*)-**2** with vinyl Gilman reagent.

Chapter 4

Studies Toward the Synthesis of Ring A: References

[1] P. Vogel, J. Cossy, J. Plumet, O. Arjona. "Derivatives of 7-Oxabicyclo[2.2.1]heptane in Nature and as Useful Synthetic Intermediates", *Tetrahedron,* **1999**, *55*, 13521-13642.

[2] M. Lautens, K. Fagnou, S. Hiebert. "Transition Metal-Catalyzed Enantioselective Ring-Opening Reactions of Oxabicyclic Alkenes", *Account of Chemical Research*, **2003**, *36*, 48-58.

[3] S. P. Forsey, D. Rajapaksa, N. J. Taylor, R. Rodrigo. "Comprehensive Synthetic Route to Eight Diastereomeric *Podophyllum* Lignans", *Journal of Organic Chemistry,* **1989**, *544*, 4280-4290.

[4] C.-C. Feng, M. Nandi, T. Sambaiah, C.-H. Cheng. "Nickel-Catalyzed Highly Stereoselective Ring Opening of 7-Oxa- and Azanorbornenes with Organic Halides", *Journal of Organic Chemistry*, **1999**, *64*, 3538-3543.

[5] R. G. Arrayás, S. Cabrera, J. C. Carretero. "Copper-Catalyzed Anti-Stereocontrolled Ring Opening of Oxabicyclic Alkenes with Grignard Reagents", *Organic Letters*, **2003**, *5*, 1333-1336.

[6] M. Lautens, P. Chiu. "Regioselective Nucleophilic Ring Opening of Oxabicyclic Compounds", *Tetrahedron Letters*, **1993**, *34*, 773-776

[7] O. Arjona, R. Menchaca, J. Plumet. "Building a Small Polypropionate Library. Synthesis of All Possible Stereotetrads (Building Blocks for Polyketide Synthesis) from Furan", *Journal of Organic Chemistry*, **2001**, *66*, 2400-2413.

[8] M. Koreeda, K-Y. Jung, J. Ichita. "Diels-Alder reactions of 3,4-Dialkoxyfurans: An Application to the Highly Efficient Synthesis of (+)-Methyl Triacetylshikimate", *Journal of the Chemical Society Perkin Transcations 1*, **1989**, 11, 2129-2131.

[9] Y. Tanoue, M. Hamada, N. Kai, T. Nagai, K. Sakata, M. "Hashimoto. Ring Opening of Cyclic Ethers by Sulfuric Acid-Acetic Anhydride", *Journal of Heterocyclic Chemistry*, **2000**, *37*, 1351-1353.

[10] S. Ogawa, H. Aoyama, T. Sato. "Synthesis of an Ether-Linked Alkyl 5a-Carba-β-D-glucoside, a 5a-Carba-β-D-galactoside, a 2-Acetamido-2-deoxy-5a-carba-β-D-glucoside, and an Alkyl 5a'-Carba-β-lactoside", *Carbohydrate Research*, **2002**, *337*, 1979-1992.

[11] J. Luo, H. Hart. "Linear Acene Derivatives. New Routes to Pentacene and Napthacene and the First Synthesis of a Triptycene with Two Anthracene Moieties", *Journal of Organic Chemistry*, **1987**, *52*, 4833-4836.

[12] P. Vogel, D. Fattori, F. Gasparini, C. Le Drain. "Optically Pure 7-Oxabicyclo[2.2.1]hept-5-en-2-yl Derivatives ("Naked Sugars") as New Chirons", *Synlett*, **1990**, 173-185.

[13] C. Le Drain, J.-P. Vionnet, P. Vogel. "Total Syntheses of (-)-Corduritol B ((-)-1L-Cyclohex-5-ene-1,3/2,4-tetrol) and of (+)-Conduritol F ((+)-1D-Cyclohex-5-ene-1,2,4/3-tetrol).

Determination of the Absolute Configuration of (+)-Leucanthemitol)", *Helvetica Chemica Acta*, **1990**, *73*, 161-168

[14] O. Arjona, A. de Dios, R. F. de la Pradilla, J. Plumet. "Highly Diasteroselective Bis-Hydroxylation of a Protected Conduritol B: A Short Route to *myo*-Inositol Derivatives", *Tetrahedron Letters*, **1991**, *32*, 7309-7312.

[15] O. Arjona, A. Candilejo, A. de Dios, R. F. de la Pradilla, J. Plumet. "Osmium-Mediated Asymmetric Synthesis of Glycosyl-myo-inositols from Oxanorbornanes", *Journal of Organic Chemistry*, **1992**, *57*, 6097-6099.

[16] F. G. Kitson, B. S. Larsen, C. N. McEwen. "Gas Chromatography and Mass Spectrometry: A Practical Guide", Academic Press, California, **1996**, 283, 228, 164, ISBN 0-12-483385-3.

[17] C. Pasquarello, S. Picasso, R. Demange, M. Malissard, E. G. Berger, P. Vogel. "The C-Disaccharide α-C(1-3)-Mannopyranoside of *N*-Acetylgalactosamine Is an Inhibitor of Glycohydrolases and of Human a-1,3-Fucosyltransferase VI. Its Epimer α-(1-3)-Mannopyranoside of *N*-Acetyltalosamine Is Not", *Journal of Organic Chemistry*, **2000**, *65*, 4251-4260.

[18] C. Le Drain, P. Vogel. "Acid-Catalyzed Rearrangement of 5,6-exo-Epoxy-7-oxabicyclo[2.2.1]hept-2-yl Derivatives. Migratory Aptitudes of Acyl vs. Alkyl Groups in Wagner-Meerwein Transpositions", *Helvetica Chimica Acta*, **1987**, *70*, 1703-1720.

[19] T. C. McMorris, M. D. Staake, M. J. Kelner. "Synthesis and Biological Activity of Enantiomers of Antitumor Irofulven", *Journal of Organic Chemistry*, **2004**, *69*, 619-623.

[20] T. Takahashi, T. Namiki, Y. Takeuchi, T. Koizumi. "A New Synthetic Route to Methyl (-)-Shikimate by Asymmetric Diels-Alder Reaction of $(S)_s$-3-(2-Pyridylsulfinyl)Acrylate", *Chemical and Pharmaceutical Bulletin*, **1988**, *36*, 3213-3215; T. Takahashi, H. Kotsubo, A. Lyobe, T. Namiki, T. Koizumi**,** "A New Synthetic Approach to Pseudo-sugars by Asymmetric Diels-Alder Reaction. Synthesis of Optically Pure Pseudo-β-D-Mannopyranose, 1-Amino-1-deoxypseudo-α-D-Mannopyranose and Pseudo-α-L-Mannopyranose Derivatives", *Journal of the Chemical Society Perkin Transactions 1*, **1990**, 3065-3072.

[21] J. D. Rainer, Q. Xu. "A Novel Anionic Condensation, Fragmentation, and Elimination Reaction of Bicyclo[2.2.1]heptenone Ring Systems", *Organic Letters*, **1999**, *1*, 27-29.

[22] G. Vidari, S. Beszant, J. El Merabet, M. Bovolenta, G. Zanoni. "$FeCl_3$ and $ZrCl_4$ regiochemically controlled biomimetic-like cyclizations of simple isoprenoid epoxyolefins", *Tetrahedron Letters*, **2002**, *43*, 2687-2690.

[23] O. Arjona, F. Iradier, R. M. Mañas, J. Plumet. "Synthesis of a Protected Derivative of (±)-1-(hydroxymethyl)conduritol C from 2-(hydroxymethyl)furan", *Tetrahedron Letters*, **1998**, *39*, 8335-8336.

[24] A. K. Mandal, N. R. Soni, K. R. Ratnam. "Boron Trifluoride Etherate/Iodide as a Mild, Convenient and Regioselective Ether Cleaving Reagent", *Synthesis*, **1985**, *3*, 274-275.

[25] G. Mehta, S. S. Ramesh. "Quest for Inosito-inositols: Synthesis of Novel, Annulated and Conformationally Locked Inositols", *Tetrahedron Letters*, **2003**, *44*, 3105-3108.

[26] H. W. Gschwend, M. J. Hillman, B. Kisis, R. K. Rodebaugh. "Intramolecular Diels-Alder Reactions. Synthesis of 3a-Phenylisoindolines as Analgesic Templates", *Journal of Organic Chemistry*, **1976**, *41*(1), 104-110.

[27] J. March. "Advanced Organic Chemistry: Reactions, Mechanisms and Structure", (4th Ed.), John Wiley and Sons, N.Y., **1992**, 971, ISBN 0-471-58148-8.

[28] M. Curini, F. Epifano, M. C. Marcotullio, O. Rosati, M. Nocchetti. "Preparation and Deprotection of 1,1-Diacetates (Acylals) Using Zirconium Sulfophenyl Phosphate as Catalyst", *Tetrahedron Letters*, **2002**, *43*, 2709-2711.

[29] M. Koreeda, K.-Y. Jung, M. Hirota. "A Novel Regio- and Stereocontrolled Synthesis of Diol Epoxide and *trans*-Dihydrodiol Metabolites of Polycyclic Aromatic Hydrocarbons. An Application to the Synthesis of the Bay-Region *syn*- and *anti*- Diol Epoxides of the Carcinogen 1,4-Dimethylphenanthrene", *Journal of the American Chemical Society*, **1990**, *112*, 7413-7414.

[30] M. Koreeda, R. Gopalaswamy. "Regio- and Stereocontrolled Synthesis of the Bay-Region anti-Diol Epoxide Metabolites of the Potent Carcinogens Benzo[*a*]pyrene and 7,12-Dimethylbenz[*a*]anthracene", *Journal of the American Chemical Society,* **1995**, *117*, 10595-10596.

[31] R. Gopalaswamy, M. Koreeda. "On the Mechanism of the Stereo- and Regioselective Ether-ring Opening of 1,2,3,4-Tetrahydro-1β, 4β-epoxy-2α,3α-carbonyldioxy Arene Systems with Boron Tribromide", *Tetrahedron Letters*, **1996**, *37*, 3651-3654 and references therein.

[32] H. Mosimann, P. Vogel, A. A. Pinkerton, K. Kirschbaum. "Highly Stereoselective Synthesis of Perhydro-8a-(hydroxymethyl)-phenanthrene-1,2,4,5,7,8-hexol and Derivatives", *Journal of Organic Chemistry*, **1997**, *62*, 3002-3007.

[33] N. Jotterand, P. Vogel, K. Schenk. "Total Asymmetric Synthesis of Doubly Branched Carba-hexopyranoses and Amino Derivatives Starting from the Diels-Alder Adducts of Maleic Anhydride to Furfuryl Esters", *Helvetica Chimica Acta*, **1999**, *82*, 821-847.

[34] A. F. Barrero, E. J. Alvarez-Manzaneda, M. Mar Herrador, R. Alvarez-Manzaneda, J. Quilez, R. Chahboun, P. Linares, A. R. Rivas. "The First Route Toward Oxygenated Monocarbocyclic Terpenoids: Synthesis of Elegansidiol, a New Sesquiterpene from *Santolina elegans*", *Tetrahedron Letters*, **1999**, *40*, 8273-8276.

[35] A. F. Barrero, E. J. Alvarez-Manzaneda, R. Chahboun, A. R. Rivas, P. L. Palomino. "Synthesis of Natural Oxygenated Monocarbocyclic Sesquiterpenoids from 6,7-Epoxygeranyl Acetate", *Tetrahedron*, **2000**, *56*, 6099-6113.

[36] J. W. J. F. Thuring, G. H. L. Nefkens, B. Zwannenburg. "Asymmetric Synthesis of All Stereoisomers of the Strigol Analogue GR24. Dependence of Absolute Configuration on Stimulatory Activity of *Striga hermonthica* and *Orobanche crenata* Seen Germination", *Journal of Agricultural Food Chemistry*, **1997**, *45*, 2278-2283.

[37] C. Tanyeli, A. Tosun, E. Turkut, B. Sezen. "Manganese(III) Acetate Promoted Acetoxylation of Various α,β-Unsaturated Cyclopentanones", *Tetrahedron*, **2003**, *59*, 1055-1058.

[38] C. Tanyeli, E. Turkut, İ. M. Akhmedov. "Chemoenzymatic Synthesis of α'- and α-Acetoxylated Cyclic Ketones", *Tetrahedron: Asymmetry*, **2004**, 1729-1733.

[39] D. H. Williams, I. Fleming. "Spectroscopic Methods in Organic Chemistry", (5th Ed.), McGraw-Hilll, London, **1995**, 6-8, ISBN 0-07-709147-7.

[40] R. J. K. Taylor (Ed.). "Organocopper Reagents: A Practical Approach", Oxford University Press, New York, **1994**, 4-15, ISBN 0-19-855757-4.

[41] H. Gilman, R. G. Jones, L. A. Woods. "The Preparation of Methylcopper and Some Observations on the Decomposition of Organocopper Compounds", *Journal of Organic Chemistry*, **1952**, *17*, 1630-1634.

[42] H. O. House, W. L. Respess, G. M. Whitesides. "The Chemistry of Carbanions. XII. The Role of Copper in the Conjugate Addition of Organometallic Reagents", *Journal of Organic Chemistry*, **1966**, *31*, 3128-3141.

[43] S. Woodward. "Decoding the 'Black Box' Reactivity That Is Organocuprate Conjugate Addition Chemistry", *Chemical Society Reviews*, **2000**, *29*, 393-401.

[44] E. J. Corey, N. W. Boaz. "Evidence For a Reversible d,π*-Complexation, β-Cupration Sequence in the Conjugate Addition Reaction of Gilman Reagents With α,β-Enones", *Tetrahedron Letters*, **1985**, *26*, 6015-6018.

[44] M. Kato, M. Watanabe, B. Vogler, B. Z. Awen, Y. Masuda, Y. Tooyama, A. Yoshikoshi. "The Use of 4,4-Disubstituted Nopinones for Natural-Product Synthesis. Synthesis of Elemanoid Sesquiterpenes", *Journal of Organic Chemistry*, **1991**, *56*, 7071-7076.

[45] D. Trauner, J. W. Bats, A. Werner, J. Mulzer. "Synthesis of Enantiomerically Pure Morphine Alkaloids: The Hydrophenanthrene Route", *Journal of Organic Chemistry*, **1998**, *63*, 5908-5918.

[46] Y. Yamamoto. "Selective Synthesis by Use of Lewis Acids in the Presence of Organocopper and Related Reagents", *Angewandte Chemie International Edition*, **1986**, *25*, 947-1038.

[47] B. H. Lipshutz, E. L. Ellsworth, T. J. Siahaan. "The Role of $BF_3.Et_2O$ in Reactions of Lower Order (Gilman) Organocuprates", *Journal of the American Chemical Society*, **1989**, *111*, 1351-1358.

[48] A. B. Smith, N. K. Dunlap, G. A. Sulikowski. "Cuprate Additions to 5-Methoxycyclopentenones: A Novel Stereoelectronic Effect", *Tetrahedron Letters*, **1988**, *29*, 439-442.

[49] A. B. Smith, P. R. Trumper. "Theoretical Evaluation of Stereoelectronic Diastereofacial Selectivity in the Conjugate Addition of Cuprates to 5-Substituted Cyclopentenones", *Tetrahedron Letters*, **1988**, *29*, 443-446.

Chapter 5

Studies Towards the δ-Lactone Ring C of Salvinorin A

Ring **C** of salvinorin A (**1**) contains the 6-(furan-3-yl)-tetrahydropyran-2-one δ-lactone skeleton and retrosynthetic analysis of **1** involving disconnection at ring **B** [(Scheme 5.1, top), shown in detail; Scheme 1.21 (Section 1.7)], gave the α,β-unsaturated lactone 6-(furan-3-yl)-5,6-dihydro-4-methyl-3-vinylpyran-2-one (*S*)-**6**. This convergent precursor contains the C(8) stereocenter of the target product and has same functionality as ring **C** without specific stereochemistry at the C(3)/C(4) olefin. The chiral center in **6** at C(6) is attached to both the 3'-furyl substituent and carboxylic functionality of the δ-lactone ring, and the (*S*)-configuration is required for the asymmetric synthesis of the natural product **1**.

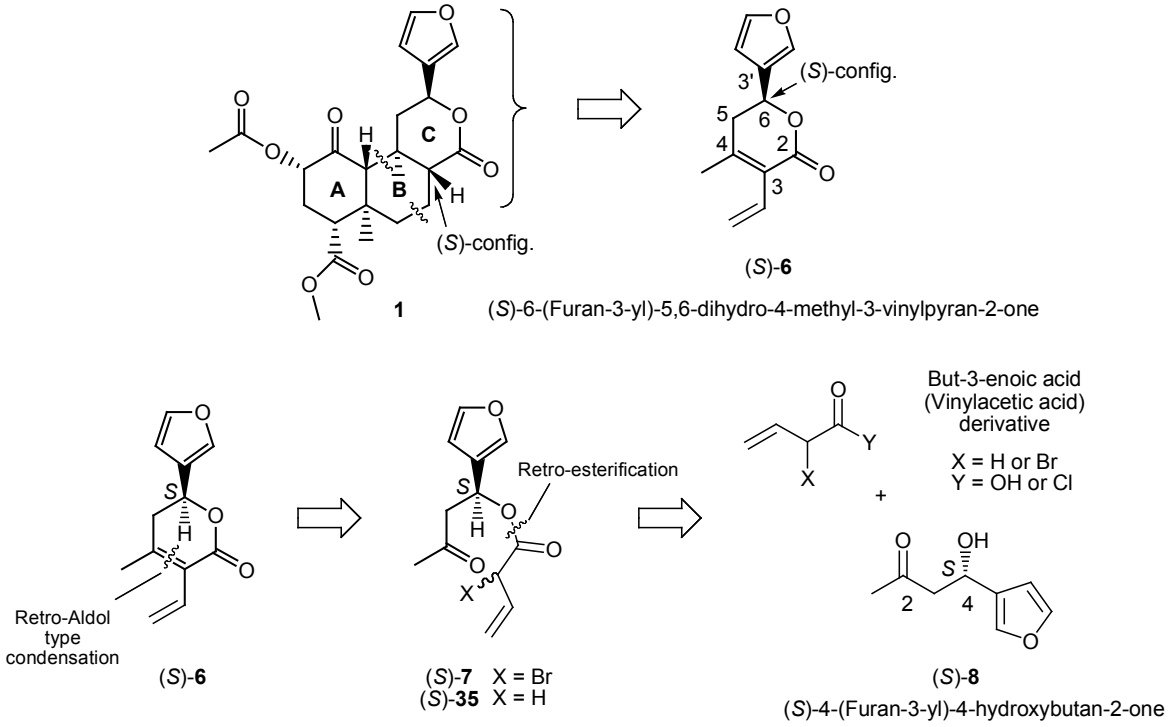

Scheme 5.1: Top; Disconnection of ring **B** gave the α,β-unsaturated lactone (*S*)-**6** as a convergent precursor for the synthesis of **1**. Bottom; Cleavage of the C(3)/C(4) olefin shows (*S*)-**35** (X = H) or (*S*)-**7** (X = Br) as a possible synthons for a retro-aldol type condensation; cleavage of the ester indicates the furyl alcohol (*S*)-**8** and a vinylacetic acid derivative as potential starting materials for the preparation of **7**.

The synthesis of **6** was not found in the literature and no direct methodology could be found for the incorporation of the 3-furyl moiety at C(6) and vinyl substituent at C(3) during the formation of the unsaturated δ-lactone ring. Disconnection of **6** to accessible starting materials involved cleavage at the

olefin and ester functionalities (Scheme 5.1, bottom). Intramolecular cyclization of an ester sidechain with a nearby carbonyl has been facilitated by an aldol or Reformatski reaction in a number of reported syntheses [1, 2] resulting in δ-lactone fragments. Likewise, the preparation of lactone **6** was thought possible by ring closure of a vinylacetic ester indicating that (*S*)-1-(furan-3-yl)-3-oxobutyl but-3-enoate (*S*)-**35** or (*S*)-1-(furan-3-yl)-3-oxobutyl 2-bromobut-3-enoate (*S*)-**7** are possible as retro-aldol type synthons. Disconnection of the ester shows the furyl alcohol (*S*)-4-(furan-3-yl)-4-hydroxybutan-2-one (*S*)-**8** as an accessible starting material for the synthesis of (*S*)-**6**.

The δ-lactone 6-(furan-3-yl)-tetrahydropyran-2-one unit (Ring **C**) of **1** is common to a range of tricyclic Labdane natural products (Section 1.4.4, Figures 1.21 to 1.24) and this moiety has been found to significantly contribute to the bioactivity of *trans-neo*-clerodanes **1** (Section 1.3.2, Figure 1.15) and bacchotricuneatin A (Section 1.4.4, Figure 1.24).

The following section briefly discusses the role of the 3-furyl group as a precursor for highly oxygenated furanones in natural product syntheses and mentions the significance of the pyranofuran-type structures as pharmacophores in some bioactive products. This is followed by a short literature review of the synthetic methods towards the racemic and non-racemic 6-(furan-3-yl)-5,6-dihydro-pyran-2-ones unit. The last section describes the synthesis of racemic **6** (*R*,*S*)-6-(furan-3-yl)-5,6-dihydro-4-methyl-3-vinylpyran-2-one and details an investigation of appropriate vinylacetic acid derivatives to achieve acylation and ring closure of **8**, with preliminary studies and strategies towards the introduction of chirality in **6**. Conclusions and further work completes the research presented in this thesis. Experimental and instrumentation details are found in Chapter 6.

5.1 Synthetic Strategies Towards 6-(Furan-3-yl)-5,6-dihydro-pyran-2-ones

The 3-furyl group is present at C(12) on the clerodane backbone of a large number of components isolated from *Salvia divinorum* so far (Section 1.1, Figure 1.2) and furyl or furanone type C(12) substituents are a common feature of clerodane natural products [3]. Synthetic strategies that introduce the 3-furyl substituent at C(12) on the clerodane core have been reported by a number of groups [4, 5, 6] who use the furan as a precursor to access the C(12) β-substituted γ-hydroxyfuran-2(5*H*)-one moiety, present in pyranofuranone containing clerodane compounds. This transformation is achieved by oxidation of the furan using photochemical methods, as illustrated in the final transformation for the

preparation of the gram-positive antibacterial 16-hydroxycleroda-3,13(14)*Z*-dien-15,16-olide (Scheme 5.2, top) reported by Hagiwara *et al.* [4], also mentioned in (Section 1.6.1).

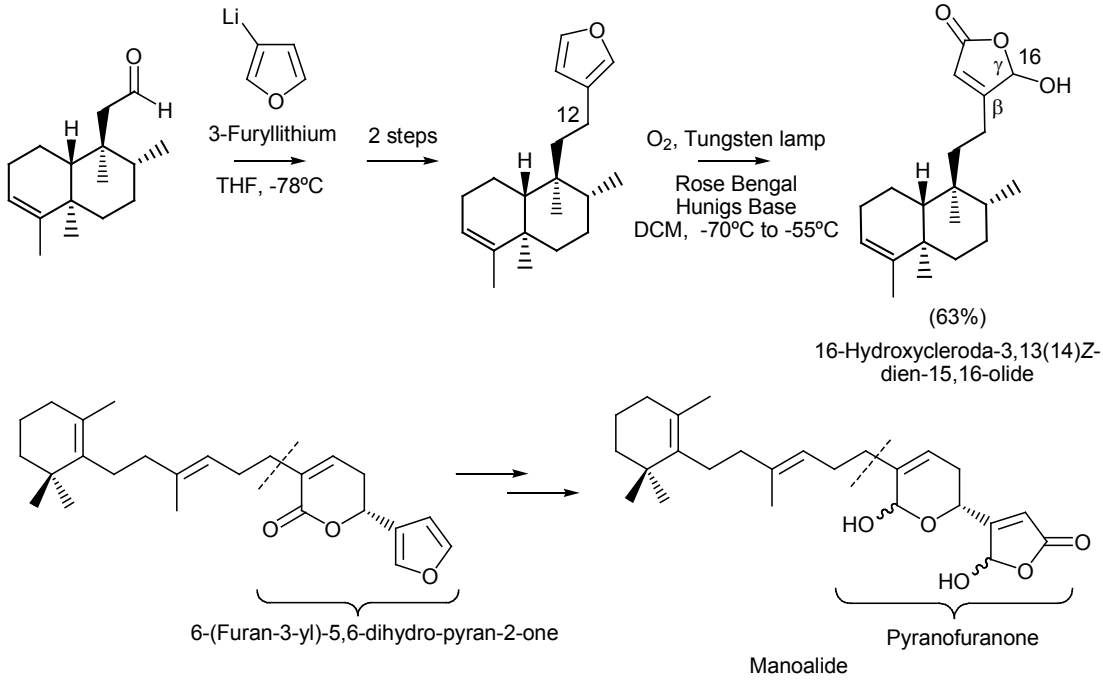

Scheme 5.2: Top; Hagiwara *et al.* [4] incorporate the 3-furyl group on the bicyclic aldehyde at C(12) using 3-furyl lithium followed by deoxygenation in two steps. Oxidation of furan to the γ-hydroxyfuran-2(5H)-one was achieved using photochemical methods to give the clerodane 16-hydroxycleroda-3,13(14)*Z*-dien-15,16-olide. Bottom; de Rosa *et al.* [7] have prepared 6-(furan-3-yl)-5,6-dihydro-pyran-2-ones as a means of accessing the bioactive pyranofuranone unit of manoalide.

Non-racemic 6-(furan-3-yl)-5,6-dihydro-pyran-2-ones have been prepared by de Rosa *et al.* [7] as intermediates to access the pharmacophoric pyranofuranone groups of some powerful anti-inflammatory marine compounds such as manoalide (Scheme 5.2, bottom). A brief literature review was undertaken on synthetic strategies toward the 6-(furan-3-yl)-5,6-dihydro-pyran-2-ones core, with focus on the incorporation of the furan group and methods for asymmetric synthesis.

The 3-furyl substituted δ-lactone has been prepared by Hagiwara *et al.* [8] in their synthesis of (-)-methyl barbascoate and the simple but costly 3-furyllithium nucleophile was used to incorporate this heterocycle as also shown in Scheme 1.15. This methodology has been adopted by a number of researchers [4, 5, 8, 9] for the introduction of the furyl substituent during the total synthesis of Labdane diterpenoids. An effective protocol has been used by Liu *et al.* [10] to construct of the CD ring system of the limonoid mexicanolide. Oxidative cleavage of a chiral hexahydro-1H-indene-1,2-diol derivative

using periodic acid (HIO_4) produced the δ-hydroxy lactone and subsequent reaction with 3-furyl lithium at -78ºC was reported to produce the furyl lactone as a single diastereoisomer in 43% with *syn*-oriented C(8a) and C(1) substituents (Scheme 5.3). Transformation to the convergent 1-(furan-3-yl)-6,7,8,8a-tetrahydro-6,8a-dimethyl-5-methylene-1H-isochromen-3(5*H*)-one precursor was achieved in low yield in four steps. The reported selectivity in the organolithium addition is likely due to the orientation of the C(8a) methyl group and products reported by Liu *et al.* [10] were prepared as a racemic (1*R,*6*R,*8a*R*/1*S,*6*S*,8a*S*)-mixture with the (*R,R,R*)-enantiomer shown in Scheme 5.3 as found in mexicanolide.

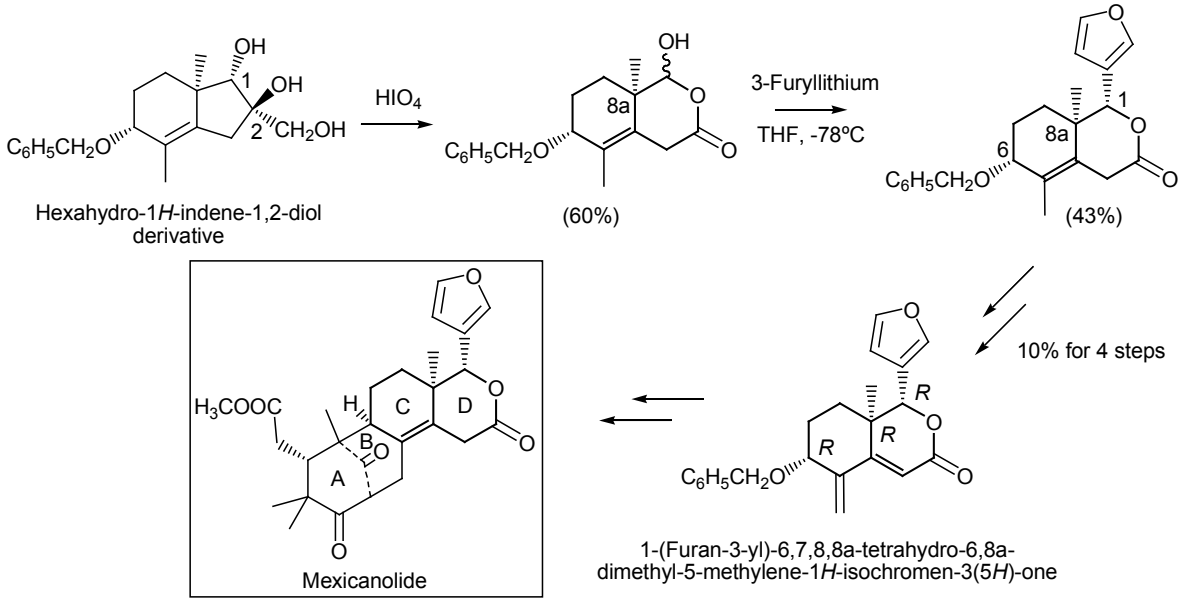

Scheme 5.3: Preparation of the CD ring system of mexicanolide was achieved by Liu *et al.* [10] using HIO_4 diol cleavage, followed by reaction with 3-furyllithium. The racemic precursor was prepared in a further four steps and the synthetic sequence is shown for the (*R*,*R*,*R*)-enantiomer as observed in mexicanolide.

Fernándes-Mateos *et al.* [11] have reported a simple preparation of the limanoid DL-pyroangolensolide by reaction of the lithium enolate of 2,6-dimethylcyclohenenone with 3-furaldehyde to give the *syn*-addition product exclusively (Scheme 5.4), and the authors suggest complexation with the lithium ion to aid this process. Acetylation followed by intramolecular aldol-type cyclization of the 1,3-acetoxyketone with LDA followed by dehydration with $SOCl_2$ was reported to produce the racemic α,β-unsaturated δ-lactone unit of the natural product [11] in excellent yields. A similar process has been reported by Shing *et al.* [6] for the preparation of quassinoid α,β-unsaturated lactone units.

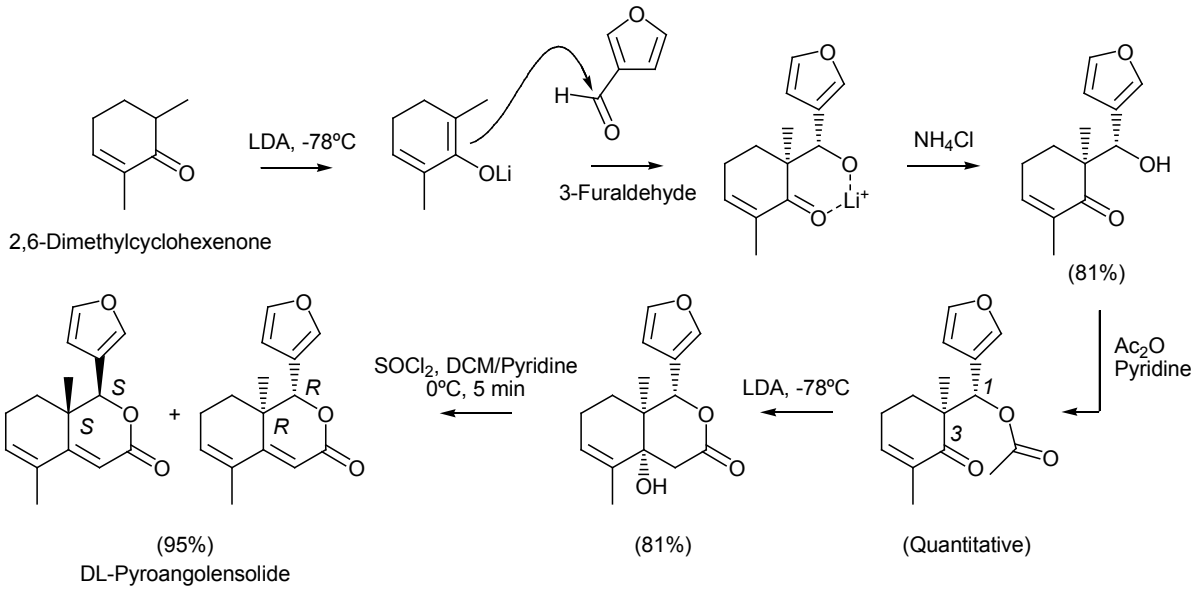

Scheme 5.4: Fernándes-Mateos *et al.* [11] constructed DL-pyroangolenolide, shown as the (*R*)-enantiomer, using the aldol addition with furaldehyde followed by a base-mediated intramolecular aldol-type cyclization of the 1,3-acetoxyketone followed by dehydration.

Syntheses reported by Liu *et al.* [10] and Fernándes-Mateos *et al.* [11] describe strategies toward the racemic 6-(furan-3-yl)-5,6-dihydro-pyran-2-ones and with *syn*-diastereoselectivity in the fused bicyclic products. De Rosa *et al.* [7] have reported a high yielding and stereoselective approach to a range of monocyclic 6-(furan-3-yl)-5,6-dihydro-pyran-2-ones using a Ti(IV)/(*R*)-BINOL catalyzed enantioselective aldol condensation of *O*-silyl dienolates to 3-furaldehyde, producing the (*R*)-furfurol products. Quantitative cyclization to the β-ketolactone was reported using K_2CO_3/MeOH and efficient interconversion to the α,β-unsaturated δ-lactone was achieved in a further two steps (Scheme 5.5).

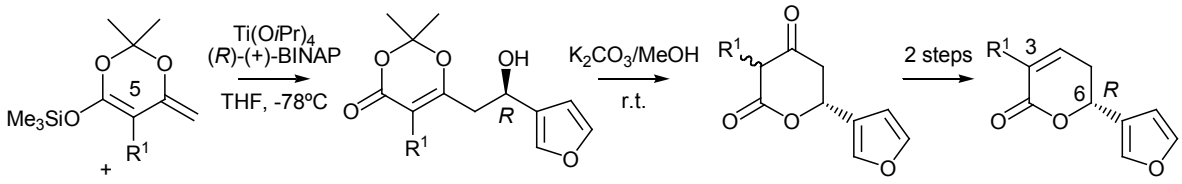

R^1	Yield (%)	e.e. (%)
H	76	91
Me	50	88
CH_2Ph	45	25

Scheme 5.5: De Rosa *et al.* [7] describe the stereoselective aldol reaction between 3-furaldehyde and *O*-silyl dienolates using Ti(IV)/(*R*)-BINAP catalysis to produce the (*R*)-furfurol in good yield, and subsequent cyclization with K_2CO_3/MeOH followed by functional group modification gave (*R*)-6-(furan-3-yl)-5,6-dihydro-pyran-2-ones as the optically enriched products.

De Rosa *et al.* [7] report highest yields and stereoselectivity using the C(5) unsubstituted dienolate (R^1 = H), and reduced yield and selectivity were noted with increasing substituent size (R^1 = Me, CH_2Ph). The same group later published chiral aldol studies involving a range of aryl aldehydes [12], offering a suitable approach for the preparation of a range of 6-aryl-5,6-dihydro-pyran-2-ones. A similar synthetic sequence to prepare 6-(furan-2-yl)-5,6-dihydro-pyran-2-ones has been described by Cahard *et al.* [13] as intermediates for the synthesis of (2*Z*)-terpenoic acids.

The syntheses reported by de Rosa *et al.* [7, 12] use the (*R*)-BINOL titanium complex, and the (*S*)-aldol product is accessible using the (*S*)-BINOL ligand *via* the same methodology. This approach represents a direct stereoselective pathway to the 6-(furan-3-yl)-5,6-dihydro-pyran-2-one system, but was not used for the synthesis of **6**. The *O*-silyl dienolate starting material required to introduce C(3) vinyl and C(4) methyl substituents is not readily accessible from commercial sources, indicating a custom dienolate synthesis or further transformation on the cyclized δ-lactone product would be necessary. For this reason, an intramolecular aldol-type ester ring closure was investigated as proposed in Scheme 5.1, involving the reaction of readily available vinyl acetic and crotonic carboxylates with the furfurol **8**. Preliminary synthetic studies using the inexpensive 2-furaldehyde were conducted and are presented in the following section, followed by the presentation of the final pathway towards the racemic **6** from **8**.

5.2 Synthesis of (R,S)-6-(Furan-3-yl)-5,6-dihydro-4-methyl-3-vinylpyran-2-one (6)

5.2.1 Preliminary δ-Lactone Research Using a 2-Furaldehyde Model

The β-keto-alcohol system in **8** can be generated by the aldol reaction between acetone and the furyl aldehyde, and reaction proceeds by the removal of a α-carbonyl proton followed by nucleophilic reaction of the anion with the aldehyde carbonyl (Scheme 5.6). A mild procedure for the aldol addition of aromatic aldehydes to acetone has been reported in studies by Shokat *et al.* [14] at 0ºC and is performed neat with a catalytic portion of NaOH. These conditions were applied to the reaction of acetone with the inexpensive model compound 2-furaldehyde. Optimization of reaction conditions using GC-MS monitoring allowed the preparation of 4-(furan-2-yl)-4-hydroxybutan-2-one **36** ($M^{+\cdot}$ *m/z* 154, t_R = 16:61 min) in >92% yield by warming from -10 to -5ºC over 30 min, followed by neutralization with 0.5 M HCl. At reaction temperatures above -5ºC, the formation of a major by-product showing a molecular ion for the α,β-unsaturated furyl ketone (*E*)-4-(furan-2-yl)but-3-en-2-one ($M^{+\cdot}$ *m/z* 136, t_R = 16:75 min) was

more predominant in GC-MS analysis and is the result of base catalyzed dehydration as typically occurs in the aldol *condensation* [15]. Dehydration of **36** was facile in the presence of acidic and basic reagents at ambient temperature and occurred to a small extent during storage at -18ºC.

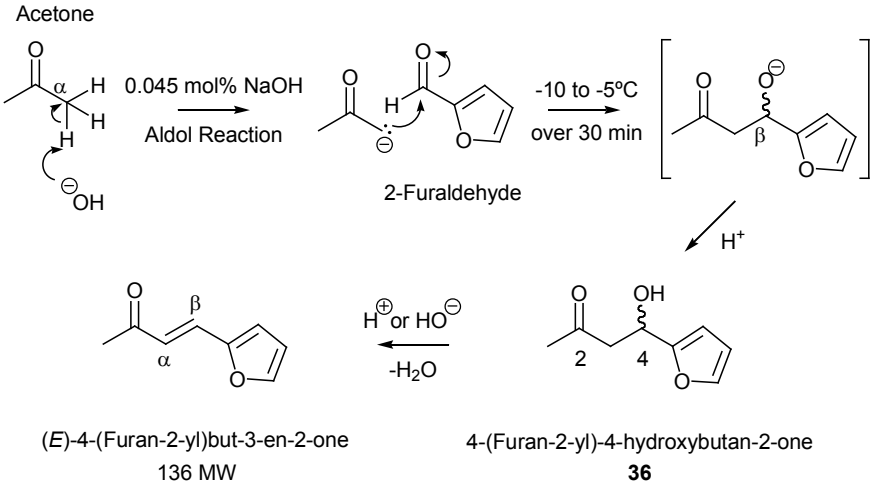

Scheme 5.6: The aldol reaction proceeds by first removal of the α-carbonyl proton with a hydroxide anion, shown above using the example acetone, followed by reaction at the carbonyl of 2-furaldehyde to give the β-hydroxy ketone **36**. Condensation involving the loss of water across C(4)/C(3) can occur under acidic or basic conditions to give the α,β-unsaturated ketone (*E*)-4-(furan-2-yl)but-3-en-2-one.

Due to the facile tendency of **36** towards dehydration, a very mild or neutral procedure was required for the esterification of the C(4) alcohol to the vinyl acetate ester to form **35**. Esterification using the Mitsunobu protocol was attempted between **36** and vinyl acetic acid under conditions described Couladouros *et al.* [16] (DEAD, Ph_3P, toluene, 45ºC) resulting in a number of failures and further literature searches revealed a mild preparation of vinyl acetic esters from crotonyl chlorides [17, 18]. Ozeki *et al.* [17] have reported a double bond shift from the α,β- to the β,γ- position in the reaction of crotonyl chloride in presence of TEA with an alcohol, as a related process to the Einhorn reaction. A later publication by Iwakura *et al.* [14] describe improvements in this process by performing the reaction in THF at 20ºC and report the deconjugated *i*-BuOH ester to form in >98% as shown in Scheme 5.6 (top).

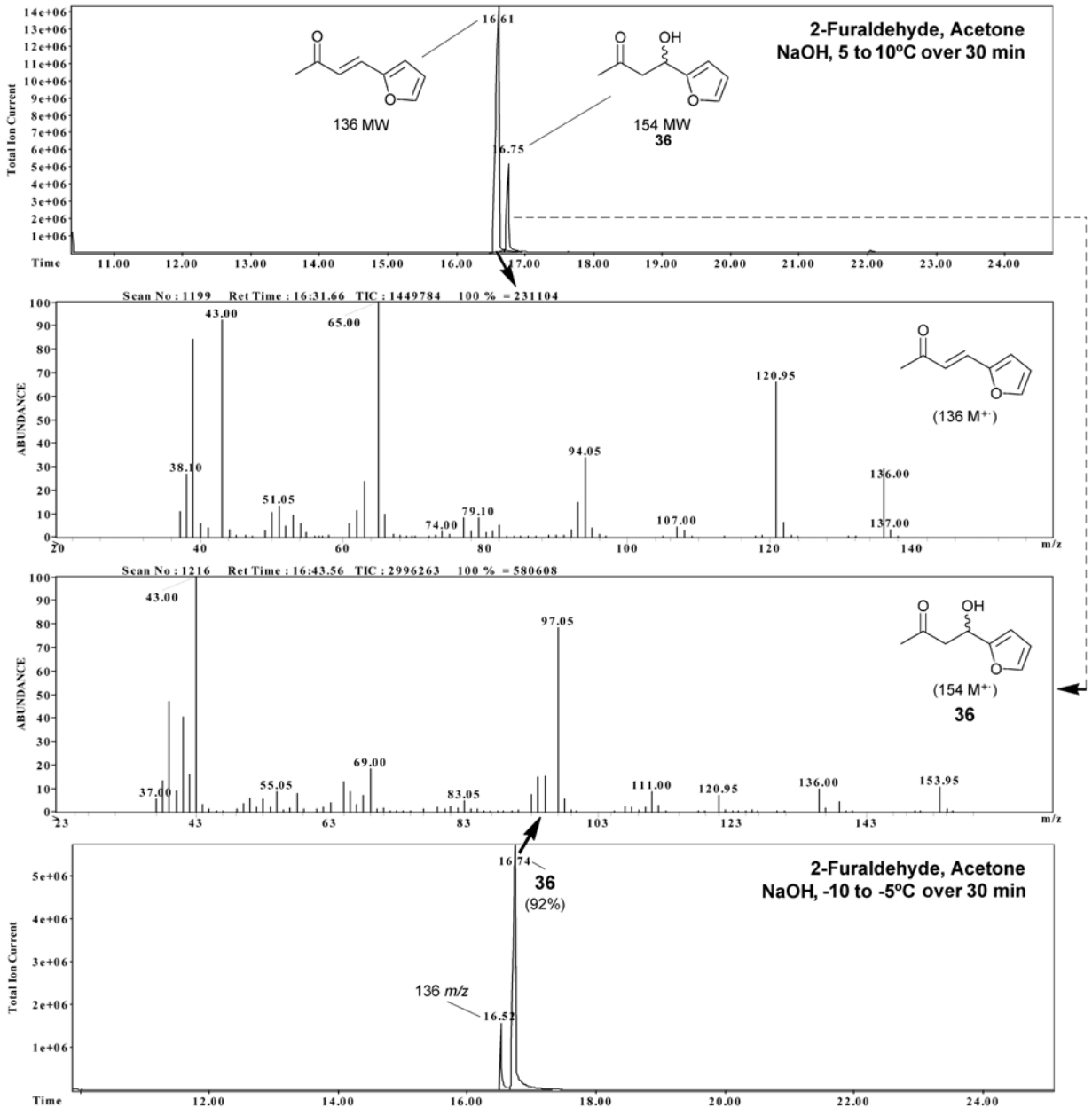

Figure 5.1: Top; The aldol condensation product at ($M^{+\cdot}$ *m/z* 136, t_R = 16:61 min) formed predominately upon the reaction of acetone with 2-furalehyde at 5 to 10ºC over 30 min, in the presence of a catalytic amount of NaOH. Bottom; Reaction from -10 to -5ºC over 30 min gave the desired alcohol **36** in 92% yield and the identity was confirmed by a *m/z* 154 molecular ion at t_R = 16:75 min.

The authors suggest this reaction to proceed by hydrogen abstraction of the β-methyl group resulting in dehydrochlorination and rearrangement to a ketene intermediate, as supported by experimental results revealing the slow addition of acid chloride to a mixture of amine and alcohol to give highest conversion to the β,γ- conjugated ester. To date this methodology appears not to have been used in the preparation of larger organic molecules.

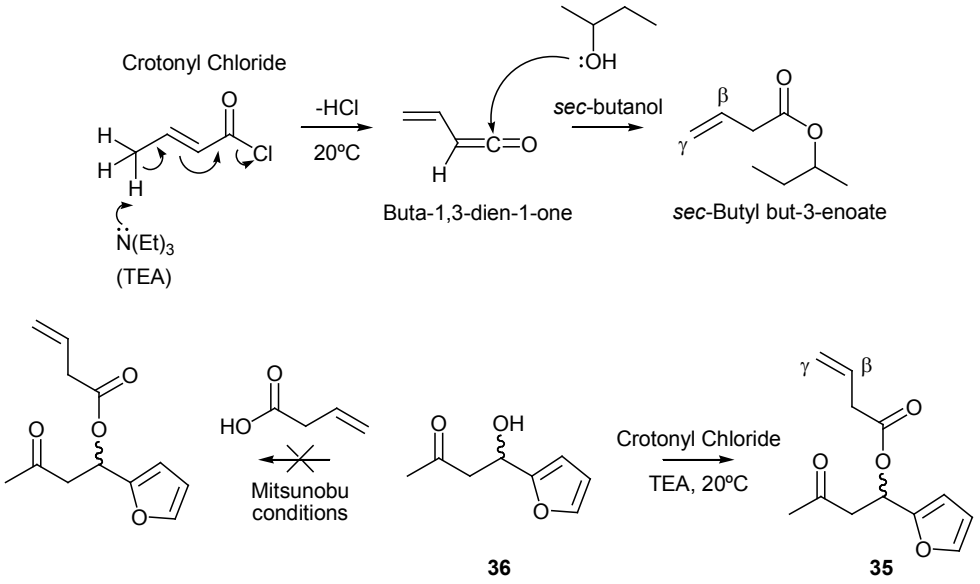

Scheme 5.7: Top; The esterification of crotonyl chloride and *sec*-butanol in the presence of TEA has been reported by Iwakura *et al.* [18] to proceed with double bond migration to the β,γ-position *via* the buta-1,3-dien-1-one ketene intermediate. Bottom; The furfurol **36** underwent decomposition during esterification with vinyl acetic acid using Mitsunobu conditions. Methodology described by Iwakura *et al.* [18] was subsequently employed to give **35** in >94% under mild conditions.

Crotonyl chloride was prepared according to procedures by Jeffery and Vogel [19] and reacted with the furfurol **36** under conditions described by Iwakura *et al.* [18] provided clean conversion to the β,γ-unsaturated ester **35** in nearly quantitative yield (Scheme 5.7, bottom) as indicated by a single peak at t_R = 18.93 min in GC-MS analysis (Appendix 5.1) containing a molecular ion at *m/z* 222 in agreement with **35**. A small amount of the α,β-unsaturated furyl ketone was also observed in the crude GC trace at t_R = 16.52 min and was removed upon washings with NH_4Cl. The structure of **35** was positively confirmed by ^{1}H NMR analysis which shows terminal vinylic protons H(4_A) and H(4_B) at δ 5.15 and 5.09 respectively and the H(3) proton as a complex multiplet at δ 5.85 in close agreement with Chemdraw predictions. A listing of ^{1}H NMR chemical shifts for this model intermediate is shown in Appendix 5.1. ^{13}C NMR analysis shows signals in the alkane region for C(1') and C(2') at δ 64.6 and 45.8 respectively

in support of the structure **35** and carbonyl, ester and aromatic signals are present and are assigned in Figure 5.2. Experimental procedures for the preparation of the model compound are included in Section 6.9.2.

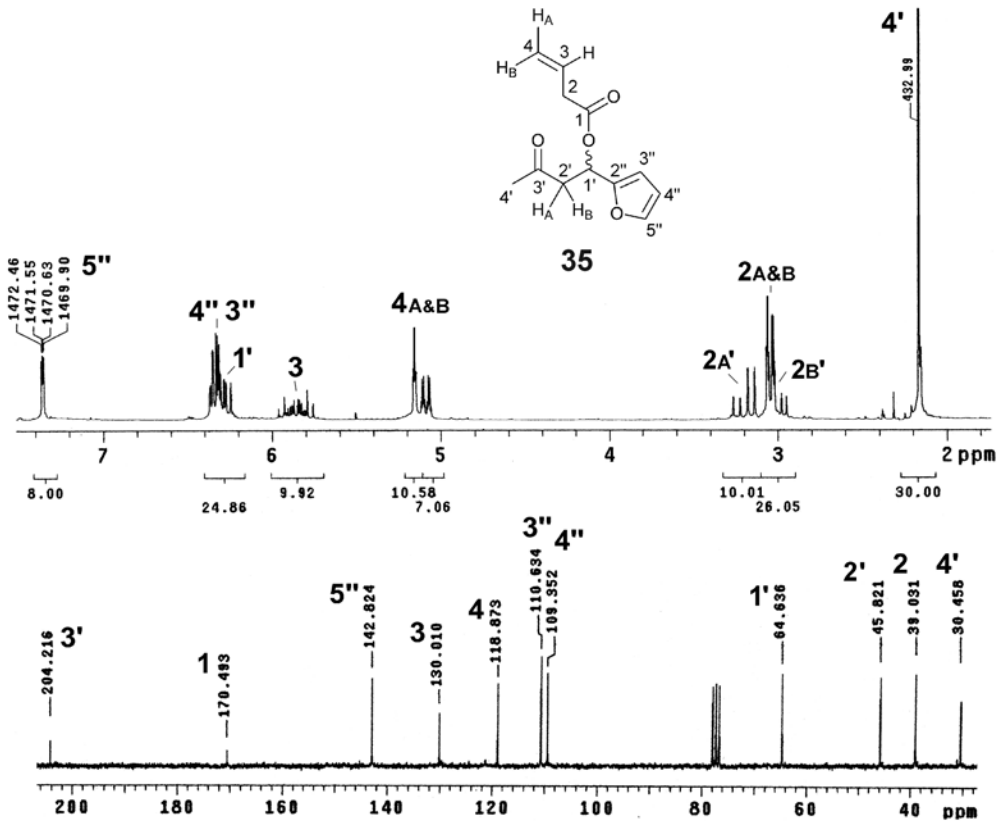

Figure 5.2: 200 MHz ^{1}H NMR analysis is shown for **36** with structural assignments and integral regions. The 50 MHz ^{13}C NMR spectrum is also shown indicating the expected resonances for **36** in agreement with Chemdraw predictions. The assigned structure is also shown.

Intramolecular ring closure of the vinyl ester was attempted on **35** (Scheme 5.8) using LDA at -78ºC following procedures described by Fernándes-Mateos *et al.* [11]. This method failed to produce the lactone even at higher temperatures (-25ºC) (Appendix 5.1), with dehydration to the familiar α,β-unsaturated ketone at t_R = 16.52 min predominating upon exposure of **35** to basic conditions. This result indicated that the deconjugation protocol could be a very facile pathway to **6** although the incorporation of an activating or reactive substituent at the α-position to the ester is required to more effectively complete the δ-lactone ring closure. The following section gives a few relevant literature examples of intramolecular lactone formation using α-activated esters and also details the final successful approach to the racemic **6** using readily available precursors.

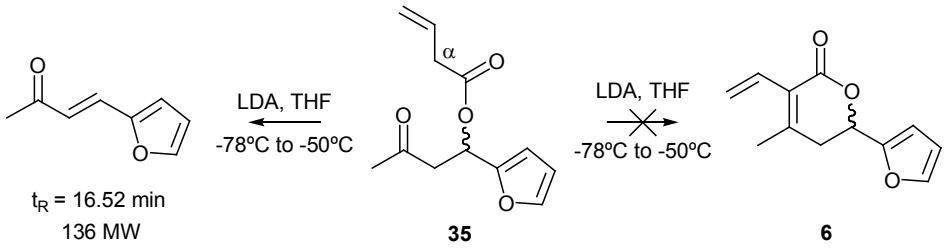

Scheme 5.8: Attempted lactone ring closure with LDA did not give the desired cyclic product **6** and instead the α,β-unsaturated dehydration product was formed as indicated by GC-MS monitoring (Appendix 5.1).

5.2.2 Preparation of 1-(Furan-3-yl)-3-oxobutyl 2-bromobut-3-enoate (7)

After the failed lactone formation of **35** using LDA, other methodologies for this transformation involving α-ester activating substituents were researched and will be discussed. Lactone formation using an α-bromo ester has been described by Iwadate *et al.* [20] in the stereoselective synthesis of steroids from the withanolide family. The bromoacetate was treated with triethylphosphite ($PO(OEt)_3$) (Arbusov reaction) to form the diethylphosphonate intermediate followed by Wittig-Horner ring closure using NaH in THF to give the 5,6-dihydro-pyran-2-one system (Scheme 5.9, top).

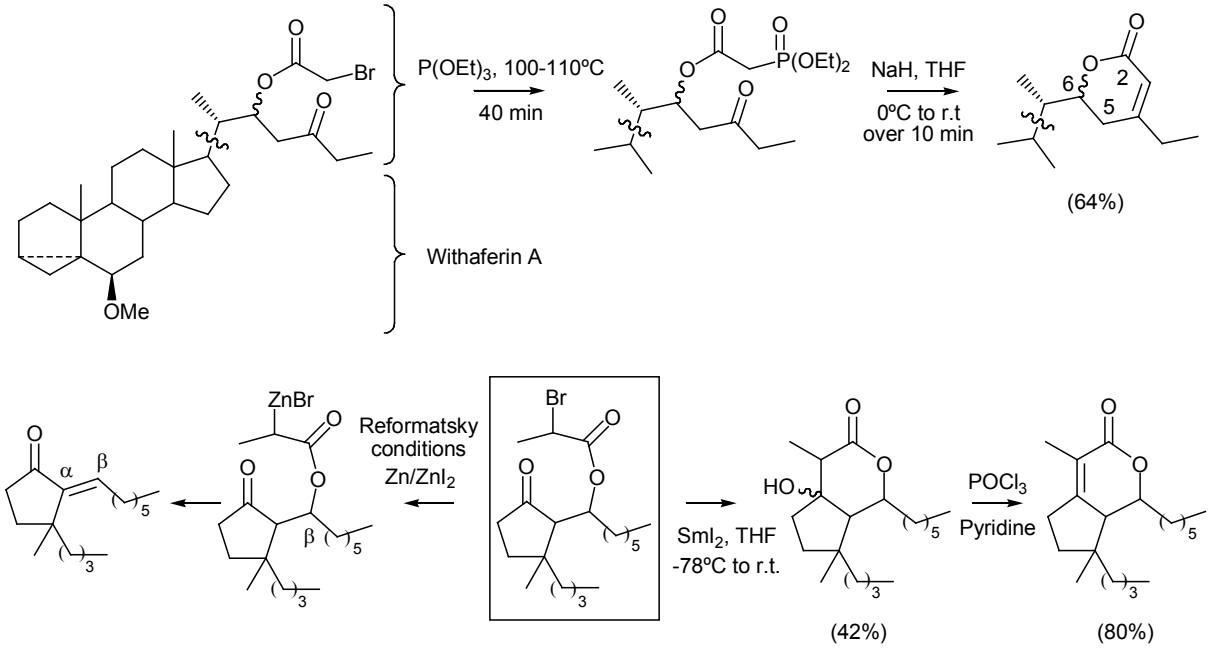

Scheme 5.9: Top; Iwadate *et al.* [20] have reported an intramolecular cyclization by reaction of the α-bromoester with $PO(OEt)_3$ followed by Wittig-Horner ring closure using NaH. Bottom; Zhu *et al.* [1] discuss failed attempts at

lactone ring closure using Reformatsky-type conditions and have achieved lactone formation by reaction with SmI_2 followed by dehydration with $POCl_3$.

A similar intramolecular α-bromoester cyclization has been used by Zhu *et al.* [1] for the preparation of bicyclic lactone systems during their studies towards a total synthesis of clavulactone and reports the β-acetoxy ketone to be labile to β-elimination in acidic and basic environments. Disappointing results were reported under Reformatsky-type conditions using Zn/ZnI_2 (Scheme 5.9, bottom) which resulted in the α,β-unsaturated product [1] and the authors achieved facile ring closure to the lactone using SmI_2 followed by dehydration using $POCl_3$ in pyridine.

Fortunately, relevant literature for the preparation of α-bromo-β,γ-unsaturated esters was described by Cardillo *et al.* [21] using a similar deconjugation pathway as shown in Scheme 5.7. The reaction of (*Z*)-2-bromobut-2-enoyl chloride with a mixture of TEA and benzyl alcohol (BnOH) in Et_2O at -78ºC was reported to give quantitative conversion to the ester in a 30:70 mixture of α,β-:β,γ- products [21].

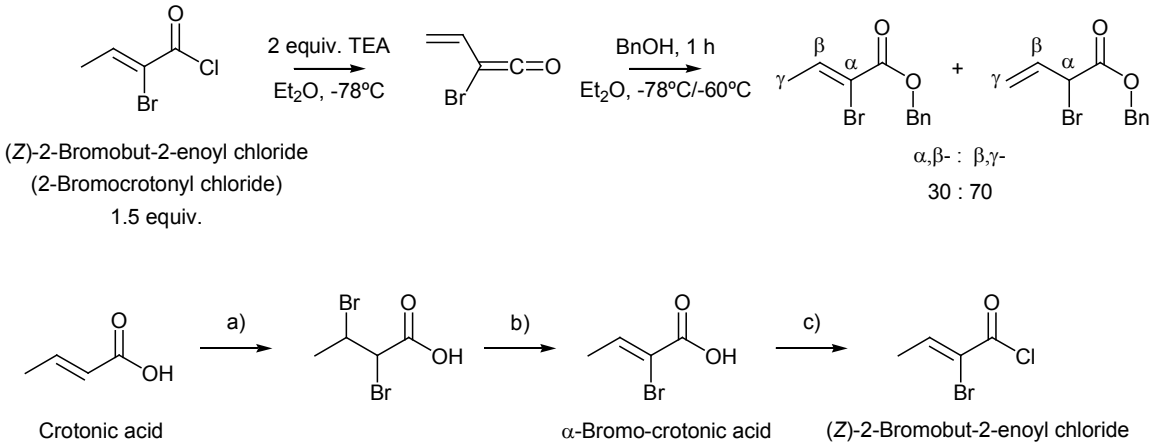

a) DCM, 1.1 equiv. Br_2, 24 h, 96% b) Pyridine, 100ºC, 4 h, 72% c) $SOCl_2$, reflux, 2 h, 67%.

Scheme 5.10: Top; Cardillo *et al.* [21] report double bond migration of (*Z*)-2-bromobut-2-enoyl chloride during esterification with BnOH in the presence of TEA to give 70% of the β,γ-unsaturated α-bromo ester. Bottom; Brominaton and dehydrohalogenation of crotonic acid was achieved in 96% and 72% yield respectively under conditions described by Pfeiffer [22] to give α-bromo-crotonic acid. Conversion to the acid chloride was achieved by heating with $SOCl_2$ using procedures by Zitrin *et al.* [23], and the pure product was distilled in 67% yield (Section 6.9.1).

α-Bromocrotonic acid was prepared in two steps from crotonic acid following literature by Pfeiffer [22]. The bromination of crotonic acid was achieved using Br_2 in DCM (96%) and

dehydrohalogenation upon heating with pyridine regenerated the α,β-unsaturated product to produce α-bromocrotonic acid in 72% yield as a light brown powder with m.p. 104-105ºC in agreement with the literature value (m.p. 105ºC, [22]). Heating of α-bromocrotonic acid with thionyl chloride ($SOCl_2$) gave the acid chloride (*Z*)-2-bromobut-2-enoyl chloride (67% yield) that distilled at 164-170ºC in agreement with the literature preparation described by Zitrin *et al.* [23] (Section 6.9.1). 4-(Furan-3-yl)-4-hydroxybutan-2-one **8** was prepared by the aldol reaction between acetone and 3-furaldehyde using optimised conditions from those shown for the model compound **36** (Scheme 5.6), involving warming from –9 to –6ºC over 40 min. The aldol addition product **8** was prepared in >98% yield as confirmed by a molecular ($M^{+\cdot}$ *m/z* 154) at t_R = 10:63 min in GC-MS analysis of the crude reaction extract (Appendix 5.3).

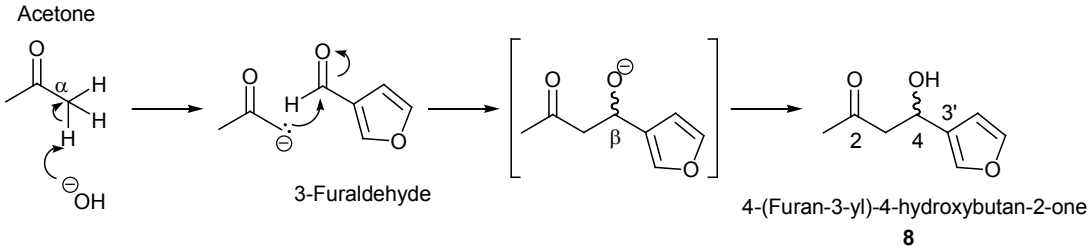

a) 1% NaOH solution dropwise at -9ºC, 0.06 mol% NaOH with respect to 3-furaldehyde b) -9 to -6ºC over 40 min c) 0.5 M HCl to pH 7, 98% yield **8**.

Scheme 5.11: Optimal conditions for the aldol reaction between 3-furaldehyde and acetone was conducted from –9 to –6ºC with a catalytic amount of NaOH to produce the furfurol **8** in >98% yield.

^{1}H NMR analysis (Figure 5.3) of **8** shows H(2') and H(5') protons at δ 7.33 and 7.22 respectively with an integral region equal to two protons, and the H(4') signal appears upfield at δ 6.34 with an integral region of one proton, in agreement with the C(3') substituted furan in **8**. The H(4) proton on the butanone chain appears as a double-doublet at δ 5.07 ($J_{4,3A}$ = 8.7 Hz, $J_{4,3B}$ = 3.9 Hz) with coupling constants equal to those observed in double-doublets for H(3_A) ($J_{3A,4}$ = 8.7 Hz, $J_{3A,3B}$ = 17.3 Hz) and H(3_B) ($J_{3B,4}$ = 3.9 Hz, $J_{3A,3B}$ = 17.3 Hz) at δ 2.75 and 2.85. The structure of **8** was confirmed by COSY correlations (Figure 5.3) between the H(5')/H(4') and H(2')/H(4') furan signals as well as cross-peaks between H(4)/H(3) in agreement with the observed ^{1}H NMR coupling constants. ^{13}C NMR data is shown in Appendix 5.4 and shows a C(2) carbonyl signal at δ 209 as well as the expected furan signals in the aromatic region (δ 140 to 100) in agreement with **8**. DEPT 135 NMR is also shown in Appendix 5.4 and features a negatively oriented C(3) peak at δ 50.5 in support of the 3-furfurol structure **8**.

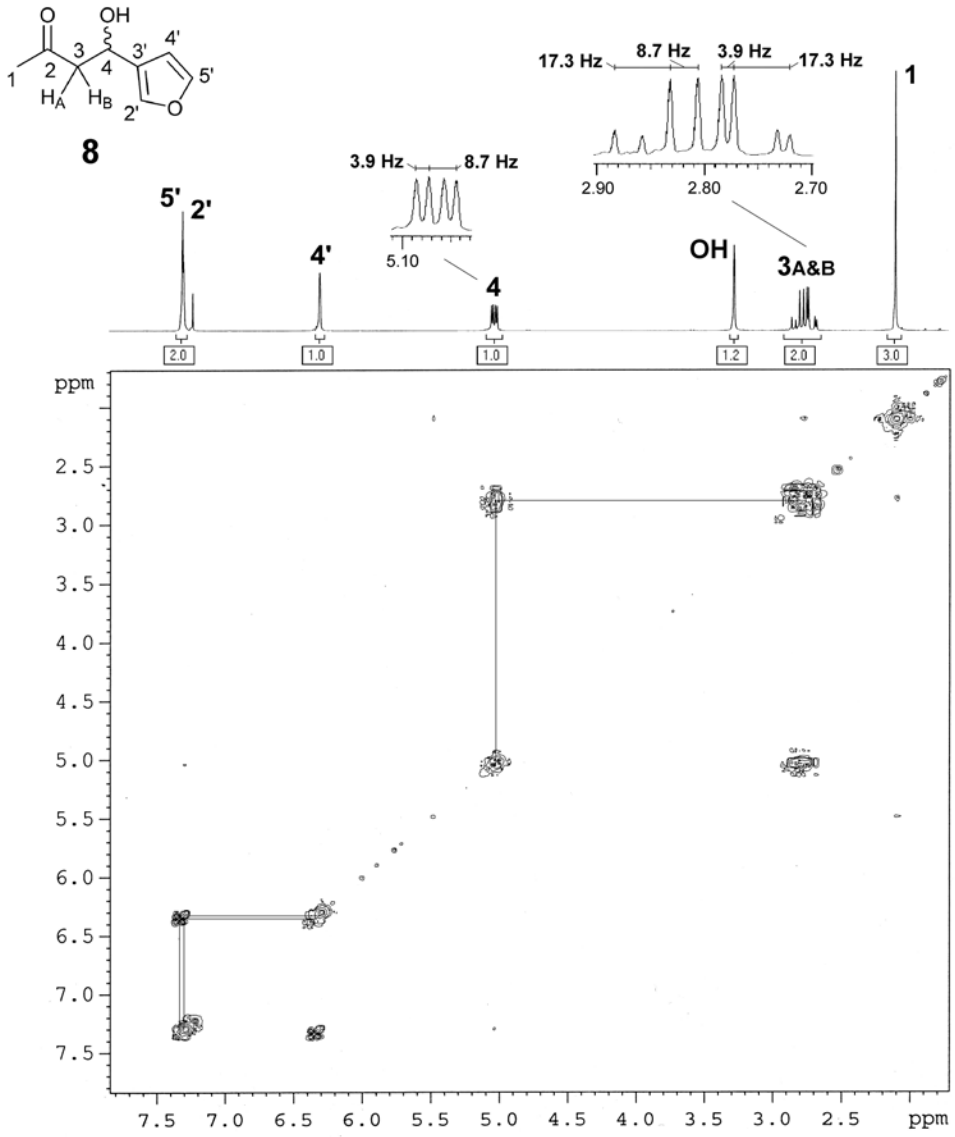

Figure 5.3: 300 MHz ^{1}H COSY NMR analysis of **8** with structural assignments.

Under conditions described by Cardillo *et al.* [21], the drop-wise addition of (*Z*)-2-bromobut-2-enoyl chloride to a mixture of **8** and TEA was carried out in Et_2O at -78ºC (Scheme 5.12). The formation of the ketene was accompanied by the appearance of a deep blue colour, which gradually progressed to dark red as esterification took place and the product **7** was isolated as a red coloured resin in 92% isolated yield. GC-MS analysis of the product mixture (Figure 5.4) indicated a major product at 13:95 min with $M^{+\cdot}$ *m/z* 300, 302 in agreement with the brominated product 1-(furan-3-yl)-3-oxobutyl 2-bromobut-3-enoate (**7**) and other small peaks at t_R = 14:41 and 15:01 min showed the same molecular ion indicative of *syn* and *anti* C(1')/C(2) structural isomers. Results for this reaction were surprisingly

reproducible given that the reaction mixture had a tendency to cake and required mechanical stirring to ensure proper mixing.

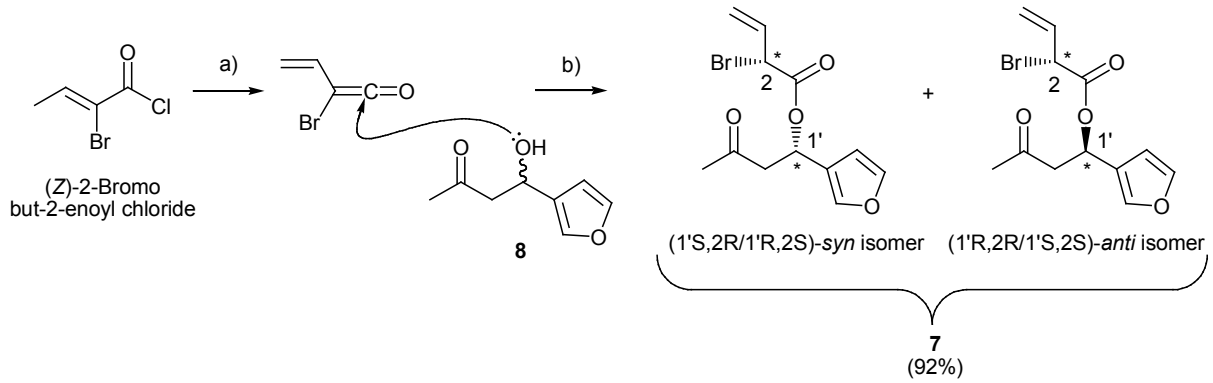

a) TEA, -78ºC, Et_2O b) -78ºC, 45 min, 92% yield

Scheme 5.12: Preparation of **7** was achieved in 92% yield from the reaction of (*Z*)-2-bromobut-2-enoyl chloride with **8** in the presence of TEA at -78ºC.

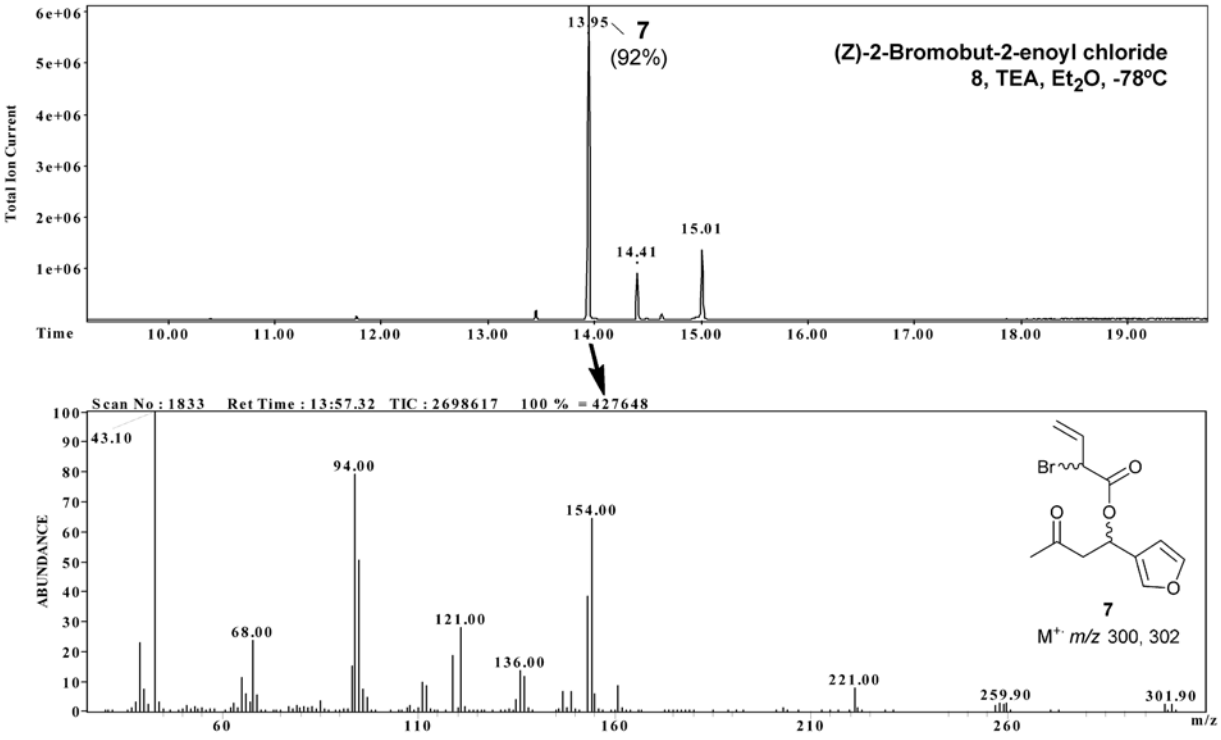

Figure 5.4: GC-MS analysis of the crude esterification of **8** using (*Z*)-2-bromobut-2-enoyl chloride and TEA in Et_2O at -78ºC showing the formation of **7** as the major product at t_R = 13:95 min.

^{1}H NMR analysis of the crude material (Figure 5.5) showed only characteristic signals for the β,γ-unsubstituted ester product, featuring terminal olefinic signals H(4_A) ($J_{4A,3}$ = 10.2 Hz, $J_{4A,4B}$ = 3.4 Hz) at δ 5.27 and H(4_B) ($J_{4B,3}$ = 17.0 Hz, $J_{4B,4A}$ = ~4.5 Hz) at δ 5.37 which may also be coupled with the

vinylic H(2) proton as inferred from the larger geminal coupling for H(4_B). ^{1}H NMR integral regions were found to be in agreement with the expected number of protons for **7** and ^{13}C NMR analysis features C(3') ketone and C(1) ester signals at δ 204.0 and 167.0 in support of the desired product. The expected double-doublet for the furfurol proton H(1') is apparent at δ 6.26 ($J_{1',2A'}$ = 8.1 Hz, $J_{1',2B'}$ = 5.2 Hz) and the notable absence of signals due to structurally related impurities indicates that thermal double-bond isomerization is facile during GC separation and the ester product was in fact obtained as a single olefin isomer.

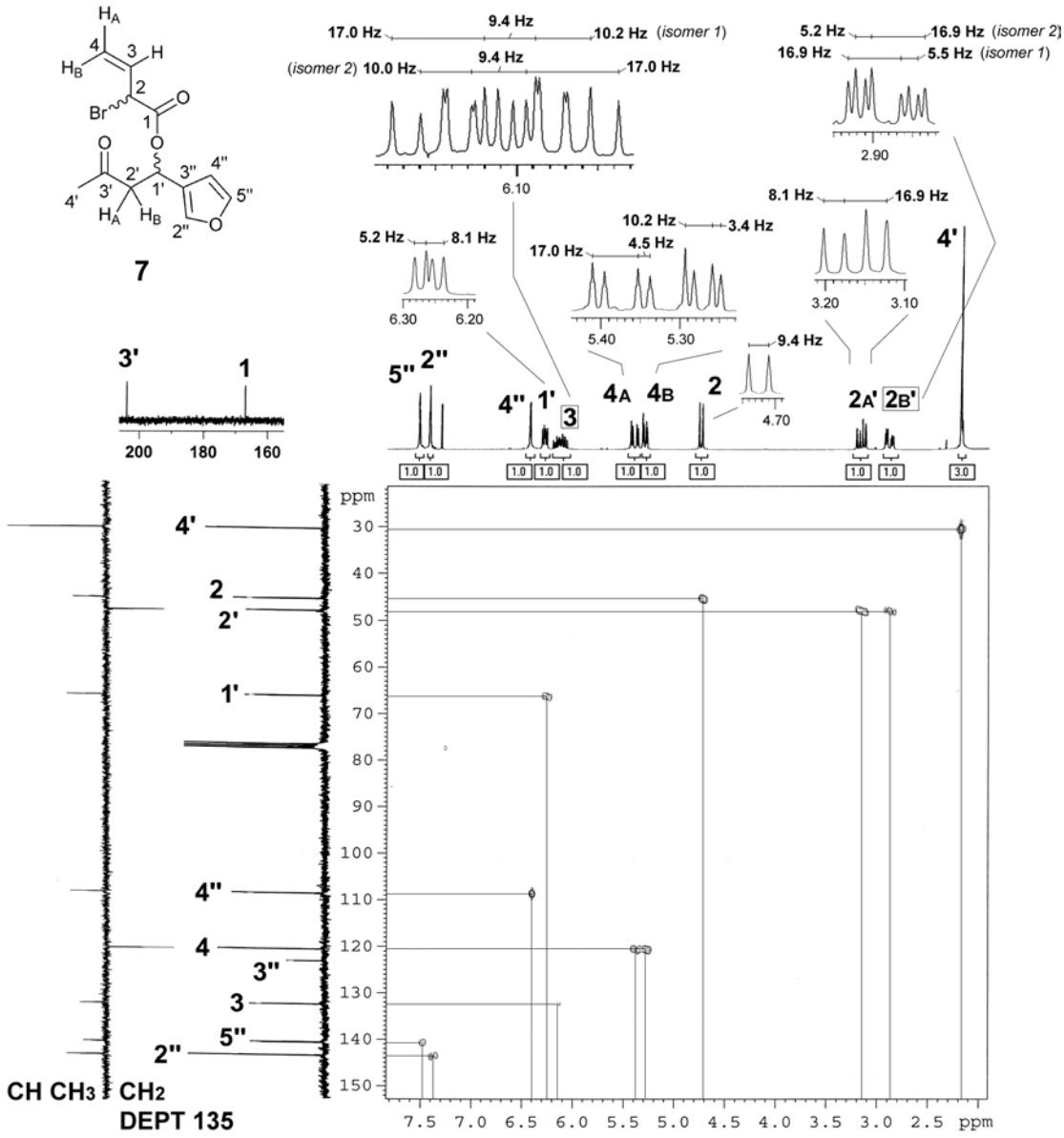

Figure 5.5: 300 MHz ^{1}H/75 MHz ^{13}C HMQC NMR analysis of **7** with structural assignments. The DEPT 135 NMR spectrum of **7** is also shown.

Two sets of clearly resolved but overlapping double-double-doublets are seen for the H(3) olefin signal at δ 6.11 ($J_{3,4B}$ = 17.0 Hz, $J_{3,4A}$ = 10.2 Hz, $J_{3,2}$ = 9.4 Hz, 1H, H-3, *isomer 1*) and δ 6.09 ($J_{3,4B}$ = 17.0 Hz, $J_{3,4A}$ = 10.0 Hz, $J_{3,2}$ = 9.4 Hz, 1H, H-3, *isomer 2*) in closer proximity to the (2) chiral center, suggesting that **7** exists as C(1')/C(2) *syn*/*anti*-diastereomers in nearly equal ratio (Scheme 5.12). Overlapping double-doublets are also observed for the H(2_B') proton signals of each isomer at δ 2.89 ($J_{2B',2A'}$ = 16.9 Hz, $J_{2B',1'}$ = 5.2 Hz, 1H, *isomer 1*) and δ 2.88 ($J_{2B',2A'}$ = 16.9 Hz, $J_{2B',1'}$ = 5.5 Hz, *isomer 2*) in support of this conclusion, and all other ^{1}H NMR signals are completely overlapped including the H(2_A') double-doublet ($J_{2A',2B'}$ = 16.9 Hz, $J_{2A',1'}$ = 8.1 Hz) at δ 3.16.

Structural NMR assignments for **7** were made using HMQC NMR data (Figure 5.5) which features cross peaks for C(2') at δ 48.0 correlating to the H(2') methylene protons, as well as C(4) at δ 120.6 correlating to the H(4) olefin protons and both ^{13}C NMR signals appear negatively oriented in DEPT 135 data in agreement with the structure of **7**. A closer look at the ^{13}C NMR spectrum showed two sets of signals of almost equal intensity for each diastereomer and these chemical shifts are labeled on the HMBC spectrum shown in Appendix 5.5 although each isomer was not individually assigned. COSY NMR of **7** (Appendix 5.6) was found to contain the expected correlations between H(1') with H(2_A')/H(2_B'), as well as H(3) with H(4_A)/H(4_B)/H(2).

Formation of the α,β-unsaturated ester (*Z*)-1-(furan-3-yl)-3-oxobutyl 2-bromobut-2-enoate (**37**) was encouraged during the esterification of **8** at temperatures above -78ºC, or upon the exclusion of TEA from the reaction mixture. Isomerization from the β,γ-unsaturated compound **7** to the conjugated ester **37** was facile during purification attempts by vacuum distillation and FCC on SiO_2 (pentane:EtOAc, 4:1) (Scheme 5.13) as shown by the appearance of a peak in GC-MS analysis (t_R = 14:24 min) with molecular ions *m/z* 300, 302 corresponding to an isomer of **8** (Appendix 5.7). The conjugated ester **37** was isolated in high purity after multiple FCC elutions and the identity of the product was confirmed by COSY NMR analysis (Figure 5.6) to be a single compound. Cross-peaks are observed between the H(3) olefinic quartet at δ 7.34 ($J_{3,4}$ = 6.8 Hz) and the H(4) methyl group which appears as a large doublet at δ 1.93 ($J_{4,3}$ = 6.8 Hz) and integrates as three protons. The expected correlations are also observed for the H(1') signal at 6.28 and H(2_A')/H(2_B') at δ 3.20 and 2.91. NMR assignments for **37** were confirmed by HMQC and DEPT 135 analyses as shown in Appendix 5.8.

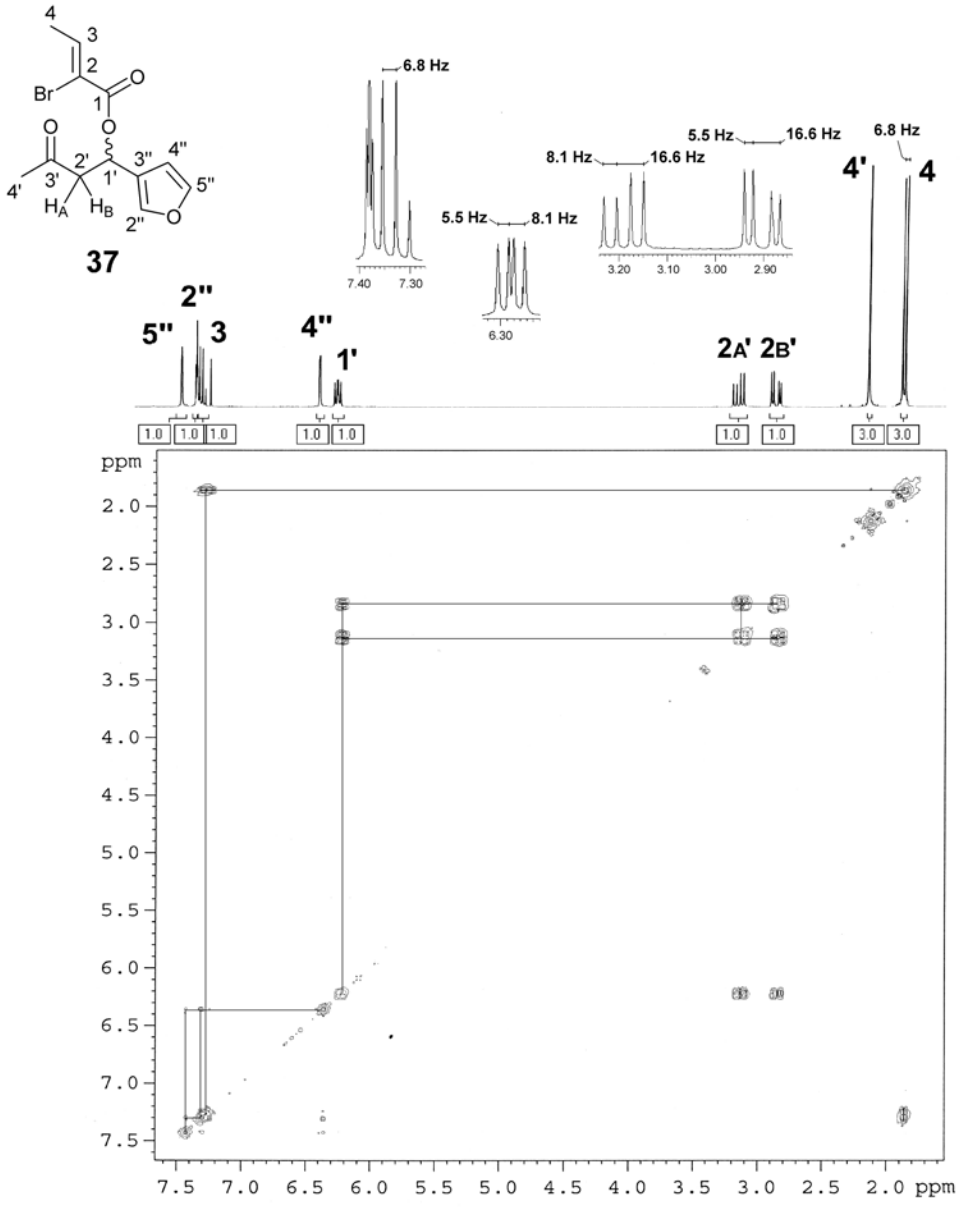

Figure 5.6: 300 MHz ^{1}H COSY NMR of the conjugated ester **37**.

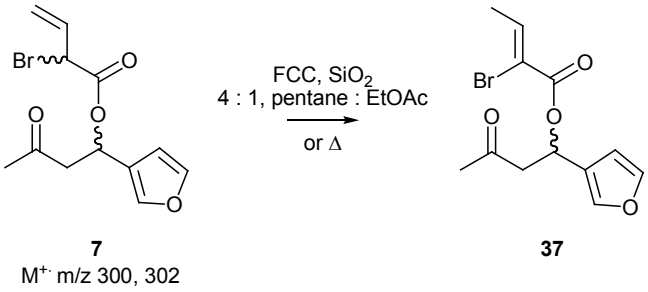

Scheme 5.13: Isomerization of **7** to the α,β-unsaturated ester **37** occurred during column chromatography or heating of **7**.

Following the development of a simple approach to the α-bromo-β,γ-ester **7**, studies towards the δ-lactone ring closure were pursued using the halogen as a point for metal insertion so it may act as a nucleophile for intramolecular reaction with the ketone carbonyl. The next section describes the formation of the cyclic ester **6** by mean of intramolecular ring closure using the zinc mediated Reformatsky reaction and outlines the relevant literature.

*5.2.3 Preparation of 6-(Furan-3-yl)-5,6-dihydro-4-methyl-3-vinylpyran-2-one (**6**)*

Although studies by Zhu *et al.* [1] (Scheme 5.9, bottom) report the organozinc approach to be unsuccessful for the bromoacetyl lactone closure, the allylic organozinc system present in **7** offers a higher degree of stabilization for the organometallic product due to electron delocalization involving the olefin. For this reason, functionalized allylic zinc reagents have been exploited in synthesis and literature by Knochel *et al.* [24] gives a discussion of the history and scope of organozinc chemistry, highlighting the selective nucleophilicity of RZnX type organozinc towards aldehyde, ketone and acid chloride carbonyl electrophiles, but relative inertness to ester groups. As such, the reactivity of organozinc compounds can allow compatibility for the presence of both ester and organozinc functionalities in the same system. In many ways the organozinc nucleophile behaves like a Grignard reagent and studies by Vaughan *et al.* [25] on the Reformatsky reaction of ethyl 2-bromo-2-methylpropanoate suggest that the bromozinc enolate of the ester to be the reactive intermediate involved in this system (Scheme 5.14, top). This conclusion was based on their IR studies showing the disappearance of the ester absorbance at 1730 cm^{-1} and appearance of zinc-oxygen absorption band at 1525cm^{-1}.

Dreiding *et al.* [26] have prepared the Reformatsky reagent from methyl 4-bromocrotonate in a number of solvents and report solvent effects to influence γ- or α-addition of the allyl organozinc to the carbonyl during the reaction with a range of cyclohexanones. Reactions conducted in 1,2-dimethoxyethane (1,2-DME) were reported to occur at the γ-position to give the cyclohexanol product in 39% yield. Saponification followed by dehydration with Ac_2O/HCOOH was reported to yield the endocyclic cyclohexenone in 57% with a small amount of the exocyclic conjugated carboxylic acid (15%) (Scheme 5.14, middle).

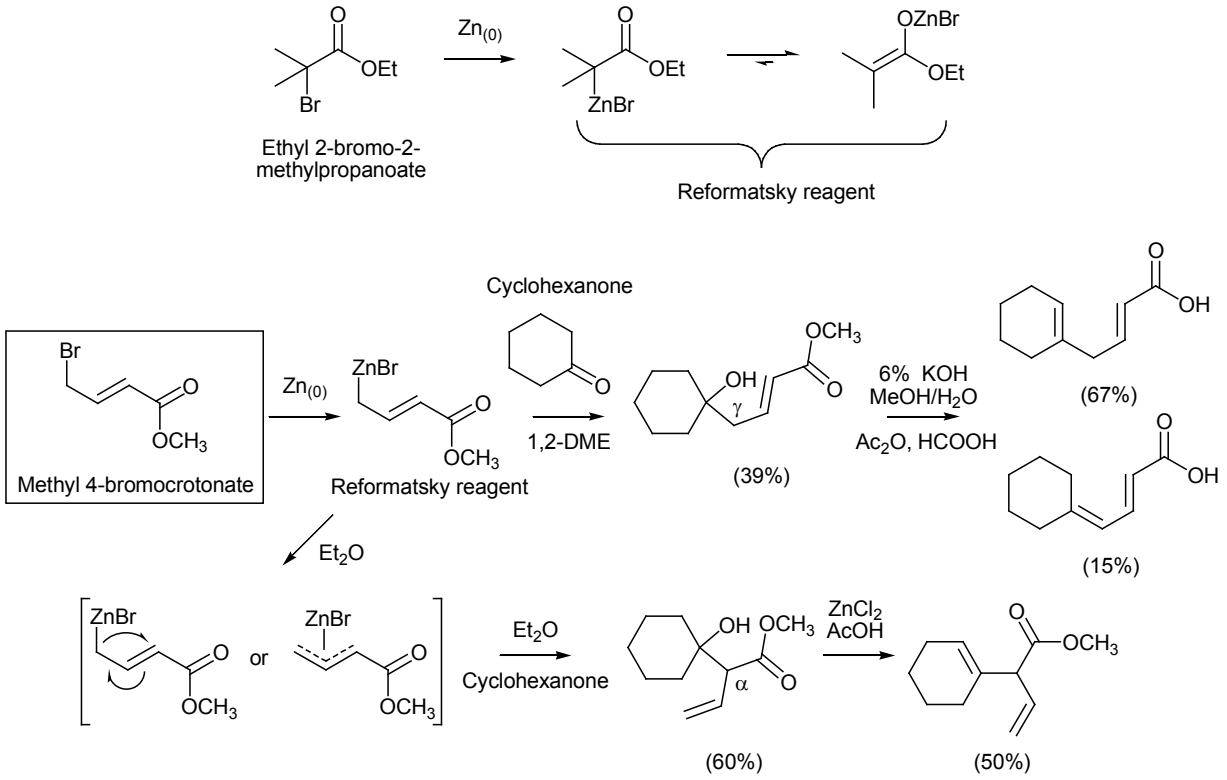

Scheme 5.14: Top; Vaughan *et al.* [25] report the preparation of the ethyl 2-bromo-2-methylpropanoate Reformatsky reagent and suggest the organozinc compound to exist as the bromozinc enolate based on IR experiments. Middle and bottom; Dreiding *et al.* [26] report the reaction between the methyl 4-bromoacetate Reformatsky reagent and cyclohexanone to yield the γ-addition product when conducted in 1,2-DME. The α-addition product predominated upon reaction in Et_2O and the alcohol was successfully dehydrated to the endocyclic product.

The authors report reactions conducted in Et_2O to behave differently, producing the α-addition product with cyclohexanone in 60% yield (Scheme 5.14, bottom) which was dehydrated using $ZnCl_2$/AcOH to form the endocyclic cyclohexenone product exclusively in 50% yield. More hindered substituted cyclohexanones were reported to yield the γ-product preferentially and the authors suggest steric hinderence and solvent effects to be determining factors in this type of Reformatsky reaction, but do not comment on whether a metalide shift or stabilized allyl complex are involved as intermediates.

It was hoped that the Reformatsky reagent prepared from the vinyl ester **7** (Scheme 5.15) would intramolecularly react with the C(3') carbonyl to form the energetically favoured six-membered ring. The C(4) alcohol intermediate can be dehydrated under acidic conditions or using methodology described by Dreiding *et al.* [26] to give the convergent target **6**. A proposed mechanism is shown in Scheme 5.15 and involves the bromozinc enolate as described in studies by Vaughan *et al.* [25].

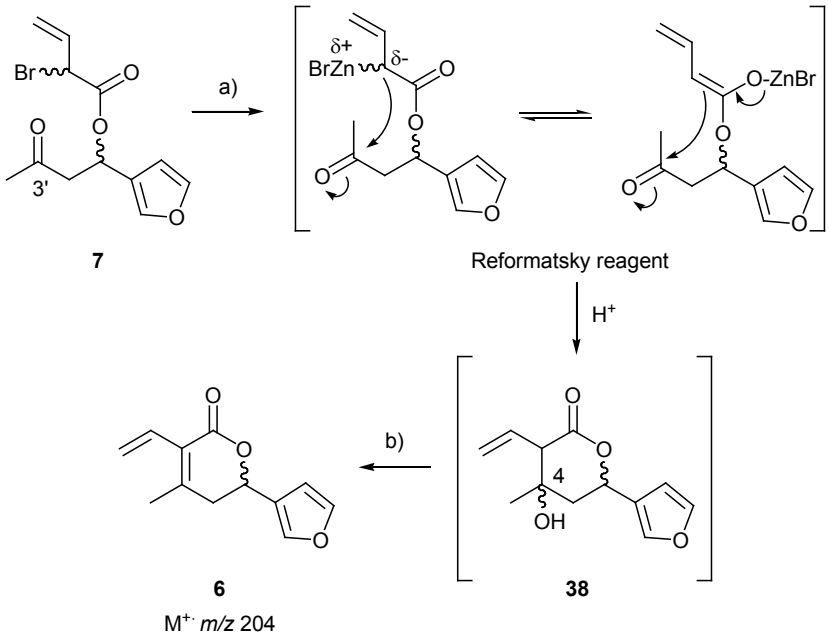

a) THF, Rieke Zinc (3 equiv.) at 0ºC then 70ºC for 5 h b) 2 M HCl, r.t., 1 h, 92%.

Scheme 5.15: Lactone closure of **7** was achieved by formation of the Reformatsky reagent using Rieke Zinc to affect intramolecular ring closure with the C(3) ketone and a proposed mechanism is shown based in research by Vaughan *et al.* [25]. The alcohol C(4) **38** was not observed and the conjugated dihydro-pyranone **6** was isolated in 92% after stirring with 2 M HCl at ambient temperature.

An experimental procedure for the Reformatsky mediated ring closure of **7** was adapted from the literature by Knochel *et al.* [24]. Commercially available Rieke Zinc (5%w/v suspension in THF, Aldrich) was used as a highly reactive form of zinc metal to improve the yield of organozinc formation and the reaction was conducted in THF rather than Et_2O to give a larger solvent boiling range. Reaction of the ester **7** with three equivalents of Rieke Zinc in dry THF at 0ºC and no detectible lactone formation was observed by GC-MS monitoring during warming to 40ºC. The reaction was heated at reflux, which was required for five hours for complete consumption of the halide, then the mixture was quenched in 2 M HCl and allowed to stir for 1 h. GC-MS analysis of the Et_2O extract showed a single major product at t_R = 14:17 min with a molecular ion at *m/z* 204 in agreement with the dehydrated product **6**. The intermediate alcohol **38** was not observed in the GC trace indicating that prolonged stirring in the acidic quenching mixture was sufficient to achieve selective dehydration for a single diene product. The major product was purified by FCC on SiO_2 using gradient elution with pentane:EtOAc (20:1 to 8:1) to yield a deep yellow resin in high recovery.

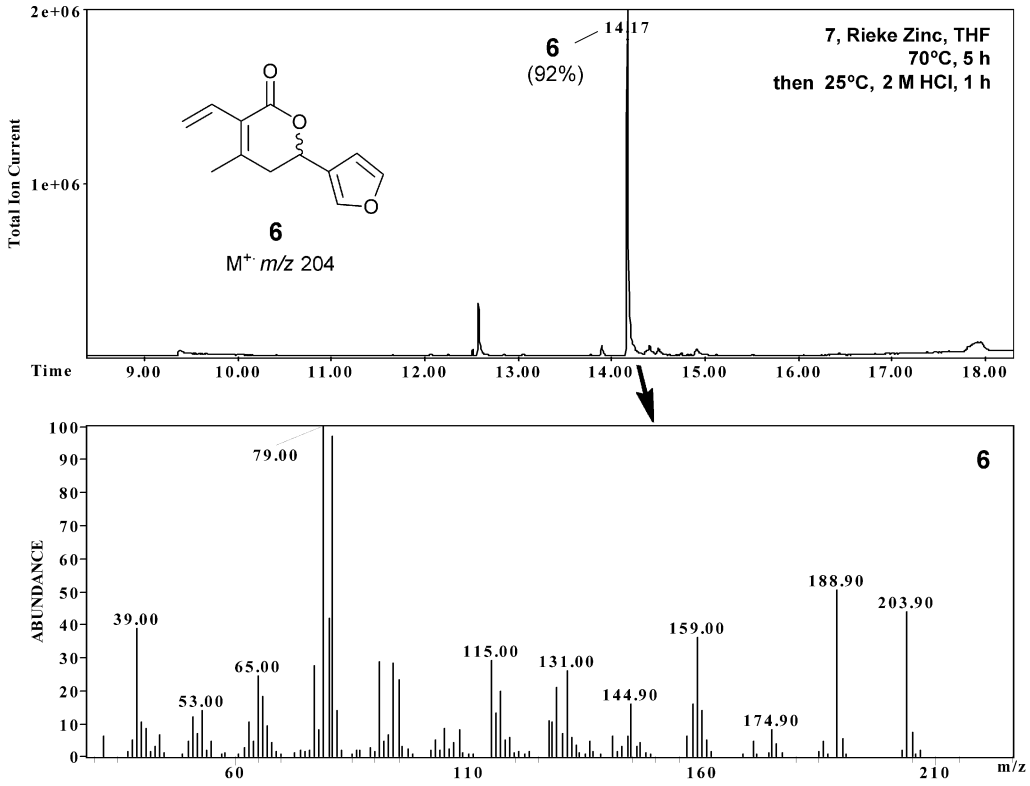

Figure 5.7: GC-MS analysis of the crude Reformatsky product mixture shows the formation of the target dihydro-pyranone **6** as the major product at t_R = 14:17 min in 92% yield, as identified by a $M^{+\cdot}$ ion at *m/z* 204.

^{1}H NMR characterization (Figure 5.8) indicated a single compound with the expected number of signals at frequencies in close agreement with predicted Chemdraw values for **6**. Broad peaks for the protonated furan signals at δ 7.49 (H-5'), 7.42 (H-2') and 6.45 (H-4') are present in the same regions as seen in **7** and **8**, and the H(9) methyl signal is present as a 3H singlet at δ 2.11 with an integral area of three protons. This suggests that the endocyclic dehydration of **38** had occurred and the presence of double-doublets at δ 2.78 ($J_{5A,5B}$ = 18.1 Hz, $J_{5A,6}$ = 11.5 Hz) and 2.54 ($J_{5B,5A}$ = 18.1 Hz, $J_{5B,6}$ = 3.8 Hz) for H(5_A) and H(5_B) respectively confirmed that the olefin is in conjugation with the ester carbonyl, consistent with the 6-(furan-3-yl)-5,6-dihydro-4-methyl-3-vinylpyran-2-one product **6**. The H(6) methine signal appears as a double-doublet at δ 5.35 ($J_{6,5A}$ = 11.5 Hz, $J_{6,5B}$ = 3.8 Hz) and coupling constants are consistent with those observed for the H(5) protons. The terminal olefinic protons H(8_A) and H(8_B) are present as broad double-doublets at δ 5.72 ($J_{8B,7}$ = 17.7 Hz) and δ 5.47 ($J_{8A,7}$ = 11.5 Hz) and the H(7) olefin appears as a double-doublet at δ 6.55 ($J_{7,8B}$ = 17.7 Hz, $J_{7,8A}$ = 11.5 Hz), consistent with C(3) vinyl substituent on the dihydro-pyranone **6**.

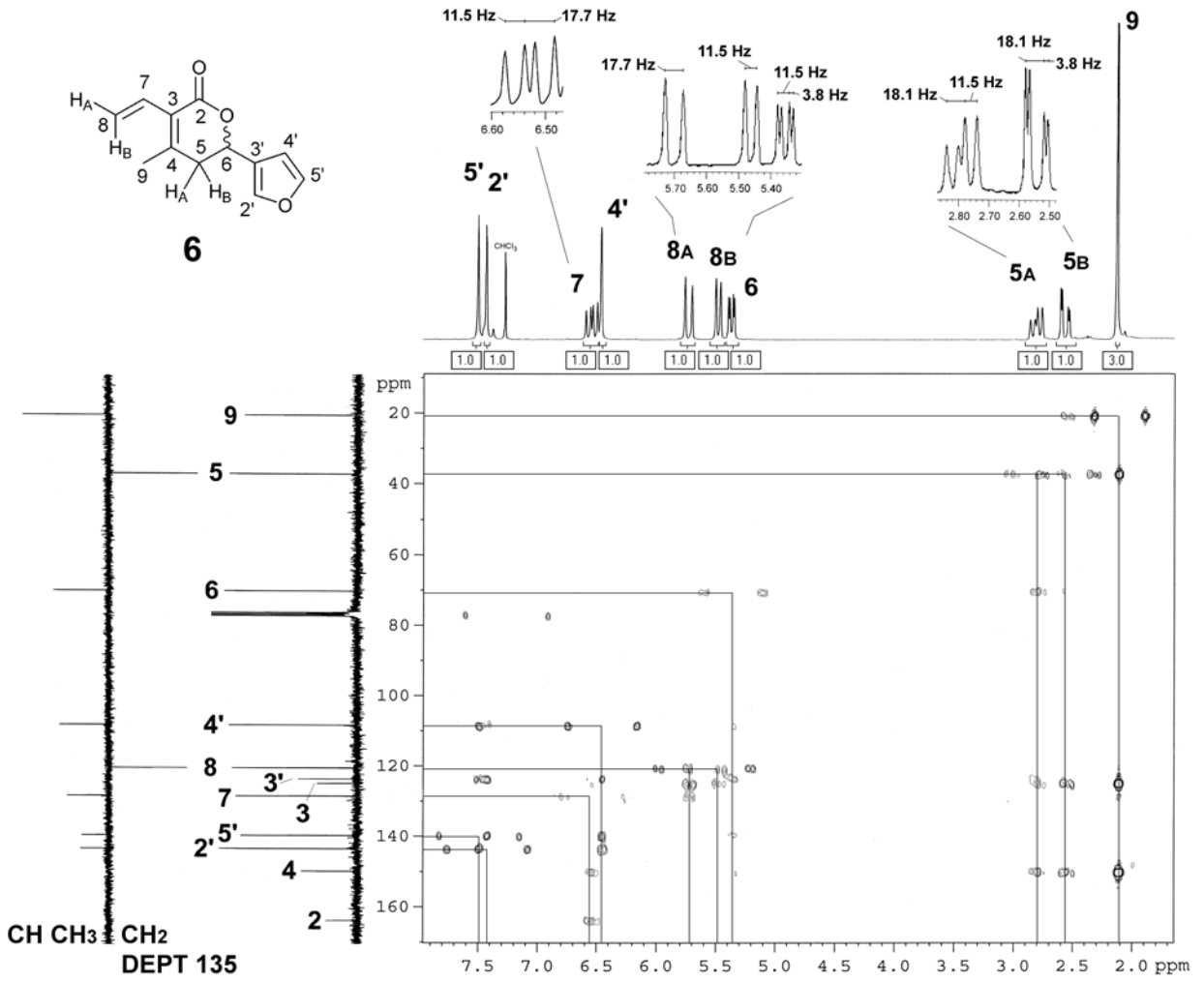

Figure 5.8: 300MHz ^{1}H/75 MHz ^{13}C HMQC NMR analysis of **6** with structural assignments shown. DEPT 135 NMR data is also included.

^{13}C and DEPT 135 NMR analyses (Figure 5.8) were used to confirm signals due to non-protonated carbons C(2), C(4), C(3) and C(3'), as well as the methylene carbons C(8) and C(5). The connectivity of **6** was verified and NMR structural assignment made using HMBC analysis (Figure 5.8). The H(9) methyl shows strong long range correlations to C(5), C(8) and C(4) at δ 37.7, 121.0 and 150.3 respectively and H(5_A)/H(5_B) methylene signals show cross-peaks with C(6) at δ 70.8, C(8) and C(4). Attachment of the vinyl group was confirmed by correlation of the H(8_A)/H(8_B) methylene signals with C(3) (δ 125.4) and C(7) (δ 128.9), and COSY correlations (Appendix 5.9) as well HMQC NMR data (Appendix 5.10) support the assigned structure of **6**. The chemical formula of **6** was confirmed by ESI-HRMS to provide an accurate mass for the $[M + Na]^{+\cdot}$ ion $C_{12}H_{12}O_3Na$ in agreement to three decimal places of the theoretical value (227.0684 calc., *m/z* 227.0677 found).

The surprising absence of the alcohol **38** in the crude product mixture of **6** prompted a brief study involving quenching of the Reformatsky reaction with alternate media to address whether dehydration to the C(3)/C(4) olefin occurs spontaneously or is mediated by the acidic conditions. Conditions for the reaction between Rieke zinc and **7** were followed as described in Scheme 5.15 and the reaction was quenched in a biphasic solution of 1 M HCl/Et_2O and allowed to stir for only 15 min before workup and purification by FCC on SiO_2 as described for **6**. GC-MS analysis indicated one major product at t_R = 14:49 min that featured a molecular ion at *m/z* 222 in agreement with the molecular weight of the alcohol **38**. A smaller peak at t_R = 14:37 min was found to have an almost identical EI-MS fragmentation to the major product and can be identified as one of a number of possible C(3)/C(4)/C(6) diastereoisomers (Scheme 5.16).

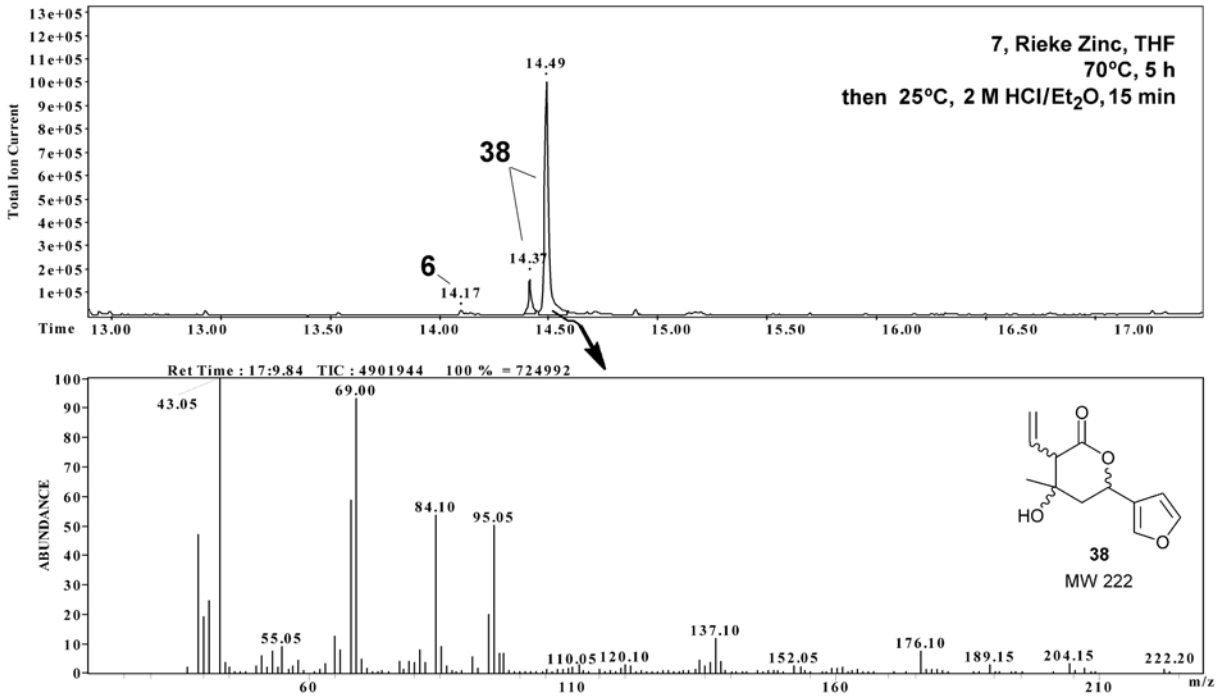

Figure 5.9: GC-MS analysis for the Reformatsky reaction of **7** shows two diastereoisomers of the alcohol **38**.

The major product was characterized using HMQC and DEPT 135 NMR data (Appendix 5.11) and confirmed as the C(4) substituted δ-lactone by the appearance of a doublet at δ 3.00 ($J_{4,3}$ = 9.1 Hz) corresponding to the H(3) proton at the α-carbonyl position. The presence of a C(4) quaternary signal in the aliphatic region at δ 71.1, as well as a broad hydroxy resonance at δ 2.50 are in agreement with the assigned structure of **38**. The minor isomer could not be fully characterized by NMR analysis and energy minimized models were calculated using Chem3D (MM2) to provide a comparison of the steric energy of various conformations of **38** (Scheme 5.16). The (6*S*)-**38** diasteromer of the δ-lactone is present in **1**

and was modeled for each C(3)/(C4) distomer to indicate the *trans*-C(3)/C(4) geometry as sterically favoured compared to the *cis*- oriented methyl and vinyl groups. ^{1}H NMR signals for the major isomer of **38** include a double-doublet for H(6) at δ 5.73 ($J_{6,5B}$ = 11.9 Hz, $J_{6,5A}$ = 3.4 Hz) indicative of a *trans*-diaxial relationship between H(6)/(5_B) as observed in **3** (Section 4.2, Figure 4.7). Energy minimized structures for the chair conformer of (3*R*,4*R*,6*S*)-**38** and (3*S*,4*S*,6*S*)-**38** were calculated to have similar values (Scheme 5.16) and in the case of (3*S*,4*S*,6*S*)-**38** an alternate pseudo-chair conformation was found as a theoretically favored geometry showing a gauche H(6)/H(5) arrangement.

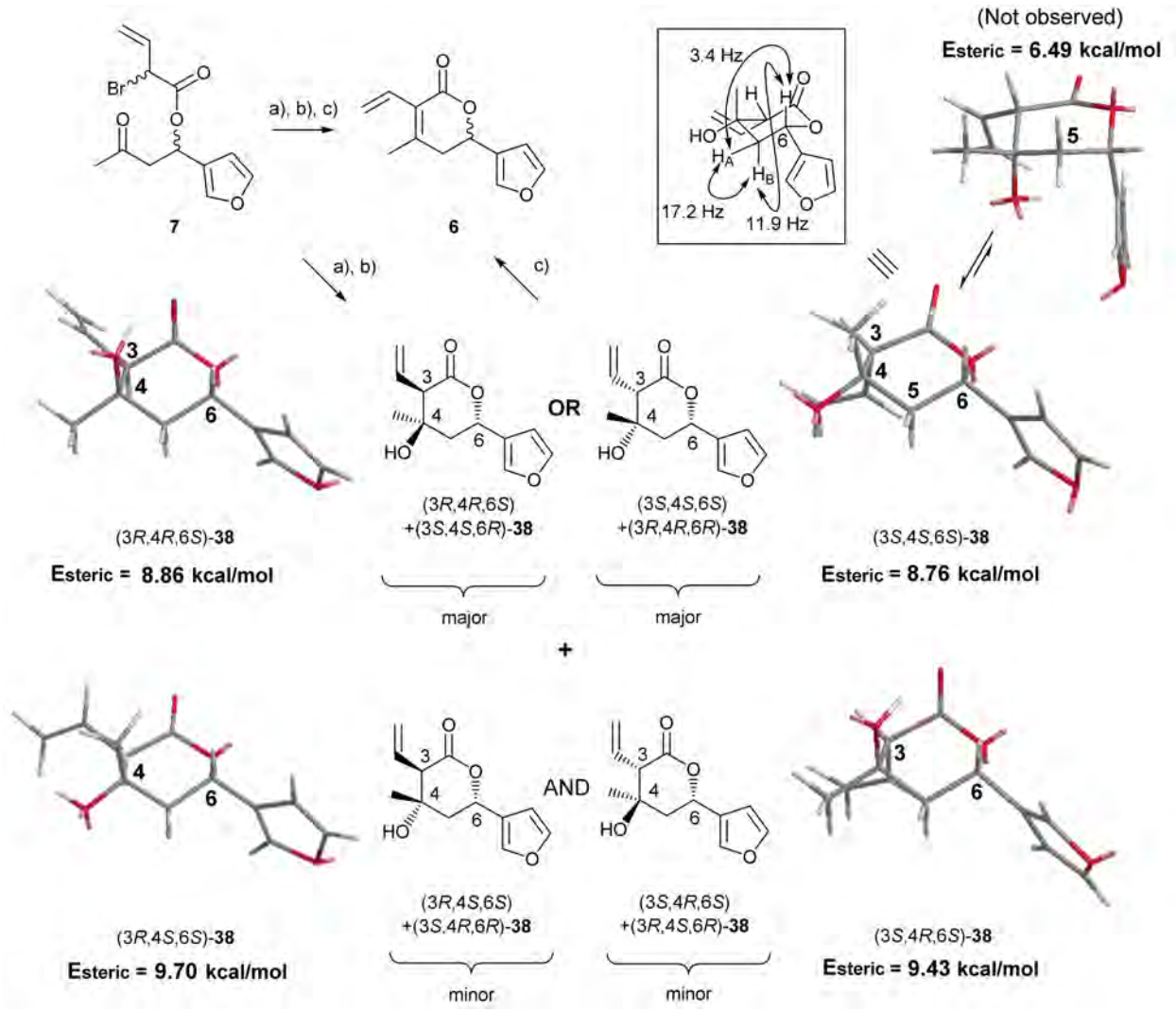

a) THF, 3 equiv. Rieke Zinc in THF at 0ºC, 70ºC for 5 h b) 1 M HCl/Et_2O, 15 min c) 2 M HCl, r.t., 1 h, 92%.

Scheme 5.16: Lactone closure of **7** was achieved under Reformatsky conditions and the alcohol **38** was isolated upon quenching in 1 M HCl/Et_2O. Energy minimized models of the chair conformations for diastereoisomers of **38** were calculated using Chem3D (MM2) and are shown with values for steric energy. The *trans*-C(3)/C(4) products (3*R*,4*R*,6*S*)-**38** and (3*S*,4*S*,6*S*)-**38** were calculated as the favoured isomer.

Contrary to this result, coupling constants characteristic of the gauche conformation between H(6)/H(5), as seen in C(5)-epi-**3** (Section 4.2, Figure 4.10), were not observed. Both the major and minor isomers were found to have similar coupling constants (Appendix 5.11) in agreement with the calculated chair geometry for the *anti*-C(3)/C(4) products of **38**. Experiments to differentiate (3*R*,4*R*,6*S*)-**38** from (3*S*,4*S*,6*S*)-**38** isomers were not pursued due to time constraints.

Positive identification of the alcohol **38** indicates that the 2 M HCl quenching solution, described the procedure shown in Scheme 5.16, provides a sufficiently acidic environment for dehydration of **38** to yield the α,β-unsaturated product **6** exclusively. Since **38** formed as a single isomer in high yield (92%) and purity, this pathway appears advantageous as a direct preparation of δ-lactones with analogous functionality.

In conclusion an efficient and high yielding synthesis for the racemic precursor 6-(furan-3-yl)-5,6-dihydro-4-methyl-3-vinylpyran-2-one (**6**) has been developed using cheap and readily available precursors. Relevant intermediates and products have been fully characterized by NMR and MS analysis and analytical data is listed in Section 6.9.3. The work presented in Chapter 4 and Chapter 5 has been published as a journal manuscript [27] and this section in the current work concludes the synthetic studies completed in this project. Preliminary studies towards the (6*S*)-**6** chiral precursor are outlined in the following section with a discussion of future work and concluding remarks.

5.3 Preliminary Studies Towards the Synthesis of (S)-6-(Furan-3-yl)-5,6-dihydro-4-methyl-3-vinylpyran-2-one ((S)-6) and Future Work

Preliminary efforts towards the stereoselective synthesis of **6** have involved the investigation of a chiral aldol reaction between acetone and 3-furaldehyde. The catalytic asymmetric aldol reaction has been reviewed by Machajewski *et al.* [28] and is a very valuable tool in organic synthesis. The C(4) alcohol is a newly created stereocenter of the aldol product **8** and correlates to the C(6) chiral center of **6** and the C(8) stereocenter of **1**. The (*S*)-**4** configuration is desired for the asymmetric natural product synthesis and asymmetric catalysis using the amino acid proline was researched in hope that the commercially available catalyst could be conveniently recycled.

Asymmetric synthesis using L-proline has been described in Chapter 1 (Scheme 1.3) and recently List *et al.* [29] have shown that L-proline can often be used alone for enantioselective reactions since the molecule is bifunctional, containing both the acidic carboxylic acid and basic amine functional

groups. The scope of proline catalyzed organic reactions is reviewed in literature by List [30] along with a proposed mechanism addressing the bi-functional role of proline in the aldol reaction of acetone, as shown in Scheme 5.17. Crossed-aldol proline catalysis has since been used by Pihko *et al.* [31] for the preparation of chiral lactones in excellent enantioselectivity (>99% *ee*) and further studies have been discussed by Peng *et al.* [32] who conduct their experiments in aqueous micelles.

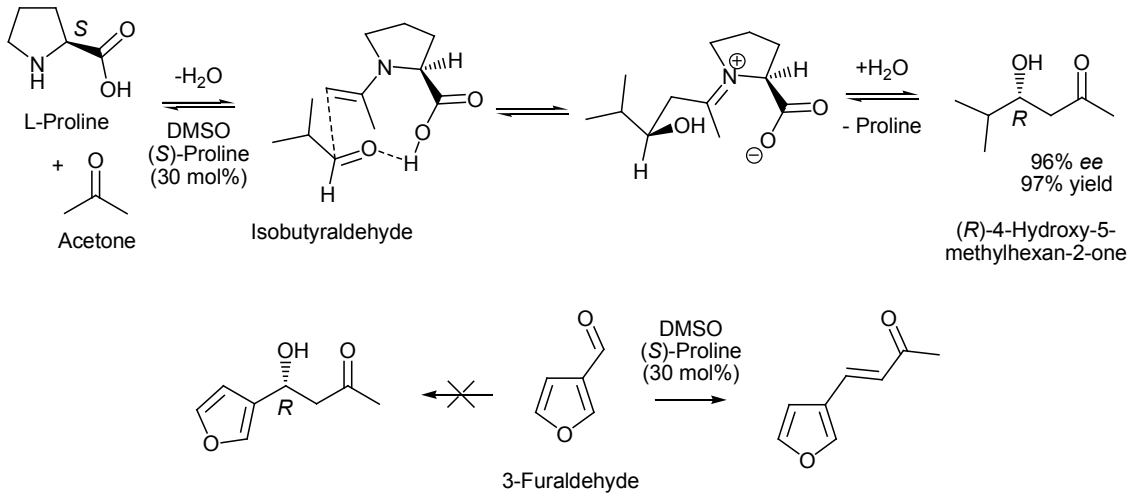

Scheme 5.17: Top; A proposed mechanism by List *et al.* [29] for the L-proline catalyzed aldol addition, shown using the reactants acetone and isobutyraldehyde which have been reported to produce the (*R*)-4-hydroxy-5-methylhexan-2-one in high optical and yield. Bottom; The reaction of 3-furaldehyde did not produce the optically enriched alcohol and only the dehydration product was observed.

The reaction 3-furaldehyde with acetone was carried out in the presence of L-proline following methodology by List *et al.* [29] and GC-MS monitoring revealed that the aldol alcohol was not formed and only a small amount (<5%) of the dehydrated α,β-unsaturated product was detected. Other methods to introduce chirality into the 1,3-ketoalcohol system were sought including resolution of the racemic mixture. Kinetic resolution of racemic furfuryl alcohols using the Sharpless reagent ($Ti(OiPr)_4$/*t*-BuO_2H/L-(+)-DIPT) has been discussed by Kobayashi *et al.* [33] to access enantiomerically pure (1*R*,3*R*)-1-(furan-2-yl)-3-(tetrahydro-2H-pyran-2-yloxy)butan-1-ol in excellent yield. Reaction of 2-furyllithium with the optically pure aldehyde (*R*)-3-(tetrahydro-2H-pyran-2-yloxy)butanal was reported to produce the racemic C(1) alcohol and diastereoselective oxidation of the (1*S*)-enantiomer allowed the isolation of the optically enriched (1*R*,3*R*)-enantiomer in high yield (Scheme 5.18).

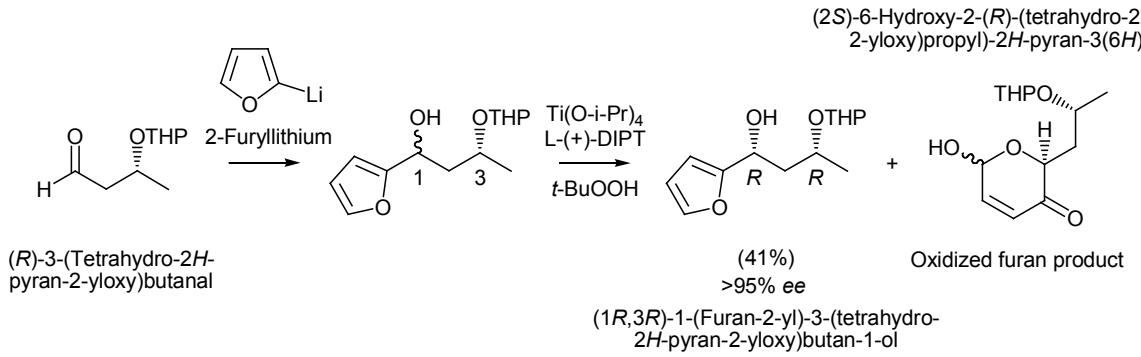

Scheme 5.18: Kobayashi *et al.* [33] have prepared (1*R*,3*R*)-1-(furan-2-yl)-3-(tetrahydro-2H-pyran-2-yloxy)butan-1-ol in high optical purity by kinetic resolution of the racemic C(1) alcohol in excellent yield.

It occurred that the single enantiomer (*S*)-**6** can be obtained by either a chiral aldol reaction with selectivity for the (*S*)-**8** enantiomer, kinetic resolution as described above, or by chemoenzymatic hydrolysis of the ester **7** or pyranone **6** as has been briefly mentioned at the end of Section 4.1.2. These directions are a focus for future studies to complete an asymmetric synthesis of the convergent precursor (*S*)-**6**.

The final goal in this synthesis is the joining of ring **A** and **C** and current ideas for this last transformation are proposed. The Gilman addition to **2** is described in Section 4.5 and this step allows for trapping of the TMS-enolate as an intermediate reactant for the subsequent reaction (Scheme 5.19).

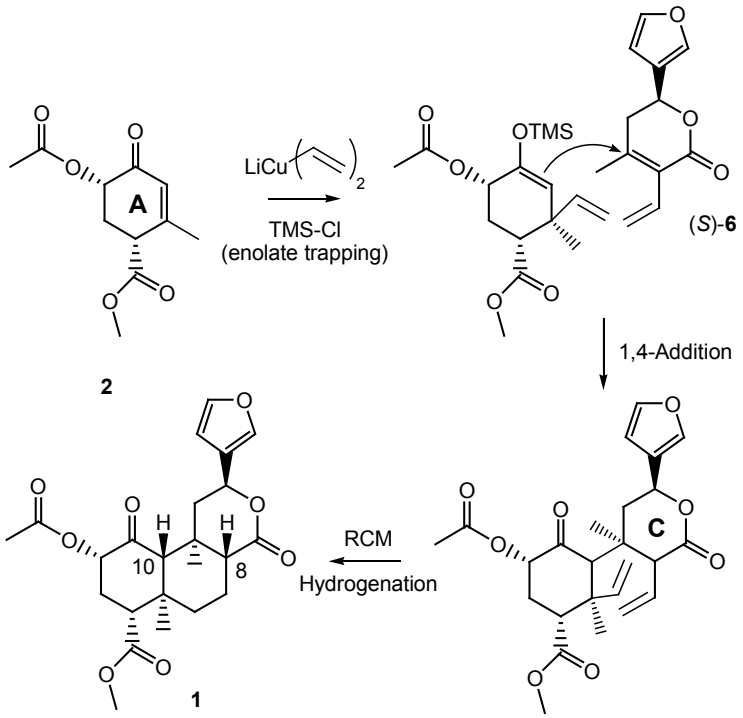

Scheme 5.19: Proposed synthetic methodology for the joining of rings **A** and **C** to prepare the target **1**.

1,4-Addition of the enolate to (*S*)-**6** provides the terminal dienes from both convergent molecules for ring closure metathesis (RCM) using Grubbs ruthenium based catalysts [34]. Hydrogenation of the metathesised product is proposed to yield the natural product **1** leaving an ambiguous stereochemical outcome at chiral centers adjacent to the C(8) ester and C(10) ketone carbonyls, which can be equilibrated to their most stable configuration **1** under basic conditions if necessary.

5.4 Thesis Conclusions

In the current work, a novel synthetic pathway towards the *trans*-neoclerodane natural product salvinorin A (**1**) has been investigated using primarily newly synthesized molecules. Products and intermediates were characterized using NMR and MS analyses and the final products confirmed by HRMS. An asymmetric synthesis has been completed for the ketone ring **A** of the diterpene **1** and a successful pathway to the lactone ring **C** has been devised using racemic precursors. These new compounds have been synthesised as convergent precursors to be used in a totally non-linear synthesis of the neoclerodane backbone of **1**.

In Chapter 2 a simple sequence for the preparation of 3-furylamines (**5**) has been devised and provided access to a large number 3-furylamine containing structures that were previously scarce in the literature due to their complicated preparation and low stability. The chemical stability of secondary substituted 3-furylamines has been shown to be low, although the tertiary substituted compounds were revealed to be synthetically useful as they can be stored and distilled. A trend towards greater stability was encountered upon increasing the size of the amine group and this result was considered during the selection of an appropriate chiral auxiliary for the commencement of an asymmetric synthesis. 3-Furylamine moieties were incorporated into optically pure amine auxiliaries to be used as chiral dienes for a D-A approach toward ring **A**, as suggested from the retrosynthetic analysis of **1**.

In Chapter 3 the Diels-Alder reaction between selected non-chiral 3-furylamines and methyl acrylate were thoroughly investigated. The reactivity of 3-furylamines towards Diels-Alder cycloaddition in organic reaction media was generally low when conducted in hydrocarbon solvents (hexane, benzene, toluene) but excellent results were achieved in the chlorinated solvent DCM. Diels-Alder reactions when conducted in water were found to give the best results and an increase in solvent polarity was accompanied by enhancement of the reaction rate to give a high yield of cycloadducts in short reaction times. Hydrolysis of the enamine cycloadducts occurred *in situ* allowing alkyl substituted 3-furylamines

to be reacted quantitatively and without polymerization of reactive intermediates. The preparation of useful quantities of the 7-oxanorbornanone intermediate **4** was achieved using this aqueous methodology, which also proved general for the reaction of larger aralkyl substituted 3-furylamines. Ephedrine derived 3-furylamines were found be reactive Diels-Alder dienes in DCM or water and the optically enriched ketones **4a-b** were quantitated using chiral gas chromatographic analysis. The absolute stereochemistry of the major enantiomer was determined by derivatization of **28** followed by identification of the single recrystallized diastereoisomer (1*S*,2*S*,4*S*,5*S*)-**29.HClO$_4$** using x-ray crystallography. Comparison with chiral gas chromatography results demonstrated that both ephedrine isomers direct facial Diels-Alder selectivity towards the (1*S*,4*S*)-**4** products. This indicates that the optically enriched *exo*-bicyclic ketone **4b** has the correct stereochemistry to be used in an asymmetric synthesis of **1**. The preparation of non-racemic 3-furylamines and application as Diels-Alder dienes represents a previously unreported strategy towards chiral 7-oxanorbornanes as useful chiral intermediates for organic synthesis.

Chapter 4 focuses on synthetic transformations of the 7-oxanorbornane structure **4**. The reactivity of the new compounds **4a-b** towards ether bridge cleavage required an in depth study addressing mechanistic reasoning for the occurrence of a number of unwanted rearrangement by-products. Under basic conditions the ketone **4** underwent C-C cleavage to produce the five-membered heterocycle and C-O cleavage was accomplished using BBr_3 followed by quenching in collidine to yield the cyclohexenone **3**. Stereochemistry at the C(5) α-carbonyl position was retained in the ether cleavage product of **4b** but not in the *endo*-isomer **4a** and this could be due to intramolecular Lewis-acid attraction in the intermediate boron complex. The acetylation of **3** was accomplished as a one-pot procedure by the addition of AcCl to the 1 M collidine/DCM quenching mixture to yield **2** in moderate yield. The isolation of **2** and **3** demanded HPLC separation and further investigation is necessary to develop a mild and high yielding ether cleavage procedure to allow simple access to **2** in larger reaction scales.

Chapter 5 begins the synthesis of a convergent precursor for lactone ring **C** of **1**. A simple process for the preparation of β,γ-unsaturated esters was used in the synthesis of the lactone ring and esterification of the furfurol **8** with α-bromocrotonyl chloride in the presence of TEA gave the deconjugated α-bromoester exclusively. Preparation of the Reformatsky reagent using Rieke Zinc facilitated intramolecular ring closure, followed by stirring in 2 M HCl to produce the α,β-unsaturated dihydropyranone **6**. Since the racemic alcohol **8** was employed in this synthesis, the racemic product was obtained and is labeled as (*R*,*S*)-**6** in Scheme 5.20. Further asymmetric strategies are required to prepare the non-racemic precursor (*S*)-**6**. The synthetic protocol used for the preparation of the lactone skeleton is a direct and high yielding synthesis for a functional unit that is commonly incorporated in range of

reported natural products and could be a useful synthetic intermediate in a number syntheses involving this moiety.

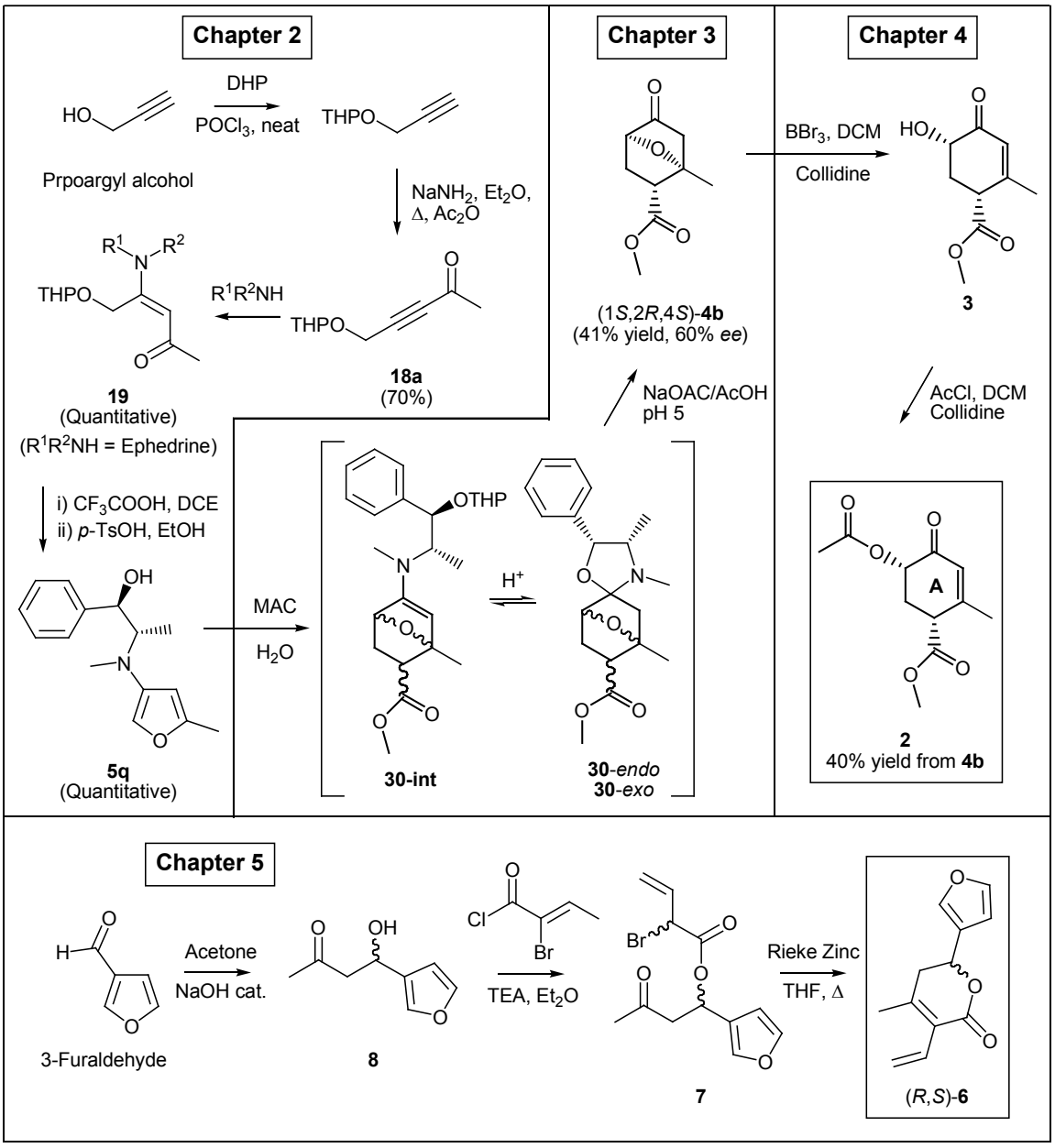

Scheme 5.20: A summary of the synthesis presented in Chapters 2-5.

In conclusion, significant progress has been made towards a novel asymmetric synthesis of natural product salvinorin A (**1**). Recent research by Scheerer *et al.* [35] describes the completion of an asymmetric synthesis for **1** by a more linear methodology involving the construction of a chiral macrocycle followed by a transannular cyclization to the fused tricyclic ring system. The current work

pursues a completely convergent synthetic route to the *trans*-neoclerodane skeleton, a challenge that most synthetic chemists avoid due to the potential for dead-ends due to the unexpected reactivity, inertness or rearrangements of intermediates. Nevertheless, the synthetic work discussed has not presented any challenges that cannot overcome by persistence and a basic understanding of the reaction mechanism. An entirely convergent synthesis for clerodane diterpenes is highly desirable to access the bioactive natural products of this family in the laboratory. It is hoped that the current work provides a significant contribution towards this accomplishment.

Chapter 5

Studies Towards the δ-Lactone Ring C: References

[1] Q. Zhu, L. Qiao, Y. Wu, Y.-L. Wu, "Studies Towards the Total Synthesis of Clavulactone". *Journal of Organic Chemistry*. **2001**, *66*, 2692-2699

[2] M. Sanchez, F. Barmejo. "Stereoselective Approach to the BCD Framework of Richardianidins via Intramolecular Reformatski-Type Reaction Promoted by Diethylaluminium Chloride", *Tetrahedron Letters*, **1997**, *38*, 5057-5060.

[3] A. T. Merritt, S. V. Ley. "Clerodane Diterpenoids", *Natural Product Reports* **1992**, *9*, 243-287.

[4] H. Hagiwara, K. Inome, H. Uda. "A Total Synthesis of an Antibacterial Clerodane, 16-Hydroxycleroda-3,13(14)*Z*-dien-15,16-olide", *Journal of the Chemical Society Perkin Transactions I*, **1995**, 757-764.

[5] P. A. Zoretic, H. Fang, A. A. Ribeiro, G. Dubay. "Synthesis of Acuminolide and 17-*O*-Acetylacuminolide from (+)-Sclareolide", *Journal of Organic Chemistry*, **1998**, *63*, 1156-1161.

[6] T. K. M. Shing, Y. Ting. "Synthesis of Optically Active Tetracyclic Quassinoid Skeleton", *Journal of the Chemical Socety Perkin Transactions 1*, **1994**, 1625-1631.

[7] M. de Rosa, R. Dell'Aglio, A. Soriente, A. Scettri. "Efficient Synthesis of Chiral Non-racemic 6-(furan-3-yl)-5,6-dihydro-pyran-2-ones". *Tetrahedron Asymmetry* **1999**, *10*, 3659-3662.

[8] H. Hagiwara, K. Hamano, M. Nozawa, T. Hoshi, T. Suzuki, F. Kido. "The First Total Synthesis of (-)-Methyl Barbascoate", *Journal of Organic Chemistry*, **2005**, *70*, 2250-2255.

[9] T. Tokoroyama, R. Kanazawa, S. Yamamoto, T. Kamikawa, H. Suenaga, M. Miyabe. "Synthetic Studies on Terpenoid Compounds. XXXIII. A Total Synthesis of (±)-15,16-Epoxy-*cis*-cleroda-3,13(16),14-triene". *Bulletin of the Chemical Society of Japan*, **1990**, *63*, 1720-1728.

[10] H.-J. Liu, T. Dieck-Abularach. "Studies Towards the Total Synthesis of Mexicanolide. Stereoselective Construction of the CD Ring Segment for a Convergent Approach", *Heterocycles*, **1987**, *25*, 245-249.

[11] A. Fernández-Mateos, M. G. Benito, G. P. Coca, R. R. González, C. T. Hernández. "Synthesis of dl-Pyroangolensolide", *Tetrahedron*, **1995**, *51*, 7521-7526.

[12] M. de Rosa, A. Soriente, A. Scettri. "Enantioselective Aldol Condensation of *O*-Silyl Dienolates to Aldehydes Mediated by Chiral BINOL-Titanium Complexes". *Tetrahedron Asymmetry*, **2000**, *11*, 3187-3195.

[13] D. Cahard, M. Mammeri, J.-M. Poirier, L. Duhamel. "A General Synthesis of (2*Z*)-Terpenoic Acids", *Tetrahedron Letters*, **2000**, *41*, 3619-3622.

[14] K. Shokat, T. Uno, P. G. Schultz. "Mechanistic Studies of an Antibody-Catalyzed Elimination Reaction", *Journal of the American Chemical Society*, **1994**, *116*, 2261-2270.

[15] J. McMurry, "Organic Chemistry" (4th edition), Brooks and Cole publishing, USA. **1996**, 897-909, ISBN 0-534-23832-7.

[16] E. A. Couladouros, I. C, Soufli, V. I. Moutsos, R. K. Chadha. "Total Synthesis of Combretastatins D", *Chemistry, A European Journal*, **1998**, *4*, 33-43.

[17] T. Ozeki, M. Kusaka. "Vinylacetic Acid Ester Formation in the Reaction of Crotonoyl Chloride with Alcohol in the Presence of *t*-Amine". *Bulletin of the Chemical Society of Japan*, **1966**, *39*, 1995-1998.

[18] Y. Iwakura, F. Toda, R. Iwata, Y. Torii. "Formation of 3-Butenoates from Crotonyl Chloride in the Presence of Amines". *Bulletin of the Chemical Society of Japan*, **1969**, *42*, 841-842.

[19] G. H. Jeffery, A. I. Vogel. "Physical Properties and Chemical Constitution. Part XVI. Ethylenic Compounds", *Journal of the American Chemical Society*, **1948**, 658-673.

[20] H. Iwadate, K. Gamoh, Y. Fujimoto, N. Ikekawa. "Stereochemistry in the Hydrogenation of Steoidal (22*R*)- and (22*S*)-Δ^{24}-26,22-Lactones". *Chemical and Pharmaceutical Bulletin*, **1986**, *34*, 2061-2065.

[21] G. Cardillo, A. De Simone, A. Mingardi, C. Tomasini. "Synthesis of β,γ-Unsaturated Esters From α,β-Unsaturated Acid Chlorides", *Synlett*, **1995**, 11, 1131-1132.

[22] Pfeiffer, P. "Umlagerungen Stereoisomer Äthylenverbindungen". *Berichte der Deutschen Chemischen Gesellschaft*, **1910**, *43*, 3039-3048.

[23] Klein, J., Zitrin, S. "The Reaction of Grignard Reagents with α-Bromocrotonic and α-Bromocinnamic Acids", *Journal of Organic Chemistry*, **1970**, *35*, 666-669.

[24] P. Knochel and P. Jones (Ed.). "Organozinc Reagents, A Practical Approach", Oxford University Press, New York, **1999**, 3-12, 25-26, ISBN 0 19 850121 8.

[25] W. R. Vaughan, S. C. Bernstein, M. E. Lorber. "The Reformatsky Reaction. I. Zinc and Ethyl α-Bromoisobutyrate", *Journal of Organic Chemistry*, **1965**, *30*, 1790-1795.

[26] A. S. Dreiding, R. J. Pratt. "α- and γ-Additions in the Reformatsky Reaction with Methyl γ-Bromocrotonate", *Journal of the American Chemical Society*, **1953**, *75*, 3717-3723.

[27] A. R. Lingham, H. M. Hügel, T. J. Rook. Diels-Alder Reactions of 3-Furylamines in Organic and Aqueous Solvents. *Australian Journal of Chemistry*, **2006**, *59*, 336-339; A. R. Lingham, H. M. Hügel, T. J. Rook. Studies Towards the Synthesis of Salvinorin A. *Australian Journal of Chemistry*, **2006**, *59*, 340-348.

[28] T. D. Machajewski, C.-H. Wong. "The Catalytic Asymmetric Aldol Reaction", *Angewandte Chemie International Edition*, **2000**, *39*, 1352-1374.

[29] B. List, R. A. Lerner, C. F. Barbas III. "Proline-Catalyzed Direct Asymmetric Aldol Reactions", *Journal of the American Chemical Society*, **2000**, *122*, 2395-2396; B. List, P. Pojarliev, C.

Castello. "Proline-Catalyzed Asymmetric Aldol Reactions Between Ketones and α-Unsubstituted Aldehydes", *Organic Letters*, **2001**, *3*, 573-575.

[30] B. List. "Proline-Catalyzed Asymmetric Reactions", *Tetrahedron*, **2002**, *58*, 5573-5590.

[31] P. M. Pihko, A. Erkkilä. "Enantioselective Synthesis of Prelactone B using a Proline-Catalyzed Crossed-Aldol Reaction", *Tetrahedron Letters*, **2003**, *44*, 7607-7609.

[32] Y.-Y. Peng, Q.-P. Ding, Z. Li, P. G. Wang, J.-P. Cheng. "Proline Catalyzed Aldol Reactions in Aqueous Micelles: An Environmentally Friendly Reaction System", *Tetrahedron Letters*, **2003**, *44*, 3871-3875.

[33] A. Y. Kobayashi, M. Matsuumi. "First Total Synthesis of Grahamimycin", *Journal of Organic Chemistry*, **2000**, *65*, 7221-7224.

[34] M. Jorgensen, E. K. Iversen, A. L. Paulsen, R. Madsen. "Efficient Synthesis of Enantiopure Conduritols by Ring-Closing Metathesis", *Journal of Organic Chemistry*, **2001**, *66*, 4630-4634.

[35] J. R. Scheerer, J. F. Lawrence, G. C. Wang, D. A. Evans. "Asymmetric Synthesis of Salvinorin A, A Potent K-Opioid Receptor Agonist". *Journal of the American Chemical Society*, **2007**, *129*, 8968-8969.

Chapter 6

Experimental Procedures and Methodology

Chemical structures and 3D molecular models included in this thesis were constructed using ChemOffice 8.0 (Cambridgesoft). Gas-chromatographic-mass-spectrometry data shown was analysed using W-search (Frank Antolasic, www.w-search.com) and processing of NMR spectra was performed using X-Win NMR (Bruker) and the scanned images are included.

Unless noted, materials were obtained from Aldrich Chemical Co. and used without further purification. Diethyl ether and THF were dried first with CaH_2, then distilled from sodium/benzophenone before use. Dry acetone (BDH) was obtained by refluxing over $KMnO_4$ followed by distillation and storage over molecular sieves (4Å). Triethylamine was dried over KOH pellets before use. ^{1}H and ^{13}C NMR spectra were recorded on a Varian Gemini 2000 (200 MHz) and a Bruker Avance 300 (300 MHz) NMR spectrometer and are indirectly referenced to TMS via $CHCl_3$. FT-IR spectra were recorded on a Perkin-Elmer Spectrum 2000 Fourier transform IR spectrometer. GC-MS data was recorded using a Hewlett Packard 6890 GC with BPX-5 column, and Hewlett Packard 5973 Mass Selective Detector. Chiral GC separation was achieved using a diEt-TBS-β-CD column (MeGA, Italy), 20 m, 0.25 mm x 0.25 μm (film thickness). Semipreparative HPLC was performed using a Varian Prostar (Model 210), with Phenomenex C18 column (250 x 10 mm, 5μ ODS (3), 50 x 10 mm, 5u ODS (3) guard column). Separation was achieved using MeCN:H_2O (55:45) at 3.5 mL/min flow rate, with UV-Vis detection. Reactions performed under ultrasonic irradiation were performed using a Elma Transsonic Digital S, 40kHz variable power ultrasonic bath. Optical rotations were determined on a Perkin-Elmer 241 MC Polarimeter at 690nm wavelength using a medium pressure mercury lamp at 20°C and at the concentration *c* (g/100 mL).

Single crystal X-ray crystal structures of **4b** and (1*S*,2*S*,4*S*,5*S*)-**29** were obtained by Associate Professor Jonathan White, Bio21 Institute, University of Melbourne, Melbourne, Australia. Data was collected on a Bruker Smart Apex diffractometer, with CCD area detection and a Enraf Nonius FR590. The structures were solved by the direct method: SHELXTL (Bruker AXS Incorporated, v6, 12, 2001) and refined by full matrix least squares method: SHELXL97 (Scheldrick, University of Gottingen, Germany, 1997).

NOE correlated NMR spectrometry of **3** and C(5)-***epi*-3** was performed by Dr. Jo Cosgriff and Dr. Rodger Mulder at CSIRO, Molecular Science, Clayton, Australia using a Bruker Avance 500 (500 MHz) NMR spectrometer.

*6.1 Preparation of 5-methyl-3-bromofuran (**10**) from 2-furoic acid methyl ester by optimized literature methodology.*

The preparation of 2,3-dibromofuran was performed via an optimized procedure from patent US3714197 [1]. The final transformation to **10** was achieved following methodology reported by Katsumura *et al.* [2]. Product were separated and identified by GC-MS using Method 1 (Section 6.10).

6.1.1 Preparation of 2,3-dibromofuran (16) *[1].*

Preparation of 2,3-dibromofuroic acid methyl ester ***(14).***

To methyl-2-furoate (50.0 g, 0.38 mol) in boiling chloroform (100 mL) was added elemental bromine (177 g, 2.8 equiv.) drop-wise over 20 min. The solution was heated to reflux for 16 h then nitrogen was bubbled through the hot solution for approx. 2 h to remove dissolved HBr and excess bromine. The solvent and excess bromine was removed to leave 2,3-dibromofuroic acid methyl ester (**14**) as a viscous light orange oil in nearly quantitative yield (113.4 g, <97% yield) by GC-MS and ^{1}H NMR. ^{1}H NMR (200 MHz, $CDCl_3$): δ 7.17 (arom. s, 1H), 3.89 (s, 3H). ^{13}C NMR (50 MHz, $CDCl_3$): δ 181.7, 157.5, 146.0, 128.5, 103.9, 52.6. MS *m/z* (relative intensity) 287 (2.4), 286 (32.0), 285 (5.0), 284 (M^+, 65.6), 282 (34.1), 256 (5.2), 255 (49.8), 254 (11.0), 253 (100), 252 (5.8), 251 (52.9), 241 (1.7), 228 (6.4), 227 (2.6), 226 (13.2), 225 (4.3), 224 (6.9), 223 (2.1), 215 (2.0), 213 (4.4), 211 (2.3), 199 (11.9), 197 (24.4), 195 (12.8), 175 (8.4), 173 (7.5), 149 (4.3), 147 (5.9), 146 (5.8), 145 (1.8), 144 (6.0), 119 (2.8), 118 (26.0), 117 (5.4), 116 (26.2), 115 (2.7), 106 (1.9), 104 (2.0), 93 (3.2), 81 (2.2), 79 (2.2), 65 (2.1), 59 (8.3), 53 (7.6), 52 (1.8), 51 (3.6), 38 (1.6), 37 (18.6), 36 (3.1). (t_R = 21.59 min)

Preparation of 2,3-dibromofuroic acid (**15**).

To a vigorously stirred solution of NaOH (195 mL, 4M aq. solution) warmed to 50°C was added **14** (45.0 g, 160 mmol) portion wise. The solution was warmed to 70°C, allowed to stir for 2.5 h then cooled in a salt/ice bath. Et_2O (300 mL) was added to the stirred solution followed by the slow addition of HCl (73 g, conc.) in ice (110 g), keeping the mixture below 5°C. The ethereal layer was separated and the aqueous layer extracted with Et_2O (4 x 75 mL). The combined organic layers were washed with $Na_2S_2O_4$ (2 x 75 mL, 5% aq. solution) then dried with $MgSO_4$ and evaporated to leave 2,3-dibromofuroic acid (**15**, 35.2 g, Yield 82%). The saponified material was recrystallized from water (10 g / 800 mL).

(m.p. 168-169°C, lit. 167-168°C, [3]). ^{1}H NMR (200 MHz, $CDCl_3$): δ 7.31 (arom. s, 1H). ^{13}C NMR (50 MHz, $CDCl_3$): δ carbonyl abs., 159.6, 127.2, 120.0, 114.0. MS *m/z* (relative intensity) 273 (3.1), 272 (50.0), 271 (5.7), 270 (M^+, 100), 268 (49.9), 255 (5.3), 253 (11.1), 251 (5.7), 244 (1.7), 242 (1.6), 240 (1.8), 227 (1.5), 226 (3.2), 225 (2.8), 224 (1.7), 200 (2.1), 199 (10.1), 198 (1.9), 197 (18.1), 195 (8.8), 192 (2.0), 191 (2.7), 190 (2.4), 189 (2.3), 163 (5.2), 161 (5.4), 146 (2.3), 144 (2.6), 135 (11.8), 134 (2.1), 133 (12.7), 132 (2.1), 119 (14.8), 117 (16.3), 116 (21.8), 115 (2.4), 107 (2.5), 106 (1.6), 105 (2.7), 104 (1.7), 93 (2.8), 91 (2.2), 82 (1.8), 81 (3.2), 79 (3.5), 66 (1.9), 65 (1.5), 53 (8.0), 45 (11.3), 44 (2.2), 39 (1.5), 38 (9.8), 37 (23.0), 36 (4.6), 32 (1.7). (t_R = 23.28 min)

Preparation of 2,3-dibromofuran (**16**).

Purified **15** (10 g, 37.2 mmol) was added to quinoline (40 mL) and copper powder (4 g). The solution was stirred briefly, then submersed in a preheated oil bath (180°C) without stirring for 10 min, or until CO_2 evolution slowed. The solution was immediately cooled in an ice bath and quenched by the addition of ice cold HCl (70 mL, 5 M aq.) with stirring followed by Et_2O (70 mL). The biphasic mixture was then filtered with suction and the filtrate washed thoroughly with Et_2O. The organic layer was separated and the aqueous layer extracted with Et_2O (2 x 75 mL). The combined organic layers were extracted with HCl (2 x 50 mL, 0.5 M aq.), dried with $MgSO_4$ and evaporated to leave a dark oil (7.2 g). Analysis by NMR showed the oil to be 2,3-dibromofuran (**16**) along with small amounts of polymeric material present in the baseline. The product was kept at -25°C, protected from UV exposure, and carefully bulb distilled before use. (Yield 86%, b.p. 58°C @ 15 mmHg, lit. 58°C @ 12 mmHg [4]). ^{1}H NMR (200 MHz, $CDCl_3$) : δ 7.37 (d, *J* = 2.2 Hz, 1H), 6.42 (d, *J* = 2.2 Hz, 1H). ^{13}C NMR (50 MHz, $CDCl_3$): δ 144.8, 123.3, 115.7, 101.8. MS *m/z* (relative intensity) 229 (2.4), 228 (49.7), 227 (5.0), 226 (M^+, 100), 224 (52.4), 200 (3.6), 199 (5.1), 198 (6.6), 197 (10.1), 196 (3.3), 195 (5.4), 120 (1.9), 119 (53.8), 118 (17.5), 117 (55.3), 116 (16.0), 113 (2.6), 93 (4.0), 91 (3.9), 81 (7.5), 79 (7.4), 38 (22.9), 37 (22.4), 36 (4.3). (t_R = 13.95 min)

6.1.2 Preparation of 4-bromo-2-methyl furan (10) [2].

Preparation of 2,3-bromo-5-methyl furan (**12**).

Under an inert atmosphere (N_2), *n*-BuLi (4.5 mmol, 2.75 mL, 1.6 M in hexanes) was added drop-wise to a solution of diisopropylamine (4.5 mmol, 0.45 g) in THF (25 mL) at 0°C. The solution was stirred at 0°C for 10 min then cooled to -15°C followed by the slow addition of freshly distilled 2,3-dibromofuran (1.0g, 4.5 mmol). After stirring for 12 min, iodomethane (4.5 mmol, 0.635 g) was added

dropwise and the solution allowed to reach room temperature. A potion of 2,3-bromo-5-methyl furan (**12**) was characterized by spectroscopic analysis and the remaining material was reacted further from the same mixture. ^{1}H NMR (200 MHz, $CDCl_3$): δ 6.27 (arom. s, 1H), 2.28 (s, 3H). ^{13}C NMR (50 MHz, $CDCl_3$): δ 151.9, 120.0, 114.7, 97.8, 12.2. MS *m/z* (relative intensity) 243 (2.7), 242 (50.0), 241 (8.4), 240 (M^+, 100), 239 (8.6), 238 (52.2), 237 (2.8), 213 (4.7), 213 (4.7), 212 (1.6), 211 (9.5), 209 (4.9), 199 (2.3), 197 (4.1), 195 (2.1), 162 (3.6), 161 (59.7), 160 (4.2), 159 (63.2), 157 (2.3), 134 (3.7), 132 (6.4), 131 (86.0), 130 (3.2), 120 (2.2), 119 (3.1), 118 (8.0), 117 (4.2), 116 (7.5), 115 (2.0), 109 (3.1), 107 (4.9), 106 (2.1), 105 (2.3), 104 (2.1), 81 (4.8), 80 (4.9), 79 (8.2), 66 (2.2), 65 (2.2), 53 (3.4), 52 (34.0), 51 (80.3), 50 (36.7), 49 (9.1), 43 (15.3), 42 (2.1), 39 (1.8), 38 (3.3), 37 (10.4), 36 (2.4). (t_R = 16.13 min)

Preparation of 4-bromo-2-methyl furan (**10**).

The solution of **12** from the previous step was cooled to -78°C whilst maintaining an inert atmosphere. ^{t}BuLi (4.5 mmol, 2.75 mL, 1.6 M in hexanes) was added dropwise and the solution allowed to stir for 8 min, followed by quenching with wet THF, followed by the addition of H_2O (20 mL). The solution was extracted with DCM (3 x 50 mL), dried with $MgSO_4$ then evaporated under vacuum to leave a dark oil (0.64 g). 4-Bromo-2-methyl furan (**10**) was distilled as a clear oil (0.54 g, 76%) which which was stable for months when stored in a freezer and protected from UV light. (b.p. 120-124°C). ^{1}H NMR (200 MHz, $CDCl_3$): δ 7.17 (arom. m, 1H), 6.26 (arom. m, 1H), 2.20 (s, 3H). ^{13}C NMR (50 MHz, $CDCl_3$): δ 149.1, 140.6, 113.3, 95.8, 11.4. MS *m/z* (relative intensity) 163 (6.0), 162 (97.4), 161 (50.1), 160 (M^+, 100), 159 (46.4), 133 (14.3), 131 (15.0), 119 (4.2), 117 (4.4), 107 (2.3), 105 (2.6), 82 (4.7), 81 (66.4), 80 (5.5), 79 (5.3), 61 (1.6), 54 (4.7), 53 (96.3), 52 (37.2), 51 (59.9), 50 (35.6), 49 (8.9), 43 (13.3), 42 (2.4), 39 (4.2), 38 (10.2), 37 (8.6). (t_R = 6.55 min)

6.2 Preparation of 3-furylamines by coupling of amines to aryl halide.

6.2.1 Preparation of 4-(5-Methylfuran-3-yl)morpholine **(5a)** *by Pd(dba)$_3$/Di-t-butyl-orthodiphenylphosphine using optimized methodology based on Wolfe et al.* [5]**.**

A flame dried flask was charged with $Pd(dba)_3$ (15 μm, 13.8 mg), P(t-Bu)$_2$-o-biphenyl (60 μm, 17.9 mg) and ^{t}BuONa (230 mg, 2.4 mmol) under a nitrogen atmosphere. Morpholine (110 mg, 1.2 mmol), **10** (190 mg, 1.2 mmol) and dry toluene (4 mL) were added sequentially and the solution heated to 70°C. Reaction monitoring by GC-MS showed maximum to conversion **5a** (30%), identified by a molecular *m/z* 167 ion, achieved after 4 h with large amounts of decomposition. After cooling to ambient temperature, Et_2O (20 mL) was added and the solution was washed with brine (2 x 10 mL). Attempts to

isolate the aminofuran by column chromatography led to decomposition, even after deactivation of the silica with triethylamine in ethyl acetate. The GC-MS spectrum of **5a** is listed in 6.4.3.

6.3 Attempted preparation of 3-furylamines from 5-methyl-furan-3-one.

*6.3.1 Preparation of 5-Methylfuran-3-one (***16***) following methodology by Cui et al.* **[6].**

n-BuLi (120 mmol, 1.6 M in hexanes) was added drop-wise to a solution of diisopropylamine (12.12 g, 120 mmol) in dry THF at –30°C under a nitrogen atmosphere. The stirred solution was allowed to warm to 0°C and stirred for 15 min after which time it was cooled to –30°C and dry acetone (6.96 g, 120 mmol) was added drop-wise. After stirring for a further 25 min, the solution was cooled to –50°C and ethylchloro acetate (7.44 g, 60 mmol) was added slowly. The solution was allowed to warm to room temperature, quenched with saturated ammonium chloride solution and extracted with diethyl ether (3 x 75 mL). The combined extracts were concentrated with gentle vacuum to leave a red sweet smelling oil (7.6 g). The oil was transferred to a silica column (4 cm diam., 40 cm length) and 20 x 20 mL fractions eluted with 5:1 hexane:EtOAc. The eluent was changed to 1:1 hexane:EtOAc and the next 10 fractions combined and evaporated to give 5-methyl-furan-3-one (**16**, 1.21 g, 10.3%) as a distinct smelling pale yellow oil. The identity of the compound was confirmed by ^{1}H NMR analysis which was consistent with that reported in the literature [7]. ^{1}H NMR (200 MHz, $CDCl_3$): δ 5.43 (1H, br. s), 4.45 (2H, br. s), 2.19 (3H, br. s). ^{13}C NMR (50 MHz, $CDCl_3$): δ 203.2, 191.9, 105.1, 75.6, 16.9.

*6.3.2 Attempted preparation of 1-(5-Methylfuran-3-yl)pyrrolidine (***5d***).*

To a solution of 5-methyl-furan-3-one (0.5 g, 5.0 mmol) in benzene (40 mL) was added freshly distilled pyrrolidine (0.36 g, 5.0 mmol) and molecular sieves (4Å). After stirring overnight at room temperature, analysis by GC-MS showed some decomposition but mainly starting materials. Heating to reflux for 5 h using a Dean-Stark apparatus led to complete decomposition of the starting materials as indicated by GC-MS monitoring.

6.4 Preparation of non-chiral 3-furylamines by tandem Michael addition/enaminone cyclization.

Product and intermediates were separated and identified by GC-MS using *Method 1*.

6.4.1 Preparation of THP protected ketoalkynols (18a-c) as Michael acceptors.

Preparation of 3-(tetrahydropyran-2-yloxyprop)-1-yne (**17**) *following methodology by Henbest et al.* [8].

$POCl_3$ (100 mg, 1.21 mmol) was added to a neat mixture of propargyl alcohol (8.4 g, 150 mmol) and 3,4-dihydro-2*H*-pyran (12.6 g, 150 mmol) and stirred whilst cooling in an ice bath until no more heat evolved. The ice bath was removed and the mixture stirred at room temperature for a further 2 h. Several NaOH pellets were added and the 3-(tetrahydropyran-2-yloxy)prop-1-yne (**17**) was distilled directly from the reaction vessel under vacuum (19 g, 90% yield, b.p. 28°C @ 25 mmHg). ^{1}H NMR (200 MHz, $CDCl_3$): δ 4.82 (m, 1H), 4.27 (d, *J* = 2.4 Hz, 1H), 4.25 (d, *J* = 2.4 Hz, 1H), 3.84 (m, 1H), 3.56 (m, 1H), 2.41 (t, *J* = 2.4 Hz, 1H), 1.85-1.45 (br. m., 6H). ^{13}C NMR (50 MHz, $CDCl_3$): δ 97.0, 79.9, 74.2, 62.2, 54.2, 30.4, 25.5, 19.2. MS *m/z* (relative intensity) 140 (M^+,1.1), 139 (10.9), 111 (1.0), 101 (5.0), 97 (1.9), 95 (1.7), 86 (6.4), 85 (100), 84 (3.9), 83 (9.6), 82 (12.9), 81 (9.0), 79 (5.8), 77 (1.2), 71 (1.6), 70 (2.1), 69 (7.7), 68 (3.6), 67 (10.3), 66 (2.8), 65 (2.1), 58 (1.4), 57 (25.9), 56 (44.1), 55 (29.4), 54 (7.6), 53 (11.9), 44 (1.7), 43 (10.6), 41 (36.0), 40 (4.3), 39 (39.6), 38 (4.0), 37 (1.5), 31 (4.1). (t_R = 15:56 min).

Preparation of 5-(tetrahydropyran-2-yloxy)pent-3-yn-2-one (**18a**) *and 6-(tetrahydropyran-2-yloxy)hex-4-yn-3-one* (**18b**) *under conditions reported by Duranti et al.* [9].

3-(Tetrahydropyran-2-yloxy)prop-1-yne **17** (28 g, 200 mmol) was added drop-wise under inert atmosphere to a stirred mixture of sodamide (7.8 g, 200 mmol) in anhydrous ether (150 mL). The mixture was refluxed for 5 h. The suspension was diluted with 200 mL anhydrous ether and poured into a vigorously stirred solution of acetic anhydride (20.4 g, 200 mmol) in anhydrous ether (300 mL), the temperature being kept between –5 and –10°C. The mixture was allowed to reach room temperature and the white solid was separated by filtration. The solvent was evaporated under reduced pressure and any unreacted materials were removed using a high vacuum oil pump and gentle heating on a water bath (60°C). The product 5-(tetrahydropyran-2-yloxy)pent-3-yn-2-one (**18a**) was obtained as a red oil (25 g, Yield 70%). ^{1}H NMR (200 MHz, $CDCl_3$): δ 4.78 (m, 1H), 4.40 (s, 2H), 3.81 (m, 1H), 3.56 (m, 1H), 2.34 (s, 3H), 1.85-1.45 (br. m., 6H). ^{13}C NMR (50 MHz, $CDCl_3$): δ 184.2, 97.3, 87.9, 85.3, 62.1, 53.9, 32.7, 30.2, 25.4, 19.0. MS *m/z* (relative intensity) 182 (M^+, 0.6), 181 (4.9), 139 (1.8), 128 (1.8), 127 (24.3), 126

(1.5), 125 (3.6), 124 (5.7), 121 (2.0), 112 (2.2), 109 (6.7), 108 (1.7), 107 (2.0), 102 (2.5), 101 (36.8), 100 (2.6), 99 (4.2), 98 (3.8), 97 (3.5), 96 (1.3), 95 (8.6), 93 (2.3), 91 (1.2), 86 (6.4), 85 (100), 84 (6.2), 83 (27.9), 82 (89.6), 81 (23.7), 79 (3.2), 77 (1.8), 71 (4.8), 70 (1.8), 69 (6.1), 68 (3.4), 67 (20.5), 66 (21.1), 65 (2.3), 63 (1.3), 59 (1.0), 58 (1.2), 57 (20.8), 56 (40.5), 55 (49.2), 54 (6.4), 53 (67.6), 52 (4.4), 51 (6.7), 50 (3.6), 45 (1.6), 44 (4.9), 43 (85.4), 42 (10.5), 41 (51.3), 40 (3.8), 39 (23.1), 38 (7.9), 37 (1.8), 31 (7.5). (t_R = 21:91 min).

The same method as outlined above was used to produce 6-(tetrahydropyran-2-yloxy)hex-4-yn-3-one (**18b**) using propanoic anhydride. ^{1}H NMR (200 MHz, $CDCl_3$): δ 4.78 (m, 1H), 4.40 (s, 2H), 3.81 (m, 1H), 3.56 (m, 1H), 2.58 (q, *J* = 7.4 Hz, 2H), 1.85-1.45 (br. m., 6H), 1.12 (t, *J* = 7.4 Hz, 3H). ^{13}C NMR (50 MHz, $CDCl_3$): δ 188.1, 97.3, 88.1, 84.8, 62.2, 54.0, 38.8, 30.2, 25.4, 19.0, 8.0.

Preparation of 4-(tetrahydropyran-2-yloxy)but-2-ynal (**18c**) *using methodology described by Journet et al.* [10].

A solution of **17** (7 g, 50 mmol) in dry THF (100 mL) was cooled to –40°C under a dry nitrogen atmosphere. *n*-BuLi (32 mL, 50 mmol, 1.6 M in hexane) was then added dropwise and the solution stirred at between –30°C and –40°C for 30 min. Anhydrous DMF (7.8 mL, 100 mmol) was added at once and the solution allowed to warm to room temperature. Stirring was continued at room temperature for an additional 30 min, and the solution was then poured into a vigorously stirred biphasic solution of KH_2PO_4 (250 mL, 10% aq.) and Et_2O (200 mL) at 5°C. The organic layer was separated and the aqueous layer extracted with Et_2O (2 x 75 mL). The combined organic phases were dried, filtered and concentrated to leave a viscous oil which was warmed on a water bath (60°C) under high vacuum to remove starting materials. 4-(Tetrahydropyran-2-yloxy)but-2-ynal (**18c**) was obtained as a yellow oil (7.1 g, Yield 84%) and used without further purification.

*6.4.2 Preparation of the 4-amino-5-(tetrahydropyran-2-yloxy)alkenones (***19a-n***) by 1,4-Michael-type addition of amines to the alkynones* **18a-c.**

Example 1: Preparation of 4-morpholino-5-(tetrahydropyran-2-yloxy)pent-3-en-2-one (**19a**)

Morpholine (0.24 g, 2.8 mmol), was added dropwise with stirring to neat 5-(tetrahydropyran-2-yloxy)pent-3-yn-2-one (0.50 g, 2.8 mmol) **18a** while cooling in a cold water bath (10°C). The viscous oil was then allowed to stir at room temperature for 2 h. Yield of **19a** via GCMS was >98%. ^{1}H NMR (200 MHz, $CDCl_3$): δ 5.29 (d, 1H, *J* = 11.9 Hz, H-5_A), 5.20 (s, 1H, H-3), 4.71 (d, 1H, *J* = 11.9 Hz, H-5_B), 4.68

(m, 1H, H-2'), 3.85 (m, 1H, H-6_A), 3.73 (t, 4H, *J* = 5.0 Hz, H-1''), 3.55 (m, 1H, H-6_B), 3.35 (m, 4H, H-2''), 2.1 (s, 3H, H-1), 1.9 – 1.4, (m, 6H, H-3', H-4', H-5'). ^{13}C NMR (50 MHz, $CDCl_3$): δ 195.9 (C-2), 158.8 (C-4), 100.0 (C-2'), 98.2 (C-3), 66.6 (C-2''), 63.5 (C-5), 60.8 (C-6'), 47.0 (C-1''), 32.3 (C-1), 31.0 (C-3'), 25.5 (C-5'), 20.2 (C-4'). MS *m/z* (relative intensity) 269 (M^+ 3.1), 210 (3.8), 186 (10.8), 185 (100), 184 (38.5), 170 (15.4), 169 (16.2), 168 (27.7), 167 (12.3), 166 (3.8), 157 (4.6), 156 (51.5), 154 (7.7), 152 (15.4), 150 (6.2), 143 (7.7), 142 (89.2), 140 (3.8), 138 (6.9), 137 (4.6), 136 (3.1), 127 (11.5), 126 (60.0), 124 (9.2), 114 (9.2), 112 (9.2), 110 (9.2), 109 (11.5), 108 (3.8), 98 (4.6), 97 (7.7), 96 (6.9), 92 (4.6), 86 (16.2), 85 (37.7), 84 (13.1), 83 (8.5), 82 (6.2), 81 (3.8), 80 (3.8), 70 (4.6), 69 (4.6), 68 (6.2), 67 (14.6), 57 (11.5), 56 (7.7), 55 (14.6), 54 (5.4), 43 (25.4), 42 (5.4), 41 (15.4). (t_R = 29:56 min).

Compounds **19a,b,d,f-k** were also prepared using the procedure described above and NMR data is included in Appendix 6.1.

Example 2: 4-Dibenzylamino-5-(tetrahydropyran-2-yloxy)pent-3-en-2-one (**19e**).

Dibenzylamine (0.54 g, 2.7 mmol), was added to **18a** (0.50 g, 2.8 mmol) **3**, and stirred for 45 min in a warm water bath (70°C). The oil was allowed to stir for an additional 8 h at room temperature and yield of **19e** via GC-MS and ^{1}H NMR was 97%. The material produced was a dark viscous resin and was used directly for further reactions. ^{1}H NMR (200 MHz, $CDCl_3$): δ 7.40 - 7.07 (m, 10H, H-3'', H-4'', H-5''), 5.28 (d, 1H, *J* = 11.5 Hz, H-5_A), 5.20 (s, 1H, H-3), 4.87 (d, 1H, *J* = 11.5 Hz, H-5_B), 4.74 (m, 1H, H-2'), 4.49 (AB quartet, 4H, *J* = 5.7 Hz, H-1''), 3.78 (m, 1H, H-6_A), 3.44 (m, 1H, H-6_B), 1.95 (s, 3H, H-1), 1.76 -1.30 (m, 6H, H-3', H-4', H-5'). ^{13}C NMR (50 MHz, $CDCl_3$): δ 195.6 (C-2), 158.8 (C-4), 136.7 (C-2''), 128.9 (C-4''), 127.6 (C-3''), 127.0 (C-5''), 99.9 (C-2'), 97.8 (C-3), 63.1 (C-5), 61.1 (C-6), 52.8 (C-1''), 32.4 (C-1), 30.8 (C-3'), 25.5 (C-5'), 19.9 (C-4'). MS *m/z* (relative intensity) 379 (M^+ 0.5), 336 (0.5), 296 (2.3), 295 (13.1), 294 (6.2), 288 (4.6), 280 (1.5), 279 (2.3), 278 (5.4), 277 (4.6), 276 (1.5), 262 (1.5), 252 (3.1), 236 (3.8), 234 (3.1), 232 (1.5), 205 (10.8), 204 (78.5), 189 (1.5), 188 (16.2), 186 (7.7), 162 (10.8), 160 (1.5), 158 (1.5), 146 (4.6), 144 (5.4), 143 (1.5), 132 (1.5), 117 (2.3), 115 (1.5), 106 (1.5), 105 (1.5), 104 (2.3), 92 (16.2), 91 (100), 85 (26.2), 67 (3.8), 65 (6.2), 57 (3.8), 55 (2.3), 43 (5.4), 41 (3.8).

Compound **19c** was also prepared using the procedure described above and NMR data is included in Appendix 6.1.

Example 3: 3-Diethylamino-4-(tetrahydropyran-2-yloxy)but-2-enal (**19m**).

4-(Tetrahydropyran-2-yloxy) but-2-ynal **18c** (0.50 g, 3.0 mmol) was added dropwise over 15 min to a solution of diethylamine (0.22 g, 3.0 mmol) in dry THF (40 mL) at 5°C. The solution was allowed to reach room temperature and was stirred for an additional 4 h. The solvent was removed under vacuum to leave a light yellow oil. Yield of **19m** via GC-MS and ^{1}H NMR was 94% and the crude material was used in further reactions without purification. ^{1}H NMR (200 MHz, $CDCl_3$): δ 9.62 (d, 1H, *J* = 8.3 Hz, C-1), 5.24 (d, 1H, *J* = 8.3 Hz, H-2), 4.66 (m, 1H, H-2'), 4.58 (s, 2H, H-4), 3.80 (m, 1H, H-6_A), 3.53 (m, 1H, H-6_B), 3.32 (quartet, 4H, *J* = 7.0 Hz, H-1''), 1.90 – 1.40 (m, 8H, H-3', H-4', H-5'), 1.18 (t, 6H, *J* = 7.1 Hz, H-2''). ^{13}C NMR (200 MHz, $CDCl_3$): δ 187.5 (C-1), 159.7 (C-3), 102.8 (C-2'), 98.1 (C-2), 62.7 (C-4), 59.8 (C-6'), 44.4 (C-1''), 30.5 (C-3'), 25.4 (C-5'), 19.5 (C-4'), 12.8 (C-2''). MS *m/z* (relative intensity) 241 (M^+ 1.0), 212 (1.0), 208 (1.5), 207 (5.4), 182 (1.5), 158 (3.1), 157 (8.5), 156 (27.7), 147 (1.5), 142 (4.6), 141 (17.7), 140 (30.0), 139 (3.1), 138 (3.1), 129 (6.2), 128 (75.4), 126 (10.0), 125 (2.3), 124 (23.1), 122 (7.7), 114 (3.1), 113 (13.1), 112 (52.3), 110 (13.8), 108 (2.3), 105 (1.5), 100 (6.2), 99 (3.8), 98 (17.7), 97 (6.2), 96 (13.8), 95 (2.3), 94 (3.8), 86 (8.5), 85 (87.7), 84 (33.1), 83 (19.2), 82 (17.7), 81 (3.8), 80 (3.1), 74 (3.8), 73 (10.0), 72 (19.2), 71 (19.2), 70 (55.4), 69 (23.8), 68 (19.2), 67 (27.7), 58 (20.8), 57 (56.9), 56 (41.5), 55 (43.8), 54 (21.5), 53 (7.7), 45 (3.8), 44 (27.7), 43 (53.8), 42 (64.6), 41 (100).

Compounds **19l-n** were also prepared using the procedure described above and NMR data is included in Appendix 6.1.

*6.4.3 Cyclisation of 4-amino-5-(tetrahydropyran-2-yloxy)pent-3-en-2-one (***19a-n***) to 3-furylamines.*

Example 1: Preparation of 4-(5-methylfuran-3-yl)morpholine (**5a**).

Anhydrous trifluoroacetic acid (2 mL) was added to **19a** (0.50 g, 2.8 mmol) in DCE (20 mL). The solution was then stirred for 40 min at room temperature and gradually became deep red. The organic layer was extracted with H_2O (4 x 50 mL) and the combined aqueous extracts were extracted once with chloroform. Crushed ice (100 g) was added to the aqueous layer followed by the rapid addition of NaOH (NaOH, 4 M aq.) to pH 14. The chilled aqueous solution was immediately extracted with Et_2O (3 x 75 mL), the combined organic layers were then dried with Na_2SO_4 and evaporated to leave **5a** in high purity and yield (0.44 g, Yield 96%). The yellow oil was bulb distilled directly before use in further reactions (b.p. 125°C @ 4mmHg) and was a white solid when stored at -10°C. IR (neat) 3140(w), 2960

(s), 2918 (s), 2855(s), 2820 (s), 2760 (m), 1755 (m), 1681 (s), 1621 (s), 1555 (m), 1451 (s), 1397 (s), 1379 (s), 1359 (m), 1332 (m), 1302 (m), 1258 (s), 1228 (m), 1178 (m), 1161 (m) and 1116 cm^{-1} (s). ^{1}H NMR (200 MHz, $CDCl_3$): δ 6.82 (s, 1H, H-2'), 5.86 (s, 1H, H-4'), 3.81 (m, 4H, H-2, H-6), 2.87 (m, 4H, H-3, H-5), 2.22 (s, 3H, H-6'). ^{13}C NMR (50 MHz, $CDCl_3$): δ 152.5 (C-5'), 141.7 (C-3'), 123.9 (C-2'), 100.2 (C-4'), 66.6 (C-2, C-6), 50.8 (C-3, C-5), 14.0 (C-6'). MS *m/z* (relative intensity) 169 (18.5), 168 (56.2), 167 (M^+ 77.9), 166 (5.6), 154 (3.2), 153 (7.6), 152 (12.0), 139 (4.4), 138 (10.4), 137 (6.4), 136 (8.4), 125 (3.2), 124 (8.4), 122 (8.0), 112 (7.2), 111 (33.7), 110 (83.1), 109 (100), 108 (12.0), 97 (2.4), 96 (4.0), 95 (4.0), 94 (6.4), 84 (4.0), 83 (4.0), 82 (10.8), 81 (15.3), 80 (16.1), 79 (4.0), 73 (2.8), 72 (2.4), 70 (4.4), 69 (4.4), 68 (4.0), 67 (6.0), 66 (4.8), 65 (3.2), 59 (2.4), 58 (2.4), 57 (5.2), 56 (4.4), 55 (8.8), 54 (8.4), 53 (8.4), 52 (3.2), 51 (3.6), 45 (9.2), 44 (49.0), 43 (14.5), 42 (9.6), 41 (17.7).; HRMS calc. for $C_9H_{14}O_2N$ 168.1025, found 168.1019. (t_R = 21:00 min)

Cyclisations to give tertiary amine products **(5a-e,i,j,l,m)** were performed using the above procedure. Modifications to this procedure for the cyclisations of secondary amine products (**5f,g,h,k,n**) involved using $CHCl_3$ in place of DCE to provide superior yields. Spectroscopic data of **5a-n** is included in Appendix 6.1 with NMR, GC-MS, HR-ESIMS and IR characterization listed. The secondary 3-furylamines were only stable for short periods in Et_2O and required derivatization by acetylation to the amides **21**.

*6.4.4 Derivatisation of Secondary 3-furylamines (***5f,g,h,k,n*).

Example: Preparation of *N*-(*n*-Butyl)-*N*-(5-methylfuran-3-yl)acetamide (**21g**)

Crude *N*-(n-butyl)-5-methylfuran-3-amine (**5g**) cyclised material was immediately dissolved in dry Et_2O (50 mL per 0.5 g furan) and one equivalent of triethylamine was added. Acetyl chloride (1.1 eq.) was added and the solution stirred for 1.5 h. The solution was then filtered and evaporated under reduced pressure followed by bulb distillation (105°C @ 0.01 mmHg) to give **21g** (Yield 84%). *N.N*'-ethylenebis[*N*-(5-methylfuran-3-yl)acetamide] (**5f**) and *N*-butyl substituted furylamines **5k,n** were produced using the same method, however acetyl chloride was substituted for acetic anhydride in the production of *N*-cyclohexyl-*N*-(5-methylfuran-2-yl)acetamide (**21h**) from **5h**.

Characterization of the 3-furylamide products (**21f,g,h,k,n**) are included in Appendix 6.1.

6.5 Preparation of chiral 3-furylamines.

Product were separated and identified by GC-MS using *Method 2*.

6.5.1 Preparation of (S)-benzyl 1-(5-methylfuran-3-yl)pyrrolidine-2-carboxylate (5o).

The proline derived (*S*)-benzyl pyrrolidine-2-carboxylate **22** [11] was used in the general furylamine synthesis as described for **5a** in Section 6.4 to yield **5o** in 30% isolated yield. This product was only characterized by GC-MS analysis. Mass spectrum *m/z* 286 (3.0), 285 (M^+, 14.2), 151 (13.4), 150 (100), 148 (2.7), 120 (1.0), 108 (5.6), 107 (1.3), 106 (1.5), 93 (1.3), 92 (1.7), 91 (12.4), 90 (0.5), 89 (0.6), 81 (1.3), 80 (1.9), 79 (1.3), 78 (0.9), 77 (1.8), 68 (1.1), 67 (1.5), 66 (1.3), 65 (3.7), 55 (1.5), 54 (1.3), 53 (3.3), 52 (1.0), 51 (1.3), 43 (2.6), 41 (1.9), 39 (1.9). (t_R = 18:87 min)

6.5.2 Preparation of (1S,2S)-2-(N-methyl-N-(5-methylfuran-3-yl)amino)-1-phenylpropan-1-ol (5p).

Preparation of 1-((2R/S,4S,5S)-3',4'-dimethyl-5'-phenyl-2'-((tetrahydro-2H-pyran-2''-yloxy)methyl)oxazolidin-2-yl)propan-2-one (**19p**).

Free base (1*S*,2*S*)-pseudoephedrine (1.62 g, 9.8 mmol) in warm (40-55°C) dry THF (15 mL) was added quickly with stirring to neat **18a** (1.95 g, 10.7 mmol) and allowed to stir at room temperature for 4 h or until the Michael addition was complete as monitored by GC-MS. The THF was removed under vacuum to leave **19p** as a viscous yellow resin. Yield via GC-MS was 99%. The crude reaction material was used without further purification. ^{1}H NMR (300 MHz, $CDCl_3$): δ 7.50-7.25 (m, 5H), 7.50-7.25 (m, 5H), 4.67 (s, 1H), 4.67 (s, 1H), 4.44 (d, 1H, *J* = 8.7 Hz), 4.44 (d, 1H, *J* = 8.7 Hz), 4.02 (d, 1H, *J* = 10.6 Hz), 3.97 (d, 1H, *J* = 10.6 Hz), 3.87 (m, 1H), 3.87 (m, 1H), 3.56 (m, 1H), 3.56 (m, 1H), 3.57 (d, 1H, *J*1 = 10.6 Hz), 3.49 (d, 1H, *J* = 10.6 Hz), 2.95-2.75 (m, 2H), 2.95-2.75 (m, 2H), 2.46 (s, 3H), 2.44 (s, 3H), 2.29 (s, 3H), 2.27 (s, 3H), 1.90-1.47 (m, 6H), 1.90-1.47 (m, 6H), 1.06 (d, 3H, *J* = 6.0 Hz), 1.06 (d, 3H, *J* = 6.0 Hz). ^{13}C NMR (75 MHz, $CDCl_3$): δ 207.4, 207.3, 139.6, 139.6, 128.4, 128.4, 128.2, 128.2, 127.0, 127.0, 99.5, 99.5, 96.4, 96.4, 85.9, 85.8, 72.6, 72.1, 70.4, 69.9, 65.2, 65.2, 62.3, 62.1, 46.5, 46.0, 49.8, 49.7, 32.3, 32.3, 32.2, 32.1, 30.7, 30.7, 25.6, 25.6, 19.4, 19.3, 15.1, 14.9. Mass spectrum *m/z* 347 (M^+, 0.1), 346 (0.1), 290 (3.0), 246 (2.3), 234 (1.6), 233 (16.7), 232 (100.0), 207 (1.0), 205 (13.5), 190 (1.0), 188 (1.5), 174 (5.6), 160 (0.4), 149 (9.3), 148 (93.0), 147 (4.8), 146 (3.2), 144 (1.6), 133 (6.3), 132 (3.2), 131 (4.0), 119 (1.2), 118 (26.9), 117 (19.0), 116 (1.2), 115 (5.1), 114 (2.4), 105 (4.0), 91 (11.9), 85 (19.8), 76 (2.4), 67 (3.2), 58 (5.6), 57 (7.9), 56 (17.5), 55 (6.3), 43 (27.8). (t_R = 23:63 min)

Signals for the enamine form of **19p**, methyl 5-(*N*-((1*S*,2*S*)-1-hydroxy-1-phenylpropan-2-yl)-*N*-methylamino)-1-methyl-7-oxa-bicyclo[2.2.1]hept-5-ene-2-carboxylate, were not observed.

The (1*R*,2*S*)-ephedrine isomer was used to prepare 1-((2*R/S,*4*S*,5*R*)-3',4'-dimethyl-5'-phenyl-2'-((tetrahydro-2H-pyran-2''-yloxy)methyl)oxazolidin-2-yl)propan-2-one **19q** following the same procedure. Major ions in GC-MS fragmentation were identical to **19p** and ^{1}H NMR spectra showed broadened indistinguishable signals due to a mixture of diastereoisomers (Appendix 2.10) and equilibration to the enamine form methyl 5-(*N*-((1*R*,2*S*)-1-hydroxy-1-phenylpropan-2-yl)-*N*-methylamino)-1-methyl-7-oxa-bicyclo[2.2.1]hept-5-ene-2-carboxylate. The GC-MS trace of **19q** is shown in Chapter 2, Figure 2.16. Mass spectrum *m/z* 347 (M^+, 0.1), 290 (1.0), 246 (1.0), 234 (1.6), 233 (16.7), 232 (93.7), 207 (1.0), 206 (2.4), 205 (13.5), 204 (1.6), 190 (1.0), 189 (2.4), 188 (1.5), 176 (1.0), 174 (5.6), 160 (1.0), 149 (10.3), 148 (100), 147 (4.8), 146 (3.2), 144 (1.6), 133 (6.3), 132 (3.2), 131 (4.0), 130 (1.6), 119 (3.2), 118 (34.9), 117 (19.0), 116 (3.2), 115 (7.1), 114 (2.4), 105 (4.0), 103 (2.4), 91 (11.9), 85 (19.8), 81 (1.6), 79 (1.6), 78 (2.4). (t_R = 23:56 min).

Preparation of (1S,2S)-2-(N-methyl-N-(5-methylfuran-3-yl)amino)-1-phenylpropan-1-ol (**5p**).

Freshly prepared **19p** was dissolved in DCE (135 mL). Anhydrous trifluoroacetic acid (5 mL) was added in one portion and the solution stirred at ambient temperature for 40 min upon which time the solution had become dark red in color. The solution was then poured into a mixture of NaOH (100 mL, 5 M aq.) and ice (300 g) and immediately shaken vigorously in a separating funnel. The organic layer was separated and the aqueous layer extracted with DCM (3 x 100 mL). The combined organic layers contain *N*,5-dimethyl-*N*-((1*S*,2*S*)-1-phenyl-1-(tetrahydro-2H-pyran-2-yloxy)propan-2-yl)furan-3-amine (**5p-THP**) and require deprotection. *Removal of the THP- group*: The combined organic layers containing **5p-THP** were evaporated and the residue was re-dissolved in ethanol (200 mL). *p*-Toluene sulphonic acid (4.0 g, 23.3 mmol) was added in one portion and the solution stirred for 4 h at 60°C. The ethanol was then evaporated under vacuum and the residue dissolved in HCl (250mL, 1 M aq.). The aqueous solution was extracted with DCM (3 x 150 mL), and the organic layers re-extracted with HCl (3 x 100 mL, 1M aq.). The combined aqueous phases were extracted once more with DCM (50 mL) and ice (200g) was added to chill the solution to 5°C. The solution was then basified with ice cold NaOH (3 M aq.) to pH 14, followed by a final extraction with DCM (4 x 100 mL). The organic phases were combined and upon evaporation **5p** was obtained as a viscous, dark-yellow oil (2.26g, 94% overall yield calculated from pseudoephedrine, >97% pure GCMS). Discolouration and impurities of (1*S*,2*S*)-pseudoephedrine were removed by dissolving the material in Et_2O and rapidly eluting the solution through short silica column deactivated with triethylamine. ^{1}H NMR (300 MHz; $CDCl_3$) δ 7.45-7.25 (5H,

m, H-2', H-3', H-4', H-5', H-6'), 6.87 (1H, s, H-2''), 5.94 (1H, s, H-4''), 4.46 (1H, d, *J* = 9.6 Hz, H-1), 3.48 (1H, s, OH), 3.26 (1H, dq, *J*1 = 6.6 Hz, *J*2 = 9.6 Hz, H-2), 2.60 (3H, s, NC$\underline{H}_3$), 2.24 (3H, s, H-6''), 0.81 (3H, d, *J* = 6.6 Hz, H-3). ^{13}C NMR (75 MHz; $CDCl_3$) δ 152.5 (C-5''), 141.5 (C-1'), 140.9 (C-3''), 128.6 (C-3', C-5'), 128.2 (C-4'), 127.5 (C-2', C-6'), 125.5 (C-2''), 101.3 (C-4''), 75.1 (C-1), 64.8 (C-2), 33.0 (N$\underline{C}H_3$), 14.1 (C-6''), 10.0 (C-3). Mass spectrum *m/z* 245 (M^+ 1.0), 184 (1.0), 139 (11.1), 138 (100), 124 (1.6), 123 (2.4), 122 (1.6), 120 (1.6), 108 (4.0), 105 (1.6), 97 (3.2), 96 (8.7), 95 (3.2), 94 (6.3), 91 (2.4), 82 (1.6), 81 (4.0), 80 (3.2), 77 (8.7), 68 (2.4), 67 (1.6), 66 (1.6), 57 (1.6), 56 (2.4), 55 (1.6), 53 (3.2), 51 (4.0), 43 (7.9), 42 (11.9). (t_R = 21:14 min).

The ephedrine stereoisomer (1*R*,2*S*)-2-(*N*-methyl-*N*-(5-methylfuran-3-yl) **5q** was prepared in >98% yield following an identical procedure from **19q**. ^{1}H NMR (300 MHz; $CDCl_3$) δ 7.45-7.25 (5H, m, H-2', H-3', H-4', H-5', H-6'), 6.86 (1H, s, H-2''), 5.93 (1H, s, H-4''), 4.45 (1H, d, *J* = 9.7 Hz, H-1), 4.04 (1H, s, OH), 3.26 (1H, dq, *J*1 = 6.5 Hz, *J*2 = 9.7 Hz, H-2), 2.60 (3H, s, NC$\underline{H}_3$), 2.24 (3H, s, H-6''), 0.81 (3H, d, *J* = 6.5 Hz, H-3). ^{13}C NMR (75 MHz; $CDCl_3$) δ 152.4 (C-5''), 141.5 (C-1'), 140.7 (C-3''), 128.5 (C-3', C-5'), 128.1 (C-4'), 127.5 (C-2', C-6'), 125.5 (C-2''), 101.2 (C-4''), 75.1 (C-1), 64.7 (C-2), 32.9 (N$\underline{C}H_3$), 14.0 (C-6''), 9.9 (C-3). (t_R = 21:31 min).

6.6 Diels-Alder reactions of 3-furylamines

Product were separated and identified by GC-MS using *Method 2* unless otherwise specified.

6.6.1 Diels-Alder reactions in organic solvents; Preparation of (1R,2R,4R)/(1S,2S,4S)-methyl 1-methyl-5-oxo-7-oxa-bicyclo[2.2.1]heptane-2-carboxylate **(4a).**

Procedure 1: To **5a** (200 mg, 1.2 mmol) in toluene (10 mL) was added MAC (310 mg, 36 mmol) and the solution heated to 110°C for 8 h. The solution was then evaporated under vacuum and re-dissolved in DCM (20 mL) followed washing with brine and the combined aqueous phases were re-extracted with DCM (2 x 10 mL). All organic phases were recombined and dried over Na_2SO_4, then evaporated to leave a dark resin (65 mg) consisting of 85% 1-methyl-5-(5-methyl-3-morpholin-4-yl-furan-2-yl)-5-morpholin-4-yl-7-oxa-bicyclo[2.2.1]heptane-2-carboxylic acid methyl ester **26** by GC-MS analysis. ^{1}H NMR (300 MHz; $CDCl_3$) δ 6.06 (1H, s, H-4'), 5.28 (1H, d, *J* = 5.9 Hz, H-4), 3.74 (3H, s, H-10), 3.71 (4H, m, H-2'', 6''), 3.64 (4H, m, H-2''', H-6'''), 3.21 (1H, d, *J* = 12.5 Hz, H-2), 2.76 (4H, m, H-5'', H-3''), 2.64 (1H, d, J = 13.2 Hz, H-6_A), 2.38 (2H, m, 5_A''', 3_A'''), 2.23 (2H, m, 5_B''', 3_B'''), 2.22 (1H, m, H-3_A), 2.20 (3H, s, H6'), 1.76 (1H, d, *J* = 13.2 Hz, H-6_B), 1.56 (1H, dd, *J*1 = 12.5 Hz, *J*2 = 5.9 Hz, H-3_B), 1.43 (3H, s, H-9). ^{13}C NMR (75 MHz; $CDCl_3$) δ 175.5 (C-7), 149.7 (C-2'), 144.2 (C-5'),

137.1 (C-3'), 102.2 (C-4'), 86.9 (C-1), 79.8 (C-4), 71.3 (C-5), 67.5 (C-5'', C-3''), 67.3 (C-5''', C-3'''), 54.4 (C-2'', C-6''), 51.7 (C-10), 49.9 (C-2''', C-6'''), 43.6 (C-2), 36.3 (C-6), 24.5 (C-3), 17.9 (C- 6'), 14.1 (C-9). Mass spectrum *m/z* M^+ not observed, 252 (1.0), 249 (1.5), 248 (13.5), 247 (82.1), 233 (1.0), 232 (6.4), 230 (1.0), 218 (2.5), 216 (5.7), 204 (16.8), 202 (9.5),190 (12.5), 189 (42.2), 188 (12.0), 187 (2.1), 180 (3.5), 176 (6.8), 175 (24.7), 174 (100), 171 (4.5), 167 (2.1), 162 (8.0), 160 (12.8), 148 (11.6), 147 (42.4), 146 (33.9), 132 (7.5), 119(10.7), 109 (14.0), 91 (11.5), 79 (11.1), 77 (14.5), 65 (14.7), 53 (27.5), 52 (10.1), 51 (13.4), 43 (80.0), 41 (11.9), 39 (19.2).

Procedure 2: Freshly distilled 4-(5-methylfuran-3-yl)morpholine **5a** (200 mg, 1.2 mmol) was added to DCM (10mL) at ambient temperature, followed by MAC (210 mg, 2.4 mmol). The solution was allowed to stir at room temperature for 8hr then DCM (30 mL) was added and the reaction mixture vigorously shaken with HCl (0.5M, 3 x 20 mL). The aqueous acidic layers were re-extracted with DCM (2 x 20 mL) and the combined organic phases dried with Na_2SO_4 and evaporated to leave methyl 1-methyl-5-oxo-7-oxa-bicyclo[2.2.1]heptane-2-carboxylate **4a:4b** as a 4:1 mixture of diastereomers (205 mg, combined yield 93%). The **4a** diastereoisomer was purifed by column chromatography using 10:1 pentane:ethylacetate. (**4a**, *endo* R_f = 0.38; **4b**, *exo* R_f = 0.12). *Endo*-(1*R*,2*R*,4*R*)/(1*S*,2*S*,4*S*)-methyl 1-methyl-5-oxo-7-oxa-bicyclo[2.2.1]heptane-2-carboxylate (**4a**). Pale yellow oil. IR (neat)/cm^{-1} 2956w, 1767s, 1733s, 1438w, 1388w, 1353w, 1320w, 1252w, 1203m, 1178m, 1149w, 1052w. ^{1}H NMR (300 MHz, $CDCl_3$): δ 4.37 (d, 1H, *J* = 6.6 Hz, broad, H-4), 3.72 (s, 1H, H-10), 2.88 (ddd, 1H, *J*1 = 11.4 Hz, *J*2 = 5.4 Hz, *J*3 = 2.1 Hz, H-2), 2.39 (d, 1H, *J* = 17.8 Hz, H-6_A), 2.33 (ddd, 1H, *J*1 = 13.4 Hz, *J*2 = 6.6 Hz, *J*3 = 5.4 Hz H-3_A), 2.17 (apparent d, 1H, *J* = 18.4 Hz, H-6_B), 2.16 (dd, 1H, *J*1 = 13.4 Hz, *J*2 = 5.4 Hz, H-3_B), 1.7 (s, 3H, H-9). ^{13}C NMR (75 MHz, $CDCl_3$): δ 210.3 (C-5), 172.2 (C-8), 86.0 (C-1), 81.4 (C-4), 52.5 (C-10), 51.0 (C-2), 46.0 (C-6), 30.9 (C-3), 21.5 (C-9). Mass Spectrum *m/z* 184 (M^+ 6.3), 156 (7.9), 153 (14.3), 152 (12.7), 141 (1.6), 140 (7.1), 138 (11.1), 128 (13.5), 127 (4.0), 125 (3.2), 124 (12.7), 115 (1.6), 114 (11.7), 113 (42.1), 112 (6.3), 111 (41.3), 110 (7.9), 109 (4.0), 100 (2.4), 99 (15.9), 98 (100), 97 (24.6), 96 (27.0), 95 (18.3), 87 (9.5), 86 (2.4), 85 (9.5), 84 (4.0), 83 (46.0), 82 (17.5), 81 (14.3), 80 (4.8), 79 (7.9), 73 (7.9), 72 (1.6), 71 (9.5), 70 (6.3), 69 (50.8), 68 (37.3), 67 (30.2), 65 (1.6), 59 (23.8), 58 (5.6), 57 (3.2), 56 (3.2), 55 (51.6), 54 (6.3), 53 (22.2), 52 (3.2), 51 (5.6), 50 (2.4), 45 (4.8), 44 (3.2), 43 (84.1). (t_R = 11:19 min)

6.6.2 Diels-Alder reactions in aqueous media; Preparation of (1R,2S,4R)/(1S,2R,4S)-methyl 1-methyl-5-oxo-7-oxa-bicyclo[2.2.1]heptane-2-carboxylate **(4b).**

General procedure for the Diels-Alder reaction of 3-furylamines in aqueous media

Method 1: Freshly distilled **5a** (100 mg, 0.60 mmol) was added to distilled water (20 mL) at ambient temperature, followed by MAC (78 mg, 0.91 mmol). The solution was allowed to stir at room temperature for 2 h and was then extracted with DCM (3 x 100 mL). The organic extracts were washed with HCl (0.5M, 3 x 20 mL) and the aqueous phases were re-extracted with DCM (2 x 10 mL). The combined organic layers were dried with $MgSO_4$ and evaporated to leave a 2.5:1 mixture of **4a:4b** diastereomers (127 mg, yield 84%).

Method 2: Freshly distilled *N*,*N*-diisopropyl-5-methylfuran-3-amine **5c** (100 mg, 0.55 mmol) was added to a 3 M solution of LiCl (20 mL) at ambient temperature, followed by MAC (71 mg, 0.83 mmol). The solution was allowed to stir at room temperature for 2 h then extracted with DCM (3 x 40 mL). The combined organic extracts were washed with HCl (0.5 M, 2 x 20 mL), dried with $MgSO_4$ and evaporated to leave *exo*-(1*R*,2*S*,4*R*)/(1*S*,2*R*,4*S*)-methyl 1-methyl-5-oxo-7-oxa-bicyclo[2.2.1]heptane-2-carboxylate (**4b**) as the major product in a 2:1 mixture with **4a** (93 mg, combined yield 91%, d.r. 1:2). The ketone **4b** was separated by column chromatography using 10:1 pentane:ethylacetate, (**4a**, *endo* $R_f = 0.38$; **4b**, *exo* $R_f = 0.12$) and formed white needle like crystals upon crystallization in Et_2O, whereas the **4a** compound was a pale yellow oil at room temperature. *Exo*-(1*R*,2*S*,4*R*)/(1*S*,2*R*,4*S*)-methyl 1-methyl-5-oxo-7-oxa-bicyclo[2.2.1]heptane-2-carboxylate (**4b**). White crystalline solid, m.p. 104 – 105°C. IR (KBr disk)/cm^{-1} 3033m, 2961w, 1762s, 1731s, 1441m, 1431m, 1392s, 1362s, 1253m, 1222m, 1199s, 1171s, 1148m, 1077w, 1038m, 1006s. ^{1}H NMR (300 MHz; $CDCl_3$) δ 4.47 (1H, d, *J* = 6.4 Hz, H-4), 3.73 (3H, s, H-10), 2.80 (1H, dd, *J*1 = 8.7 Hz, *J*2 = 5.1 Hz, H-2), 2.52 (1H, apparent dt, *J*1 = 13.4 Hz, *J*2 = 5.9 Hz, H-3_A), 2.25 (2H, m, AB quartet, H-6), 1.94 (1H, dd, *J*1 = 13.4 Hz, *J*2 = 8.7 Hz, H-3_B), 1.55 (3H, s, H-9). ^{13}C NMR (75 MHz; $CDCl_3$) δ 211.0 (C-5), 173.0 (C-8), 86.3 (C-1), 80.7 (C-4), 52.3 (C-10), 50.5 (C-6), 49.4 (C-2), 30.7 (C-3), 19.3 (C-9). Mass Spectrum *m/z* 185 (1.6), 184 (M^+ 9.5), 157 (3.2), 156 (17.5), 154 (2.4), 153 (27.8), 152 (15.9), 141 (7.1), 140 (14.3), 139 (1.6), 138 (22.2), 129 (1.6), 128 (27.0), 127 (7.9), 125 (3.2), 124 (27.0), 123 (3.2), 115 (1.6), 114 (18.3), 113 (65.1), 111 (59.5), 110 (6.3), 109 (4.8), 100 (1.6), 99 (15.9), 98 (98.4), 97 (39.7), 96 (41.3), 95 (17.5), 87 (10.3), 86 (3.2), 85 (11.1), 84 (5.6), 83 (66.7), 82 (23.0), 81 (21.4), 80 (9.5), 79 (11.9), 78 (3.2), 77 (2.4), 73 (11.1), 72 (3.2), 71 (7.9), 70 (4.8), 69 (68.3), 68 (44.4), 67 (51.6), 66 (2.4), 65 (5.6), 59 (30.2), 58 (5.6), 57 (4.0), 56 (6.3), 55 (63.5), 54 (8.7), 53 (18.3), 52 (3.2), 51 (6.3), 50 (3.2), 45 (6.3), 44 (11.1), 43 (100), 42 (19.0), 41 (85.7). HRMS calc. for $C_9H_{12}O_4Na[M]^{+\cdot}$ 207.0633. Found 207.0631. (t_R = 11:35 min)

Crystal Data for **4b**.

Empirical Formula	$C_9H_{12}O_4$
Formula Weight (g/mol)	184.19
Melting Point (^oC)	104-105
Crystal Colour	Colourless
Crystal Description	Block
Crystal Class	Triclinic
Space Group	P-1
a(Å)	7.2235(10)
b(Å)	8.1158(11)
c(Å)	8.3058(12)
$\alpha(^o)$	75.273(2)
$\beta(^o)$	74.540(3)
$\gamma(^o)$	86.114(2)
Density (g/m^3)	1.348
Crystal Size (mm)	0.50, 0.15, 0.10
Volume ($Å^3$)	453.89
Z	2
$\mu(mm^{-1})$	0.106
F(000), e	196
θ range, ^{o}	2.59-25.0
Index ranges	$-8 \leq h \leq 8, -9 \leq k \leq 9, -6 \leq l \leq 9$
Reflections collected/unique	2428/1583 [R(int)=0.0587]
Data/restraints/parameters	1583/0/121
Goodness of fit on F^2	1.029
Final R indices [$I>2\sigma(I)$]	$R1 = 0.0529$, $wR2 = 0.1351$
R indices (all data)	$R1 = 0.0605$, $wR2 = 0.1414$

6.6.3 General procedure for the Diels-Alder reaction of 3-furylamines in ionic liquid DIMCARB.

Freshly distilled *N*,*N*-diisopropyl-5-methylfuran-3-amine **5c** (100 mg, 0.55 mmol) was dissolved in DIMCARB (10 mL) then MAC (78 mg, 0.91 mmol) was added in one portion. The solution was allowed to stir at room temperature for 1 h, evaporated and then re-dissolved in DCM (30 mL). The organic solution was washed with HCl (0.5M, 3 x 20 mL) and the aqueous phases were re-extracted with DCM (2 x 10 mL). The combined organic layers were dried with $MgSO_4$ and evaporated to leave a 3:7 ratio of **4a**:**4b** (135 mg, yield 95%).

*6.6.4 General procedure for the Diels-Alder reaction ephedrine derived furans (***5p** *and* **5q***) in DCM.*

Example: Diels-Alder reaction of (1*S*,2*S*)-2-(*N*-methyl-*N*-(5-methylfuran-3-yl)amino)-1-phenylpropan-1-ol (**5p**) with MAC in DCM.

The furan **5p** (150 mg, 0.61 mmol) was dissolved in DCM (20 mL) and cooled to –78°C. MAC (210 mg, 2.45 mmol) was then added and the solution was allowed to warm to –50°C where it was kept for 2 h, then gradually warmed to room temperature and stirred overnight. Evaporation of the solvent and excess MAC under vacuum gave diastereomers of optically enriched *endo*-(1*S*,4*S*,5*S*)/(1*R*,4*R*,5*R*)-methyl 3',4,4'*S*-trimethyl-5'*S*-phenylspiro[7-oxa-bicyclo[2.2.1]heptane-2,2'-[1,3]oxazolidine]-5-carboxylate (**28-*endo***) as a viscous red semisolid (196 mg, Yield >97%, *endo*:*exo* d.r. >99:1). ^{1}H NMR (300 MHz, $CDCl_3$): δ 7.40-7.22 (5H, m, arom., H-2'', H-3'', H-4'', H-5'', H-6''), δ4.60 (1H, d, *J* = 9.1 Hz, H-5'), 4.54 (1H, d, *J* = 6.2 Hz, H-1), 3.73 (3H, s, H-10), 3.05 (1H, dq, *J*1 = 6.7 Hz, *J*2 = 9.1 Hz, H-4'), 2.70 (1H, ddd, *J* = 11.4 Hz, *J* = 5.7 Hz, *J* = 1.9 Hz, H-5), 2.55 (1H, m, H-6_A), 2.46 (3H, s, NC$\underline{H}_3$), 2.43 (1H, m, H-3_A), 2.04 (1H, ddd, *J* = 11.4 Hz, *J* = 6.2 Hz, *J* = 5.7 Hz, H-6_B), 1.85 (1H, d, broad, *J* = 14.4 Hz, H-3_B), 1.64 (3H, s, H-9), 1.26 (3H, d, *J* = 6.7 Hz, H-6'). ^{13}C NMR (300 MHz, $CDCl_3$): δ 173.2 (C-8), 140.9 (C-1''), 128.6 (C-5'', C-3''), 127.5 (C-6'', C-2''), 126.0 (C-4''), 108.8 (C-2/2'), 85.3 (C-4), 83.1 (C-1), 81.8 (C-5'), 67.1 (C-4'), 52.1 (C-10), 51.8 (C-5), 41.7 (C-3), 33.9 (N$\underline{C}H_3$), 29.8 (C-6), 21.0 (C-9), 13.9 (C-6'). EI-MS (relative intensity) 331 (M^+ 3.5), 301 (2.0), 300 (9.2), 290 (2.4), 289 (20.8), 288 (100), 273 (2.1), 272 (12.3), 261 (1.3), 260 (2.7), 257 (1.1), 256 (4.7), 246 (1.0), 245 (4.3), 244 (1.3), 228 (1.8), 217 (1.6), 216 (5.5), 205 (1.3), 204 (7.8), 203 (1.1), 202 (5.8), 197 (2.0), 189 (5.5), 174 (2.4), 154 (1.0), 149 (7.4), 148 (68.7), 147 (3.3), 146 (3.9), 145 (1.1), 144 (1.2), 141 (11.8), 138 (2.6), 133 (4.7), 132 (2.7), 131 (4.9), 130 (2.2), 129 (1.1), 127 (1.0), 124 (1.0), 123 (1.2), 119 (3.2), 118 (34.0), 117 (27.2), 116 (3.7), 115 (8.9), 113 (4.6), 111 (1.2), 110 (2.6), 109 (10.7), 108 (1.4), 107 (1.0), 105 (4.5), 104 (1.3),

103 (3.6), 98 (1.4), 97 (2.4), 96 (1.7), 95 (4.7), 94 (1.1), 92 (1.7), 91 (14.3), 90 (1.3), 89 (2.3), 85 (2.3), 83 (2.3), 82 (3.2), 80 (1.0), 79 (4.0), 78 (2.5), 77 (6.8), 73 (1.0), 71 (1.4), 70 (1.5), 69 (7.4), 68 (3.1), 67 (5.2), 65 (4.1), 63 (1.3), 59 (4.4), 58 (4.6), 57 (1.9), 56 (14.7), 55 (10.3), 54 (1.5), 53 (4.4), 51 (2.2), 45 (1.0), 44 (1.8), 43 (11.4), 42 (11.0), 41 (13.3), 40 (1.6), 39 (5.5), 32 (1.5), 30 (1.2). HRESI calc. for $C_{19}H_{26}NO_4$ 332.1862, found 332.1855. (t_R = 16:27 min). (**28-*exo***, t_R = 16:59 min).

Signals for the enamine methyl 5-(*N*-((1*S*,2*S*)-1-hydroxy-1-phenylpropan-2-yl)-*N*-methylamino)-1-methyl-7-oxa-bicyclo[2.2.1]hept-5-ene-2-carboxylate (**28-int**) were not observed.

An identical procedure was used for the reaction of **5q** in DCM to prepare a mixture of diastereoisomers of (1*S*,4*S*,5*S*)/(1*R*,4*R*,5*R*)-methyl 3',4,4'*S*-trimethyl-5'*R*-phenylspiro[7-oxa-bicyclo[2.2.1]heptane-2,2'-[1,3]oxazolidine]-5-carboxylate (**30-*endo***, t_R = 20:69 min, *Method 1*; t_R = 16:25 min, *Method 2*) and (1*S*,4*S*,5*R*)/(1*R*,4*R*,5*S*)- methyl 3',4,4'*S*-trimethyl-5'*R*-phenylspiro[7-oxa-bicyclo[2.2.1]heptane-2,2'-[1,3]oxazolidine]-5-carboxylate (**30-*exo***, t_R = 21:75 min; *Method 1*; t_R = 16:57 min, *Method 2*) (95% combined yield) in a diastereomeric ratio of 4:1 according to GC-MS analysis. EI-MS (relative intensity) 331 (M^+ 0.6), 301 (0.7), 300 (3.7), 290 (1.3), 289 (8.4), 288 (44.3), 273 (0.9), 272 (5.9), 261 (0.5), 260 (1.6), 257 (0.6), 256 (3.7), 246 (0.6), 245 (3.1), 244 (0.9), 228 (1.0), 217 (1.0), 216 (6.8), 205 (1.3), 204 (7.0), 202 (4.8), 200 (0.6), 197 (2.5), 190 (1.2), 189 (4.9), 176 (1.3), 174 (3.5), 159 (1.4), 158 (0.9), 149 (12.1), 148 (100), 146 (5.4), 145 (2.2), 144 (1.7), 143 (1.0), 142 (2.9), 141 (23.5), 139 (0.6), 138 (3.1), 133 (6.4), 132 (4.7), 131 (4.9), 130 (2.2), 129 (1.1), 127 (1.0), 124 (1.0), 123 (1.2), 119 (3.2), 118 (36.7), 117 (32.2), 116 (6.2), 115 (12.6), 113 (8.2), 111 (2.0), 110 (4.1), 109 (22.2), 108 (3.7), 107 (2.3), 105 (7.9), 104 (2.0), 103 (5.8), 98 (2.6), 97 (3.8), 96 (3.0), 95 (6.3), 94 (1.9), 92 (2.1), 91 (20.9), 90 (2.7), 89 (3.5), 85 (2.3), 83 (2.3), 82 (6.2), 80 (1.0), 79 (8.0), 78 (4.5), 77 (10.9), 73 (1.0), 71 (1.4), 70 (3.5), 69 (12.7), 68 (7.5), 67 (9.2), 65 (6.6), 63 (1.3), 59 (12.6), 58 (10.4), 57 (4.0), 56 (33.9), 55 (20.8), 54 (3.8), 53 (9.2), 51 (4.2), 45 (2.0), 44 (1.8), 43 (25.4), 42 (23.9), 41 (24.4), 40 (3.2), 39 (12.8), 32 (1.5), 30 (1.2). HRESI calc. for $C_{19}H_{26}NO_4$ 332.1862, found 332.1855.

6.6.5 Confirmation of Absolute Stereochemistry in Diels-Alder Reaction of **5p** *and* **5q.**

Preparation of methyl 5-(N-((1S,2S)-1-hydroxy-1-phenylpropan-2-yl)-N-methylamino)-1-methyl-7-oxa-bicyclo[2.2.1]heptane-2-carboxylate (**29**) *using conditions described by Hutchins et al.* [12]

To glacial acetic acid (35 mL), $NaBH_4$ (0.87 g, 23.0 mmol, crushed pellets) was added portion wise with cooling in an ice bath and stirred until the evolution of hydrogen ceased. A solution of **28-*endo*** (2.55 g, 77 mmol), (prepared from **5p,** Section 6.6.4), in glacial acetic acid (17 mL) was added drop-

wise, followed by the portion-wise addition of $NaBH_4$ (0.50 g, 13.2 mmol, crushed pellets). After stirring for a further 4 h at ambient temperature, the mixture was poured into H_2O (200 mL) and carefully neutralized with $NaHCO_3$ (saturated aqueous solution). The neutralized solution was extracted with DCM (3 x 75 mL) and the combined extracts dried over Na_2SO_4. Evaporation of under vacuum gave a red resin which after bulb distillation (150°C @ 0.1mmHg) yielded (1*S*,2*S*,4*S*,5*S*)-methyl 5-(*N*-((1*S*,2*S*)-1-hydroxy-1-phenylpropan-2-yl)-*N*-methylamino)-1-methyl-7-oxa-bicyclo[2.2.1]heptane-2-carboxylate, (1*S*,2*S*,4*S*,5*S*)-**29-*endo***, as a viscous yellow resin (1.8 g, Yield 70%) in a 10:1 ratio with the (1*R*,2*R*,4*R*,5*R*)-**29-*endo*** diastereoisomer. ^{1}H NMR (300 MHz; $CDCl_3$) δ 7.35-7.22 (5H, arom. m, H-2'', H-3'', H-4'', H-5'', H-6''), 4.40 (1H, dd, , *J*1 = 5.6 Hz, *J*2 = 4.7 Hz, H-4), 4.27 (1H, d, *J* = 9.6 Hz, H-1'), 3.78 (3H, s, H-10), 3.12 (1H, m, H-5), 2.78 (1H, m, H-2), 2.76 (1H, m, H-3_A), 2.64 (1H, dq, *J*1 = 9.6 Hz, *J*2 = 6.7 Hz , H-2'), 2.10 (3H, s, H-4'), 2.03 (1H, m, H-3_B), 1.64 (2H, m, H-6), 1.57 (3H, s, H-9), 0.66 (3H, d, *J* = 6.7 Hz, H-3'). ^{13}C NMR (75 MHz; $CDCl_3$) δ 172.7 (C-8), 142.3 (C-1''), 128.4 (C-5'', C-3''), 127.8 (C-6'', C-2''), 127.5 (C-4''), 87.0 (C-1), 79.4 (C-4), 74.5 (C-1'), 64.9 (C-5), 63.2 (C-2'), 53.3 (C-2), 52.5 (C-10), 38.3 (C-6), 33.2 (N<u>C</u>H$_3$), 28.0 (C-3), 21.6 (C-9), 7.5 (C-3'). EI-MS (relative intensity) 333 (M^+ not observed), 302 (3.4), 228 (2.5), 227 (21.0), 226 (100), 182 (1.9), 168 (2.0), 166 (1.1), 151 (2.3), 148 (3.5), 142 (1.0), 141 (1.6), 140 (10.0), 138 (2.0), 137 (5.9), 125 (1.1), 124 (4.1), 123 (2.0), 117 (1.5), 110 (2.7), 109 (4.0), 108 (1.4), 107 (2.0), 105 (1.8), 98 (1.1), 96 (2.2), 95 (2.0), 94 (1.2), 93 (1.5), 91 (3.1), 84 (3.9), 83 (1.3), 82 (2.4), 81 (6.1), 79 (4.7), 77 (3.6), 67 (1.2), 59 (1.7), 58 (11.6), 57 (2.0), 56 (2.0), 55 (2.0), 43 (3.7), 42 (3.3). HRESI calc. for $C_{19}H_{28}NO_4$ 334.2018 found 334.2013.

Full ^{1}H NMR characterization of (1*R*,2*R*,4*R*,5*R*)-**29-*endo*** was not obtained and ^{13}C NMR signals for this minor diastereoisomer are included here. ^{13}C (75 MHz; $CDCl_3$) δ172.7, 142.3, 128.4, 127.9, 127.5, 87.1, 78.6, 75.1, 65.1, 63.2, 53.1, 52.2, 38.9, 33.2, 28.7, 21.7, 6.7.

Preparation of (1S,2S,4S,5S)-methyl 5-(N-((1S,2S)-1-hydroxy-1-phenylpropan-2-yl)-N-methylamino)-1-methyl-7-oxa-bicyclo[2.2.1]heptane-2-carboxylate perchlorate salt (1*S*,2*S*,4*S*,5*S*)-**29.HClO$_4$** [13].

To the above 10:1 mixture of (1*S*,2*S*,4*S*,5*S*)-**29-*endo*** and (1*R*,2*R*,4*R*,5*R*)-**29-*endo*** (1.0 g, 30.0 mmol) in dry Et_2O was bubbled HCl gas by means of the Kipps generator. A white hygroscopic salt precipitated which was quickly filtered and dried in a vacuum dessicator over drying silica. The hydrochloride salt was dissolved in acetonitrile (20 mL) and silver perchlorate (620 mg, 30.0 mmol) was added as the solution was gently warmed (50°C). After 10 min, the solution was filtered and the salt crystallized by slow evaporation of solvent. Recrystallization from hot EtOH gave colourless needles that showed only a single diastereoisomer by ^{13}C NMR analysis. One final crystallization was performed from MECN by the slow diffusion of Et_2O to give pure (1*S*,2*S*,4*S*,5*S*)-**29.HClO$_4$** as colourless plates

which were showed only a single diastereomer by ^{13}C NMR analysis. (m.p. 227°C). ^{1}H NMR (300 MHz; CD_3CN) δ 7.27 (5H, arom. br. s., H-2'', H-3'', H-4'', H-5'', H-6''), 4.76 (1H, s, OH), 4.75 (1H, m, H-4), 4.74 (1H, d, *J* = 10.1 Hz, H-1'), 3.91 (1H, m, *J* = 5.3 Hz, H-5), 3.78 (3H, s, H-10), 3.47 (1H, m, H-2'), 2.95 (1H, apparent t., H-2), 2.87 (3H, s, $N\underline{C}H_3$), 2.30 (2H, m, H-3), 1.95 (2H, m, H-6), 1.54 (3H, s, H-9), 1.02 (3H, d, *J* = 6.8 Hz, H-3'). ^{13}C NMR (75 MHz; CD_3CN) δ 174.8 (C-8), 140.1 (C-1''), 130.0 (C-4''), 129.7 (C-3'', C-5''), 128.3 (C-2'', C-6''), 88.4 (C-1), 77.0 (C-4), 72.5 (C-1'), 67.8 (C-2'), 65.3 (C-5), 53.5 (C-10), 52.5 (C-2), 35.6 (C-6), 35.1 ($N\underline{C}H_3$), 30.7 (C-3), 20.8 (C-9), 8.7 (C-3').

Crystal structure data for **29.$HClO_4$**.

Empirical Formula	$C_{19}H_{28}ClNO_8$
Formula Weight (g/mol)	433.87
Melting Point (°C)	300 (dec.)
Crystal Colour	Colourless
Crystal Description	Plates
Crystal Class	orthorhombic
Space Group	P212121
a(Å)	8.511(2)
b(Å)	15.356(5)
c(Å)	15.839(3)
α(°)	90.00
β(°)	90.00
γ(°)	90.00
Density (g/m^3)	1.392
Crystal Size (mm)	0.20 x 0.10 x 0.02
Volume (Å^3)	2070.1(9)
Z	4
μ(mm^{-1})	2.043
F(000), e	920
θ range, °	4.01-64.92
Index ranges	$-1 \leq h \leq 9$, $-18 \leq k \leq 0$, $-1 \leq l \leq 18$
Reflections collected/unique	2462/2365 [R(int) = 0.0230]
Data/restraints/parameters	2365/0/275
Goodness of fit on F^2	1.071
Final R indices [I>2σ(I)]	*R*1 = 0.0496, *wR*2 = 0.1271
R indices (all data)	*R*1 = 0.0608, *wR*2 = 0.1371

*6.6.6 General procedure for the hydrolysis of ephedrine derived oxazolidines (***28** *and* **30***).*

Example: Preparation of (1*S*,2*S*,4*S*)-methyl 1-methyl-5-oxo-7-oxa-bicyclo[2.2.1]heptane-2-carboxylate (1*S*,2*S*,4*S*)-**4a**.

To a solution of acetic acid (0.5 mL), sodium acetate (3 g), H_2O (15 mL) was added **28-*endo*** (196 mg, 0.61 mmol), as a mixture of diastereoisomers obtained from **5p** (Section 6.6.4), and the solution heated with stirring in an oil bath at 70°C. After 2 h the solution was cooled and extracted with DCM (3 x 75 mL). The ketone *endo*-(1*S*,2*S*,4*S*) methyl 1-methyl-5-oxo-7-oxa-bicyclo[2.2.1]heptane-2-carboxylate (1*S*,2*S*,4*S*)-**4a** was purified as a pale yellow oil by flash column chromatography using pentane:EtOAc (5:1) (101 mg, Yield 90%, 85% *ee*, >98% pure GC-MS).

*6.6.7 General procedure for the Diels-Alder reaction ephedrine derived furans (***5p** *and* **5q***) in H_2O.*

Example: Diels-Alder reaction of (1*S*,2*R*)-2-(*N*-methyl-*N*-(5-methylfuran-3-yl)amino)-1-phenylpropan-1-ol (**5q**) with MAC in H_2O

The furan **5q** (100 mg, 0.41 mmol) was added to H_2O (10 mL) and irradiated in an ultrasonic bath (80% power) maintained between 15-25°C. MAC (157 mg, 1.80 mmol) was added drop-wise over 5 min and the solution irradiated for a further 95 min. The excess methyl acrylate was removed under high vacuum at room temperature and the solution extracted with DCM (3 x 35 mL). The product mixture was shown by GC-MS to contain both the ketones **4a-b** and diastereomers of optically enriched **30-*endo*** and **30-*exo*** in a 1:1 ratio and formed as a viscous red semisolid upon evaporation (110 mg, 86%, d.r. 1:1).

An identical procedure was used for the reaction of **5p** to prepare **28-*endo*** and **28-*exo*** as a 9:1 mixture of diastereoisomers (106 mg, 84%, d.r. 9:1).

*6.6.8 Preparation of (***1*S*,2*R*,4*S*)-methyl 1-methyl-5-oxo-7-oxa-bicyclo[2.2.1]heptane-2-carboxylate (+)-(***1*S*,2*S*,4*S*)-4b.**

Following the general methodology outlined in Section 6.6.6, a 1:1 mixture of **30-*endo***:**30-*exo*** (110 mg) was added to a solution of acetic acid (0.5 mL) and sodium acetate (3.0 g) in H_2O (15 mL) with heating at 70°C for 2 h. Extraction with DCM (3 x 75 mL) followed by evaporation gave a brown resin that was purified by flash column chromatography on SiO_2 (pentane:EtOAc, 10:1) to provide (1*S*,2*S*,4*S*)-

4a (30 mg, 40% yield, 18% *ee*) and (1*S*,2*R*,4*S*)-**4b** (31 mg, 41% yield, 60% *ee*). The optically enhanced (1*S*,2*R*,4*S*)-**4b** was crystallized from Et_2O at -18°C until the supernatant solution was enriched to enantiomeric purity as indicated by chiral GC-MS. The Et_2O was evaporated to dryness to leave optically pure (1*S*,2*R*,4*S*)-methyl 1-methyl-5-oxo-7-oxa-bicyclo[2.2.1]heptane-2-carboxylate (1*S*,2*R*,4*S*)-**4b** (14.5 mg, >99% *ee*) $[\alpha]_D$ = + 1.72° (*c* = 1.45, chloroform) in 19% yield from **5q**.

Calculation for the specific optical rotation of (1*S*,2*R*,4*S*)-**4b** is as follows;

14.5 mg of (1*S*,2*R*,4*S*)-**4b** was dissolved in 1.0 mL of $CHCl_3$ to provide a solution of c = 1.45 g/100 mL. The equation for specific optical rotation according to Hallas [14] is

$$[\alpha]_D^T = \frac{100\alpha}{l \times c}$$

and the measured optical rotation at c = 1.45 g/100 mL was stable at +0.025 after 24 measurements at 5 min intervals. The specific optical rotation is thus calculated as follows,

$$[\alpha]_D^{25} = \frac{100 \times (+0.025)}{1 \times 1.45} = +1.72^o$$

A sample at half the concentation (14.5 mg in 2.0 mL $CHCl_3$) c = 0.725 g/100 mL was prepared from the previous sample and a stable rotation value of + 0.011 was recorded after 23 measurements at 5 min intervals. The specific optical rotation is this calculated as follows,

$$[\alpha]_D^{25} = \frac{100 \times (+0.011)}{1 \times 0.725} = +1.52^o$$

The specific optical rotation was taken as the first measurement conducted at the higher concentration due the accumulation of error upon serial dilution to the second concentration and sample transfer procedure. The second measurement is simply to confirm the sign of the rotation value, determined to be dextrorotatory or (+).

6.7 Ether opening reactions of methyl 1-methyl-5-oxo-7-oxa-bicyclo[2.2.1]heptane-2-carboxylates **4a** *and* **4b.**

Product were separated and identified by GC-MS using *Method 2 unless otherwise specified*.

6.7.1 Acid induced ring opening reactions.

Preparation of methyl 4-acetoxy-2-methylbenzoate from **4b** *using conditions reported by Ogawa et al.* [15].

The ketone **4b** (56 mg, 0.30 mmol) was added to a solution of glacial acetic acid (0.52 mL), acetic anhydride (0.32 mL) and H_2SO_4 (conc., 0.034 g). The solution was stirred overnight then poured into dH_2O (20 mL) and extracted with ethyl acetate (3 x 25 mL). The organic extracts were dried with Na_2SO_4 and evaporated to leave methyl 4-acetoxy-2-methylbenzoate in high purity. (57 mg, Yield 90%, 91% Match NIST98 library). ^{1}H NMR (300 MHz, $CDCl_3$): δ 7.95 (arom. m, 1H, H-6), 6.99 (m, 2H, H-3, H-5), 3.88 (s, 3H, H-10), 2.61 (s, 3H, H-10), 2.30 (s, 3H, H-9). ^{13}C NMR (75 MHz, $CDCl_3$): δ 169.1 (C-8), 167.4 (C-7), 153.4 (C-4), 142.8 (C-2), 132.5 (C-6), 127.2 (C-1), 124.7 (C-3), 119.1 (C-5), 52.0 (C-11), 22.1 (C-10), 21.3 (C-9). Mass Spectrum *m/z* 209 (1.9), 208 (M^+, 15.6), 177 (6.8), 167 (8.2), 166 (74.9), 165 (6.9), 151 (2.1), 149 (1.1), 137 (2.5), 136 (11.1), 135 (100), 134 (33.0), 121 (1.4), 109 (1.2), 108 (1.7), 107 (12.0), 106 (5.3), 105 (6.3), 89 (1.3), 79 (3.0), 78 (5.9), 77 (14.7), 66 (1.4), 65 (1.3), 63 (2.6), 53 (1.9), 52 (3.1), 51 (4.5), 50 (1.7), 43 (12.0), 39 (1.8).

6.7.2 Base induced ring opening reactions

Preparation of 3-[(3-t-butyl-dimethyl-silanyloxy)-5-methyl-furan-2-yl]-propionic acid methyl ester (**31**) *from* **4a** *using condition reported by Le Drain et al.* [16].

To **4a** (100 mg, 0.54 mmol) in dry benzene (1.0 mL) under an inert (N_2) atmosphere was added 1.0 mL of a solution of $CF_3SO_3Si(t\text{-Bu})Me_2$ (0.43 g, 1.63 mmol) and triethylamine (0.21 g, 2.12 mmol, NaOH dry) in benzene (1.5 mL) and the solution stirred at ambient temperature for 4 hours. The remaining regent in benzene was added and the solution stirred for an additional 2 h before pouring into Et_2O (15 mL) and washing with HCl (10 mL, 1 M) followed by $NaHCO_3$ (5% aq. solution). The organic phase was evaporated under reduced pressure and the resin subject to column chromatography on silica gel (5:1 hexane:EtOAc) to afford **31** as a yellow oil (111 mg, 69% yield). ^{1}H NMR (300 MHz, $CDCl_3$):

δ5 .66 (s, 1H, H-4'), 3.70 (s, 3H, H-4), 2.85 (apparent t., *J* = 8.5 Hz, 2H, H-2), 2.60 (apparent t, *J* = 8.5 Hz, 2H, H-3), 2.16 (s, 3H, H-6'), 0.96 (s, 9H, H-4'', H-5'', H-6''), 0.14 (s, 6H, H-1'', H-2''). ^{13}C NMR (75 MHz, CDCl3) : δ173.6 (C-1), 148.2 (C-2'), 138.4 (C-3'), 136.9 (H-5'), 103.2 (H-4'), 51.8 (C-4), 32.8 (C-2), 25.8 (C-4'', C-5'', C-6''), 20.7 (C-3), 18.2 (C-3''), 14.2 (C-6'), -4.5 (C-1'', C-2''). Mass Spectrum *m/z* 299 (4.0), 298 (M^+ 18.3), 283 (1.6), 267 (1.6), 243 (3.2), 242 (10.3), 241 (60.3), 227 (4.8), 226 (15.1), 225 (81.0), 209 (4.8), 200 (4.8), 199 (19.0), 183 (4.0), 181 (4.8), 169 (9.5), 168 (3.2), 167 (25.4), 153 (4.8), 151 (3.2), 136 (3.2), 135 (31.7), 132 (3.2), 131 (37.3), 125 (3.2), 123 (3.2), 112 (1.6), 111 (27.0), 109 (3.2), 107 (4.8), 99 (4.8), 97 (3.2), 95 (1.6), 91 (5.6), 90 (7.9), 89 (98.4), 85 (4.8), 84 (5.6), 83 (4.8), 77 (4.8), 76 (2.4), 75 (23.8), 74 (9.5), 73 (100), 69 (2.4), 67 (1.6), 61 (3.2), 60 (2.4), 59 (34.9), 58 (4.8), 57 (6.3), 55 (7.1), 45 (10.3), 43 (18.3). (t_R = 13:46 min)

Preparation of methyl 3-(2,3-dihydro-5-methyl-3-oxofuran-2-yl)propanoate (**32**) *from* **4a** *using conditions reported by Takahashi et al.* [17].

A solution of **4a** (100 mg, 0.54 mmol) in dry THF (2.5 mL) under an inert (N_2) atmosphere was cooled to -78°C in a dry ice/acetone bath. LHMDS (1.35 mmol, 1.35 mL, 1 M in THF) was then added dropwise and the solution stirred at -50°C for 1.5 hours. An additional volume of LHMDS (0.95 mmol, 0.95 mL, 1 M in THF) was added and the solution stirred at -45°C for 30 min. The mixture was then quenched with ammonium chloride (saturated solution), and extracted with DCM (3 x 20 mL). The combined organic layers were evaporated and the product was subject to column chromatography on silica gel column (2cm diam., 20 mL length) using 5:3 pentane:EtOAc. 20 mL fractions were collected and fractions 14 to 17 contained pure **32**. (63 mg, Yield 63%). ^{1}H NMR (300 MHz, $CDCl_3$): δ 5.44 (s, 1H, H-4'), 4.49 (dd, *J*1 = 4.9 Hz, *J*2 = 7.7 Hz, 1H, H-2'), 3.67 (s, 3H, H-4), 2.46 (m, 2H, H-2), 2.27 (m, 1H, H-3_A), 2.23 (s, 3H, H-6'), 2.02 (apparent sextet, *J* = 7.7 Hz, 1H, H-3_B). ^{13}C NMR (75 MHz, $CDCl_3$): δ 204.3 (s, C-3'), 190.5 (s, C-5'), 173.1 (s, C-1), 104.6 (d, C-4'), 85.0 (d, C-2'), 52.0 (q, C-4), 29.2 (t, C-2), 26.4 (t, C-3), 17.0 (q, C-6'). Mass Spectrum *m/z* 185 (3.2), 184 (M^+ 26.2), 154 (2.4), 153 (33.3), 152 (34.9), 125 (14.3), 124 (19.0), 123 (2.4), 112 (7.1), 111 (100), 110 (15.9), 99 (4.0), 98 (42.9), 97 (4.0), 95 (1.6), 88 (2.4), 87 (3.2), 85 (20.6), 83 (2.4), 82 (1.6), 81 (2.4), 71 (11.9), 69 (14.3), 68 (58.7), 67 (6.3), 59 (13.5), 57 (11.9), 56 (5.6), 55 (81.0), 53 (4.8), 45 (2.4), 43 (42.9), 42 (11.1). (t_R = 12:21 min)

6.7.3 Lewis-Acid catalysed ring opening reactions.

Preparation of methyl 5,5-diacetoxy-1-methyl-7-oxa-bicyclo[2.2.1]heptane-2-carboxylate (**33**) *from* **4b** *using conditions reported by Gschwend et al.* [18].

Under dry atmosphere (N_2), **4b** (50 mg, 0.27 mmol) was dissolved in DCM (10 mL) and Ac_2O (0.5 mL) was added in one portion. The solution was cooled to -78°C and $BF_3.Et_2O$ (0.1 mL) was added dropwise. The solution was allowed to reach room temperature and stirred overnight. The solution was then washed with Na_2CO_3 (2 x10 mL, 10% aq. solution) and dried with Na_2SO_4. Evaporation under high vacuum gave a dark oil (77 mg) which was subjected to chromatography on silica gel using pentane:EtOAc (4:1) to give **33** (35 mg, Yield 45%). ^{1}H NMR (300 MHz, $CDCl_3$): δ 5.10 (d, *J* = 5.6 Hz, 1H, H-4), 3.69 (s, 3H, H-12), 2.67 (dd, *J*1 = 5.6 Hz, *J*2 = 8.6 Hz, 1H, H-2), 2.27 (m, 1H, H-3_A), 2.25 (m, 2H, H-6), 2.05 (s, 3H, H-2'), 2.05 (s, 3H, H-2''), 1.95 (m, 1H, H-3_B), 1.41 (s, 3H, H-11). ^{13}C NMR (75 MHz, $CDCl_3$): δ173.4 (C-8), 169.0 (C-1'), 168.7 (C-1''), 107.9 (C-5), 86.0 (C-1), 81.3 (C-4), 52.7 (C-6), 52.1 (C-10), 49.3 (C-2), 29.9 (C-3), 21.7 (C-2'), 21.3 (C-2''), 18.6 (C-9). Mass Spectrum *m/z* 286 (M^+, not observed), 243 (5.5), 227 (1.1), 213 (4.1), 203 (1.5), 202 (9.7), 201 (87.7), 196 (1.5), 195 (12.8), 185 (6.6), 184 (21.0), 183 (24.1), 170 (2.7), 169 (17.4), 168 (1.7), 167 (16.0), 166 (1.4), 159 (2.5), 158 (2.7), 157 (2.9), 156 (12.1), 155 (7.6), 154 (2.6), 153 (25.9), 152 (18.7), 151 (50.5), 143 (2.1), 142 (10.6), 141 (37.8), 140 (25.7), 139 (4.3), 138 (11.3), 137 (3.3), 136 (1.2), 135 (1.2), 135 (12.1), 129 (3.8), 128 (13.0), 127 (8.8), 126 (2.3), 125 (18.8), 124 (14.2), 123 (13.8), 117 (2.8), 116 (12.3), 115 (1.5), 114 (8.7), 113 (26.0), 112 (4.1), 111 (19.1), 110 (9.4), 109 (4.5), 108 (2.0), 107 (6.4), 100 (1.1), 99 (7.2), 98 (55.3), 97 (17.1), 96 (15.7), 95 (12.1), 93 (1.3), 87 (3.9), 86 (1.4), 85 (5.2), 84 (1.8), 83 (15.8), 82 (7.6), 81 (5.3), 80 (3.0), 79 (5.0), 77 (1.1), 73 (3.0), 71 (3.2), 70 (1.6), 69 (11.6), 68 (9.8), 67 (7.6), 65 (1.5), 59 (5.9), 58 (1.0), 55 (11.9), 54 (1.1), 53 (4.0), 45 (1.3), 44 (2.6), 43 (100), 42 (3.6), 41 (8.8), 40 (1.3), 39 (4.7). (t_R = 13:49 min)

6.8 Synthesis of the Ring A precursor (1*R*,5*S*)/(1*S*,5*R*)-methyl 5-acetoxy-2-methyl-4-oxocyclohex-2-enecarboxylate (2).

*Preparation of methyl (*1*R,*5*S)/(*1*S,*5*R)-5-hydroxy-2-methyl-4-oxo-2-cyclohexane-1-carboxylate* (**3**) *from* **4b** *using optimized conditions from those described by Barrero et al.* [19].

To solution of **4b** (75 mg, 0.41 mmol) in dry DCM (100 mL) at -1°C was added BBr_3 (0.3 mL, 0.30 mmol, 1 M solution in DCM) at once under dry N_2. The solution was stirred at -1°C for 10 min then poured quickly into a well stirred quenching solution of collidine (3 g) in DCM (25 mL, LR) at 25 to

30°C. The solution was stirred at ambient temperature for 35 min, then extracted with HCl (3 x 75 mL, 1 M aq.) to give a mixture of compounds as a yellow/brown resin. The sample was purified by semi preparative HPLC (t_R = 5.1 min, λ_{max} = 235 nm) to give **3** as a colourless oil (46 mg, 61% yield). IR (neat)/cm^{-1} 3452m, 2956w, 2922w, 2856w, 1735s, 1683s, 1438m, 1379w, 1261m, 1197m, 1164m, 1106s. ^{1}H NMR (300 MHz, $CDCl_3$): δ 6.05 (s, 1H, H-3), 4.15 (dd, *J*1 = 13.6 Hz, *J*2 = 5.6 Hz, 1H, H-5), 3.78 (s, 3H, H-9), 3.55 (m, 1H, H-1), 2.59 (dt, *J*1 = 12.4 Hz, *J*2 = 5.6 Hz, 1H, H-6_A), 2.14 (apparent quartet, *J* = ~12.4 Hz, 1H, H-6_B), 1.98 (s, 3H, H-8). ^{13}C NMR (75 MHz, $CDCl_3$): δ 198.4 (C-4), 172.0 (C-7), 158.9 (C-2), 125.9 (C-3), 71.2 (C-5), 52.7 (C-9), 47.4 (C-1), 34.4 (C-6), 22.2 (C-8). Mass Spectrum *m/z* 184 (M^+ 1.4), 153 (2.2), 141 (7.2), 140 (72.5), 125 (2.2), 124 (2.9), 113 (7.2), 112 (100), 109 (7.2), 108 (2.2), 98 (3.6), 97 (66.7), 96 (2.9), 95 (9.4), 82 (2.2), 81 (2.9), 80 (1.4), 79 (4.3), 78 (1.4), 77 (5.1), 69 (5.8), 68 (1.4), 67 (8.7), 66 (1.4), 65 (2.9), 59 (2.9), 55 (5.8), 54 (1.4), 53 (11.6), 52 (2.9), 51 (3.6), 43 (3.6), 41 (13.0), 40 (1.4), 39 (10.1). HRESI calc. for $C_9H_{12}O_4Na$ 207.0633, found 207.0627. (t_R = 12:15 min)

*Preparation of (*1*R,*5*S)/(*1*S,*5*R)-methyl 5-acetoxy-2-methyl-4-oxocyclohex-2-enecarboxylate* (**2**).

From the above procedure, acetyl chloride (2 mL) was added to **3** in the collidine/DCM quench mixture and the solution was stirred for an additional 35 min. The solution was then extracted with HCl (3 x 75 mL, 1 M) and the organic layer evaporated to leave a brown viscous resin. The sample was purified by semi preparative HPLC (t_R = 7.2 min, λ_{max} = 235 nm) to afford **2** as a pale yellow oil (37 mg, 40% yield). IR (neat)/cm^{-1} 2925m, 2857w, 1742s, 1692s, 1634m, 1442m, 1379m, 1222s, 1169s, 1078s. ^{1}H NMR (300 MHz, $CDCl_3$): δ 6.02 (s, 1H, H-3), 5.32 (dd, *J*1 = 11.9 Hz, *J*2 = 6.4 Hz, 1H, H-5), 3.77 (s, 3H, H-11), 3.58 (m, 1H, H-1), 2.44 (m, 2H, H-6), 2.17 (s, 3H, H-9), 1.98 (s, 3H, H-10). ^{13}C NMR (75 MHz, $CDCl_3$): δ 192.2 (C-4), 171.8 (C-7), 170.3 (C-8), 157.1 (C-2), 127.7 (C-3), 71.8 (C-5), 52.8 (C-11), 47.1 (C-1), 31.7 (C-6), 22.2 (C-10), 21.0 (C-9). Mass Spectrum *m/z* 226 (0.1), 184 (2.2), 166 (2.2), 153 (10.1), 151 (5.8), 141 (8.0), 140 (89.9), 135 (4.3), 125 (1.4), 124 (1.4), 123 (13.0), 113 (4.3), 112 (100), 109 (8.7), 108 (1.4), 107 (4.3), 97 (20.3), 96 (2.9), 95 (16.7), 85 (1.4), 81 (1.4), 80 (1.4), 79 (7.2), 78 (1.4), 77 (5.1), 69 (2.2), 68 (1.4), 67 (13.0), 66 (1.4), 65 (2.9), 59 (4.3), 55 (2.9), 53 (1.4), 52 (1.4), 43 (35.5), 41 (7.2), 39 (1.4). HRESI calc. for $C_{11}H_{14}O_5Na$ 249.0739, found 249.0734. (t_R = 13:39 min)

Epimerization of **3** *to* (1*R*,5*R*)/(1*S*,5*S*)*-methyl-5-hydroxy-2-methyl-4-oxocyclohex-2-enecarboxylate* (C(5)-*epi*-**3**).

The α-ketol **3** (20 mg) was subject to column chromatography on silica gel using pentane:EtOAc (1:1). Upon elution, the material in the middle fractions contained an equal mixture of **3**:C(5)-*epi*-**3**. (**3** R_f

= 0.61, C(5)-*epi*-**3** R_f = 0.60). C(5)-*epi*-**3**: ^{1}H NMR (300 MHz, $CDCl_3$): δ 6.04 (s, 1H, H-3), 4.39 (dd, *J*1 = 13.3 Hz, *J*2 = 5.5 Hz, 1H, H-5), 3.79 (s, 3H, H-9), 3.41 (apparent d., *J* = 6.0 Hz, 1H, H-1), 2.69 (ddd, *J*1 = 13.3 Hz, *J*2 = 5.5 Hz, *J*3 = 1.8 Hz, 1H, H-6_B), 2.12 (dt, *J*1 = 13.3 Hz, *J*2 = 6.0 Hz, 1H, H-6_A), 2.16, (s, 3H, H-8). ^{13}C NMR (75 MHz, $CDCl_3$): δ 199.1 (C-4), 171.4 (C-7), 158.7 (C-2), 126.0 (C-3), 69.1 (C-5), 52.9 (C-9), 46.7 (C-1), 34.2 (C-6), 24.2 (C-8). (t_R = 12:16 min)

Characterization of (1*S*,2*R*,5*S*)/(1*R*,2*S*,5*R*)-*methyl 2-bromo-5-hydroxy-2-methyl-4-oxocyclohexanecarboxylate* (*cis*-**34**), (1*S*,2*S*,5*S*)/(1*R*,2*R*,5*R*)-*methyl 2-bromo-5-hydroxy-2-methyl-4-oxocyclohexanecarboxylate* (*trans*-**34**).

Purification of ring cleavage mixtures by semi-preparative HPLC led to the isolation of mixtures containing *cis*-**34** and *trans*-**34** as a pale yellow oil (t_R = 6.2 min, λ_{max} = 225 nm). *cis*-**34**: ^{1}H NMR (300 MHz, $CDCl_3$): δ 4.47 (d, *J*1 = 6.2 Hz, 1H, H-5), 3.75 (s, 3H, H-9), 2.80 (dd, *J*1 = 8.7 Hz, *J*2 = 5.3 Hz, 1H, H-1), 2.52 (ddd, *J*1 = 13.4 Hz, *J*2 = 6.2 Hz, *J*3 = 5.3 Hz, 1H, H-6_A), 2.26 (AB quartet, *J* = 17. Hz, 2H, H-3), 1.95 (dd, *J*1 = 13.4 Hz, *J*2 = 8.7 Hz, 1H, H-6_B), 1.55 (s, 3H, H-8). ^{13}C NMR (75 MHz, $CDCl_3$): δ 209.8 (C-4), 171.8 (C-7), 79.5 (C-5), 51.1 (C-9), 49.3 (C-3), 48.2 (C-1), 42.9 (C-2), 29.5 (C-6), 18.1 (C-8). (t_R = 13:06 min). *trans*-**34**: ^{1}H NMR (300 MHz, $CDCl_3$): δ 4.23 (dd, *J*1 = 11.9 Hz, *J*2 = 7.7 Hz, 1H, H-5), 3.79 (s, 3H, H-9), 3.52 (dd, *J*1 = 13.2 Hz, *J*2 = 3.4 Hz, 1H, H-1), 3.16 (AB quartet, 2H, H-3), 2.54 (m, 1H, H-6_A), 1.93 (m, 1H, H-6_B), 1.84 (s, 3H, H-8). (t_R = 13:08 min).

6.9 Preparation of 6-(furan-3-yl)-tetrahydro-4-hydroxy-4-methyl-3-vinylpyran-2-one (6) as a convergent precursor to ring C

Intermediates in the preparation **6** were identified by GC-MS analysis using Method 2 unless otherwise mentioned.

6.9.1 Preparation of but-2-enoic acid derivatives.

Preparation of (E)-but-2-enoyl chloride (crotonyl chloride) following methodology by Jeffery et al. [28].

To neat $SOCl_2$ (150 g, 1.26 mol), (*E*)-but-2-enoic acid (95g, 1.10 mol) was added portionwise over 1h. During the addition, large amounts of HCl were evolved and the reaction was endothermic. The solution was heated to reflux for an additional 30 min then fractionally distilled, collecting crotonyl chloride between 110-120°C in agreement with the literature.

Preparation of (*E*)-2-bromobut-2-enoyl chloride by method of Pfeiffer *et al.* [20] and Klein *et al.* [21] in a three-step procedure.

2,3-Dibromobutanoic acid [20].

To a solution of crotonic acid (20.0 g, 0.23 mol) in DCM (500 mL) was added elemental bromine (41.0 g, 0.26 mol) portion-wise over a period of 20 min. The solution was allowed to stir overnight then evaporated to dryness. The residual solvent and bromine were removed under high vacuum to give 2,3-dibromobutanoic acid (56.1 g) as a pale orange solid. ^{1}H NMR analysis showed the material to be 96% pure, m.p.83-85°C (lit.87°C). ^{1}H NMR (200 MHz, $CDCl_3$): δ 10.89 (b, OH), 4.42 (m, 1H), 4.41 (s, 1H), 1.94 (m, 3H).

(E)-2-Bromobutenoic acid [20].

2,3-Dibromobutanoic acid (56 g, 0.23 mol) was dissolved in pyridine (120 mL) and heated to reflux on a steam cone for 4 h with occasional agitation. Additional pyridine (70 mL) was added at this point to prevent the solution from caking, and the mixture heated for an additional 2 h. The reflux apparatus was then arranged as a distillation and 80% of the pyridine was distilled. The remaining solvent was removed under high vacuum and the residue triturated with Et_2O (3 x 150 mL). The residual material was acidified with HCl (30 mL, 1 M) and extracted once with ether. Combined organic extracts were then thoroughly shaken with HCl (3 x 150 mL, 2 M), dried over Na_2SO_4 and evaporated to dryness to leave (*E*)-2-bromobutanoic acid as a pale brown powder (27.6 g) in 72% overall yield from crotonic acid. m.p. 104-105°C after recrystallization from water (lit. 105°C). ^{1}H NMR (300 MHz, $CDCl_3$): δ 7.57 (q, *J* = 6.9 Hz, 1H), 1.99 (d, *J* = 6.9 Hz, 3H). ^{13}C NMR (75 MHz, $CDCl_3$): δ 167.0, 144.7, 116.9, 18.4.

(E)-2-Bromo-but-2-enoyl chloride [21].

To (*E*)-2-bromobutanoic acid (20 g, 0.12 mol) was added $SOCl_2$ (36 mL) and the solution heated at reflux for 2 h. The solution was then distilled under dry nitrogen to yield (*E*)-2-bromobut-2-enoyl chloride (b.p. 164-170°C, lit. 168°C, 14.8 g, 67%), which was pure by ^{1}H and ^{13}C NMR analysis. ^{1}H NMR (300 MHz, $CDCl_3$): δ 7.87 (q, *J* = 6.8 Hz, 1H), 2.11 (d, *J* = 6.8 Hz, 3H). ^{13}C NMR (50 MHz, $CDCl_3$): δ 161.9, 151.6, 120.6, 19.3.

6.9.2 Model studies toward Ring C using 2-furaldehyde.

Preparation of 4-(furan-2-yl)-4-hydroxybutan-2-one (**35**) *under conditions described by Shokat et al.* [22].

To a solution of 2-furaldehyde (6.4 g, 66.2 mmol) in acetone (120 mL) was added a NaOH (12 mL, 1% solution) dropwise between –5 to -10°C. Stirring was continued for 30min, before neutralization with 0.5M HCl. The solution was concentrated *in vacuo* and the residue dissolved in water (100 mL) then extracted with ether (3 x 100 mL). The combined organic extracts were dried with Na_2SO_4 and concentrated to **35** in 93% purity by GC-MS analysis. Mass Spectrum *m/z* 155 (1.0), 154 (M^+, 11.0), 139 (4.1), 137 (1.2), 136 (8.8), 120 (5.8), 112 (2.4), 111 (8.5), 110 (1.9), 108 (1.8), 107 (2.0), 98 (4.9), 97 (80.7), 95, (14.8), 94 (14.7), 93 (7.2), 85 (1.1), 84 (1.1), 83 (4.3), 82 (1.1), 81 (2.1), 80 (1.0), 79 (1.9), 77 (0.8), 71 (1.3), 70 (1.2), 69 (17.7), 68 (7.2), 67 (2.9), 66 (8.1), 65 (10.0), 64 (1.5), 63 (3.0), 58 (7.2), 57 (1.5), 55 (8.6), 53 (5.6), 52 (1.7), 51 (5.1), 50 (3.2), 44 (3.1), 43 (100), 41 (40.7), 40 (8.2), 39 (46.6), 38 (12.6). (tR = 16:75, *Method 1*)

Preparation of 1-(furan-2-yl)-3-oxobutyl but-3-enoate (**36**) *under conditions described by Iwakura et al.* [23].

To the aldol product **35** (3.0 g, 19.5 mmol) and TEA (2.2 g, 21.4 mmol) in dry THF (20 mL), crotonyl chloride (2.0 g, 19.5 mmol) was added drop-wise with occasional cooling to keep the solution at 20°C. After a further 30 min stirring, the amine hydrochloride was filtered and the filter cake washed with Et_2O (3 x 25 mL). The ethereal washes were extracted with HCl (3 x 75 mL, 1M), washed with NH_4Cl then dried over Na_2SO_4. Evaporation gave **36** (3.9 g) in 90% yield. NMR and GCMS data showed no detectable conjugated ester product. ^{1}H NMR (200 MHz, $CDCl_3$): δ 7.33 (arom. m, 1H), 6.33 (arom. m, 1H), 6.30 (arom. m, 1H), 6.27 (m, 1H), 5.85 (m, H), 5.13 (m, 1H), 5.05 (dq, *J*1 = 6.9 Hz, *J*2 = 1.4 Hz, 1H), 3.08 (m, 1H), 3.02 (m, 1H), 3.02 (m, 2H), 2.14 (s, 3H). ^{13}C NMR (50 MHz, CDCl3): δ 204.2, 170.4, 151.4, 142.7, 130.0, 118.8, 110.6, 109.2, 64.6, 45.7, 38.9, 30.4. Mass Spectrum *m/z* 222 (M^+, 0.3), 154 (2.4), 153 (17.0), 137 (1.8), 136 (1.1), 120 (1.8), 111 (3.7), 97 (4.5), 96 (1.1), 95 (9.9), 94 (7.8), 93 (4.7), 85 (9.7), 69 (5.5), 68 (1.6), 67 (1.1), 66 (4.2), 65 (5.7), 63 (1.1), 53 (1.1), 51 (1.3), 44 (2.7), 43 (100), 41 (28.8), 40 (5.1), 39 (21.4), 38 (3.6).

6.9.3 Preparation of the Ring C precursor 6-(furan-3-yl)-5,6-dihydro-4-methyl-3-vinylpyran-2-one (6) from 3-furaldehyde.

Preparation of 4-(furan-3-yl)-4-hydroxybutan-2-one (**8**).

To a solution of 3-furaldehyde (1.0g, 10.4 mol) in acetone (18) was added a 1% NaOH solution (2.5 mL) dropwise at -9°C to. Stirring was continued for 40min as the solution temperature was slightly increased to –6°C, before neutralization with 0.5M HCl. The solution was concentrated *in vacuo* and the residue dissolved in water (100 mL) then extracted with ether (3 x 100 mL). The combined organic extracts were dried with Na_2SO_4 and concentrated to leave **8** (1.60 g, >98% yield) as a yellow resin. ^{1}H NMR (300 MHz, $CDCl_3$): δ 7.33 (arom. br. s, 1H, H-5''), 7.32 (arom. br. s, 1H, H-2''), 6.34 (arom. m, 1H, H-4'), 5.07 (dd, 1H, *J*1 = 8.7 Hz , *J*2 = 4.0 Hz, H-4), 3.32 (m, br. s, 1H, OH), 2.85 (double AB quartet, 2H, *J*1 = 17.3 Hz , *J*2 = 8.7 Hz, H-3_A), 2.75 (double AB quartet, 2H, *J*1 = 17.3 Hz , *J*2 = 4.0 Hz, H-3_B), 2.14 (s, 3H, H-1). ^{13}C NMR (75 MHz, $CDCl_3$): δ 208.7 (C-2), 143.2 (C-2'), 138.8 (C-5'), 127.5 (C-3'), 108.3 (C-4'), 62.7 (C-4), 50.5 (C-3), 30.5 (C-1). Mass Spectrum *m/z* 155 (2.3), 154 (M^+ 16.9), 139 (2.3), 136 (2.3), 126 (2.3), 121 (4.6), 113 (2.3), 111 (16.2), 107 (2.3), 98 (3.1), 97 (53.1), 96 (56.9), 95 (28.5), 94 (15.4), 93 (10.8), 83 (6.1), 81 (2.3), 79 (2.3), 71 (3.1), 70 (3.1), 69 (64.6), 68 (12.3), 67 (4.6), 66 (6.9), 65 (10.0), 63 (4.6), 58 (15.4), 55 (9.2), 53 (6.1), 51 (7.7), 50 (4.6), 44 (3.1), 43 (100), 42 (18.5), 41 (51.5), 40 (9.2), 39 (52.3), 38 (13.8), 37 (4.6). (t_R = 10:63 min).

Preparation of 1-(furan-3-yl)-3-oxobutyl 2-bromobut-3-enoate (**7**) *under conditions described by Cardillo et al.* [24].

The alcohol **8** (1.0 g, 6.5 mmol) was added to dry Et_2O (6 mL) then cooled to -78°C in a dry ice/acetone bath under inert atmosphere (N_2). TEA (2.1 g, 21 mmol) was then added, followed by (*E*)-2-bromo-but-2-enoyl chloride (1.9 g, 10 mmol) in Et_2O (3 mL) in one portion. An additional volume of Et_2O (3 mL) was added then the mixture was allowed to stir at –78ºC for 45 min followed by vacuum filtration. The filter cake was washed with Et_2O (2 x 25 mL, LR), cooled to at -78ºC and allowed to stand at -50ºC until all precipitate had formed, then filtered under suction once more. The ethereal solution was washed with HCl (3 x 20 mL, 1 M), dried with Na_2SO_4 and evaporated to leave the β,γ- unsaturated ester **7** (1.8 g, Yield 92%) as a 1:1 mixture of *syn* and *anti* diastereoisomers. IR (neat)/cm^{-1} 3136w, 2985w, 2917w, 1741s, 1724s, 1624m, 1504m, 1419m, 1369m, 1315m, 1289m, 1252s, 1201s, 1148s, 1092m, 1037s. ^{1}H NMR (300 MHz, $CDCl_3$): δ 7.48 (arom. m, 2H, H-5''), 7.38 (arom. m, 2H, H-2''), 6.40 (arom. m, 2H, H-4''), 6.26 (dd, 2H, *J*1 = 8.1 Hz, *J*2 = 5.2 Hz, H-1'), 6.11 (ddd, *J*1 = 17.0 Hz, *J*2 = 10.2 Hz, *J*2 = 9.4 Hz, 1H, H-3, *isomer 1*), 6.09 (ddd, *J*1 = 17.0 Hz, *J*2 = 10.0 Hz, *J*2 = 9.4 Hz, 1H, H-3, *isomer 2*), 5.37

(dd, 2H, *J*1 = 17.0 Hz , *J*2 = 4.5 Hz, H-4_A), 5.27 (dd, 2H, *J*1 = 10.2 Hz, *J*2 = 3.4 Hz, H-4_B), 4.73 (d, 2H, *J* = 9.4 Hz, H-2), 3.16 (dd, 2H, *J*1 = 16.9 Hz, *J*2 = 8.1 Hz, H-2_A'), 2.89 (dd, *J*1 = 16.9 Hz, *J*2 = 5.2 Hz, 1H, H-2_B', *isomer 1*), 2.88 (dd, 1H, *J*1 = 16.9 Hz, *J*2 = 5.5 Hz-H-2_B', *isomer 2*), 2.18 (s, 6H-H-4'). ^{13}C NMR (75 MHz, $CDCl_3$): δ 204.0 (C-3'), 204.0 (C-3'), 167.0 (C-1), 166.9 (C-1), 143.0 (C-2''), 143.0 (C-2''), 140.7 (C-5''), 140.6 (C-5''), 132.5 (C-3), 132.5 (C-3), 123.2 (C-3''), 123.2 (C-3''), 120.6 (C-4), 120.6 (C-4), 108.6 (C-4''), 108.6 (C-4''), 66.3 (C-1'), 66.2 (C-1'), 48.0 (C-2'), 47.9 (C-2'), 45.4 (C-2), 45.3 (C-2), 30.5 (C-4'), 30.5 (C-4'). Mass Spectrum *m/z* 302 (1.0), 300 (M^+ 1.0), 260 (1.0), 259 (1.0), 258 (1.0), 257 (1.0), 221 (4.6), 161 (6.1), 155 (3.8), 154 (50.0), 153 (30.0), 149 (4.6), 147 (4.6), 137 (9.2), 136 (9.2), 135 (2.3), 121 (22.3), 119 (15.4), 112 (7.7), 111 (7.7), 97 (3.8), 96 (6.9), 95 (46.2), 94 (72.3), 93 (12.3), 85 (2.3), 69 (3.8), 68 (21.5), 67 (2.3), 66 (4.6), 65 (9.2), 62 (1.5), 43 (100), 40 (6.2), 39 (1.5), 38 (20.8). (t_R = 13:95 min).

Preparation of (*Z*)-1-(furan-3-yl)-3-oxobutyl 2-bromobut-2-enoate (**37**) (α,β-unsaturated by-product).

The above procedure was performed using pyridine at 0°C to give **37** in quantitative yield. ^{1}H NMR (300 MHz, $CDCl_3$): δ 7.50 (arom. m, 1H, H-5''), 7.38 (arom. m, 1H, H-2''), 7.34 (quartet, 1H, *J* = 6.8 Hz, H-3), 6.42 (arom. m, 1H, H-4''), 6.28 (dd, 1H, *J*1 = 8.1 Hz, *J*2 = 5.5 Hz, H-1'), 3.20 (dd, 1H, *J*1 = 16.6 Hz, *J*2 = 8.1 Hz, H-2_A'), 2.91 (dd, 1H, *J*1 = 16.6 Hz, *J*2 = 5.5 Hz, H-2_B'), 2.20 (s, 3H, H-4'), 1.93 (d, 3H, *J* = 6.8 Hz, H-4). ^{13}C NMR (75 MHz, $CDCl_3$) : δ 204.3 (C-3'), 161.4 (C-1), 143 .5 (C-2''), 142.0 (C-3), 140.8 (C-5''), 123.6 (C-3''), 117.2 (C-2), 108.7 (C-4''), 66.5 (C-1'), 48.2 (C-2'), 30.5 (C-4'), 17.9 (C-4). Mass Spectrum *m/z* 303 (1.6), 302 (M^+ 11.3), 301 (1.6), 300 (11.8), 260 (4.1), 259 (2.0), 258 (4.4), 257 (1.6), 161 (1.4), 155 (1.3), 154 (12.6), 153 (71.2), 150 (3.9), 149 (83.5), 148 (5.0), 147 (85.4), 137 (6.6), 136 (30.0), 135 (4.6), 122 (2.0), 121 (32.6), 120 (1.5), 119 (16.6), 112 (2.4), 111 (3.7), 110 (1.7), 108 (3.9), 107 (1.8), 97 (1.6), 96 (11.6), 95 (88.2), 94 (90.3), 93 (26.2), 92 (1.3), 85 (4.3), 81 (1.3), 79 (2.0), 77 (2.0), 69 (2.6), 68 (7.0), 67 (4.9), 66 (8.1), 65 (15.2), 64 (1.2), 63 (3.1), 55 (1.1), 53 (4.4), 51 (2.3), 50 (1.2), 44 (2.4), 43 (100), 41 (2.8), 40 (7.2), 39 (35.8), 38 (4.5), 37 (1.3). (t_R = 14:42 min).

Preparation of 6-(furan-3-yl)-5,6-dihydro-4-methyl-3-vinylpyran-2-one (**6**) from **7**.

A solution of **7** (1.0 g, 6.0 mmol) in dry THF (40 mL) was cooled to 0°C and a Rieke zinc (120mg, 18.0 mmol) suspension in THF (2.5 mL) was added in one portion. The solution was heated to reflux for 5 h then cooled before quenching in HCl (30 mL, 2 M). After stirring in acid for 1 h, H_2O (50 mL) was added and the solution extracted with Et_2O (3 x 50 mL). The combined organic extracts were dried over Na_2SO_4 then concentrated to leave **6** (1.4 g, Yield 92%) as a deep yellow resin. IR (neat)/cm^{-1} 3147w, 2972w, 2933w, 1713s, 1629s, 1505m, 1430m, 1376m, 1260s, 1162s, 1122m, 1098m, 1061m,

1034s. ^{1}H NMR (300 MHz, $CDCl_3$): δ 7.49 (arom. m, 1H, H-5'), 7.42 (arom. m, 1H, H-2'), 6.55 (dd, 1H, *J*1 = 17.7 Hz, *J*2 = 11.5 Hz, H-7), 6.45 (arom. m, 1H, H-4'), 5.72 (d, 1H, *J* = 17.7 Hz, H-8_A), 5.47 (d, 1H, *J* = 11.5 Hz, H-8_B), 5.35 (dd, 1H, *J*1 = 11.5 Hz, *J*2 = 3.8 Hz, H-6), 2.78 (dd, 1H, *J*1 = 18.1 Hz, *J*2 = 11.5 Hz, H-5_A), 2.54 (dd, 1H, *J*1 = 18.1 Hz, *J*2 = 3.8 Hz, H-5_B), 2.11 (s, 3H, H-9). ^{13}C NMR (75 MHz, $CDCl_3$): δ 164.2 (C-2), 150.3 (C-4), 143.9 (C-2'), 140.2 (C-5'), 128.9 (C-7), 125.4 (C-3), 124.1 (C-3'), 121.0 (C-8), 108.8 (C-4'), 70.8 (C-6), 37.7 (C-5), 21.1 (C-9). Mass Spectrum *m/z* 205 (6.1), 204 (M^+ 41.5), 203 (2.3), 190 (4.6), 189 (46.2), 186 (2.3), 185 (1.0), 176 (3.1), 175 (4.6), 171 (3.8), 161 (4.6), 160 (9.2), 159 (33.1), 158 (13.8), 157 (6.1), 147 (2.3), 146 (1.5), 145 (13.8), 144 (5.4), 143 (2.3), 141 (6.1), 136 (4.6), 133 (3.8), 132 (3.8), 131 (25.4), 130 (5.4), 129 (20.0), 128 (8.5), 127 (10.0), 119 (4.6), 118 (4.6), 117 (18.5), 116 (13.1), 115 (29.2), 108 (6.1), 107 (2.3), 105 (2.3), 105 (6.1), 103 (4.6), 95 (20.8), 94 (22.3), 93 (7.7), 92 (2.3), 91 (30.0), 89 (3.1), 82 (13.1), 81 (88.5), 80 (42.3), 79 (100), 78 (6.1), 77 (27.7), 75 (7.7), 69 (1.5), 68 (3.1), 67 (7.7), 66 (17.7), 65 (27.7), 64 (3.1), 63 (11.5), 55 (4.6), 54 (2.3), 53 (13.8), 52 (8.5), 51 (13.1), 49 (5.4), 44 (5.4), 41 (8.5), 40 (10.8), 39 (36.2). HRESI calc. for $C_{12}H_{12}O_3Na$ 227.0684, found 227.0677. (t_R = 14:17 min).

Preparation of 6-(furan-3-yl)-tetrahydro-4-hydroxy-4-methyl-3-vinylpyran-2-one (**38**).

Reformatski intermediates **38** were obtained by quenching the Rieke Zinc solution in a biphasic mixture of Et_2O (30 mL) and HCl (30 mL, 1 M), followed by stirring for 15 min. Separation of the ethereal layer and drying over Na_2SO_4 gave a mixture of intermediates that were separated by flash column chromatography on silica gel using gradient elution with pentane:EtOAc (20:1 to 8:1). **38** was isolated as a 1:1 mixture of diastereomers. ^{1}H NMR (300 MHz, $CDCl_3$): δ 7.45 (arom. m, 1H, H-2'), 7.42 (arom. m, 1H, H-5'), 6.44 (arom. m, 1H, H-4'), 5.94 (dt, 1H, *J*1 = 17.2 Hz, *J*2 = 9.6 Hz, H-7), 5.73 (dd, 1H, *J*1 = 11.9 Hz, *J*2 = 3.4 Hz, H-6), 5.52 (d, 1H, *J* = 9.6 Hz, H-8_A), 5.29 (d, 1H, *J* = 17.2 Hz, H-8_B), 2.95 (d, 1H, *J* = 9.1 Hz, H-3), 2.50 (OH), 2.24 (dd, 1H, *J*1 = 14.2 Hz, *J*2 = 3.4 Hz, H-5_A), 2.05 (dd, 1H, *J*1 = 14.2 Hz, *J*2 = 11.9 Hz, H-5_B), 1.37 (s, 3H, H-9). ^{13}C NMR (75 MHz, $CDCl_3$): δ 171.4 (C-2), 143.7 (C-2'), 139.7 (C-5'), 130.1 (C-7), 124.6 (C-3'), 122.8 (C-8), 108.5 (C-4'), 71.1 (C-6), 70.4 (C-4), 56.6 (C-3), 42.6 (C-5), 28.3 (C-9). Mass Spectrum *m/z* 222 (M^+ 1.5), 204 (2.3), 189 (1.5), 176 (7.7), 160 (1.5), 153 (1.5), 152 (2.3), 138 (3.8), 137 (12.3), 136 (3.1), 135 (2.3), 134 (3.8), 121 (1.5), 120 (2.3), 111 (2.3), 110 (1.5), 97 (6.2), 96 (6.9), 95 (49.2), 94 (17.7), 93 (3.8), 92 (3.1), 91 (4.6), 85 (9.2), 84 (55.4), 82 (3.1), 81 (7.7), 80 (3.1), 79 (3.8), 77 (3.8), 70 (4.6), 69 (93.1), 68 (59.2), 66 (6.9), 65 (12.3), 63 (3.1), 58 (3.8), 57 (2.3), 55 (8.5), 54 (15.4), 53 (6.9), 52 (1.5), 51 (5.4), 50 (1.5), 44 (3.1), 43 (100), 41 (24.6), 40 (18.5), 39 (46.2). (t_R = 14:49 min).

6.10 Experimental Methods Used for Chromatographic Separation.

6.10.1 Gas Chromatorgraphy Mass Spectroscopy. (GC-MS)

Instrument 1

GC:	Hewlett Packard 5890 GC
MS:	Hewlett Packard 5970 Mass Selective Detector
Voltage:	70eV
Flow (He)	0.5 mL/min
Split ratio:	50:1
Column:	Type: BPX-5
	Length: 30m
	Internal Diameter: 0.25mm
	Film Thickness: 0.25um.

Instrument 2

GC:	Hewlett Packard 6890 GC	
MS:	Hewlett Packard 5973 Mass Selective Detector	
Voltage:	70eV	
Flow (He)	0.5 mL/min	
Split ratio:	50:1	
Column:	Type: BPX-5	
	Length: 25m	
	Internal Diameter:	0.25mm
	Film Thickness:	0.25um

Method 1:	Starting temperature:	50°C
	Ramp Rate:	10°C/min
	Final temperature:	280°C
	Hold time:	20 min.

Method 2:	Starting temperature:	70°C
	Ramp Rate:	10°C/min
	Final temperature:	280°C
	Hold time:	20 min.

6.10.2 Chiral Gas Chromatography

Instrument 1

GC:	Hewlett Packard 5890 GC
Carrier gas:	H_2
Make up gas:	N_2
Injector:	220°C
Detector (FID): 230°C	
Column pressure:	5.9 psi
Column flow:	1.33 mL/min.
Linear Velocity:	40.07 cm/sec.
Total flow:	69 mL/min.
Split ratio:	50:1

Column:	Type: Et-TBS-β-CD column (MeGA, Italy).	
	Length:	20m
	Internal Diameter:	0.25mm
	Film Thickness:	0.25um

Method:	Starting temperature:	60°C
	Ramp Rate:	2°C/min.
	Final temperature:	180°C
	Hold time:	30 min.

6.10.3 Semi Preparative High Performance Liquid Chromatography

HPLC:	Varian Prostar (Model 210).
Guard column:	50 x 10 mm, 5 micron filter.
Analytical column:	Phenomenex C-18, 250 x 10 mm, prodigy 5 micron ODS (3), 100A.
Solvent A:	Acetonitrile.
Solvent B:	Water.
Solvent ratio (A:B):	55:45
Flow rate:	3.5 mL/min.
Pressure:	2900 psi.

Chapter 6

Experimental Procedures and Methodology: References

[1] B. Majoie. "2,3-Dibromofuran by Bromination of Furancarboxaldehydes", Societe de Recherches Industrielles ("SORI"), Patent U.S. 3,714,197, **1971**, CAN: 74:76318, AN: 1971:76318.

[2] Katsumura, S., Ichikawa, K., Mori, H. "Synthesis of Tetrasubstituted Butenolide, Bromobeckerelide by Regioselective Lithiation of Furan Followed by Photosensitized Oxygenation of α-Silylfuran". *Chemistry Letters*, **1993**, *9*, 1525-1528.

[3] D. J. Chadwick, J. Chambers, D. Meakins, R. L. Snowden. "Esters of Furan-, Thiophen- and *N*-Methylpyrrole-2-carboxylic Acids, Bromination of Methyl Furan-2-carboxylate, Furan-2-carbaldehyde, and Thiophen-2-carbaldehyde in the Presence of Aluminium Chloride", *Journal Chemical Society Perkin Transactions I*, **1973**, 1766-1773.

[4] M.-C. Zaluski, M. Robba, M. Bonhomme, " No 314 Synthese de Dèrivès Dicarbonylès Furanniques II. Preparation par l'Intermèdiaire, d'Organolithiens. *Bulletin de la Sociètè Chimique de France*, **1970**, 5, 1838-1946.

[5] J. P. Wolfe, H. Tomori, J. P. Sadighi, J. Yin, S. L. Buchwald. "Simple, Efficient Catalyst System for the Palladium-Catalyzed Amination of Aryl Chlorides, Bromides and Triflates", *Journal of Organic Chemistry*, **2000**, *65*, 1158-1174; M. C. Harris, S. L. Buchwald. "One-Pot Synthesis of Unsymmetrical Triarylamines from Aniline Precursors", *Journal of Organic Chemistry*, **2000**, *65*, 5327-5333.

[6] J.-N. Cui, T. Ema, T. Sakai, M. Utaka. "Control of Enantioselectivity in the Bakers Yeast Asymmetric Reduction of γ-Chloro-β-diketones to γ-Chloro-(*S*)-β-hydroxy ketones", *Tetrahedron Asymmetry*, **1998**, *9*, 2681-2692.

[7] A. Hofmann, W.v. Philipsborn, C. H. Eugster, C.H. "NMR.-Untersuchungen an einfachen Furenidonsystemen. Synthese den unsubstituierten Δ^2-Furenidons-(4) (β-Hydroxyfuran)". *Helvetica Chimica Acta*, **1965**, *48*, 1322-1331.

[8] H. B. Henbest, E. R. H. Jones, I. M. S. Walls. "Researches on Acetylenic Compounds. Part XXVI. Further Reformatsky Reactions with Propargyl Bromides", *Journal of the Chemical Society*, **1950**, 3646-3650.

[9] E. Duranti, C. Balsamini. "Synthesis of 4-Oxo-2-alkyn-1-ols", *Synthesis*, **1974**, 357-358.

[10] M. Journet, D. Cai, L. M. di Michele, R. D. Larsen. "Highly Efficient Synthesis of α,β-Acetylenic Aldehydes From Terminal Alkynes Using DMF As the Formylating Reagent", *Tetrahedron Letters*, **1998**, *39*, 6427-6428.

[11] D. Enders, H. Eichenauer. "Assymetrische Synthesen via metallierte chirale Hydrazone. Enantioselective Alkylierung von cyclischen Ketonen und Aldehyden", *Chemie Berichte*, **1979**, *112*, 2933-2960.

[12] R. O. Hutchins, W.-Y. Su, R. Sivakumar, F. Cistone, Y. P. Stercho. "Stereoselective Reductions of Substituted Cyclohexyl and Cyclopentyl Carbon-Nitrogen π Systems with Hydride Reagents". *Journal of Organic Chemistry*, **1983**, *48*, 3412-3422.

[13] Steven Priver, private communication.

[14] G. Hallas. "Organic Stereochemistry", McGraw-Hill publishing Co. Ltd., England, **1965**, 40, 4, 53.

[15] S. Ogawa, H. Aoyama, T. Sato. "Synthesis of an Ether-Linked Alkyl 5a-Carba-β-D-glucoside, a 5a-Carba-β-D-galactoside, a 2-Acetamido-2-deoxy-5a-carba-β-D-glucoside, and an Alkyl 5a'-Carba-β-lactoside", *Carbohydrate Research*, **2002**, *337*, 1979-1992.

[16] C. Le Drain, J.-P. Vionnet, P. Vogel. "Total Syntheses of (-)-Corduritol B ((-)-1L-Cyclohex-5-ene-1,3/2,4-tetrol) and of (+)-Conduritol F ((+)-1D-Cyclohex-5-ene-1,2,4/3-tetrol). Determination of the Absolute Configuration of (+)-Leucanthemitol)", *Helvetica Chemica Acta*, **1990**, *73*, 161-168

[17] T. Takahashi, T. Namiki, Y. Takeuchi, T. Koizumi. "A New Synthetic Route to Methyl (-)-Shikimate by Asymmetric Diels-Alder Reaction of $(S)_s$-3-(2-Pyridylsulfinyl)Acrylate", *Chemical and Pharmaceutical Bulletin*, **1988**, *36*, 3213-3215.

[18] H. W. Gschwend, M. J. Hillman, B. Kisis, R. K. Rodebaugh. "Intramolecular Diels-Alder Reactions. Synthesis of 3a-Phenylisoindolines as Analgesic Templates", *Journal of Organic Chemistry*, **1976**, *41*, 104-110.

[19] A. F. Barrero, E. J. Alvarez-Manzaneda, R. Chahboun, A. R. Rivas, P. L. Palomino. "Synthesis of Natural Oxygenated Monocarbocyclic Sesquiterpenoids from 6,7-Epoxygeranyl Acetate", *Tetrahedron*, **2000**, *56*, 6099-6113.

[20] Pfeiffer, P. "Umlagerungen Stereoisomer Äthylenverbindungen". *Berichte der Deutschen Chemischen Gesellschaft*, **1910**, *43*, 3039-3048.

[21] Klein, J., Zitrin, S. "The Reaction of Grignard Reagents with α-Bromocrotonic and α-Bromocinnamic Acids", *Journal of Organic Chemistry*, **1970**, *35*, 666-669.

[22] K. Shokat, T. Uno, P. G. Schultz. "Mechanistic Studies of an Antibody-Catalyzed Elimination Reaction", *Journal of the American Chemical Society*, **1994**, *116*, 2261-2270.

[23] Y. Iwakura, F. Toda, R. Iwata, Y. Torii. "Formation of 3-Butenoates from Crotonyl Chloride in the Presence of Amines". *Bulletin of the Chemical Society of Japan*, **1969**, *42*, 841-842.

[24] G. Cardillo, A. De Simone, A. Mingardi, C. Tomasini. "Synthesis of β,γ-Unsaturated Esters From α,β-Unsaturated Acid Chlorides", *Synlett*, **1995**, *11*, 1131-1132.

Chapter 1
Introduction: Appendices

Appendix 1.1:

Chemical Transmission: The structure and function of neurons and neurotransmitters.

Signal processes of the central nervous system rely on cells called neurons. The cell body of the neuron, called the soma contains the nucleus and organelles similar to that of a normal cell, however the morphological features consist of a long branching pathway called an axon connecting to a bulb like terminal. Multiple shorter branches called dendrites are responsible for the reception of nerve impulses from other neurons and respond to an action potential. The axon terminal is closely situated to a neighboring neuron, providing a junction for chemical communication between cells called a synapse. Upon the reception of sufficient potential through the dendrites, the axon hillock initiates a second potential, which travels down the axon to the terminal. Neurotransmitters contained in vesicles at the terminal are then released and travel from the pre-synaptic membrane into a narrow gap between cells called the synaptic cleft. Proteins act as selective receptors within the post-synaptic membrane of the neighboring cell (including neuron, muscle cell or gland cell) and bind to neurotransmitters in a structure specific manner. The entire process takes approximately 1 millisecond. If binding results in excitation (activation, agonism) of the receptor site, depolarization of the membrane occurs and a new potential is created through the movement of ions through channels. Binding can also result in inhibition (deactivation, antagonism) of the receptor protein, leading to hyperpolarization and signal blockage. Modulatory action at a receptor site leads to a change the postsynaptic cells response to other connected synapses.

Synaptic transmission is quite complex, since each axon terminal can contain many neurotransmitters, thousands of synapses can converge on a single neuron, or a single axon terminal can affect many neurons. Reception of the released neurotransmitters is also complex and for each receptor family there are usually many receptor subtypes. Different neurotransmitters have different synaptic action in that some can bind at a broad range of receptors with varying degrees of agonist or antagonistic action. Endogenous neurotransmitters are synthesized within the body and can be separated into four categories:

- The amino acid neurotransmitters are the most common in the body. Excitatory amino acids include glutamate and aspartate, and inhibitory amino acids include glycine and γ-amino-butyric acid (GABA). GABA is the major inhibitory neurotransmitter in the CNS and plays an important role in

regulatory functions, anxiety/mood, analgesia (pain), sleep and cognition. Binding of GABA to its receptors increases membrane potential by either opening up ligand-gated Cl^- channels ($GABA_A$-receptor), or by activating an internal G-protein and second messenger that leads to the removal of K^+ by active transport ($GABA_B$-receptor). Both modes of ion diffusion counteract excitation.

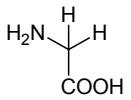

Glycine

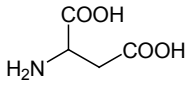

Aspartate

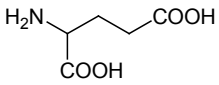

Glutamate

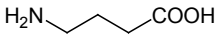

γ-Aminobutyrate (GABA)

-The monoamine neurotransmitters are produced from amino acids at the terminal via a short series of enzymatic steps. Dopamine is produced from tyrosine via L-DOPA and is involved in mood, motor activity and cognitive functions (learning and memory). It also plays a crucial role in reward-reinforcement, and reward-related incentive learning. Dopamine receptors modulate hippocampal ACh release [1] and receptor signaling pathways in the nucleus accumbens caused by repeated use of drugs, are hypothesized to produce tolerance to the rewarding effects of receptor stimulation, leading to increased drug intake to satisfy reward-reinforcement pathway [1].

Serotonin (5-hydroxytryptophan or 5-HT) is produced from tryptophan and governs body temperature, sleep and feeding. Serotonin acts at an array of receptors that are found in both the central and peripheral nervous systems. 5-HT has been implicated in depression, anxiety, social phobia and obsessive-compulsive disorders. The effects of 5-HT are felt most predominately in the cardiovascular system, with additional effects in the respiratory system and the intestines. There are several types of 5-HT receptors, most of which are coupled to G-proteins that effect the activities of either adenylate cyclase or phospholipase Cγ. The catecholamine receptors are termed the α- and β-adronergic receptors and couple to intracellular G-proteins.

Norepinephrine is produced from dopamine and is primarily active in the locus coeruleus, which monitors external stimuli and responses. Regulates mood, blood pressure, state of alertness and feelings of pleasure. Difficulty concentrating and feelings of apathy and depression results from problems associated with the norepinephrine transmitter. Epinephrine is produced from norepinephrine and is involved in the physiological response to threatening or exciting conditions (short-term stress reactions). It increases heart rate, dilates pupils and is also involved in the regulation of blood sugar levels.

Most amine neurotransmitters are removed from the synaptic cleft by transport mechanisms and catabolized for re-uptake into the pre-synaptic terminal by catechol-O-methyltransferase and monoamine oxidase.

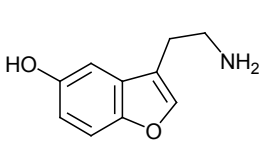

Serotonin (5-HT)

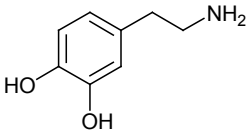

Dopamine

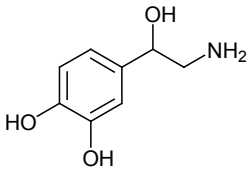

Norepinephrine

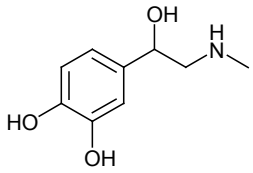

Epinephrine

-Acetylcholine (ACh) is synthesized from choline and acetyl-CoA through the action of choline acetyltransferase. It is the major neurotransmitter in the peripheral nervous system and is usually excitatory, however the release of Ach in hippocampus plays also part in the generation of mood and the acquisition of short-term memory.

Binding of acetylcholine to its receptors opens up ligand-gated sodium channels. The resulting influx of Na^+ ions reduces membrane potential which if sufficient will cause an action potential to be generated in the postsynaptic cell. Acetylcholine however is removed rapidly from the synapse by enzymatic metabolism by acetylcholinesterase and not reused. Acetylcholine controls the release of the pituitary hormone vasopressin and is involved in protective and regulatory functions. Two main classes of ACh receptors are the muscarinic and nicotinic receptors.

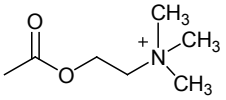

Acetylcholine

-Peptides neurotransmitters (neuropeptides) are far more potent than others and are responsible for mediating sensory and emotional responses including hunger, thirst, sex drive, pleasure and pain. Neuropeptides can be predominately found in the brain and gut and differ from those previously discussed in that they are synthesized from huge precursors (about 300 amino acids) in the nucleus of the cell. Translation by ribosomes in cell bodies or dendrites produces the prepropeptide, which is cleaved into smaller fragments by peptidases during axonal transportation in vesicles to the terminal. The lengthy biosynthesis and transportation processes determine that the release at the terminal is not quick. There is no evidence to suggest that transport mechanisms exist for the reuptake of peptide transmitters and once released the peptide is catabolised by membrane peptidases [2]. The earliest neuropeptide to be studied was substance P, which is a sensory neurotransmitter in the spinal chord involved in the

perception of pain. Opioid neuropeptides include endorphins, enkephalins and dynorphins and are so called since they bind to the same to the same postsynaptic receptors as opium derivatives. The release of substance P is inhibited by opioid peptides, which hyperpolarize the postsynaptic membrane and prevent transmission of pain signals back to the brain. Almost all of the neuropeptide receptors belong to the rhodopsin or glucagons-vasoactive intestinal peptide/calcitonin G-protein-coupled receptor family.

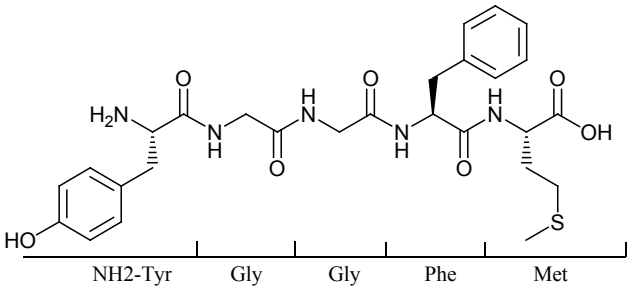

Met-Enkephalin

Leu-Enkephalin	NH_2-Tyr-Gly-Gly-Phe-Leu
β-Endorphin	NH_2-Tyr-Gly-Gly-Phe-Met-Thr-Ser-Glu-Lys-Ser-Gln-Thr-Pro-Leu-Val-Thr-Leu-Phe-Lys-Asn-Ala-Ile-Ile-Lys-Asn-Ala-Tyr-Lys-Lys-Gly-Glu
Dynorphin	NH_2-Tyr-Gly-Gly-Phe-Leu-Arg-Arg-Ile-Arg-Pro-Lys-Leu-Lys-Trp-Asp-Asn-Gln
Substance P	NH_2-Met-Leu-Gly-Phe-Phe-Gln-Gln-Pro-Lys-Pro-Arg

[1] A. Sidhu, M. Laruelle, P. Vernier. "Dopamine Receptors and Transporters", Marcel Dekker, ISBN: 0824708547.

[2] R. A. Webster (Ed.). "*Neurotransmitters, Drugs and Brain Function"*, John Wiley and Sons Ltd., **2001**, 251-264. ISBN:0471978191.

Chapter 2

Synthesis of 3-Furylamines: Appendices

Appendix 2.1: EIMS of the polyhalogenated products identified by the isotope pattern in the largest fragment. The predicted isotope pattern was calculated using 'Isotope 1.0' (F. Antolasic, RMIT).

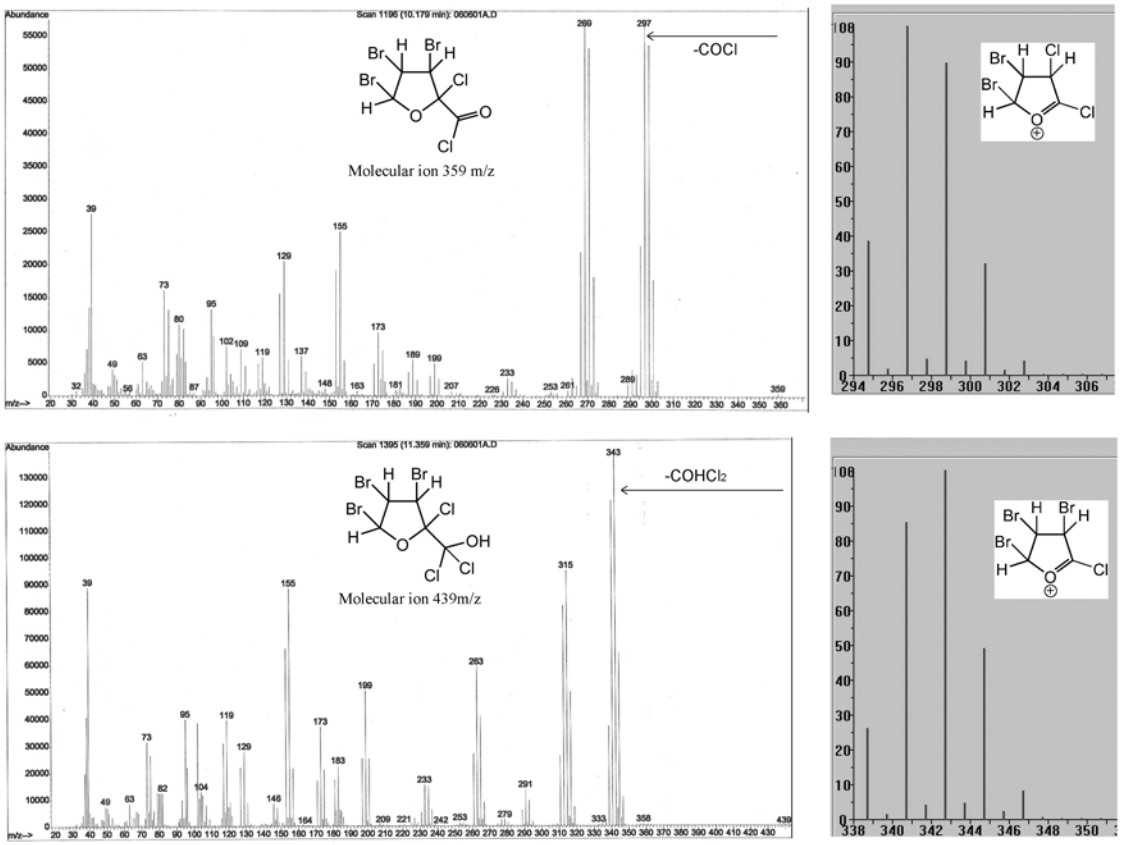

Appendix 2.2: Mass spectra of the 5-bromofuran-2-carbaldehyde **8** and the hydrolysis product upon Wolf-Kishner reduction of **11**.

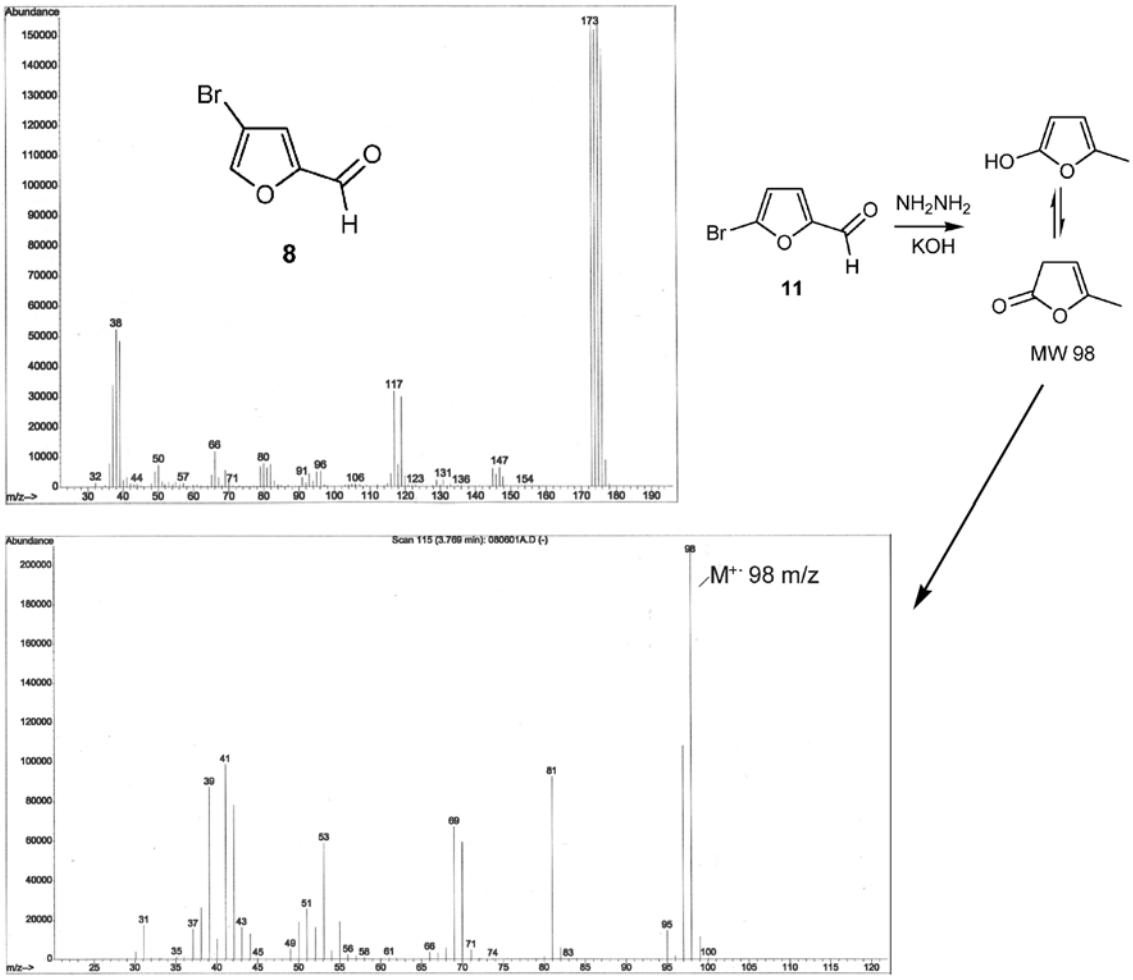

Appendix 2.3: Possible fragmentation pathway for the enaminone **19a**. This pathway is characteristic for the enaminones **19a-n** and major fragments are included in the experimental data.

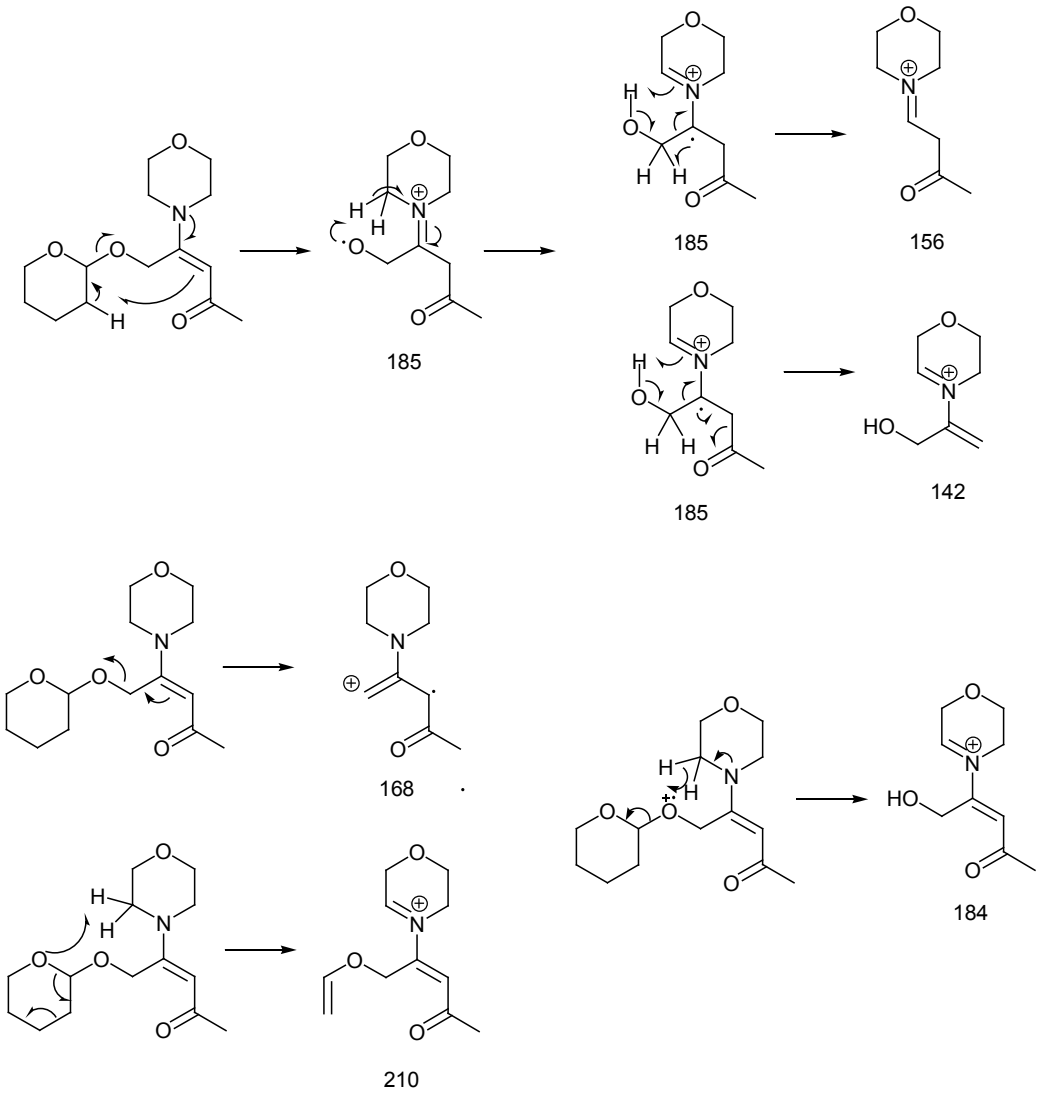

Appendix 2.4: 300MHz COSY NMR of the *E*- and *Z*- isomers of 3-(*n*-butylamino)-4-(tetrahydropyran-2-yloxy)but-2-enal **19n**.

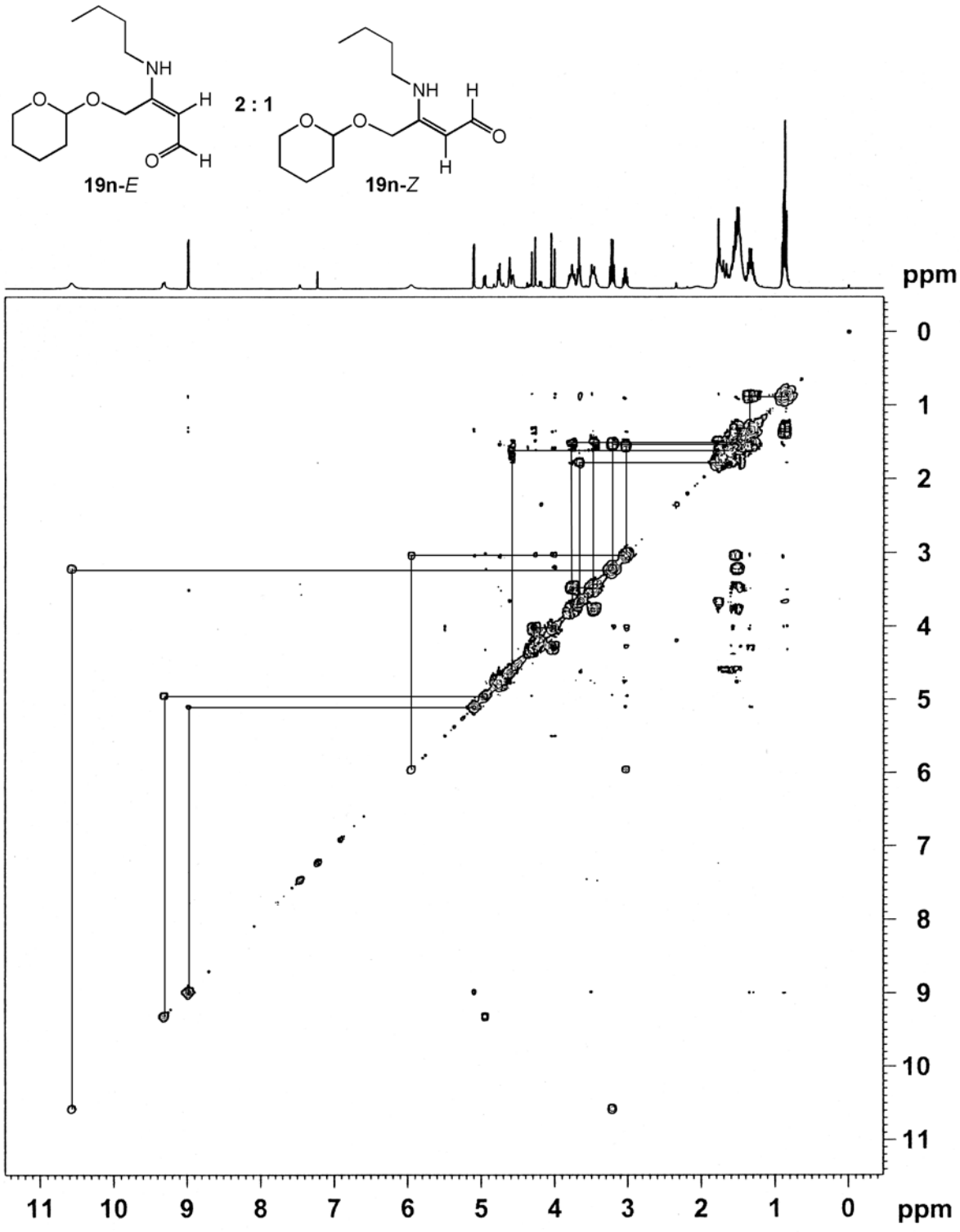

Appendix 2.5: Possible fragmentation pathway for the furan **5a**. This pathway is characteristic for the furans and major fragments are included in the experimental data.

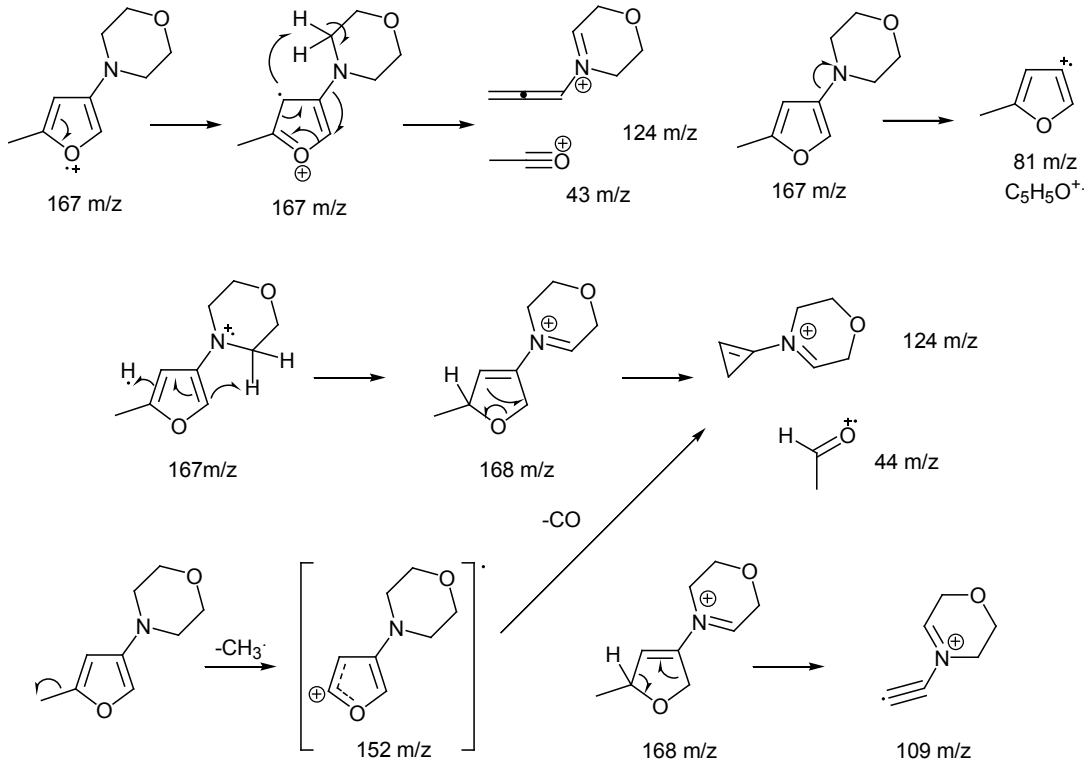

Appendix 2.6: 50MHz ^{13}C and 200MHz ^{1}H NMR of *N,N*-diethyl-furan-3-amine **5l**, and EIMS fragmentation data.

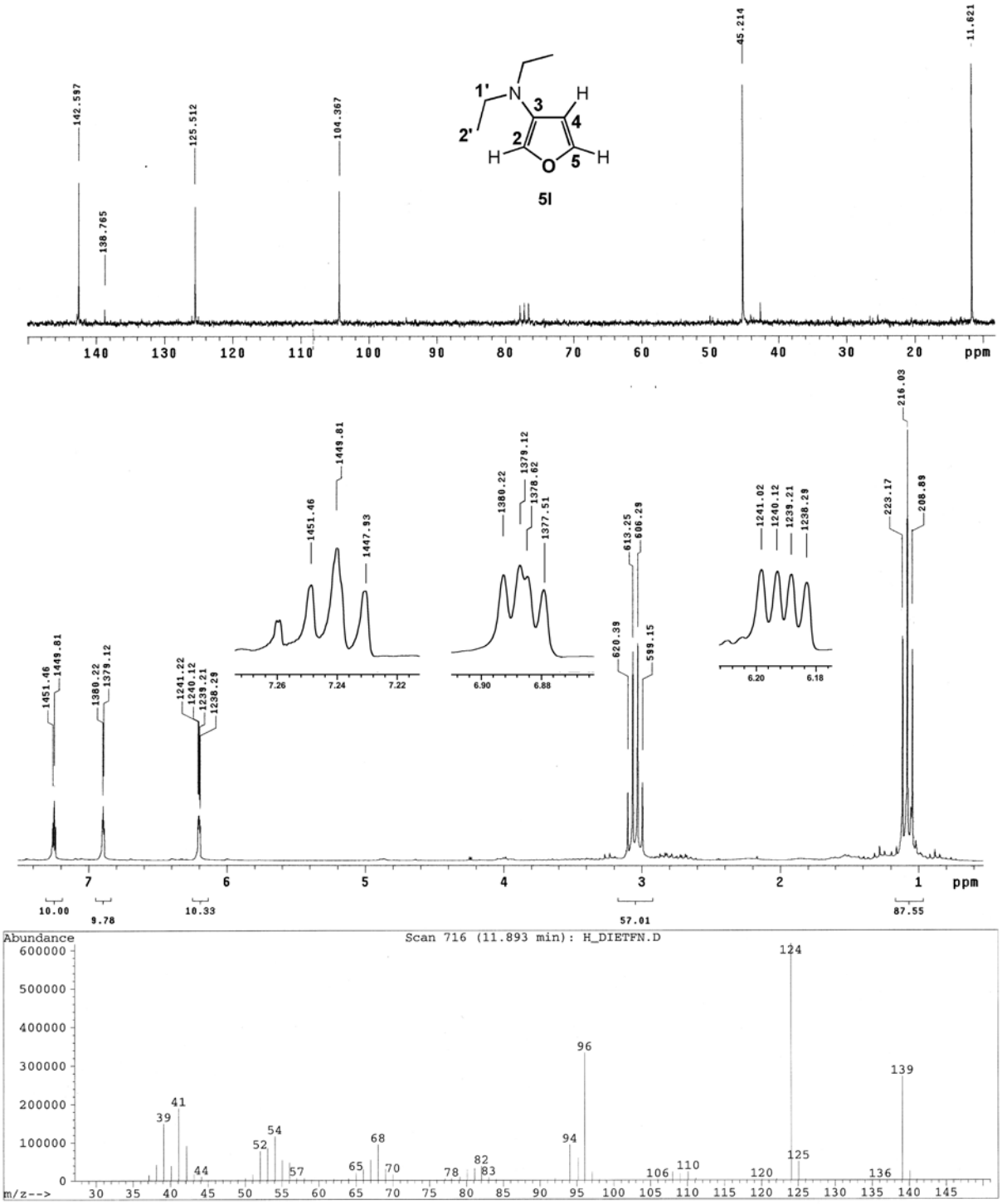

Appendix 2.7: 50MHz ^{13}C and 200MHz ^{1}H NMR of *N*-(*n*-butyl)-*N*-(5-methylfuran-3-yl)acetamide **21g**, and EIMS fragmentation data.

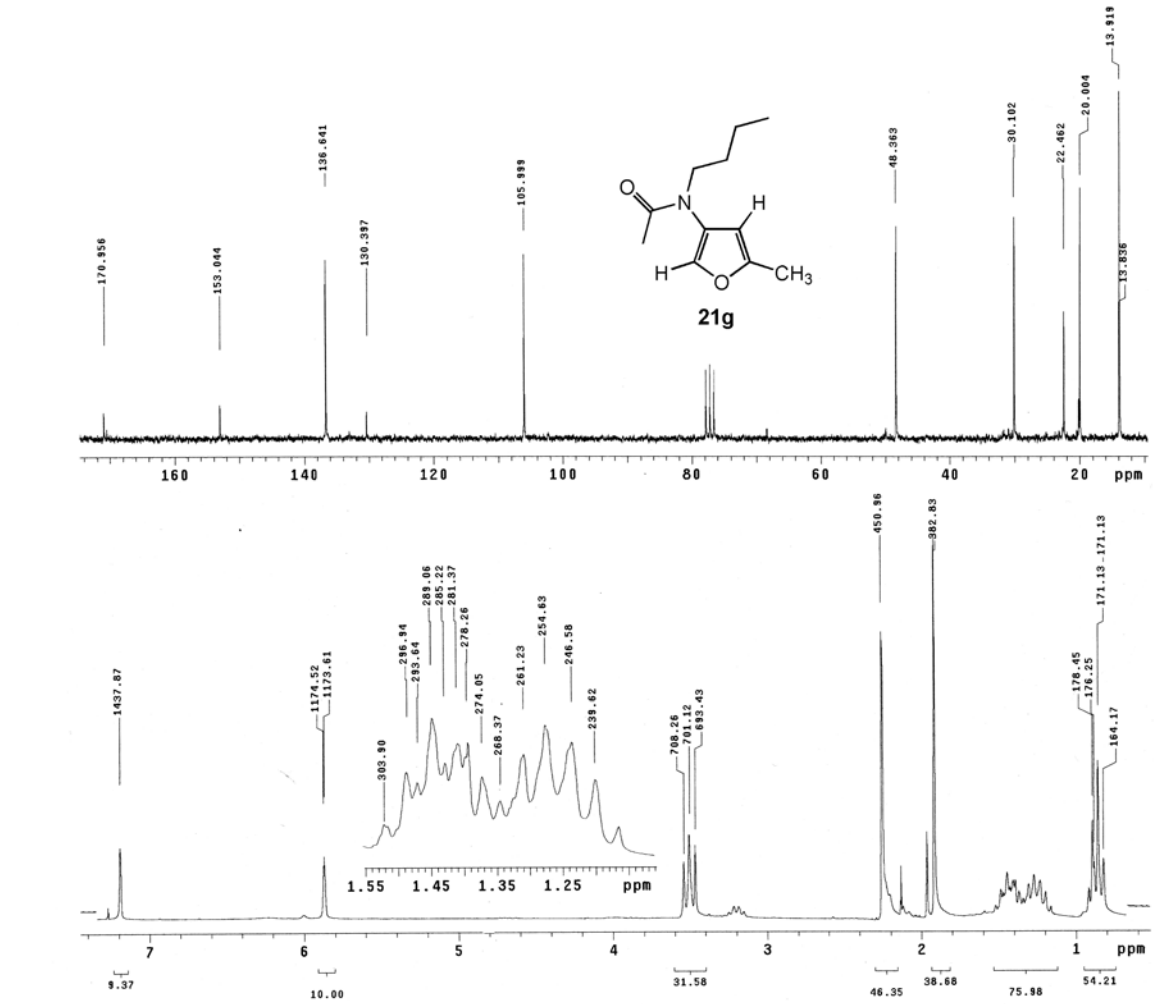

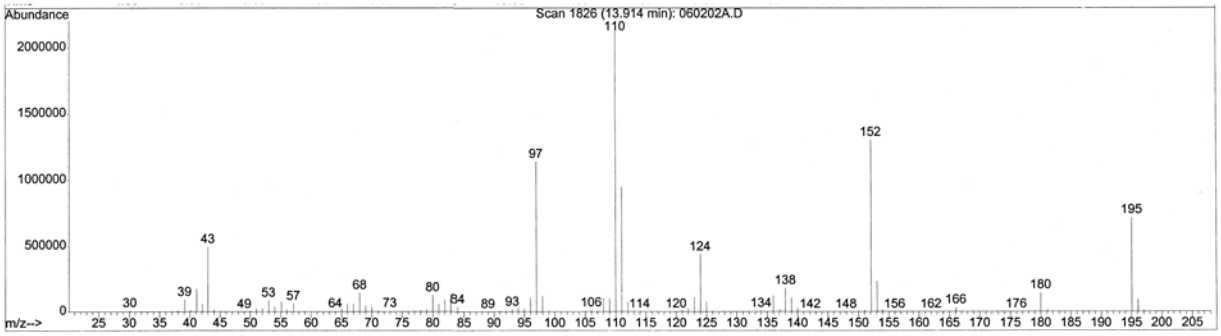

Appendix 2.8: ^{1}H NMR, ^{13}C NMR and GC-MS of a mixture of diastereoisomers of 1-((2*R/S*,4*S*,5*S*)-3',4'-dimethyl-5'-phenyl-2'-((tetrahydro-2H-pyran-2''-yloxy)methyl)oxazolidin-2-yl)propan-2-one **19p**

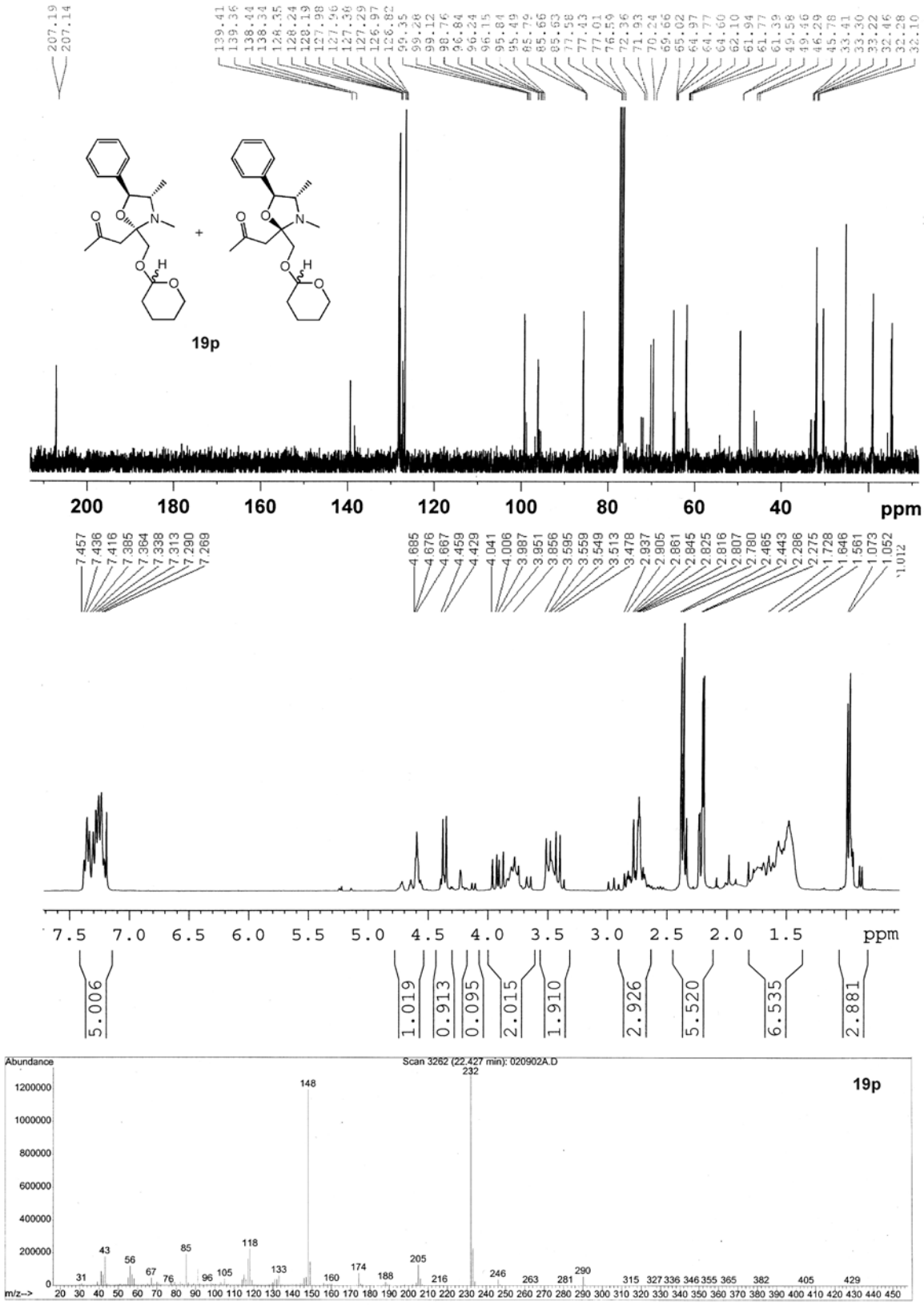

Appendix 2.9: 300MHz ^{1}H COSY NMR of C(2'') isomers of 1-((2*R/S*,4*S*,5*S*)-3',4'-dimethyl-5'-phenyl-2'-((tetrahydro-2H-pyran-2''-yloxy)methyl)oxazolidin-2-yl)propan-2-one (**19p**).

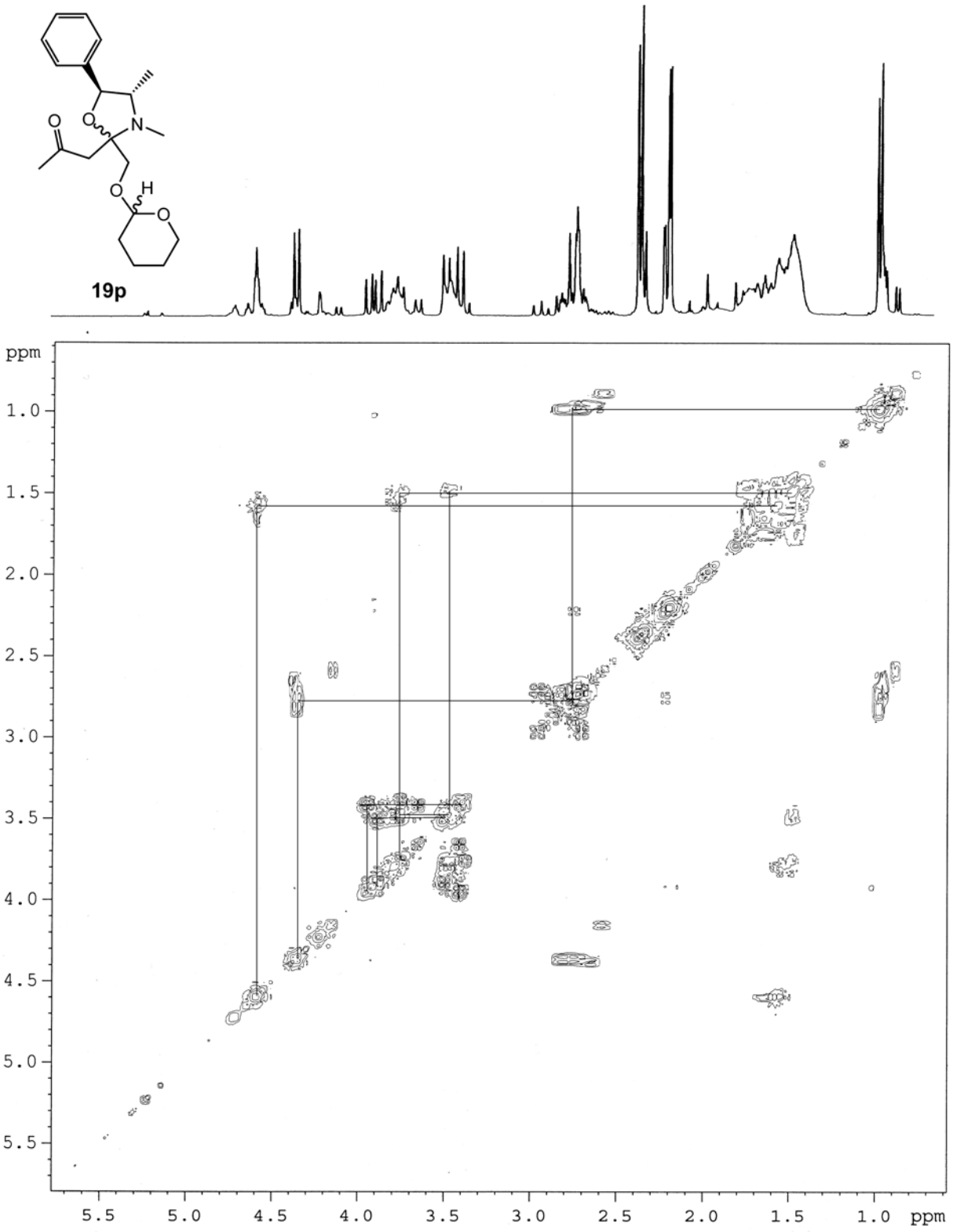

Appendix 2.10: Top; 300MHz ^{1}H NMR of **19q**, 1-((2*R*/*S*,4*S*,5*R*)-3,4-dimethyl-5-phenyl-2-((tetrahydro-2H-pyran-2-yloxy)methyl)oxazolidin-2-yl)propan-2-one. Bottom; ^{1}H NMR and GC-MS data of the cyclization mixture showing the **5q-THP** intermediate at 16.59 min with a characteristic *m*/z 85 THP fragment ion but no molecular ion. Two sets of ^{1}H signals can be seen in **5q-THP** and are due to C(2')-diastereoisomers at the THP group.

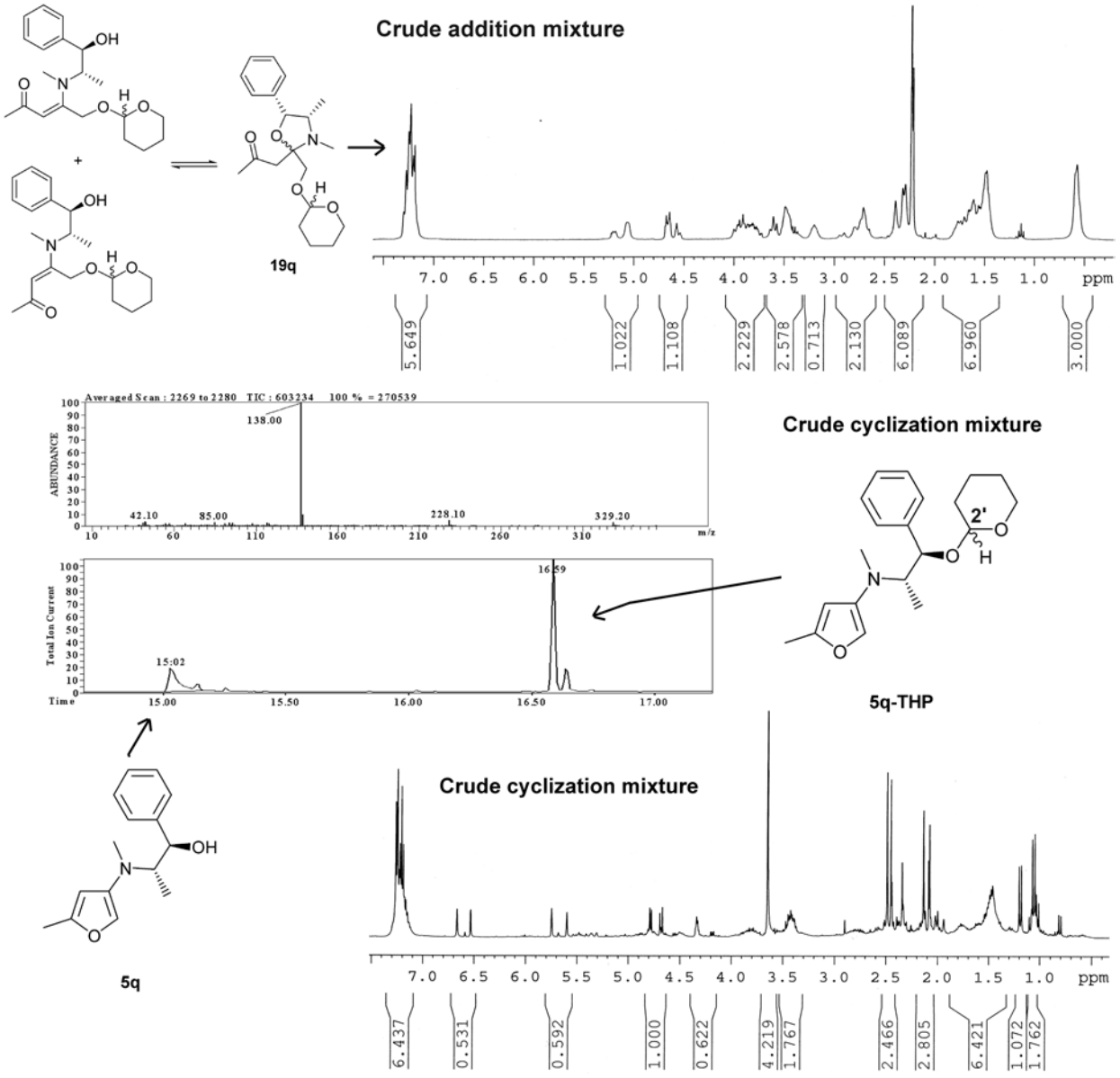

Chapter 3

Diels-Alder Reactions of 3-Furylamines: Appendices

Appendix 3.1: 200 MHz ^{1}H NMR homo-decoupling experiments of **4a**.

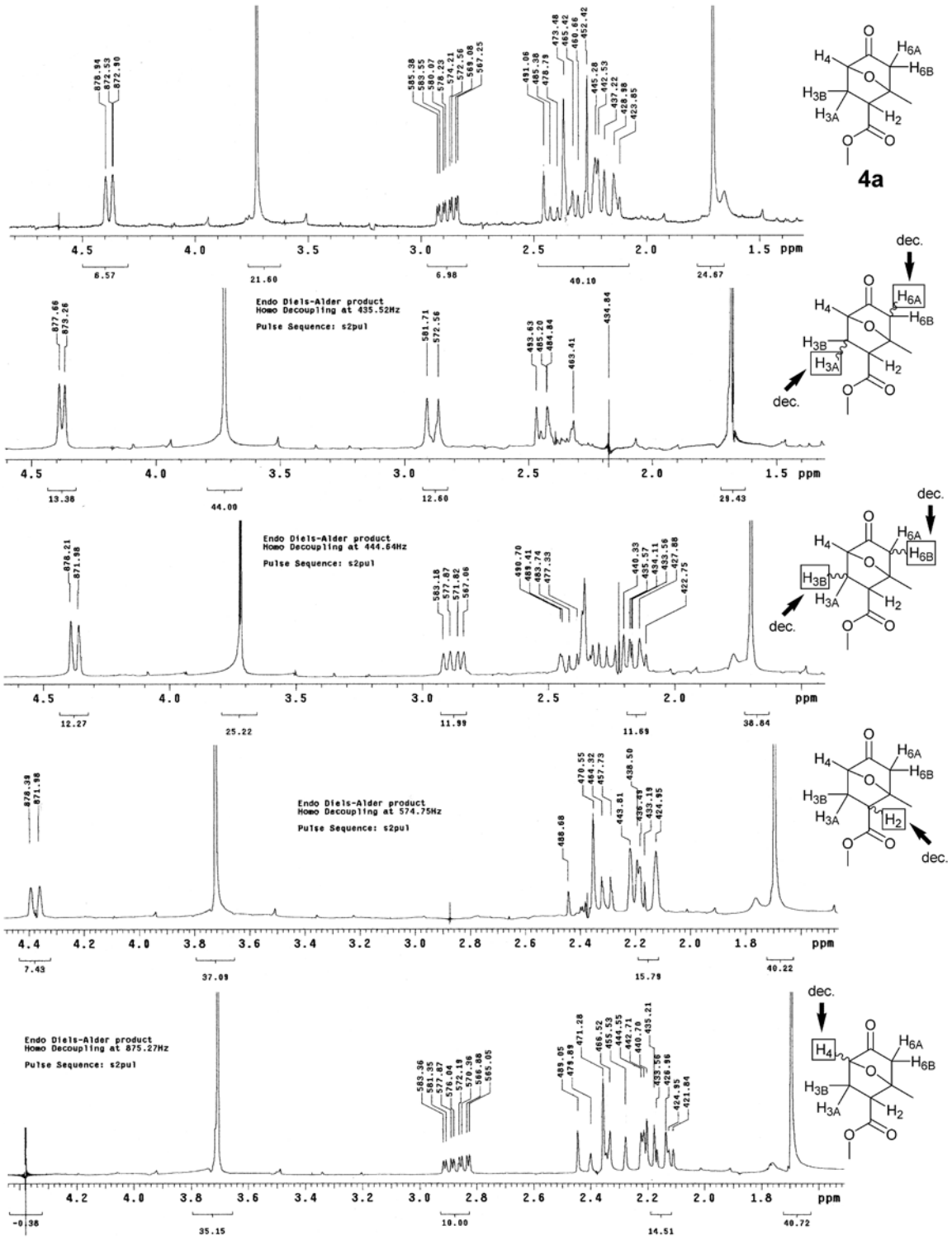

Appendix 3.2: 500 MHz ^{1}H/125 MHz ^{13}C HMBC NMR spectrum of **4a** and 125MHz ^{13}C NMR of **4a** with peak labels.

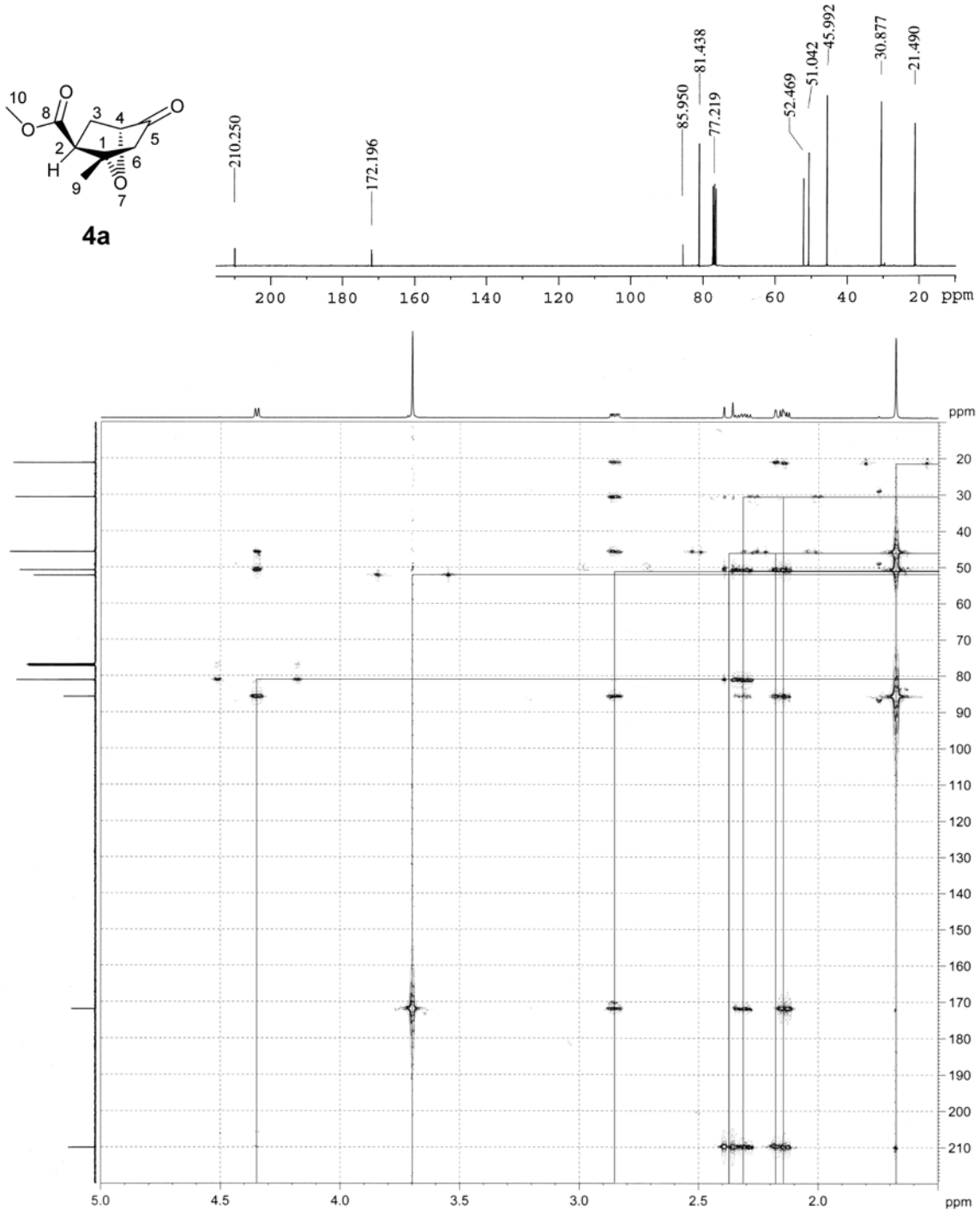

Appendix 3.3: GC traces for the GC-MS analysis of the crude D-A reaction mixture between **5a** and MAC in DCM at –78 to 0ºC (top) and 4ºC (bottom).

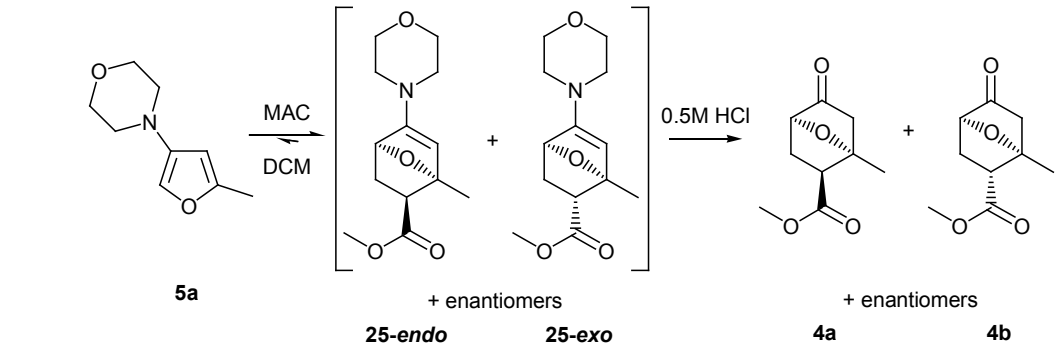

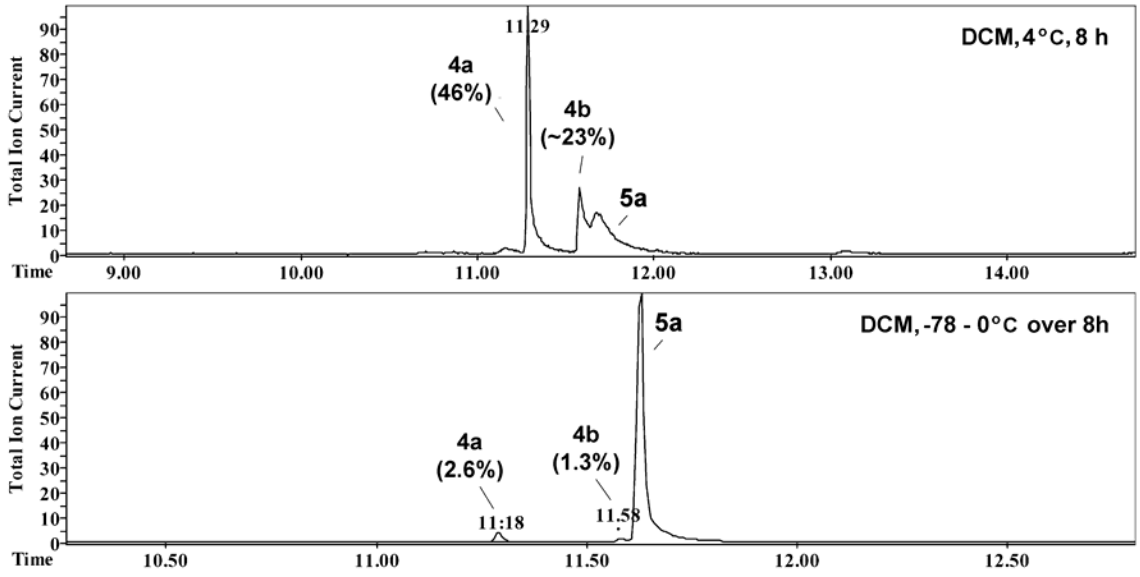

Appendix 3.4: 200MHz ^{1}H and 50 MHz ^{13}C NMR of **4b**, and 300 MHz ^{1}H/75 MHz ^{13}C HMQC NMR analysis. GC-MS data for **4b** is also shown.

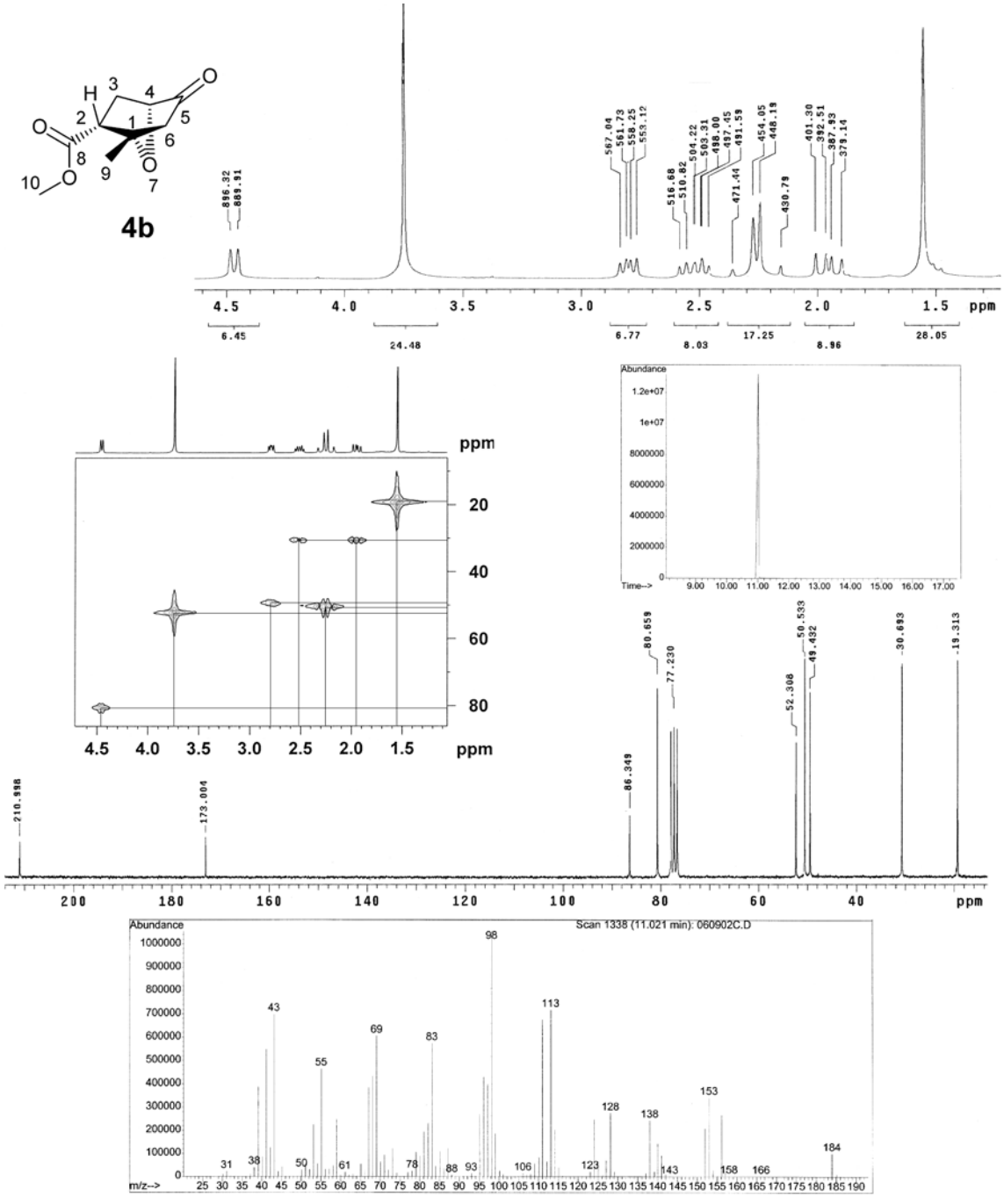

Appendix 3.5: A summary of bond distances and the X-ray crystal CIF file is shown for **4b**. The atom numbering produced in the CIF file used to describe the X-ray crystal data of **4b** is slightly different from that discussed throughout chapter 3 and alternate numbering used in the crystal structure data of *exo*-methyl 1-methyl-5-oxo-7-oxa-bicyclo[2.2.1]heptane-2-carboxylate **4b** is shown below.

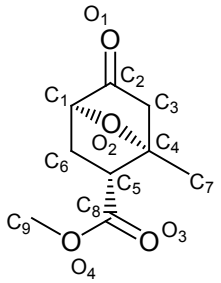

Bond distances are listed and are close to distances quoted by Allen *et al*. [88]

Atom 1	Atom 2	Exp. (Å)	Lit. $d^{[88]}$ (Å)	Closest functional group	
O2	C1	1.434(2)	1.429	Csp_2-O(2) $(C)_2$-**C**H-**O**-C	
O2	C4	1.451(2)	1.452	Csp_2-O(2) $(C)_3$-**C**-**O**-C	
O4	C8	1.337(2)	1.336	Csp_2-O(2) C-**C**(=O)-**O**-C	
O4	C9	1.440(2)	1.448	Csp_3-O(2) C-C(=O)-**O**-**C**H_3	
O3	C8	1.201(2)	1.196	Csp_2=O(1) C-**C**(=**O**)-O-C	
O1	C2	1.200(2)	1.211	Csp_2=O(1) $(C)_2$-**C=O**	cyclohexanone
C8	C5	1.497(2)	1.497	Csp_3-Csp_3 **C-C**(=O)(-OC)	acyclic esters
C5	C6	1.541(2)	1.535	Csp_3-Csp_3 **C-C**	cyclohexane
C5	C4	1.564(2)	1.556	Csp_3-Csp_3 $(C)_3$-**C**-**CH-**$(C)_2$	
C4	C3	1.537(3)	1.535	Csp_3-Csp_3 **C-C**	cyclohexane
C2	C3	1.507(3)	1.509	Csp_3-Csp_3 **C_2-C**=O	C_6+ rings
C2	C1	1.517(3)	1.514	Csp_3-Csp_3 **C_2-C**=O	cyclopentanone
C6	C1	1.529(3)	1.535	Csp_3-Csp_3 **C-C**	cyclohexane
C4	C7	1.502(2)			

X-ray crystal CIF data:

```
_audit_creation_method          SHELXL-97
_chemical_name_systematic
'methyl 1-methyl-5-oxo-7-oxa-bicyclo[2.2.1]heptane-2-carboxylate'
_chemical_name_common           ?
_chemical_melting_point         377
_chemical_formula_moiety        ?
_chemical_formula_sum           'C9 H12 O4'
_chemical_formula_weight        184.19

loop_
```

```
_atom_type_symbol
_atom_type_description
_atom_type_scat_dispersion_real
_atom_type_scat_dispersion_imag
_atom_type_scat_source
C C 0.0033 0.0016 'International Tables Vol C Tables 4.2.6.8 and 6.1.1.4'
H H 0.0000 0.0000 'International Tables Vol C Tables 4.2.6.8 and 6.1.1.4'
O O 0.0106 0.0060 'International Tables Vol C Tables 4.2.6.8 and 6.1.1.4'

_symmetry_cell_setting          triclinic
_symmetry_space_group_name_H-M   'P -1'
_symmetry_int_tables_number     2

loop_
_symmetry_equiv_pos_as_xyz
'x, y, z'
'-x, -y, -z'

_cell_length_a                 7.2235(10)
_cell_length_b                 8.1158(11)
_cell_length_c                 8.3058(12)
_cell_angle_alpha               75.273(2)
_cell_angle_beta               74.540(3)
_cell_angle_gamma                86.114(2)
_cell_volume                   453.89(11)
_cell_formula_units_Z          2
_cell_measurement_temperature    293(2)
_cell_measurement_reflns_used    966
_cell_measurement_theta_min      2.59
_cell_measurement_theta_max      26.53
_exptl_crystal_description       block
_exptl_crystal_colour           colourless
_exptl_crystal_size_min         0.10
_exptl_crystal_size_mid         0.15
_exptl_crystal_size_max         0.50
_exptl_crystal_density_meas      ?
_exptl_crystal_density_diffrn    1.348
_exptl_crystal_density_method    'not measured'
_exptl_crystal_F_000            196
_exptl_absorpt_coefficient_mu    0.106
_exptl_absorpt_correction_type   none
_exptl_absorpt_correction_T_min  ?
_exptl_absorpt_correction_T_max  ?
_exptl_absorpt_process_details   ?

_exptl_special_details
;
 ?
;

_diffrn_ambient_temperature      293(2)
_diffrn_radiation_probe          x-ray
_diffrn_radiation_type           MoK\a
```

```
_diffrn_radiation_wavelength     0.71073
_diffrn_source                   'sealed tube'
_diffrn_radiation_monochromator  graphite
_diffrn_measurement_device_type  'CCD area detector'
_diffrn_measurement_method       'phi and omega scans'
_diffrn_detector_area_resol_mean ?
_diffrn_standards_number         ?
_diffrn_standards_interval_count ?
_diffrn_standards_interval_time  ?
_diffrn_standards_decay_%        ?
_diffrn_reflns_number            2428
_diffrn_reflns_av_R_equivalents  0.0587
_diffrn_reflns_av_sigmaI/netI    0.0477
_diffrn_reflns_limit_h_min       -8
_diffrn_reflns_limit_h_max       8
_diffrn_reflns_limit_k_min       -9
_diffrn_reflns_limit_k_max       9
_diffrn_reflns_limit_l_min       -6
_diffrn_reflns_limit_l_max       9
_diffrn_reflns_theta_min         2.59
_diffrn_reflns_theta_max         25.00
_reflns_number_total             1583
_reflns_number_gt                1311
_reflns_threshold_expression     >2sigma(I)

_computing_data_collection       'Bruker SMART'
_computing_cell_refinement       'Bruker SMART'
_computing_data_reduction        'Bruker SAINT'
_computing_structure_solution    'Bruker SHELXTL'
_computing_structure_refinement  'Bruker SHELXTL'
_computing_molecular_graphics    'Bruker SHELXTL'
_computing_publication_material  'Bruker SHELXTL'

_refine_special_details
;
 Refinement of F^2^ against ALL reflections.  The weighted R-factor wR and
 goodness of fit S are based on F^2^, conventional R-factors R are based
 on F, with F set to zero for negative F^2^. The threshold expression of
 F^2^ > 2sigma(F^2^) is used only for calculating R-factors(gt) etc. and is
 not relevant to the choice of reflections for refinement.  R-factors based
 on F^2^ are statistically about twice as large as those based on F, and R-
 factors based on ALL data will be even larger.
;

_refine_ls_structure_factor_coef Fsqd
_refine_ls_matrix_type           full
_refine_ls_weighting_scheme      calc
_refine_ls_weighting_details
'calc w=1/[\s^2^(Fo^2^)+(0.0803P)^2^+0.0000P] where P=(Fo^2^+2Fc^2^)/3'
_atom_sites_solution_primary     direct
_atom_sites_solution_secondary   difmap
_atom_sites_solution_hydrogens   geom
_refine_ls_hydrogen_treatment    mixed
```

```
_refine_ls_extinction_method     SHELXL
_refine_ls_extinction_coef       0.027(11)
_refine_ls_extinction_expression Fc^*^=kFc[1+0.001xFc^2^\l^3^/sin(2\q)]^-1/4^
_refine_ls_number_reflns         1583
_refine_ls_number_parameters     121
_refine_ls_number_restraints     0
_refine_ls_R_factor_all          0.0605
_refine_ls_R_factor_gt           0.0529
_refine_ls_wR_factor_ref         0.1414
_refine_ls_wR_factor_gt          0.1351
_refine_ls_goodness_of_fit_ref   1.029
_refine_ls_restrained_S_all      1.029
_refine_ls_shift/su_max          0.000
_refine_ls_shift/su_mean         0.000

loop_
_atom_site_label
_atom_site_type_symbol
_atom_site_fract_x
_atom_site_fract_y
_atom_site_fract_z
_atom_site_U_iso_or_equiv
_atom_site_adp_type
_atom_site_occupancy
_atom_site_symmetry_multiplicity
_atom_site_calc_flag
_atom_site_refinement_flags
_atom_site_disorder_assembly
_atom_site_disorder_group
O2 O 0.19794(18) 0.38773(15) 0.55710(16) 0.0517(4) Uani 1 1 d . . .
O4 O 0.38542(18) -0.05322(15) 0.85346(18) 0.0534(4) Uani 1 1 d . . .
O3 O 0.56481(18) 0.14141(16) 0.6395(2) 0.0661(5) Uani 1 1 d . . .
O1 O -0.0597(2) 0.63082(19) 0.8229(2) 0.0745(5) Uani 1 1 d . . .
C8 C 0.4233(3) 0.1057(2) 0.7566(2) 0.0433(5) Uani 1 1 d . . .
C5 C 0.2674(2) 0.2268(2) 0.8108(2) 0.0420(5) Uani 1 1 d . . .
H5 H 0.2048 0.1872 0.9340 0.050 Uiso 1 1 calc R . .
C4 C 0.1155(2) 0.2493(2) 0.7034(2) 0.0441(5) Uani 1 1 d . . .
C2 C 0.0159(3) 0.5143(2) 0.7655(3) 0.0535(5) Uani 1 1 d . . .
C6 C 0.3393(3) 0.4110(2) 0.7698(3) 0.0517(5) Uani 1 1 d . . .
H6A H 0.3166 0.4517 0.8736 0.062 Uiso 1 1 calc R . .
H6B H 0.4752 0.4204 0.7116 0.062 Uiso 1 1 calc R . .
C1 C 0.2175(3) 0.5081(2) 0.6514(3) 0.0534(6) Uani 1 1 d . . .
H1 H 0.2697 0.6190 0.5797 0.064 Uiso 1 1 calc R . .
C3 C -0.0607(3) 0.3378(3) 0.7960(3) 0.0548(6) Uani 1 1 d . . .
H3A H -0.1677 0.3399 0.7455 0.066 Uiso 1 1 calc R . .
H3B H -0.1007 0.2827 0.9180 0.066 Uiso 1 1 calc R . .
C9 C 0.5214(3) -0.1813(2) 0.8048(3) 0.0661(6) Uani 1 1 d . . .
H9A H 0.5110 -0.1996 0.6978 0.099 Uiso 1 1 calc R . .
H9B H 0.4947 -0.2858 0.8927 0.099 Uiso 1 1 calc R . .
H9C H 0.6491 -0.1440 0.7914 0.099 Uiso 1 1 calc R . .
C7 C 0.0747(3) 0.0988(3) 0.6438(3) 0.0617(6) Uani 1 1 d . . .
H7A H -0.0190 0.1300 0.5782 0.093 Uiso 1 1 calc R . .
H7B H 0.0260 0.0066 0.7420 0.093 Uiso 1 1 calc R . .
```

H7C H 0.1910 0.0638 0.5730 0.093 Uiso 1 1 calc R . .

loop_
_atom_site_aniso_label
_atom_site_aniso_U_11
_atom_site_aniso_U_22
_atom_site_aniso_U_33
_atom_site_aniso_U_23
_atom_site_aniso_U_13
_atom_site_aniso_U_12
O2 0.0640(9) 0.0463(8) 0.0371(7) -0.0041(6) -0.0065(6) 0.0027(6)
O4 0.0530(8) 0.0389(7) 0.0575(9) 0.0014(6) -0.0089(6) 0.0001(6)
O3 0.0521(9) 0.0488(8) 0.0749(11) -0.0019(8) 0.0092(8) 0.0001(6)
O1 0.0941(12) 0.0626(10) 0.0627(10) -0.0207(8) -0.0162(9) 0.0324(8)
C8 0.0427(10) 0.0392(10) 0.0446(11) -0.0034(8) -0.0108(9) -0.0045(8)
C5 0.0431(10) 0.0404(10) 0.0380(10) -0.0052(8) -0.0059(8) -0.0049(8)
C4 0.0420(10) 0.0414(10) 0.0430(11) -0.0043(8) -0.0066(8) -0.0016(8)
C2 0.0675(13) 0.0479(11) 0.0400(10) -0.0065(9) -0.0136(9) 0.0178(9)
C6 0.0514(11) 0.0436(11) 0.0585(13) -0.0142(9) -0.0088(9) -0.0042(8)
C1 0.0681(13) 0.0331(9) 0.0492(12) -0.0047(9) -0.0033(10) -0.0007(8)
C3 0.0453(11) 0.0601(12) 0.0513(12) -0.0063(10) -0.0077(9) 0.0053(9)
C9 0.0725(15) 0.0417(11) 0.0772(16) -0.0050(11) -0.0190(12) 0.0094(10)
C7 0.0574(13) 0.0582(12) 0.0780(16) -0.0238(12) -0.0247(11) -0.0023(10)

_geom_special_details
;
All esds (except the esd in the dihedral angle between two l.s. planes)
are estimated using the full covariance matrix. The cell esds are taken
into account individually in the estimation of esds in distances, angles
and torsion angles; correlations between esds in cell parameters are only
used when they are defined by crystal symmetry. An approximate (isotropic)
treatment of cell esds is used for estimating esds involving l.s. planes.
;

loop_
_geom_bond_atom_site_label_1
_geom_bond_atom_site_label_2
_geom_bond_distance
_geom_bond_site_symmetry_2
_geom_bond_publ_flag
O2 C1 1.434(2) . ?
O2 C4 1.451(2) . ?
O4 C8 1.337(2) . ?
O4 C9 1.440(2) . ?
O3 C8 1.201(2) . ?
O1 C2 1.200(2) . ?
C8 C5 1.497(2) . ?
C5 C6 1.541(2) . ?
C5 C4 1.564(2) . ?
C5 H5 0.9800 . ?
C4 C7 1.502(2) . ?
C4 C3 1.537(3) . ?
C2 C3 1.507(3) . ?

C2 C1 1.517(3) . ?
C6 C1 1.529(3) . ?
C6 H6A 0.9700 . ?
C6 H6B 0.9700 . ?
C1 H1 0.9800 . ?
C3 H3A 0.9700 . ?
C3 H3B 0.9700 . ?
C9 H9A 0.9600 . ?
C9 H9B 0.9600 . ?
C9 H9C 0.9600 . ?
C7 H7A 0.9600 . ?
C7 H7B 0.9600 . ?
C7 H7C 0.9600 . ?

loop_
_geom_angle_atom_site_label_1
_geom_angle_atom_site_label_2
_geom_angle_atom_site_label_3
_geom_angle
_geom_angle_site_symmetry_1
_geom_angle_site_symmetry_3
_geom_angle_publ_flag
C1 O2 C4 97.76(12) . . ?
C8 O4 C9 115.88(15) . . ?
O3 C8 O4 122.49(17) . . ?
O3 C8 C5 125.88(16) . . ?
O4 C8 C5 111.62(15) . . ?
C8 C5 C6 113.02(14) . . ?
C8 C5 C4 111.56(15) . . ?
C6 C5 C4 101.42(14) . . ?
C8 C5 H5 110.2 . . ?
C6 C5 H5 110.2 . . ?
C4 C5 H5 110.2 . . ?
O2 C4 C7 110.56(16) . . ?
O2 C4 C3 100.89(14) . . ?
C7 C4 C3 116.02(15) . . ?
O2 C4 C5 101.76(12) . . ?
C7 C4 C5 117.86(15) . . ?
C3 C4 C5 107.50(16) . . ?
O1 C2 C3 128.85(19) . . ?
O1 C2 C1 127.6(2) . . ?
C3 C2 C1 103.49(15) . . ?
C1 C6 C5 102.15(14) . . ?
C1 C6 H6A 111.3 . . ?
C5 C6 H6A 111.3 . . ?
C1 C6 H6B 111.3 . . ?
C5 C6 H6B 111.3 . . ?
H6A C6 H6B 109.2 . . ?
O2 C1 C2 102.40(15) . . ?
O2 C1 C6 102.75(14) . . ?
C2 C1 C6 106.17(17) . . ?
O2 C1 H1 114.7 . . ?
C2 C1 H1 114.7 . . ?

C6 C1 H1 114.7 . . ?
C2 C3 C4 101.62(15) . . ?
C2 C3 H3A 111.4 . . ?
C4 C3 H3A 111.4 . . ?
C2 C3 H3B 111.4 . . ?
C4 C3 H3B 111.4 . . ?
H3A C3 H3B 109.3 . . ?
O4 C9 H9A 109.5 . . ?
O4 C9 H9B 109.5 . . ?
H9A C9 H9B 109.5 . . ?
O4 C9 H9C 109.5 . . ?
H9A C9 H9C 109.5 . . ?
H9B C9 H9C 109.5 . . ?
C4 C7 H7A 109.5 . . ?
C4 C7 H7B 109.5 . . ?
H7A C7 H7B 109.5 . . ?
C4 C7 H7C 109.5 . . ?
H7A C7 H7C 109.5 . . ?
H7B C7 H7C 109.5 . . ?

loop_
_geom_torsion_atom_site_label_1
_geom_torsion_atom_site_label_2
_geom_torsion_atom_site_label_3
_geom_torsion_atom_site_label_4
_geom_torsion
_geom_torsion_site_symmetry_1
_geom_torsion_site_symmetry_2
_geom_torsion_site_symmetry_3
_geom_torsion_site_symmetry_4
_geom_torsion_publ_flag
C9 O4 C8 O3 -2.4(3) . . . . ?
C9 O4 C8 C5 176.40(16) . . . . ?
O3 C8 C5 C6 -28.6(3) . . . . ?
O4 C8 C5 C6 152.70(16) . . . . ?
O3 C8 C5 C4 85.0(2) . . . . ?
O4 C8 C5 C4 -93.77(17) . . . . ?
C1 O2 C4 C7 179.27(15) . . . . ?
C1 O2 C4 C3 55.95(16) . . . . ?
C1 O2 C4 C5 -54.72(15) . . . . ?
C8 C5 C4 O2 -88.23(15) . . . . ?
C6 C5 C4 O2 32.35(16) . . . . ?
C8 C5 C4 C7 32.8(2) . . . . ?
C6 C5 C4 C7 153.41(16) . . . . ?
C8 C5 C4 C3 166.23(14) . . . . ?
C6 C5 C4 C3 -73.19(17) . . . . ?
C8 C5 C6 C1 120.65(16) . . . . ?
C4 C5 C6 C1 1.10(17) . . . . ?
C4 O2 C1 C2 -53.79(16) . . . . ?
C4 O2 C1 C6 56.21(16) . . . . ?
O1 C2 C1 O2 -152.25(19) . . . . ?
C3 C2 C1 O2 30.56(19) . . . . ?
O1 C2 C1 C6 100.3(2) . . . . ?

C3 C2 C1 C6 -76.84(18) . . . . ?
C5 C6 C1 O2 -34.87(17) . . . . ?
C5 C6 C1 C2 72.28(17) . . . . ?
O1 C2 C3 C4 -173.5(2) . . . . ?
C1 C2 C3 C4 3.7(2) . . . . ?
O2 C4 C3 C2 -36.26(18) . . . . ?
C7 C4 C3 C2 -155.72(18) . . . . ?
C5 C4 C3 C2 69.90(17) . . . . ?

_diffrn_measured_fraction_theta_max 0.986
_diffrn_reflns_theta_full 25.00
_diffrn_measured_fraction_theta_full 0.986
_refine_diff_density_max 0.244
_refine_diff_density_min -0.202
_refine_diff_density_rms 0.049
_chemical_compound_source 'Produced Synthetically'
_exptl_crystal_recrystallization_method Ether

Appendix 3.6: 200 MHz ^{1}H NMR and 50 MHz ^{13}C NMR spectra of **26** with GC-MS data.

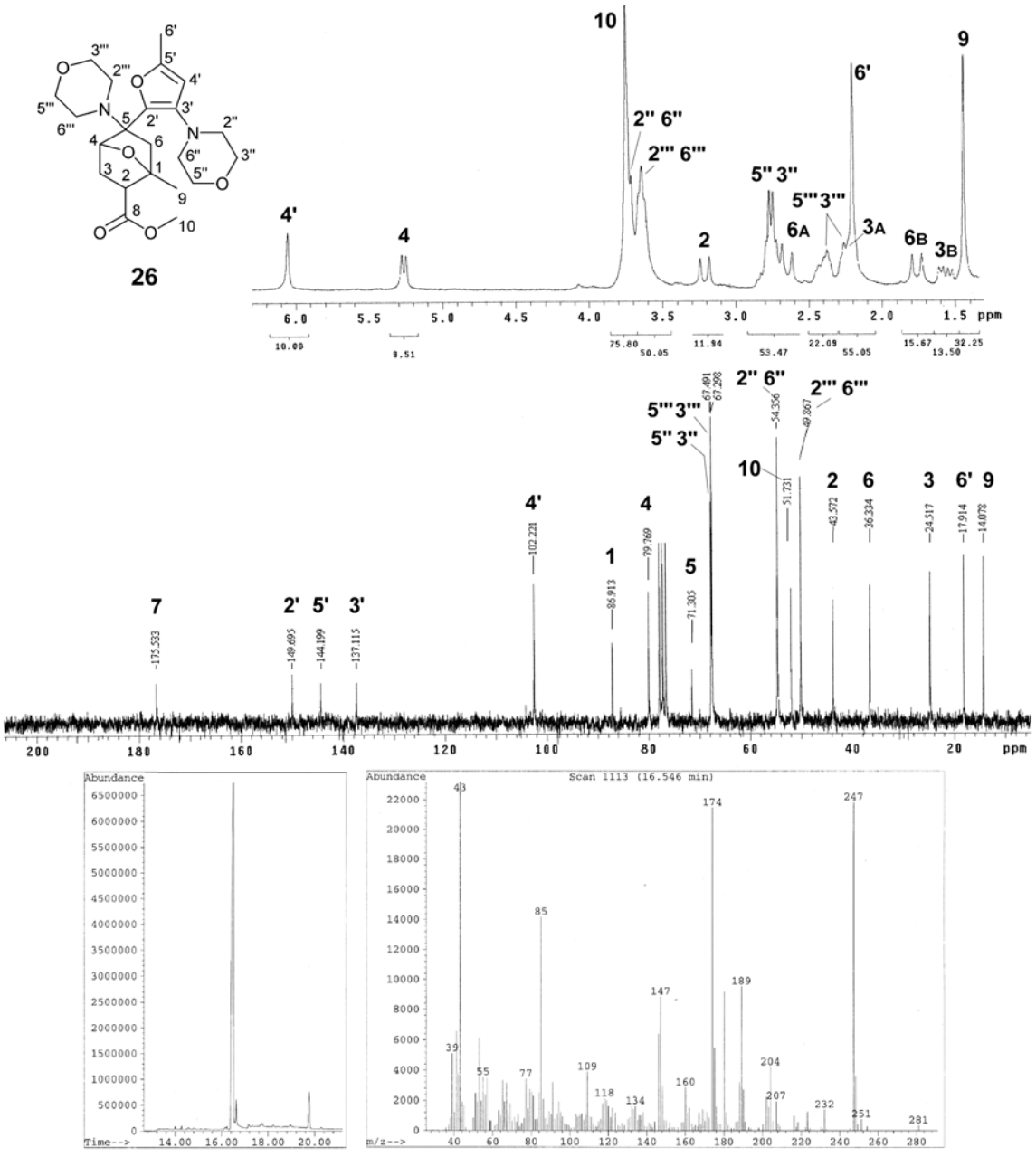

Appendix 3.7: GC traces for the GC-MS analysis of the crude D-A reaction mixture between **5a** and MAC in H_2O at 2ºC (top) and 25ºC (bottom).

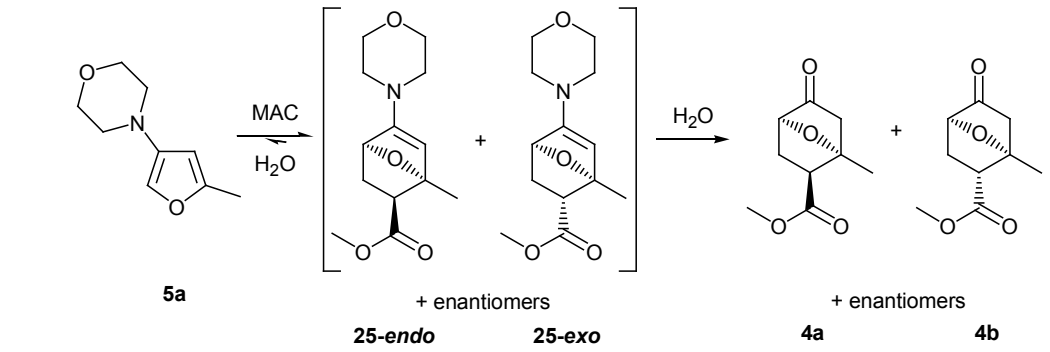

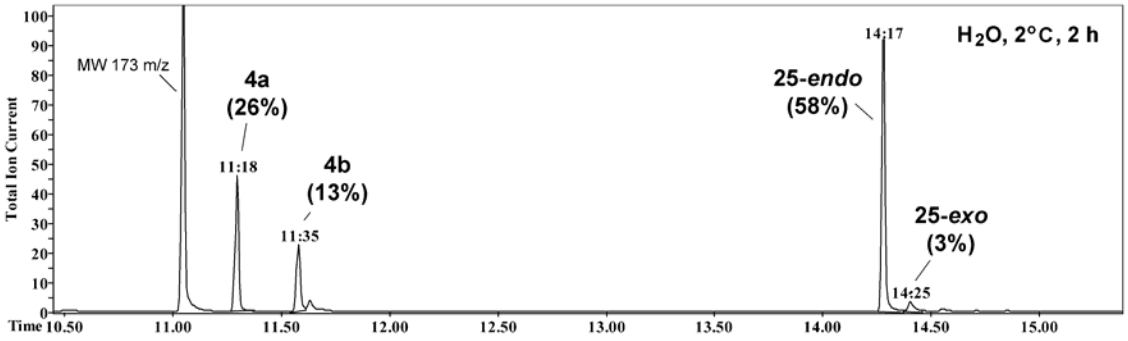

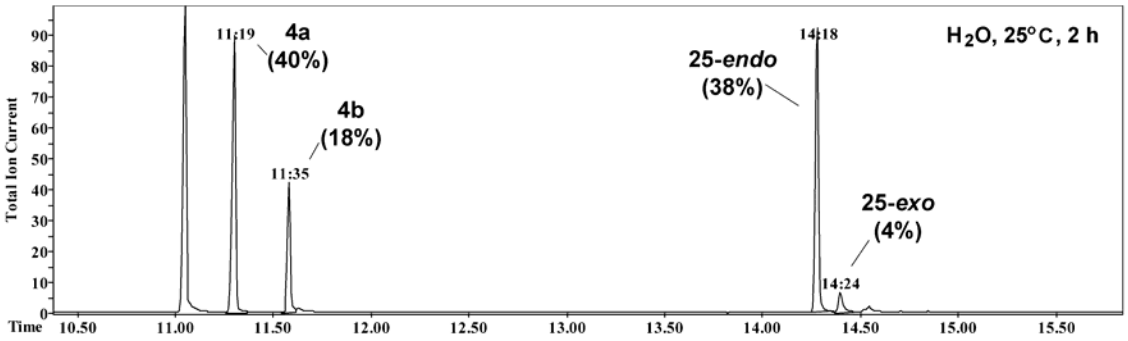

Appendix 3.8: GC traces for the GC-MS analysis of the crude D-A reaction mixture between **5b** and MAC in H_2O (top), 3.0 M LiCl (second from top), 0.1 M CH_3COOH (second from bottom) and DIMCARB (bottom) at 25ºC.

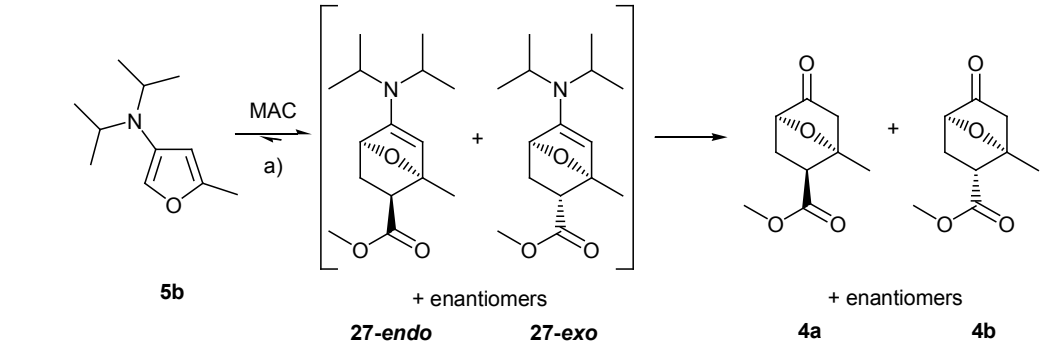

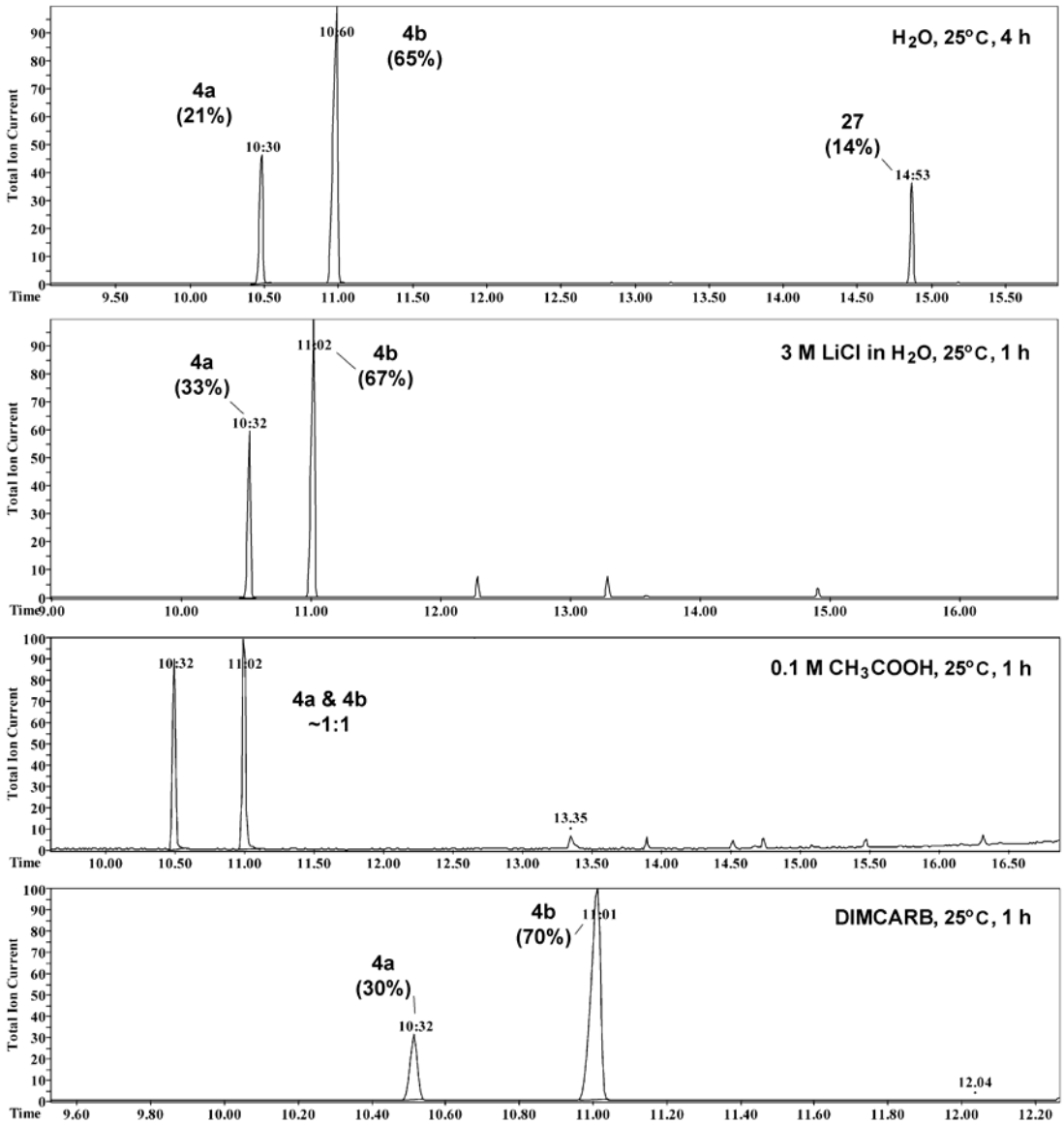

Appendix 3.9: GC-MS data for the crude D-A reaction between **5p** and MAC in DCM.

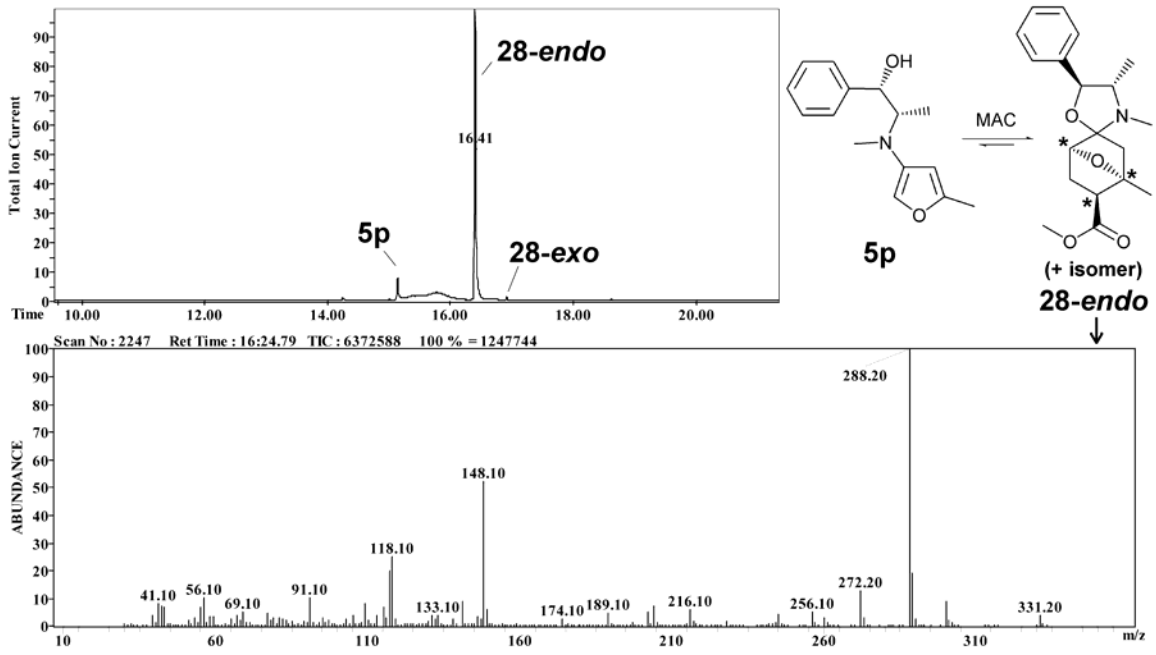

Appendix 3.10: 300 MHz COSY NMR analysis for **28**-*endo* with assignments for the major diastereoisomer. The 75 MHz ^{13}C NMR for **28**-*endo* in $CDCl_3$ and the hydrochloride salt of **28**-*endo* in D_2O is also shown.

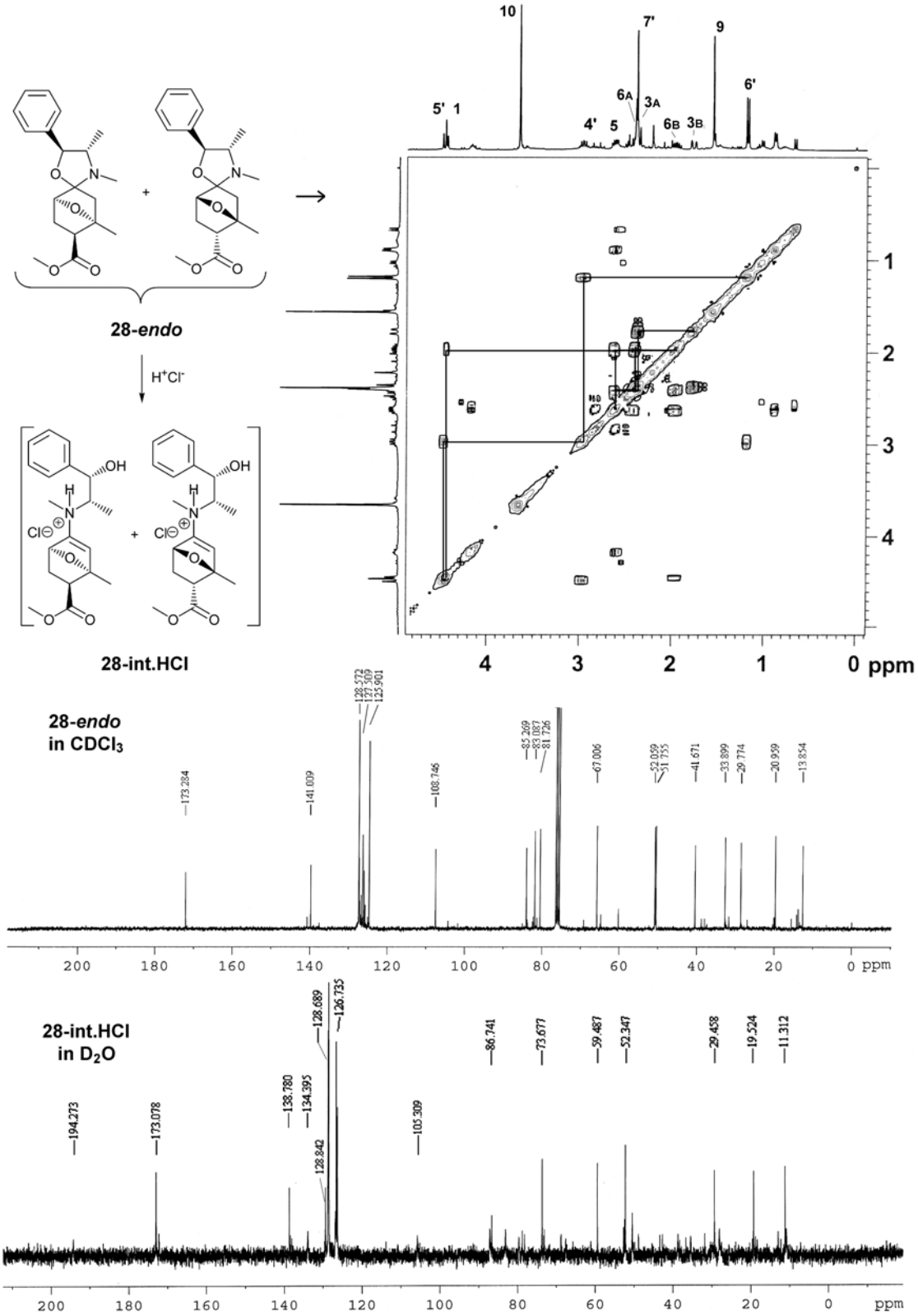

Appendix 3.11: 300 MHz ^{1}H/ 75 MHz ^{13}C HMBC NMR of **28**-*endo* with ^{1}H expansions.

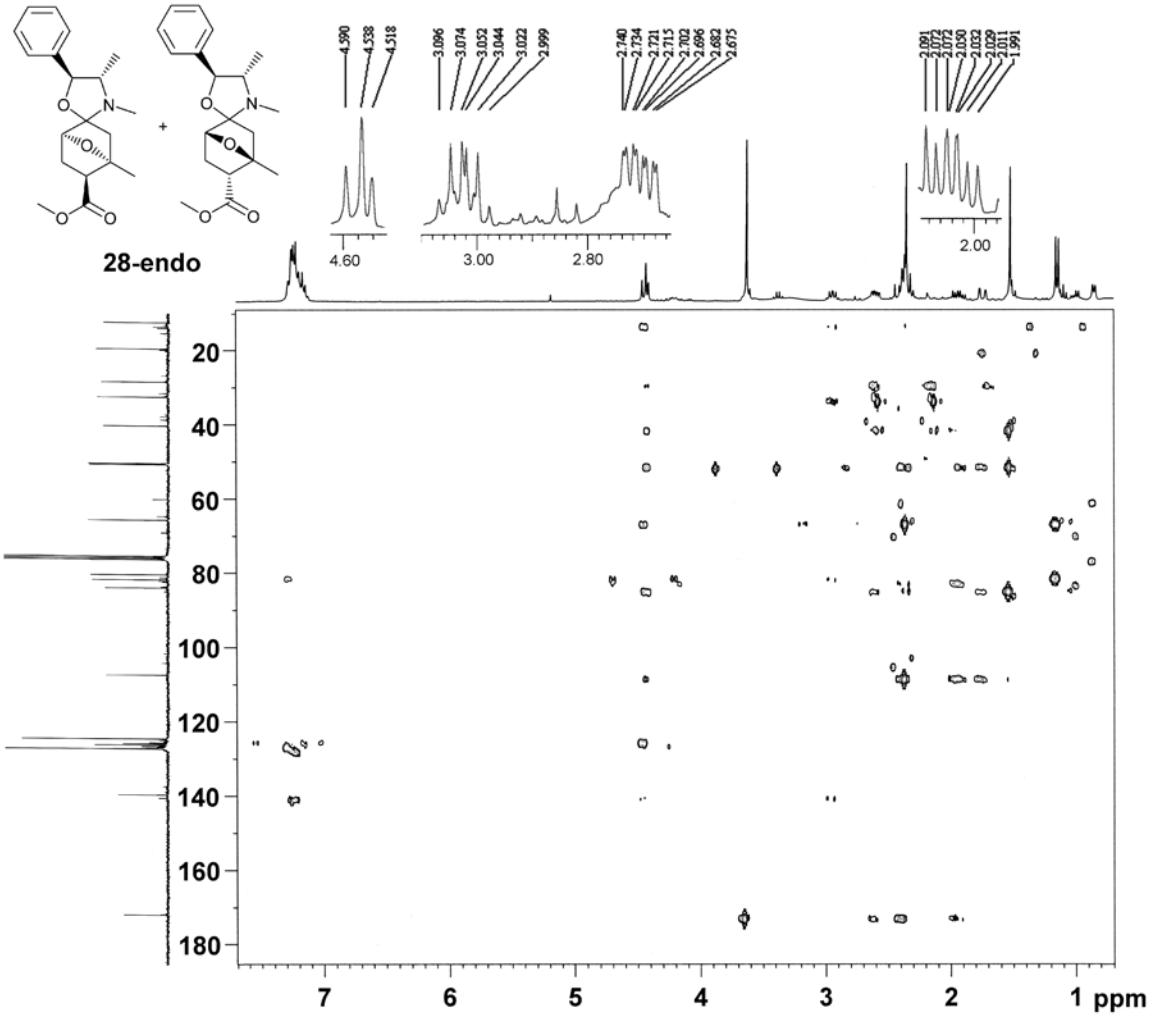

Appendix 3.12: 300 MHz ^{1}H COSY NMR analysis of **29** with structure assignments for the major isomer. The GC-MS data for **29** is also shown.

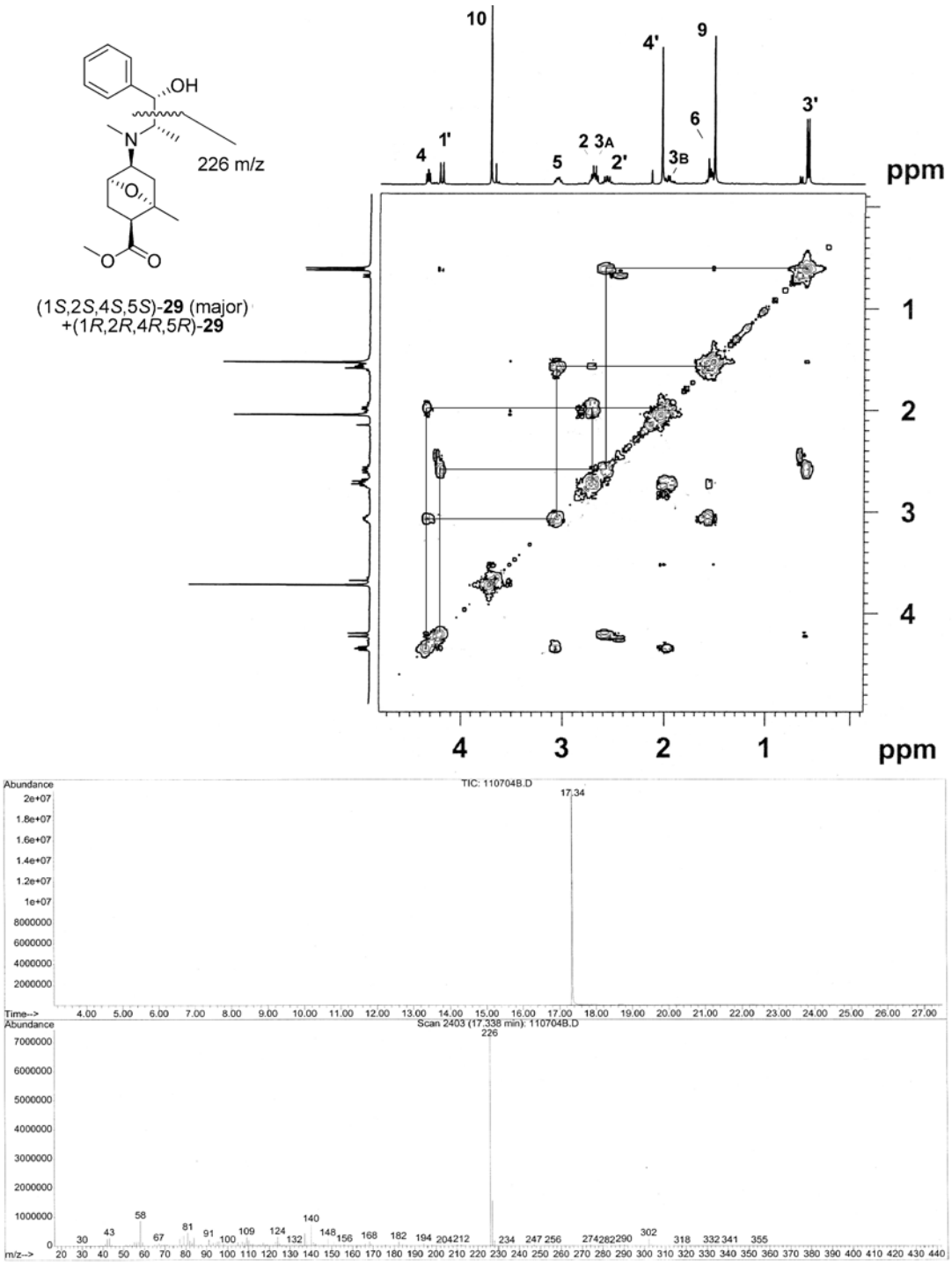

Appendix 3.13: 75 MHz ^{13}C NMR Analysis and 300 MHz ^{1}H/ 75 MHz ^{13}C HMBC NMR analysis of **29**. ^{1}H expansions are also shown.

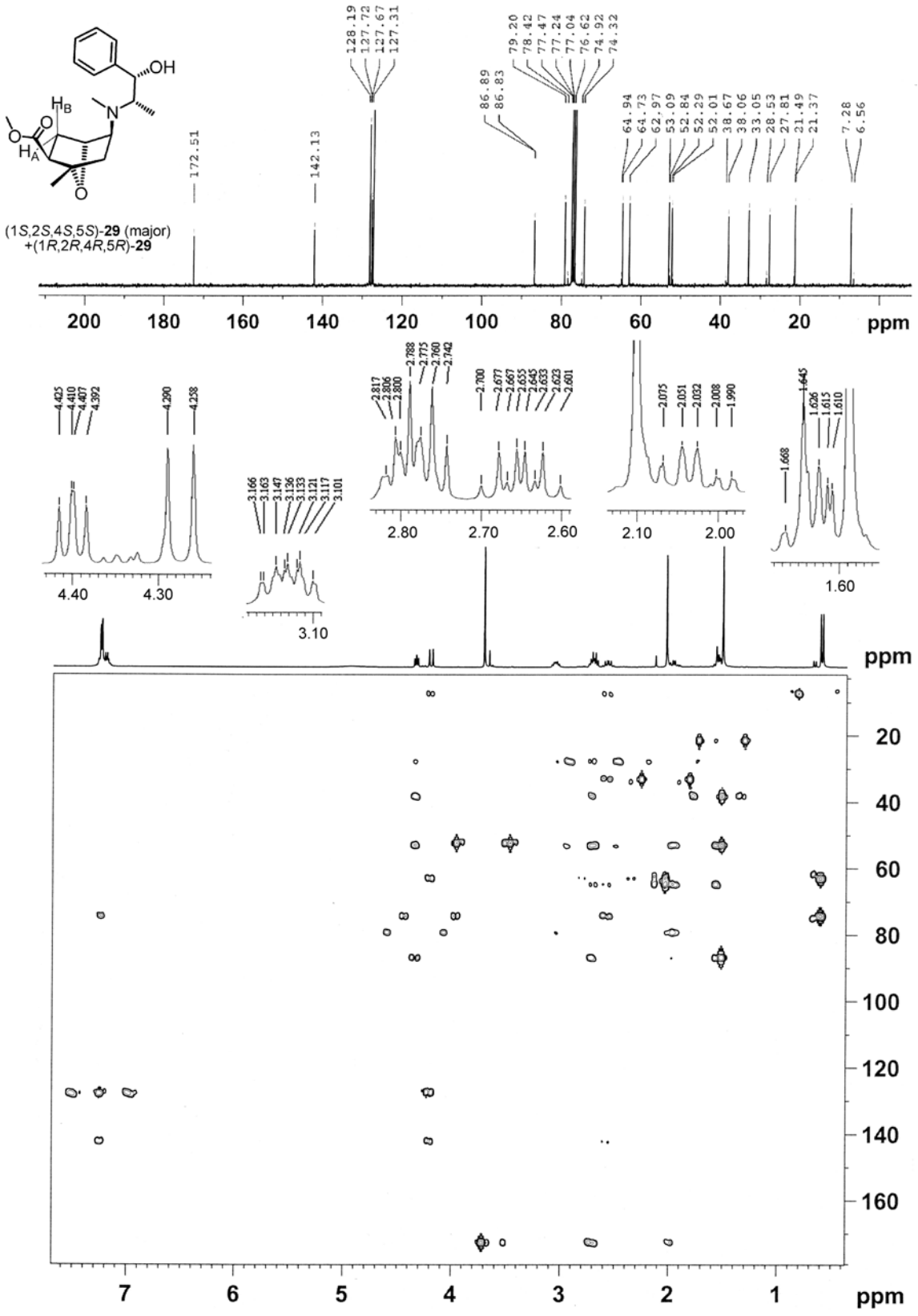

Appendix 3.14: 300 MHz ^{1}H/75 MHz ^{13}C HMQC NMR, 300 MHz COSY NMR and 300 MHz ^{1}H/75 MHz ^{13}C HMBC NMR spectra of the pure isomer (1*S*,2*S*,4*S*,5*S*)-**29.HClO$_4$**. DEPT 135 data is also shown.

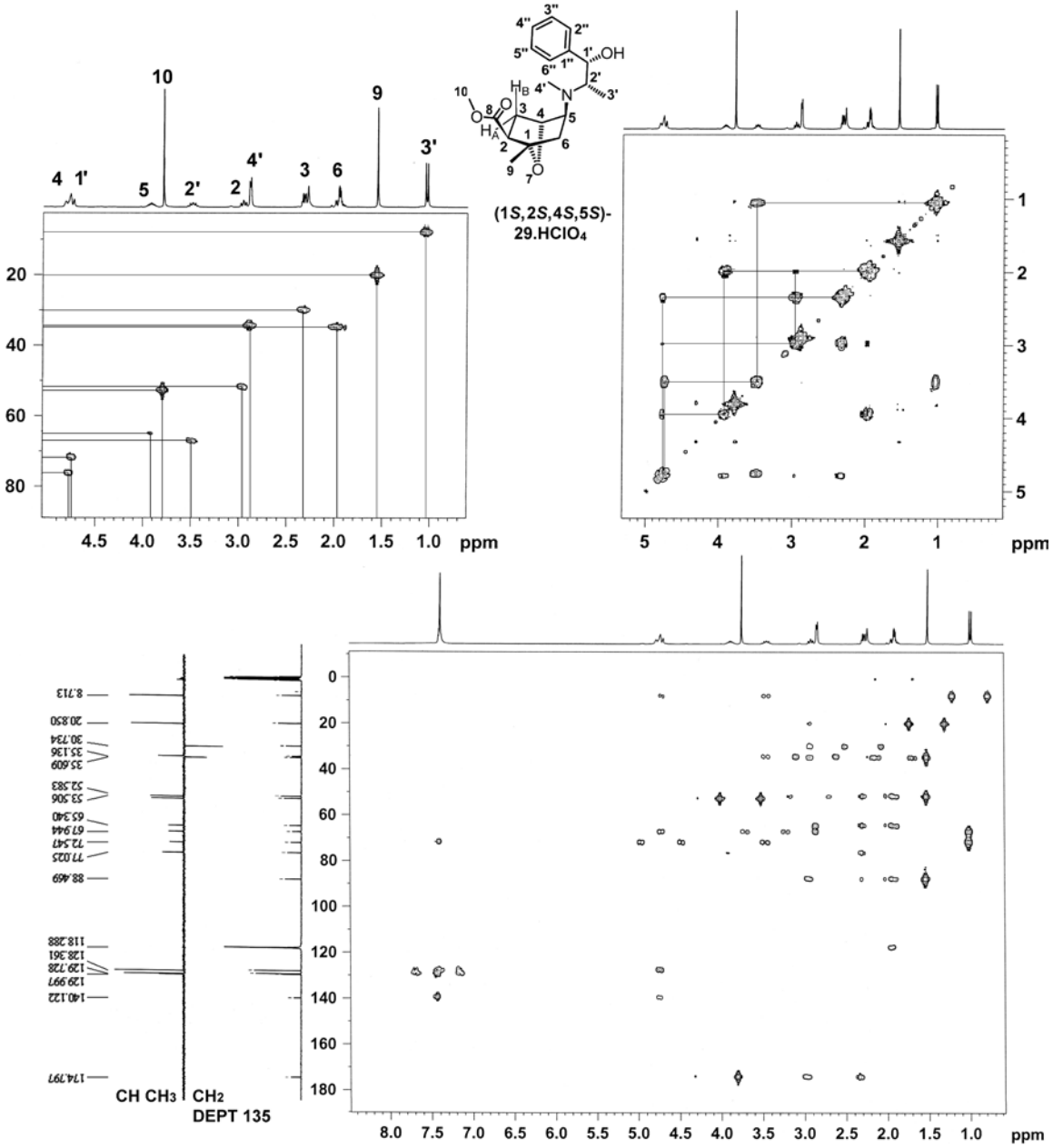

Appendix 3.15: A summary of bond distances and the X-ray crystal CIF file is shown for (1*S*,2*S*,4*S*,5*S*)-**29.HClO$_4$**. The atom numbering produced in the CIF file used to describe the X-ray crystal data is slightly different from that used throughout the discussion in Chapter 3 and alternate numbering used in the crystal structure data of (1*S*,2*S*,4*S*,5*S)*-methyl- 5-(N-((1*S*,2*S*)-1-hydroxy-1-phenylpropan-2-yl)-N-methylamino)-1-methyl-7-oxa-bicyclo[2.2.1]heptane-2-carboxylate perchlorate salt (1*S*,2*S*,4*S*,5*S*)-**29.HClO$_4$** is shown below.

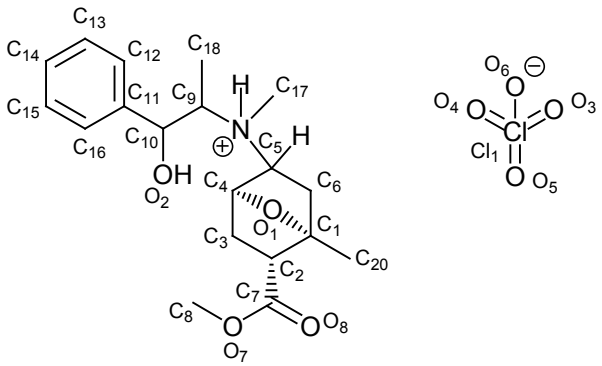

Atom 1	Atom 2	Exp. *d* (Å)	Lit. *d*[88] (Å)	Closest functional group	
O6	Cl1	1.418(5)	1.414	**Cl**-**O**	$ClO4^-$
O5	Cl1	1.393(5)			
Cl1	O3	1.389(4)			
Cl1	O4	1.430(4)			
O2	C10	1.416(5)	1.432	Csp_3-O(2) C_2-**C**H-**O**H	
O1	C4	1.429(5)	1.429	Csp_2-O(2) $(C)_2$-**C**H-**O**-C	
O1	C1	1.464(5)	1.452	Csp_2-O(2) $(C)_3$-**C**-**O**-C	
N1	C17	1.503(5)	1.502	Csp_3-N(4) $\mathbf{C}_3$-**N**H^+	
N1	C5	1.513(5)			
N1	C9	1.521(5)			
C3	C4	1.526(6)	1.535	Csp_3-Csp_3 **C**-**C**	cyclohexane
C3	C2	1.526(6)	1.535	Csp_3-Csp_3 **C**-**C**	cyclohexane
C11	C12	1.374(6)	1.380	*Car*=*Car* H-**C**=**C**-H	aromatic
C11	C16	1.394(6)	1.397	*Car*=*Car* C-**C**=**C**-C	aromatic
C12	C13	1.384(7)			
C15	C14	1.381(9)			
C16	C15	1.389(7)			
C13	C14	1.371(9)			
C11	C10	1.507(6)	1.510	Csp_3-*Car* C-**C**H_2-**C**ar	
C5	C4	1.539(5)	1.535	Csp_3-Csp_3 **C**-**C**	cyclohexane
C5	C6	1.545(5)	1.543	Csp_3-Csp_3 **C**-**C**	cyclopentane
C1	C6	1.531(5)	1.535	Csp_3-Csp_3 **C**-**C**	cyclohexane
C1	C2	1.545(5)	1.543	Csp_3-Csp_3 **C**-**C**	cyclopentane

C2	C7	1.506(6)	1.497	Csp_3-Csp_3 **C-C**(=O)(-OC) acyclic esters
C10	C9	1.537(6)	1.542	Csp_3-Csp_3 C_2-**C**H-**C**H-C_2
C9	C18	1.526(6)	1.524	Csp_3-Csp_3 C_2-**C**H-**C**H_3
C7	O8	1.198(5)	1.196	Csp_2=O(1) C-**C**(=**O**)-O-C
C7	O7	1.324(5)	1.336	Csp_2-O(2) C-**C**(=O)-**O**-C
O7	C8	1.451(5)	1.448	Csp_3-O(2) C-C(=O)-**O**-**C**H_3
C1	C20	1.487(6)		

X-ray crystal CIF data:

```
_audit_creation_method            SHELXL-97
_chemical_name_systematic
;
 ?
;
_chemical_name_common             ?
_chemical_melting_point           ?
_chemical_formula_moiety          ?
_chemical_formula_sum
 'C19 H28 Cl N O8'
_chemical_formula_weight          433.87

loop_
 _atom_type_symbol
 _atom_type_description
 _atom_type_scat_dispersion_real
 _atom_type_scat_dispersion_imag
 _atom_type_scat_source
 'C'  'C'   0.0181   0.0091
 'International Tables Vol C Tables 4.2.6.8 and 6.1.1.4'
 'H'  'H'   0.0000   0.0000
 'International Tables Vol C Tables 4.2.6.8 and 6.1.1.4'
 'N'  'N'   0.0311   0.0180
 'International Tables Vol C Tables 4.2.6.8 and 6.1.1.4'
 'O'  'O'   0.0492   0.0322
 'International Tables Vol C Tables 4.2.6.8 and 6.1.1.4'
 'Cl'  'Cl'   0.3639   0.7018
 'International Tables Vol C Tables 4.2.6.8 and 6.1.1.4'

_symmetry_cell_setting            'orthorhombic'
_symmetry_space_group_name_H-M    P212121

loop_
 _symmetry_equiv_pos_as_xyz
 'x, y, z'
 '-x+1/2, -y, z+1/2'
 'x+1/2, -y+1/2, -z'
 '-x, y+1/2, -z+1/2'

_cell_length_a                    8.511(2)
```

```
_cell_length_b                  15.356(5)
_cell_length_c                  15.839(3)
_cell_angle_alpha                90.00
_cell_angle_beta                 90.00
_cell_angle_gamma                 90.00
_cell_volume                    2070.1(9)
_cell_formula_units_Z            4
_cell_measurement_temperature     293(2)
_cell_measurement_reflns_used     25
_cell_measurement_theta_min       15
_cell_measurement_theta_max       25

_exptl_crystal_description       'plate'
_exptl_crystal_colour            'colourless'
_exptl_crystal_size_max           0.2
_exptl_crystal_size_mid           0.1
_exptl_crystal_size_min           0.02
_exptl_crystal_density_meas       ?
_exptl_crystal_density_diffrn     1.392
_exptl_crystal_density_method     'not measured'
_exptl_crystal_F_000              920
_exptl_absorpt_coefficient_mu     2.043
_exptl_absorpt_correction_type    'analytical'
_exptl_absorpt_correction_T_min   0.7624
_exptl_absorpt_correction_T_max   0.9604
_exptl_absorpt_process_details    'WingX'

_exptl_special_details
;
 ?
;

_diffrn_ambient_temperature       293(2)
_diffrn_radiation_wavelength      1.54180
_diffrn_radiation_type            CuK\a
_diffrn_radiation_source          'fine-focus sealed tube'
'audit_creation_method           'WinGX-Routine XCAD4'
_audit_creation_date             2004-08-30
_diffrn_radiation_monochromator  graphite
_diffrn_radiation_probe          x-ray
_diffrn_source                   'Enraf Nonius FR590'
_diffrn_detector                 'scintillation LiI'
_diffrn_detector_dtime           1.195
_diffrn_measurement_device       '\k-geometry diffractometer'
_diffrn_measurement_device_type  'Enraf Nonius CAD4'
_diffrn_measurement_method       'non-profiled omega/2theta scans'
_diffrn_standards_number         3
_diffrn_standards_interval_time  160
_diffrn_standards_decay_%        1
_diffrn_reflns_number            2462
_diffrn_reflns_av_R_equivalents   0.0230
_diffrn_reflns_av_sigmaI/netI     0.0313
_diffrn_reflns_limit_h_min        -1
```

```
_diffrn_reflns_limit_h_max       9
_diffrn_reflns_limit_k_min       -18
_diffrn_reflns_limit_k_max       0
_diffrn_reflns_limit_l_min       -1
_diffrn_reflns_limit_l_max       18
_diffrn_reflns_theta_min         4.01
_diffrn_reflns_theta_max         64.92
_reflns_number_total             2365
_reflns_number_gt                2006
_reflns_threshold_expression     >2sigma(I)

_computing_data_collection       ?
_computing_cell_refinement       ?
_computing_data_reduction        ?
_computing_structure_solution    ?
_computing_structure_refinement   'SHELXL-97 (Sheldrick, 1997)'
_computing_molecular_graphics    ?
_computing_publication_material   ?

_refine_special_details
;
 Refinement of F^2^ against ALL reflections.  The weighted R-factor wR and
 goodness of fit S are based on F^2^, conventional R-factors R are based
 on F, with F set to zero for negative F^2^. The threshold expression of
 F^2^ > 2sigma(F^2^) is used only for calculating R-factors(gt) etc. and is
 not relevant to the choice of reflections for refinement.  R-factors based
 on F^2^ are statistically about twice as large as those based on F, and R-
 factors based on ALL data will be even larger.
;

_refine_ls_structure_factor_coef  Fsqd
_refine_ls_matrix_type           full
_refine_ls_weighting_scheme      calc
_refine_ls_weighting_details
 'calc w=1/[\s^2^(Fo^2^)+(0.0878P)^2^+0.2825P] where P=(Fo^2^+2Fc^2^)/3'
_atom_sites_solution_primary     direct
_atom_sites_solution_secondary    difmap
_atom_sites_solution_hydrogens    geom
_refine_ls_hydrogen_treatment    mixed
_refine_ls_extinction_method     SHELXL
_refine_ls_extinction_coef       0.0011(3)
_refine_ls_extinction_expression
 'Fc^*^=kFc[1+0.001xFc^2^\l^3^/sin(2\q)]^-1/4^'
_refine_ls_abs_structure_details
 'Flack H D (1983), Acta Cryst. A39, 876-881'
_refine_ls_abs_structure_Flack    0.00(3)
_refine_ls_number_reflns         2365
_refine_ls_number_parameters     275
_refine_ls_number_restraints     0
_refine_ls_R_factor_all          0.0608
_refine_ls_R_factor_gt           0.0496
_refine_ls_wR_factor_ref         0.1371
_refine_ls_wR_factor_gt          0.1271
```

```
_refine_ls_goodness_of_fit_ref    1.071
_refine_ls_restrained_S_all       1.071
_refine_ls_shift/su_max           0.000
_refine_ls_shift/su_mean          0.000

loop_
 _atom_site_label
 _atom_site_type_symbol
 _atom_site_fract_x
 _atom_site_fract_y
 _atom_site_fract_z
 _atom_site_U_iso_or_equiv
 _atom_site_adp_type
 _atom_site_occupancy
 _atom_site_symmetry_multiplicity
 _atom_site_calc_flag
 _atom_site_refinement_flags
 _atom_site_disorder_assembly
 _atom_site_disorder_group
H1 H 0.316(5) -0.039(2) 0.125(2) 0.032(10) Uiso 1 1 d . . .
O6 O 0.9119(7) 0.7454(3) 0.1749(4) 0.133(2) Uani 1 1 d . . .
O5 O 0.7120(9) 0.7727(4) 0.0797(3) 0.135(2) Uani 1 1 d . . .
Cl1 Cl 0.77073(15) 0.71368(7) 0.13861(7) 0.0568(3) Uani 1 1 d . . .
O2 O 0.5625(4) -0.0230(2) 0.14945(19) 0.0482(8) Uani 1 1 d . . .
O1 O -0.1188(3) 0.00263(19) 0.1100(2) 0.0489(8) Uani 1 1 d . . .
N1 N 0.2753(4) -0.0757(2) 0.1633(2) 0.0364(7) Uani 1 1 d . . .
C3 C 0.0923(5) -0.0022(3) 0.0182(2) 0.0449(10) Uani 1 1 d . . .
H3A H 0.0469 -0.0153 -0.0365 0.054 Uiso 1 1 calc R . .
H3B H 0.2041 -0.0145 0.0168 0.054 Uiso 1 1 calc R . .
C11 C 0.6446(5) -0.0379(3) 0.2962(3) 0.0411(9) Uani 1 1 d . . .
C5 C 0.1045(5) -0.0496(2) 0.1716(2) 0.0359(9) Uani 1 1 d . . .
H5 H 0.0537 -0.0877 0.2131 0.043 Uiso 1 1 calc R . .
C1 C -0.0275(5) 0.0810(2) 0.1292(3) 0.0413(9) Uani 1 1 d . . .
C6 C 0.0805(5) 0.0461(2) 0.1987(2) 0.0376(9) Uani 1 1 d . . .
H6A H 0.0309 0.0499 0.2537 0.045 Uiso 1 1 calc R . .
H6B H 0.1795 0.0775 0.2000 0.045 Uiso 1 1 calc R . .
C2 C 0.0600(5) 0.0918(3) 0.0444(2) 0.0423(10) Uani 1 1 d . . .
H2A H -0.0137 0.1168 0.0035 0.051 Uiso 1 1 calc R . .
C16 C 0.6335(6) 0.0486(3) 0.3224(3) 0.0516(11) Uani 1 1 d . . .
H16 H 0.5604 0.0857 0.2977 0.062 Uiso 1 1 calc R . .
C10 C 0.5438(5) -0.0712(3) 0.2250(2) 0.0396(9) Uani 1 1 d . . .
H10 H 0.5712 -0.1321 0.2139 0.048 Uiso 1 1 calc R . .
C9 C 0.3674(5) -0.0657(3) 0.2450(2) 0.0376(9) Uani 1 1 d . . .
H9 H 0.3461 -0.0074 0.2675 0.045 Uiso 1 1 calc R . .
C17 C 0.2890(6) -0.1647(3) 0.1247(3) 0.0561(12) Uani 1 1 d . . .
H17A H 0.2276 -0.2053 0.1568 0.084 Uiso 1 1 calc R . .
H17B H 0.3971 -0.1826 0.1249 0.084 Uiso 1 1 calc R . .
H17C H 0.2511 -0.1631 0.0676 0.084 Uiso 1 1 calc R . .
C18 C 0.3180(6) -0.1319(4) 0.3117(3) 0.0663(15) Uani 1 1 d . . .
H18A H 0.2072 -0.1268 0.3219 0.099 Uiso 1 1 calc R . .
H18B H 0.3743 -0.1210 0.3631 0.099 Uiso 1 1 calc R . .
H18C H 0.3413 -0.1896 0.2920 0.099 Uiso 1 1 calc R . .
C4 C 0.0104(5) -0.0525(3) 0.0887(3) 0.0448(10) Uani 1 1 d . . .
```

H4 H -0.0213 -0.1115 0.0722 0.054 Uiso 1 1 calc R . .
C12 C 0.7538(6) -0.0913(3) 0.3336(3) 0.0596(12) Uani 1 1 d . . .
H12 H 0.7612 -0.1492 0.3169 0.072 Uiso 1 1 calc R . .
C15 C 0.7323(7) 0.0789(3) 0.3857(3) 0.0678(15) Uani 1 1 d . . .
H15 H 0.7241 0.1363 0.4036 0.081 Uiso 1 1 calc R . .
O4 O 0.6607(7) 0.7060(3) 0.2064(3) 0.1081(17) Uani 1 1 d . . .
C7 C 0.1989(5) 0.1522(3) 0.0511(3) 0.0451(10) Uani 1 1 d . . .
O3 O 0.7961(8) 0.6309(3) 0.1061(3) 0.1153(18) Uani 1 1 d . . .
C13 C 0.8529(7) -0.0600(5) 0.3959(3) 0.0757(17) Uani 1 1 d . . .
H13 H 0.9271 -0.0968 0.4201 0.091 Uiso 1 1 calc R . .
C14 C 0.8426(8) 0.0248(5) 0.4223(3) 0.0797(18) Uani 1 1 d . . .
H14 H 0.9089 0.0457 0.4644 0.096 Uiso 1 1 calc R . .
O7 O 0.3300(3) 0.11242(19) 0.0742(2) 0.0519(8) Uani 1 1 d . . .
O8 O 0.1917(5) 0.2295(2) 0.0413(3) 0.0805(12) Uani 1 1 d . . .
C20 C -0.1280(5) 0.1562(3) 0.1533(3) 0.0569(12) Uani 1 1 d . . .
H20A H -0.1838 0.1768 0.1045 0.085 Uiso 1 1 calc R . .
H20B H -0.0632 0.2022 0.1752 0.085 Uiso 1 1 calc R . .
H20C H -0.2018 0.1383 0.1957 0.085 Uiso 1 1 calc R . .
C8 C 0.4631(6) 0.1685(3) 0.0924(4) 0.0676(14) Uani 1 1 d . . .
H8A H 0.4838 0.2050 0.0444 0.101 Uiso 1 1 calc R . .
H8C H 0.5538 0.1334 0.1041 0.101 Uiso 1 1 calc R . .
H8B H 0.4396 0.2041 0.1405 0.101 Uiso 1 1 calc R . .
H2 H 0.654(6) -0.021(3) 0.140(3) 0.044(13) Uiso 1 1 d . . .

loop_
 _atom_site_aniso_label
 _atom_site_aniso_U_11
 _atom_site_aniso_U_22
 _atom_site_aniso_U_33
 _atom_site_aniso_U_23
 _atom_site_aniso_U_13
 _atom_site_aniso_U_12
O6 0.101(4) 0.122(4) 0.176(5) 0.005(4) -0.045(4) -0.048(3)
O5 0.160(5) 0.139(4) 0.108(3) 0.054(3) 0.002(4) 0.056(5)
Cl1 0.0621(7) 0.0525(6) 0.0558(6) 0.0003(5) -0.0008(6) 0.0028(6)
O2 0.0289(15) 0.075(2) 0.0408(16) 0.0139(14) 0.0022(14) 0.0021(15)
O1 0.0240(12) 0.0548(17) 0.0679(19) 0.0041(15) -0.0046(15) -0.0073(13)
N1 0.0294(16) 0.0357(15) 0.0442(17) -0.0017(14) -0.0012(16) -0.0034(14)
C3 0.037(2) 0.060(2) 0.038(2) -0.0075(19) -0.0068(19) -0.009(2)
C11 0.030(2) 0.050(2) 0.043(2) 0.0109(19) 0.0024(19) -0.0026(18)
C5 0.0283(18) 0.0365(19) 0.0430(19) 0.0028(17) 0.0045(17) -0.0058(17)
C1 0.0258(19) 0.047(2) 0.051(2) 0.0052(19) -0.0017(19) -0.0046(17)
C6 0.028(2) 0.046(2) 0.0379(18) 0.0003(17) 0.0008(17) 0.0027(17)
C2 0.033(2) 0.053(2) 0.041(2) 0.0082(18) -0.0088(19) -0.002(2)
C16 0.051(3) 0.053(2) 0.051(2) 0.004(2) 0.002(2) -0.011(2)
C10 0.032(2) 0.043(2) 0.044(2) 0.0036(17) -0.0013(18) 0.0046(18)
C9 0.034(2) 0.0405(19) 0.0382(19) 0.0080(17) -0.0004(18) -0.0035(17)
C17 0.055(3) 0.045(2) 0.069(3) -0.017(2) -0.006(3) 0.007(2)
C18 0.049(3) 0.089(3) 0.060(3) 0.036(3) -0.004(3) -0.015(3)
C4 0.033(2) 0.050(2) 0.051(2) -0.007(2) -0.008(2) -0.0073(19)
C12 0.047(3) 0.073(3) 0.059(3) 0.018(2) -0.010(2) 0.005(2)
C15 0.079(4) 0.071(3) 0.053(3) -0.005(2) 0.007(3) -0.034(3)
O4 0.124(4) 0.095(3) 0.105(3) -0.004(3) 0.046(3) -0.015(3)

C7 0.039(2) 0.055(3) 0.041(2) 0.0111(18) 0.003(2) -0.005(2)
O3 0.141(5) 0.086(3) 0.119(3) -0.043(3) -0.012(4) 0.024(3)
C13 0.053(3) 0.116(5) 0.059(3) 0.030(3) -0.016(3) -0.004(3)
C14 0.070(4) 0.119(5) 0.050(3) 0.011(3) -0.010(3) -0.042(4)
O7 0.0281(14) 0.0512(17) 0.076(2) 0.0118(16) -0.0077(16) -0.0079(13)
O8 0.065(2) 0.0485(19) 0.128(3) 0.028(2) -0.022(3) -0.0075(19)
C20 0.037(2) 0.055(2) 0.078(3) 0.002(2) 0.004(3) 0.014(2)
C8 0.038(2) 0.065(3) 0.100(4) 0.007(3) 0.000(3) -0.023(2)

_geom_special_details
;
All esds (except the esd in the dihedral angle between two l.s. planes)
are estimated using the full covariance matrix. The cell esds are taken
into account individually in the estimation of esds in distances, angles
and torsion angles; correlations between esds in cell parameters are only
used when they are defined by crystal symmetry. An approximate (isotropic)
treatment of cell esds is used for estimating esds involving l.s. planes.
;

loop_
_geom_bond_atom_site_label_1
_geom_bond_atom_site_label_2
_geom_bond_distance
_geom_bond_site_symmetry_2
_geom_bond_publ_flag
O6 Cl1 1.418(5) . ?
O5 Cl1 1.393(5) . ?
Cl1 O3 1.389(4) . ?
Cl1 O4 1.430(4) . ?
O2 C10 1.416(5) . ?
O2 H2 0.79(5) . ?
O1 C4 1.429(5) . ?
O1 C1 1.464(5) . ?
N1 C17 1.503(5) . ?
N1 C5 1.513(5) . ?
N1 C9 1.521(5) . ?
N1 H1 0.90(4) . ?
C3 C4 1.526(6) . ?
C3 C2 1.526(6) . ?
C3 H3A 0.9700 . ?
C3 H3B 0.9700 . ?
C11 C12 1.374(6) . ?
C11 C16 1.394(6) . ?
C11 C10 1.507(6) . ?
C5 C4 1.539(5) . ?
C5 C6 1.545(5) . ?
C5 H5 0.9800 . ?
C1 C20 1.487(6) . ?
C1 C6 1.531(5) . ?
C1 C2 1.545(5) . ?
C6 H6A 0.9700 . ?
C6 H6B 0.9700 . ?
C2 C7 1.506(6) . ?

```
C2 H2A 0.9800 . ?
C16 C15 1.389(7) . ?
C16 H16 0.9300 . ?
C10 C9 1.537(6) . ?
C10 H10 0.9800 . ?
C9 C18 1.526(6) . ?
C9 H9 0.9800 . ?
C17 H17A 0.9600 . ?
C17 H17B 0.9600 . ?
C17 H17C 0.9600 . ?
C18 H18A 0.9600 . ?
C18 H18B 0.9600 . ?
C18 H18C 0.9600 . ?
C4 H4 0.9800 . ?
C12 C13 1.384(7) . ?
C12 H12 0.9300 . ?
C15 C14 1.381(9) . ?
C15 H15 0.9300 . ?
C7 O8 1.198(5) . ?
C7 O7 1.324(5) . ?
C13 C14 1.371(9) . ?
C13 H13 0.9300 . ?
C14 H14 0.9300 . ?
O7 C8 1.451(5) . ?
C20 H20A 0.9600 . ?
C20 H20B 0.9600 . ?
C20 H20C 0.9600 . ?
C8 H8A 0.9600 . ?
C8 H8C 0.9600 . ?
C8 H8B 0.9600 . ?

loop_
 _geom_angle_atom_site_label_1
 _geom_angle_atom_site_label_2
 _geom_angle_atom_site_label_3
 _geom_angle
 _geom_angle_site_symmetry_1
 _geom_angle_site_symmetry_3
 _geom_angle_publ_flag
O3 Cl1 O5 113.8(4) . . ?
O3 Cl1 O6 109.5(4) . . ?
O5 Cl1 O6 110.6(4) . . ?
O3 Cl1 O4 107.7(3) . . ?
O5 Cl1 O4 108.8(4) . . ?
O6 Cl1 O4 106.2(4) . . ?
C10 O2 H2 107(4) . . ?
C4 O1 C1 97.3(3) . . ?
C17 N1 C5 110.5(3) . . ?
C17 N1 C9 113.5(3) . . ?
C5 N1 C9 113.2(3) . . ?
C17 N1 H1 106(2) . . ?
C5 N1 H1 105(3) . . ?
C9 N1 H1 108(2) . . ?
```

C4 C3 C2 101.4(3) . . ?
C4 C3 H3A 111.5 . . ?
C2 C3 H3A 111.5 . . ?
C4 C3 H3B 111.5 . . ?
C2 C3 H3B 111.5 . . ?
H3A C3 H3B 109.3 . . ?
C12 C11 C16 119.1(4) . . ?
C12 C11 C10 120.4(4) . . ?
C16 C11 C10 120.5(4) . . ?
N1 C5 C4 114.7(3) . . ?
N1 C5 C6 113.8(3) . . ?
C4 C5 C6 101.3(3) . . ?
N1 C5 H5 108.9 . . ?
C4 C5 H5 108.9 . . ?
C6 C5 H5 108.9 . . ?
O1 C1 C20 112.8(3) . . ?
O1 C1 C6 100.4(3) . . ?
C20 C1 C6 115.6(4) . . ?
O1 C1 C2 99.4(3) . . ?
C20 C1 C2 114.6(4) . . ?
C6 C1 C2 111.9(3) . . ?
C1 C6 C5 102.3(3) . . ?
C1 C6 H6A 111.3 . . ?
C5 C6 H6A 111.3 . . ?
C1 C6 H6B 111.3 . . ?
C5 C6 H6B 111.3 . . ?
H6A C6 H6B 109.2 . . ?
C7 C2 C3 117.4(4) . . ?
C7 C2 C1 112.5(3) . . ?
C3 C2 C1 102.8(3) . . ?
C7 C2 H2A 107.9 . . ?
C3 C2 H2A 107.9 . . ?
C1 C2 H2A 107.9 . . ?
C15 C16 C11 119.5(5) . . ?
C15 C16 H16 120.2 . . ?
C11 C16 H16 120.2 . . ?
O2 C10 C11 113.0(3) . . ?
O2 C10 C9 104.8(3) . . ?
C11 C10 C9 112.5(3) . . ?
O2 C10 H10 108.8 . . ?
C11 C10 H10 108.8 . . ?
C9 C10 H10 108.8 . . ?
N1 C9 C18 112.3(3) . . ?
N1 C9 C10 108.8(3) . . ?
C18 C9 C10 112.1(4) . . ?
N1 C9 H9 107.8 . . ?
C18 C9 H9 107.8 . . ?
C10 C9 H9 107.8 . . ?
N1 C17 H17A 109.5 . . ?
N1 C17 H17B 109.5 . . ?
H17A C17 H17B 109.5 . . ?
N1 C17 H17C 109.5 . . ?
H17A C17 H17C 109.5 . . ?

H17B C17 H17C 109.5 . . ?
C9 C18 H18A 109.5 . . ?
C9 C18 H18B 109.5 . . ?
H18A C18 H18B 109.5 . . ?
C9 C18 H18C 109.5 . . ?
H18A C18 H18C 109.5 . . ?
H18B C18 H18C 109.5 . . ?
O1 C4 C3 102.9(3) . . ?
O1 C4 C5 100.5(3) . . ?
C3 C4 C5 111.8(3) . . ?
O1 C4 H4 113.5 . . ?
C3 C4 H4 113.5 . . ?
C5 C4 H4 113.5 . . ?
C11 C12 C13 120.8(5) . . ?
C11 C12 H12 119.6 . . ?
C13 C12 H12 119.6 . . ?
C14 C15 C16 120.9(5) . . ?
C14 C15 H15 119.5 . . ?
C16 C15 H15 119.5 . . ?
O8 C7 O7 122.4(4) . . ?
O8 C7 C2 124.1(5) . . ?
O7 C7 C2 113.4(3) . . ?
C14 C13 C12 120.5(6) . . ?
C14 C13 H13 119.7 . . ?
C12 C13 H13 119.7 . . ?
C13 C14 C15 119.1(5) . . ?
C13 C14 H14 120.4 . . ?
C15 C14 H14 120.4 . . ?
C7 O7 C8 116.0(3) . . ?
C1 C20 H20A 109.5 . . ?
C1 C20 H20B 109.5 . . ?
H20A C20 H20B 109.5 . . ?
C1 C20 H20C 109.5 . . ?
H20A C20 H20C 109.5 . . ?
H20B C20 H20C 109.5 . . ?
O7 C8 H8A 109.5 . . ?
O7 C8 H8C 109.5 . . ?
H8A C8 H8C 109.5 . . ?
O7 C8 H8B 109.5 . . ?
H8A C8 H8B 109.5 . . ?
H8C C8 H8B 109.5 . . ?

loop_
 _geom_torsion_atom_site_label_1
 _geom_torsion_atom_site_label_2
 _geom_torsion_atom_site_label_3
 _geom_torsion_atom_site_label_4
 _geom_torsion
 _geom_torsion_site_symmetry_1
 _geom_torsion_site_symmetry_2
 _geom_torsion_site_symmetry_3
 _geom_torsion_site_symmetry_4
 _geom_torsion_publ_flag

C17 N1 C5 C4 -55.6(4) . . . . ?
C9 N1 C5 C4 175.8(3) . . . . ?
C17 N1 C5 C6 -171.6(3) . . . . ?
C9 N1 C5 C6 59.8(4) . . . . ?
C4 O1 C1 C20 178.8(4) . . . . ?
C4 O1 C1 C6 -57.6(3) . . . . ?
C4 O1 C1 C2 57.0(3) . . . . ?
O1 C1 C6 C5 32.8(3) . . . . ?
C20 C1 C6 C5 154.4(3) . . . . ?
C2 C1 C6 C5 -71.9(4) . . . . ?
N1 C5 C6 C1 125.6(3) . . . . ?
C4 C5 C6 C1 2.1(4) . . . . ?
C4 C3 C2 C7 127.3(4) . . . . ?
C4 C3 C2 C1 3.3(4) . . . . ?
O1 C1 C2 C7 -163.7(3) . . . . ?
C20 C1 C2 C7 75.9(5) . . . . ?
C6 C1 C2 C7 -58.3(5) . . . . ?
O1 C1 C2 C3 -36.5(4) . . . . ?
C20 C1 C2 C3 -156.9(4) . . . . ?
C6 C1 C2 C3 68.9(4) . . . . ?
C12 C11 C16 C15 -0.1(6) . . . . ?
C10 C11 C16 C15 -177.2(4) . . . . ?
C12 C11 C10 O2 -120.5(4) . . . . ?
C16 C11 C10 O2 56.6(5) . . . . ?
C12 C11 C10 C9 121.0(4) . . . . ?
C16 C11 C10 C9 -61.9(5) . . . . ?
C17 N1 C9 C18 -57.6(5) . . . . ?
C5 N1 C9 C18 69.5(4) . . . . ?
C17 N1 C9 C10 67.1(4) . . . . ?
C5 N1 C9 C10 -165.9(3) . . . . ?
O2 C10 C9 N1 41.0(4) . . . . ?
C11 C10 C9 N1 164.2(3) . . . . ?
O2 C10 C9 C18 165.8(4) . . . . ?
C11 C10 C9 C18 -71.0(5) . . . . ?
C1 O1 C4 C3 -56.4(3) . . . . ?
C1 O1 C4 C5 59.1(3) . . . . ?
C2 C3 C4 O1 32.3(4) . . . . ?
C2 C3 C4 C5 -74.8(4) . . . . ?
N1 C5 C4 O1 -160.2(3) . . . . ?
C6 C5 C4 O1 -37.3(3) . . . . ?
N1 C5 C4 C3 -51.6(5) . . . . ?
C6 C5 C4 C3 71.3(4) . . . . ?
C16 C11 C12 C13 -0.7(7) . . . . ?
C10 C11 C12 C13 176.4(4) . . . . ?
C11 C16 C15 C14 0.7(7) . . . . ?
C3 C2 C7 O8 152.6(5) . . . . ?
C1 C2 C7 O8 -88.5(5) . . . . ?
C3 C2 C7 O7 -31.5(5) . . . . ?
C1 C2 C7 O7 87.5(5) . . . . ?
C11 C12 C13 C14 0.9(8) . . . . ?
C12 C13 C14 C15 -0.3(8) . . . . ?
C16 C15 C14 C13 -0.5(8) . . . . ?
O8 C7 O7 C8 3.7(7) . . . . ?

C2 C7 O7 C8 -172.4(4) . . . . ?

_diffrn_measured_fraction_theta_max 1.000
_diffrn_reflns_theta_full 64.92
_diffrn_measured_fraction_theta_full 1.000
_refine_diff_density_max 0.341
_refine_diff_density_min -0.257
_refine_diff_density_rms 0.050

Appendix 3.16: GC-MS data for the crude D-A reaction between **5q** and MAC in DCM.

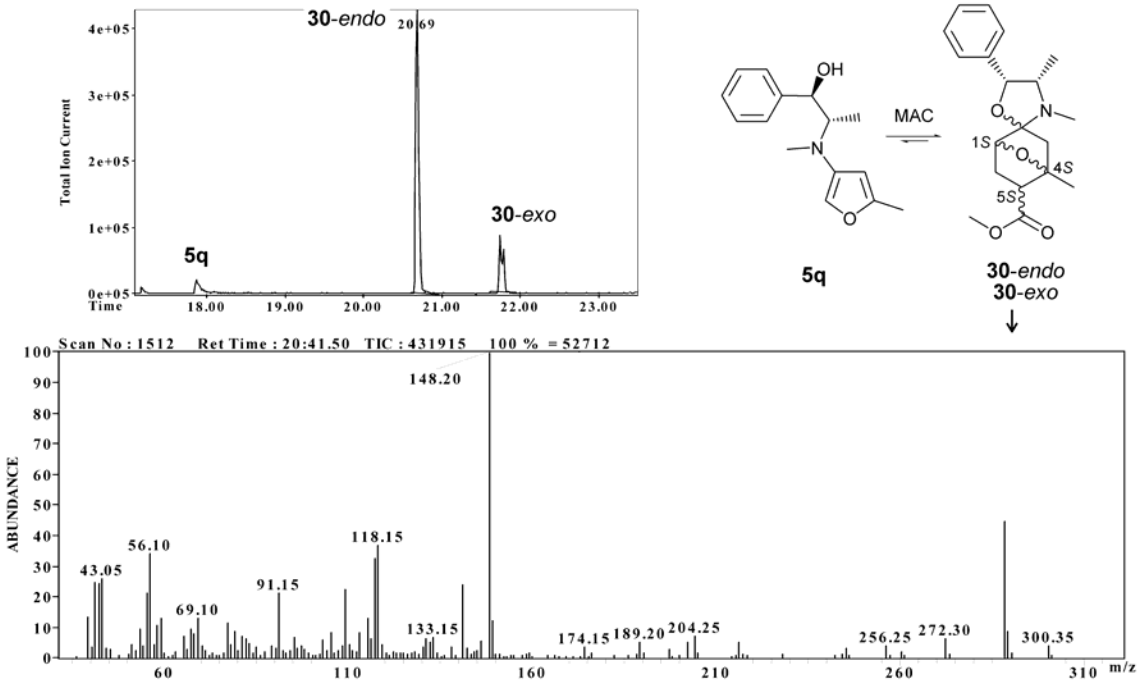

Appendix 3.17: GC-MS data for the crude D-A reaction between **5p** and MAC in H_2O with ultrasonic irradiation.

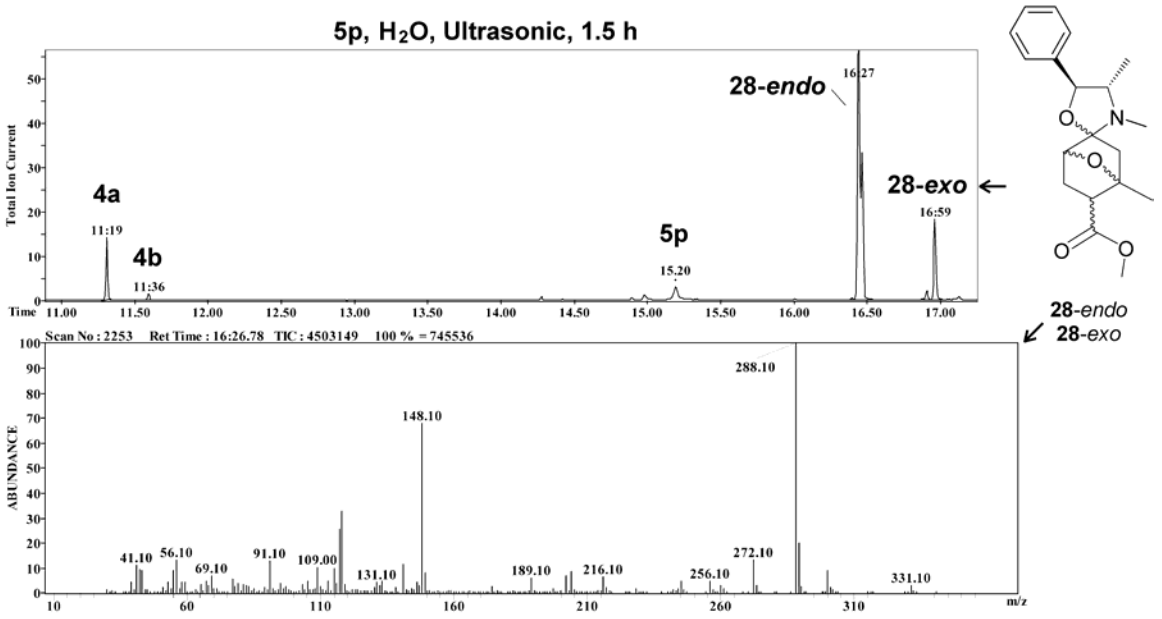

Appendix 3.18: GC-MS data for the crude D-A reaction between **5q** and MAC in H_2O and 3.0 M LiCl with ultrasonic irradiation.

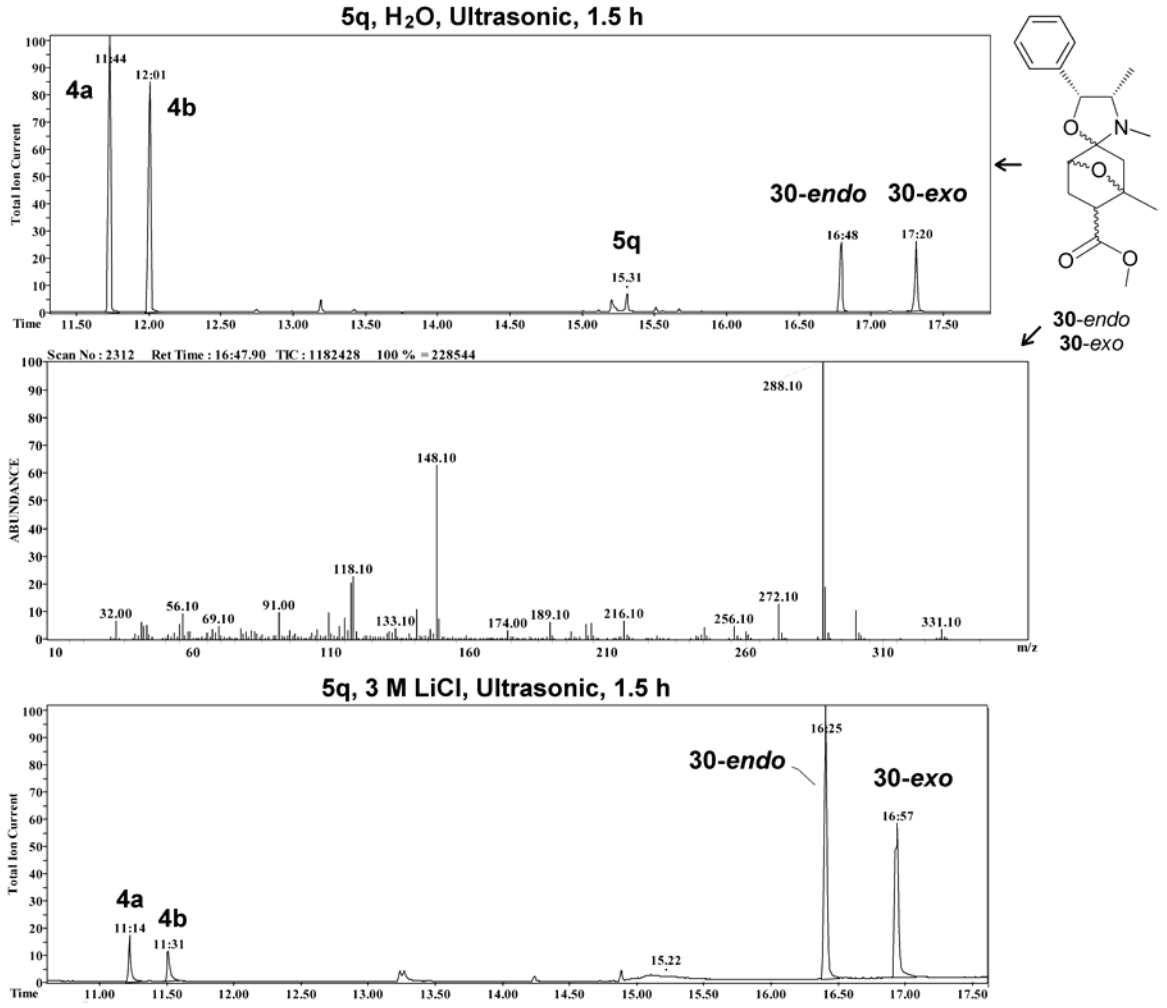

Chapter 4

Studies Toward the Synthesis of Ring A: Appendices

Appendix 4.1: 300 MHz ^{1}H/75 MHz ^{13}C HMQC NMR and DEPT 135 NMR analysis of **31**.

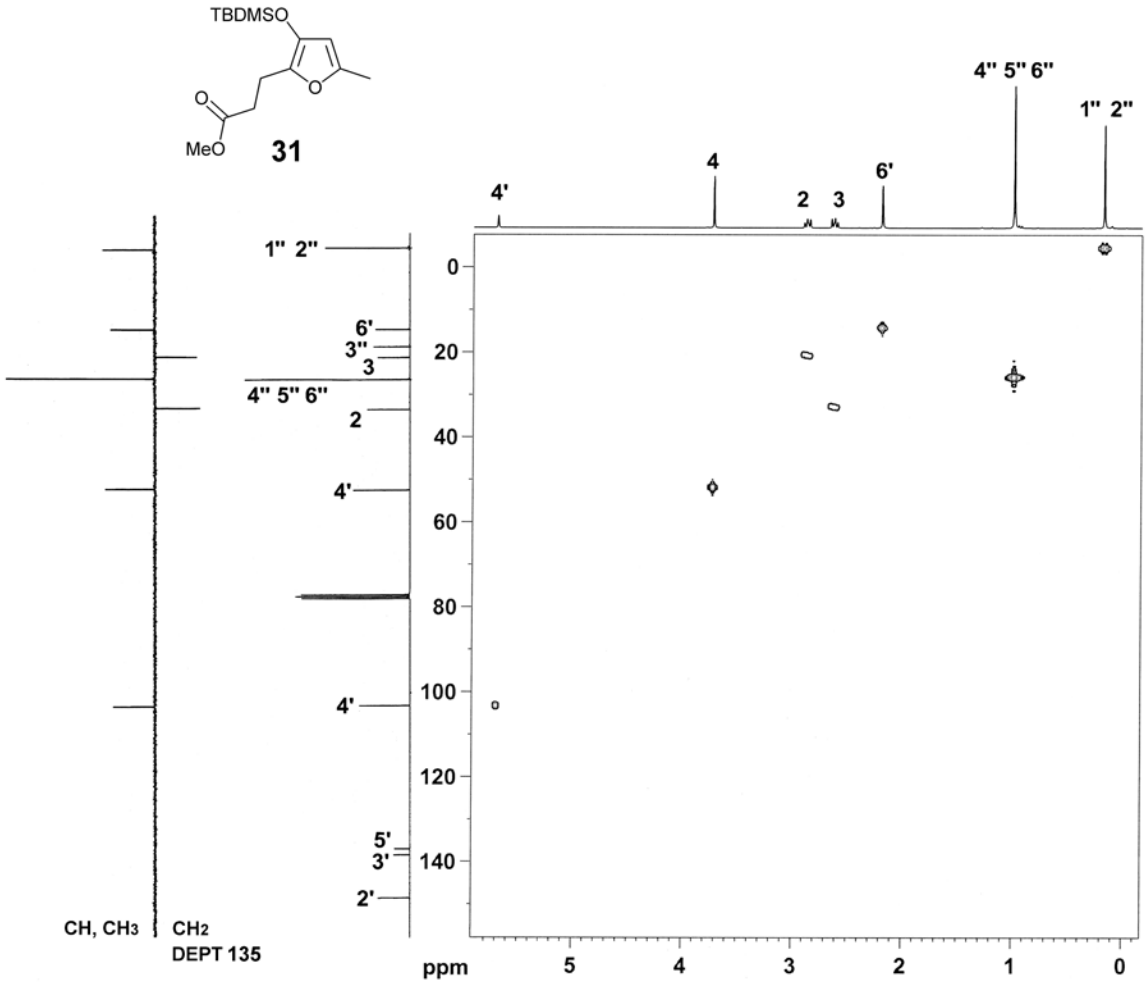

Appendix 4.2: 300 MHz ^{1}H COSY NMR of **32** and the GC-MS analysis for the crude reaction of **4a** with LHMDS in THF (-78°C to -45°C over 2 h) to give **32** in 56%. The EI-MS spectrum of **32** (t_R = 12:21 min) is shown below.

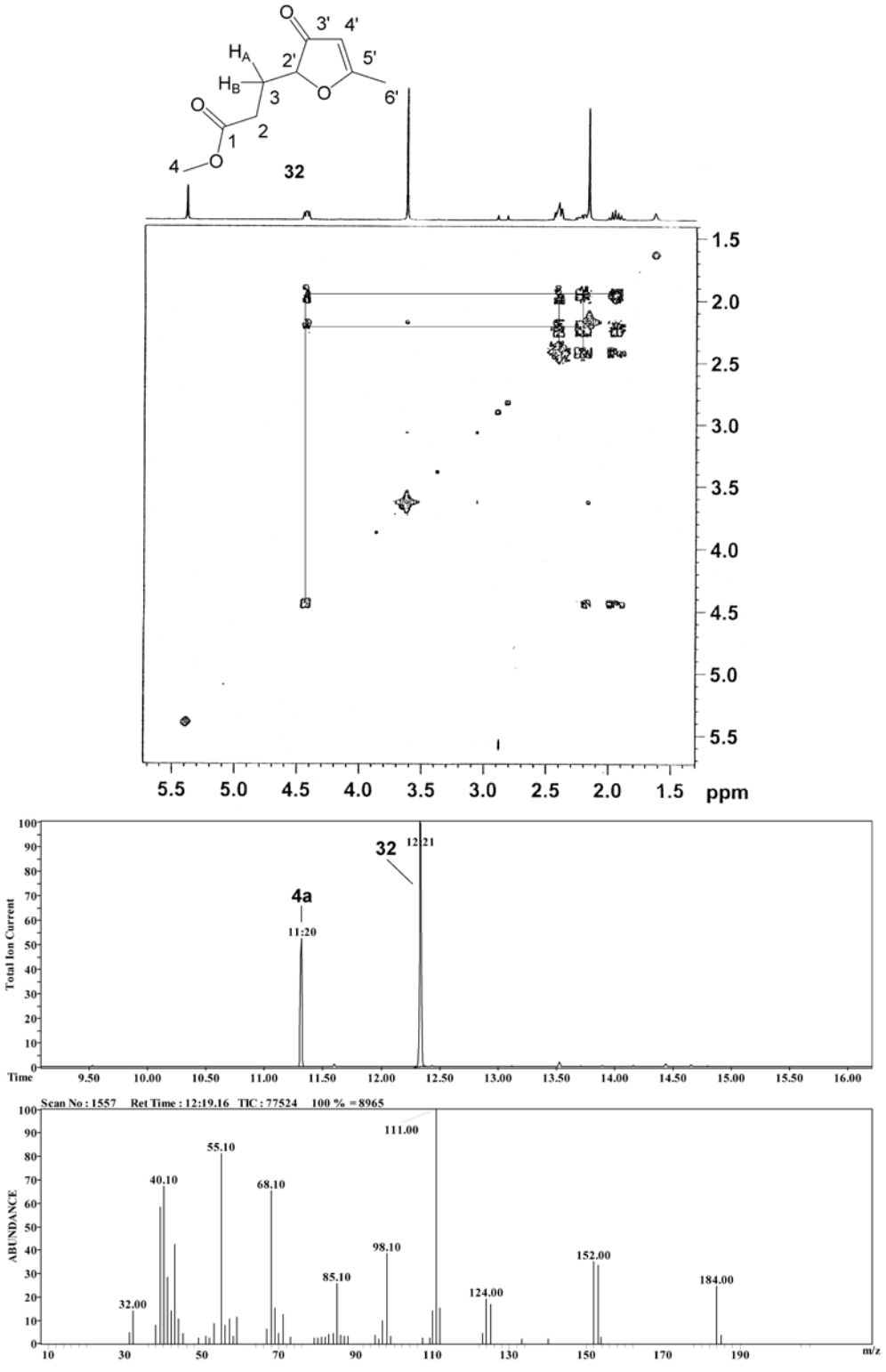

Appendix 4.3: GC-MS analysis of the crude desilylation mixture of **31** using TBAF which shows the formation of **32** as a minor component.

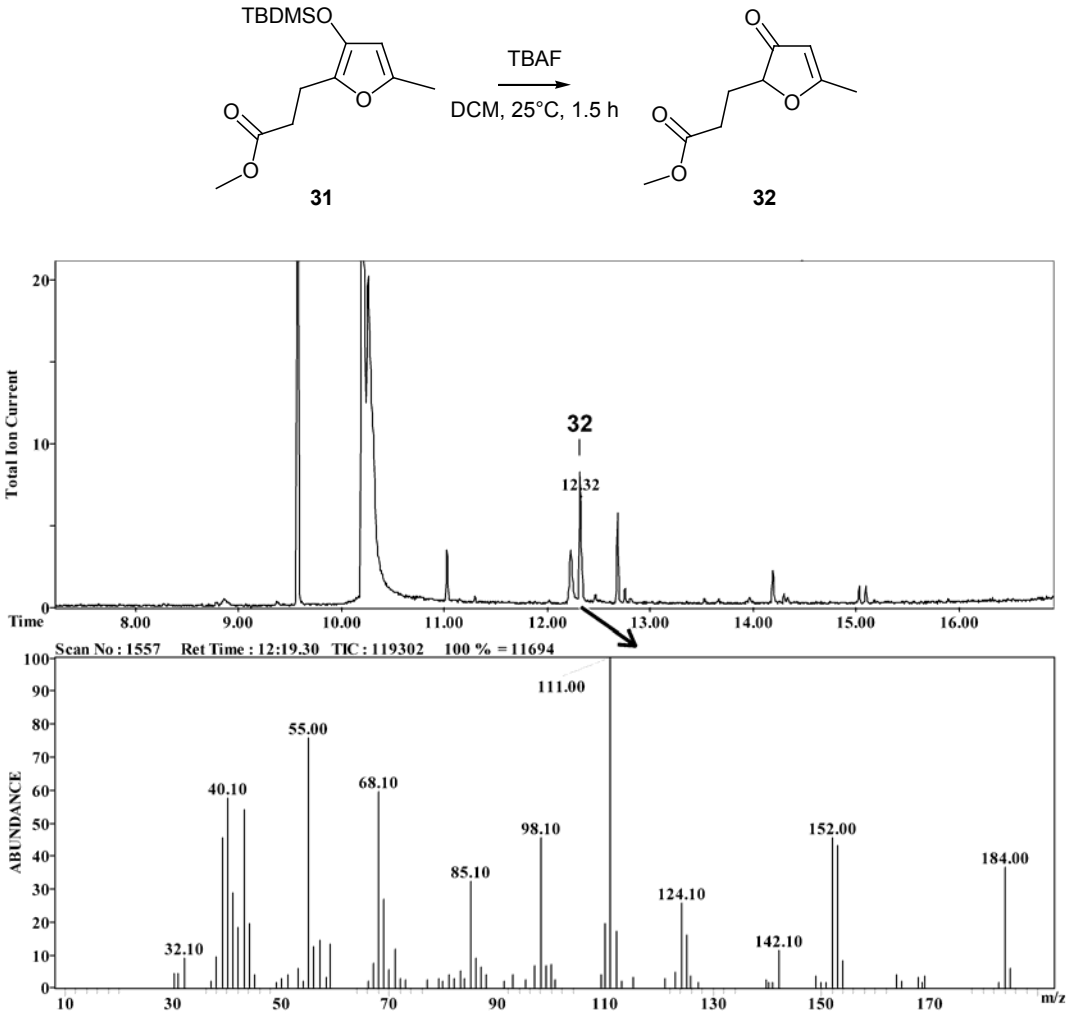

Appendix 4.4: 300 MHz ^{1}H/75 MHz ^{13}C HMQC and DEPT 135 NMR data of **33** with ^{13}C assignments.

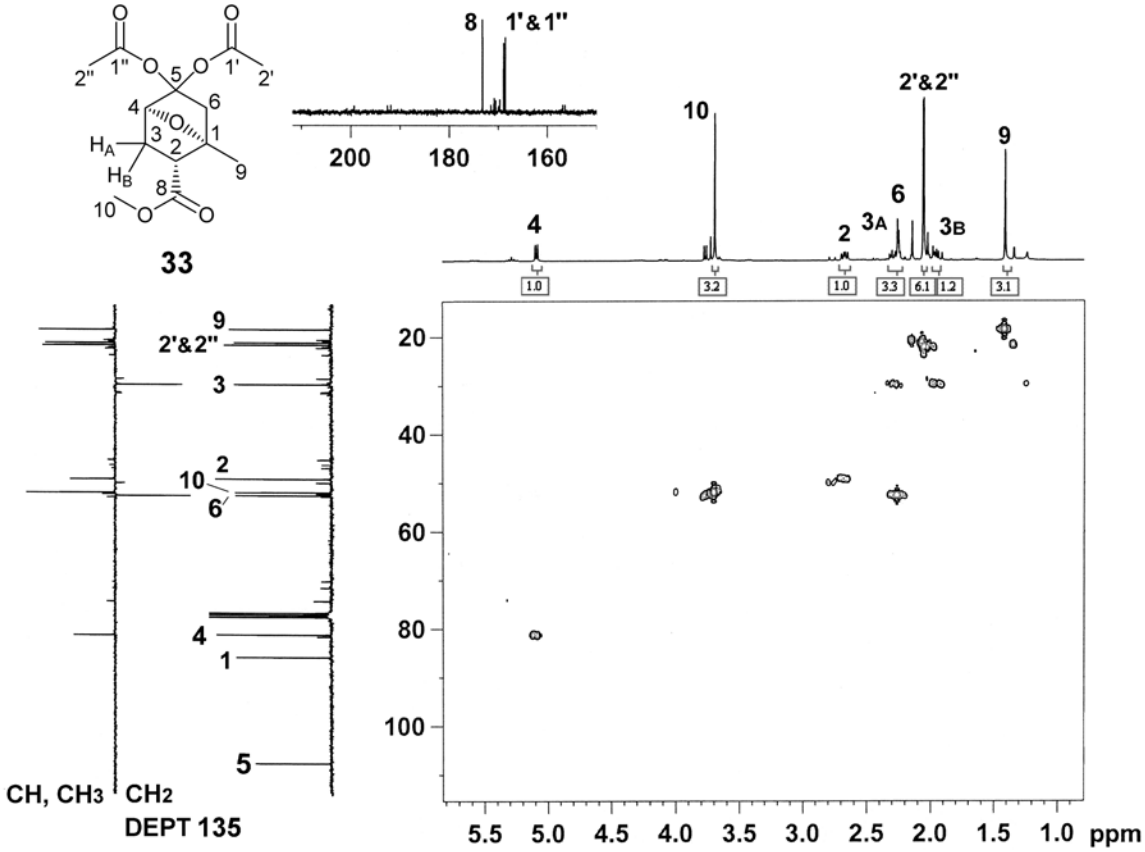

Appendix 4.5: 300 MHz ^{1}H/75 MHz ^{13}C HMBC and DEPT 135 NMR of **3** with structural assignments.

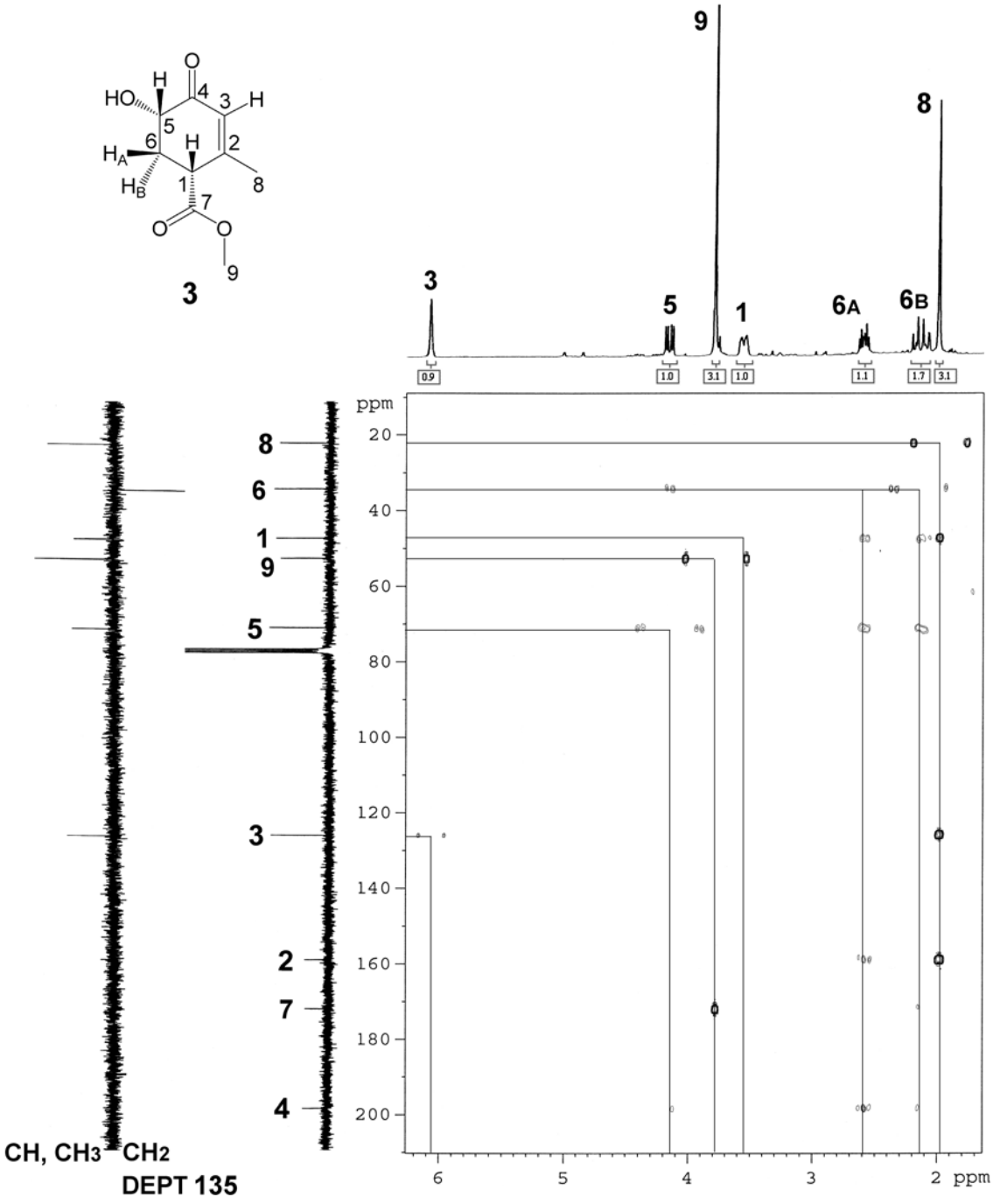

Appendix 4.6: 300 MHz ^{1}H COSY NMR of a 2:1 mixture of **3** and C(5)-*epi*-**3**. ^{13}C NMR data is also shown.

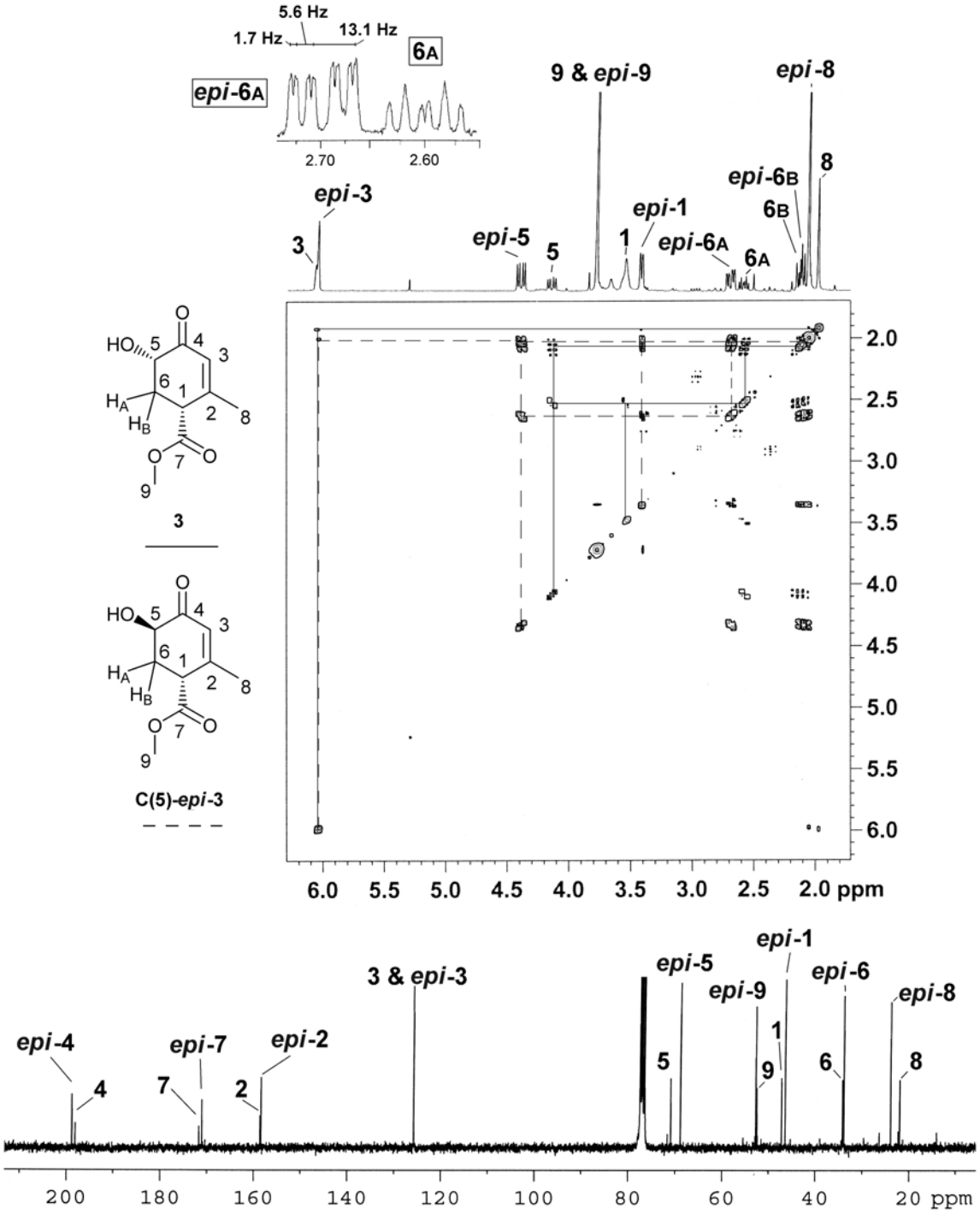

Appendix 4.7: GC-MS for a fraction collected from the FCC purification of **2** on SiO_2 (8:1, pentane:EtOAc) shows a mixture of **2** and C(5)-*epi*-**2** due to C(5) epimerization on the stationary phase. The C(5)-*epi*-**2** isomer at t_R = 13:29 min was verified by EI-MS showing almost identical fragmentation to **2,** however no molecular ion was observed for C(5)-*epi*-**2**.

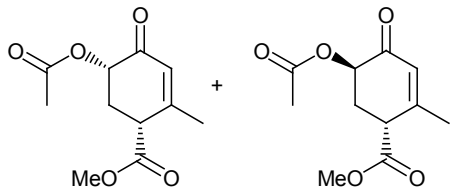

2 C(5)-*epi*-**2**

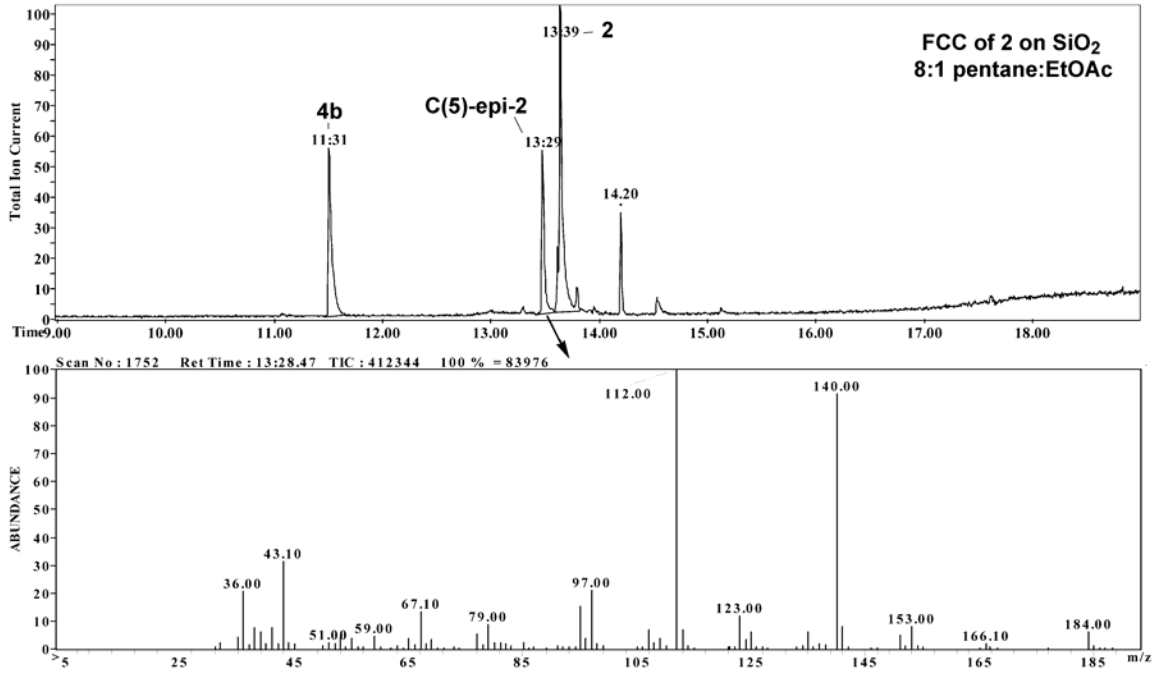

Appendix 4.8: 300 MHz ^{1}H COSY NMR of **2** with structural assignments.

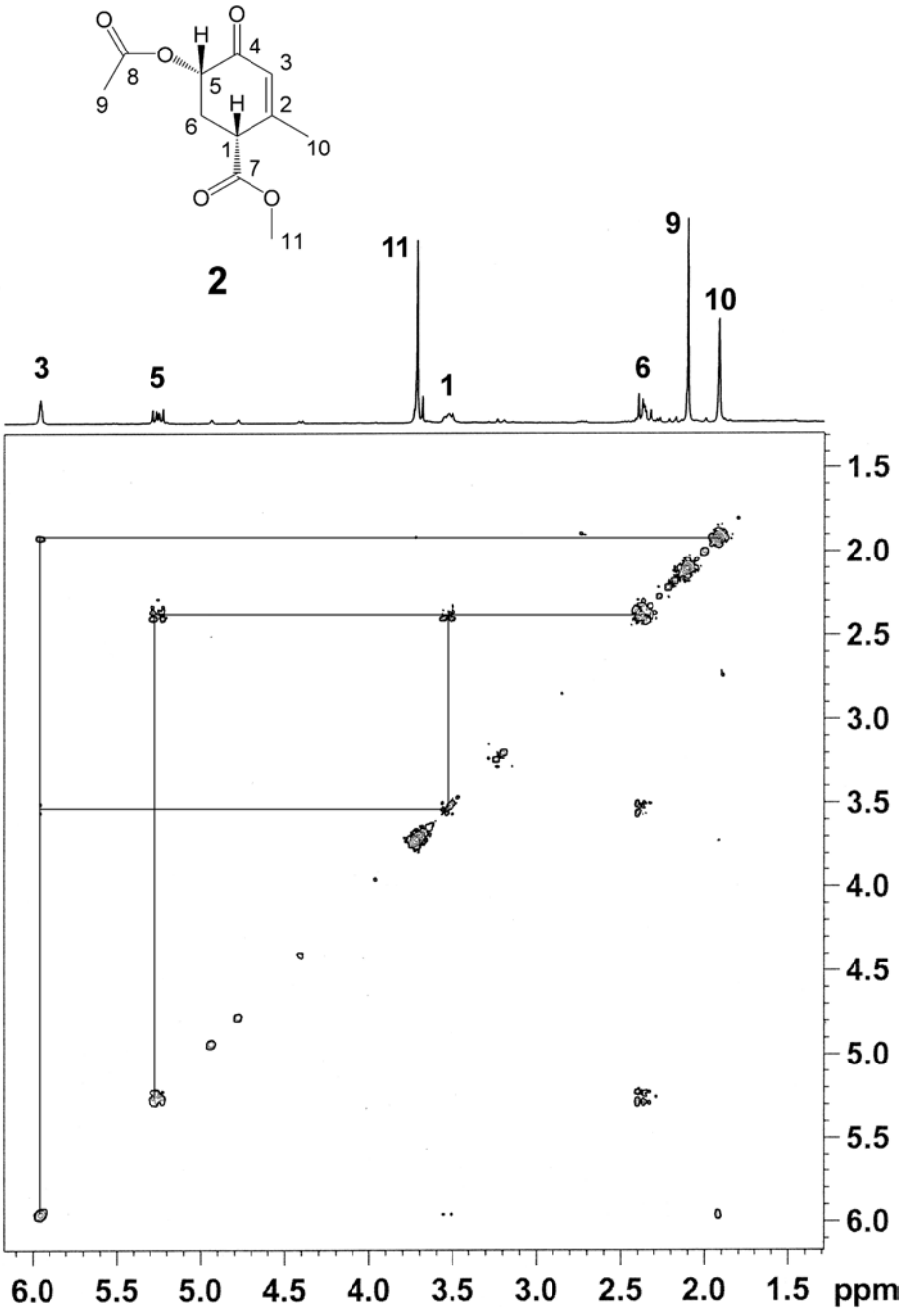

Appendix 4.9: 300 MHz ^{1}H/75 MHz ^{13}C HMBC and DEPT 135 NMR of **2** with structural assignments.

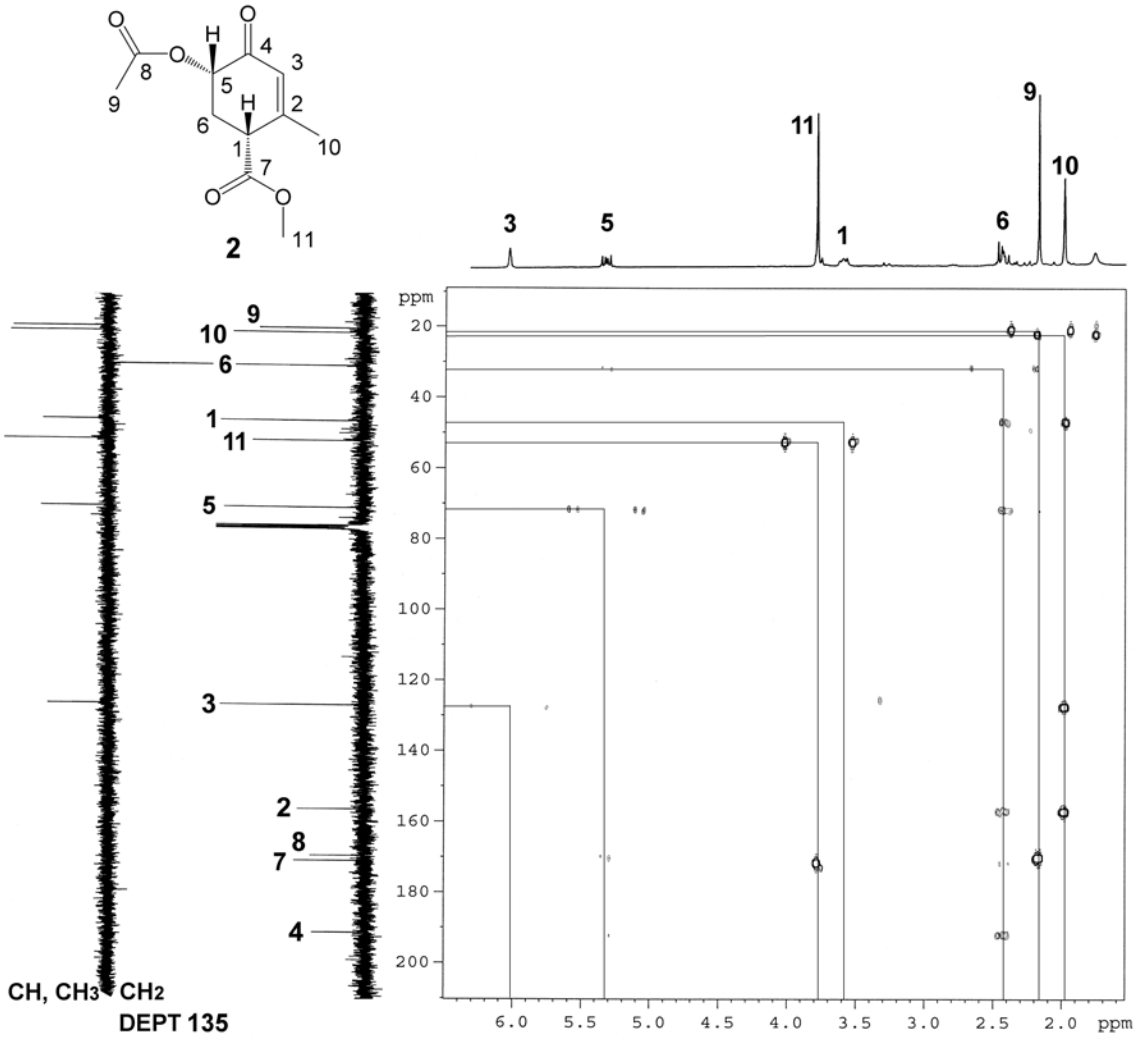

Appendix 4.10: 300 MHz ^{1}H COSY NMR analysis of 1.0:0.7 ratio of *cis*:*trans* **34** with assignments for the *trans*-**34** isomer shown.

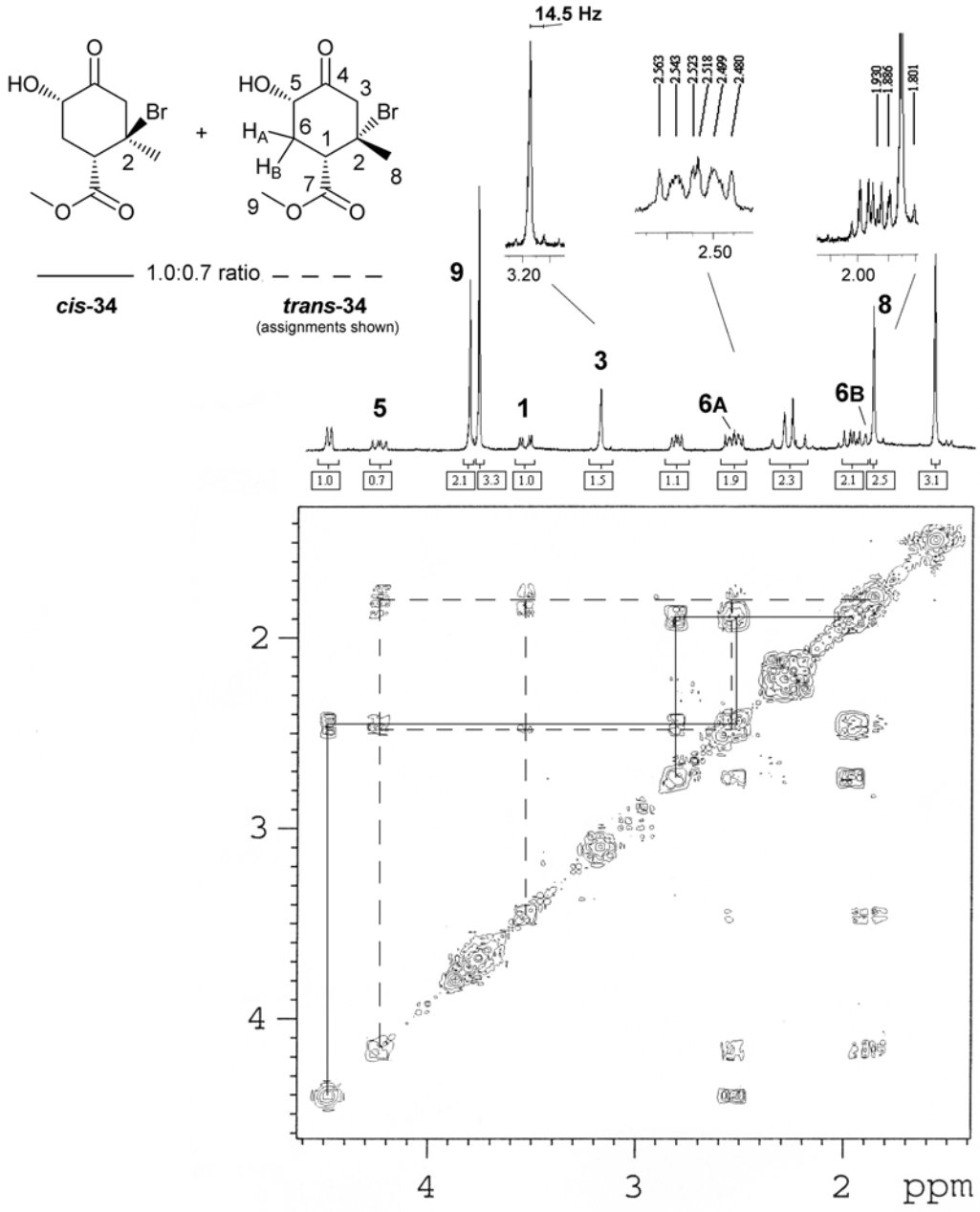

Appendix 4.11: ^{13}C NMR of a 1.0:0.3 mixture of *cis*:*trans* **34** with assignments for the major *cis*-**34** isomer. DEPT 135 NMR data is also included but shows only distinguishable signals for the major *cis*-**34** isomer.

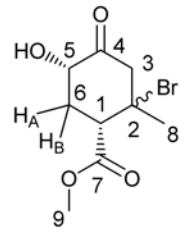

34

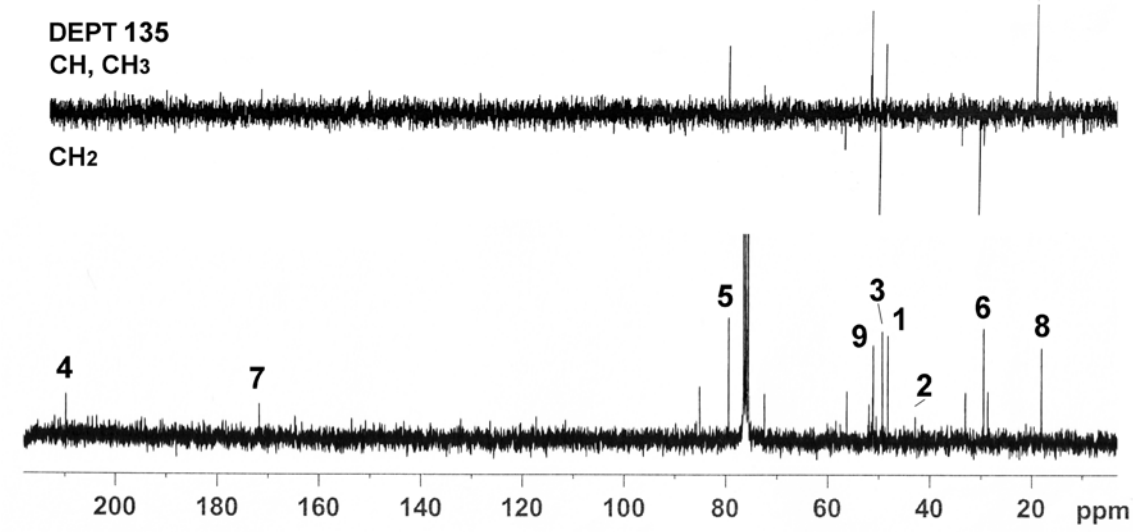

Chapter 5

Studies Towards the δ-Lactone Ring C of (1): Appendices

Appendix 5.1: GC-MS of the crude esterification mixture using **36** and crotonyl chloride with TEA. EI-MS of the product **35** (t_R = 16:52 min) is shown. The GC trace of an attempted LDA lactone closure of **35** is shown at the bottom.

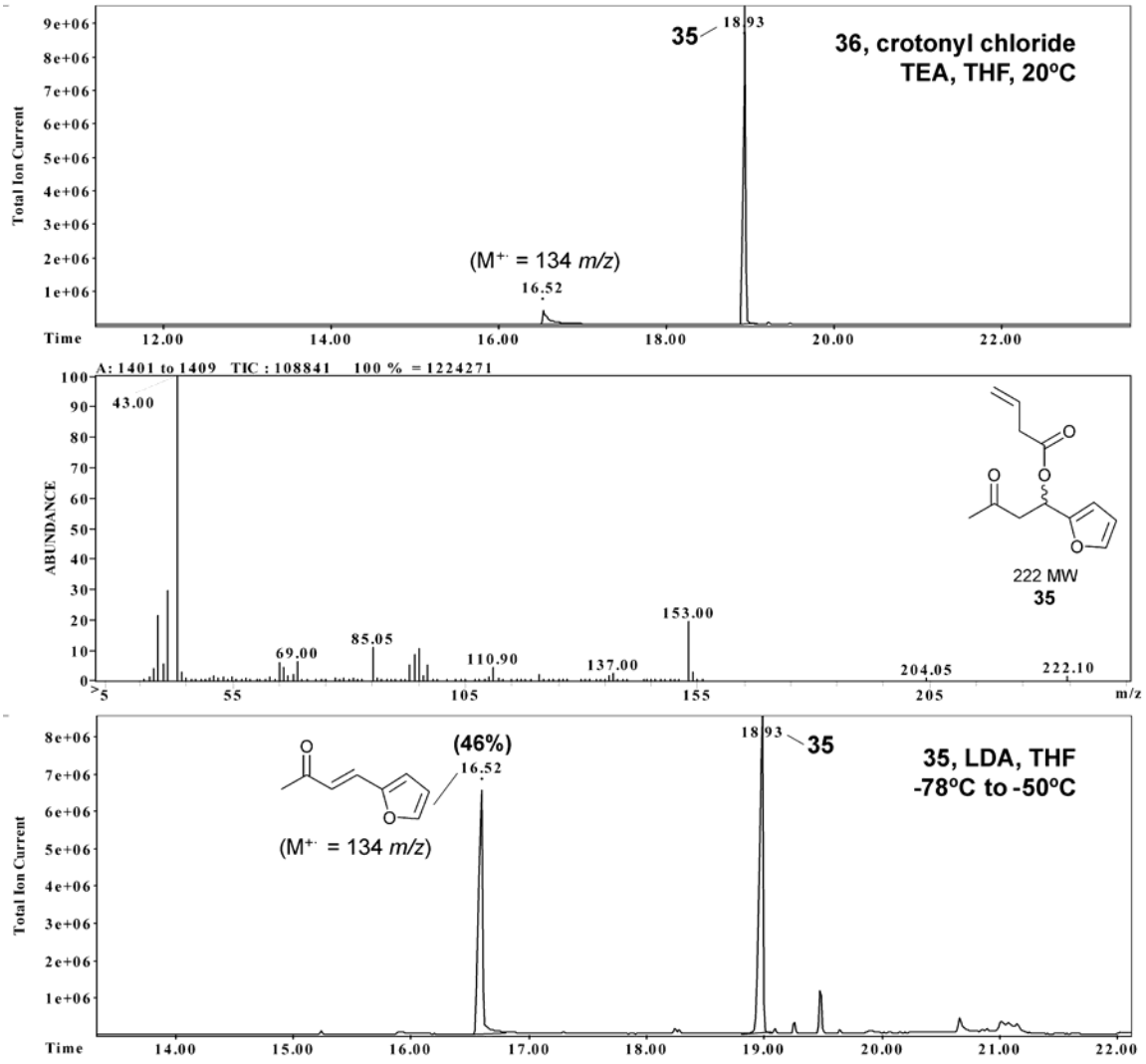

Appendix 5.2: 200 MHz ^{1}H NMR analysis of **36** with structural assignments.

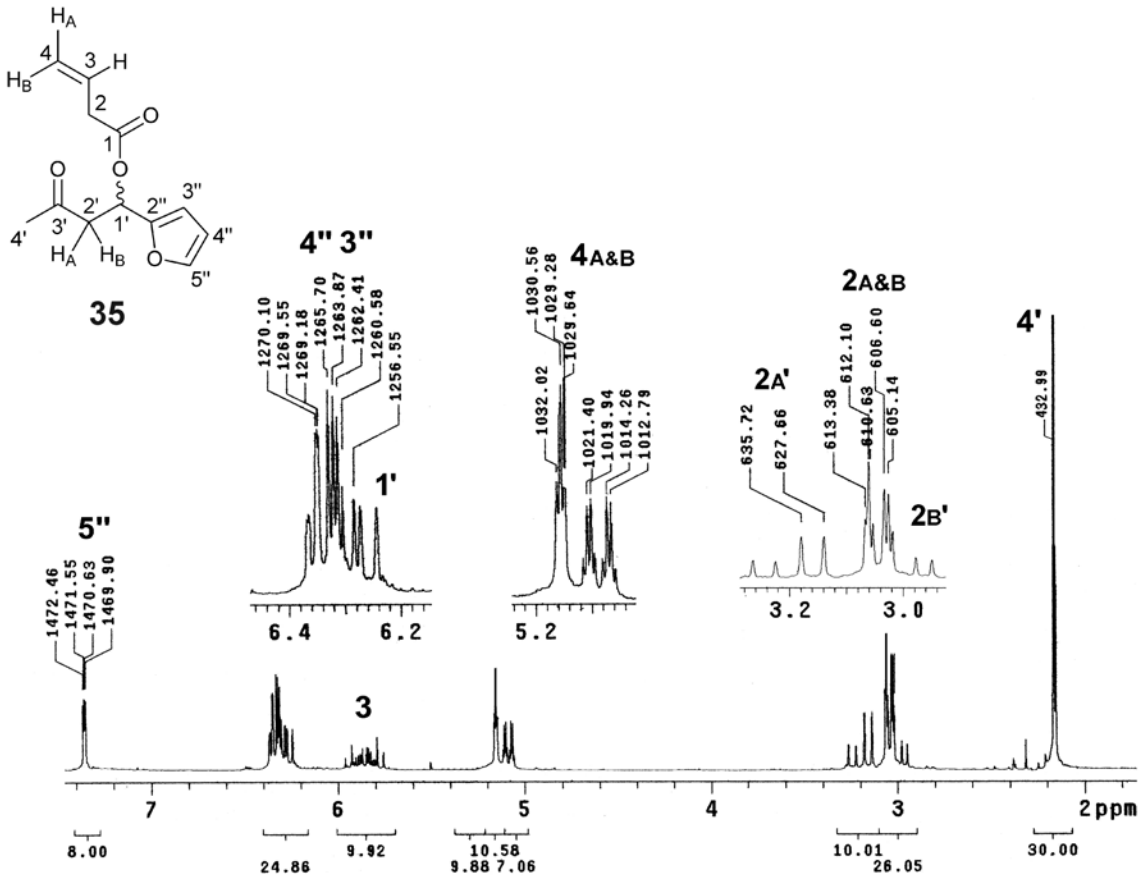

Appendix 5.3: GC-MS analysis of the crude aldol product **8** (t_R = 10:63 min).

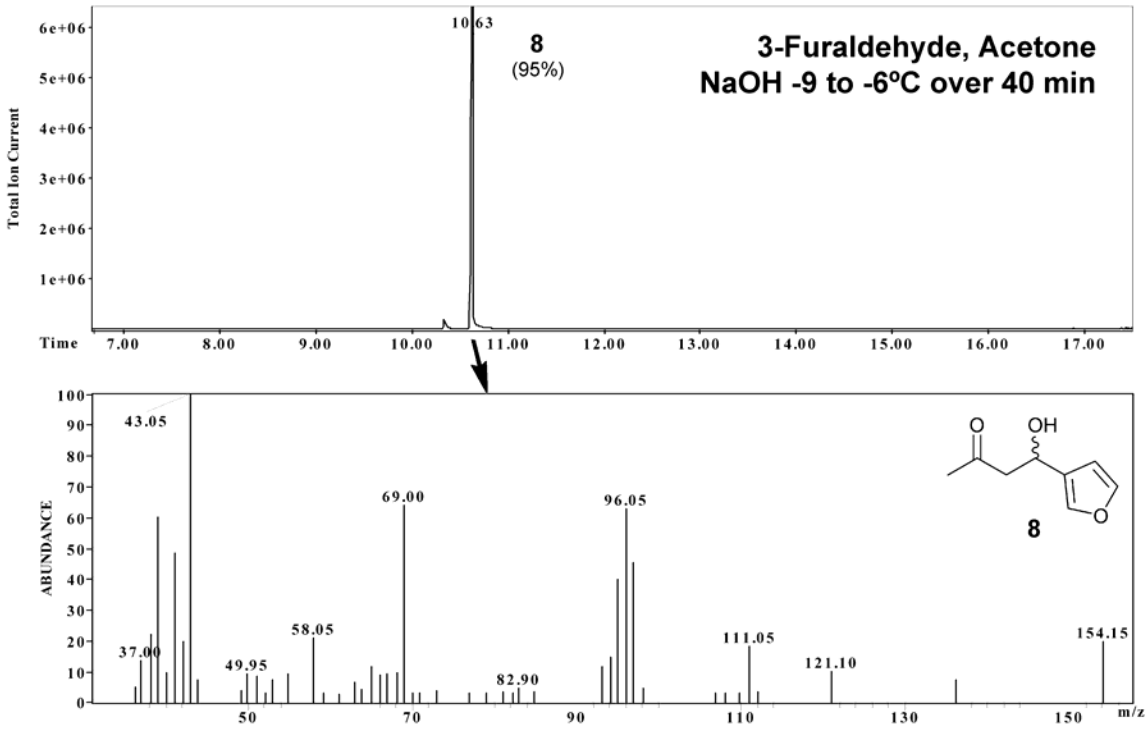

Appendix 5.4: 75 MHz ^{13}C and DEPT 135 NMR data of **8** with ^{13}C assignments.

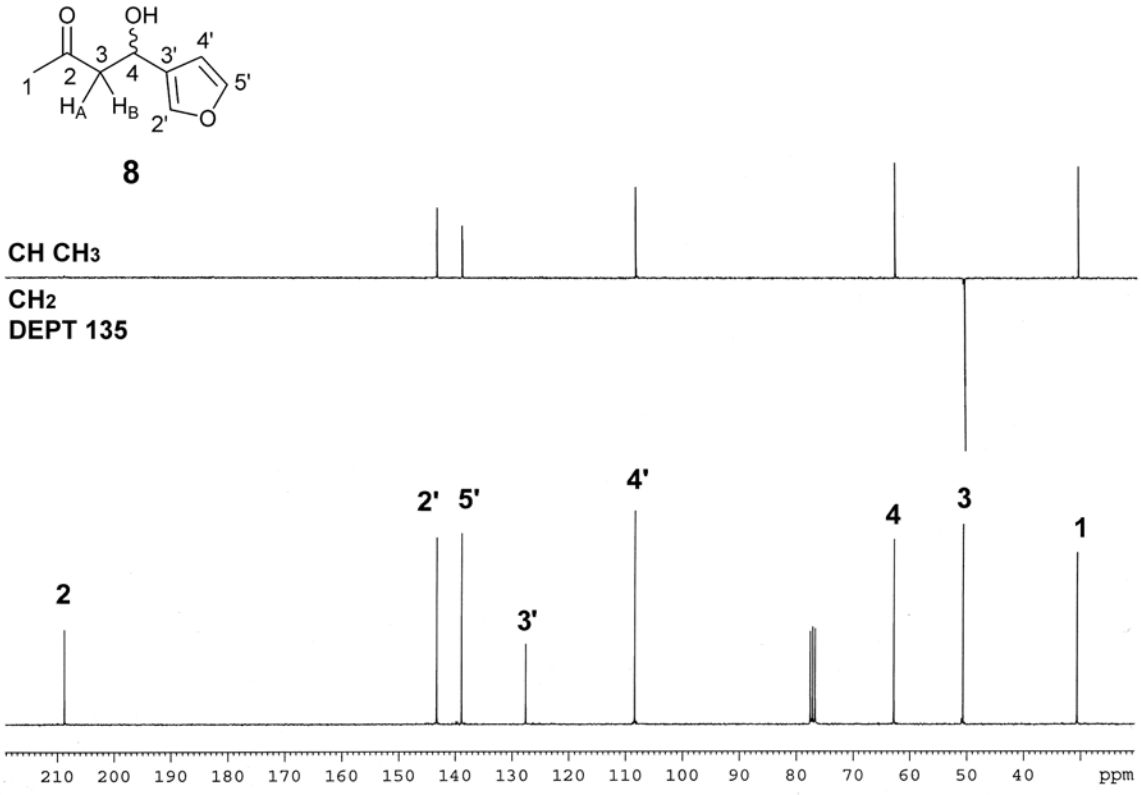

Appendix 5.5: 300 MHz ^{1}H/75 MHz ^{13}C HMBC NMR of **7** with ^{1}H structural assignments.

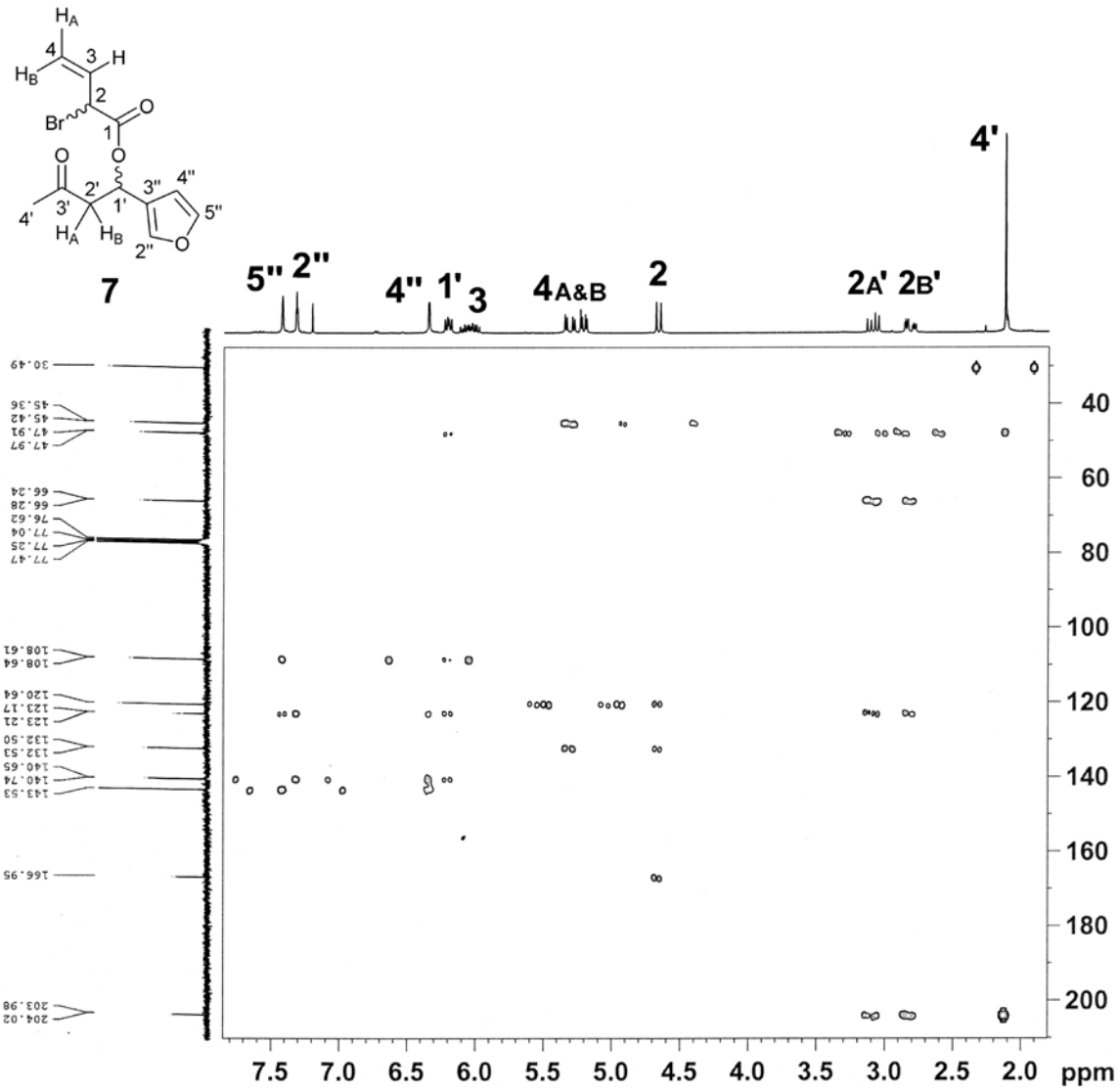

Appendix 5.6: 300 MHz ^{1}H COSY NMR of **7** with structural assignments.

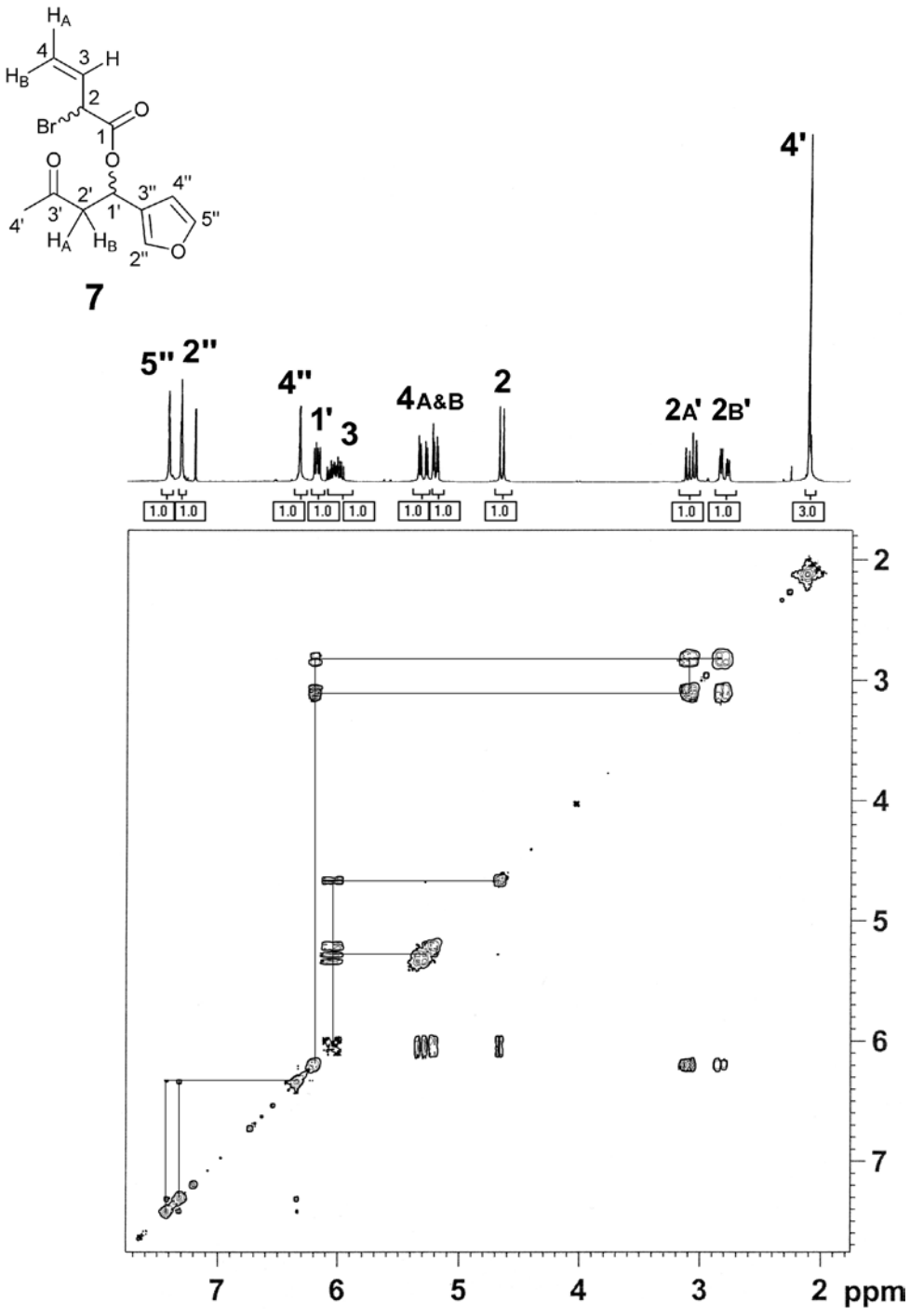

Appendix 5.7: FCC of the crude mixture of **7** led to isomerization to the α,β-unsaturated **37**. EI-MS spectra of **37** is also shown.

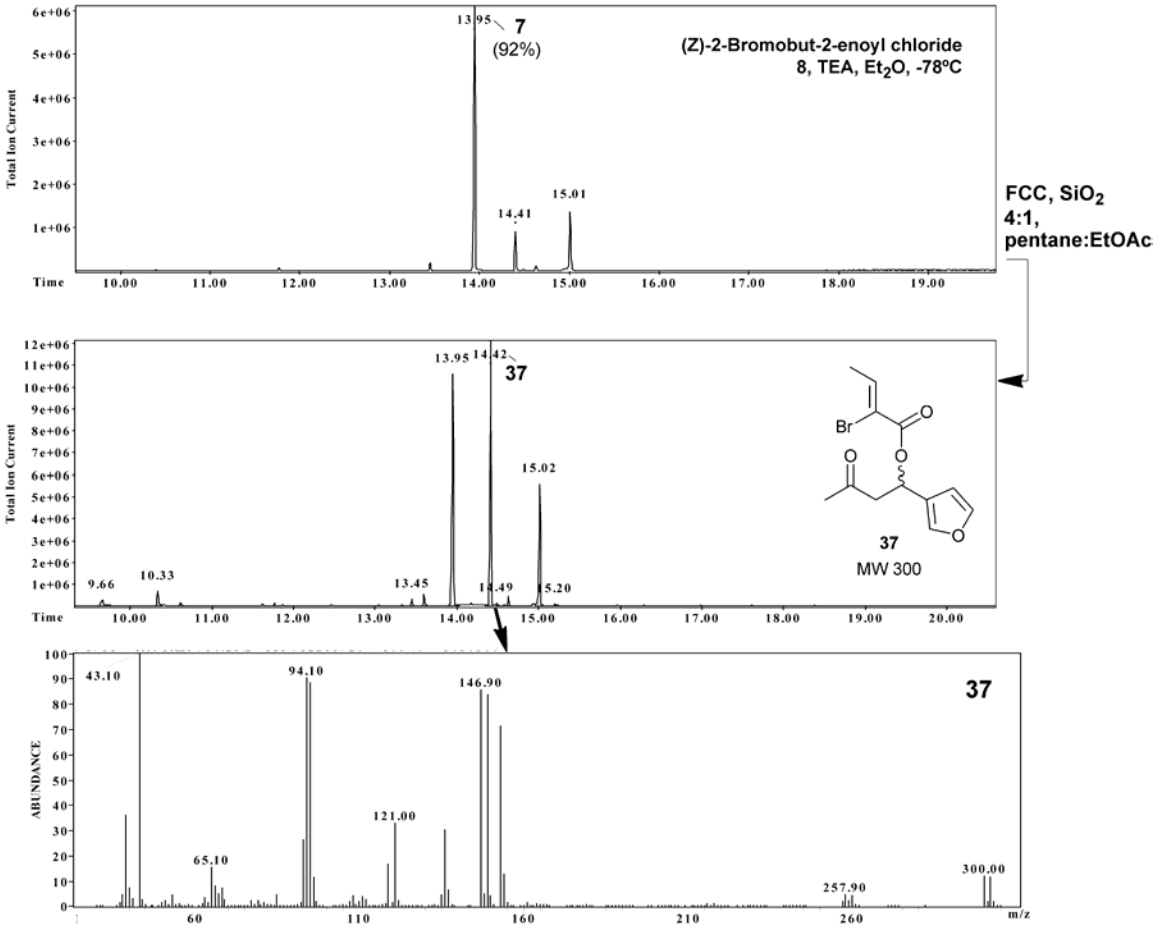

Appendix 5.8: 300 MHz ^{1}H/75 MHz ^{13}C HMQC and DEPT 135 NMR of **37** with structural assignments.

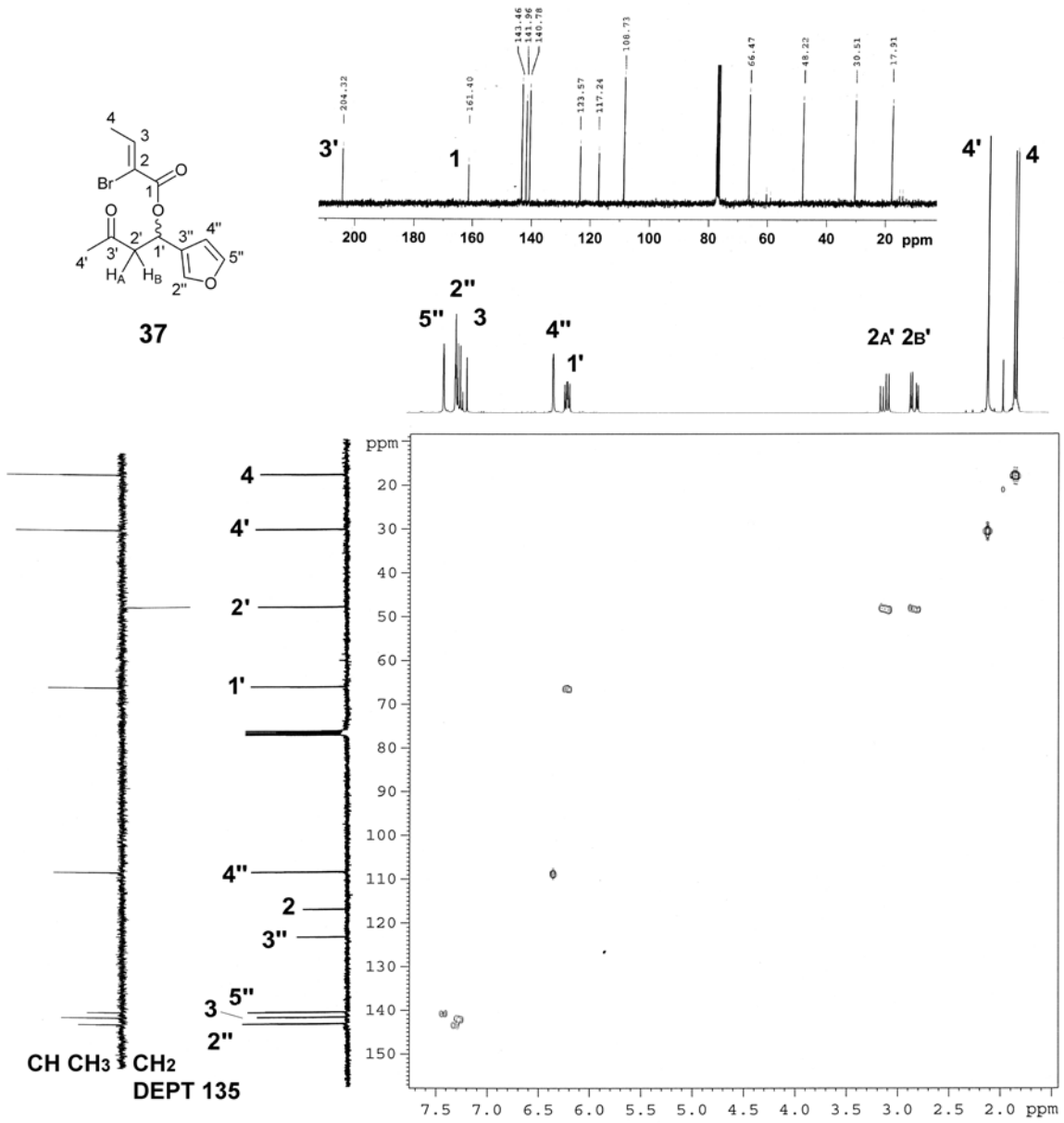

Appendix 5.9: 300 MHz ^{1}H COSY NMR of **6** with structural assignments.

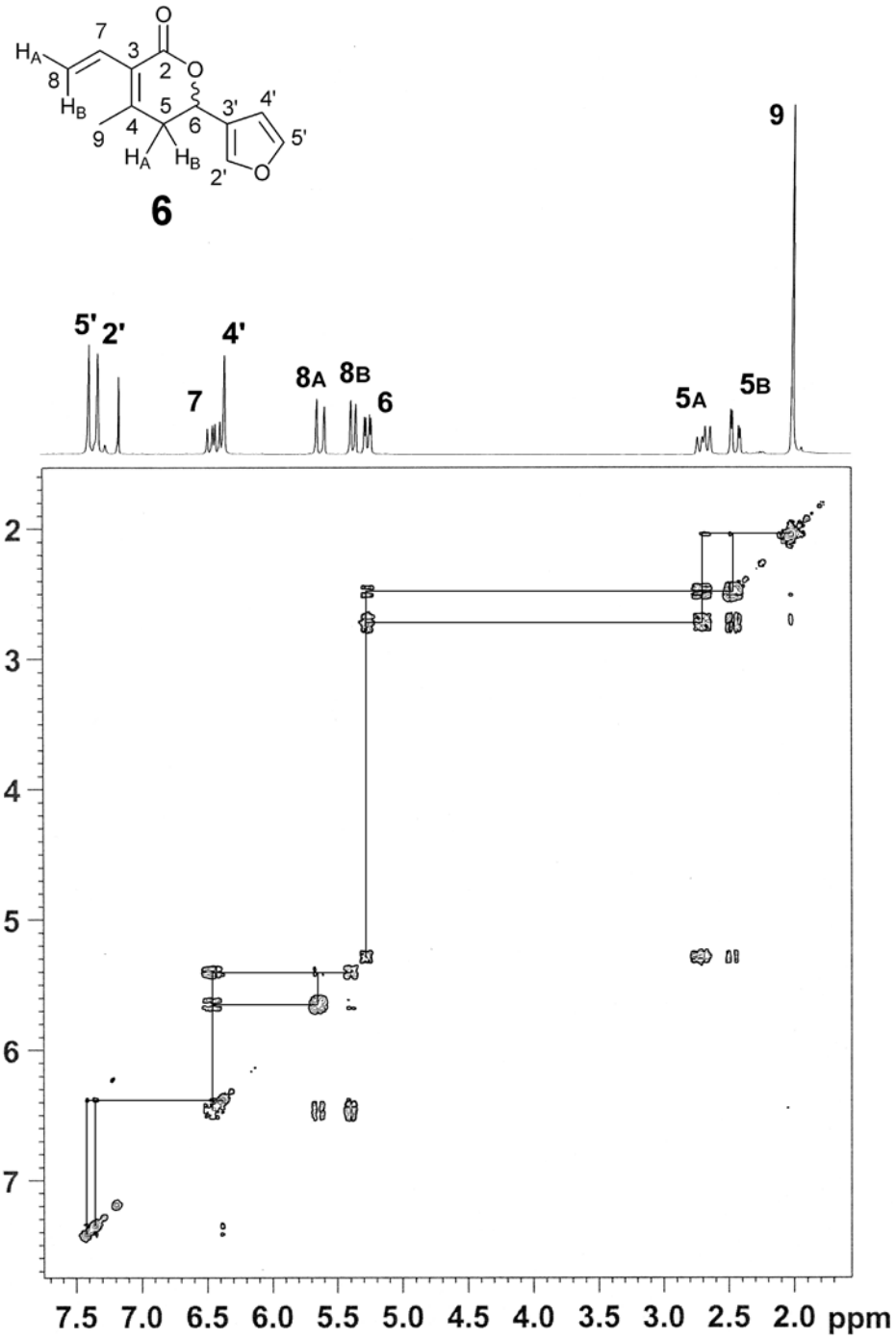

Appendix 5.10: 300 MHz ^{1}H/75 MHz ^{13}C HMQC NMR of **37** with structural assignments.

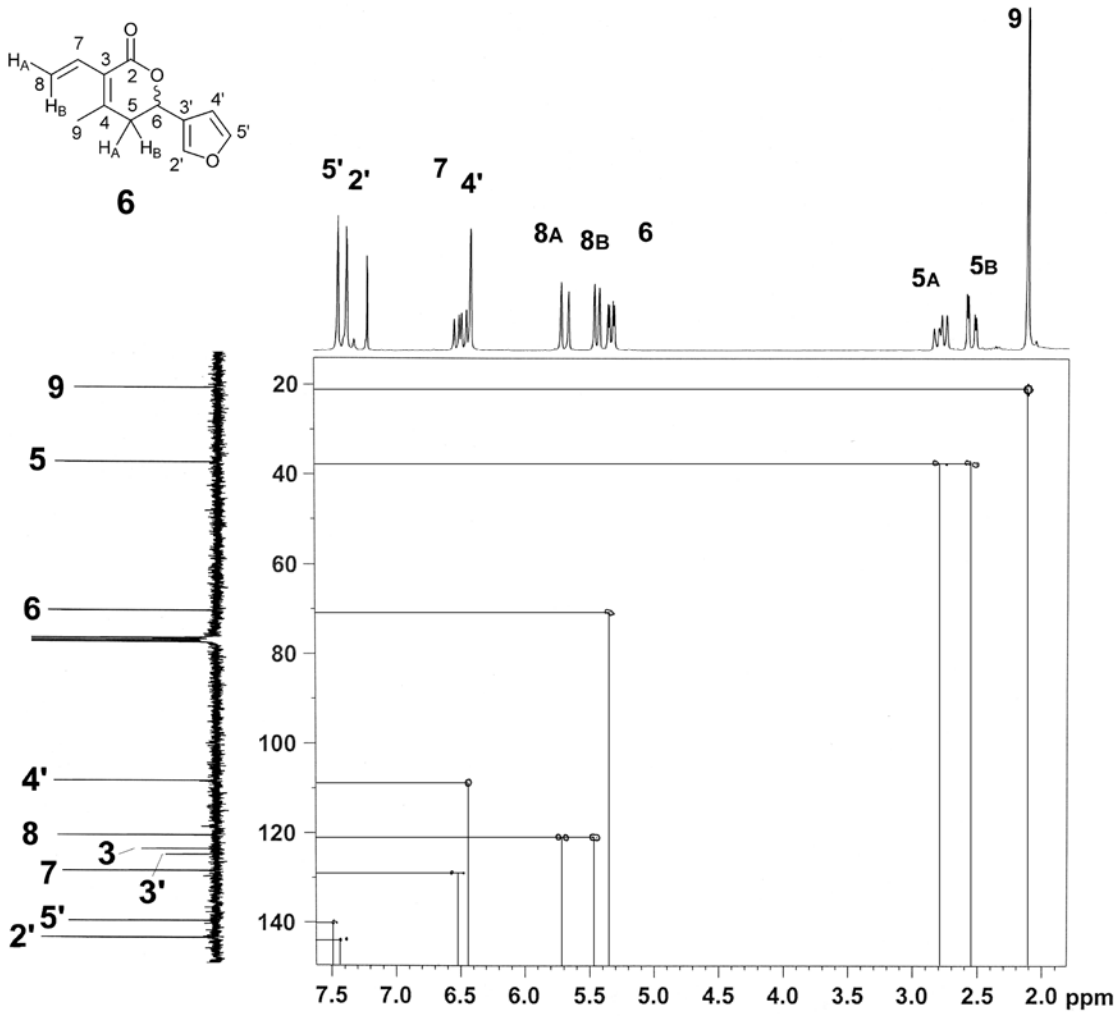

Appendix 5.11: 300 MHz ^{1}H/75 MHz ^{13}C HMQC and DEPT 135 NMR of **38** with structural assignments.

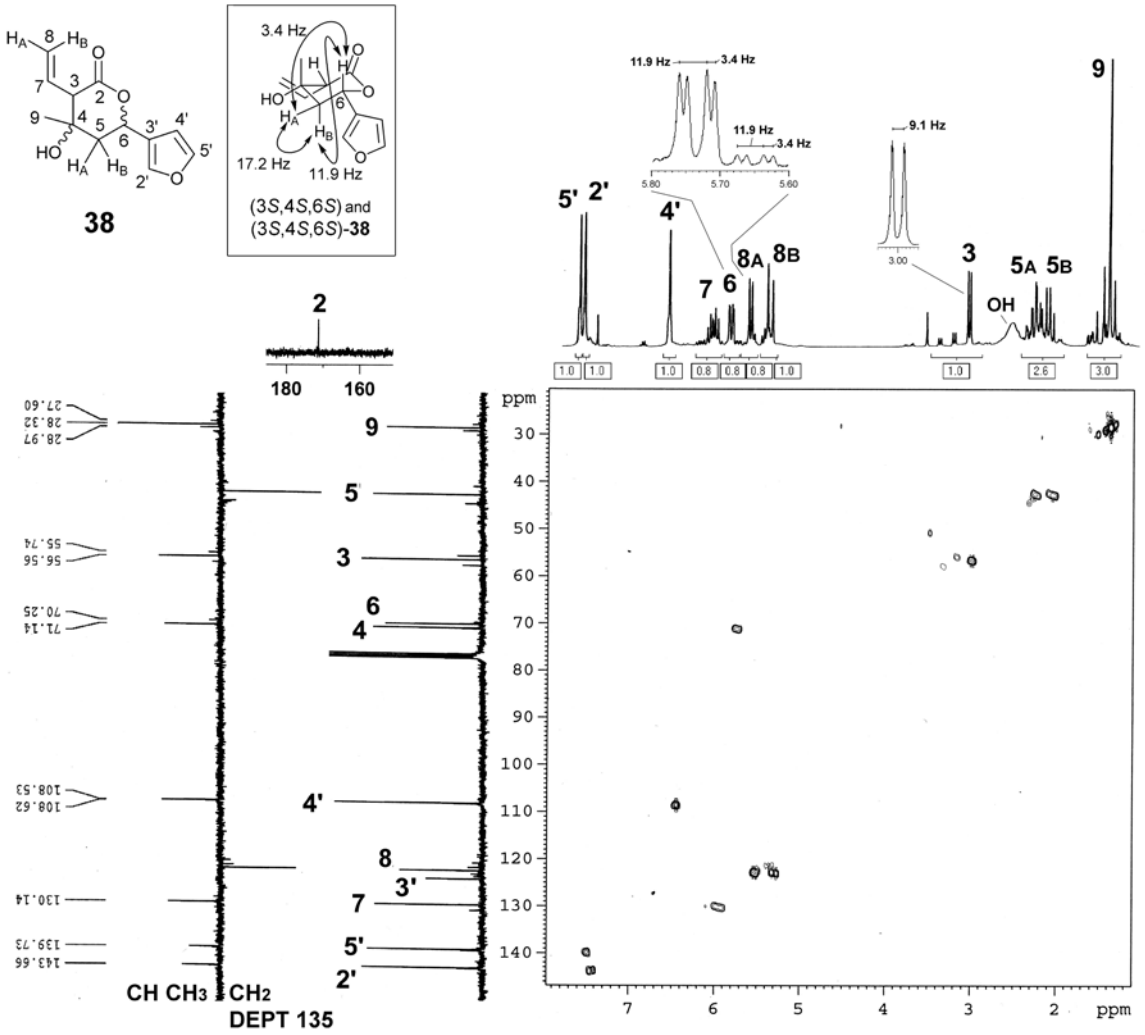

Chapter 6

Experimental Procedures and Methodology

Appendix 6.1: *Characterisation data for 3-furylamines and intermediates 19, 4 and 21.*

4-Morpholino-5-(tetrahydropyran-2-yloxy)pent-3-en-2-one **(19*a*)**

^{1}H NMR (200MHz, $CDCl_3$): δ 5.29 (d, 1H, J = 11.9Hz), 5.20 (s, 1H), 4.71 (d, 1H, J = 11.9Hz), 4.68 (m, 1H), 3.85 (m, 1H), 3.73 (t, 4H, J = 5.0Hz), 3.55 (m, 1H), 3.35 (m, 4H), 2.1 (s, 3H), 1.9 – 1.4, (m, 6H). ^{13}C NMR (200MHz, $CDCl_3$): δ 195.9, 158.8, 100.0, 98.2, 66.6, 63.5, 60.8, 47.0, 32.3, 31.0, 25.5, 20.2. MS *m/z* (relative intensity) 269 (M^+ 3.1), 210 (3.8), 186 (10.8), 185 (100), 184 (38.5), 170 (15.4), 169 (16.2), 168 (27.7), 167 (12.3), 166 (3.8), 157 (4.6), 156 (51.5), 154 (7.7), 152 (15.4), 150 (6.2), 143 (7.7), 142 (89.2), 140 (3.8), 138 (6.9), 137 (4.6), 136 (3.1), 127 (11.5), 126 (60.0), 124 (9.2), 114 (9.2), 112 (9.2), 110 (9.2), 109 (11.5), 108 (3.8), 98 (4.6), 97 (7.7), 96 (6.9), 92 (4.6), 86 (16.2), 85 (37.7), 84 (13.1), 83 (8.5), 82 (6.2), 81 (3.8), 80 (3.8), 70 (4.6), 69 (4.6), 68 (6.2), 67 (14.6), 57 (11.5), 56 (7.7), 55 (14.6), 54 (5.4), 43 (25.4), 42 (5.4), 41 (15.4).

4-(5-Methylfuran-3-yl)morpholine **(5*a*)**

IR (neat) 3140(w), 2960 (s), 2918 (s), 2855(s), 2820 (s), 2760 (m), 1755 (m), 1681 (s), 1621 (s), 1555 (m), 1451 (s), 1397 (s), 1379 (s), 1359 (m), 1332 (m), 1302 (m), 1258 (s), 1228 (m), 1178 (m), 1161 (m) and 1116 cm^{-1} (s). ^{1}H NMR (200MHz, $CDCl_3$): δ 6.82 (s, 1H), 5.86 (s, 1H), 3.81 (m, 4H), 2.87 (m, 4H), 2.22 (s, 3H). ^{13}C NMR (200MHz, $CDCl_3$): δ 152.5, 141.7, 123.9, 100.2, 66.6, 50.8, 14.0. MS *m/z* (relative intensity) 169 (18.5), 168 (56.2), 167 (M^+ 77.9), 166 (5.6), 154 (3.2), 153 (7.6), 152 (12.0), 139 (4.4), 138 (10.4), 137 (6.4), 136 (8.4), 125 (3.2), 124 (8.4), 122 (8.0), 112 (7.2), 111 (33.7), 110 (83.1), 109 (100), 108 (12.0), 97 (2.4), 96 (4.0), 95 (4.0), 94 (6.4), 84 (4.0), 83 (4.0), 82 (10.8), 81 (15.3), 80 (16.1), 79 (4.0), 73 (2.8), 72 (2.4), 70 (4.4), 69 (4.4), 68 (4.0), 67 (6.0), 66 (4.8), 65 (3.2), 59 (2.4), 58 (2.4), 57 (5.2), 56 (4.4), 55 (8.8), 54 (8.4), 53 (8.4), 52 (3.2), 51 (3.6), 45 (9.2), 44 (49.0), 43 (14.5), 42 (9.6), 41 (17.7).; HRMS calc. for $C_9H_{14}NO_2$ 168.1025, found 168.1019.

4-Diethylamino-5-(tetrahydropyran-2-yloxy)pent-3-en-2-one **(19*b*)**

^{1}H NMR (200MHz, $CDCl_3$): δ 5.10 (d, 1H, J = 11.3Hz), 4.94 (s, 1H), 4.67 (m, 1H), 4.58 (d, 1H, J = 11.3Hz), 3.75 (m, 1H), 3.40 (m, 1H), 3.21 (quartet, 4H, J = 7.4Hz), 1.93 (s, 3H), 1.72 - 1.28 (m, 6H),

1.05 (t, 6H, J = 7.0Hz). ^{13}C NMR (200MHz, $CDCl_3$): δ 194.1, 157.4, 99.5, 95.2, 62.6, 60.7, 43.8, 31.8, 30.5, 25.2, 19.6, 12.7. MS *m/z* (relative intensity) 255 (M^+ 7.7), 226 (3.8), 212 (3.8), 196 (10.8), 172 (10.8), 171 (100), 170 (57.7), 157 (2.3), 156 (27.7), 155 (26.9), 154 (41.5), 153 (12.3), 152 (2.3), 143 (7.7), 142 (99.0), 140 (16.9), 139 (3.8), 138 (32.3), 136 (9.2), 129 (7.7), 128 (90.8), 127 (3.1), 126 (29.2), 125 (4.6), 124 (13.1), 114 (4.6), 113 (9.2), 112 (99.0), 111 (9.2), 110 (36.9), 98 (12.3), 97 (16.9), 96 (15.4), 86 (6.2), 85 (53.8), 84 (28.5), 83 (15.4), 82 (13.8), 81 (4.6), 80 (2.3), 74 (4.6), 72 (23.8), 71 (3.8), 70 (18.5), 69 (6.2), 68 (10.8), 67 (15.4), 58 (6.2), 57 (12.3), 56 (13.8), 55 (13.8), 54 (6.9), 53 (3.1), 44 (6.9), 43 (32.3), 42 (16.2), 41 (19.2)

N,N-Diethyl-5-methylfuran-3-amine **(5*b*)**

IR (neat) 3142 (w), 2972 (s), 2933 (s), 2872 (m), 2825 (m), 1755 (m), 1622 (s), 1553 (m), 1447 (s), 1376 (s), 1283 (m), 1183 (m) and 1111 cm^{-1}(s). ^{1}H NMR (200MHz, $CDCl_3$): δ 6.75 (s, 1H), 5.83 (s. 1H), 3.03 (quartet, 4H, J = 7.2Hz), 2.22 (s, 3H), 1.08 (t, 6H, J = 7.2Hz). ^{13}C NMR (200MHz, $CDCl_3$): δ 151.9, 139.5, 123.5, 100.8, 45.1, 14.0, 11.7. MS *m/z* (relative intensity) 154 (7.7), 153 (M^+ 72.3), 139 (9.2), 138 (100), 124 (5.4), 111 (3.8), 110 (41.5), 109 (7.7), 108 (6.9), 96 (3.8), 95 (2.3), 83 (4.6), 82 (6.9), 81 (3.8), 80 (5.4), 68 (7.7), 67 (4.6), 66 (4.6), 56 (4.6), 55 (3.1), 54 (2.3), 53 (3.8), 43 (6.9), 41 (4.6).; HRMS calc. for $C_9H_{16}NO$ 154.1232, found 154.1229.

4-(Diisopropylamino)-5-(tetrahydropyran-2-yloxy)pent-3-en-2-one **(19*c*)**

^{1}H NMR (200MHz, $CDCl_3$): δ 5.30 (d, 1H, J = 11.5Hz), 5.20 (s, 1H), 4.74 (m. 1H), 4.61 (d, 1H, J = 11.5Hz), 3.95 (septet, 2H, J = 6.9Hz), 3.81 (m, 1H), 3.49 (m, 1H), 2.01 (s, 3H), 1.82 – 1.35 (m, 6H), 1.25 (d, 6H, J = 7.0Hz), 1.23 (d, 6H, 7.0Hz). ^{13}C NMR (200MHz, $CDCl_3$): δ 193.7, 156.7, 99.7, 98.3, 63.0, 61.7, 48.1, 32.3, 30.8, 25.4, 20.4, 19.8. MS *m/z* (relative intensity) 283 (M^+ 2.8), 254 (1.0), 241 (2.3), 240 (15.9), 244 (1.0), 210 (1.0), 200 (3.3), 199 (27.6), 198 (5.6), 184 (15.9), 183 (3.7), 182 (9.3), 181 (3.3), 170 (3.3), 168 (4.7), 166 (4.2), 157 (9.8), 156 (100), 142 (4.2), 141 (2.3), 140 (21.0), 139 (1.9), 138 (7.9), 126 (7.5), 125 (2.3), 124 (9.3), 115 (2.8), 114 (40.2), 112 (2.3), 110 (2.3), 100 (5.1), 99 (2.8), 98 (25.7), 97 (8.4), 96 (9.3), 86 (4.2), 85 (53.3), 84 (25.2), 83 (4.7), 82 (4.7), 81 (2.3), 72 (9.8), 71 (3.7), 70 (3.7), 68 (4.2), 67 (8.4), 58 (3.7), 57 (8.4), 56 (2.8), 55 (8.4), 54 (2.3), 44 (3.7), 43 (30.8), 42 (8.4), 41 (15.9).

N,N-Diisopropyl-5-methylfuran-3-amine **(5*c*)**

IR (neat) 2971 (s), 2932 (m), 2873 (m), 1750 (w), 1619 (s), 1546 (m), 1513 (w), 1456 (m), 1381 (m), 1364 (m), 1328 (w), 1305 (m), 1271 (m), 1181 (m) and 1115 cm^{-1}(s). ^{1}H NMR (200MHz, $CDCl_3$): δ 6.88 (s, 1H), 5.88 (s, 1H), 3.40 (septet, 2H, J = 6.6Hz), 2.22 (s, 3H), 1.11 (d, 12H, J = 6.8Hz). ^{13}C NMR (200MHz, $CDCl_3$): δ 150.8, 134.9, 129.0, 104.5, 48.6, 21.1, 14.0. MS *m/z* (relative intensity) 182 (7.7), 181 (M^+ 45.4), 167 (10.0), 166 (61.5), 139 (1.5), 138 (9.2), 125 (12.3), 124 (100), 123 (7.7), 122 (10.8), 110 (2.3), 109 (2.3), 108 (7.7), 106 (3.8), 97 (2.3), 96 (10.0), 95 (2.3), 94 (4.6), 84 (2.3), 83 (3.8), 82 (10.8), 81 (6.9), 80 (4.6), 79 (4.6), 69 (1.5), 68 (8.4), 67 (2.3), 66 (4.6), 55 (3.8), 54 (2.3), 53 (5.4), 44 (3.8), 43 (13.1), 42 (5.4).; HRMS calc. for $C_{11}H_{20}NO$ 182.1545, found 182.1541.

4-(Pyrrolidin-1-yl)-5-(tetrahydropyran-2-yloxy)pent-3-en-2-one **(19*d*)**

^{1}H NMR (200MHz, $CDCl_3$): δ 5.14 (d, 1H, J = 10.9Hz), 4.93 (s, 1H), 4.76 (m, 1H), 4.75 (d, 1H, J = 10.9Hz), 3.89 (m, 1H), 3.58 (m, 2H), 3.53 (m, 1H), 3.18 (m, 2H), 2.04 (s, 3H), 1.90 (m, 4H), 1.80 – 1.39 (m, 6H). ^{13}C NMR (200MHz, $CDCl_3$): δ 194.5, 156.8, 100.1, 96.5, 63.1, 62.8, 48.2, 31.9, 30.8, 25.6, 24.9, 20.0. MS *m/z* (relative intensity) 254 (2.3), 253 (M^+ 15.4), 224 (6.2), 210 (2.3), 194 (10.0), 170 (10.0), 169 (100), 168 (97.7), 154 (30), 153 (33.8), 152 (45.4), 151 (50.0), 150 (30.8), 141 (6.2), 140 (70.0), 138 (14.6), 136 (17.7), 134 (6.2), 127 (6.2), 126 (61.5), 124 (12.3), 123 (16.9), 122 (6.2), 112 (6.2), 111 (33.1), 110 (70.8), 109 (6.2), 108 (6.2), 85 (16.9), 84 (16.2), 83 (19.2), 82 (6.2), 81 (6.9), 80 (6.2), 72 (5.4), 71 (7.7), 70 (53.8), 69 (5.4), 68 (10.8), 67 (10.8), 57 (6.9), 56 (3.8), 55 (16.9), 54 (6.9), 53 (4.6), 43 (23.8), 42 (5.4), 41 (17.7)

1-(5-Methylfuran-3-yl)pyrrolidine **(5*d*)**

IR (neat) 3139 (w), 3106 (w), 2967 (s), 2919 (s), 2875 (s), 2814 (s), 1625 (s), 1557 (m), 1459 (m), 1402 (s), 1358 (m), 1327 (m), 1168 (m), 1152 (m) and 1106 cm^{-1}(s). ^{1}H NMR (200MHz, $CDCl_3$): δ 6.72 (s, 1H), 5.80 (s, 1H), 3.01 (m, 4H), 2.22 (s, 3H), 1.93 (m, 4H). ^{13}C NMR (200MHz, $CDCl_3$): δ 152.0, 139.7, 121.6, 100.6, 50.5, 24.9, 14.0. MS *m/z* (relative intensity) 152 (10.8), 151 (M^+ 100), 150 (89.2), 149 (3.1), 148 (3.1), 136 (7.7), 123 (10.8), 122 (20.0), 120 (2.3), 110 (2.3), 109 (6.2), 108 (33.8), 106 (2.3), 96 (4.6), 95 (16.2), 94 (13.1), 93 (2.3), 82 (2.3), 81 (8.5), 80 (10.8), 79 (2.3), 70 (3.1), 68 (9.2), 67 (7.7), 66 (4.6), 65 (2.3), 55 (4.6), 54 (3.1), 53 (8.5), 52 (3.1), 51 (3.1), 43 (6.2), 41 (12.3).; HRMS calc. for $C_9H_{14}NO$ 152.1075, found 152.1070.

4-Dibenzylamino-5-(tetrahydropyran-2-yloxy)pent-3-en-2-one **(19*e*)**

^{1}H NMR (200MHz, $CDCl_3$): δ 7.40 - 7.07 (m, 10H), 5.28 (d, 1H, J = 11.5Hz), 5.20 (s, 1H), 4.87 (d, 1H, J = 11.5Hz), 4.74 (m, 1H), 4.49 (AB quartet, 4H, J = 5.7Hz), 3.78 (m, 1H), 3.44 (m, 1H), 1.95 (s, 3H), 1.76 – 1.30 (m, 6H). ^{13}C NMR (200MHz, $CDCl_3$): δ 195.6, 158.8, 136.7, 128.9, 127.6, 127.0, 99.9, 97.8, 63.1, 61.1, 52.8, 32.4, 30.8, 25.5, 19.9. MS *m/z* (relative intensity) 379 (M^+ 0.5), 336 (0.5), 296 (2.3), 295 (13.1), 294 (6.2), 288 (4.6), 280 (1.5), 279 (2.3), 278 (5.4), 277 (4.6), 276 (1.5), 262 (1.5), 252 (3.1), 236 (3.8), 234 (3.1), 232 (1.5), 205 (10.8), 204 (78.5), 189 (1.5), 188 (16.2), 186 (7.7), 162 (10.8), 160 (1.5), 158 (1.5), 146 (4.6), 144 (5.4), 143 (1.5), 132 (1.5), 117 (2.3), 115 (1.5), 106 (1.5), 105 (1.5), 104 (2.3), 92 (16.2), 91 (100), 85 (26.2), 67 (3.8), 65 (6.2), 57 (3.8), 55 (2.3), 43 (5.4), 41 (3.8)

N,*N*-Dibenzyl-5-methylfuran-3-amine **(5*e*)**

IR (neat) 3057 (m), 3026 (m), 2937 (m), 2920 (m), 2882 (m), 2844 (m), 1623 (s), 1493 (s), 1454 (s), 1395 (m), 1371 (m), 1352 (m), 1224 (m), 1161 (m), 1134 (m), 1101 (m) and 1080 cm^{-1}(m). ^{1}H NMR (200MHz, $CDCl_3$): δ 7.50 – 7.10, (m, 10H), 6.68 (s, 1H), 5.87 (s, 1H), 4.20 (s, 4H), 2.21, (s, 3H). ^{13}C NMR (200MHz, $CDCl_3$): δ 151.8, 140.9, 138.9, 128.6, 127.9, 127.2, 123.5, 100.8, 56.1, 14.1. MS *m/z* (relative intensity) 278 (15.4), 277 (M^+ 71.5), 276 (20.0), 186 (50.8), 185 (2.3), 184 (3.8), 170 (3.8), 168 (1.5), 167 (6.9), 159 (5.4), 158 (33.8), 157 (3.1), 156 (3.1), 144 (14.6), 143 (9.2), 142 (2.3), 130 (2.3), 129 (3.8), 128 (2.3), 117 (3.1), 116 (3.1), 115 (4.6), 108 (3.1), 104 (2.3), 92 (8.5), 91 (100), 90 (3.8), 89 (5.4), 77 (2.3), 65 (14.6), 53 (1.5), 51 (1.5), 43 (5.4).; HRMS calc. for $C_{19}H_{20}NO$ 278.1545, found 278.1538.

4,4'-Ethylenediiminobis[5-(tetrahydropyran-2-yloxy)pent-3-en-2-one] **(19*f*)**

^{1}H NMR (200MHz, $CDCl_3$): δ 5.12 (s, 2H), 4.58 (m, 2H), 4.23 (d, 2H, J = 13.2Hz), 3.92 (d, 2H, J = 13.2Hz), 3.75 (m, 2H), 3.47 (m, 2H), 3.41 (m, 4H), 1.97 (s, 6H), 1.85 – 1.35 (m, 12H). ^{13}C NMR (200MHz, $CDCl_3$): δ 196.9, 160.1, 97.9, 95.2, 65.0, 62.3, 43.7, 30.3, 29.3, 25.2, 19.2. MS *m/z* (relative intensity) 424 (M^+ 1), 381 (1.5), 340 (2.3), 323 (2.3), 322 (3.5), 267 (2.3), 257 (1.5), 256 (11.5), 255 (1.5), 240 (2.3), 239 (6.9), 238 (3.8), 226 (4.6), 225 (33.1), 221 (2.3), 220 (2.3), 213 (6.9), 212 (5.4), 209 (6.2), 207 (10.8), 201 (2.3), 200 (16.9), 197 (3.8), 196 (1.5), 195 (6.2), 183 (2.3), 182 (4.6), 181 (3.1), 179 (1.5), 165 (3.1), 152 (2.3), 151 (1.5), 142 (15.4), 141 (59.2), 140 (3.8), 130 (3.1), 129 (41.5), 128 (79.2), 127 (4.6), 126 (13.1), 125 (42.3), 124 (4.6), 123 (8.5), 117 (3.8), 116 (66.9), 115 (4.6), 114 (3.8), 113 (4.6), 112 (9.2), 111 (12.3), 110 (12.3), 100 (11.5), 99 (3.8), 98 (16.2), 97 (3.8), 96 (6.2), 86 (12.3),

85 (100), 84 (9.2), 83 (6.9), 82 (16.9), 71 (3.1), 70 (4.6), 69 (3.1), 68 (6.2), 67 (20.0), 57 (17.7), 56 (3.8), 55 (11.5), 43 (23.1), 41 (14.6)

N,*N*'-Bis(5-methylfuran-3-yl)ethylenediamine **(5*f*)**

MS *m/z* (relative intensity) 221 (13.1), 220 (M^+ 77.7), 191 (10.7), 190 (56.9), 182 (2.3), 178 (3.4), 177 (17.7), 176 (3.8), 175 (6.2), 174 (10.7), 172 (3.1), 162 (6.9), 161 (3.1), 160 (3.8), 149 (9.2), 148 (60.0), 147 (100), 146 (7.7), 134 (5.4), 133 (5.4), 132 (6.2), 124 (3.1), 120 (5.4), 119 (5.4), 118 (8.5), 117 (3.1), 111 (13.1), 110 (25.4), 109 (6.2), 108 (7.7), 106 (3.1), 105 (2.3), 103 (2.3), 98 (3.1), 96 (3.1), 91 (5.4), 89 (4.6), 85 (2.3), 83 (3.8), 81 (3.8), 80 (4.6), 79 (3.8), 78 (2.3), 77 (4.6), 69 (2.3), 68 (5.4), 67 (2.3), 66 (4.6), 65 (4.6), 63 (3.1), 53 (7.7), 52 (2.1), 51 (3.8), 44 (14.6), 43 (20.8), 42 (3.8), 41 (5.4)

N.*N*'-Ethylenebis[N-(5-methylfuran-3-yl)acetamide] **(21*f*)**

IR (neat) 3414 (w), 3167 (w), 3127 (s), 3104 (s), 2985 (m), 2947 (s), 2915 (s), 2853 (w), 1667 (s), 1613 (s), 1556 (m), 1431 (s), 1397 (s), 1296 (s), 1263 (m), 1237 (s), 1203 (m), 1186 (m) and 1128 cm^{-1}(s). ^1H NMR (200MHz, $CDCl_3$): δ 7.41 (s, 2H), 5.98 (s, 2H), 3.69 (s, 4H), 2.28 (s, 6H), 1.91 (s, 6H). ^{13}C NMR (200MHz, $CDCl_3$): δ 171.7, 153.0, 137.5, 130.3, 105.8, 46.7, 22.5, 14.0. MS *m/z* (relative intensity) 305 (1.5), 304 (M^+ 10.0), 262 (3.1), 246 (1.5), 245 (13.8), 219 (3.1), 166 (15.4), 165 (40.0), 153 (2.3), 140 (3.1), 139 (33.8), 124 (12.3), 123 (46.9), 122 (3.8), 111 (10.8), 110 (100), 109 (8.5), 108 (10.8), 98 (1.5), 97 (22.3), 82 (3.1), 81 (2.3), 80 (9.2), 68 (3.1), 67 (2.3), 66 (2.3), 55 (2.3), 53 (2.3), 43 (25.4), 41 (3.1).; HRMS calc. for $C_{16}H_{20}N_2O_4Na$ 327.1321, found 327.1317.

4-n-Butylamino-5-(tetrahydropyran-2-yloxy)pent-3-en-2-one **(19*g*)**

^1H NMR (200MHz, $CDCl_3$): δ 5.15 (s, 1H), 4.65 (m, 1H), 4.30 (d, 1H, J = 13.4Hz), 4.00 (d, 1H, J = 13.4Hz), 3.80 (m, 1H), 3.52 (m, 1H), 3.25 (AB quartet, 2H, J= 6.4Hz), 2.05 (s, 1H), 1.87-1.49 (m, 8H), 1.40 (sextet, 2H, J = 7.3Hz), 0.91 (t, 3H, J= 7.1Hz). ^{13}C NMR (200MHz, $CDCl_3$): δ 196.4, 161.1, 98.1, 93.6, 64.9, 62.3, 42.7, 32.5, 30.5, 29.3, 25.5, 20.1, 19.2, 13.9. MS *m/z* (relative intensity) 255 (M^+ 5.7), 212 (2.5), 198 (2.0), 182 (9.3), 172 (10.6), 171 (100), 170 (39.0), 156 (29.3), 155 (15.4), 154 (26.0), 142 (27.6), 141 (6.5), 140 (77.2), 138 (7.7), 129 (7.3), 128 (51.2), 126 (12.2), 124 (14.6), 115 (4.9), 114 (52.0), 113 (91.9), 112 (30.1), 111 (9.8), 110 (23.6), 100 (8.9), 99 (9.8), 98 (88.6), 97 (20.3), 96, (12.2), 86 (8.1), 85 (81.3), 84 (69.1), 83 (8.9), 82 (10.6), 81 (4.1), 80 (2.8), 72 (8.1), 71 (11.4), 70 (50.0), 69 (7.0), 68 (10.6), 67 (22.4), 58 (13.0), 57 (33.0), 56 (7.3), 55 (17.1), 54 (5.7), 44 (4.1), 43 (38.2), 42 (9.8), 41 (31.9)

N-(n-Butyl)-5-methylfuran-3-amine **(5*g*)**

MS *m/z* (relative intensity) 154 (4.8), 153 (M^+ 43.7), 138 (4.0), 124 (4.8), 111(42.1), 110 (100), 97 (17.5), 96 (7.1), 84 (3.2), 83 (7.9), 82 (7.1), 81 (3.2), 80 (5.6), 70 (3.2), 69 (3.2), 68 (14.3), 67 (4.8), 66 (3.2), 55 (6.3), 54 (2.4), 53 (4.8), 43 (11.1), 42 (3.2), 41 (11.1)

N-(n-Butyl)-*N*-(5-methylfuran-3-yl)acetamide **(21*g*)**

IR (neat) 3322 (w), 3109 (w), 2959 (s), 2932 (s), 2873 (m), 1722 (w), 1666 (s), 1615 (s), 1548 (w), 1408 (s), 1367 (s), 1302 (s), 1228 (s), 1180 (w) and 1133 cm^{-1}(m). ^{1}H NMR (200MHz, $CDCl_3$): δ 7.17 (s, 1H), 5.85 (s, 1H), 3.49 (t, 2H, J = 7.7Hz), 2.23 (s, 3H), 1.89 (s, 3H), 1.40 (m, 2H,), 1.25 (sextet, 2H, J = 7.3Hz), 0.83 (t, 3H, J = 7.3Hz). ^{13}C NMR (200MHz, $CDCl_3$): δ 171.0, 153.0, 136.6, 130.4, 106.0, 48.4, 30.1, 22.5, 20.0, 13.9, 13.8. MS *m/z* (relative intensity) 196 (4.0), 195 (M^+ 33.3), 180 (6.3), 152 (61.1), 151 (11.1), 139 (4.8), 138 (7.9), 136 (5.5), 125 (3.2), 124 (20.6), 123 (4.8), 111 (44.4), 110 (100), 98 (5.6), 97 (53.2), 83 (4.0), 82 (4.0), 80 (6.3), 68 (6.3), 55 (3.2), 54 (4.0), 43 (23.0).; HRMS calc. for $C_{11}H_{18}NO_2$ 196.1337, found 196.1334.

4-Cyclohexylamino-5-(tetrahydropyran-2-yloxy)pent-3-en-2-one **(19*h*)**

^{1}H NMR (200MHz, $CDCl_3$): δ 5.15 (s, 1H), 4.68 (m, 1H), 4.35 (d, 1H, J = 13.2Hz), 4.02 (d, 1H, J = 13.2Hz), 3.85 (m, 1H), 3.55 (m, 1H), 3.45 (m, 1H), 2.04 (s, 1H), 1.95 – 1.15 (m, 16H). ^{13}C NMR (200MHz, $CDCl_3$): δ 196.1, 159.9, 98.1, 93.4, 64.8, 62.2, 51.6, 34.4, 34.3, 30.5, 29.3, 25.4, 24.6, 19.1. MS *m/z* (relative intensity) 282 (1.0), 281 (M^+ 5.4), 238 (1.5), 208 (3.8), 198 (9.2), 197 (56.9), 196 (16.2), 182 (16.2), 181 (48.5), 180 (12.3), 179 (8.5), 168 (6.9), 167 (3.8), 166 (28.5), 164 (6.9), 162 (3.1), 154 (12.3), 152 (1.5), 150 (2.3), 139 (6.2), 138 (50.8), 137 (6.9), 136 (45.4), 126 (6.2), 124 (13.8), 123 (2.3), 122 (3.1), 116 (9.5), 115 (14.6), 114 (77.7), 110 (4.6), 108 (4.6), 102 (2.3), 101 (6.2), 100 (100), 99 (6.2), 98 (26.9), 97 (12.3), 96 (6.2), 95 (1.5), 94 (6.2), 86 (3.8), 85 (46.2), 84 (43.1), 83 (14.6), 82 (8.5), 81 (7.7), 80 (4.6), 79 (3.8), 74 (3.1), 72 (3.8), 71 (6.2), 70 (4.6), 68 (5.4), 67 (18.5), 58 (18.5), 57 (12.3), 56 (6.2), 55 (29.2), 54 (4.6), 53 (3.8), 43 (20.0), 42 (3.8), 41 (21.5)

N-Cyclohexyl-5-methylfuran-3-amine **(5*h*)**

MS *m/z* (relative intensity) 180 (11.5), 179 (M^+ 100), 178 (5.4), 164 (6.9), 151 (1.5), 150 (15.4), 138 (4.6), 137 (10.0), 136 (56.9), 134 (3.1), 124 (9.2), 123 (6.9), 122 (5.4), 120 (2.3), 118 (3.1), 117 (3.1), 110 (15.4), 109 (1.5), 108 (21.5), 107 (1.5), 106 (3.1), 98 (45.4), 97 (69.2), 96 (4.6), 95 (2.3), 94

(19.2), 93 (12.3), 91 (2.3), 83 (3.1), 82 (4.6), 81 (4.6), 80 (11.5), 79 (3.1), 70 (3.1), 69 (6.9), 68 (15.4), 67 (5.4), 66 (3.1), 56 (2.3), 55 (13.1), 54 (3.8), 53 (6.2), 43 (13.1), 41 (14.6)

N-Cyclohexyl-N-(5-methylfuran-2-yl)acetamide **(21*h*)**

IR (neat) 3105 (w), 2930 (s), 2856 (s), 1726 (w), 1660 (s), 1614 (s), 1544 (m), 1451 (m), 1399 (s), 1375 (s), 1345 (m), 1313 (s), 1283 (m), 1245 (m) and 1132 cm^{-1}(m). ^{1}H NMR (200MHz, $CDCl_3$): δ 7.10 (s, 1H), 5.78 (s, 1H), 4.43 (tt, 1H, J = 11.9Hz, J = 3.8Hz), 2.26 (s, 3H), 1.85 (s, 3H), 1.80 – 0.75 (m, 10H). ^{13}C NMR (200MHz, $CDCl_3$): δ 170.9, 152.7, 138.1, 126.6, 108.1, 52.9, 31.3, 25.7, 25.5, 23.1, 13.9. MS *m/z* (relative intensity) 222 (3.1), 221 (M^+ 20.8), 206 (2.3), 179 (4.6), 178 (20.0), 164 (1.5), 150 (3.8), 141 (4.6), 140 (55.4), 139 (22.3), 137 (3.1), 136 (16.9), 134 (2.3), 124 (10.0), 123 (2.3), 122 (1.5), 110 (2.3) , 108 (6.9), 98 (23.8), 97 (100), 96 (2.3), 94 (4.6), 93 (2.3), 83 (2.3), 82 (1.5), 81 (3.1), 80 (4.6), 79 (2.3), 69 (3.1), 68 (4.6), 67 (3.8), 66 (1.5), 55 (10.0), 54 (2.3), 53 (4.6), 43 (16.9), 41 (8.5).; HRMS calc. for $C_{13}H_{19}NO_2Na$ 244.1314, found 244.1311.

5-Morpholino-6-(tetrahydropyran-2-yloxy)hex-4-en-3-one **(19*i*)**

^{1}H NMR (200MHz, $CDCl_3$): δ 5.33 (d, 1H, J = 12.1Hz), 5.19 (s, 1H), 4.71 (m, 1H), 4.66 (d, 1H, J = 12.1Hz), 3.85 (m, 1H), 3.73 (t, 4H, J = 4.9Hz), 3.50 (m, 1H), 3.34 (m, 4H), 2.35 (quartet, 2H, 7.3Hz), 1.90 – 1.35 (m, 6H), 1.05 (t, 3H, 7.3Hz). ^{13}C NMR (200MHz, $CDCl_3$): δ 199.2, 158.5, 100.1, 97.8, 66.6, 63.5, 61.1, 47.0, 37.8, 31.0, 25.5, 20.2, 9.5. MS *m/z* (relative intensity) 283 (M^+ 2.3), 254 (2.3), 224 (3.1), 200 (9.2), 199 (82.3), 198 (36.2), 183 (8.5), 182 (15.4), 181 (6.9), 171 (9.2), 170 (100), 168 (5.4), 166 (5.4), 154 (8.5), 152 (12.3), 143 (8.5), 142 (90.8), 140 (6.2), 127 (12.3), 126 (25.4), 124 (8.5), 123 (4.6), 114 (8.5), 112 (10.0), 98 (2.3), 97 (3.8), 96 (4.6), 95 (3.8), 94 (3.8), 86 (11.5), 85 (36.2), 84 (7.7), 83 (5.4), 82 (3.8), 70 (3.8), 69 (3.1), 68 (3.8), 67 (14.6), 57 (29.2), 56 (6.9), 55 (13.1), 54 (3.8), 43 (8.5), 41 (13.8)

4-(5-Ethylfuran-3-yl)morpholine **(5*i*)**.

IR (neat) 3136 (w), 2968 (s), 2855 (s), 2821 (m), 1703 (w), 1618 (s), 1551 (w), 1451 (m), 1399 (m), 1378 (m), 1359 (w), 1257 (s), 1161 (m) and 1117 cm^{-1}(s). ^{1}H NMR (200MHz, $CDCl_3$): δ 6.83 (s, 1H), 5.86 (s, 1H), 3.80 (m, 4H), 2.89 (m, 4H), 2.56 (quartet, 2H, J = 7.5Hz), 1.19 (t, 3H, J = 7.5Hz). ^{13}C NMR (200MHz, $CDCl_3$): δ 158.1, 141.5, 123.8, 98.7, 66.7, 50.8, 21.8, 12.1. MS *m/z* (relative intensity) 182 (12.3), 181 (M^+ 97.7), 180 (4.2), 166 (19.2), 152 (13.1), 150 (9.2), 138 (3.8), 136 (3.1), 125 (6.2), 124 (34.6), 123 (100), 122 (20.0), 109 (6.2), 108 (52.3), 96 (4.6), 95 (7.7), 94 (14.6), 81 (3.8), 80 (9.2),

79 (3.1), 67 (6.2), 66 (4.6), 65 (4.6), 57 (3.8), 55 (3.1), 54 (3.8), 53 (7.7), 42 (2.3), 41 (7.7).; HRMS calc. for $C_{10}H_{16}NO_2$ 182.1181, found 182.1176.

5-Diethylamino-6-(tetrahydro-2-yloxy)hex-4-ene-3-one **(19*j*)**

^{1}H NMR (200MHz, $CDCl_3$): δ5.31 (d, 1H, J = 11.2Hz), 5.07 (s, 1H), 4.81 (m, 1H), 4.68 (d, 1H, J = 11.2Hz), 3.85 (m, 1H), 3.55 (m, 1H), 3.34 (quartet, 4H, J = 7.3Hz), 2.34 (quartet, 2H, J = 7.3Hz), 1.90 – 1.40 (m, 6H), 1.18 (t, 6H, 7.3Hz), 1.07 (t, 3H, J = 7.3Hz). ^{13}C NMR (200MHz, $CDCl_3$): δ 198.2, 157.5, 100.2, 95.1, 63.3, 61.5, 44.1, 37.8, 30.9, 25.6, 20.1, 13.1, 10.0. MS *m/z* (relative intensity) 269 (M^+ 3.1), 240 (2.3), 210 (4.6), 186 (6.2), 185 (56.2), 184 (31.5), 170 (3.8), 169 (10.0), 168 (16.2), 167 (6.9), 157 (9.2), 156 (100), 154 (5.4), 152 (10.0), 150 (2.3), 140 (20.0), 138 (11.5), 129 (2.9), 128 (83.1), 126 (6.9), 124 (6.9), 113 (6.9), 112 (31.5), 111 (6.9), 110 (13.8), 100 (9.2), 98 (6.9), 97 (3.1), 96 (6.9), 86 (3.8), 85 (32.3), 84 (7.7), 83 (5.4), 82 (5.4), 72 (11.5), 70 (7.7), 69 (2.3), 68 (5.4), 67 (10.0), 58 (3.8), 57 (26.2), 56 (8.5), 55 (8.5), 54 (3.8), 44 (3.1), 43 (6.2), 42 (8.5), 41 (11.5).

N,*N*,5-Triethylfuran-3-amine **(5*j*)**

IR (neat) 3142 (w), 2971 (s), 2935 (s), 2874 (s), 1755 (m), 1702 (w), 1618 (s), 1550 (m), 1519 (w), 1462 (s), 1402 (s), 1374 (s), 1277 (m), 1179 (s) and 1113 cm^{-1}(s). ^{1}H NMR (200MHz, $CDCl_3$): δ 6.76 (s, 1H), 5.83 (s, 1H), 3.03 (quartet, 4H, J = 7.1Hz), 2.57 (quartet, 2H, J = 7.5Hz), 1.21 (t, 3H, 7.5Hz), 1.08 (t, 6H, J = 7.1Hz). ^{13}C NMR (200MHz, $CDCl_3$): δ 157.6, 138.3, 123.4, 99.1, 45.1, 21.9, 12.1, 11.7. MS *m/z* (relative intensity) 168 (6.9), 167 (M^+ 52.3), 153 (12.3), 152 (100), 138 (5.4), 125 (3.1), 124 (31.5), 123 (3.8), 122 (3.8), 110 (2.3), 109 (2.3), 108 (6.9), 96 (4.6), 95 (5.4), 94 (3.8), 82 (6.2), 81 (4.6), 80 (6.2), 79 (2.3), 68 (2.3), 67 (4.6), 66 (2.3), 57 (4.6), 56 (5.4), 55 (3.8), 54 (2.3), 53 (5.4), 43 (2.3), 41 (4.6).; HRMS calc. for $C_{10}H_{18}NO$ 168.1388, found 168.1385.

5-(n-Butylamino)-6-(tetrahydropyran-2-yloxy)hex-4-en-3-one **(19*k*)**

^{1}H NMR (200MHz, $CDCl_3$): δ5.16 (s, 1H), 4.65 (m, 1H), 4.31 (d, 1H, J = 13.4Hz), 4.01 (d, 1H, J = 13.4Hz), 3.80 (m, 1H), 3.50 (m, 1H), 3.24 (quartet, 2H, J = 6.6Hz), 2.28 (quartet, 2H, J = 7.5Hz), 1.90 – 1.50 (m, 8H), 1.40 (septet, 2H, J = 8.1Hz), 1.07 (t, 3H, J = 7.5Hz), 0.90 (t, 3H, 7.3Hz). ^{13}C NMR (200MHz, $CDCl_3$): δ 200.1, 161.1, 98.1, 92.6, 65.0, 62.8, 42.7, 35.2, 32.4, 30.5, 25.4, 20.1, 19.2, 13.8, 10.0. MS *m/z* (relative intensity) 269 (M^+ 1.9), 212 (1.9), 196 (3.3), 186 (6.1), 185 (46.7), 184 (23.4), 169 (7.0), 168 (12.6), 167 (4.7), 157 (10.3), 156 (100), 155 (4.2), 154 (35.5), 142 (7.9), 140 (14.0), 138 (10.7), 129 (4.7), 128 (45.8), 127 (37.4), 126 (4.7), 125 (5.6), 124 (12.6), 114 (3.7), 113 (4.7), 112 (17.8),

111 (7.9), 110 (8.4), 100 (4.2), 99 (5.6), 98 (72.9), 97 (5.6), 96 (9.3), 95 (3.7), 86 (4.7), 85 (49.5), 84 (21.0), 83 (9.3), 82 (8.4), 81 (2.3), 72 (7.5), 71 (7.5), 70 (28.5), 69 (7.0), 68 (7.5), 67 (17.8), 58 (3.7), 57 (39.3), 56 (7.9), 55 (22.4), 54 (6.1), 53 (4.2), 43 (11.2), 42 (6.1), 41 (23.4)

N-(n-Butyl)-5-ethylfuran-3-amine **(5*k*)**

MS *m/z* (relative intensity) 168 (6.2), 167 (M^+ 52.3), 152 (6.2), 138 (6.2), 126 (3.1), 125 (41.5), 124 (100), 111 (13.1), 110 (6.9), 108 (6.9), 97 (3.1), 96 (18.5), 95 (2.3), 83 (3.1), 82 (11.5), 81 (6.2), 80 (7.7), 68 (5.4), 67 (5.4), 66 (2.3), 57 (6.2), 55 (4.6), 53 (4.6), 41 (7.7)

N-(n-Butyl)-N-(5-ethylfuran-3-yl)acetamide **(21*k*)**

IR (neat) 3109 (w), 2960 (s), 2933 (s), 2874 (s), 1761 (w), 1664 (s), 1611 (s), 1543 (w), 1406 (s), 1301 (m), 1227 (m) and 1136 cm^{-1}(m). ^{1}H NMR (200MHz, $CDCl_3$): δ 7.20 (s, 1H), 5.86 (s, 1H), 3.51 (t, 2H, J = 7.1Hz), 2.60 (quartet, 2H, J = 7.5Hz), 1.92 (s, 3H), 1.43 (quintet, 2H, J = 7.5Hz), 1.24 (septet, 2H, J = 7.0Hz), 1.20 (t, 3H, 7.5Hz), 0.86 (t, 3H, 7.1Hz). ^{13}C NMR (200MHz, $CDCl_3$): d 171.0, 158.7, 136.6, 130.3, 104.4, 48.4, 30.2, 22.5, 21.7, 20.0, 14.0, 11.9.
MS *m/z* (relative intensity) 210 (4.6), 209 (M^+ 30.8), 194 (5.4), 180 (7.7), 167 (3.8), 166 (6.2), 153 (10.0), 152 (52.3), 150 (4.6), 139 (3.8), 138 (23.1), 137 (5.4), 125 (35.4), 124 (100), 112 (3.8), 111 (30.8), 110 (6.2), 108 (6.9), 97 (23.1), 96 (10.0), 94 (3.8), 82 (6.2), 81 (3.8), 80 (6.2), 68 (3.1), 67 (3.1), 57 (9.2), 55 (3.8), 53 (3.8), 43 (16.9), 41 (7.7).; HRMS calc. for $C_{12}H_{19}NO_2Na$ 232.1313, found 132.1310.

3-Morpholino-4-(tetrahydropyran-2-yloxy)but-2-enal **(19*l*)**

^{1}H NMR (200MHz, $CDCl_3$): δ9.70 (d, 1H, J = 8.1Hz), 5.28 (d, 1H, J = 8.1Hz), 4.64 (m, 1H), 4.62 (AB quartet, 2H, 7.0Hz), 3.80 (m, 1H), 3.71 (m, 4H), 3.50 (m, 4H), 1.95 – 1.6 (m, 9H). ^{13}C NMR (200MHz, $CDCl_3$): δ 188.2, 160.6, 104.5, 98.2, 66.5, 63.1, 59.6, 47.1, 30.6, 25.3, 19.7. MS *m/z* (relative intensity) 255 (M^+ 2.3), 226 (2.3), 196 (3.1), 172 (7.7), 171 (100), 170 (43.8), 156 (2.3), 155 (26.2), 154 (45.4), 153 (16.2), 152 (6.2), 143 (3.1), 142 (25.4), 140 (7.7), 138 (22.3), 136 (9.2), 127 (15.4), 126 (45.4), 125 (3.1), 124 (16.2), 123 (2.3), 122 (3.8), 114 (3.8), 113 (9.2), 112 (23.8), 111 (3.1), 110 (8.5), 108 (5.4), 106 (1.5), 100 (1.5), 99 (2.3), 98 (6.2), 97 (11.5), 96 (18.5), 95 (26.2), 94 (12.3), 87 (4.6), 86 (16.9), 85 (45.4), 84 (12.3), 83 (9.2), 82 (11.5), 81 (4.6), 80 (3.8), 72 (3.1), 71 (3.8), 70 (10.0), 69 (15.4), 68 (13.1), 67 (26.2), 66 (2.3), 65 (1.5), 58 (3.8), 57 (21.5), 56 (16.9), 55 (30.0), 54 (12.3), 53 (6.2), 52 (2.3), 45 (6.2), 44 (4.6), 43 (19.2), 42 (19.2), 41 (42.3).

4-(Furan-3-yl)morpholine **(5*l*)**

IR (neat) 3454 (w), 3145 (w), 2960 (m), 2915 (m), 2895 (m), 2856 (m), 2823 (m), 1596 (s), 1508 (w), 1452 (m), 1393 (m), 1381 (m), 1359 (w), 1330 (m), 1303 (w), 1272 (m), 1251 (s), 1211 (w), 1182 (w), 1160 (m) and 1119 cm^{-1}(s). ^{1}H NMR (200MHz, $CDCl_3$): δ7.32 (m, 1H), 7.00 (m, 1H), 6.28 (m, 1H), 3.84 (m, 4H), 2.94 (m, 4H). ^{13}C NMR (200MHz, $CDCl_3$): δ143.4, 141.3, 126.1, 104.0, 66.5, 50.7. MS *m/z* (relative intensity) 154 (3.1), 153 (M^+ 40.0), 138 (6.2), 124 (5.4), 122 (9.2), 97 (2.3), 96 (10.8), 95 (100), 94 (28.5), 69 (2.3), 68 (5.4), 67 (14.6), 66 (5.4), 65 (2.3), 55 (2.3), 54 (6.1), 53 (6.1), 52 (6.1), 45 (2.3), 44 (1.5), 43 (5.4), 42 (7.7), 41 (21.5).; HREIMS calc. $C_8H_{11}NO_2$ 153.0790, Found 153.0786.

3-Diethylamino-4-(tetrahydropyran-2-yloxy)but-2-enal **(19*m*)**

^{1}H NMR (200MHz, $CDCl_3$): δ9.62 (d, 1H, J = 8.3Hz), 5.24 (d, 1H, J = 8.3Hz), 4.66 (m, 1H), 4.58 (s, 2H), 3.80 (m, 1H), 3.53 (m, 1H), 3.32 (quartet, 4H, J = 7.0Hz), 1.90 – 1.40 (m, 8H), 1.18 (t, 6H, J = 7.1Hz). ^{13}C NMR (200MHz, $CDCl_3$): δ187.5, 159.7, 102.8, 98.1, 62.7, 59.8, 44.4, 30.5, 25.4, 19.5, 12.8. MS *m/z* (relative intensity) 241 (M^+ 1.0), 212 (1.0), 208 (1.5), 207 (5.4), 182 (1.5), 158 (3.1), 157 (8.5), 156 (27.7), 147 (1.5), 142 (4.6), 141 (17.7), 140 (30.0), 139 (3.1), 138 (3.1), 129 (6.2), 128 (75.4), 126 (10.0), 125 (2.3), 124 (23.1), 122 (7.7), 114 (3.1), 113 (13.1), 112 (52.3), 110 (13.8), 108 (2.3), 105 (1.5), 100 (6.2), 99 (3.8), 98 (17.7), 97 (6.2), 96 (13.8), 95 (2.3), 94 (3.8), 86 (8.5), 85 (87.7), 84 (33.1), 83 (19.2), 82 (17.7), 81 (3.8), 80 (3.1), 74 (3.8), 73 (10.0), 72 (19.2), 71 (19.2), 70 (55.4), 69 (23.8), 68 (19.2), 67 (27.7), 58 (20.8), 57 (56.9), 56 (41.5), 55 (43.8), 54 (21.5), 53 (7.7), 45 (3.8), 44 (27.7), 43 (53.8), 42 (64.6), 41 (100).

N,*N*-Diethylfuran-3-amine **(5*m*)**

IR (neat) 3148 (w), 2972 (s), 2934 (m), 2873 (m), 2831 (m), 1599 (s), 1508 (w), 1450 (m), 1378 (m), 1341 (m), 1274 (m), 1194 (w), 1165 (s), 1118 (w) and 1066 cm^{-1}(m). ^{1}H NMR (200MHz, $CDCl_3$): δ7.25 (m, 1H), 6.90 (m, 1H), 6.20 (m, 1H), 3.05 (quartet, 4H, J = 7.0Hz), 1.08 (t, 6H, J = 7.1Hz). ^{13}C NMR (200MHz, $CDCl_3$): δ 142.6, 138.8, 125.5, 104.4, 45.2, 11.6. MS *m/z* (relative intensity) 140 (3.8), 139 (M^+ 43.8), 125 (7.7), 124 (100), 110 (3.1), 109 (2.3), 108 (3.1), 97 (3.1), 96 (53.8), 95 (9.2), 94 (14.6), 82 (6.2), 81 (4.6), 80 (4.6), 70 (2.3), 69 (4.6), 68 (14.6), 67 (8.5), 66 (4.6), 65 (3.1), 56 (7.7), 55 (7.7), 54 (18.5), 53 (13.1), 52 (12.3), 51 (1.5), 43 (2.1), 42 (13.8), 41 (30.0).;EIMS: Calc $C_8H_{13}NO$ 139.0997, Found 139.0994.

3-(n-Butylamino)-4-(tetrahydropyran –2-yloxy)but-2-enal **(19*n*)**

^{1}H NMR (200MHz, $CDCl_3$): *E)* δ9.37 (d, 1H, J = 6.8Hz), 5.01 (d, 1H, J = 6.8), 4.77 (AB quartet, 1H, J = 19.8Hz, C = 15.5Hz), 4.67 (AB quartet, 1H, J = 19.8Hz, C = 15.5Hz), 4.63 (m, 1H), 3.17 (AB quartet, 2H, J = 5.3Hz), 0.92 (m, 3H) ; *Z)* 9.03 (d, 1H, J = 2.6Hz), 5.15 (d, 1H, J = 2.6Hz), 4.66 (m, 1H), 4.34 (d, 1H, J = 13.9Hz, C = 54.9Hz), 4.07 (d, 1H, J = 13.9Hz, C = 54.9Hz), 3.10 (AB quartet, 2H), 0.80 (m, 3H) ; *E + Z)* 3.81 (m, 1H), 3.56 (m, 1H), 1.9 – 1.5 (m, 6H), 1.41 (quintet, 2H, J = 7.1Hz). ^{13}C NMR (200MHz, $CDCl_3$): δ 186.9, 185.4, 162.9, 161.6, 99.7, 98.2, 94.5, 64.3, 63.4, 62.3, 43.0, 42.8, 32.3, 30.6, 30.4, 30.3, 25.4, 25.2, 20.3, 20.1, 20.0, 19.1. MS *m/z* (relative intensity) 241 (M^+ 1.0), 168 (1.5), 158 (3.1), 151 (26.9), 156 (13.1), 141 (6.2), 140 (10.0), 128 (3.8), 127 (1.5), 126 (22.3), 124 (3.1), 115 (3.8), 114 (7.7), 113 (10.8), 112 (10.8), 111 (1.5), 110 (8.5), 101 (2.3), 100 (31.5), 99 (31.5), 98 (38.5), 97 (7.7), 96 (9.2), 87 (2.3), 86 (11.5), 85 (87.7), 84 (28.5), 83 (11.5), 82 (9.2), 73 (3.1), 72 (6.9), 71 (33.1), 70 (73.8), 69 (13.8), 68 (13.1), 67 (28.5), 58 (8.5), 57 (58.5), 56 (23.1), 55 (27.7), 54 (15.4), 53 (5.4), 52 (1.5), 51 (1.5), 49 (3.1), 44 (9.2), 43 (40), 42 (13.1), 41 (100).

N-(n-Butyl)furan-3-amine **(5*n*)**

MS *m/z* (relative intensity) 140 (3.1), 139 (M^+ 27.7), 124 (1.5), 110 (4.6), 97 (18.5), 96 (100), 94 (2.3), 83 (4.6), 80 (3.1), 69 (4.6), 68 (5.4), 67 (2.3), 55 (3.1), 54 (7.7), 53 (2.3), 52 (3.1), 42 (3.8), 41 (13.8).

N-(n-Butyl)-*N*-(furan-3-yl)acetamide **(21*n*)**

IR (neat) 3482 (w), 3317 (w), 3131 (w), 2959 (m), 2933 (m), 2873 (m), 1751 (w), 1722 (w), 1663 (s), 1592 (m), 1509 (w), 1439 (m), 1403 (s), 1378 (m), 1368 (m), 1303 (m), 1256 (w), 1223 (m), 1115(w). ^{1}H NMR (200MHz, $CDCl_3$): δ7.37 (m, 1H), 7.35 (m, 1H), 6.26 (m, 1H), 3.51 (t, 2H, J = 7.1Hz), 1.88 (s, 3H), 1.43 (quintet, 2H, J = 8.1Hz), 1.25 (sextet, 2H, J = 7.1Hz), 0.87 (t, 3H, 7.1Hz). ^{13}C NMR (200MHz, $CDCl_3$): δ 170.9, 143.5, 138.5, 129.9, 110.1, 48.4, 30.0, 22.4, 19.9, 13.9. MS *m/z* (relative intensity) 182 (1.0), 181 (M^+ 10), 166 (3.1), 153 (3.8), 152 (26.2), 139 (4.6), 138 (5.4), 125 (3.1), 124 (3.1), 111 (5.4), 110 (8.5), 98 (2.3), 97 (32.3), 96 (100), 95 (3.1), 94 (3.8), 83 (12.3), 80 (1.5), 69 (2.3), 68 (3.1), 67 (3.8), 55 (3.1), 54 (3.8), 53 (2.3), 52 (1.5), 43 (31.5), 42 (3.8), 41 (12.3).; HRESMS: calc $C_{10}H_{15}NO_2Na$ 204.1001, Found 204.0991.